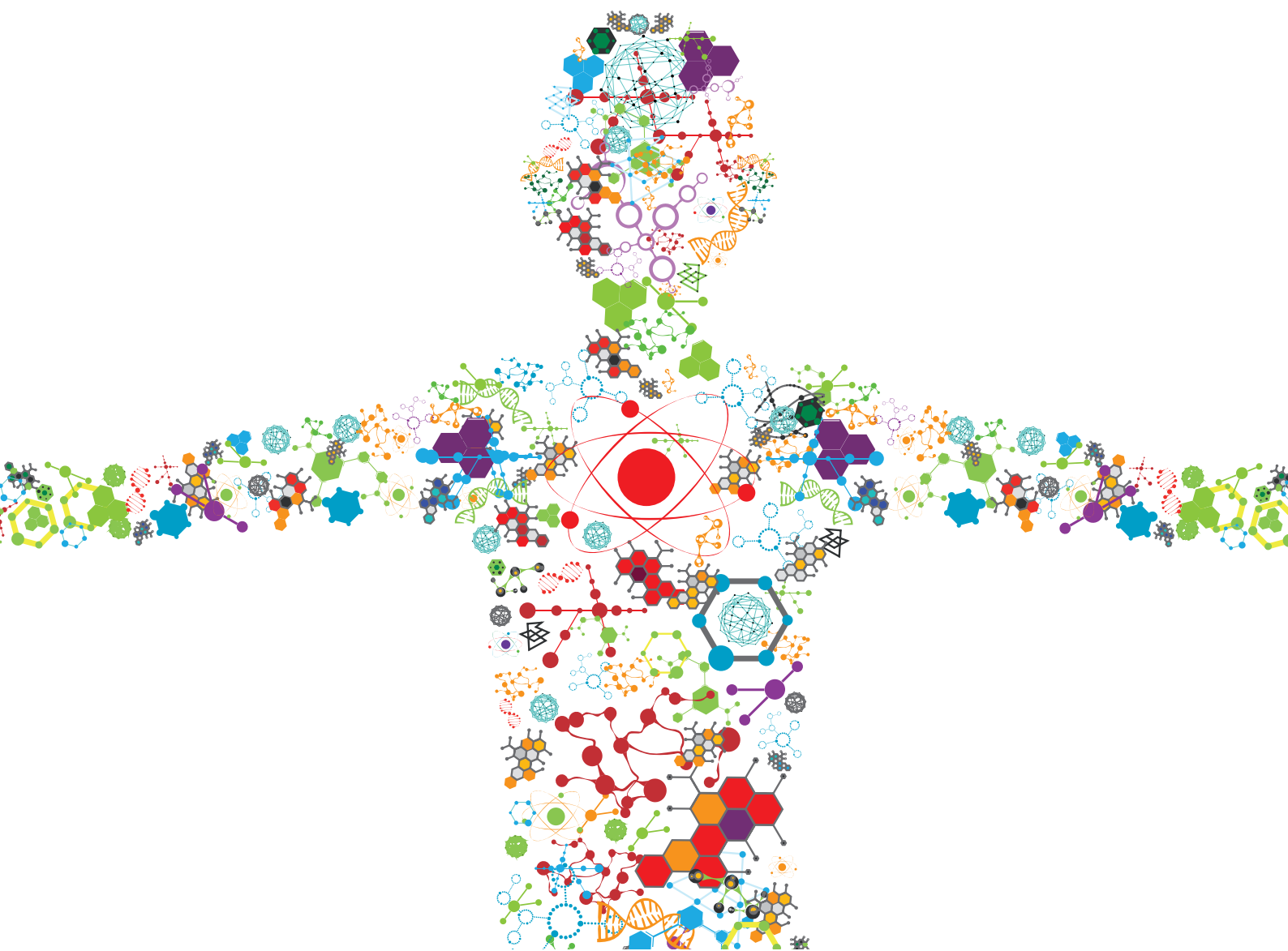


USE OF 3D MODELS IN DRUG DEVELOPMENT AND PRECISION MEDICINE: ADVANCES AND OUTLOOK

EDITED BY: Luigi Bonacina, Adriele Prina-Mello, Dania Movia and
Davide Staedler

PUBLISHED IN: Frontiers in Bioengineering and Biotechnology





frontiers

Frontiers eBook Copyright Statement

The copyright in the text of individual articles in this eBook is the property of their respective authors or their respective institutions or funders. The copyright in graphics and images within each article may be subject to copyright of other parties. In both cases this is subject to a license granted to Frontiers.

The compilation of articles constituting this eBook is the property of Frontiers.

Each article within this eBook, and the eBook itself, are published under the most recent version of the Creative Commons CC-BY licence.

The version current at the date of publication of this eBook is CC-BY 4.0. If the CC-BY licence is updated, the licence granted by Frontiers is automatically updated to the new version.

When exercising any right under the CC-BY licence, Frontiers must be attributed as the original publisher of the article or eBook, as applicable.

Authors have the responsibility of ensuring that any graphics or other materials which are the property of others may be included in the CC-BY licence, but this should be checked before relying on the CC-BY licence to reproduce those materials. Any copyright notices relating to those materials must be complied with.

Copyright and source acknowledgement notices may not be removed and must be displayed in any copy, derivative work or partial copy which includes the elements in question.

All copyright, and all rights therein, are protected by national and international copyright laws. The above represents a summary only. For further information please read Frontiers' Conditions for Website Use and Copyright Statement, and the applicable CC-BY licence.

ISSN 1664-8714

ISBN 978-2-88966-692-8

DOI 10.3389/978-2-88966-692-8

About Frontiers

Frontiers is more than just an open-access publisher of scholarly articles: it is a pioneering approach to the world of academia, radically improving the way scholarly research is managed. The grand vision of Frontiers is a world where all people have an equal opportunity to seek, share and generate knowledge. Frontiers provides immediate and permanent online open access to all its publications, but this alone is not enough to realize our grand goals.

Frontiers Journal Series

The Frontiers Journal Series is a multi-tier and interdisciplinary set of open-access, online journals, promising a paradigm shift from the current review, selection and dissemination processes in academic publishing. All Frontiers journals are driven by researchers for researchers; therefore, they constitute a service to the scholarly community. At the same time, the Frontiers Journal Series operates on a revolutionary invention, the tiered publishing system, initially addressing specific communities of scholars, and gradually climbing up to broader public understanding, thus serving the interests of the lay society, too.

Dedication to Quality

Each Frontiers article is a landmark of the highest quality, thanks to genuinely collaborative interactions between authors and review editors, who include some of the world's best academicians. Research must be certified by peers before entering a stream of knowledge that may eventually reach the public - and shape society; therefore, Frontiers only applies the most rigorous and unbiased reviews. Frontiers revolutionizes research publishing by freely delivering the most outstanding research, evaluated with no bias from both the academic and social point of view. By applying the most advanced information technologies, Frontiers is catapulting scholarly publishing into a new generation.

What are Frontiers Research Topics?

Frontiers Research Topics are very popular trademarks of the Frontiers Journals Series: they are collections of at least ten articles, all centered on a particular subject. With their unique mix of varied contributions from Original Research to Review Articles, Frontiers Research Topics unify the most influential researchers, the latest key findings and historical advances in a hot research area! Find out more on how to host your own Frontiers Research Topic or contribute to one as an author by contacting the Frontiers Editorial Office: frontiersin.org/about/contact

USE OF 3D MODELS IN DRUG DEVELOPMENT AND PRECISION MEDICINE: ADVANCES AND OUTLOOK

Topic Editors:

Luigi Bonacina, Université de Genève, Switzerland

Adriele Prina-Mello, Trinity College Dublin, Ireland

Dania Movia, Trinity College Dublin, Ireland

Davide Staedler, University of Lausanne, Switzerland

Dr. Davide Staedler is CEO of TIBIO Sagl, a consulting company, and chief scientific officer of Scitec Research S.A., a private analytical laboratory. All other Topic Editors declare no competing interests with regards to the Research Topic subject.

Citation: Bonacina, L., Prina-Mello, A., Movia, D., Staedler, D., eds. (2021). Use of 3D Models in Drug Development and Precision Medicine: Advances and Outlook. Lausanne: Frontiers Media SA. doi: 10.3389/978-2-88966-692-8

Table of Contents

04	<i>Editorial: Use of 3D Models in Drug Development and Precision Medicine - Advances and Outlook</i>	Adriele Prina-Mello, Luigi Bonacina, Davide Staedler and Dania Movia
06	<i>Cell Culture Based in vitro Test Systems for Anticancer Drug Screening</i>	Kristina V. Kitaeva, Catrin S. Rutland, Albert A. Rizvanov and Valeriya V. Solovyeva
15	<i>In vitro Alternatives to Acute Inhalation Toxicity Studies in Animal Models—A Perspective</i>	Dania Movia, Solene Bruni-Favier and Adriele Prina-Mello
25	<i>Impact of Culture Medium on Cellular Interactions in in vitro Co-culture Systems</i>	Michelle A. M. Vis, Keita Ito and Sandra Hofmann
33	<i>A Systematic Approach to Review of in vitro Methods in Brain Tumour Research (SATO RI-BTR): Development of a Preliminary Checklist for Evaluating Quality and Human Relevance</i>	Mike Bracher, Geoffrey J. Pilkington, C. Oliver Hanemann and Karen Pilkington
50	<i>Advanced Microfluidic Models of Cancer and Immune Cell Extravasation: A Systematic Review of the Literature</i>	Carlotta Mondadori, Martina Crippa, Matteo Moretti, Christian Candrian, Silvia Lopa and Chiara Arrigoni
69	<i>Organoids to Study Intestinal Nutrient Transport, Drug Uptake and Metabolism – Update to the Human Model and Expansion of Applications</i>	Tamara Zietek, Pieter Giesbertz, Maren Ewers, Florian Reichart, Michael Weinmüller, Elisabeth Urbauer, Dirk Haller, Ihsan Ekin Demir, Güralp O. Ceyhan, Horst Kessler and Eva Rath
83	<i>Ex vivo Live Cell Imaging of Nanoparticle-Cell Interactions in the Mouse Lung</i>	Fernanda Ramos-Gomes, Nathalia Ferreira, Alexander Kraupner, Frauke Alves and M. Andrea Markus
97	<i>Mechanical Stimulation: A Crucial Element of Organ-on-Chip Models</i>	Clare L. Thompson, Su Fu, Hannah K. Heywood, Martin M. Knight and Stephen D. Thorpe
115	<i>Building Scaffolds for Tubular Tissue Engineering</i>	Alexander J. Boys, Sarah L. Barron, Damyan Tilev and Roisin M. Owens
135	<i>Mass Generation, Neuron Labeling, and 3D Imaging of Minibrains</i>	Subashika Govindan, Laura Batti, Samira F. Osterop, Luc Stoppini and Adrien Roux



Editorial: Use of 3D Models in Drug Development and Precision Medicine - Advances and Outlook

Adriale Prina-Mello^{1,2*}, Luigi Bonacina³, Davide Staedler⁴ and Dania Movia^{1*}

¹ Laboratory for Biological Characterisation of Advanced Materials (LBCAM), Department of Clinical Medicine, Trinity College Dublin, Trinity Translational Medicine Institute, Dublin, Ireland, ² Advanced Materials and BioEngineering Research (AMBER) Centre, Centre for Research on Adaptive Nanostructures and Nanodevices (CRANN) Institute, Trinity College Dublin, Dublin, Ireland, ³ Department of Applied Physics, Université de Genève, Genève, Switzerland, ⁴ Department of Biomedical Sciences, University of Lausanne, Lausanne, Switzerland

Keywords: organ-on-chip, mini-organ, 3D culture, scaffold-based cell culture, organoid, drug discovery and development

Editorial on the Research Topic

Use of 3D Models in Drug Development and Precision Medicine: Advances and Outlook

Three-dimensional (3D) *in vitro* models in the drug development pipeline can help selecting the most promising and safe drug candidates at the pre-clinical stage, prior to clinical trials, reducing and sometimes even replacing animal studies in accordance with the “3Rs (Reduction, Refinement and Replacement) principle” (Herrmann and Jayne, 2019). Several types of 3D *in vitro* cultures have been developed for this purpose, including advanced models such as organ-on-chips and microfluidic models (Sontheimer-Phelps et al., 2019; Peck et al., 2020), organoids (Kim et al., 2020), and mini-organs (Lawlor et al., 2020). These models have also opened many new opportunities and research directions in the drug discovery space. For example, 3D organoids generated from cells harvested from patients can be applied toward a personalized medicine approach. Moreover, the development and translational investigation of new therapies or treatments for degenerative or regenerative applications, can be expedited by tissue engineering solutions powered by the current knowledge in 3D *in vitro* modeling. This facilitates drug formulation and screening with a direct input into the regulatory science and industrial technological innovation pipeline.

This Research Topic covers the areas of the development, use and validation of *in vitro* 3D models where novel methodologies and findings demonstrate the key role of three-dimensionality in biology, and provide a platform to increase the success rate in translating new diagnostic and treatment solutions into real clinical innovative approaches to the benefit of patients. This Research Topic features five review and perspective articles, which elucidate the multiple facets of the field of alternative models in drug discovery and provide critical considerations for its short- and long-term development. These reviews are complemented by three original research articles, which help contextualizing the challenges and the potential of the state-of-the-art in 3D *in vitro* modeling.

In the cancer research area, Kitaeva et al. contributed with a review on advanced *in vitro* models. This manuscript provides an in-depth comparison of different methodologies including two- and three-dimensional cultures, Boyden chambers, microfluidic systems, and 3D bioprinting. Mondadori et al. performed a systematic literature review updated to January 2020 on the microfluidic models available for the study of cancer and immune cells extravasation highlighting the key role of biophysical, biochemical, and environmental factors in the several studies analyzed. Similarly, Bracher et al. discuss the need for a systematic approach to review *in vitro* methods in brain tumor research. This approach would enable to identify relevant appraisal criteria to aid planning and/or evaluation of brain tumor studies using advanced *in vitro* methods.

In the tissue engineering field, the review by Thompson et al. provides insights on commercially

OPEN ACCESS

Edited and reviewed by:

Gianni Ciofani,
Italian Institute of Technology (IIT), Italy

*Correspondence:

Adriale Prina-Mello
prinamea@tcd.ie
Dania Movia
dmovia@tcd.ie

Specialty section:

This article was submitted to
Nanobiotechnology,
a section of the journal
Frontiers in Bioengineering and
Biotechnology

Received: 26 January 2021

Accepted: 08 February 2021

Published: 03 March 2021

Citation:

Prina-Mello A, Bonacina L, Staedler D
and Movia D (2021) Editorial: Use of
3D Models in Drug Development and
Precision Medicine - Advances and
Outlook.
Front. Bioeng. Biotechnol. 9:658941.
doi: 10.3389/fbioe.2021.658941

available organ-on-chip platforms incorporating active biomechanical stimulation. The authors highlight instances where mechanical stimuli can drastically alter a given biochemical response with relevance to pre-clinical studies. They also critically discuss which level of approximation of the *in vivo* conditions is sufficient for the proposed screening applications. In their review entitled “Building Scaffolds for Tubular Tissue Engineering,” Boys et al. from University of Cambridge, discuss some of state-of-the-art methods for producing hollow and tubular systems. The latter deem essential to provide crucial tissue structures including vasculature, the intestines, and the trachea. The authors carefully review different methodologies such as casting, electrospinning, rolling, 3D printing, and decellularization.

In the lung research area, Movia et al. present a perspective article on the status and the outlook of *in vitro* respiratory models for toxicity studies. Notably this contribution provides a compendium of regulatory information useful for all researchers in the field. Ramos-Gomes et al. took a distinct perspective for their contribution to the topic, by introducing a novel method to study nanoparticle-cell interactions in the lung. This work details a clever imaging protocol to obtain time-series at high spatial resolution in an *ex vivo* system. The authors discuss the potential of this approach for assessing novel therapeutic strategies with a special emphasis on nanomedicine.

In the organoids and mini-organs field, Zietek et al. describe the applicability of 3D organoids for *in vitro* investigation of intestinal biochemical processes related to transport and

metabolism of nutrients and drugs. The authors, relying on a wide range of methodologies, provide a thorough assessment of the robustness and reliability of intestinal organoids. Whereas, Govindan et al. detail the step-by-step procedure leading to the generation of human mini-brains (i.e., 3D brain *in vitro* spheroid models comprising of neurons and glial cells, generated from human induced pluripotent neural stem cells) and the protocols to successfully label projection neurons, perform immunohistochemistry and 3D imaging at large scales.

In conclusion, this Research Topic provides an extended overview of the advanced *in vitro* approaches that can be applied to drug development and precision medicine. We are sure the reader will find this Research Topic as a useful reference for state-of-the-art in the fast-growing field of 3D cultures, organ-on-chip, organoids and mini-organs and their use in the relevant toxicology, bioengineering, and biomedical fields.

AUTHOR CONTRIBUTIONS

All authors contributed to the drafting and finalization of the editorial.

FUNDING

This work has been supported, in parts, by the European Union's HORIZON 2020 Framework Programme under Grant Agreements Nos. 760928 and 761104.

REFERENCES

- Herrmann, K., and Jayne, K. (2019). *Animal Experimentation: Working Towards a Paradigm Change*. Boston, MA: Brill. doi: 10.1163/9789004391192
- Kim, J., Koo, B.-K., and Knoblich, J. A. (2020). Human organoids: model systems for human biology and medicine. *Nat. Rev. Mol. Cell Biol.* 21, 571–584. doi: 10.1038/s41580-020-0259-3
- Lawlor, K. T., Vanslambrouck, J. M., Higgins, J. W., Chambon, A., Bishard, K., Arndt, D., et al. (2020). Cellular extrusion bioprinting improves kidney organoid reproducibility and conformation. *Nat. Mater.* 20, 260–271. doi: 10.1038/s41563-020-00853-9
- Peck, R. W., Hinojosa, C. D., and Hamilton, G. A. (2020). Organs-on-chips in clinical pharmacology: putting the patient into the center of treatment selection and drug development. *Clin. Pharmacol. Ther.* 107, 181–185. doi: 10.1002/cpt.1688

- Sontheimer-Phelps, A., Hassell, B. A., and Ingber, D. E. (2019). Modelling cancer in microfluidic human organs-on-chips. *Nat. Rev. Cancer* 19, 65–81. doi: 10.1038/s41568-018-0104-6

Conflict of Interest: The authors declare that the research was conducted in the absence of any commercial or financial relationships that could be construed as a potential conflict of interest.

Copyright © 2021 Prina-Mello, Bonacina, Staedler and Movia. This is an open-access article distributed under the terms of the Creative Commons Attribution License (CC BY). The use, distribution or reproduction in other forums is permitted, provided the original author(s) and the copyright owner(s) are credited and that the original publication in this journal is cited, in accordance with accepted academic practice. No use, distribution or reproduction is permitted which does not comply with these terms.



Cell Culture Based *in vitro* Test Systems for Anticancer Drug Screening

Kristina V. Kitaeva¹, Catrin S. Rutland², Albert A. Rizvanov^{1,2} and Valeriya V. Solovyeva^{1*}

¹ Institute of Fundamental Medicine and Biology, Kazan Federal University, Kazan, Russia, ² School of Veterinary Medicine and Science, University of Nottingham, Nottingham, United Kingdom

OPEN ACCESS

Edited by:

Adriale Prina-Mello,
Trinity College Dublin, Ireland

Reviewed by:

Fransisca Leonard,
Houston Methodist Research
Institute, United States
Francesca Bianchini,
University of Florence, Italy

*Correspondence:

Valeriya V. Solovyeva
solovyovavv@gmail.com

Specialty section:

This article was submitted to
Nanobiotechnology,
a section of the journal
Frontiers in Bioengineering and
Biotechnology

Received: 26 November 2019

Accepted: 24 March 2020

Published: 09 April 2020

Citation:

Kitaeva KV, Rutland CS,
Rizvanov AA and Solovyeva VV (2020)
Cell Culture Based *in vitro* Test
Systems for Anticancer Drug
Screening.
Front. Bioeng. Biotechnol. 8:322.
doi: 10.3389/fbioe.2020.00322

The development of new high-tech systems for screening anticancer drugs is one of the main problems of preclinical screening. Poor correlation between preclinical *in vitro* and *in vivo* data with clinical trials remains a major concern. The choice of the correct tumor model at the stage of *in vitro* testing provides reduction in both financial and time costs during later stages due to the timely screening of ineffective agents. In view of the growing incidence of oncology, increasing the pace of the creation, development and testing of new antitumor agents, the improvement and expansion of new high-tech systems for preclinical *in vitro* screening is becoming very important. The pharmaceutical industry presently relies on several widely used *in vitro* models, including two-dimensional models, three-dimensional models, microfluidic systems, Boyden's chamber and models created using 3D bioprinting. This review outlines and describes these tumor models including their use in research, in addition to their characteristics. This review therefore gives an insight into *in vitro* based testing which is of interest to researchers and clinicians from differing fields including pharmacy, preclinical studies and cell biology.

Keywords: drug screening, two-dimensional cultures, three-dimensional cultures, microfluidic systems, Boyden chamber, tumor microenvironment, 3D bioprinting

INTRODUCTION

The number of patients diagnosed with cancer is increasing worldwide and one of the most important challenges remains the development of effective, safe and economically viable antitumor drugs. Clinical approval for drugs tested in preclinical studies enabling them to enter phase I clinical trials is essential. Currently, potential anticancer drugs have a very low rate of gaining clinical approval at around 7%, much lower than drugs for other diseases (Hay et al., 2014). Given the high cost and duration of anticancer drug clinical development it is necessary to develop new, more effective preclinical platforms for screening antitumor compounds (Imamura et al., 2015).

In vitro tumor models are a necessary tool in not only the search for new substances showing antitumor activity but additionally for assessing their effectiveness. Realistic *in vitro* models of tumors enable more detailed primary screening of potential antitumor drugs thus preventing drugs with insufficient antitumor activity from entering preclinical animal testing. Pharmacological testing on animal models is carried out to assess bioavailability, toxicity at specific doses and therapeutic efficacy of compounds (Stevens and Baker, 2009). According to industry standards, any novel drugs must undergo preclinical trials using animal models before being admitted to human

clinical trials. However, the use of animal models can cause a number of problems including high cost, differential responses due to physiological variations between species, and limitations in test availability and feasibility (Bileckot et al., 1991). This presents an opportunity and a requirement for the creation of more high-tech *in vitro* models to assess the therapeutic efficacy of antitumor drugs.

TUMOR MICROENVIRONMENT

The behavior of the tumor in the body is determined by cells within the tumor and stromal tumor microenvironment (TME) and the extracellular matrix (ECM), which provides structural support for cells in the extracellular space (Chiantore et al., 2015). The TME is characterized by a low extracellular pH and a high level of hypoxia, both factors moderate dormant phenotypes of tumor cells. As a result, these factors are associated with development of therapy resistance and poor prognosis of tumor-bearing patients (Peppicelli et al., 2017; Butturini et al., 2019). The tumor biological characteristics are similar to the chronically unhealed wound with constant inflammation, which contributes toward tumorigenesis, tumor progression and metastasis (Gal et al., 2017). Attracted by the tumor stromal microenvironment, other cell types also play a key role in not only tumor progression and metastasis, but also in the formation of resistance to therapies (Wu and Dai, 2017). Within the TME many other cellular components reside including immune cells (T-lymphocytes, B-lymphocytes, neutrophils, natural killer cells (NK-cells) and macrophages), endothelial cells associated with the tumor, fibroblasts, myofibroblasts, adipocytes, pericytes and mesenchymal stem/stromal cells (MSCs) (Chiantore et al., 2015).

The stromal cells and fibroblasts within the TME are known to secrete growth factors and chemokines, which support the growth and survival of malignant cells and additionally function as chemoattractants that stimulate the migration of other cells into the tumor (Hanahan and Coussens, 2012). MSCs are involved throughout every stage of tumor development: avoiding immunological surveillance, stimulating tumor angiogenesis, developing resistance to therapy, invasion and metastasis, as well as inducing the transition of tumor cells into a low-differentiated state and the formation of stem tumor cells (Sun et al., 2014). Of great interest is the interaction between immune cells and tumor cells, this is primarily due to the dual role of immune cells and the factors they produce. Immune reactions prevent and inhibit the development of tumors, however, recent evidence suggests that immune cells in the tumor microenvironment closely interact with transformed malignant cells, thus promoting oncogenesis (Payne et al., 2014).

An important component of TME is the ECM, consisting of components with various physical and biochemical properties, including proteins, glycoproteins, proteoglycans and polysaccharides (Insua-Rodriguez and Oskarsson, 2016). ECM provides physical support for TME cells, and also it is a source of key growth factors. In the late stages of the ECM become disorganized. ECM modulates the behavior of stromal cells in the tumor microenvironment, which leads to

the induction of inflammatory reactions and the growth of new blood vessels (Trivanovic et al., 2016).

Thus, the study of the tumor as a complex environment can make a significant contribution to improving the quality of cancer treatment, as can the development of new diagnosis and personalized therapeutic methodologies (Chulpanova et al., 2018a,b,c), alongside the creation of new, realistic tumor models for the effective screening of new substances exhibiting potential antitumor activity.

TWO-DIMENSIONAL CULTURES

Until the 1980s, the National Cancer Institute (NCI) used *in vivo* mouse models of P388 or L1210V leukemia for systematic screening of drugs (Waud, 2011). These models possessed high levels of productivity and stability, were convenient for data interpretation, and were relatively inexpensive. Despite these qualities, a significant drawback to these models was the inability to identify potential antitumor substances aimed at treating solid tumors. This drawback was taken into account, and by the end of the 80s, an *in vitro* panel for drug screening was developed, consisting of 60 different human cell lines originating from tumors (leukemia, melanoma, tumors of the central nervous system, cancer of the lungs, colon, ovaries, breast, kidney, and prostate), which was called NCI60 (Mingaleeva et al., 2013).

Testing a drug of interest using the NCI60 panel involves the application of two-dimensional (2D) tumor cell cultures, grown in a monolayer on a flat surface (Takimoto, 2003). During the first stage of screening, testing is carried out on the three cell lines that are frequently the most sensitive to drug therapy, MCF7 (breast adenocarcinoma), NCI-H460 (lung carcinoma) and SF-268 (glioma) (Blatt et al., 2013). The cytotoxicity of the test substance is determined using the pink anionic dye sulforodamine B. If the test substance inhibits the growth of at least one cell line, testing proceeds to the next stage comprising of the full 60 cell line panel (Mingaleeva et al., 2013). In 2017, the NCI ALMANAC database was created based on screening results using the NCI60 panel¹. The database helped identify new effective combinations of existing antitumor drugs and new clinical trials were launched (Holbeck et al., 2017).

By analogy with the NCI60 panel, the Japanese Foundation for Cancer Research (JFCR) developed a panel in the 1990s consisting of 30 tumor lines from the NCI60 panel, plus nine tumor cell lines specific to the Japanese population, specifically gastric cancer cells (St-4, MKN-1, MKN-7, MKN-28, MKN-45, and MKN-74) and breast cancer cells (HBC-4, HBC-5, and BSY-1). Thus, the panel included 39 cell lines and was therefore called JFCR39 (Nakatsu et al., 2007). However, during clinical trials, it became apparent that drugs that have shown high efficacy in 2D *in vitro* models do not always work or can have a low efficacy in oncology patients (Shoemaker, 2006). This phenomenon is partially explained by the fact that cells grown in 2D cultures do not have a complex three-dimensional tissue architecture and do not exactly reflect the complex interactions

¹ <https://dtp.cancer.gov/ncialmanac>

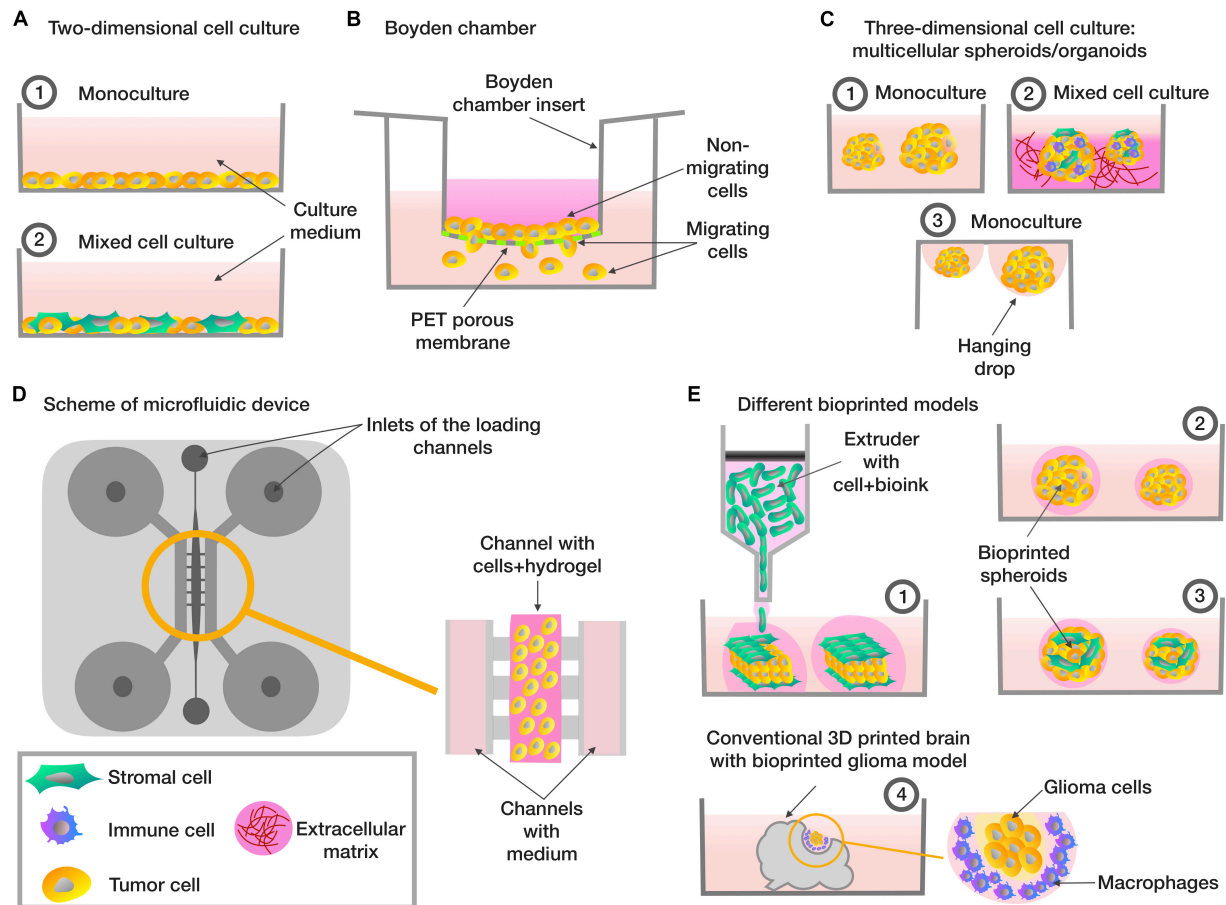


FIGURE 1 | Different types of *in vitro* tumor models. **(A)** Two-dimensional cell cultures based on monolayer (1) consisting of tumor cells (2) co-culture included tumor and stromal cells. **(B)** The Boyden chamber scheme, analyzing the ability of cells to migrate – cells with high invasive potential pass through the porous membrane. **(C)** Three-dimensional cellular models based on multicellular spheroids/organoids: (1) spheroids consisting of tumor cells (2) a tumor stroma model based on the co-cultivation of several types of cells on extracellular matrix model or on the organoid-based manner (3) spheroids created using the hanging drops method. **(D)** Scheme of microfluidic system that evaluates the invasive potential of tumor cells – a mixture of hydrogel and cells is placed in the central channel, into the lateral channels placed the enriched/depleted factors medium depending on the purpose of the experiment. **(E)** Tumor bioprinting models (1) a tumor model, which is a layer of tumor cells located between the layers of stromal cells (2) bioprinted spheroids consisting of tumor cells (3) bioprinted spheroids, which are a model of the tumor stroma, consisting of tumor cells mixed with stromal cells (4) a glioma model, consisting of conventional 3D-printed model of the brain with glioma cells and macrophages embedded in.

between TME or ECM and cells which exist in the body (Figure 1A; Rizvanov et al., 2010).

BOYDEN CHAMBER

The Boyden chamber is a chamber consisting of two compartments filled with medium and separated by a microporous membrane (Falasca et al., 2011). Boyden chamber is a convenient tool for the study of chemotaxis, assessing cell motility and invasion (Figure 1B). Thus, the Boyden chamber was used to assess cell motility in a study on the effect of free paclitaxel and paclitaxel-loaded pyromellitic nanorods on reducing the growth and invasiveness of melanoma cells (Clemente et al., 2019). Wessely et al. (2019) also tested the use of the Boyden chamber to evaluate and compare the

invasive activity of spheroids containing only tumor cells and spheroids containing a mixture of tumor and stem cells. Another study examined the adhesion and cytoskeletal migration of HT1080 fibrosarcoma cells and LX2 line stellate cells in a three-dimensional system using fibronectin, Matrigel and type I collagen as chemoattractants (Tovari et al., 2014). However, despite the ease of use of the Boyden chamber, researchers are increasingly turning to more advanced systems that take into account a greater number of TME conditions, in particular, microfluidic systems.

THREE-DIMENSIONAL CULTURES

It is known that 2D cultures do not fully reflect the pathophysiology of tumor cells and the actual level of resistance

TABLE 1 | Comparative characteristics of cell culture test systems for anticancer drug screening.

Tumor model	Advantages	Disadvantages	Application	Cell type	References
Two-dimensional mono cell cultures	Simple test system for rapid cost effective screening of multiple compounds or libraries	Do not have a complex three-dimensional tissue architecture, complex interactions between TME or ECM and cells	Anticancer drug screening	NCI60 panel	(Shoemaker, 2006)
Boyden's chamber	Possibility to study the effect of the test substance on the invasiveness and migration potential of tumor cells	The lack of direct intercellular interactions (the study of paracrine factors only) important for TME	Chemotaxis, assessing cell motility and invasion studies	JFCR39 panel 2D cultures (melanoma, fibrosarcoma and other cell types)	(Nakatsu et al., 2007) (Tovari et al., 2014; Clemente et al., 2019)
Microfluidic systems	Can reproduce a specific fluid flow, constant temperature, flow pressure and chemical gradients characteristic of <i>in vivo</i> systems	Expensive consumables and equipment, non-standardized protocols	Migration/invasion and extravasation studies	Spheroids (tumor or tumor and stem cells) 2D cultures (lung adenocarcinoma cells, breast tumor cells and other cell types) Co-culture (CAFs + NSCLC cells) Breast or liver cancer spheroids	(Kaneda et al., 2019; Wessely et al., 2019) (Chen et al., 2010; Wang et al., 2013; Anguiano et al., 2017) (Yu et al., 2016) (Yu et al., 2010; Zuchowska et al., 2017)
Three-dimensional spheroids	Can reproduce paracrine and direct intercellular interaction, complex three-dimensional architecture and hypoxic conditions in the center of the spheroid	Do not accurately reproduce interaction between ECM and cells. Difficult to standardize.	Anticancer drug screening, invasion studies	One cell type (breast, liver cancer cells, head and neck squamous cell carcinoma and other cell types)	(Uchida et al., 2010; Imamura et al., 2015; Melissaridou et al., 2019)
Three-dimensional organoids	Accurately reproduce <i>in vivo</i> tumor architecture	Difficulty in creating large numbers of homogeneous organoids for high-throughput drug screening	Anticancer drug screening, invasion and extravasation studies	Several cell types (colorectal carcinoma + fibroblasts/endothelial cells) Organoids derived from lung cancer/prostate cancer bone metastasis/bladder cancer tissues Cerebral glioma/medulloblastoma organoids derived from induced pluripotent stem cells (iPSCs) Colon cancer organoids derived from cancer stem cells (CSCs)	(Zoetemelk et al., 2019) (Kim et al., 2019; Mullenders et al., 2019; Nelson et al., 2020) (Linkous et al., 2019; Ballabio et al., 2020) (Otte et al., 2019)
Co-cultures on scaffolds	Complex three-dimensional tissue architecture, complex interactions between TME or ECM and cells	Poor reproducibility and similarity to <i>in vivo</i> tumor architecture	Anticancer drug screening, invasion studies, cell infiltration studies	Co-culture of NSCLC cells + fibroblasts + immune cells on Matrigel Co-culture of PDAC cell lines + CAFs surrounding by oligomeric type I collagen	(Osswald et al., 2019) (Puls et al., 2018)

(Continued)

TABLE 1 | Continued

Tumor model	Advantages	Disadvantages	Application	Cell type	References
3D Bioprinting	Reproducing of complex three-dimensional tissue architecture, mimicking chemical environments in tumor, complex interactions between TME or ECM and cells, possibility to create standardized cellular structures for high-throughput drug screening	Expensive consumables and equipment, low precision of cell positioning	Anticancer drug screening, tumor cell invasion and angiogenesis studies	Co-culture of breast cancer cells + GM637 fibroblasts on reconstitutable tissue matrix scaffold (TMS) Co-culture of A549 lung carcinoma cells + HUVEC	(Rijal and Li, 2017) (Meng et al., 2019)
				Co-culture of glioblastoma cells and glioblastoma-associated macrophages (GAMs) Co-culture of breast cancer MCF-7/MDA-MB-468 cells and MCF-12A organoid	(Heinrich et al., 2019) (Reid et al., 2019)

to radiotherapy or chemotherapy in the tumor niche in the *in vivo* system (Chen et al., 2012; **Table 1**). Studies have shown that gene expression profiles as well as treatment responses in multicellular spheroid 3D models are more similar to the *in vivo* situation (Riedl et al., 2017). For example, liver tumor cells in 3D culture have high resistance to drug treatment, similar to the resistance of solid tumors *in vivo* (Uchida et al., 2010). Thus, the BT-549, BT-474, and T-47D breast cancer cell lines cultured as spheroids showed greater resistance to paclitaxel and doxorubicin compared to cells in a 2D culture (Imamura et al., 2015). Cells of squamous cell carcinoma originating from the head and neck (lines LK0902, LK0917, and LK1108) cultured as spheroids were shown to be less sensitivity to cisplatin when compared with 2D cultures. Also in cell lines LK0917 and LK1108, resistance to cetuximab was observed, mediated by culturing in the form of spheroids (Melissaridou et al., 2019). When culturing HCT-116, SW-620, and DLD-1 cells in the form of spheroids or in co-culture with fibroblasts and endothelial cells, their resistance to 5-fluorouracil, regorafenib, and erlotinib preparations increases (Zoetemelk et al., 2019).

It is known that the TME may significantly change the susceptibility of tumor cells to drugs. To solve this problem, new methods were developed for culturing cells using the ECM to model spatial organization, as well as adding various types of cells included in the TME to the culture (Kitaeva et al., 2019). 3D co-cultures of non-small cell lung cancer (NSCLC) and fibroblasts embedded in a Matrigel or encapsulated in alginate are used as models in drug discovery for analysis of immune cell infiltration (Osswald et al., 2019). Also, described is a high-potential tumor spheroid model drug screening, which consists of pancreatic ductal adenocarcinoma (PDAC) cell lines (Panc-1 and BxPC-3) and cancer-associated fibroblasts (CAFs) surrounding by oligomeric type I collagen (Oligomer) for creation of the interstitial ECM supports definition (Puls et al., 2018).

An alternative way to create a novel 3D tumor-tissue model is organoid manner. One of the first of developed spheroid method was a mammospheres, described Dontu et al. (2003). The novel *in vitro* system allowed the propagation of mammary stem and progenitor cells into functional ductal/acinar structures (Dontu et al., 2003). Organoids can be received by two main types of stem cells: pluripotent embryonic stem cells and their synthetic induced pluripotent stem cell counterparts and organ-restricted adult stem cells (Clevers, 2016). Also, organoids received by cultivation small tissue fragments and explants on matrixes or from cultured or sorted cells assembled to organoids *in vitro* (Hu et al., 2018). Organoids from primary lung cancer tissues demonstrated the high reproduction levels of histological and genetic characteristics of *in situ* tissue and their high ability for using them in patient-specific drug trials (Kim et al., 2019). Organoid manner was used for modeling PDAC from patient derived xenografts (PDX) tumors (Nelson et al., 2020) and organoids derived from patient prostate cancer bone metastasis (Lee et al., 2020). Organoids derived from patients with bladder cancer were tested with epirubicin, mitomycin C, gemcitabine, vincristine, doxorubicin, and cisplatin, this model was presented as a prospective model of human bladder cancer (Mullenders et al., 2019; **Figure 1C**).

MICROFLUIDIC SYSTEMS

Microfluidic systems are prospective models for reconstructing the migration, microenvironment, and microcirculation of cells in tumor tissue. Microfluidic systems are small devices that can reproduce a specific fluid flow, constant temperature, fresh medium, flow pressure and chemical gradients characteristic of *in vivo* systems (Ruzycka et al., 2019; **Figure 1D**).

The microfluidic system using collagen-matrigel hydrogel matrices made it possible to reproduce the microenvironment and experimental conditions for studying the migration and invasion of H1299 lung adenocarcinoma cells. At the same time, Matrigel in low concentrations facilitated the migration of H1299 cells, however, at a high concentration Matrigel slowed the migration of cells, possibly due to their excessive attachment. It has also been shown that the use of antibody-based integrin blockers significantly modulated the mechanisms of H1299 cell migration (Anguiano et al., 2017). A microfluidic system with an incessant supply of nutrient medium through a syringe pump has also been described. It is used to study the effect of the matrix metalloproteinase inhibitor (GM6001) on the formation of invadopodia in A549 lung cancer cells, which is characteristic of cells during invasion (Wang et al., 2013). Microfluidic systems also make it possible to obtain a metastatic model of a tumor, such as breast cancer, which allows the study of antitumor drugs effects on the inhibition of tumor cell migration (Mi et al., 2016). To simulate the extravasation process, a microfluidic system was constructed containing two microfluidic channels and a porous membrane sandwiched between them. The first channel represents the vascular equivalent and contains primary endothelial cells isolated from the pulmonary artery. The second channel acts as a reservoir for collecting migratory tumor cells. In this case, endothelial cells showed *in vivo*-like behavior under flow conditions. The introduced GFP-labeled tumor cells of epithelial or mesenchymal origin were detected using vital imaging, which showed tightly attached tumor cells to the endothelial membrane (Kuhlbach et al., 2018).

3D BIOPRINTING

One of the types of three-dimensional cultures is 3D bioprinting, which enables researchers to create various situations that mimic the processes that occur in the TME (Lee et al., 2016; Truong et al., 2018). 3D bioprinting technology enables the creation of standardized test-systems for screening anticancer drugs (Kingsley et al., 2019; **Figure 1E**). For example, a model of human hepatoma created using 3D bioprinting was more resistant to an anti-CD147 monoclonal antibody (Metuzumab) than a similar model created on a microfluidic system (Li et al., 2019).

An interesting approach is the combination of several types of cells, tumor and stromal, in a 3D bioprinting model. Breast cancer cells and fibroblasts cultured in 3D bioprinting spheroids as part of an alginate-gelatin hydrogel maintained viability for more than 30 days and were resistant to paclitaxel, which was not observed in 3D bioprinting monocultures of breast cancer cells (Jiang et al., 2018). The trophic role of stromal or immune cells has been

shown in other studies. The presence of MSCs in 3D bioprinting hydrogel constructs supported breast cancer cell viability after exposure of doxorubicin (Wang et al., 2018). Application of 3D bioprinting technology also allows immune cell behavior studies in TME. In a 3D bioprinting model, glioblastoma cells were shown to actively recruit macrophages and polarize them in glioblastoma-associated macrophages (GAMs), which in turn contributed to the proliferation and invasiveness of glioblastoma cells (Heinrich et al., 2019). 3D-bioprinting models of breast and pancreatic cancer containing the stromal component (human umbilical vessel epithelial cells (HUVEC), fibroblasts, MSCs) and an ECM analog were described. The resulting 3D bioprinting models repeated the behavior of tumors *in vivo* and *in situ* (Langer et al., 2019).

The using of 3D bioprinting also enables designs that simulate tumor vascularization. 3D organotypic microfluidic platform, integrated with hydrogel biomaterials, were obtained in order to simulate the vascular niche of glioma stem cells (GSCs) obtained from patients (Truong et al., 2018). It has been shown that the microvascular network enhances invasion, supports the proliferation rate and the classic GSCs phenotype (Truong et al., 2018). A three-dimensional model of GSCs is described in the composition of a porous hydrogel containing gelatin, alginate and fibrinogen. GSCs actively proliferated, retained viability and biological properties (nestin expression, differentiation ability) in the resulting 3D bioprinting *in vitro* model, and also had resistance to the cytotoxic effect of temozolomide in contrast to 2D culture. An increase in vascular endothelial growth factor (VEGF) secretion in the first 3 weeks of cultivation was also noted, which indicates the induction of tumor angiogenesis mechanisms (Dai et al., 2016). 3D bioprinting capsules with programmable VEGF and EGF outputs also mimics tumor vascularization. The programmed release of growth factors facilitates control over cell migration and the process of angiogenesis, therefore it is possible to get a dynamic system for the study of metastatic processes (Meng et al., 2019).

Thus, the designs obtained using 3D bioprinting enable us to simulate various processes occurring in TME. Further studies in the field of 3D bioprinting, standardization and validation of the developed tumor models will allow the creation of high-efficiency 3D tumor models in order to obtain new fundamental knowledge about the mechanisms of carcinogenesis and also to more accurately screen potential anticancer drugs and aid individual selection of drugs (Knowlton et al., 2015).

CONCLUSION

In recent decades, preclinical trials of antitumor agents have undergone significant changes, in particular, much attention has been focused on the modernization of screening protocols for cell cultures. The widespread use of *in vitro* models in preclinical practice was facilitated by the development of the NCI60 panel. Even after more than 30 years, this model is still actively used for screening anticancer drugs as a reference *in vitro* testing method. However, as knowledge of intercellular interactions within the tumor deepened, as well as the low reliability of testing

potential anticancer drugs on the NCI60 panel, in the field of preclinical screening, the need arose to develop more complex and high-tech models. Three-dimensional cultures, representing spheroids and spheroid-like formations grown under various cultivation conditions, partially satisfied this request. Three-dimensional cultures compensated for some of the shortcomings of two-dimensional cultures, in particular those associated with intercellular interactions and interactions with the extracellular scaffold. However, conventional three-dimensional cultures are not quite suitable for assessing the effect of anticancer drugs on important processes as migration, invasion and chemotaxis; such studies require the use of additional devices, for example, chips in microfluidic systems and the Boyden chamber. One of the trends of the last decade has been the use of 3D bioprinting, thanks to which, in theory, it is possible to print fabric with the desired architecture with a sufficiently high resolution. Although at the moment there is no universal protocol for printing this or a standard type of tumor tissue used with it, interest in this technology and the importance of its further development are not weakening. Researchers working in the developing new screening models field may liken the situation to the Greek mythology of Odysseus, finding themselves between Scylla and Charybdis – when the model must be complex enough to take into account

most of the microenvironment factors, but at the same time be reproducible, with the ability to correctly interpret the screening results. Existing trends in science, particularly in the field of preclinical screening, are heading precisely toward complicating the models being developed, drawing an analogy, the course for Scylla, which turned out to be a competent choice for Odysseus.

AUTHOR CONTRIBUTIONS

VS, KK, and AR conceptualization. KK and VS writing – original draft preparation. VS, CR, and AR writing – review and editing. KK visualization. VS and AR supervision.

FUNDING

This study was supported by the Russian Foundation for Basic Research (RFBR) grant 18-04-01133. Albert Rizvanov was funded by the subsidy allocated to Kazan Federal University for the state assignment in the sphere of scientific activities. Kazan Federal University was supported by the Russian Government Program of Competitive Growth.

REFERENCES

- Anguiano, M., Castilla, C., Maska, M., Eder, C., Pelaez, R., Morales, X., et al. (2017). Characterization of three-dimensional cancer cell migration in mixed collagen-Matrigel scaffolds using microfluidics and image analysis. *PLoS One* 12:e0171417. doi: 10.1371/journal.pone.0171417
- Ballabio, C., Anderle, M., Giansello, M., Lago, C., Miele, E., Cardano, M., et al. (2020). Modeling medulloblastoma in vivo and with human cerebellar organoids. *Nat. Commun.* 11:583. doi: 10.1038/s41467-019-13989-3
- Bilek, R., Masson, C., Ntsiba, H., Mbongo, J. A., Biendo, M., Yala, F., et al. (1991). [Prospective study of rheumatic manifestations in human immunodeficiency virus infection. Apropos of 26 cases in Congo]. *Rev. Rhum. Mal. Osteoartic.* 58, 163–168.
- Blatt, N. L., Mingaleeva, R. N., Khaiboullina, S. F., Lombardi, V. C., and Rizvanov, A. A. (2013). Application of cell and tissue culture systems for anticancer drug screening. *World Appl. Sci. J.* 23, 315–325. doi: 10.5829/idosi.wasj.2013.23.03.13064
- Butturini, E., Carcereri de Prati, A., Boriero, D., and Mariotto, S. (2019). Tumor dormancy and interplay with hypoxic tumor microenvironment. *Int. J. Mol. Sci.* 20:4305. doi: 10.3390/ijms20174305
- Chen, L., Xiao, Z., Meng, Y., Zhao, Y., Han, J., Su, G., et al. (2012). The enhancement of cancer stem cell properties of MCF-7 cells in 3D collagen scaffolds for modeling of cancer and anti-cancer drugs. *Biomaterials* 33, 1437–1444. doi: 10.1016/j.biomaterials.2011.10.056
- Chen, M. C., Gupta, M., and Cheung, K. C. (2010). Alginate-based microfluidic system for tumor spheroid formation and anticancer agent screening. *Biomed. Microdevices* 12, 647–654. doi: 10.1007/s10544-010-9417-2
- Chiantore, M. V., Mangino, G., Zangrillo, M. S., Iuliano, M., Affabris, E., Fiorucci, G., et al. (2015). Role of the microenvironment in tumorigenesis: focus on virus-induced tumors. *Curr. Med. Chem.* 22, 958–974.
- Chulpanova, D. S., Kitaeva, K. V., James, V., Rizvanov, A. A., and Solovyeva, V. V. (2018a). Therapeutic prospects of extracellular vesicles in cancer treatment. *Front. Immunol.* 9:1534. doi: 10.3389/fimmu.2018.01534
- Chulpanova, D. S., Kitaeva, K. V., Tazetdinova, L. G., James, V., Rizvanov, A. A., and Solovyeva, V. V. (2018b). Application of mesenchymal stem cells for therapeutic agent delivery in anti-tumor treatment. *Front. Pharmacol.* 9:259. doi: 10.3389/fphar.2018.00259
- Chulpanova, D. S., Solovyeva, V. V., Kitaeva, K. V., Dunham, S. P., Khaiboullina, S. F., and Rizvanov, A. A. (2018c). Recombinant viruses for cancer therapy. *Biomedicines* 6:94. doi: 10.3390/biomedicines6040094
- Clemente, N., Argenziano, M., Gigliotti, C. L., Ferrara, B., Boggio, E., Chiochetti, A., et al. (2019). Paclitaxel-loaded nanospheres inhibit growth and angiogenesis in melanoma cell models. *Front. Pharmacol.* 10:776. doi: 10.3389/fphar.2019.00776
- Clevers, H. (2016). Modeling development and disease with organoids. *Cell* 165, 1586–1597. doi: 10.1016/j.cell.2016.05.082
- Dai, X., Ma, C., Lan, Q., and Xu, T. (2016). 3D bioprinted glioma stem cells for brain tumor model and applications of drug susceptibility. *Biofabrication* 8:045005. doi: 10.1088/1758-5090/8/4/045005
- Dontu, G., Al-Hajj, M., Abdallah, W. M., Clarke, M. F., and Wicha, M. S. (2003). Stem cells in normal breast development and breast cancer. *Cell Prolif.* 36(Suppl. 1), 59–72. doi: 10.1046/j.1365-2184.36.s.1.6.x
- Falasca, M., Raimondi, C., and Maffucci, T. (2011). Boyden chamber. *Methods Mol. Biol.* 769, 87–95. doi: 10.1007/978-1-61779-207-6_7
- Gal, P., Varinska, L., Faber, L., Novak, S., Szabo, P., Mitrengova, P., et al. (2017). How signaling molecules regulate tumor microenvironment: parallels to wound repair. *Molecules* 22:1818. doi: 10.3390/molecules22111818
- Hanahan, D., and Coussens, L. M. (2012). Accessories to the crime: functions of cells recruited to the tumor microenvironment. *Cancer Cell* 21, 309–322. doi: 10.1016/j.ccr.2012.02.022
- Hay, M., Thomas, D. W., Craighead, J. L., Economides, C., and Rosenthal, J. (2014). Clinical development success rates for investigational drugs. *Nat. Biotechnol.* 32, 40–51. doi: 10.1038/nbt.2786
- Heinrich, M. A., Bansal, R., Lammers, T., Zhang, Y. S., Michel Schiffelers, R., and Prakash, J. (2019). 3D-bioprinted mini-brain: a glioblastoma model to study cellular interactions and therapeutics. *Adv. Mater.* 31:e1806590. doi: 10.1002/adma.201806590
- Holbeck, S. L., Camalier, R., Crowell, J. A., Govindharajulu, J. P., Hollingshead, M., Anderson, L. W., et al. (2017). The national cancer institute ALMANAC: a comprehensive screening resource for the detection of anticancer drug pairs with enhanced therapeutic activity. *Cancer Res.* 77, 3564–3576. doi: 10.1158/0008-5472.CAN-17-0489
- Hu, J. L., Todhunter, M. E., LaBarge, M. A., and Gartner, Z. J. (2018). Opportunities for organoids as new models of aging. *J. Cell. Biol.* 217, 39–50. doi: 10.1083/jcb.201709054

- Imamura, Y., Mukohara, T., Shimono, Y., Funakoshi, Y., Chayahara, N., Toyoda, M., et al. (2015). Comparison of 2D- and 3D-culture models as drug-testing platforms in breast cancer. *Oncol. Rep.* 33, 1837–1843. doi: 10.3892/or.2015.3767
- Insua-Rodriguez, J., and Oskarsson, T. (2016). The extracellular matrix in breast cancer. *Adv. Drug Deliv. Rev.* 97, 41–55. doi: 10.1016/j.addr.2015.12.017
- Jiang, T., Munguia-Lopez, J., Flores-Torres, S., Grant, J., Vijayakumar, S., De Leon-Rodriguez, A., et al. (2018). Bioprintable alginate/gelatin hydrogel 3D *in vitro* model systems induce cell spheroid formation. *J. Vis. Exp.* 137:e57826. doi: 10.3791/57826
- Kaneda, S., Kawada, J., Shinohara, M., Kumemura, M., Ueno, R., Kawamoto, T., et al. (2019). Boyden chamber-based compartmentalized tumor spheroid culture system to implement localized anticancer drug treatment. *Biomicrofluidics* 13:054111. doi: 10.1063/1.5125650
- Kim, M., Mun, H., Sung, C. O., Cho, E. J., Jeon, H. J., Chun, S. M., et al. (2019). Patient-derived lung cancer organoids as *in vitro* cancer models for therapeutic screening. *Nat. Commun.* 10:3991. doi: 10.1038/s41467-019-11867-6
- Kingsley, D. M., Roberge, C. L., Rudkouskaya, A., Faulkner, D. E., Barroso, M., Intes, X., et al. (2019). Laser-Based 3D bioprinting for spatial and size control of tumor spheroids and embryoid bodies. *Acta Biomater.* 95, 357–370. doi: 10.1016/j.actbio.2019.02.014
- Kitaeva, K. V., Prudnikov, T. S., Gomzikova, M. O., Kletukhina, S. K., James, V., Rizvanov, A. A., et al. (2019). Analysis of the interaction and proliferative activity of adenocarcinoma, peripheral blood mononuclear and mesenchymal stromal cells after co-cultivation *in vitro*. *BioNanoScience* 9, 502–509. doi: 10.1007/s12668-019-00625-z
- Knowlton, S., Onal, S., Yu, C. H., Zhao, J. J., and Tasoglu, S. (2015). Bioprinting for cancer research. *Trends Biotechnol.* 33, 504–513. doi: 10.1016/j.tibtech.2015.06.007
- Kuhlbach, C., da Luz, S., Baganz, F., Hass, V. C., and Mueller, M. M. (2018). A microfluidic system for the investigation of tumor cell extravasation. *Bioengineering* 5:40. doi: 10.3390/bioengineering5020040
- Langer, E. M., Allen-Petersen, B. L., King, S. M., Kendsersky, N. D., Turnidge, M. A., Kuziel, G. M., et al. (2019). Modeling tumor phenotypes *in vitro* with three-dimensional bioprinting. *Cell Rep.* 26, 608.e6–623.e6. doi: 10.1016/j.celrep.2018.12.090
- Lee, S., Burner, D. N., Mendoza, T. R., Muldong, M. T., Arreola, C., Wu, C. N., et al. (2020). Establishment and analysis of three-dimensional (3D) organoids derived from patient prostate cancer bone metastasis specimens and their xenografts. *J. Vis. Exp.* 156:e60367. doi: 10.3791/60367
- Lee, V. K., Yoo, S., Zou, H., Friedel, R., and Dai, G. (2016). 3D bio-printed model of glioblastoma-vascular niche. *Tissue Eng. A* 22, S60–S61.
- Li, Y., Zhang, T., Pang, Y., Li, L., Chen, Z. N., and Sun, W. (2019). 3D bioprinting of hepatoma cells and application with microfluidics for pharmacodynamic test of Metuzumab. *Biofabrication* 11:034102. doi: 10.1088/1758-5090/ab256c
- Linkous, A., Balamatsias, D., Snuderl, M., Edwards, L., Miyaguchi, K., Milner, T., et al. (2019). Modeling patient-derived glioblastoma with cerebral organoids. *Cell Rep.* 26, 3203.e5–3211.e5. doi: 10.1016/j.celrep.2019.02.063
- Melissaridou, S., Wiechec, E., Magan, M., Jain, M. V., Chung, M. K., Farnebo, L., et al. (2019). The effect of 2D and 3D cell cultures on treatment response, EMT profile and stem cell features in head and neck cancer. *Cancer Cell Int.* 19:16. doi: 10.1186/s12935-019-0733-1
- Meng, F., Meyer, C. M., Joung, D., Vallera, D. A., McAlpine, M. C., and Panoskaltis-Mortari, A. (2019). 3D bioprinted *in vitro* metastatic models via reconstruction of tumor microenvironments. *Adv. Mater.* 31:e1806899. doi: 10.1002/adma.201806899
- Mi, S., Du, Z., Xu, Y., Wu, Z., Qian, X., Zhang, M., et al. (2016). Microfluidic co-culture system for cancer migratory analysis and anti-metastatic drugs screening. *Sci. Rep.* 6:35544. doi: 10.1038/srep35544
- Mingaleeva, R. N., Solovieva, V. V., Blatt, N. L., and Rizvanov, A. A. (2013). Application of cell and tissue cultures for potential anti-cancer/oncology drugs screening *in vitro*. *Cell. Transpl. Tissue Eng.* 8, 20–28.
- Mullenders, J., de Jongh, E., Brousal, A., Roosen, M., Blom, J. P. A., Begthel, H., et al. (2019). Mouse and human urothelial cancer organoids: a tool for bladder cancer research. *Proc. Natl. Acad. Sci. U.S.A.* 116, 4567–4574. doi: 10.1073/pnas.1803595116
- Nakatsu, N., Nakamura, T., Yamazaki, K., Sadahiro, S., Makuuchi, H., Kanno, J., et al. (2007). Evaluation of action mechanisms of toxic chemicals using JFCR39, a panel of human cancer cell lines. *Mol. Pharmacol.* 72, 1171–1180. doi: 10.1124/mol.107.038836
- Nelson, S. R., Zhang, C., Roche, S., O'Neill, F., Swan, N., Luo, Y., et al. (2020). Modelling of pancreatic cancer biology: transcriptomic signature for 3D PDX-derived organoids and primary cell line organoid development. *Sci. Rep.* 10:2778. doi: 10.1038/s41598-020-59368-7
- Osswald, A., Hedrich, V., and Sommergruber, W. (2019). 3D-3 tumor models in drug discovery for analysis of immune cell infiltration. *Methods Mol. Biol.* 1953, 151–162. doi: 10.1007/978-1-4939-9145-7_10
- Otte, J., Dizdar, L., Behrens, B., Goering, W., Knoefel, W. T., Wruck, W., et al. (2019). FGF signalling in the self-renewal of colon cancer organoids. *Sci. Rep.* 9:17365. doi: 10.1038/s41598-019-53907-7
- Payne, K. K., Bear, H. D., and Manjili, M. H. (2014). Adoptive cellular therapy of cancer: exploring innate and adaptive cellular crosstalk to improve anti-tumor efficacy. *Future Oncol.* 10, 1779–1794. doi: 10.2217/fon.14.97
- Peppicelli, S., Andreucci, E., Ruzzolini, J., Laurenzana, A., Margheri, F., Fibbi, G., et al. (2017). The acidic microenvironment as a possible niche of dormant tumor cells. *Cell. Mol. Life Sci.* 74, 2761–2771. doi: 10.1007/s00018-017-2496-y
- Puls, T. J., Tan, X., Husain, M., Whittington, C. F., Fishel, M. L., and Voytik-Harbin, S. L. (2018). Development of a novel 3D tumor-tissue invasion model for high-throughput, high-content phenotypic drug screening. *Sci. Rep.* 8:13039. doi: 10.1038/s41598-018-31138-6
- Reid, J. A., Palmer, X. L., Mollica, P. A., Northam, N., Sachs, P. C., and Bruno, R. D. (2019). A 3D bioprinter platform for mechanistic analysis of tumoroids and chimeric mammary organoids. *Sci. Rep.* 9:7466. doi: 10.1038/s41598-019-43922-z
- Riedl, A., Schleiderer, M., Pudelko, K., Stadler, M., Walter, S., Unterleuthner, D., et al. (2017). Comparison of cancer cells in 2D vs 3D culture reveals differences in AKT-mTOR-S6K signaling and drug responses. *J. Cell Sci.* 130, 203–218. doi: 10.1242/jcs.188102
- Rijal, G., and Li, W. (2017). A versatile 3D tissue matrix scaffold system for tumor modeling and drug screening. *Sci. Adv.* 3:e1700764. doi: 10.1126/sciadv.1700764
- Rizvanov, A. A., Yalvac, M. E., Shafigullina, A. K., Salafutdinov, F. I. I., Blatt, N. L., Sahin, F., et al. (2010). Interaction and self-organization of human mesenchymal stem cells and neuro-blastoma SH-SY5Y cells under co-culture conditions: a novel system for modeling cancer cell micro-environment. *Eur. J. Pharm. Biopharm.* 76, 253–259. doi: 10.1016/j.ejpb.2010.05.012
- Ruzicka, M., Cimpan, M. R., Rios-Mondragon, I., and Grudzinski, I. P. (2019). Microfluidics for studying metastatic patterns of lung cancer. *J. Nanobiotechnol.* 17:71. doi: 10.1186/s12951-019-0492-0
- Shoemaker, R. H. (2006). The NCI60 human tumour cell line anticancer drug screen. *Nat. Rev. Cancer* 6, 813–823. doi: 10.1038/nrc1951
- Stevens, J. L., and Baker, T. K. (2009). The future of drug safety testing: expanding the view and narrowing the focus. *Drug Discov. Today* 14, 162–167. doi: 10.1016/j.drudis.2008.11.009
- Sun, Z., Wang, S., and Zhao, R. C. (2014). The roles of mesenchymal stem cells in tumor inflammatory microenvironment. *J. Hematol. Oncol.* 7:14. doi: 10.1186/1756-8722-7-14
- Takimoto, C. H. (2003). Anticancer drug development at the US National Cancer Institute. *Cancer Chemother. Pharmacol.* 52(Suppl. 1), S29–S33. doi: 10.1007/s00280-003-0623-y
- Tovari, J., Futosi, K., Bartal, A., Tatrai, E., Gacs, A., Kenessey, I., et al. (2014). Boyden chamber-based method for characterizing the distribution of adhesions and cytoskeletal structure in HT1080 fibrosarcoma cells. *Cell Adh. Migr.* 8, 509–516. doi: 10.4161/cam.28734
- Trivanovic, D., Krstic, J., Djordjevic, I. O., Mojsilovic, S., Santibanez, J. F., Bugarski, D., et al. (2016). The roles of mesenchymal stromal/stem cells in tumor microenvironment associated with inflammation. *Mediators Inflamm.* 2016:7314016. doi: 10.1155/2016/7314016
- Truong, D., Fiorelli, R., Barrientos, E. S., Melendez, E. L., Sanai, N., Mehta, S., et al. (2018). A three-dimensional (3D) organotypic microfluidic model for glioma stem cells - Vascular interactions. *Biomaterials* 198, 63–77. doi: 10.1016/j.biomaterials.2018.07.048
- Uchida, Y., Tanaka, S., Aihara, A., Adikrisna, R., Yoshitake, K., Matsumura, S., et al. (2010). Analogy between sphere forming ability and stemness of human hepatoma cells. *Oncol. Rep.* 24, 1147–1151. doi: 10.3892/or_00000966

- Wang, S., Li, E., Gao, Y., Wang, Y., Guo, Z., He, J., et al. (2013). Study on invadopodia formation for lung carcinoma invasion with a microfluidic 3D culture device. *PLoS One* 8:e56448. doi: 10.1371/journal.pone.0056448
- Wang, Y., Shi, W., Kuss, M., Mirza, S., Qi, D. J., Krasnoslobodtsev, A., et al. (2018). 3D bioprinting of breast cancer models for drug resistance study. *ACS Biomater. Sci. Eng.* 4, 4401–4411. doi: 10.1021/acsbiomaterials.8b01277
- Waud, W. R. (2011). “Murine L1210 and P388 leukemias,” in *Tumor Models in Cancer Research*, ed. B. Teicher, (Totowa, NJ: Humana), 23–41.
- Wessely, A., Waltera, A., Reichert, T. E., Stockl, S., Grassel, S., and Bauer, R. J. (2019). Induction of ALP and MMP9 activity facilitates invasive behavior in heterogeneous human BMSC and HNSCC 3D spheroids. *FASEB J.* 33, 11884–11893. doi: 10.1096/fj.201900925R
- Wu, T., and Dai, Y. (2017). Tumor microenvironment and therapeutic response. *Cancer Lett.* 387, 61–68. doi: 10.1016/j.canlet.2016.01.043
- Yu, L., Chen, M. C., and Cheung, K. C. (2010). Droplet-based microfluidic system for multicellular tumor spheroid formation and anticancer drug testing. *Lab. Chip* 10, 2424–2432. doi: 10.1039/c004590j
- Yu, T., Guo, Z., Fan, H., Song, J., Liu, Y., Gao, Z., et al. (2016). Cancer-associated fibroblasts promote non-small cell lung cancer cell invasion by upregulation of glucose-regulated protein 78 (GRP78) expression in an integrated bionic microfluidic device. *Oncotarget* 7, 25593–25603. doi: 10.18632/oncotarget.8232
- Zoetemelk, M., Rausch, M., Colin, D. J., Dormond, O., and Nowak-Sliwinska, P. (2019). Short-term 3D culture systems of various complexity for treatment optimization of colorectal carcinoma. *Sci. Rep.* 9:7103. doi: 10.1038/s41598-019-42836-0
- Zuchowska, A., Kwapiszewska, K., Chudy, M., Dybko, A., and Brzozka, Z. (2017). Studies of anticancer drug cytotoxicity based on long-term HepG2 spheroid culture in a microfluidic system. *Electrophoresis* 38, 1206–1216. doi: 10.1002/elps.201600417

Conflict of Interest: The authors declare that the research was conducted in the absence of any commercial or financial relationships that could be construed as a potential conflict of interest.

Copyright © 2020 Kitaeva, Rutland, Rizvanov and Solovyeva. This is an open-access article distributed under the terms of the Creative Commons Attribution License (CC BY). The use, distribution or reproduction in other forums is permitted, provided the original author(s) and the copyright owner(s) are credited and that the original publication in this journal is cited, in accordance with accepted academic practice. No use, distribution or reproduction is permitted which does not comply with these terms.



In vitro Alternatives to Acute Inhalation Toxicity Studies in Animal Models—A Perspective

Dania Movia^{1*}, Solene Bruni-Favier¹ and Adriele Prina-Mello^{1,2}

¹ Laboratory for Biological Characterisation of Advanced Materials (LBCAM), Department of Clinical Medicine, Trinity Translational Medicine Institute, Trinity College, The University of Dublin, Dublin, Ireland, ² AMBER Centre, CRANN Institute, Trinity College, The University of Dublin, Dublin, Ireland

OPEN ACCESS

Edited by:

João Conde,
New University of Lisbon, Portugal

Reviewed by:

Robert Landsiedel,
BASF, Germany
Il Je Yu,
Independent Researcher, Icheon,
South Korea

*Correspondence:

Dania Movia
dmovia@tcd.ie

Specialty section:

This article was submitted to
Nanobiotechnology,
a section of the journal
Frontiers in Bioengineering and
Biotechnology

Received: 25 February 2020

Accepted: 07 May 2020

Published: 03 June 2020

Citation:

Movia D, Bruni-Favier S and
Prina-Mello A (2020) *In vitro*
Alternatives to Acute Inhalation
Toxicity Studies in Animal Models—A
Perspective.
Front. Bioeng. Biotechnol. 8:549.
doi: 10.3389/fbioe.2020.00549

When assessing the risk and hazard of a non-pharmaceutical compound, the first step is determining acute toxicity, including toxicity following inhalation. Inhalation is a major exposure route for humans, and the respiratory epithelium is the first tissue that inhaled substances directly interact with. Acute inhalation toxicity testing for regulatory purposes is currently performed only in rats and/or mice according to OECD TG403, TG436, and TG433 test guidelines. Such tests are biased by the differences in the respiratory tract architecture and function across species, making it difficult to draw conclusions on the potential hazard of inhaled compounds in humans. Research efforts have been therefore focused on developing alternative, human-relevant models, with emphasis on the creation of advanced *In vitro* models. To date, there is no *In vitro* model that has been accepted by regulatory agencies as a stand-alone replacement for inhalation toxicity testing in animals. Here, we provide a brief introduction to current OECD test guidelines for acute inhalation toxicity, the interspecies differences affecting the predictive value of such tests, and the current regulatory efforts to advance alternative approaches to animal-based inhalation toxicity studies. We then list the steps that should allow overcoming the current challenges in validating *In vitro* alternatives for the successful replacement of animal-based inhalation toxicity studies. These steps are inclusive and descriptive, and should be detailed when adopting in house-produced 3D cell models for inhalation tests. Hence, we provide a checklist of key parameters that should be reported in any future scientific publications for reproducibility and transparency.

Keywords: toxicity testing alternatives, inhalation studies, *In vitro* alternatives, air-liquid interface (ALI) culture, lung epithelium

INTRODUCTION

Inhalation is a major exposure route for humans, where the respiratory tract serves as both target tissue and portal of entry (POE) to the systemic circulation for inhaled substances. REACH (Registration, Evaluation, Authorization, and Restriction of Chemicals) states that testing for acute inhalation toxicity is mandatory for all substances manufactured or imported at quantities above 10 tons per year when (i) human exposure is possible via this route or (ii) the physico-chemical

properties of the substance indicate that such exposure may occur¹. In this scenario, acute inhalation toxicity testing provides the data used for both hazard identification and risk assessment.

Current Regulatory Test Guidelines for Acute Inhalation Toxicity

According to the Organization for Economic Co-operation and Development (OECD), acute inhalation toxicity testing is performed to define the effects of inhaled substances on (i) the respiratory tract (local toxicity) and/or (ii) the whole body (systemic toxicity) (OECD, 2018a).

Acute inhalation toxicity studies are currently conducted in animals by using the OECD methods TG403, TG436, and TG433. According to these methods, healthy young adult rats are the preferred animal model, and justification should be provided if other species are used (OECD, 2009a). Animals are exposed to the test compound as a gas, vapor, aerosol, or a mixture thereof. Nose-only exposure is generally recommended (OECD, 2009a). In special cases, whole-body exposure can be used, but this should be justified in the study report. Principles, advantage and disadvantages of the nose-only and whole-body exposure techniques are described in OECD Guidance Document 39 (OECD, 2018a). For both techniques, a single exposure is applied to each animal, with each exposure lasting up to 6 h in rats but not exceeding 4 h in mice. Animal observation is conducted for at least 14 days after exposure.

The endpoint of OECD TG403 and TG436 is “death.” A full description of these test guidelines is available on the OECD website (OECD, 2009b,c) and in Arts et al. (2008). In order to reduce the number of animals used and to improve their welfare (3Rs principle), an alternative fixed concentration procedure (FCP) was proposed in 2004 (draft OECD TG433²), where the endpoint “death” was replaced with “evident toxicity.” A previous study had demonstrated, in fact, that the performance of the FCP method in estimating the toxic class of inhaled substances was comparable to that of TG403 and TG436 tests (Stallard et al., 2003). However, the FCP test was dropped from the OECD workplan in 2007, due to suspected gender influences in the data generated, and the “subjective nature” of the tested endpoint. Conversely, few years later, scientists demonstrated that gender differences did not have any significant impact on the performance of the FCP test (Stallard et al., 2011). In parallel, an international working group that included 19 organizations around the world, led by the UK NC3Rs, developed the criteria to make “evident toxicity” into an objective and transferable endpoint. The working group carried out a large-scale analysis of inhalation toxicity data from 188 substances, and developed guidelines to support the recognition and use of “evident toxicity.” Such guidelines are described in Sewell et al. (2015). The scientific evidence provided by these two studies, supported the approval of the FCP method as OECD method in

2017 (OECD TG433). It should be noted here that, validation of the FCP method was critical at regulatory level for addressing the need for an OECD-approved inhalation toxicity test method that would satisfy the guidelines of Directive 2010/63/EU (EU, 2010). The latter states, *in vivo* testing methods should avoid, as far as possible, death as an endpoint, due to the severe suffering caused on the animal during the period prior to death.

Interspecies Differences in the Respiratory Tract—How Does This Affect Acute Inhalation Toxicity Tests?

Species-specific differences can have important implications in acute inhalation toxicity testing, making it difficult to draw conclusions on the potential hazard of inhaled compounds in humans, for the reasons highlighted below.

When using animal models, two parameters are known to influence the local toxic effects of inhaled substances in the respiratory tract: (i) the pattern of deposition of the test substance, followed by (ii) the specific pathways by which the compound is cleared from the lungs. Animal models differ from humans in both aspects (Pauluhn, 2003). On one hand, the deposition of inhaled substances depends upon air-flow dynamics, which is different across species. Interspecies differences affecting air-flow dynamics include: the gross anatomy and geometry of airways in both the upper and lower respiratory tract (Parent, 2015), airway dimensions (e.g., length and diameter) (Hofmann et al., 1989), and respiratory physiology (e.g., breathing mode and ventilation rates). On the other hand, substance clearance is affected by tissue volumes, cell types and their location in the respiratory tract, mucus composition and distribution, macrophage-triggered clearance, biochemical mechanisms of airway activation, and enzyme-dependent metabolic processes. All the properties abovementioned are highly species dependent (Miller et al., 1993; Bogdanffy and Keller, 1999; Sarangapani et al., 2002).

In the following section, the specific differences between humans and the preferred animal model used in the three OECD accepted methods (rats) are briefly summarized.

Implications in the Use of Rodents in the OECD Tests

In the last two decades scientists have demonstrated that the relevance of using rats (the preferred animal model in OECD tests) for assessing hazard and risk of chemicals in humans, is scientifically debatable (Harkema, 1991; Mauderly, 1997; Phalen et al., 2008; Creton et al., 2010; Chamanza and Wright, 2015; Mowat et al., 2017). For example, recently, a review of 52 inhalation toxicity studies conducted in rodents, showed that the results obtained from such studies lack relevance to humans (Mowat et al., 2017),

Probably the most obvious and significant difference between humans and rodents is the anatomy of their lungs. Rat lungs have a monopodial branching system with no respiratory bronchioles; whereas, the human respiratory tract has a symmetric branching. This results in compound/particle deposition mainly at the bifurcation points of the human lungs, a phenomenon that cannot be mimicked in rodent models. Also, rat airway diameter is smaller than human one. Thus, insoluble solid aerosols can

¹REACH. Annex VIII: Standard Information Requirements for Substances Manufactured or Imported in Quantities of 10 Tonnes or More. Available online at: <https://reachonline.eu/reach/en/annex-viii.html> (accessed April 2020).

²Available online at: <http://www.oecd.org/chemicalsafety/testing/32035886.pdf> (last accessed April 2020).

lead to an obstruction of the rat airways and, subsequently, to animal death, at the highest tested doses, even when the compound under investigation is non-toxic to humans (Hofmann et al., 2018).

Furthermore, the breathing mode of humans is different from rodents. Humans are oronasal breathers, while rodents are obligate nose breathers. This strongly influence how inhaled particle and gas deposit in the respiratory tract, and the subsequent toxicities detected. For example, there is less filtering of particles and gases in oral breathing compared to nasal breathing, resulting in a greater delivery of material to the peripheral airways of humans compared to rodents.

Differences in compound metabolism are also striking (Bogdanffy and Keller, 1999; Sarangapani et al., 2002; Oesch et al., 2019). Cytochrome P450 in the nasal mucosa and lower respiratory tract of humans is poorly efficient, as compared to that of most animal species, including mice and rats. Clearance via carboxylesterase activity is also particularly ineffective in humans as compared to rodents. On the other hand, phase II enzymes (e.g., epoxide hydrolase and glutathione S-transferase) are more active in humans than in rodents, enabling a clearance of inhaled compounds that cannot be replicated in the rat/mice models used in the OECD tests.

Finally, reflex reactions that are of a protective nature in rodents, can limit the animal exposure to the chemicals under investigation. Reflex reactions range from mechanisms where the animal use its own fur as a filter to aerosol exposure, causing dosimetry issues in whole-body exposure techniques (reviewed in Pauluhn, 2003), to the stimulation of the parasympathetic system, resulting in reactions that can be confused with early toxic effects, such as decrease in ventilation rate, heartbeat, blood pressure, and body temperature of the animal.

The OECD is aware of the interspecies differences listed above and their negative influence on the predictivity of the existing inhalation toxicity tests. Subsequently, a new test for determining acute inhalation toxicity has been recently brought forward for validation and OECD adoption (Jackson et al., 2018). Such test adopts the EpiAirway™ model, a ready-to-use, three-dimensional (3D) *In vitro* mucociliary tissue model consisting of normal, human-derived tracheal/bronchial epithelial cells cultured at the Air-Liquid Interface (ALI). The test under development could, therefore, provide a human-relevant *In vitro* alternative to current, animal-based acute inhalation toxicity studies.

In vitro Alternatives to Acute Inhalation Toxicity Studies in Animals

Considering the limitations of animal models in predicting the safety of inhaled substances in humans, research efforts have focused on developing human-relevant models, with particular emphasis on *In vitro* models, such as the EpiAirway™ model mentioned above. Our perspective focuses on the steps that should allow these models to increase the predictive value of acute inhalation toxicity testing, by overcoming some of the shortfalls of animal models. Indeed, inadequate physico-chemical characterization of the test compound and dosimetry

can also lead to unpredictable results in inhalation toxicity tests. However, our manuscript does not address issues associated with exposure technology, test compound characterization and dosimetry, as these have already been identified and described in detail elsewhere (Dorato and Wolff, 1991; Oberdorster, 1996; Pauluhn, 2003, 2005; Wong, 2007; Phalen and Mendez, 2009; Clippinger et al., 2018b; Hofmann et al., 2018).

Human-relevant *In vitro* models allow reproducing distinctive properties and mechanisms of the human lung epithelium that define the clearance of inhaled compounds in humans. The properties/mechanisms reproduced include tissue volumes, cell and mucus composition, human-specific aspects of macrophage-triggered clearance, and unique human biochemical and enzyme-dependent processes. To date, the most advanced *In vitro* approaches for animal replacement detect local toxicity. Thus, this manuscript focuses solely on such endpoint.

Numerous reviews on *In vitro* inhalation toxicity testing models have been published in the last decade (Berube et al., 2009; Creton et al., 2010; Gordon et al., 2015; Clippinger et al., 2018b; Lacroix et al., 2018; Upadhyay and Palmberg, 2018). These models can be grouped in three main categories: (i) cell cultures, including commercially available, 3D *In vitro* lung models; (ii) lung-on-a-chip models, and (iii) *ex vivo* human precision-cut lung slices. Various case studies demonstrate that it is possible to reproduce specific regions of the human respiratory tract and their responses *In vitro*. For example, in 2018, the US Environmental Protection Agency (EPA) has publicly recognized the value of an alternative approach based on an *In vitro* model of the human lung epithelium (the MucilAir™ model), to refine inhalation risk assessment for the pesticide chlorothalonil, as well as for other contact irritants (EPA, 2018). However, currently there is no *In vitro* model that has been accepted by regulatory agencies as a stand-alone replacement for animal tests in acute inhalation toxicity studies, and the issues associated with interspecies differences remain unsolved.

Regulatory Efforts to Advance Alternative Approaches to Animal-Based Inhalation Toxicity Studies

In the last years, regulatory efforts have been focused on advancing the alternative approaches for replacing animal use in acute inhalation toxicity testing, as reported by Clippinger et al. (2018b) and Krewski et al. (2020). For example, an Interagency Coordinating Committee on the Validation of Alternative Methods (ICCVAM)³ has been formally established in US in 2000, with the aim of (i) evaluating existing *in vivo*, *in silico*, and *In vitro* tests for acute systemic toxicity, and (ii) developing a strategic roadmap⁴ where *In vitro* and *in silico* approaches enable the reduction, or the full replacement, of current *in vivo* tests. Similarly, the Office of Pesticide Programs (OPP) of EPA has committed to significantly reduce the number

³Available online at: <https://ntp.niehs.nih.gov/whatwestudy/niceatm/iccvam/iccvam-agencies/index.html> (accessed April 2020).

⁴Available online at: https://ntp.niehs.nih.gov/whatwestudy/niceatm/natl-strategy/index.html?utm_source=direct&utm_medium=prod&utm_campaign=ntpgolinks&utm_term=natl-strategy (accessed April 2020).

of animals used for acute inhalation toxicity testing in the agrochemical registration process (EPA, 2016)⁵. EPA has also announced that funding to studies in mammals will be ended by 2035.

In Europe, in 2016, the Netherlands National Committee for the protection of animals used for scientific purposes (NCad) announced that animal studies for safety research on chemical substances, food ingredients, pesticides, and medicines (including veterinary medicines) will be phased out in the Netherlands by 2025 (NCad, 2016). This ambitious objective is backed up also by the European Commission. In 2005, the European Partnership for Alternative Approaches to Animal Testing (EPAA) was established, with the aim to replace, reduce and refine (3Rs concept) animal use in regulatory testing. Furthermore, Directive 2010/63/EU (EU, 2010) explicitly incorporates the 3Rs concept in European legislation, and establishes the European Union Reference Laboratory—European Centre for the Validation of Alternative Methods (EURL—ECVAM) at the Joint Research Centre (JRC) as support to the development, validation, and acceptance of alternative methods. The European Commission is also currently funding several research projects in the alternatives field (e.g., EU-ToxRisk).

Globally, the International Cooperation on Alternative Test Methods (ICATM) was established. ICATM includes governmental organizations from Europe, US, Canada, Japan, South Korea, Brazil, and China.

Although all initiatives above create a momentum toward the replacement of animal testing, the translational rate of *In vitro* alternatives into regulator-approved methods is poor. Thus, one could question the predictive value of such alternatives. The reality is, validation of *In vitro* testing methods for animal replacement is currently a gray area (Griesinger et al., 2016). Regulatory authorities grant validation to *In vitro* alternative tests upon demonstration of their ability to predict *in vivo* animal-derived data, the quality and reliability of which is sometimes poor (Sauer et al., 2013). The scientific relevance of using animal data as benchmark for a human-relevant model is also debatable (Griesinger et al., 2016; Cryan et al., 2019), since the interspecies differences described in the previous sections negatively affect the animal-to-human data correlation. In Europe, the mandatory steps for validation are: (i) endorsement from the European validation authority, i.e., the EURL—ECVAM; (ii) formal test methods via large international collaboration platforms, such as the OECD or the International Council on Harmonization; (iii) regulatory acceptance; and (iv) deletion of the animal test. Thus, the current validation process is tremendously demanding, taking an average of 10 years and costing up to 1 million dollars (Hartung, 2013). This approach raises the bar to an unaffordable level for small technology providers and universities, creating a translational “valley of death.” Predictive, human-relevant *In vitro* platforms are published in peer-reviewed scientific journals, but do not go through the validation process.

In this context, the following section presents the authors’ perspective on how, in our view, it may be possible to overcome the current challenges in validating *In vitro* alternatives for the successful replacement of animal-based inhalation toxicity testing studies.

DISCUSSION

Although in some cases *In vitro* alternative tests are at an advanced stage of development (e.g., the EpiAirway™ model mentioned above), to date all *In vitro* alternative models for inhalation toxicity studies still fall into the category of “non-guideline methods.” Four major actions should be undertaken, in our view, to increase the uptake of *In vitro* alternative methods and meet the replacement of animal models for the definition of local toxicity in acute inhalation testing.

Firstly, *In vitro* test methods should be presented in detail to allow interpretation and use of the data from regulators. According to regulatory agencies, non-guideline methods can be used to support risk/hazard assessment of inhaled substances only if they fulfill basic requirements, such as relevance, reproducibility and predictivity. The OECD has recently formulated a guidance document (GD211) on the information that should be provided for non-guideline methods. Further to this, an annotated toxicity test method template (ToxTemp), described in full by Krebs et al. (2019, 2020), was developed, to complement the OECD GD211 guidance document and support researchers in meeting its requirements. Furthermore, the test methods and conditions under which the data are generated, must adhere to the Good *In vitro* Method Practices (GIVIMP) for the development and implementation of *In vitro* methods for regulatory use in human safety assessment (OECD, 2018b). We believe that the mandatory adoption of the ToxTemp template and GIVIMP procedures by the scientific community, will facilitate implementation of *In vitro* alternative methods for inhalation toxicity testing.

Secondly, *In vitro* alternatives must be compatible with the evaluation of markers of membrane/cell damage and cell functional competence that are relevant to known adverse outcome pathways (AOPs). As recently reviewed by Clippinger et al. (2018a), AOPs can model the mechanisms leading to adverse local and systemic effects following compound inhalation. By using cellular- and tissue-specific Key Events (KE) reported in inhalation AOPs as experimental endpoints, the authors have successfully investigated the predictive value of reconstructed human lung tissue cultures in detecting POE inflammatory effects. The results of such investigation (the details of which are described in the **Supplementary Material**) are shown in **Figure 1** and are original and unpublished data from the authors. Comparable experimental strategies have been successfully adopted by other research groups to validate the predictive value of *In vitro* alternative models (Iskandar et al., 2017; Balogh Sivars et al., 2018; Hoffmann et al., 2018; Barosova et al., 2020). In our experiments, SmallAir-HF™ and MucilAir-HF™, purchased from Epithelix Sàrl, were used (**Supplementary Figure S1**). Experimental endpoints

⁵ Available online at: <https://www.epa.gov/pesticide-registration/mixtures-equation-pilot-program-reduce-animal-testing> (accessed April 2020).

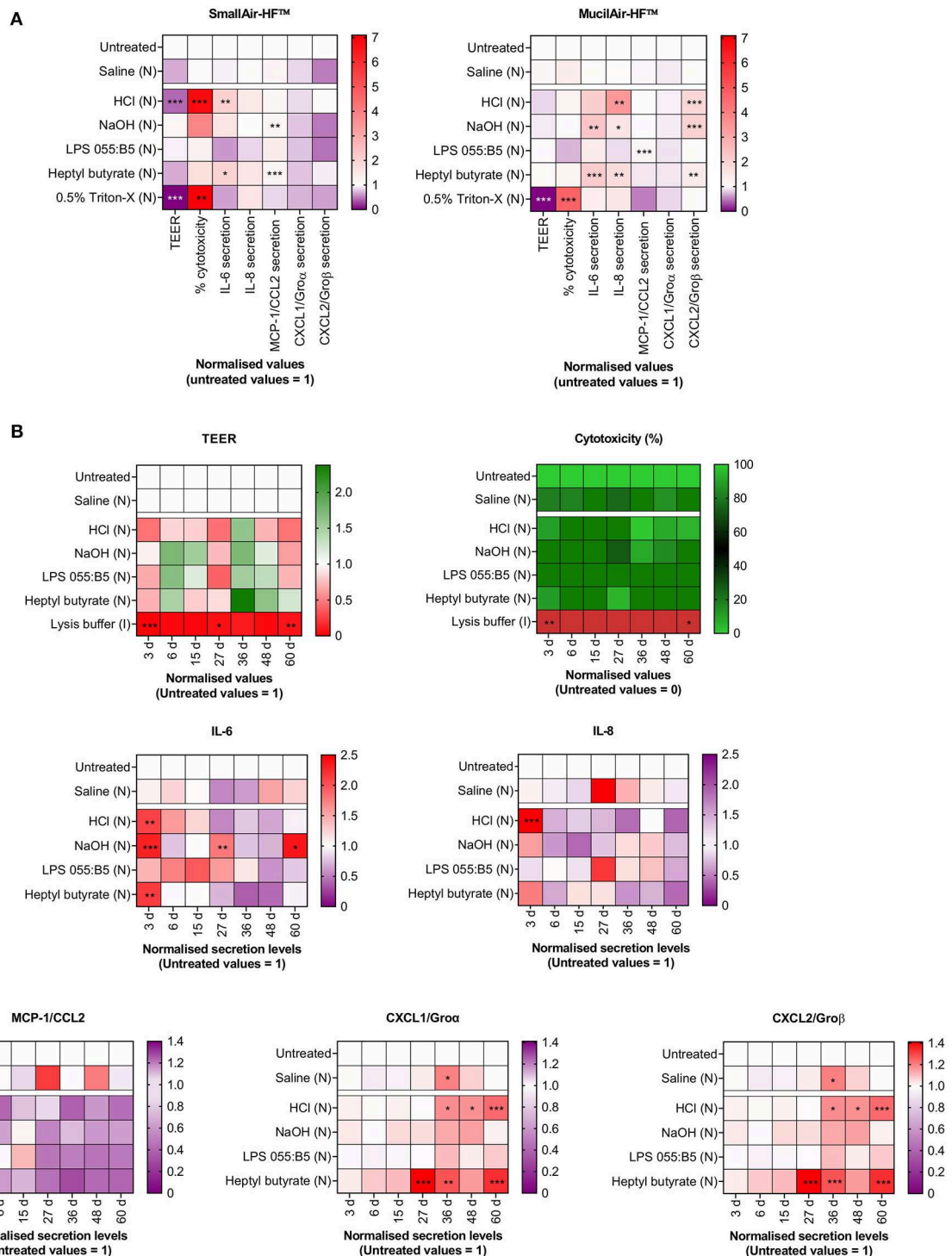


FIGURE 1 | Changes in markers of cellular- and tissue-specific KEs following a single-dose aerosol (N) exposure to benchmark substances. Cell cultures were exposed to liquid aerosols by means of a Vitrocell Cloud ALI system equipped with an Aeronex® Pro nebulizer. Cellular-specific KEs included percentage (%) cytotoxicity, cytokines (IL-6, IL-8) and chemokines (MCP-1/CCL2, CXCL1/Groα, CXCL2/Groβ) secretion. Tissue-specific KEs included epithelial barrier impairment, quantified as changes in TEER. Data are presented as mean and normalized to untreated cultures. **(A)** SmallAir-HF™ (left) and MucilAir-HF™ (right) models were exposed to benchmarks for 72 h. **(B)** MucilAir-HF™ models were exposed to benchmarks up to 60 days. **(A,B)** Symbols (*), (**), and (***) indicate $p < 0.05$, $p < 0.01$, and $p < 0.001$, respectively (two-way ANOVA followed by Dunnett post-test; comparison to the untreated controls).

included changes in: (i) percentage cytotoxicity and release of cytokines (IL-6, IL-8)/chemokines (MCP-1/CCL2, CXCL1/Gro α , CXCL2/Gro β), as markers of cellular-specific KEs; and (ii) trans-epithelial electrical resistance (TEER) as marker of a tissue-specific KE (the epithelial barrier integrity). Marker expression was evaluated after a single aerosol exposure to benchmark substances with known effects on the respiratory epithelium in humans. These included: (i) hypertonic saline solution, a biocompatible nebulization vehicle, as negative control; (ii) chemical lung irritants (hydrochloric acid, HCl, and ammonium hydroxide, NaOH); (iii) lipopolysaccharide (LPS) from *E. Coli* 055:B5, a biological contaminant to which the respiratory system is directly exposed, and that does not cause irritation unless the epithelial barrier function is impaired, such as, for example, in the presence of pre-existing medical conditions (e.g., asthma, cystic fibrosis); (iv) heptyl butyrate, which is known to be non-irritant if inhaled at doses lower than 200 mg/ml; and (v) 0.5% Triton-X or lysis buffer, which are cytotoxic compounds, as positive controls. After 72 h exposure (**Figure 1A**), benchmark compounds induced the predicted response. Saline did not induce any significant change in TEER and did not trigger cytotoxicity. Similar results were found after exposure to LPS and the non-irritant heptyl butyrate. Triton-X significantly disrupted the barrier integrity (TEER \sim 0) and caused severe cytotoxicity. Lung irritants (HCl and NaOH) caused barrier integrity disruption, cytotoxicity and/or release of inflammatory signals. The unaltered viability of untreated MucilAir-HFTM

cultures after 60 days (**Figure 1B**), together with the evident time-dependent inflammatory responses detected for the benchmarks in the same time period, suggests that the here presented *In vitro* model could be used to carry out long-term experiments as an alternative method to acute inhalation toxicity studies in animals.

Thirdly, *In vitro* acute inhalation toxicity testing should use exclusively cell cultures in ALI conditions, i.e., cultures where cells are grown in direct contact with air. ALI culturing conditions are in fact a critical element driving the *In vitro* formation of a pseudostratified epithelium that mimics the human lung epithelium functions in the best possible way (Gras et al., 2017; Hiemstra et al., 2018). Furthermore, ALI cultures should be exposed to the test compound in realistic exposure conditions by means of realistic exposure techniques (e.g., gas, vapor, aerosol). The influence of exposure methods on cell responses in ALI cultures has been described in the past by the authors (Di Cristo et al., 2018; Movia et al., 2018). This was also supported by further experiments we recently carried out on MucilAir-HFTM and SmallAir-HFTM, showing that inoculation (I) or nebulization (N) of the same compound on the apical side of the two models triggered cellular responses that significantly differed (**Figure 2**). Finally, exposure should be clearly characterized, including among the parameters particle size distribution, nominal and actual/deposited concentrations, as described in the OECD guidelines for testing acute inhalation toxicity (OECD, 2009a).

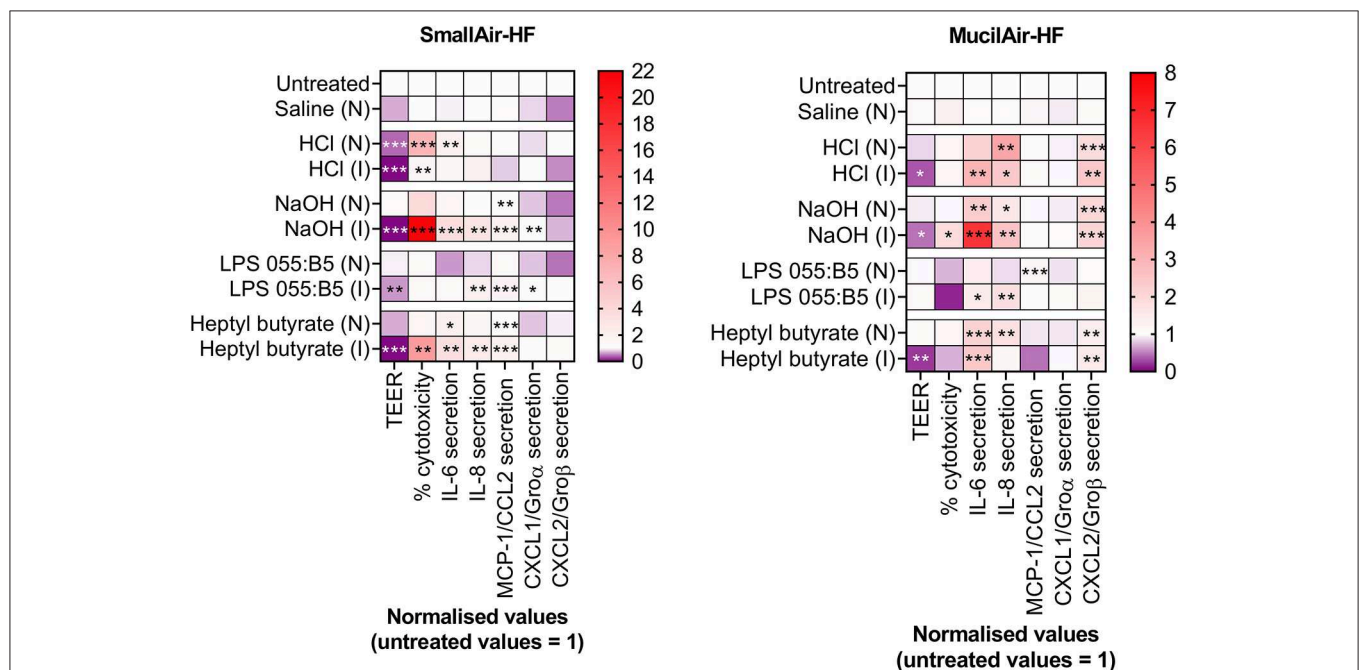


FIGURE 2 | Changes in markers of cellular- and tissue-specific KEs in SmallAir-HFTM (left) and MucilAir-HFTM (right) models following a single-dose exposure by aerosol (N) or by direct inoculation (I). Cellular-specific KE included percentage (%) cytotoxicity, cytokines (IL-6, IL-8) and chemokines (MCP-1/CCL2, CXCL1/Gro α , CXCL2/Gro β) secretion. Tissue-specific KE included epithelial barrier impairment, quantified as changes in TEER. Data are presented as mean and normalized to untreated cultures. Symbols (*), (**), and (***) indicate $p < 0.05$, $p < 0.01$, and $p < 0.001$, respectively (two-way ANOVA followed by Dunnett post-test; comparison to the untreated controls).

Fourthly, the adoption of ready-to-use ALI models of the human respiratory epithelium, reconstituted from biopsies originated from human donors, should be preferred to in-house *In vitro* systems based on immortalized cell lines. Ready-to-use systems, which are available for purchase from commercial sources (e.g., EpiAirway™, MucilAir-HF™, SmallAir-HF™), offer in fact a standardized platform, thus facilitating method validation and promoting consistency across laboratories. Furthermore, selecting donors of different age and gender, ensures that hazard/risk assessment studies address the issues of population heterogeneity and gender dimension. However, the high cost of ready-to-use systems often hinders their use in research and university labs. Within the EC scenario of the H2020-funded BIORIMA and REFINE projects, which have enabled regulatory-science dialogue and experimental evidence discussion, we have highlighted that, when using in house-produced *In vitro* models for conducting inhalation toxicity studies, it is of critical importance to report the methodologies used for the formation, characterization, exposure, verification, validation and testing of the ALI cell model. On this matter, in **Table 1**, we propose a checklist describing key parameters that, in our opinion, should be included in future scientific publications when adopting in house-produced ALI cell models to test inhaled substances. This information should be also submitted as part of section 3 of the ToxTemp document, thus ensuring reproducibility, repeatability, and a transparent assessment of the predictive value of the *In vitro* method developed. This will ultimately allow a meaningful comparison between novel, animal-free, non-guideline methods and current OECD tests.

In addressing the four points above, consideration should be also given to the respiratory tract region/s where the inhaled substance under test is more likely to deposit in humans, followed by development of an *In vitro* model that is representative of such region/s. *In vitro* models representative of different respiratory tract regions, in fact, respond differently to the same irritant insult. Our results demonstrate that the MucilAir-HF™ model was less prone than the SmallAir-HF™ culture to develop inflammatory responses following exposure to the chemical irritants HCl and NaOH (**Figure 1A**). Furthermore, to avoid any uncertainty introduced by the interspecies differences associated with the use of animal products, *In vitro* alternatives should be fully humanized. Thus, only human cells should be used, and fetal bovine serum (FBS) and animal-derived ECM proteins should be avoided, as clearly addressed in Jochems et al. (2002), Gstraunthaler (2003), Van Der Valk et al. (2004, 2018), OECD (2018b), and Oredsson et al. (2019). Cell-to-cell ratios of the human tissues, as well as the endogenous lung microbiome, should also be recapitulated.

As highlighted by the recommendations from the 2015 workshop entitled “Alternative Approaches for Identifying Acute Systemic Toxicity: Moving from Research to Regulatory Testing,” we share the view that there is still need to improve the *In vitro* models for completely replacing animal use in acute inhalation toxicity testing (Hamm et al., 2017). Based on our experience in the development of advanced ALI cultures (Movia et al., 2017, 2018, 2019; Di Cristo et al., 2018), we have identified two critical shortfalls in the ALI culture models currently commercially available or reported in the scientific

TABLE 1 | Checklist describing key parameters that should be included in scientific publications, as well as in Section 3 of the ToxTemp document, when adopting in house-produced 3D cell models to test inhaled substances.

Checklist descriptor	3D cell culture parameter	Information to be provided
Culturing substrate	Scaffold-based	Scaffold material and structure
	Scaffold-free	Specialized cell culture plates or lab equipment (e.g. 3D printing) used
Cells	Cell types	Mono- or co-culture, primary cells, immortalized and/or carcinogenic cell lines, differentiation protocol
	Donors	Gender-balanced pool of cell donors
Cell culture formation	Methodology	Air-Liquid Interface (ALI) conditions, cell seeding on scaffolds, incorporation into matrices, liquid overlay, partially separated or mixed ALI co-cultures
	Growth time	Number of days/weeks
Cell culture manipulation	Biological cues	Medium change, mechanical cues (e.g. substrate stiffness, shear flow), soluble/chemical cues (e.g. hormones)
Biological functions of cells	Cell phenotype	Cell shape, polarity, proliferative activity, cell differentiation
Biological functions of culture	Geometry	Culture morphology (2D or 3D) and architecture, culture size.
	Stability	Viability and phenotype changes overtime
	Comparison to tissue in humans	Cell-ECM and cell-cell interactions, formation of tissue-mimetic structures, mucus production
Exposure	Exposure methodologies	Human-relevance of experimental exposure conditions
Verification	Model benchmarking	Comparison to known, human-relevant exposure scenarios
Validation	Benchmarks	Benchmark identification and validation of cell culture responses
Assay validation for toxicity/efficacy testing	Endpoints	Human-relevant endpoint definition (e.g. based on AOPs), overcoming diffusion issues (e.g. during immunostaining), positive controls
	Accuracy	Benchmark data should include information on the variability and the upper and lower limits of accuracy metrics, as suggested by Leontaridou et al. (2019)

literature. They do not incorporate either (i) the 3D tissue microenvironment, constituted by different cell types, in direct contact with each other, and the extracellular matrix (ECM); or (ii) the tissue biomechanical environment (namely, the epithelial stretching during breathing). These two parameters strongly influence local inhalation toxicity, which is mainly affected by the nature of the interactions between the inhaled substance itself and the surrounding biological environment. To overcome these shortfalls, we suggest that future research efforts would focus on developing advanced ALI cultures formed by mixed cell populations that exist on ECM-like, 3D synthetic hydrogels. Furthermore, *In vitro* ALI models should undergo cyclic mechanical strains, mimicking the forces exerted during breathing, as these have been demonstrated to correlate to the absorption of inhaled substances (Huh et al., 2010) and to the epithelium inflammatory responses (Rentzsch et al., 2017).

In conclusion, we strongly advocate for enforcing standardization within the development of *In vitro* models for inhalation toxicity testing, and the uptake of the checklist in **Table 1** within the ToxTemp framework. This will enable reproducibility and repeatability in this field, ensuring a rapid uptake of alternative methods from the regulatory agencies. It will also ensure the production of valuable data for *in silico* PBPK modeling, further supporting animal replacement in acute inhalation toxicity testing.

DATA AVAILABILITY STATEMENT

The datasets generated for this study are available on request to the corresponding author.

AUTHOR'S NOTE

The views expressed in this article are those of the authors. Mention of trade name or commercial products does not constitute endorsement or recommendation for use.

REFERENCES

- Arts, J. H., Muijsers, H., Jonker, D., Van De Sandt, J. J., Bos, P. M., and Feron, V. J. (2008). Inhalation toxicity studies: OECD guidelines in relation to REACH and scientific developments. *Exp. Toxicol. Pathol.* 60, 125–133. doi: 10.1016/j.etp.2008.01.011
- Balogh Sivars, K., Sivars, U., Hornberg, E., Zhang, H., Branden, L., Bonfante, R., et al. (2018). A 3D human airway model enables prediction of respiratory toxicity of inhaled drugs *In vitro*. *Toxicol. Sci.* 162, 301–308. doi: 10.1093/toxsci/kfx255
- Barosova, H., Maione, A. G., Septiadi, D., Sharma, M., Haeni, L., Balog, S., et al. (2020). Use of EpiAlveolar lung model to predict fibrotic potential of multiwalled carbon nanotubes. *ACS Nano*. 14, 3941–3956. doi: 10.1021/acsnano.9b06860
- Berube, K., Aufderheide, M., Breheny, D., Clothier, R., Combes, R., Duffin, R., et al. (2009). *In vitro* models of inhalation toxicity and disease. the report of a FRAME workshop. *Altern. Lab. Anim.* 37, 89–141.
- Bogdanffy, M., and Keller, D. (1999). "Metabolism of xenobiotics by the respiratory tract," in *Toxicology of the Lung, 3rd Edn.*, eds D. E. Gardner, J. D. Crapo and R. O. McClellan (Philadelphia PA: Taylor & Francis).

AUTHOR CONTRIBUTIONS

DM and AP-M conceived this study. DM designed and carried out the experimental work, with exception of ELISA experiments, which were carried out by SB-F. DM analyzed the data and discussed them with AP-M. DM drafted the paper, and AP-M revised it. All authors read and approved the final manuscript.

FUNDING

This study has been funded, in parts, by the Center for Alternatives to Animal Testing Award (CAAT Project #2018-17). Also, the research leading to these results has received funding from the European Union's HORIZON 2020 Framework Programme under Grant Agreements No. 760928 and 761104. The funders had no role in study design, data collection and analysis, decision to publish, or preparation of the manuscript.

ACKNOWLEDGMENTS

The authors thank Prof. Bengt Fadeel (Work Package leader of the EC-funded BIORIMA project) and Dr. Marco Siccardi (Work Package leader of the EC-funded REFINE project) for useful discussion and continuous support.

SUPPLEMENTARY MATERIAL

The Supplementary Material for this article can be found online at: <https://www.frontiersin.org/articles/10.3389/fbioe.2020.00549/full#supplementary-material>

Details on the experimental methods used to generate the data presented in the manuscript are reported in the **Supplementary Information**. **Supplementary Figure S1** is also reported within the **Supplementary Information** file.

- Chamanza, R., and Wright, J. A. (2015). A review of the comparative anatomy, histology, physiology and pathology of the nasal cavity of rats, mice, dogs and non-human primates. Relevance to inhalation toxicology and human health risk assessment. *J. Comp. Pathol.* 153, 287–314. doi: 10.1016/j.jcpa.2015.08.009
- Clippinger, A. J., Allen, D., Behrsing, H., Berube, K. A., Bolger, M. B., Casey, W., et al. (2018a). Pathway-based predictive approaches for non-animal assessment of acute inhalation toxicity. *Toxicol. In vitro* 52, 131–145. doi: 10.1016/j.tiv.2018.06.009
- Clippinger, A. J., Allen, D., Jarabek, A. M., Corvaro, M., Gaca, M., Gehen, S., et al. (2018b). Alternative approaches for acute inhalation toxicity testing to address global regulatory and non-regulatory data requirements: an international workshop report. *Toxicol. In vitro* 48, 53–70. doi: 10.1016/j.tiv.2017.12.011
- Creton, S., Dewhurst, I. C., Earl, L. K., Gehen, S. C., Guest, R. L., Hotchkiss, J. A., et al. (2010). Acute toxicity testing of chemicals-opportunities to avoid redundant testing and use alternative approaches. *Crit. Rev. Toxicol.* 40, 50–83. doi: 10.3109/10408440903401511
- Cryan, S.-A., Lorigan, J., and O'leary, C. (2019). "3D models as tools for inhaled drug development," in *Inhalation Aerosols-Physical and Biological Basis for Therapy, 3rd Edn.*, eds A. Hickey and H. Mansour (Boca Raton, FL: CRC Press), 16. doi: 10.1201/9781315159768-6

- Di Cristo, L., Maguire, C. M., Mc Quillan, K., Aleardi, M., Volkov, Y., Movia, D., et al. (2018). Towards the identification of an *In vitro* tool for assessing the biological behavior of aerosol supplied nanomaterials. *Int. J. Environ. Res. Public Health* 15:563. doi: 10.3390/ijerph15040563
- Dorato, M. A., and Wolff, R. K. (1991). Inhalation exposure technology, dosimetry, and regulatory issues. *Toxicol. Pathol.* 19, 373–383. doi: 10.1177/0192623391019004-106
- EPA (2016). *Process for Evaluating & Implementing Alternative Approaches to Traditional in vivo Acute Toxicity Studies for FIFRA Regulatory Use*. Available online at: https://www.epa.gov/sites/production/files/2016-03/documents/final_alternative_test_method_guidance_2-4-16.pdf (accessed May 22, 2020).
- EPA (2018). *Evaluation of a Proposed Approach to Refine Inhalation Risk Assessment for Point of Contact Toxicity: A Case Study Using a New Approach Methodology (NAM)*. Available online at: https://ntp.niehs.nih.gov/ntp/about_ntp/sacatm/2019/september/bcgn-1-epa_case_study.pdf (accessed May 22, 2020).
- EU (2010). *Directive 2010/63/EU of the European Parliament and of the Council of 22 September 2010 on the Protection of Animals Used for Scientific Purposes*.
- Gordon, S., Daneshian, M., Bouwstra, J., Caloni, F., Constant, S., Davies, D. E., et al. (2015). Non-animal models of epithelial barriers (skin, intestine and lung) in research, industrial applications and regulatory toxicology. *ALTEX* 32, 327–378. doi: 10.14573/altex.1510051
- Gras, D., Petit, A., Charriot, J., Knabe, L., Alagha, K., Gamez, A. S., et al. (2017). Epithelial ciliated beating cells essential for *ex vivo* ALI culture growth. *BMC Pulm. Med.* 17:80. doi: 10.1186/s12890-017-0423-5
- Griesinger, C., Desprez, B., Coecke, S., Casey, W., and Zuang, V. (2016). Validation of alternative *In vitro* methods to animal testing: concepts, challenges, processes and tools. *Adv. Exp. Med. Biol.* 856, 65–132. doi: 10.1007/978-3-319-33826-2_4
- Gstraunthaler, G. (2003). Alternatives to the use of fetal bovine serum: serum-free cell culture. *ALTEX* 20, 275–281.
- Hamm, J., Sullivan, K., Clippinger, A. J., Strickland, J., Bell, S., Bhattacharai, B., et al. (2017). Alternative approaches for identifying acute systemic toxicity: moving from research to regulatory testing. *Toxicol. In vitro* 41, 245–259. doi: 10.1016/j.tiv.2017.01.004
- Harkema, J. R. (1991). Comparative aspects of nasal airway anatomy: relevance to inhalation toxicology. *Toxicol. Pathol.* 19, 321–336. doi: 10.1177/0192623391019004-102
- Hartung, T. (2013). Look back in anger—what clinical studies tell us about preclinical work. *ALTEX* 30, 275–291. doi: 10.14573/altex.2013.3.275
- Hiemstra, P. S., Grootaers, G., Van Der Does, A. M., Krul, C. A. M., and Koeter, I. M. (2018). Human lung epithelial cell cultures for analysis of inhaled toxicants: lessons learned and future directions. *Toxicol. In vitro* 47, 137–146. doi: 10.1016/j.tiv.2017.11.005
- Hoffmann, W., Gradinaru, J., Farcas, L., Caul-Futy, M., Huang, S., Wiszniewski, L., et al. (2018). Establishment of a human 3D tissue-based assay for upper respiratory tract absorption. *Appl. In vitro Toxicol.* 4, 139–148. doi: 10.1089/aivt.2017.0035
- Hofmann, T., Ma-Hock, L., Teubner, W., Athas, J.-C., Neubauer, N., Wohlleben, W., et al. (2018). Reduction of acute inhalation toxicity testing in rats: the contact angle of organic pigments predicts their suffocation potential. *Appl. In vitro Toxicol.* 4, 220–228. doi: 10.1089/aivt.2018.0006
- Hofmann, W., Koblinger, L., and Martonen, T. B. (1989). Structural differences between human and rat lungs: implications for monte carlo modeling of aerosol deposition. *Health Phys.* 57, 41–46; discussion 46–47. doi: 10.1097/00004032-198907001-00005
- Huh, D., Matthews, B. D., Mammoto, A., Montoya-Zavala, M., Hsin, H. Y., and Ingber, D. E. (2010). Reconstituting organ-level lung functions on a chip. *Science* 328, 1662–1668. doi: 10.1126/science.1188302
- Iskandar, A. R., Mathis, C., Schlage, W. K., Frenzel, S., Leroy, P., Xiang, Y., et al. (2017). A systems toxicology approach for comparative assessment: biological impact of an aerosol from a candidate modified-risk tobacco product and cigarette smoke on human organotypic bronchial epithelial cultures. *Toxicol. In vitro* 39, 29–51. doi: 10.1016/j.tiv.2016.11.009
- Jackson, G. R. Jr., Maione, A. G., Klausner, M., and Hayden, P. J. (2018). Prevalidation of an acute inhalation toxicity test using the epi-airway *In vitro* human airway model. *Appl. In vitro Toxicol.* 4, 149–158. doi: 10.1089/aivt.2018.0004
- Jochems, C. E., Van Der Valk, J. B., Stafleu, F. R., and Baumans, V. (2002). The use of fetal bovine serum: ethical or scientific problem? *Altern. Lab. Anim.* 30, 219–227. doi: 10.1177/026119290203000208
- Krebs, A., Waldmann, T., Wilks, M. F., Van Vugt-Lussenburg, B. M. A., Van Der Burg, B., Terron, A., et al. (2019). Template for the description of cell-based toxicological test methods to allow evaluation and regulatory use of the data. *ALTEX* 36, 682–699. doi: 10.14573/altex.1909271
- Krebs, A., Waldmann, T., Wilks, M. F., Van Vugt-Lussenburg, B. M. A., Van Der Burg, B., Terron, A., et al. (2020). Erratum to template for the description of cell-based toxicological test methods to allow evaluation and regulatory use of the data. *ALTEX* 37:164. doi: 10.14573/altex.1909271e
- Krewski, D., Andersen, M. E., Tyshenko, M. G., Krishnan, K., Hartung, T., Boekelheide, K., et al. (2020). Toxicity testing in the 21st century: progress in the past decade and future perspectives. *Arch. Toxicol.* 94, 1–58. doi: 10.1007/s00204-019-02613-4
- Lacroix, G., Koch, W., Ritter, D., Gutleb, A. C., Larsen, S. T., Loret, T., et al. (2018). Air-liquid interface *In vitro* models for respiratory toxicology research: consensus workshop and recommendations. *Appl. In vitro Toxicol.* 4, 91–106. doi: 10.1089/aivt.2017.0034
- Leontaridou, M., Gabbert, S., and Landsiedel, R. (2019). The impact of precision uncertainty on predictive accuracy metrics of non-animal testing methods. *ALTEX* 36, 435–446. doi: 10.14573/altex.1810111
- Mauderly, J. L. (1997). Relevance of particle-induced rat lung tumors for assessing lung carcinogenic hazard and human lung cancer risk. *Environ. Health Perspect.* 105, 1337–1346. doi: 10.1289/ehp.97105s51337
- Miller, F. J., Mercer, R. R., and Crapo, J. D. (1993). Lower respiratory tract structure of laboratory animals and humans: dosimetry implications. *Aerosol. Sci. Technol.* 18, 257–271. doi: 10.1080/02786829308959603
- Movia, D., Bazou, D., and Prina-Mello, A. (2019). ALI multilayered co-cultures mimic biochemical mechanisms of the cancer cell-fibroblast cross-talk involved in NSCLC MultiDrug resistance. *BMC Cancer* 19:854. doi: 10.1186/s12885-019-6038-x
- Movia, D., Bazou, D., Volkov, Y., and Prina-Mello, A. (2018). Multilayered cultures of NSCLC cells grown at the air-liquid interface allow the efficacy testing of inhaled anti-cancer drugs. *Sci. Rep.* 8:12920. doi: 10.1038/s41598-018-31332-6
- Movia, D., Di Cristo, L., Alnemari, R., McCarthy, J. E., Moustau, H., Lamy De La Chapelle, M., et al. (2017). The curious case of how mimicking physiological complexity in *In vitro* models of the human respiratory system influences the inflammatory responses. A preliminary study focused on gold nanoparticles. *J. Interdiscip. Nanomed.* 2, 110–130. doi: 10.1002/jin.2.25
- Mowat, V., Alexander, D. J., and Pilling, A. M. (2017). A comparison of rodent and nonrodent laryngeal and tracheal bifurcation sensitivities in inhalation toxicity studies and their relevance for human exposure. *Toxicol. Pathol.* 45, 216–222. doi: 10.1177/0192623316678695
- NCad (2016). *Transition to Non-animal Research. Opportunities for the Phasing Out of Animal Procedures and the Stimulation of Innovation Without Laboratory Animals. Opinion of the Netherlands National Committee for the Protection of Animals used for Scientific Purposes (NCad)*. Available online at: <https://www.ncadierproevenbeleid.nl/documenten/rapport/2016/12/15/ncad-opinion-transition-to-non-animal-research> (accessed May 22, 2020).
- Oberdorster, G. (1996). Significance of particle parameters in the evaluation of exposure-dose-response relationships of inhaled particles. *Inhal. Toxicol.* 8, 73–89. doi: 10.1080/02726359608906690
- OECD (2009a). OECD guideline for the testing of chemicals. Available online at: <https://ntp.niehs.nih.gov/iccvam/suppdocs/feddocs/oecd/oecd-tg403.pdf> (accessed May 22, 2020).
- OECD (2009b). *Test No. 403: Acute Inhalation Toxicity*.
- OECD (2009c). *Test No. 436: Acute Inhalation Toxicity—Acute Toxic Class Method*.
- OECD (2018a). *ENV/JM/MONO(2009)28/REV1—Guidance Document on Acute Inhalation Toxicity Testing. Series on Testing and Assessment No. 39*.
- OECD (2018b). *Guidance Document on Good In vitro Method Practices (GIVIMP)*.
- Oesch, F., Fabian, E., and Landsiedel, R. (2019). Xenobiotica-metabolizing enzymes in the lung of experimental animals, man and in human lung models. *Arch. Toxicol.* 93, 3419–3489. doi: 10.1007/s00204-019-02602-7
- Oredsson, S., Coecke, S., Van Der Valk, J., and Vinken, M. (2019). What is understood by “animal-free research”? *Toxicol. In vitro* 57, 143–144. doi: 10.1016/j.tiv.2019.03.001

- Parent, R. A. (2015). *Comparative Biology of the Normal Lung*. San Diego, CA: Academic Press.
- Pauluhn, J. (2003). Overview of testing methods used in inhalation toxicity: from facts to artifacts. *Toxicol. Lett.* 140–141, 183–193. doi: 10.1016/S0378-4274(02)00509-X
- Pauluhn, J. (2005). Overview of inhalation exposure techniques: strengths and weaknesses. *Exp. Toxicol. Pathol.* 57, 111–128. doi: 10.1016/j.etp.2005.05.014
- Phalen, R. F., and Mendez, L. B. (2009). Dosimetry considerations for animal aerosol inhalation studies. *Biomarkers* 14, 63–66. doi: 10.1080/13547500902965468
- Phalen, R. F., Oldham, M. J., and Wolff, R. K. (2008). The relevance of animal models for aerosol studies. *J. Aerosol Med. Pulm. Drug Deliv.* 21, 113–124. doi: 10.1089/jamp.2007.0673
- Rentsch, I., Santos, C. L., Huhle, R., Ferreira, J. M. C., Koch, T., Schnabel, C., et al. (2017). Variable stretch reduces the pro-inflammatory response of alveolar epithelial cells. *PLoS ONE* 12:e0182369. doi: 10.1371/journal.pone.0182369
- Sarangapani, R., Clewell, H. J., Cruzan, G., and Andersen, M. E. (2002). Comparing respiratory-tract and hepatic exposure-dose relationships for metabolized inhaled vapors: a pharmacokinetic analysis. *Inhal. Toxicol.* 14, 835–854. doi: 10.1080/08958370290084656
- Sauer, U. G., Vogel, S., Hess, A., Kolle, S. N., Ma-Hock, L., Van Ravenzwaay, B., et al. (2013). *In vivo-In vitro* comparison of acute respiratory tract toxicity using human 3D airway epithelial models and human A549 and murine 3T3 monolayer cell systems. *Toxicol. In vitro* 27, 174–190. doi: 10.1016/j.tiv.2012.10.007
- Sewell, F., Ragan, I., Marczylo, T., Anderson, B., Braun, A., Casey, W., et al. (2015). A global initiative to refine acute inhalation studies through the use of 'evident toxicity' as an endpoint: towards adoption of the fixed concentration procedure. *Regul. Toxicol. Pharmacol.* 73, 770–779. doi: 10.1016/j.yrtph.2015.10.018
- Stallard, N., Price, C., Creton, S., Indans, I., Guest, R., Griffiths, D., et al. (2011). A new sighting study for the fixed concentration procedure to allow for gender differences. *Hum. Exp. Toxicol.* 30, 239–249. doi: 10.1177/0960327110370983
- Stallard, N., Whitehead, A., and Indans, I. (2003). Statistical evaluation of the fixed concentration procedure for acute inhalation toxicity assessment. *Hum. Exp. Toxicol.* 22, 575–585. doi: 10.1191/0960327103ht395oa
- Upadhyay, S., and Palmberg, L. (2018). Air-liquid interface: relevant *In vitro* models for investigating air pollutant-induced pulmonary toxicity. *Toxicol. Sci.* 164, 21–30. doi: 10.1093/toxsci/kfy053
- Van Der Valk, J., Bieback, K., Buta, C., Cochrane, B., Dirks, W. G., Fu, J., et al. (2018). Fetal Bovine Serum (FBS): past–present–future. *ALTEX* 35, 99–118. doi: 10.14573/altex.1705101
- Van Der Valk, J., Mellor, D., Brands, R., Fischer, R., Gruber, F., Gstraunthaler, G., et al. (2004). The humane collection of fetal bovine serum and possibilities for serum-free cell and tissue culture. *Toxicol. In vitro* 18, 1–12. doi: 10.1016/j.tiv.2003.08.009
- Wong, B. A. (2007). Inhalation exposure systems: design, methods and operation. *Toxicol. Pathol.* 35, 3–14. doi: 10.1080/01926230601060017

Conflict of Interest: The authors declare that the research was conducted in the absence of any commercial or financial relationships that could be construed as a potential conflict of interest.

The views expressed in this article are those of the authors. Mention of trade names or commercial products does not constitute endorsement or recommendation for use.

Copyright © 2020 Movia, Bruni-Favier and Prina-Mello. This is an open-access article distributed under the terms of the Creative Commons Attribution License (CC BY). The use, distribution or reproduction in other forums is permitted, provided the original author(s) and the copyright owner(s) are credited and that the original publication in this journal is cited, in accordance with accepted academic practice. No use, distribution or reproduction is permitted which does not comply with these terms.



Impact of Culture Medium on Cellular Interactions in *in vitro* Co-culture Systems

Michelle A. M. Vis^{1,2}, Keita Ito^{1,2} and Sandra Hofmann^{1,2*}

¹ Orthopaedic Biomechanics, Department of Biomedical Engineering, Eindhoven University of Technology, Eindhoven, Netherlands, ² Institute for Complex Molecular Systems, Eindhoven University of Technology, Eindhoven, Netherlands

OPEN ACCESS

Edited by:

Davide Staedler,
University of Lausanne, Switzerland

Reviewed by:

Sveva Bollini,
University of Genoa, Italy
Islam M. Saadeldin,
King Saud University, Saudi Arabia

*Correspondence:

Sandra Hofmann
s.hofmann@tue.nl

Specialty section:

This article was submitted to
Nanobiotechnology,
a section of the journal
Frontiers in Bioengineering and
Biotechnology

Received: 12 May 2020

Accepted: 15 July 2020

Published: 04 August 2020

Citation:

Vis MAM, Ito K and Hofmann S
(2020) Impact of Culture Medium on
Cellular Interactions in *in vitro*
Co-culture Systems.
Front. Bioeng. Biotechnol. 8:911.
doi: 10.3389/fbioe.2020.00911

Co-culturing of cells in *in vitro* tissue models is widely used to study how they interact with each other. These models serve to represent a variety of processes in the human body such as development, homeostasis, regeneration, and disease. The success of a co-culture is dependent on a large number of factors which makes it a complex and ambiguous task. This review article addresses co-culturing challenges regarding the cell culture medium used in these models, in particular concerning medium composition, volume, and exchange. The effect of medium exchange on cells is often an overlooked topic but particularly important when cell communication via soluble factors and extracellular vesicles, the so-called cell secretome (CS) is being studied. Culture medium is regularly exchanged to supply new nutrients and to eliminate waste products produced by the cells. By removing medium, important CSs are also removed. After every medium change, the cells must thus restore their auto- and paracrine communication through these CSs. This review article will also discuss the possibility to integrate biosensors into co-cultures, in particular to provide real-time information regarding media composition. Overall, the manner in which culture medium is currently used will be re-evaluated. Provided examples will be on the subject of bone tissue engineering.

Keywords: co-cultures, *in vitro* models, culture medium, medium exchange, biosensors

INTRODUCTION: *IN VITRO* TISSUE MODELS

Before culturing of cells was possible, animals were used to study human physiology and pathophysiology, in particular in medical and pharmaceutical industries (Russell and Burch, 1959). Animal models frequently failed to capture important facets of human physiology and pathophysiology and thus failed to mimic true human responses (Holmes et al., 2009). The possibility to culture human cells increased our insight into healthy and diseased states of the human body (Thomson et al., 1998; Holloway et al., 2019). First, cells were cultured in monolayers which in some cases lacked the complexity needed to study diseases and responses to drugs thoroughly (Esch et al., 2014; Fu et al., 2017; Zhang et al., 2019). Three-dimensional (3D) models enabled the creation of a cell environment closer to the natural microenvironment,

increasing the potential to predict physiological responses and also increasing complexity. For example, different 3D *in vitro* models to study osteocytes were established recently, mimicking their native environment and showing superior morphology and behavior compared to monolayer cultures, enabling future development of human disease models (Zhang et al., 2019).

The approach for the design of *in vitro* tissue models originates from tissue engineering (TE; Langer and Vacanti, 1993; Caddeo et al., 2017). TE combines cells, scaffolds, growth factors and mechanical stimuli to create tissues *in vitro*. Traditionally, TE has focused on the creation of tissue grafts for implantation. More recently, TE has been applied to develop *in vitro* tissue models. In contrast to tissue grafts that need clinically relevant sizes of engineered tissue, *in vitro* models aim to resemble the smallest functional unit of a tissue. Such *in vitro* models show potential to study processes of the human body such as development (Robin et al., 2016), homeostasis (Rossi et al., 2018), regeneration (Guzmán et al., 2014), and disease (Salamanna et al., 2016).

The development of 3D human *in vitro* models depends on the ability to partially recreate the complexity of the native microenvironment that defines cues (physical, chemical, and biological) for cell function, proliferation, and differentiation (Holmes et al., 2009). The challenge is to define the aspects of the microenvironment which are important in order to engineer the smallest functional unit that captures the interaction between key cues in the cell system which it controls (Holmes et al., 2009). Research has shifted toward improving *in vitro* models by increasing their complexity in order to understand how mature intricate tissues form (Holloway et al., 2019). An increase in complexity can be accomplished by culturing different cell types together in one culture, called co-culturing.

CO-CULTURES WITH THE APPLICATION FOR *IN VITRO* TISSUE MODELS

Co-culturing of cells is widely used to study interactions between cell populations in many fields including (but not limited to) synthetic biology (Goers et al., 2014), ecology (Jessup et al., 2004), TE both 2D and 3D (Liu et al., 2015; Paschos et al., 2015), and multi-organ microphysiological systems (Wang et al., 2017). Models have been developed for a variety of tissues such as lung (Strikoudis et al., 2019), intestine (Jalili-Firoozinezhad et al., 2019), kidney (Takasato and Little, 2017), bone (Rossi et al., 2018), embryo (Saadeldin et al., 2014), ovary (Saadeldin et al., 2015), neuron-glia (Skaper and Facci, 2018), and liver (Coll et al., 2018). Co-cultures can be used to represent both physiological and pathological tissue states. Ideally, human, or even patient-specific cells are used to create cellular environments that are more representative for humans rather than animal derived cells (Caddeo et al., 2017). Most co-culture studies involve two cell types, owing to an increased complexity in establishing a stable system when more cell types are involved (Goers et al., 2014). There are also studies reporting the use of three (Venter and Niesler, 2018; Churm et al., 2019; Lin et al., 2019) or even four cell types (Zhang et al., 2009; DesRochers et al., 2015).

Different strategies to co-culture cells in 3D exist, each allowing for a different degree of contact between the cell types. Through this contact, the cells are able to stimulate each other. Direct co-cultures facilitate physical contact between the different cell types which allows for communication through their surface receptors and gap junctions, defined as juxtacrine communication (Figure 1A). Indirect co-cultures incorporate a physical separation between cell types, such as a semi-permeable membrane in the form of a transwell system, only enabling signaling via the cell secretome (CS; Figures 1B-I). In addition, in indirect co-cultures, conditioned medium is frequently used (Figures 1B-II). Medium is first used for culturing one cell type and then transferred to the second cell type. The medium contains the CS of the first cell type, which then affects the second cell type. Conditioned medium contains numerous CSs that may positively and/or negatively regulate cell behavior (Katagiri et al., 2017). The mechanisms that support the effect of these CSs remain insufficiently defined and are highly dependent on the cell source (Marolt Presen et al., 2019).

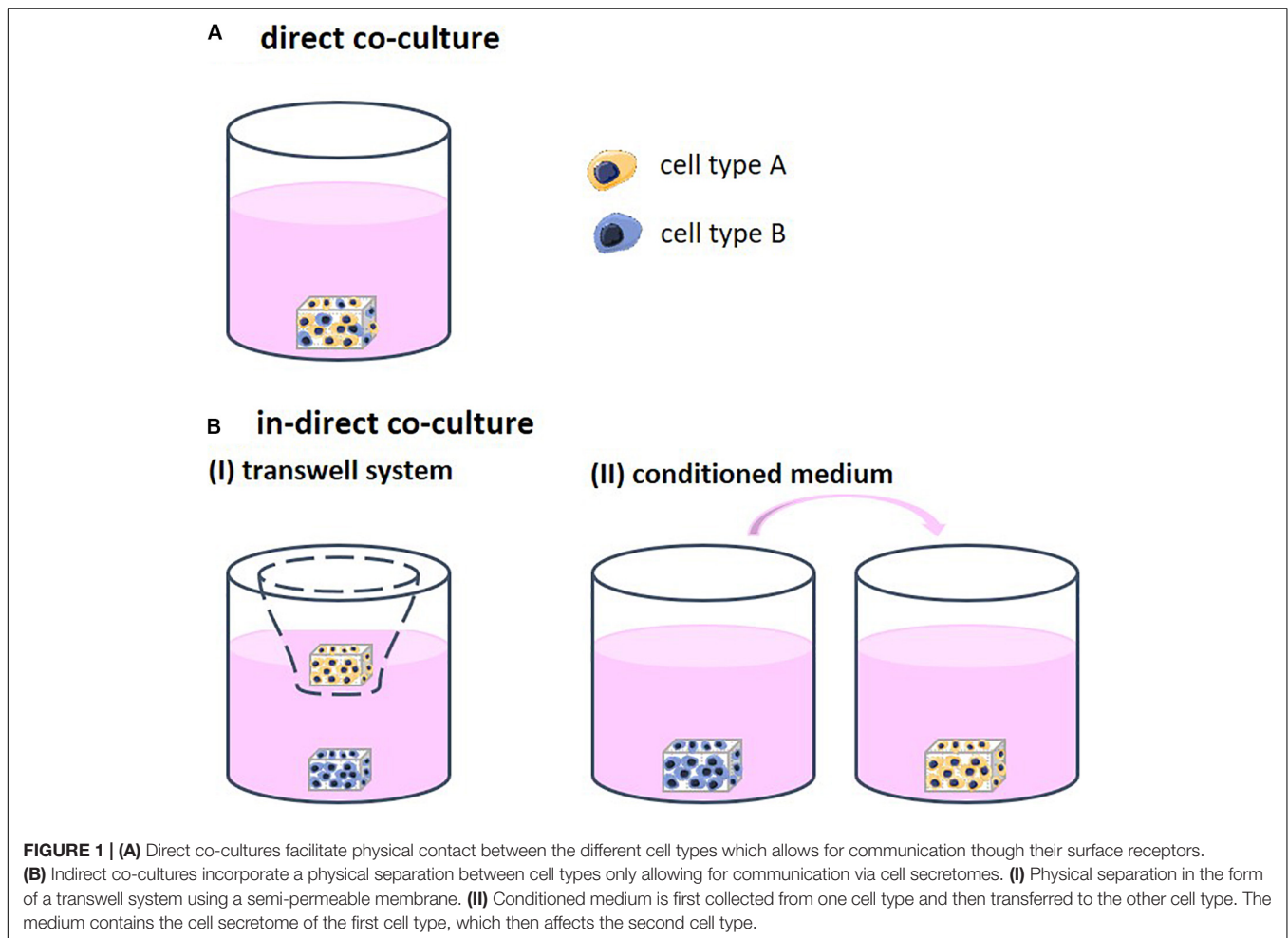
Cell secretomes ensure cell-cell communication and comprise of soluble factors and cell-derived membranous structures. These so-called extracellular vesicles (EVs), are nanosized particles (exosomes, 30–100 nm; microvesicles, 50–2000 nm; Martins et al., 2016) that transfer proteins, bioactive lipids between cells. Moreover, EVs are also capable of transferring RNA between cells, called exosomal RNA or esRNA (Lotvall and Valadi, 2007; Valadi et al., 2007). EVs are present in biological fluids and are involved in multiple physiological and pathological processes (van Niel et al., 2018). For example, EVs derived from osteogenically committed mesenchymal stromal cells were shown to induce osteogenic commitment of homotypic cells without further supplementation (Martins et al., 2016). EVs are widely studied for their potential as a cell-free therapeutic method for regeneration of numerous tissue types. Subsequently, EVs might be used to study cellular interactions *in vitro* omitting the requirement for a co-culture experiment and thus overcoming co-culture challenges. The biggest challenge of using EVs lies within the development of purification and characterization protocols (Lee et al., 2019).

Overall, co-cultures are versatile models to create cellular environments in which interactions between different cell types can be studied *in vitro*. These interactions can take place by direct contact and by exchange of soluble factors and EVs. This review article will focus on steps that can guide optimization of medium composition and volume in co-cultures with a particular focus on cell communication via the CS.

GENERAL CONSIDERATIONS REGARDING CULTURE MEDIUM IN CO-CULTURES

Selecting Culture Medium Composition

In cell culturing, culture medium is added to nourish the cells. Culture medium is a liquid nutritive substance consisting of a mixture of base medium, serum, and regulating factors. Firstly,



base medium fills the nutritional requirements of the cells. The first base medium was developed in 1959 and was defined as the Minimal Essential Medium (MEM), including 13 amino acids, 8 vitamins, 6 ionic species, and glucose (Eagle, 1959). Secondly, serum, such as fetal bovine serum (FBS) contains important basic proteins including growth factors and hormones for maintaining cell survival, growth, and proliferation (Gstraunthaler, 2003). FBS is a complex and natural mixture that is extracted from fetal blood. The use of FBS is controversial due to quality and reproducibility issues as well as animal welfare concerns which is elaborately reviewed elsewhere (van der Valk et al., 2018). Thirdly, regulating factors such as growth factors are added to the medium to guide specific and desired cell behavior such as proliferation and differentiation into a particular cell lineage. These factors are key in cell cultures as they predominantly determine cell fate. Establishing a functional and precise mixture of these culture medium ingredients is of great importance for creating *in vitro* tissue models.

Each cell type has specific needs according to its function and requires a corresponding specific medium composition. When two or more different cell types are cultured together, choosing the right medium becomes a challenge (Goers et al., 2014). Several approaches are possible, such as mixed medium,

supplemented medium and partitioned culture environments (**Figure 2A**). In a mixed medium, the medium of all used cell types is combined, possibly in different ratios. With this method, the original medium supplements might interfere with the other cell type, which is particularly important when culturing progenitor cells as these cells yet have to differentiate into the desired cell type. For instance, in a co-culture of precursors of osteoblasts and osteoclasts, the osteogenic supplements dexamethasone and β -glycerophosphate are needed for osteoblast differentiation and maturation, while these supplements have been shown to inhibit monocyte differentiation into osteoclasts (Haynesworth et al., 1996; Takeyama et al., 2001; Langenbach and Handschel, 2013). An optimum dosage of supplements has to be found in order to obtain both functional osteoblast and functional osteoclasts. Another approach could be to use a general base medium, supplemented with the soluble factors that stimulate both cell types without negatively affecting either of them (Zhu et al., 2018). This method makes it possible to modulate the medium more specifically than by just mixing two media types. The disadvantage is that it is time consuming to find suitable supplements and to optimize the combination. Additionally, a culture method that enables two physically partitioned medium

flows can be used. In this way, both cell types receive their specific medium while cell-cell contact is still possible (Robertson et al., 2014). However, this is a complicated and precise method that can mostly be performed in 2D and for certain cell types.

In multi-organ microphysiological systems, the challenge of finding the right medium is even more difficult as a variety of cell types may each have their own optimal medium and supplements. For example, in a device combining liver, lung, kidney, and adipose tissue, it was shown that addition of transforming growth factor $\beta 1$ (TGF- $\beta 1$) supported the growth of lung cells but inhibited the growth of liver cells (Zhang et al., 2009). They overcame this by using gelatin microspheres that released TGF- $\beta 1$ locally to support the lung compartment while in the circulation, low TGF- $\beta 1$ levels could be maintained (Zhang et al., 2009).

Just as important, one cell type in a co-culture naturally provides CSs that influence the other cell type. As a result, medium supplements might have to be altered in concentration or might be fully omitted (Zhu et al., 2018). For example, osteoclasts in mono-culture are derived from mononuclear cells by addition of macrophage colony-stimulating factor and receptor activator of nuclear factor kappa-B ligand. Both molecules are naturally produced by osteoblasts (Boyce and Xing, 2007). Thus, in a co-culture with osteoblasts, no additional cytokines may be needed for osteoclast formation (Schulze et al., 2018; Zhu et al., 2018).

Medium optimization is crucial but is laborious and time-consuming because of the enormous number of possible combinations. Parallel assays using micro/nano-scale devices hold great promise for evaluation and optimization of a multitude of options (Sasaki et al., 2016). For example, a sensitive platform for optimum culture media investigation was developed in which image-based profiling was combined with microdevices to achieve high-throughput evaluation of culture medium conditions (Sasaki et al., 2016). Advances in this field could be of great value to ease the inconvenience of medium optimization.

The Effect of Culture Medium Volume

Medium volume is of importance as a higher volume leads to lower concentrations of the CS (Figure 2B). In bone cell cultures, osteoblastic mineral deposition and fusion of osteoclast-precursors into osteoclasts were shown to be dependent on the medium volume (Yoshimura et al., 2017). When culturing cells, often the medium volume suggested by the manufacturer of culture plastics is used. However, this volume is not optimized for specific cell types. For example, low culture medium volumes not only have been shown to be beneficial for culturing cell types such as neuron-like cells (Shimomura et al., 2016) and adipose derived mesenchymal stem cells (Simão et al., 2019), they are also more economical. On the other hand, some culturing conditions, for example in bioreactors, might require minimal volumes to operate, which makes volume optimization impracticable. In these cases, it should be recognized that the medium volume may impact a variety of cell culture aspects (Yoshimura et al., 2017).

Medium volume is influenced by cell culture aspects such as nutrient supply, dilution, or concentration of waste products

and metabolites, and changes in oxygen level (Zhu et al., 2018). Studies have demonstrated that the oxygen concentration in medium decreases with increasing medium depth, leading to altered cell growth characteristics (Oze et al., 2012; Place et al., 2017). Moreover, it has been recognized that cell proliferation and differentiation are largely influenced by the concentration of CSs (Yoshimura et al., 2017). With different medium volumes these CSs become either more or less concentrated resulting in faster or slower proliferation and differentiation of these cells. Thus, cells might function differently when cultured in different medium volumes. Again, optimization is key but laborious and, in some cases, even impracticable. Therefore, one should be aware of the effects of medium volume. Certainly, when unexplainable results are encountered and when protocols are adjusted to up- or down-scale experiments.

THE EFFECT OF MEDIUM EXCHANGE ON CELL-CELL INTERACTIONS

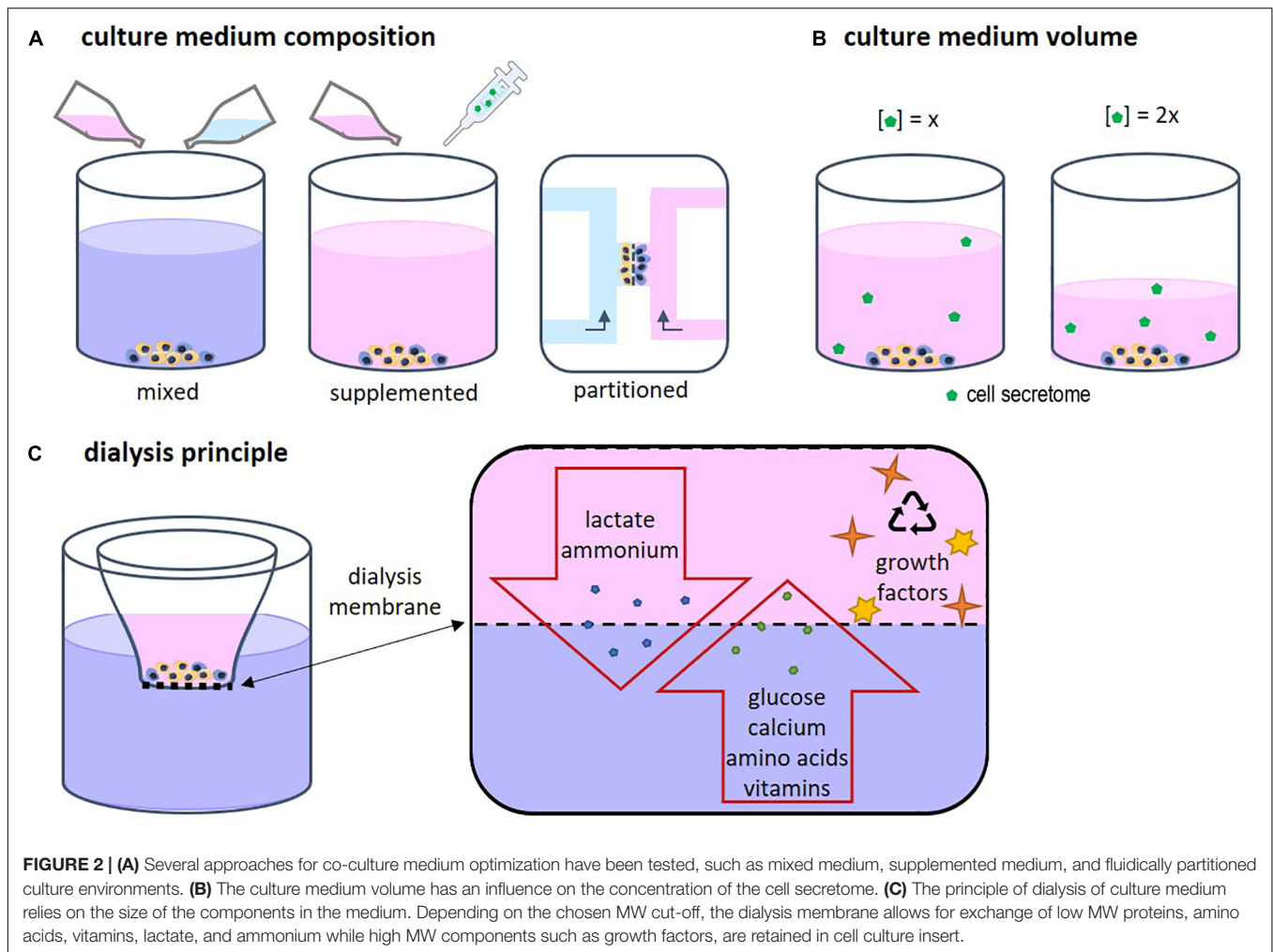
Waste Accumulation Problem

Medium is exchanged regularly to maintain nutrients and growth factors consumed by the cells and to eliminate waste products produced by the cells. Mammalian cells use glucose for energy and produce lactate as a metabolite (Ozturk et al., 1997). *In vitro*, every cell type needs a narrow pH range within 0.2 to 0.4 pH units of its optimum to grow (Paul, 1975). The production of lactic acid should not exceed the buffering capacity of the medium, because lowering the pH can inhibit cell growth (Zielke et al., 1980; Glacken et al., 1986; Ozturk et al., 1992, 1997). Also, high ammonium concentrations as a by-product of glutamine catabolism can be toxic to cells causing cytosol vacuolization and subsequent cell death (Glacken et al., 1986; Slivac et al., 2010). Exchanging the medium prevents these waste product accumulation effects.

However, after every medium exchange, also the CS is removed, and the cells must make a new effort to restore their communication by producing fresh molecules. This effort could negatively influence their behavior, not representing their natural state. The influence of medium exchange was for example investigated by measuring actin microfilament structure directly before and after medium exchange (Krüger-Genge et al., 2015). Medium exchange led to a rapid disturbance of stress fiber formation and disconnection of cell-cell contacts. Frequent medium exchange is also economically disadvantageous as medium can contain expensive additives such as growth factors and animal serum (Glacken et al., 1986). However, medium exchange cannot be prevented as nutrient deprivation and waste accumulation would lead to inevitable cell death.

Systems for Culture Medium Re-use

Driven by economical motives, re-use of medium was first described in 1977 by adding fresh nutrient supplements to used medium (Mizrahi and Avihoo, 1977). However, due to the accumulation of waste products, the medium could only be re-used once. A second re-use caused cell death.



To overcome this issue, other cell culture systems were developed in which medium was dialyzed to remove waste products. In addition, dialysis could be used to harvest cell products such as antibodies (Adamson et al., 1983). The principle of dialysis relies on the exclusion of molecules based on their size (Figure 2C). Fresh medium contains low molecular weight (MW) molecules such as nutrients, amino acids, and vitamins. Depending on the chosen MW cut-off, the dialysis membrane allows for exchange of those molecules. In this way waste products can diffuse out of the culture medium while nutrients and vitamins diffuse back in. High MW components such as growth factors are retained in the medium compartment.

The first dialysis system cultures were rather complex and large. For example, a bioreactor was developed using a 5 liter medium vessel coupled to a 2 liter perfusion system (Büntemeyer et al., 1992). Several fluid streams were connected to control waste removal, medium recycling, and nutrient supply. For the elimination of toxic waste products, a hollow fiber microfiltration system was used while nutrients were supplied by adding concentrated solutions. Most previous studies focused on mass production, generally using large scale reactors (Chen et al., 2011;

Nath et al., 2017). Recently, a simpler dialysis culture system was presented that does not require the use of pumps and vessels (Shinohara et al., 2019). A deep well culture plate including an insert with a dialysis membrane was used (Figure 2C). Successful and continuous glucose supply and lactate removal through the dialysis membrane were shown. The retaining of cytokines and autocrine factor enabled to promote endodermal differentiation of induced pluripotent stem cells (iPSCs) without daily cytokine addition. This dialysis system for re-using culture medium still is not frequently applied and mainly used for proliferation and differentiation processes of (costly) iPSCs studies (Côme et al., 2008; Nath et al., 2017; Shinohara et al., 2019). Use of these dialysis systems in other cell culturing fields requires optimization. For example, the size of medium components should be known and taken into account as high MW proteins, which are also found in FBS, will not be able to cross the dialysis membrane. In our opinion, medium dialysis could not only reduce culture costs, it could also contribute to a more physiological environment for cell proliferation and differentiation. This would especially be true for co-cultures where the interaction between different cell types is investigated, by retaining the communication factors produced by the cells.

IMPLEMENTATION OF BIOSENSORS

Combining biology and technology advances cell culturing at a rapid pace. Addition of biosensors to cell cultures is one of these beneficial combinations. Biosensors show potential for monitoring of the microenvironments in *in vitro* systems and aim at providing real-time information regarding cell viability, growth and metabolism (Pereira Rodrigues et al., 2008; Modarres et al., 2018; Young et al., 2019). For example, on-line measurement of dissolved oxygen was applied for medium optimization of mammalian cell cultures (Deshpande et al., 2004). An oxygen sensor immobilized at the bottom of each well in a 96 wells plate was successfully used to optimize the concentration of glucose, glutamine and inorganic salts. This method was highly cost effective and time efficient, automatically analyzing many samples in one go in small medium volumes.

In order to maintain cell viability, experimental validity and reproducibility, it is essential that metabolite levels are maintained within physiological limits (Place et al., 2017). For example, fluctuations in oxygen and glucose concentration can affect cell growth, differentiation and signaling (Place et al., 2017). Multiplexed sensing, recording, and processing of real-time data could provide novel insights into the optimal nutrients and culture conditions needed to grow cells (Young et al., 2019). Furthermore, real-time data analytics can be used to respond to changes in culture conditions in a closed feedback loop, adjusting inputs to obtain desired results (Young et al., 2019). Sensors could provide help in determining the status of the cell culture. For example, medium composition can be tracked for the CS as a stem cell differentiates to determine how differentiation is progressing. Accordingly, growth factors can be removed or added to encourage further differentiation (Young et al., 2019).

It needs to be mentioned that while the technology is available, not many user-friendly and affordable techniques have been implemented into *in vitro* tissue cultures. Particularly techniques developed for continuous detection of biomolecules at low physiological concentrations require thorough understanding of electrochemistry, electrical engineering, and/or optics. Implementation will require a closer collaboration between researchers of different fields, willing to combine each other's expertise, requirements, and possibilities.

REFERENCES

- Adamson, S. R., Fitzpatrick, S. L., Behie, L. A., Gaucher, G. M., and Lesser, B. H. (1983). In vitro production of high titre monoclonal antibody by hybridoma cells in dialysis culture. *Biotechnol. Lett.* 5, 573–578. doi: 10.1007/BF00130835
- Boyce, B. F., and Xing, L. (2007). The RANKL/RANK/OPG pathway. *Curr. Osteoporos. Rep.* 5, 98–104. doi: 10.1007/s11914-007-0024-y
- Büntemeyer, H., Wallerius, C., and Lehmann, J. (1992). Optimal medium use for continuous high density perfusion processes. *Cytotechnology* 9, 59–67. doi: 10.1007/BF02521732
- Caddeo, S., Boffito, M., and Sartori, S. (2017). Tissue engineering approaches in the design of healthy and pathological in vitro tissue models. *Front. Bioeng. Biotechnol.* 5:40. doi: 10.3389/fbioe.2017.00040
- Chen, G., Gulbranson, D. R., Hou, Z., Bolin, J. M., Ruotti, V., Probasco, M. D., et al. (2011). Chemically defined conditions for human iPSC derivation and culture. *Nat. Methods* 8, 424–429. doi: 10.1038/nmeth.1593

CONCLUSION

Investigating cell-cell interactions through CSs requires complex tissue cultures where different cell types are being co-cultured. Co-culturing asks for a highly specific environment meeting the requirements of all involved cell types and therefore requires a great deal of optimizing. Advances in this field bring us closer to *in vitro* models that can be used to study physiological and pathological cell-cell interactions and will allow for the development of drugs that interact with cells. We highly recommend to reconsider today's method of complete medium exchange to provide a more physiological environment to the cells. Combining current *in vitro* culturing techniques with existing technological inventions such as dialysis and biosensors could lead toward the goal of developing more complex, reproducible, nature-like *in vitro* tissue models.

AUTHOR CONTRIBUTIONS

MV and SH contributed to the conception of the review. MV wrote the first draft of the manuscript. All authors contributed to manuscript revision, read, and approved the submitted version.

FUNDING

The authors gratefully acknowledge the financial support for MV and SH by the research program TTW with project number TTW 016.Vidi.188.021, which is financed by the Dutch Organization for Scientific Research (NWO).

ACKNOWLEDGMENTS

The authors gratefully acknowledge Professor Menno Prins and Paul Vernooij for sharing their knowledge on biosensors and for their contribution to the discussions about implementation of biosensors in the cell biology field.

- Churm, R., Dunseath, G. J., Prior, S. L., Thomas, R. L., Banerjee, S., and Owens, D. R. (2019). Development and characterization of an in vitro system of the human retina using cultured cell lines. *Clin. Experiment. Ophthalmol.* 47, 1055–1062. doi: 10.1111/ceo.13578
- Coll, M., Perea, L., Boon, R., Leite, S. B., Vallverdú, J., Mannaerts, I., et al. (2018). Generation of hepatic stellate cells from human pluripotent stem cells enables in vitro modeling of liver fibrosis. *Cell Stem Cell* 23, 101.e7–113.e7. doi: 10.1016/j.stem.2018.05.027
- Côme, J., Nissan, X., Aubry, L., Tournois, J., Girard, M., Perrier, A. L., et al. (2008). Improvement of culture conditions of human embryoid bodies using a controlled perfused and dialyzed bioreactor system. *Tissue Eng. Part C Methods* 14, 289–298. doi: 10.1089/ten.tec.2008.0029
- Deshpande, R. R., Wittmann, C., and Heinzel, E. (2004). Microplates with integrated oxygen sensing for medium optimization in animal cell culture. *Cytotechnology* 46, 1–8. doi: 10.1007/s10616-004-6401-9

- DesRochers, T. M., Holmes, L., O'Donnell, L., Mattingly, C., Shuford, S., O'Rourke, M. A., et al. (2015). Macrophage incorporation into a 3D perfusion tri-culture model of human breast cancer. *J. Immunother. Cancer* 3(Suppl. 2):P401. doi: 10.1186/2051-1426-3-S2-P401
- Eagle, H. (1959). Amino acid metabolism in mammalian cell cultures. *Science* 130, 432–437. doi: 10.1126/science.130.3373.432
- Esch, M. B., Smith, A. S. T., Prot, J.-M., Oleaga, C., Hickman, J. J., and Shuler, M. L. (2014). How multi-organ microdevices can help foster drug development. *Adv. Drug Deliv. Rev.* 6, 158–169. doi: 10.1016/j.addr.2013.12.003
- Fu, J., Fernandez, D., Ferrer, M., Titus, S. A., Buehler, E., and Lal-Nag, M. A. (2017). RNAi high-throughput screening of single- and multi-cell-type tumor spheroids: a comprehensive analysis in two and three dimensions. *SLAS Discov. Adv. Life Sci. RD* 22, 525–536. doi: 10.1177/2472555217696796
- Glacken, M. W., Fleischaker, R. J., and Sinskey, A. J. (1986). Reduction of waste product excretion via nutrient control: possible strategies for maximizing product and cell yields on serum in cultures of mammalian cells. *Biotechnol. Bioeng.* 28, 1376–1389. doi: 10.1002/bit.260280912
- Goers, L., Freemont, P., and Polizzi, K. M. (2014). Co-culture systems and technologies: taking synthetic biology to the next level. *J. R. Soc. Interface* 11:20140065. doi: 10.1098/rsif.2014.0065
- Gstraunthaler, G. (2003). Alternatives to the use of fetal bovine serum: serum-free cell culture. *ALTEX* 20, 275–281.
- Guzmán, R., Nardecchia, S., Gutiérrez, M. C., Ferrer, M. L., Ramos, V., del Monte, F., et al. (2014). Chitosan scaffolds containing calcium phosphate salts and rhBMP-2: in vitro and in vivo testing for bone tissue regeneration. *PLoS One* 9:e87149. doi: 10.1371/journal.pone.0087149
- Haynesworth, S. E., Baber, M. A., and Caplan, A. I. (1996). Cytokine expression by human marrow-derived mesenchymal progenitor cells in vitro: effects of dexamethasone and IL-1 alpha. *J. Cell. Physiol.* 166, 585–592. doi: 10.1002/(sici)1097-4652(199603)166:3<585::aid-jcp13>3.0.co;2-6
- Holloway, E. M., Capeling, M. M., and Spence, J. R. (2019). Biologically inspired approaches to enhance human organoid complexity. *Dev. Camb. Engl.* 146:dev166173. doi: 10.1242/dev.166173
- Holmes, A., Brown, R., and Shakesheff, K. (2009). Engineering tissue alternatives to animals: applying tissue engineering to basic research and safety testing. *Regen. Med.* 4, 579–592. doi: 10.2217/rme.09.26
- Jalili-Firoozinezhad, S., Gazzaniga, F. S., Calamari, E. L., Camacho, D. M., Fadel, C. W., Bein, A., et al. (2019). A complex human gut microbiome cultured in an anaerobic intestine-on-a-chip. *Nat. Biomed. Eng.* 3, 520–531. doi: 10.1038/s41551-019-0397-0
- Jessup, C. M., Kassen, R., Forde, S. E., Kerr, B., Buckling, A., Rainey, P. B., et al. (2004). Big questions, small worlds: microbial model systems in ecology. *Trends Ecol. Evol.* 19, 189–197. doi: 10.1016/j.tree.2004.01.008
- Katagiri, W., Sakaguchi, K., Kawai, T., Wakayama, Y., Osugi, M., and Hibi, H. (2017). A defined mix of cytokines mimics conditioned medium from cultures of bone marrow-derived mesenchymal stem cells and elicits bone regeneration. *Cell Prolif.* 50:e12333. doi: 10.1111/cpr.12333
- Krüger-Genge, A., Fuhrmann, R., Jung, F., and Franke, R. P. (2015). Morphology of primary human venous endothelial cell cultures before and after culture medium exchange. *Clin. Hemorheol. Microcirc.* 61, 151–156. doi: 10.3233/CH-151992
- Langenbach, F., and Handschel, J. (2013). Effects of dexamethasone, ascorbic acid and β -glycerophosphate on the osteogenic differentiation of stem cells in vitro. *Stem Cell Res. Ther.* 4:117. doi: 10.1186/scrt328
- Langer, R., and Vacanti, J. P. (1993). Tissue engineering. *Science* 260, 920–926. doi: 10.1126/science.8493529
- Lee, Y. X. F., Johansson, H., Wood, M. J. A., and El Andaloussi, S. (2019). Considerations and implications in the purification of extracellular vesicles - A cautionary tale. *Front. Neurosci.* 13:1067. doi: 10.3389/fnins.2019.01067
- Lin, Y., Huang, S., Zou, R., Gao, X., Ruan, J., Weir, M. D., et al. (2019). Calcium phosphate cement scaffold with stem cell co-culture and prevascularization for dental and craniofacial bone tissue engineering. *Dent. Mater. Off. Publ. Acad. Dent. Mater.* 35, 1031–1041. doi: 10.1016/j.dental.2019.04.009
- Liu, Y., Chan, J. K. Y., and Teoh, S.-H. (2015). Review of vascularised bone tissue-engineering strategies with a focus on co-culture systems. *J. Tissue Eng. Regen. Med.* 9, 85–105. doi: 10.1002/term.1617
- Lotvall, J., and Valadi, H. (2007). Cell to cell signalling via exosomes through esRNA. *Cell Adhes. Migr.* 1, 156–158. doi: 10.4161/cam.1.3.5114
- Marolt Presen, D., Traweger, A., Gimona, M., and Redl, H. (2019). Mesenchymal stromal cell-based bone regeneration therapies: from cell transplantation and tissue engineering to therapeutic secretomes and extracellular vesicles. *Front. Bioeng. Biotechnol.* 7:352. doi: 10.3389/fbioe.2019.00352
- Martins, M., Ribeiro, D., Martins, A., Reis, R. L., and Neves, N. M. (2016). Extracellular vesicles derived from osteogenically induced human bone marrow mesenchymal stem cells can modulate lineage commitment. *Stem Cell Rep.* 6, 284–291. doi: 10.1016/j.stemcr.2016.01.001
- Mizrahi, A., and Avihoo, A. (1977). Growth medium utilization and its re-use for animal cell cultures. *J. Biol. Stand.* 5, 31–37. doi: 10.1016/0092-1157(77)90016-6
- Modarres, H. P., Janmaleki, M., Novin, M., Saliba, J., El-Hajj, F., RezayatiCharan, M., et al. (2018). In vitro models and systems for evaluating the dynamics of drug delivery to the healthy and diseased brain. *J. Controlled Release* 273, 108–130. doi: 10.1016/j.jconrel.2018.01.024
- Nath, S. C., Nagamori, E., Horie, M., and Kino-Oka, M. (2017). Culture medium refinement by dialysis for the expansion of human induced pluripotent stem cells in suspension culture. *Bioprocess Biosyst. Eng.* 40, 123–131. doi: 10.1007/s00449-016-1680-z
- Oze, H., Hirao, M., Ebina, K., Shi, K., Kawato, Y., Kaneshiro, S., et al. (2012). Impact of medium volume and oxygen concentration in the incubator on pericellular oxygen concentration and differentiation of murine chondrogenic cell culture. *In Vitro Cell. Dev. Biol. Anim.* 48, 123–130. doi: 10.1007/s11626-011-9479-3
- Ozturk, S. S., Jorjani, P., Taticek, R., Lowe, B., Shackleford, S., Ladehoff-Guiles, D., et al. (1997). "Kinetics of glucose metabolism and utilization of lactate in mammalian cell cultures," in *Animal Cell Technology: From Vaccines to Genetic Medicine*, eds M. J. T. Carrondo, B. Griffiths, and J. L. P. Moreira (Dordrecht: Springer Netherlands), 355–360. doi: 10.1007/978-94-011-5404-8_56
- Ozturk, S. S., Riley, M. R., and Palsson, B. O. (1992). Effects of ammonia and lactate on hybridoma growth, metabolism, and antibody production. *Biotechnol. Bioeng.* 39, 418–431. doi: 10.1002/bit.260390408
- Paschos, N. K., Brown, W. E., Eswaramoorthy, R., Hu, J. C., and Athanasios, K. A. (2015). Advances in tissue engineering through stem cell-based co-culture. *J. Tissue Eng. Regen. Med.* 9, 488–503. doi: 10.1002/term.1870
- Paul, J. (1975). *Cell and Tissue Culture*, 5th Edn. Edinburgh, NY: Churchill Livingstone.
- Pereira Rodrigues, N., Sakai, Y., and Fujii, T. (2008). Cell-based microfluidic biochip for the electrochemical real-time monitoring of glucose and oxygen. *Sens. Actuators B Chem.* 132, 608–613. doi: 10.1016/j.snb.2007.12.025
- Place, T. L., Domann, F. E., and Case, A. J. (2017). Limitations of oxygen delivery to cells in culture: an underappreciated problem in basic and translational research. *Free Radic. Biol. Med.* 113, 311–322. doi: 10.1016/j.freeradbiomed.2017.10.003
- Robertson, G., Bushell, T., and Zagnoni, M. (2014). Chemically induced synaptic activity between mixed primary hippocampal co-cultures in a microfluidic system. *Integr. Biol.* 6, 636–644. doi: 10.1039/C3IB40221E
- Robin, M., Almeida, C., Azaïs, T., Haye, B., Illoul, C., Lesieur, J., et al. (2016). Involvement of 3D osteoblast migration and bone apatite during in vitro early osteocytogenesis. *Bone* 88, 146–156. doi: 10.1016/j.bone.2016.04.031
- Rossi, E., Mracsko, E., Papadimitropoulos, A., Allafi, N., Reinhardt, D., Mehrkens, A., et al. (2018). An in vitro bone model to investigate the role of triggering receptor expressed on myeloid cells-2 in bone homeostasis. *Tissue Eng. Part C Methods* 24, 391–398. doi: 10.1089/ten.TEC.2018.0061
- Russell, W. M. S., and Burch, R. L. (1959). *The Principles of Humane Experimental technique*. London: Methuen & Co, 86–97.
- Saadeldin, I. M., Elsayed, A., Kim, S. J., Moon, J. H., and Lee, B. C. (2015). A spatial model showing differences between juxtacrine and paracrine mutual oocyte-granulosa cells interactions. *Indian J. Exp. Biol.* 53, 75–81.
- Saadeldin, I. M., Kim, S. J., Choi, Y. B., and Lee, B. C. (2014). Improvement of cloned embryos development by co-culturing with parthenotes: a possible role of exosomes/microvesicles for embryos paracrine communication. *Cell. Reprogramming* 16, 223–234. doi: 10.1089/cell.2014.0003
- Salamanna, F., Borsari, V., Brogini, S., Giavaresi, G., Parrilli, A., Cepollaro, S., et al. (2016). An in vitro 3D bone metastasis model by using a human bone tissue culture and human sex-related cancer cells. *Oncotarget* 7, 76966–76983. doi: 10.18632/oncotarget.12763
- Sasaki, H., Enomoto, J., Ikeda, Y., Honda, H., Fukuda, J., and Kato, R. (2016). Comparisons of cell culture medium using distribution of morphological

- features in microdevice. *J. Biosci. Bioeng.* 121, 117–123. doi: 10.1016/j.jbiosc.2015.05.011
- Schulze, S., Wehrum, D., Dieter, P., and Hempel, U. (2018). A supplement-free osteoclast-osteoblast co-culture for pre-clinical application. *J. Cell. Physiol.* 233, 4391–4400. doi: 10.1002/jcp.26076
- Shimomura, A., Iizuka-Kogo, A., Yamamoto, N., and Nomura, R. (2016). A lower volume culture method for obtaining a larger yield of neuron-like cells from mesenchymal stem cells. *Med. Mol. Morphol.* 49, 119–126. doi: 10.1007/s00795-015-0131-2
- Shinohara, M., Choi, H., Ibuki, M., Yabe, S. G., Okochi, H., Miyajima, A., et al. (2019). Endodermal differentiation of human induced pluripotent stem cells using simple dialysis culture system in suspension culture. *Regen. Ther.* 12, 14–19. doi: 10.1016/j.reth.2019.05.004
- Simão, V. A., Evangelista-Ribeiro, C. P., Brand, H., Lagass-Pereira, L., Marques, L. F., Benites-Aoki, P. H., et al. (2019). Metabolic and proliferation evaluation of human adipose-derived mesenchymal stromal cells (ASC) in different culture medium volumes: standardization of static culture. *Biologicals* 62, 93–101. doi: 10.1016/j.biologicals.2019.08.006
- Skaper, S. D., and Facci, L. (2018). Central Nervous System Neuron-Glia co-Culture Models and Application to Neuroprotective Agents. *Methods Mol. Biol. Clifton NJ* 1727, 63–80. doi: 10.1007/978-1-4939-7571-6_5
- Sliac, I., Blajie, V., Radoševic, K., Kniewald, Z., and Gaurina Srček, V. (2010). Influence of different ammonium, lactate and glutamine concentrations on CCO cell growth. *Cytotechnology* 62, 585–594. doi: 10.1007/s10616-010-9312-y
- Strikoudis, A., Cieślak, A., Loffredo, L., Chen, Y.-W., Patel, N., Saqi, A., et al. (2019). Modeling of fibrotic lung disease using 3D organoids derived from human pluripotent stem cells. *Cell Rep.* 27, 3709.e5–3723.e5. doi: 10.1016/j.celrep.2019.05.077
- Takasato, M., and Little, M. H. (2017). Making a kidney organoid using the directed differentiation of human pluripotent stem cells. *Methods Mol. Biol. Clifton NJ* 1597, 195–206. doi: 10.1007/978-1-4939-6949-4_14
- Takeyama, S., Yoshimura, Y., Deyama, Y., Sugawara, Y., Fukuda, H., and Matsumoto, A. (2001). Phosphate decreases osteoclastogenesis in coculture of osteoblast and bone marrow. *Biochem. Biophys. Res. Commun.* 282, 798–802. doi: 10.1006/bbrc.2001.4652
- Thomson, J. A., Itskovitz-Eldor, J., Shapiro, S. S., Waknitz, M. A., Swiergiel, J. J., Marshall, V. S., et al. (1998). Embryonic stem cell lines derived from human blastocysts. *Science* 282, 1145–1147. doi: 10.1126/science.282.5391.1145
- Valadi, H., Ekström, K., Bossios, A., Sjöstrand, M., Lee, J. J., and Lötvall, J. O. (2007). Exosome-mediated transfer of mRNAs and microRNAs is a novel mechanism of genetic exchange between cells. *Nat. Cell Biol.* 9, 654–659. doi: 10.1038/ncb1596
- van der Valk, J., Bieback, K., Buta, C., Cochrane, B., Dirks, W. G., Fu, J., et al. (2018). Fetal bovine serum (FBS): past - present - future. *ALTEX* 35, 99–118. doi: 10.14573/altex.1705101
- van Niel, G., D'Angelo, G., and Raposo, G. (2018). Shedding light on the cell biology of extracellular vesicles. *Nat. Rev. Mol. Cell Biol.* 19, 213–228. doi: 10.1038/nrm.2017.125
- Venter, C., and Niesler, C. (2018). A triple co-culture method to investigate the effect of macrophages and fibroblasts on myoblast proliferation and migration. *BioTechniques* 64, 52–58. doi: 10.2144/btn-2017-0100
- Wang, Y. I., Oleaga, C., Long, C. J., Esch, M. B., McAleer, C. W., Miller, P. G., et al. (2017). Self-contained, low-cost Body-on-a-Chip systems for drug development. *Exp. Biol. Med.* 242, 1701–1713. doi: 10.1177/1535370217694101
- Yoshimura, Y., Kikui, T., Hasegawa, T., Matsuno, M., Minamikawa, H., Deyama, Y., et al. (2017). How much medium do you use for cell culture? Medium volume influences mineralization and osteoclastogenesis in vitro. *Mol. Med. Rep.* 16, 429–434. doi: 10.3892/mmr.2017.6611
- Young, A. T., Rivera, K. R., Erb, P. D., and Daniele, M. A. (2019). Monitoring of Microphysiological systems: integrating sensors and real-time data analysis toward autonomous decision-making. *ACS Sens.* 4, 1454–1464. doi: 10.1021/acssensors.8b01549
- Zhang, C., Bakker, A. D., Klein-Nulend, J., and Bravenboer, N. (2019). Studies on osteocytes in their 3D native matrix versus 2D in vitro models. *Curr. Osteoporos. Rep.* 17, 207–216. doi: 10.1007/s11914-019-00521-1
- Zhang, C., Zhao, Z., Abdul Rahim, N. A., van Noort, D., and Yu, H. (2009). Towards a human-on-chip: culturing multiple cell types on a chip with compartmentalized microenvironments. *Lab. Chip* 9, 3185–3192. doi: 10.1039/b915147h
- Zhu, S., Ehnert, S., Rouß, M., Häussling, V., Aspera-Werz, R. H., Chen, T., et al. (2018). From the clinical problem to the basic research—co-culture models of osteoblasts and osteoclasts. *Int. J. Mol. Sci.* 19:E2284. doi: 10.3390/ijms19082284
- Zielke, H. R., Sumbilla, C. M., Sevdalian, D. A., Hawkins, R. L., and Ozand, P. T. (1980). Lactate: a major product of glutamine metabolism by human diploid fibroblasts. *J. Cell. Physiol.* 104, 433–441. doi: 10.1002/jcp.1041040316

Conflict of Interest: The authors declare that the research was conducted in the absence of any commercial or financial relationships that could be construed as a potential conflict of interest.

Copyright © 2020 Vis, Ito and Hofmann. This is an open-access article distributed under the terms of the Creative Commons Attribution License (CC BY). The use, distribution or reproduction in other forums is permitted, provided the original author(s) and the copyright owner(s) are credited and that the original publication in this journal is cited, in accordance with accepted academic practice. No use, distribution or reproduction is permitted which does not comply with these terms.



A Systematic Approach to Review of *in vitro* Methods in Brain Tumour Research (SAToRI-BTR): Development of a Preliminary Checklist for Evaluating Quality and Human Relevance

Mike Bracher¹, Geoffrey J. Pilkington², C. Oliver Hanemann³ and Karen Pilkington^{4*}

OPEN ACCESS

Edited by:

Gianni Ciofani,
Italian Institute of Technology (IIT), Italy

Reviewed by:

Nanasaheb D. Thorat,
University of Limerick, Ireland
Shuwen Zeng,
Centre National de la Recherche
Scientifique (CNRS), France

*Correspondence:

Karen Pilkington
karen.pilkington@port.ac.uk

Specialty section:

This article was submitted to
Nanobiotechnology,
a section of the journal
Frontiers in Bioengineering and
Biotechnology

Received: 27 March 2020

Accepted: 20 July 2020

Published: 07 August 2020

Citation:

Bracher M, Pilkington GJ,
Hanemann CO and Pilkington K
(2020) A Systematic Approach
to Review of *in vitro* Methods in Brain
Tumour Research (SAToRI-BTR):
Development of a Preliminary
Checklist for Evaluating Quality
and Human Relevance.
Front. Bioeng. Biotechnol. 8:936.
doi: 10.3389/fbioe.2020.00936

¹ School of Health Sciences, Faculty of Environmental and Life Sciences, University of Southampton, Southampton, United Kingdom, ² School of Pharmacy and Biomedical Sciences, University of Portsmouth, Portsmouth, United Kingdom, ³ Institute of Translational and Stratified Medicine, University of Plymouth, Plymouth, United Kingdom, ⁴ School of Health and Social Care Professions, University of Portsmouth, Portsmouth, United Kingdom

Background: A wide range of human *in vitro* methods have been developed and there is considerable interest in the potential of these studies to address questions related to clinical (human) use of drugs, and the pathobiology of tumours. This requires agreement on how to assess the strength of evidence available (i.e., quality and quantity) and the human-relevance of such studies. The SAToRI-BTR (Systematic Approach To Review of *in vitro* methods in Brain Tumour Research) project seeks to identify relevant appraisal criteria to aid planning and/or evaluation of brain tumour studies using *in vitro* methods.

Objectives: To identify criteria for evaluation of quality and human relevance of *in vitro* brain tumour studies; to assess the general acceptability of such criteria to senior scientists working within the field.

Methods: Stage one involved identification of potential criteria for evaluation of *in vitro* studies through: (1) an international survey of brain tumour researchers; (2) interviews with scientists, clinicians, regulators, and journal editors; (3) analysis of relevant reports, documents, and published studies. Through content analysis of findings, an initial list of criteria for quality appraisal of *in vitro* studies of brain tumours was developed. Stage two involved review of the criteria by an expert panel (Delphi process).

Results: Results of stage one indicated that methods for and quality of review of *in vitro* studies are highly variable, and that improved reporting standards are needed. 129 preliminary criteria were identified; duplicate and highly context-specific items were removed, resulting in 48 criteria for review by the expert (Delphi) panel. 37 criteria reached agreement, resulting in a provisional checklist for appraisal of *in vitro* studies in brain tumour research.

Conclusion: Through a systematic process of collating assessment criteria and subjecting these to expert review, SAToRI-BTR has resulted in preliminary guidance for appraisal of *in vitro* brain tumour studies. Further development of this guidance, including investigating strategies for adaptation and dissemination across different sub-fields of brain tumour research, as well as the wider *in vitro* field, is planned.

Keywords: *in vitro*, quality appraisal, evaluation, critical appraisal, brain tumour, cancer, systematic review

INTRODUCTION

There is currently a drive to review the use of animals in research for both scientific and ethical reasons. A wide range of *in vitro* methods have been developed and, increasingly, there are suggestions that these can replace the use of animals in research (NC3Rs, 2020). In order for *in vitro* studies to be considered for replacement of *in vivo* (animal) studies to answer questions related to the clinical (human) use of drugs and pathobiology of tumours, there must be agreement on the strength of evidence available (i.e., the quality and quantity of studies) as well as their relevance. Judging the strength of evidence requires that all relevant research is located, each research study is assessed for quality and, if appropriate, the results of the individual research studies are combined to give an overall ‘answer’ and/or a clear picture of the current research on the topic in question. This process can also reveal poor research practises, unreliable reporting of research and unnecessary replication and duplication (Hartung et al., 2019). Any such practises, if left undetected, would render efforts to replace animal research less likely to gain acceptance.

Methods for assessing clinical (human) studies are well-developed, led by organisations such as the international Cochrane collaboration (Higgins and Green, 2011). ‘Systematic reviews’ of the evidence are regularly published (over 140,000 systematic reviews are listed on PubMed as of March 2020). Well-conducted systematic reviews of clinical studies are widely used as the basis for clinical decisions.

A parallel development has taken place for animal studies. CAMARADES (Collaborative Approach to Meta-Analysis and Review of Animal Data from Experimental Studies) is an initiative to improve the design, conduct, analysis and reporting of animal experiments (CAMARADES, 2020). By means of ‘precise and robust’ overviews of existing data through systematic review and meta-analysis, CAMARADES aims to clearly demonstrate where further experiments are necessary, avoiding unnecessary replication. The CAMARADES initiative has generated interest and collaborative efforts on a global scale with five national coordinating centres. This is seen as crucial in efforts to reduce animal experimentation.

Reduction strategies, however, constitute only one of the Three Rs (Refinement, Reduction, and Replacement) – the underlying principles of ethical and humane use of animals in research (NC3Rs, 2020). The third principle, replacement, as described above, requires that a desired scientific goal is achieved by approaches other than those involving live animals, such as through use of *in vitro* studies. As with the CAMARADES initiative ‘precise and robust’ overviews of existing research are

essential to provide a clear picture of the research (Nuffield Council on BioEthics, 2005). However, as Hartung et al. observe, ‘[while] [m]any areas have developed reporting standards and checklists to support the adequate reporting of scientific efforts. . . *in vitro* research still has no generally accepted criteria. . . [and] such a culture may undermine trust in the reproducibility of animal-free methods’ (Hartung et al., 2019). Thus, there is a need to evaluate and develop current practises for assessing quantity and quality of *in vitro* studies of brain tumours and their potential to replace *in vivo* (animal) studies.

As Hartung et al. (2019) indicate, issues in reporting are not restricted to specific areas of interest (such as brain tumours) but encompass the broad field of *in vitro* research. Searches on a major scientific database (PubMed) reveal that while reviews have been published and described as systematic reviews of *in vitro* studies, many fail to apply key principles and processes expected of such studies. For example, one publication reported the databases searched and inclusion criteria, but not whether any quality criteria were applied (Laaksonen et al., 2010). A second ‘systematic review’ assessed each study based on two criteria defined by the authors (type of publication and whether there was a ‘comparable baseline’), and reported the lack of generally accepted evaluation criteria for *in vitro* studies (Xiao et al., 2011). A third review revised an existing tool for assessing diagnostic studies using four selected criteria (Deng et al., 2016). Few details are reported on exactly how these criteria were applied. Another study attempted to provide an overview of guidance systems with evaluation criteria for *in vitro* studies on chemical toxicity (Lynch et al., 2016). The criteria compared were from four sources [Animal Research: Reporting of *in vivo* Experiments (ARRIVE) (Kilkenny et al., 2010), Klimisch et al. (1997) on evaluating the quality of toxicological data; OECD Guidance Document on the Validation and International Acceptance of New or Updated Test Methods for Hazard Assessment (OECD, 2005); Toxicological Data Reliability Assessment Tool (ToxRTool) (Schneider et al., 2009)]. The criteria include reporting requirements, categories to be scored and items to be assessed. Few criteria were common to all 4 sources. Furthermore, while criteria for assessment of the quality of studies is crucial for unbiased, reliable reviews of the research literature, assessment of relevance of the technique or method employed is also a key element.

Both development of reporting standards for *in vitro* research (Hartung et al., 2019) as well as adoption of existing guidance (Pamies et al., 2017; Hartung et al., 2019) remain issues across the broad field of *in vitro* research. This study specifically focuses on brain tumour research, with the intention of providing a model for other areas. We have selected brain tumour as a particular area for study because although many brain tumours can be

cultured in the laboratory with relative ease, there are specific challenges in gaining accurate biological information from cells which have been removed from such a complex multicellular organ as the brain. Not only are brain tumour cells reliant on the non-neoplastic cells such as glial and immune cells for their resistance to therapeutics, but they are also reliant on the very special vasculature of the brain and indeed the blood brain barrier which protects against toxins but inhibits delivery of therapeutics. Provision of sophisticated, complex 3D models of the brain and its vasculature, including organoids, induced pluripotent stem cells and blood brain barrier elements for pre-clinical drug delivery and sensitivity are perhaps the most complex forms of all human tissue *in vitro* systems and, if we can produce best practise criteria for this area we can roll this out for many other areas of research.

The overall aim of the SAToRI-BTR project is to explore how *in vitro* studies could be presented as a body of knowledge in the form of a rigorous and comprehensive systematic review, to assess the potential for replacement of animal studies for answering specific questions in brain tumour research. SAToRI-BTR seeks to address these challenges by assessing reviews of existing studies (published systematic reviews) and identifying areas for potential improvement and investigating current practise and views on how *in vitro* studies of brain tumours should be assessed, leading to agreed criteria.

The aim of the study reported in this paper was to explore potential methods for the systematic identification, and assessment of quality and appropriate use of *in vitro* studies through a process involving identification of existing criteria

which were subject to expert review in order to develop draft criteria.

MATERIALS AND METHODS

The project to develop a set of appropriate criteria for assessment of quality and human relevance in *in vitro* studies of brain tumours was carried out in two stages. The first stage involved identification for potentially relevant criteria through collection and analysis of appropriate data (stage one), and the second stage focused on obtaining agreement on identified criteria by an expert panel by means of a Delphi process (stage two – see **Figure 1**).

The overall process followed that developed by the EQUATOR (Enhancing the QUALity and Transparency Of health Research) Network which was used for development and agreement on reporting guidelines for systematic reviews (PRISMA: Preferred Reporting Items for Systematic Reviews and Meta-Analyses) (Moher et al., 2009). This required documenting the need for a set of guidelines by reviewing previously published systematic reviews and the methods and reporting of these, reviewing existing literature to identify potential criteria. It also draws on the methods used to establish CONSORT (Consolidated Standards of Reporting Trials) (Moher, 1998) and the Cochrane collaboration's tool for assessing risk of bias in trials (Higgins et al., 2011).

Therefore, at stage two, these criteria were put to a panel (Delphi) of senior researchers, who were asked to rate their

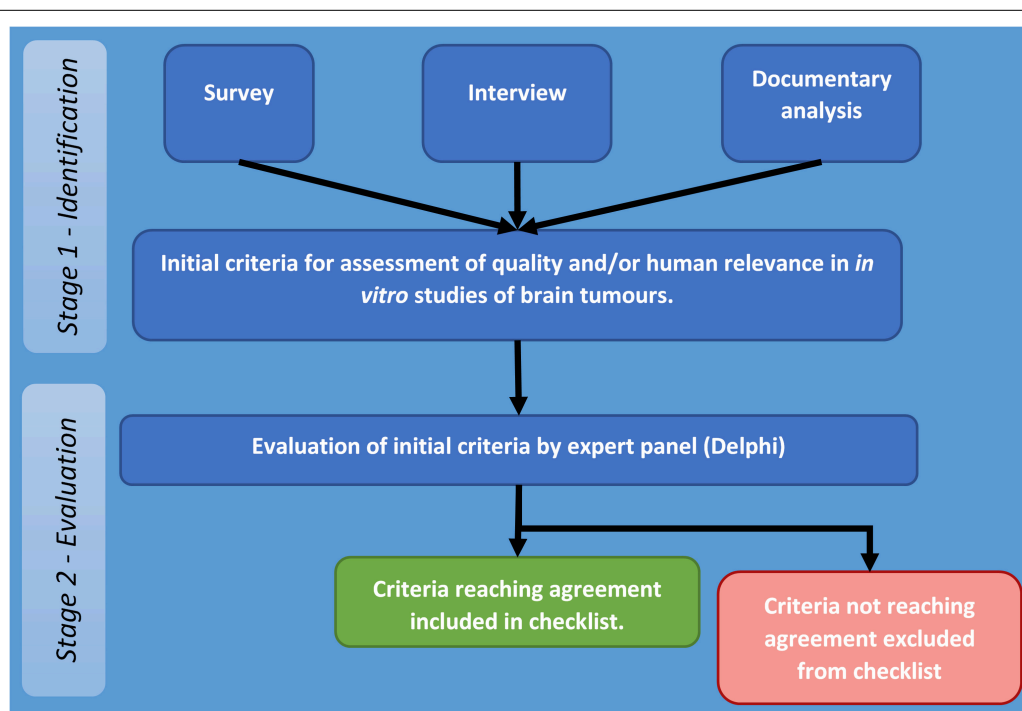


FIGURE 1 | Flow diagram of stages and procedures in identification and evaluation of criteria for assessment of quality and/or human relevance in *in vitro* studies of brain tumours.

appropriateness for assessing quality and human relevance in *in vitro* studies of brain tumours. Criteria reaching agreement form the basis of the checklist reported in this study.

Summary of the Overall Approach

- *Pre-stage (documenting the need for a set of criteria/guidelines)*
 - Search for and review of previously published systematic reviews in the field of *in vitro* cancer research.
 - Examination of all papers described as systematic reviews of *in vitro* cancer studies to assess the quality/relevance assessment tools that had been used.
- *Stage one (identifying potential criteria)*
 - Survey of senior brain tumour researchers to obtain a list of all *in vitro* techniques that are used in brain tumour research, suggested criteria, areas of agreement, relevant guidance, or quality-related initiatives.
 - Interviews with a pre-defined sample of leading and emerging researchers, journal editors, senior clinicians, funding body, and regulatory committee representatives to elicit views on how quality and relevance should be assessed.
 - Examination of peer review guidelines from major journals in the field for potential quality criteria for *in vitro* studies.
 - Identification and analysis of all documents presenting potential quality criteria.
 - Collation of the findings of the documentary analysis, and the survey and interview data.
 - Development of a draft set of criteria for assessing *in vitro* studies based on the findings of the above.
- *Stage two (gaining agreement on criteria for the guidelines)*
 - Establishment of a panel of experts in the field of brain tumour *in vitro* research.
 - Use of the Delphi method to obtain agreement on key criteria to be used for assessing *in vitro* studies.

Pre-stage

Searches were carried out using five databases for systematic reviews of *in vitro* cancer studies. All reviews that were described as a 'systematic review' and which focused solely on *in vitro* studies in any form of cancer were selected and the full-text checked for relevance. Those that met the inclusion criteria were selected and the data extracted on aspects including the focus and methods used. The full details of this review are to be published as a separate paper.

Stage One

Quality Criteria in Previously Published Systematic Reviews

All relevant systematic reviews identified in the pre-stage review were selected and the full-text checked for mention of, or reference to, quality criteria, a checklist for quality, or guidance used to judge quality and/or human relevance of included studies.

Survey of Brain Tumour Researchers

An online survey was conducted to investigate current areas of research interest/focus related to *in vitro* research; *in vitro* models and study methods used within these areas; methods for assessing quality and relevance in these areas and knowledge of any published guidelines, checklists or quality initiatives.

Questions were developed by the authors with a draft version piloted followed by further revisions before the survey was finalised. The survey was completed online, using the University of Portsmouth's online survey platform provider (Online Surveys.ac.uk) and was completed anonymously. A copy of the full set of questions in the questionnaire is available from the authors on request.

Potential participants were identified from conference abstracts for oral and poster presentations from international conferences and scientific meetings. See **Table 1** for a list of sources used to identify potential participants. Once identified, further information was sought on participants from publicly available sources such as departmental, ResearchGate, and Google Scholar web pages. Those meeting inclusion criteria and for whom contact details could be found were approached for participation. Inclusion criteria were:

- Scientist working on studies of brain tumours using *in vitro* methods.
- Evidence of further publication history within brain tumour field using *in vitro* methods beyond conference abstract through which initially identified.

Potential participants were approached through published email addresses obtained from conference abstracts, departmental or professional web pages, or other publications. Design of invitations was informed by Fan and Yan's (2010) recommendations drawn from a systematic review of factors affecting response rates in web surveys. Email invitations used a personalised salutation, identified survey tasks and salience, described how recipients were identified as potential participants, provided estimation of the time to finish the survey and gave contact details for further questions and assistance (Fan and Yan, 2010).

While no specific methodological guidance was available for conducting surveys of pre-clinical scientists, this target population was hypothesised to share many of the characteristics likely to affect participation which have been identified in previous studies with senior managers in other kinds of organisation. These include increased sensitivity to personalised responses, declining time capacity for participation due to increasing pressures from their core roles (Cycyota and Harrison, 2006), and an increasingly saturated information environment (e.g., email and social media) in which there are high levels of competition for feedback (and thus participant time). The potential vulnerability of the survey to low response in spite of efforts to implement best practise guidance formed part of the rationale for using multiple sources of data (i.e., survey, interviews, and documentary analysis) to inform the Delphi process, in order to make the project overall more resilient to the limitations of any single data collection stream.

TABLE 1 | Identification of potential participants by source.

Meeting/source	Abstracts screened (n)	Abstracts indicating <i>in vitro</i> research (n)	Potential participants excluded* (n)	Potential participants approached (n)
World Federation of Neuro-oncology Societies (WFNOS) 2017 Meeting (WFNOS, 2017a,b)	481	165	65	100
Society for Neuro-oncology (SNO) 2017 Annual Meeting (SNO, 2017a,b)	1248	224	56	168
European Association of Neuro-Oncology 13th Meeting (2018) (EANO, 2018)	446	157	61	96
British Neuro-Oncology Society (BNOS) 2017 Meeting (BNOS, 2018)	119	14	3	11
Asian Society for Neuro-Oncology (ASNO) 14th Meeting (2017) (ASNO, 2017)	240	52	27	25
Sub-Saharan Africa Neuro-Oncology Collaborative (S-SANOC) 2017 Planning Meeting (S-SANOC, 2017)	25	17	14	3
Additional (potential participants identified through other sources, e.g., team members or other neuro-oncologists)				33
Totals	2559	629	193	436

*Not *in vitro* specialist OR not neuro-oncology specialist OR no contact information available.

Interviews With Key Individuals From the *in vitro* Field

Semi-structured interviews used widely to explore in-depth contextual factors affecting practise change (e.g., regulatory, funding, and variations in clinical or scientific practise) (Carlsen et al., 2007; Gardner and Webster, 2016; Colquhoun et al., 2017). A purposive sampling frame was constructed to reflect the different roles relevant to *in vitro* research. These included scientists, clinicians, regulators, and journal editors involved with studies using *in vitro* methods (including those working in fields other than brain tumour research, e.g., other neurological disease, other forms of cancer). Participants were identified through publications, professional and regulatory activities, and via the project team. An interview guide was developed and piloted with focus on the potential helpfulness and scope of set criteria, likely extent of agreement on assessment of *in vitro* research and the specific challenges in getting guidelines widely accepted.

The interviews aimed to explore:

- Professional opinion and practise in evaluation of quality and human relevance of *in vitro* models for brain tumour research, and identify points of agreement and disagreement.
- Current practises, opinions, and resources for identifying *in vitro* studies for review in brain tumour research.
- Factors that may promote or inhibit introduction of new practises for assessment of quality and human relevance in brain tumour research.

Interviews were carried out by phone after confirming consent with the participant. All interviews were guided by a set of core questions developed through pilot interviews, with follow up questions and exploration taking place where appropriate (and depending on the expertise and interest of respective participants). The semi-structured nature of interviews therefore meant that there was some variation in the length of

interviews, number of questions asked, and in development of the interview schedule as the study progressed. Interviews were recorded and transcribed for directed content analysis in Nvivo (v12) Computer-assisted Qualitative Data Analysis Software (CAQDAS) (QSR International, 2018). Nvivo allows users to attach labels (or ‘codes’) to text, audio, video or image data, and facilitates data management through which directed content analysis can be conducted by a competent user. This involved reading across interview transcripts to identify responses relevant to the above aims (Corbin and Strauss, 2014).

Exploration of Author and Peer-Reviewer Guidance Provided by Journals

A set of relevant journals was identified using the following techniques:

- The 50 journals appearing most frequently in the results of searching the Medline database using the index term “*In vitro* Techniques+”.
- The 50 journals appearing most frequently using the search “*In vitro* Techniques+” AND “Neoplasms+” (both as index terms).
- The top 20 ranked journals from both the ‘Oncology’ and ‘Cancer Research’ categories of the Scimago Scientific Journal Rankings.

Resulting journals were combined into a single list, which after duplicate removal resulted in a set of unique journals for assessment of author and peer-review guidance. Assessment was conducted through manual exploration of journal websites, to identify publicly available information on author and peer-review guidance pertaining to quality assessment of *in vitro* methods.

Identification of Relevant Documents

Relevant documents including guidelines on the conduct and reporting of *in vitro* research, published standards were identified through the following methods:

- Previous review of published systematic reviews.
- 101 journal websites searched for general guidance on *in vitro*-relevant study reporting, and quality appraisal for specific techniques.
- Feedback from survey and interview responses.
- Searches of reporting guidance databases [e.g., US National Institutes of Health (NIH), EQUATOR Network FAIRSharing.org (2020)], the PubMed database and a commercial social networking site for scientists and researchers (ResearchGate).

All documents were loaded into NVivo software for directed content analysis.

Analysis

Survey

Descriptive statistical analysis was performed on quantitative data, and responses to free-text questions were analysed using a content analysis approach, where data are grouped into categories (e.g., cell line authentication and replication) for reporting (Krippendorff, 2018). For this aspect of the SAToRI-BTR project, data on quality and relevance criteria that are used in practice (e.g., when peer reviewing) and any quality initiatives or guidelines were extracted.

Interviews

Full interview transcripts were uploaded to Nvivo and directed content analysis of data was performed using Nvivo. Through this process, any data on quality and relevance criteria used in practice, and any quality initiatives or guidelines were identified and collated in order to inform stage two.

Documents

Directed content analysis was also performed on documents using Nvivo software.

Collation and Compilation of List of Proposed Criteria

A full list of all criteria was generated and a comparison of the criteria from documentary analysis compared with those from the survey and interviews. Any additional criteria generated from the latter were added to the list. The initial list was then further reviewed for duplicate criteria (i.e., those assessing the same or similar aspects but which were phrased in different terms which could be merged), ensuring that those criteria highlighted in several sources were retained and those that related only to a specialised technique were removed. The outcome of stage one was identification of a range of criteria for assessment of quality and/or human relevance in *in vitro* studies of brain tumours, which were organised in a taxonomy by area of focus.

Stage Two

Having identified potential assessment criteria for *in vitro* studies of brain tumours at stage one through international survey, telephone interview, and documentary analysis, stage

two involved evaluation of appropriateness of these criteria for assessment of brain tumour studies by a panel of senior scientists. The expert agreement panel (or 'Delphi') process has been used extensively in clinical and health services research to develop reporting guidance and quality assessment criteria for a range of scientific and clinical applications (Fitch et al., 2001; Boukdedid et al., 2011). Delphi allows participants to rate criteria anonymously (i.e., without knowledge of the composition of the panel, or identities of members), and to provide written feedback on them. The process occurs across multiple rounds, between which comments from all participants are also circulated so each participant is aware of the range of opinions and the reasons underlying these. Criteria reaching agreement are removed, additional criteria may be added, or existing criteria amended if they have not reached agreement (e.g., in response to suggestions from the panel). The process is anonymous and usually three rounds of the survey are sufficient to achieve reasonable agreement (Fitch et al., 2001; Hsu Chia and Brian, 2007; Boukdedid et al., 2011).

Delphi has been used both as a standalone technique to reach agreement on reporting and assessment criteria, and also as a sorting procedure to identify criteria of ongoing controversy requiring further discussion by a subsequent panel of experts (Boukdedid et al., 2011). As the aim of SAToRI-BTR is to identify agreed criteria, this method was assessed as appropriate for either outcome in terms of wider development of the project in the future.

Identification and Approach of Participants

Professors, heads of laboratories, and principal investigators who had been previously identified at either the survey or interview stages were invited to participate via personalised email and physical letter as described at the survey stage. Following indications of willingness to participate, participants were sent a link to complete the online consent form, after which they were invited to participate in the first round of the Delphi panel.

Development of Initial Criteria

Criteria identified at stage one were evaluated by expert members of the SAToRI-BTR Team and results grouped into categories for assessment by the panel.

Rating and Progression Between Rounds

Participants rated criteria on an 9-point scale: 1 (not at all relevant) to 9 (essential) to assessment of a brain tumour study'. They were invited to leave qualitative comments (e.g., on context of application, clarity of criterion etc.) (Boukdedid et al., 2011) and to suggest additional criteria for each category (see **Figure 2**).

Criteria were judged to have reached agreement according to the RAND/UCLA agreement criteria (Fitch et al., 2001, p. 58). Criteria reaching agreement were removed between rounds, additional criteria added (if suggested by participants), and existing criteria not reaching agreement changed in line with participant feedback or (in its absence) passed to the next round unchanged.

Compliance with Good Laboratory Practice (GLP)

Please don't select more than 1 answer(s) per row.

	1	2	3	4	5	6	7	8	9	
Not at all relevant to assessment of an <i>in vitro</i> brain tumour study.	<input type="checkbox"/>	<input type="checkbox"/>	<input type="checkbox"/>	<input type="checkbox"/>	<input type="checkbox"/>	<input type="checkbox"/>	<input type="checkbox"/>	<input type="checkbox"/>	<input type="checkbox"/>	Essential to assessment of an <i>in vitro</i> brain tumour study

Do you have any comments on the above criterion?

FIGURE 2 | Example of Delphi rating scale and written feedback facility.

The final outcome of stage two was a set of criteria around which agreement was obtained on their importance for the assessment of quality and relevance.

Ethical Approval

Ethical approval for the survey, interviews, and Delphi processes was granted by the University of Portsmouth Faculty of Science Ethics Committee, reference number SFEC 2018-073 (original application plus amendments).

RESULTS

Pre-stage (Review of Published Systematic Reviews of *in vitro* Studies)

The review of published systematic reviews of *in vitro* studies indicated that few were available. Not all those described as systematic applied systematic approaches to the literature. Analysis of the methods used in the reviews confirmed that there was not a widely used set of criteria for assessing quality and/or relevance of *in vitro* studies. Those that did conduct a systematic appraisal of the included studies, adapted a wide range of existing appraisal checklists. A lack of agreed criteria specific to *in vitro* studies was highlighted.

Stage One

Survey of *in vitro* Brain Tumour Researchers

A total of 436 researchers were contacted and invited to complete the online questionnaire (see **Figure 3**). Of those invited, 7.8% (34 participants) completed the survey. Sixteen were from the United States, 12 from Europe, five from the United Kingdom and one from South America. A total of 10 different countries were represented. 30 (88%) participants identified as either 'Professor/Department Head' or 'Research

Team Lead.' Mean years' experience in brain tumour research 17.6 ($SD = 10.1$, range = 3–40). 28 participants (85%) also use *in vivo* techniques. The participants recommended a range of potential quality criteria.

Interviews

Thirty-four potential participants approached via email and letter, of which 13 participants completed the interview (see **Figure 4**). The participants included/represented: professors/head of laboratories, consultant clinicians, industry, those leading quality and human relevance initiatives, regulators and journal editors. Telephone interviews totaled 414 min, with an average length of 34.46 min (range = 17–58 min, $SD = 12.92$ min).

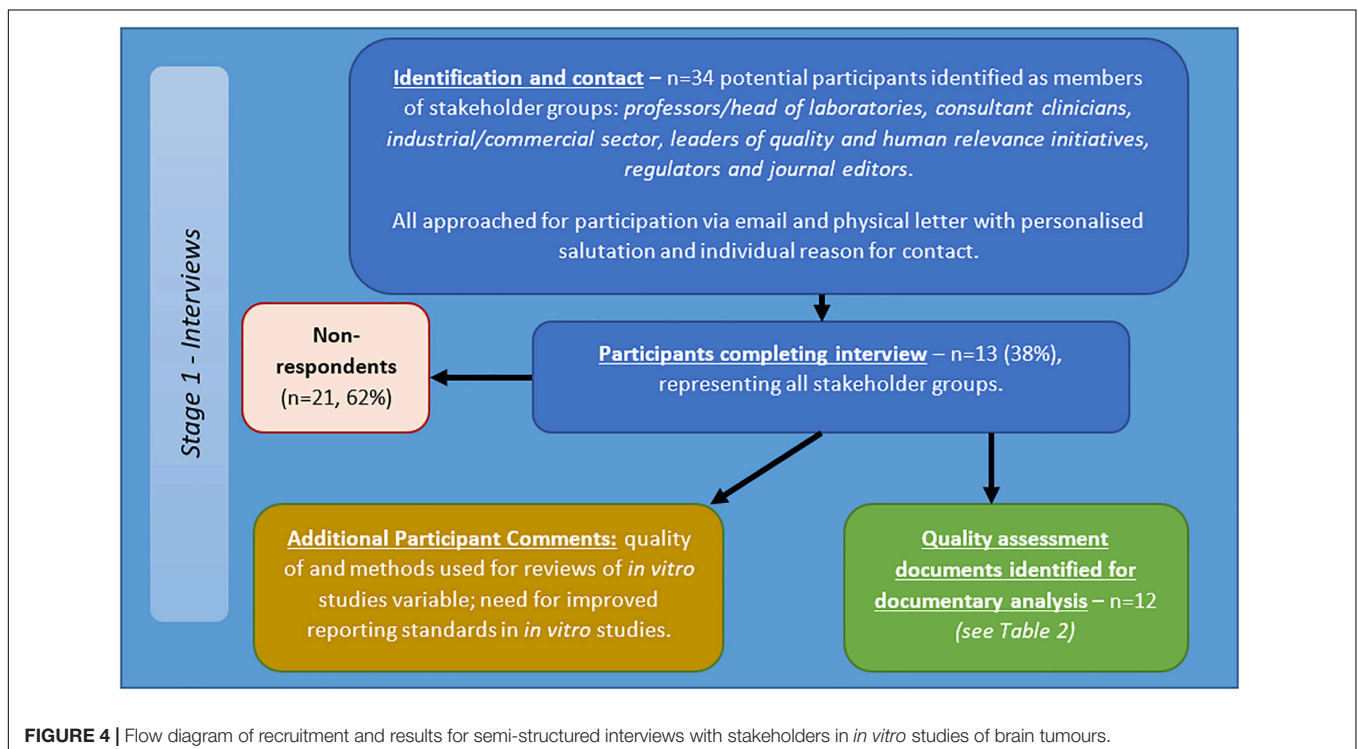
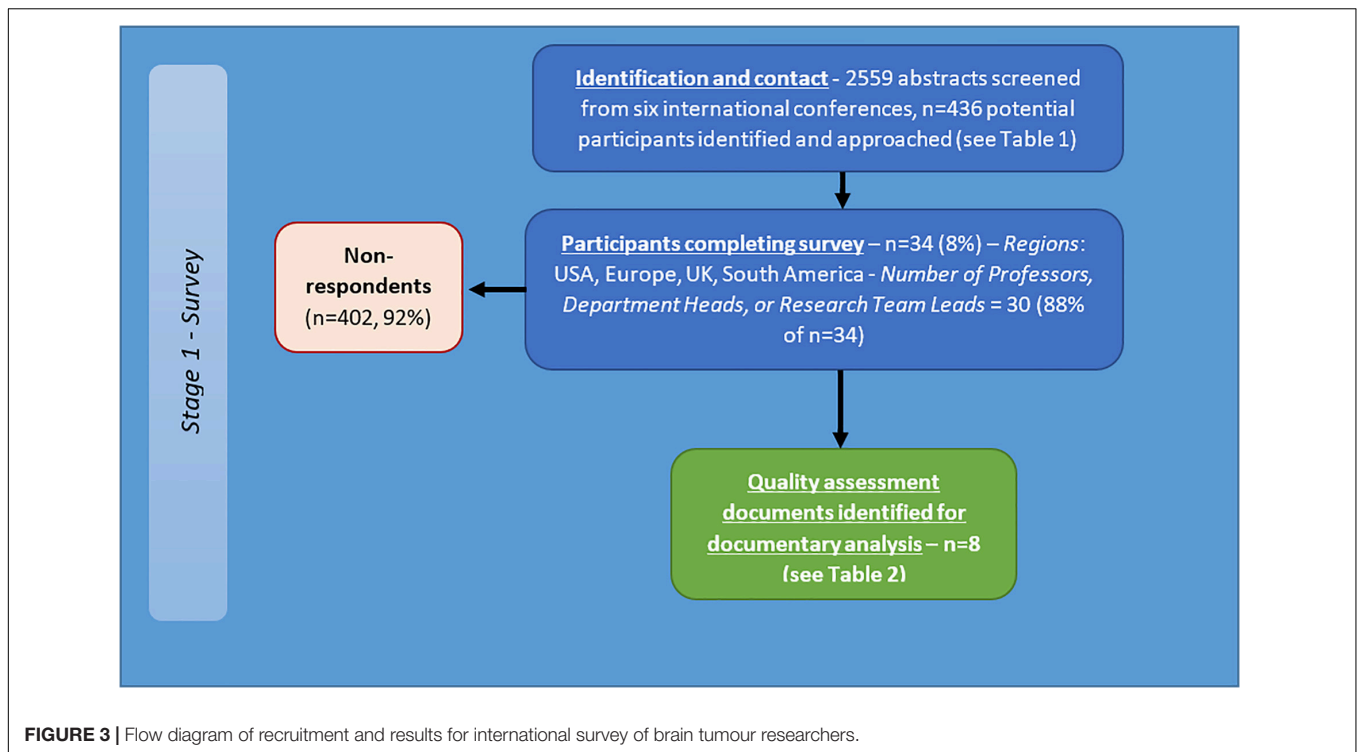
Responses indicated:

- Methods for reviews of *in vitro* studies are highly variable;
- Quality of reviews of *in vitro* studies varies;
- Need for improved reporting standards.

Participants described a number of relevant quality assurance documents and reporting standards. Views were also expressed on the involvement of clinicians and regulators in development and barriers to adoption of any suggested guidelines or quality initiatives. More detailed results are to be reported in subsequent published works.

Exploration of Author and Peer-Reviewer Guidance Provided by Journals

Of the 101 unique journal titles identified, 6 journals had been discontinued or renamed, 2 were book series and 1 journal was inaccessible. Identifying and including the replacement titles for the renamed journals resulted in a total of 96 journals currently in print and accessible which could be assessed. Fifty-eight (60%) journals did provide some guidance specific to or



relevant to *in vitro* techniques. Thirty-eight (40%) did not appear to provide any guidance accessible on the website that was specific to *in vitro* research. Established guidelines were reported by 25 journals (26%). These guidelines included those on specific techniques which could be, but are not exclusively, applied

in *in vitro* research, such as MIAME (Minimum Information About a Microarray Experiment) and STREND (Standards for Reporting Enzymology Data). Generic guidelines were also cited such as the National Institute for Health (NIH) Principles and Guidelines for Reporting Preclinical Research. Cell line

TABLE 2 | Quality assessment documents identified for analysis including sources.

Documents	Survey	Interviews	Searches of journal criteria and assessment databases
Tools for methodological quality and risk of bias (Al Saadi et al., 2016)			Y
Cell culture techniques [edited collection] (Aschner et al., 2011)			Y
Minimum information about a microarray experiment (MIAME)—toward standards for microarray data (Brazma et al., 2001)			Y
STAR methods guide (CELL Press, 2020)	Y		Y
Six checklists relating to <i>in vitro</i> models for different organs/systems [COMMERCIAL ENTERPRISE]*		Y	
Quality of reporting in systematic reviews – meta-analyses of <i>in vitro</i> studies – a systematic review protocol (Elshafay et al., 2019)			Y
Good cell culture practises and <i>in vitro</i> toxicology (Eskes et al., 2017)			Y
EU-NETVAL meeting 10–11th October 2016 (EU-NETVAL, 2016)		Y	
EU-NETVAL meeting 26th–27th November 2015 (EU-NETVAL, 2015)		Y	
GOOD <i>IN VITRO</i> METHOD PRACTISES (GIVIMP) (OECD, 2018)		Y	
EURL ECVAM workshop – inaugural meeting of EU-NETVAL members – 26–27 June 2014 (EURL ECVAM, 2014)		Y	
Guidelines for the use of cell lines in biomedical research (Geraghty et al., 2014)			Y
Perspectives on <i>in vitro</i> to <i>in vivo</i> extrapolations (Hartung, 2018)		Y	
Hartung et al. (2002) good cell culture practise ECVAM good cell culture practise task force report 1 (Hartung et al., 2002)		Y	
Definitions relating to cell line authentication (ICLAC, 2019b)	Y	Y	Y
Cell line checklist for manuscripts and grant applications (ICLAC, 2019a)	Y	Y	Y
Better reporting for better research: a checklist for reproducibility (Kenall et al., 2015)	Y	Y	Y
UKCCCR guidelines for the use of cell lines in cancer research (UKCCCR, 2000)			Y
Reporting recommendations for tumour marker prognostic studies (REMARK) (McShane et al., 2005; Altman et al., 2012)	Y	Y	Y
Enhancing reproducibility through rigour and transparency (NOT-OD-15-103) (NIH-OER, 2015)	Y		Y
Guidelines for research involving recombinant or synthetic nucleic acid molecules (NIH, 2019)	Y		Y
Principles and guidelines for reporting preclinical research (NIH, 2017)	Y		Y
Advisory document of the working group on good laboratory practise the application of the principles of GLP to <i>in vitro</i> studies (OECD, 2004)		Y	
Good cell culture practise for stem cells and stem-cell-derived models (Pamies et al., 2017)			Y
Extending a risk-of-bias approach to address <i>in vitro</i> studies – a systematic review protocol (Rooney, 2015)			Y
<i>In vitro</i> acute and developmental neurotoxicity screening – an overview of cellular platforms and high-throughput technical possibilities (Schmidt et al., 2017)			Y
Promoting coherent minimum reporting guidelines for biological and biomedical investigations – the MIBBI project (Taylor et al., 2008)			Y

*Documents marked [COMMERCIAL ENTERPRISE] were provided on condition of confidentiality of content.

authentication was referred to by 22 journals and related guidance that was cited included the UKCCCR Guidelines for the Use of Cell Lines in Cancer Research. A full list of the guidance that was located through review of the journal websites is included in **Table 2**.

For all journals still in publication and with an impact factor for 2018 ($n = 95$), the median impact factor (IF) was 4.9 (range = 0.6–223.7, IQR = 5.6). Of these: for journals citing established criteria ($n = 25$) the median was 5.2 (range = 1.9–59.1, IQR = 3.5); for journals giving general guidance ($n = 48$) the median was 4.9 (range = 1.9–41.1, IQR = 3.5); while for journals giving no specific guidance ($n = 37$) the median was 4.5 (range = 0.6–223.7, IQR = 6.7).

The analysis of author and peer-review guidance provided further evidence to support the observation of a lack of common, comprehensive, quality assessment criteria for *in vitro* studies,

by showing significant variation in the quantity and types of guidance provided by journals.

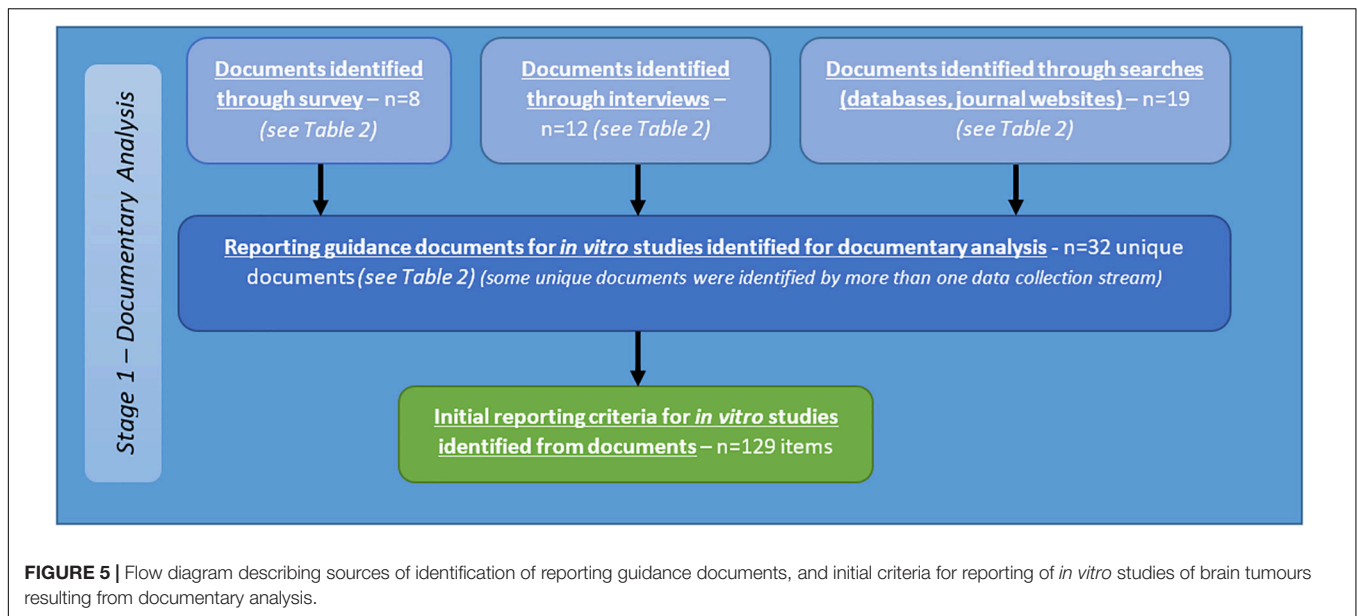
Documentary Analysis

A total of 32 documents were identified from the above sources (see **Table 2**). Criteria identified from analysis of these documents are reported below as part of the summary of all criteria identified from stage one (see **Figure 5**).

Stage Two

Compilation of Preliminary Criteria

Following completion of the survey, interview, and documentary analysis stages, potential criteria were collated using Nvivo software, through which a long list of 129 preliminary items were identified (see **Figure 6**). Duplicate and highly context



specific items were removed. Forty-one criteria were selected for assessment by expert panel (Delphi) (see **Table 3**).

Expert Panel

Of the 38 professors, heads of laboratories, and principal investigators invited to participate by personalised email and letter, 22 agreed to participate initially. 19 participants completed round one and 18 completed round two (see **Figure 6**). For a comparison of those participating in the expert panel compared with those taking part in the survey and interviews, see **Table 4**.

Delphi Assessment

Of the initial 41 criteria, agreement was achieved in round one on 28 with no agreement on 13. Seven further criteria were suggested.

For round two, based on feedback from participants, four of the 13 criteria were merged with existing criteria, nine were re-presented to Delphi group (with or without rephrasing) and the seven new criteria identified by participants were also presented to the panel. Thus, a total of 16 criteria were assessed in round two and a total of 48 criteria across the two rounds.

In round two agreement was achieved on nine (including three new criteria). No agreement was apparent on seven criteria (including four new criteria). Although the level of agreement across the two rounds of Delphi completed was high, for the remaining seven criteria, the level of agreement, even when criteria were rephrased reduced and the feedback from participants indicated that achieving agreement on these was unlikely to be feasible.

The large amount of qualitative data to analyse (comments, explanations etc.) collected should further inform the application of the criteria in practise. Further specification of criteria needs discussion and, thus, it was decided that the next stage would require an in-person meeting and discussion. A summary of the process is shown in **Table 4**, and in **Figure 6**.

DISCUSSION

This study represents a first attempt to use a systematic approach to generating a set of criteria for assessing the quality and relevance of *in vitro* brain tumour research studies. In designing the process, the aim was to combine a systematic analysis of existing guidance and practise with the implicit views of those with expertise in *in vitro* brain tumour research. By attempting to engage those involved in research in this field at an early stage and throughout the process, it was anticipated that the uptake of any resulting guidance would be optimised. It was also anticipated that focusing the study in a specific area (brain tumour research) would also increase the relevance and hence engagement with the process.

There have been a number of initiatives aimed at improving and standardising the quality and reporting of *in vitro* research, some of which are ongoing (Eskes et al., 2017; Pamies et al., 2017; OECD, 2018; Hartung et al., 2019). Full and transparent reporting is of importance as it enables the evaluation and reproduction by other researchers and thus optimises the resources that have been expended. While various initiatives have been undertaken, adoption by researchers working in the field has been low (Pamies et al., 2017). The participants taking part in the survey and interviews conducted in this study were aware of some of these initiatives but there was not universal or consistent reference to any particular set of guidance.

The intention of screening a large number of abstracts from a series of relevant recent conferences was to ensure that a large number of researchers were involved in the survey (and thus the guideline production process). Over 2,500 abstracts were screened resulting in over 400 individual senior researchers being identified but the response rate was extremely low. There may be several explanations for this: lack of perceived relevance or concern about the ultimate aim of any guidance

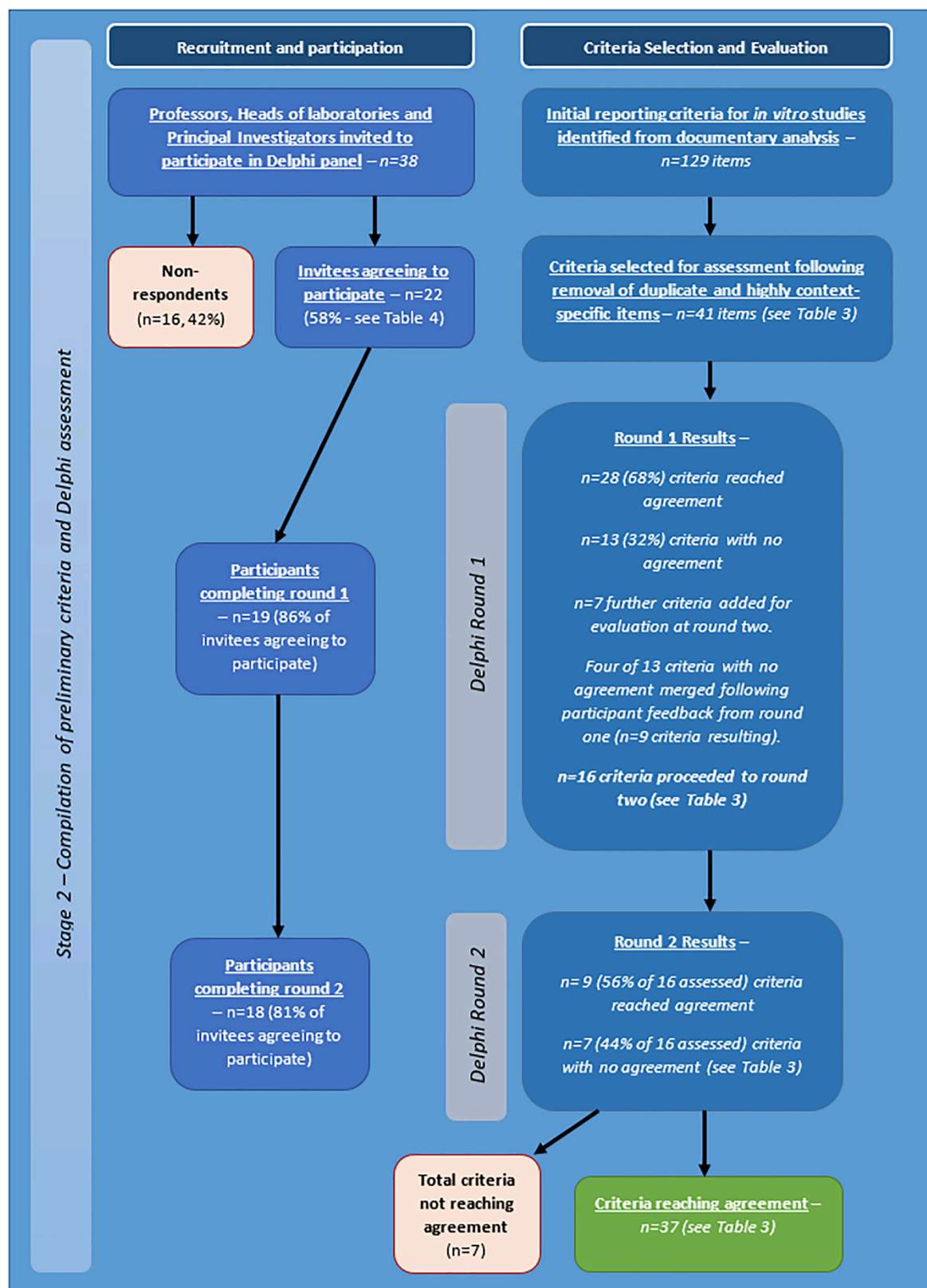


FIGURE 6 | Flow diagram describing Delphi process and outcomes.

TABLE 3 | Summary of Delphi process (italics: no agreement).

Category	Criteria Delphi round 1	Agreement (n = 19)	Median	Criteria Delphi round 2	Agreement (n = 18)	Median	Criteria reaching agreement
General	<i>Ethical approval</i>	<i>N</i>	5	<i>Changed to: Ethical approval for cells from human donors</i>	<i>N</i>	8	–
Initial set-up and processes	Compliance with Good Laboratory Practise (GLP)	Y+	9		–		Compliance with Good Laboratory Practise (GLP)
	Transportation conditions for tissues/cells	Y+	9		–		Transportation conditions for tissues/cells
	<i>Quarantine process for new cells</i>	<i>N</i>	8	Changed to: Quarantine process in place for cells introduced from other laboratories	Y+	9	Quarantine process in place for cells introduced from other laboratories
	Testing for micro-organisms	Y+	9		–		Testing for micro-organisms
	Cell authentication	Y+	9		–		Cell authentication
	Method of primary culture establishment	Y+	9		–		Method of primary culture establishment
	<i>Cell detachment and disaggregation methods</i>	<i>N</i>	7	Unchanged	Y+	7	Cell detachment and disaggregation methods
Cells	<i>Take rate of primary culture establishment</i>	<i>N</i>	6.5	<i>Changed to: Success rate for establishing primary culture</i>	<i>N</i>	8	–
	Sources of reagents	Y+	9		–		Sources of reagents
	Consistent use of reagents	Y+	9		–		Consistent use of reagents
	Origin or source of cells (whether tissue, biopsy-derived early passage or cell lines)	Y+	9		–		Origin or source of cells (whether tissue, biopsy-derived early passage or cell lines)
	Cell authenticity	Y+	9		–		Cell authenticity
	<i>Genomic stability</i>	<i>N</i>	7	Changed to: Researcher awareness of genomic instability	Y+	9	Researcher awareness of genomic instability
	Passage number (reduced heterogeneity and acquired resistance)	Y+	9				Passage number (reduced heterogeneity and acquired resistance)
Models	Cell characterisation (morphology, differentiation and antigenicity)	Y+	9				Cell characterisation (morphology, differentiation and antigenicity)
	<i>Population doubling times</i>	<i>N</i>	8	Unchanged	Y+	7	Population doubling times
	Cell viability testing	Y+	8		–		Cell viability testing
	Cryopreservation process/method	Y+	9		–		Cryopreservation process/method
	Patient-derived (human)	Y+	9		–		Patient-derived (human)
	Cellular heterogeneity	Y+	8		–		Cellular heterogeneity
	Culture conditions 1 (HEPES or CO ₂ incubation)	Y+	9		–		Culture conditions 1 (HEPES or CO ₂ incubation)
	Culture conditions 2 (temperature, oxygen, pH, and humidity)	Y+	9		–		Culture conditions 2 (temperature, oxygen, pH, and humidity)
	Serum supplementation (human, FCS/NCS or serum-free)	Y+	9		–		Serum supplementation (human, FCS/NCS, or serum-free)

(Continued)

TABLE 3 | Continued

Category	Criteria Delphi round 1	Agreement (n = 19)	Median	Criteria Delphi round 2	Agreement (n = 18)	Median	Criteria reaching agreement
	Complexity of the model (3D versus 2D)	Y+	9		–		Complexity of the model (3D versus 2D)
	<i>Vascular flow</i>	N	5	Merged *	–		–
	<i>Use of antimycotics and/or antibiotics</i>	N	7	Changed to: If used, effect of antimycotics and/or antibiotics on cell growth	Y+	7	If used, effect of antimycotics and/or antibiotics on cell growth
	<i>Tumour microenvironment (e.g., immune cells and non-neoplastic glial cells)</i>	N	8	Unchanged	N	9	–
	<i>Representation in the model of the physiology of intended patients</i>	N	7	Merged *	–		–
Assays	<i>Multimodality assays</i>	N	7	Changed to: Validation of results using multiple methods	Y+	7.5	Validation of results using multiple methods
Interpretation by authors	Functional assays (biological behaviour)	Y+	8		–		Functional assays (biological behaviour)
	Replicated assays	Y+	9		–		Replicated assays
	Appropriate controls	Y+	9		–		Appropriate controls
	<i>Therapeutic testing</i>	N	7	Merged **	–		–
	<i>Blood brain barrier</i>	N	6	Merged *	–		–
	Reproducibility of results (within-laboratory)	Y+	9		–		Reproducibility of results (within-laboratory)
	Reproducibility of results (between laboratory transferability)	Y+	8		–		Reproducibility of results (between laboratory transferability)
	Definition of the human relevance of the <i>in vitro</i> model	Y+	8		–		Definition of the human relevance of the <i>in vitro</i> model
	Demonstration of the relationship of the model to the target tissue or organ	Y+	9		–		Demonstration of the relationship of the model to the target tissue or organ
	Discussion of the limitations of the method	Y+	9		–		Discussion of the limitations of the method
Additional criteria proposed by Delphi panel members	Discussion of the limitations of the model	Y+	9		–		Discussion of the limitations of the model
		–	–	Reporting of Standard Operating Procedures (SOPs) to aid replication	Y+	9	Reporting of Standard Operating Procedures (SOPs) to aid replication
		–	–	Pathology/patient data reported or accessible	Y+	9	Pathology/patient data reported or accessible
		–	–	<i>Sampling of different regions of heterogeneous tumour</i>	N	7	–
		–	–	<i>Time interval between collecting biopsy tissue and setting up primary culture</i>	N	9	–

(Continued)

TABLE 3 | Continued

Category	Criteria Delphi round 1	Agreement (n = 19)	Median	Criteria Delphi round 2	Agreement (n = 18)	Median	Criteria reaching agreement
		–	–	Substrate on which cells are cultured	Y+	8.5	Substrate on which cells are cultured
		–	–	Assessment of imaging method used	N	7	–
		–	–	Appropriate use of bioinformatics and/or mathematical modelling	N	7	–

* Criterium merged with Demonstration of the relationship of the model to the target tissue or organ (Criteria Delphi round 1). ** Criterium merged with Multimodality assays (Criteria Delphi round 1).

TABLE 4 | Comparison of participants in survey, interviews and Delphi.

Country	Surveys	Interviews	Delphi	Minimum number of individuals participating in at least one stage	
				Brain tumour <i>in vitro</i> researchers	All participants
Belgium	1		1	1	1
Brazil	1			1	1
Germany	4	1	2	4	5
Ireland		1	2	2	2
Italy	1		1	1	1
Luxembourg	1			1	1
Netherlands	3			3	3
Norway	1		2	2	2
Poland			1	1	1
Slovenia			1	1	1
Sweden	1			1	1
United Kingdom	5	11	7	7	15
United States	16		2	16	16
Total	34	13	19	41	50

may have discouraged participation. Other practical problems such as contact emails being filtered out by organisational email servers may also have had an impact. Additionally, the field of brain tumour research has, historically, been poorly funded (House of Commons Petitions Committee [HCPC], 2016) so that researchers are likely to be focused on core issues including grant income and job security and we anticipated that they may be less inclined to become involved in research that appears more peripheral to these aspects. Because of this, we chose a study design (as summarised in **Figure 1**) which drew on multiple data collection streams to inform the criteria for Delphi assessment (survey, interview, and documentary analysis). This was to ensure that the study design was resistant to risks associated with low response rates to survey or interviews. Nevertheless, more than 30 heads of laboratories/professors from 10 different countries did participate and, overall 40 *in vitro* brain tumour experts from 13 countries contributed to at least one stage of the process. This is a significant number in a

relatively small field and these people represent experienced, senior authorities within the field. Furthermore, there was consistency in the criteria suggested in the survey, interview, and documents.

There was also consistency and a high level of agreement on the importance of each of the criteria proposed. The final outcome of the process reported in this paper is a set of 37 criteria which reached agreement as essential to consider when assessing the quality and/or human relevance of an *in vitro* study. The focus was on *in vitro* research in the brain tumour field but the majority of the criteria generated are generic and could be applied to other *in vitro* research areas, particularly those in the field of cancer.

The data collected included individual comments and feedback on each of the criteria and revealed areas where there are differences in opinions and practise which would benefit from further investigation. It will be necessary to further specify how each of the 'criteria' could best be applied in

practise as, in some cases, this is implicit and/or context-specific rather than explicit and/or universal. Thus, criteria refer to specific aspects of an *in vitro* study that should be assessed and not whether simply reporting this would constitute good practise or whether it is also necessary that the study meets a particular standard related to this aspect. For example, there was agreement on the importance of assessing ‘cellular heterogeneity’ but no specific standard of reporting or conduct is currently attached to this. The data collected will inform the next stage of the process which is to develop more detailed guidance on the application of the criteria in practise. This may require an in person meeting as is generally required for finalising guidance such as this (EQUATOR Network, 2020). Ultimately, the set of guidance generated could be disseminated and used by journals, grant awarding bodies, and peer reviewers. As has been proposed, producing and disseminating a set of agreed criteria for the assessment of *in vitro* studies will further support ‘Meaningful contributions to the body of science’ as they can be evaluated and reproduced by other researchers in the field and are more accessible to those in related fields previously (Hartung et al., 2019).

CONCLUSION

The SAToRI-BTR project drew on a range of well-established methods for identification and appraisal of current practise standards. Through a rigorous, systematic process of expert review, the project has resulted in a set of preliminary criteria for use in assessment of quality and human relevance of *in vitro* brain tumour studies. Further development of these criteria, including potential strategies for adaptation and dissemination across different sub-fields of brain tumour research, will follow. While the focus of the study remains in the brain tumour field, the initial criteria identified and the methods through which they were developed remain applicable to a broader range of fields relating to *in vitro* research. It is therefore hoped that this investigation will prove useful empirically and methodologically, both within and beyond the specific focus of brain tumour studies.

REFERENCES

- Al Saadi, T., Fala, S., Hassan Akl, H. A., El-badawy, M., Ghanem, M., Shamandy, B., et al. (2016). *Tools For Methodological Quality And Risk Of Bias Assessment For In-Vitro Studies: A Systematic Review Protocol*. Available online at: https://www.researchgate.net/institution/Vo_Truong_Toan_University/department/Faculty_of_Medicine/stats (accessed February 1, 2020).
- Altman, D. G., McShane, L. M., Sauerbrei, W., and Taube, S. E. (2012). Reporting recommendations for tumor marker prognostic studies (remark): explanation and elaboration. *PLoS Med.* 9:e1001216. doi: 10.1371/journal.pmed.1001216
- Aschner, M., Suñol, C., and Bal-Price, A. (eds) (2011). *Cell Culture Techniques*. Totowa, NJ: Humana Press.
- ASNO (2017). *The 14th Meeting of the Asian Society for Neuro-Oncology (Scientific Program)*. Available online at: <http://asno2017.jp/data/program.pdf> (accessed February 1, 2020).

DATA AVAILABILITY STATEMENT

The datasets presented in this article are not readily available because the small numbers of participants and specific nature of the responses mean that individuals may be identified. Anonymised data collated from the online survey are available on request from the authors. Requests to access the datasets should be directed to KP, karen.pilkington@port.ac.uk.

ETHICS STATEMENT

The studies involving human participants were reviewed and approved by University of Portsmouth Faculty of Science Ethics Committee, reference number SFEC 2018-073 (original application plus amendments). The patients/participants provided their written informed consent to participate in this study.

AUTHOR CONTRIBUTIONS

KP and GP conceptualised the study. MB, GP, CH, and KP contributed to the design of the study. MB conducted the data collection. MB and KP carried out the analysis. MB and KP drafted the manuscript. All authors contributed to the final version of the manuscript.

FUNDING

This study was supported by a grant from Animal Free Research UK. The funding was unrestricted and the funders had no influence on the project design, conduct or reporting.

ACKNOWLEDGMENTS

The authors gratefully acknowledge the contribution of all participants in the study who completed the survey, participated in interviews or contributed to the Delphi process.

- BNOS (2018). Abstracts from the BNOS 2017 Meeting June 21-23, 2017 John McIntyre Conference Centre. *Edinburgh. Neuro. Oncol.* 20, i1–i26. doi: 10.1093/neuonc/nox237
- Boukdedid, R., Abdoul, H., Loustau, M., Sibony, O., and Alberti, C. (2011). Using and reporting the delphi method for selecting healthcare quality indicators: a systematic review. *PLoS One* 6:e20476. doi: 10.1371/journal.pone.0020476
- Brazma, A., Hingamp, P., Quackenbush, J., Sherlock, G., Spellman, P., Stoeckert, C., et al. (2001). Minimum information about a microarray experiment (MIAME)—toward standards for microarray data. *Nat. Genet.* 29, 365–371. doi: 10.1038/ng1201-365
- CAMARADES (2020). *CAMARADES (Collaborative Approach to Meta-Analysis and Review of Animal Data from Experimental Studies)*. Available online at: <http://www.dcn.ed.ac.uk/camarades/> (accessed February 1, 2020).
- Carlsen, B., Glenton, C., and Pope, C. (2007). Thou shalt versus thou shalt not: a meta-synthesis of GPs’ attitudes to clinical practice guidelines. *Br. J. Gen. Pract.* 57, 971–978. doi: 10.3399/096016407782604820

- CELL Press (2020). *Structured Transparent Accessible Reporting (STAR)*. Available online at: <https://www.cell.com/star-methods> (accessed February 1, 2020).
- Colquhoun, H. L., Squires, J. E., Kolehmainen, N., Fraser, C., and Grimshaw, J. M. (2017). Methods for designing interventions to change healthcare professionals' behaviour: a systematic review. *Implement. Sci.* 12, 1–11. doi: 10.1186/s13012-017-0560-5
- Corbin, J., and Strauss, A. (2014). *Basics of Qualitative Research: Techniques and Procedures for Developing Grounded Theory*. New York, NY: SAGE Publications.
- Cycyota, C. S., and Harrison, D. A. (2006). What (Not) to expect when surveying executives: a meta-analysis of top manager response rates and techniques over time. *Organ. Res. Methods* 9, 133–160. doi: 10.1177/1094428105280770
- Deng, K., Zhu, C., Ma, X., Jia, H., Wei, Z., Xiao, Y., et al. (2016). Rapid discrimination of malignant breast lesions from normal tissues utilizing raman spectroscopy system: a systematic review and meta-analysis of *in vitro* studies. *PLoS One* 11:e0159860. doi: 10.1371/journal.pone.0159860
- EANO (2018). 13th meeting of the European association of neurooncology October 10–14, 2018 Stockholm. Sweden. *Neuro. Oncol.* 20, iii215–iii344. doi: 10.1093/neuonc/now139
- Elshafay, A., Omran, E., Abdelkhalik, M., El-Badry, M., Eisa, H., Fala, S., et al. (2019). Reporting quality in systematic reviews of *in vitro* studies: a systematic review. *Curr. Med. Res. Opin.* 35:1. doi: 10.1080/03007995.2019.1607270
- EQUATOR Network (2020). *Enhancing the QUALity and Transparency Of Health Research*. Available online at: <https://www.equator-network.org> (accessed March 1, 2020).
- Eskes, C., Bostrom, A.-C., Bowe, G., Coecke, S., Hartung, T., Hendriks, G., et al. (2017). Good cell culture practices & *in vitro* toxicology. *Toxicol. Vitro* 45, 272–277. doi: 10.1016/j.tiv.2017.04.022
- EU-NETVAL (2015). *Summary Record: EU-NETVAL Meeting 26th–27th November 2015, Ispra, Italy*. In (Ispra, Italy). Available online at: https://ec.europa.eu/jrc/sites/jrcsh/files/eu-netval_meeting_2015_summary_record.pdf (accessed February 1, 2020).
- EU-NETVAL (2016). *Summary Record: EU-NETVAL Meeting 10–11th October 2016, Ispra, Italy*. In (Ispra, Italy: European Commission). Available online at: https://ec.europa.eu/jrc/sites/jrcsh/files/summary_record_eu-netval_meeting_2016.pdf (accessed February 1, 2020).
- EURL ECVAM (2014). *EURL ECVAM Workshop “Inaugural Meeting of EU-NETVAL Members” 26–27 June 2014*. In (Ispra, Italy). Available online at: https://ec.europa.eu/jrc/sites/jrcsh/files/eu-netval_june_2014mm-final.pdf (accessed February 1, 2020).
- FAIRSharing.org (2020). *FAIRSharing.org*. Available online at: <https://fairsharing.org/> (accessed March 1, 2020).
- Fan, W., and Yan, Z. (2010). Factors affecting response rates of the web survey: a systematic review. *Comput. Human Behav.* 26, 132–139. doi: 10.1016/j.chb.2009.10.015
- Fitch, K., Bernstein, S. J. J., Aguilar, M. D. D., Burnand, B., LaCalle, J. R. R., Lazaro, P., et al. (2001). *The RAND / UCLA Appropriateness Method User's Manual*. Available online at: https://www.rand.org/pubs/monograph_reports/MR1269.html (accessed February 1, 2020).
- Gardner, J., and Webster, A. (2016). The social management of biomedical novelty: facilitating translation in regenerative medicine. *Soc. Sci. Med.* 156, 90–97. doi: 10.1016/j.socscimed.2016.03.025
- Geraghty, R. J., Capes-Davis, A., Davis, J. M., Downward, J., Freshney, R. I., Knezevic, I., et al. (2014). Guidelines for the use of cell lines in biomedical research. *Br. J. Cancer* 111, 1021–1046. doi: 10.1038/bjc.2014.166
- Hartung, T. (2018). Perspectives on *in vitro* to *in vivo* extrapolations. *Appl. Vitro Toxicol.* 4, 305–316. doi: 10.1089/aivt.2016.0026
- Hartung, T., Balls, M., Bardouille, C., Blanck, O., Coecke, S., Gstraunthaler, G., et al. (2002). Good cell culture practice: ECVAM good cell culture practice task force report 1. *ATLA Altern. to Lab. Anim.* 30, 407–414. doi: 10.1177/026119290203000404
- Hartung, T., De Vries, R., Hoffmann, S., Hogberg, H. T., Smirnova, L., Tsaioun, K., et al. (2019). Toward good *in vitro* reporting standards. *ALTEX* 36, 3–17. doi: 10.14573/altex.1812191
- House of Commons Petitions Committee [HCPC] (2016). *Funding For Research Into Brain Tumours*. First Report of Session 2015–16. HC 554. London: The Stationery Office Limited.
- Higgins, J., and Green, S. (eds) (2011). *Cochrane Handbook for systematic reviews of interventions. Version 5.1.0. The Cochrane Collaboration*. Available online at: <https://handbook-5-1.cochrane.org/> (accessed February 1, 2020).
- Higgins, J. P. T., Altman, D. G., Gøtzsche, P. C., Jüni, P., Moher, D., Oxman, A. D., et al. (2011). The Cochrane Collaboration's tool for assessing risk of bias in randomised trials. *BMJ* 343:928. doi: 10.1136/bmj.d5928
- Hsu Chia, C., and Brian, A. S. (2007). The delphi technique: making sense of consensus. *Pract. Assess. Res. Eval.* 12:27071. doi: 10.1576/toag.7.2.120.27071
- ICLAC (2019a). *Cell Line Checklist for Manuscripts and Grant Applications*. Available online at: https://iclac.org/wp-content/uploads/ICLAC_Cell-Line-Checklist_v2_1.docx (accessed February 1, 2020).
- ICLAC (2019b). *International Cell Line Authentication Committee - Definitions*. Available online at: <https://iclac.org/resources/definitions/> (accessed February 1, 2020).
- Kenall, A., Edmunds, S., Goodman, L., Bal, L., Flintoft, L., Shanahan, D. R., et al. (2015). Better reporting for better research: a checklist for reproducibility. *Genome Biol.* 16, 15–17. doi: 10.1186/s13059-015-0710-5
- Kilkenny, C., Browne, W. J., Cuthill, I. C., Emerson, M., and Altman, D. G. (2010). Improving bioscience research reporting: the ARRIVE guidelines for reporting animal research. *PLoS Biol.* 8:e1000412. doi: 10.1371/journal.pbio.1000412
- Klimisch, H.-J., Andreae, M., and Tillmann, U. (1997). A systematic approach for evaluating the quality of experimental toxicological and ecotoxicological data. *Regul. Toxicol. Pharmacol.* 25, 1–5. doi: 10.1006/rtp.1996.1076
- Krippendorff, K. (2018). *Content Analysis: An Introduction to Its Methodology*. New York, NY: SAGE Publications.
- Laaksonen, M., Sorsa, T., and Salo, T. (2010). Emdogain in carcinogenesis: a systematic review of *in vitro* studies. *J. Oral Sci.* 52, 1–11. doi: 10.2334/josn.52.1
- Lynch, H. N., Goodman, J. E., Tabony, J. A., and Rhomberg, L. R. (2016). Systematic comparison of study quality criteria. *Regul. Toxicol. Pharmacol.* 76, 187–198. doi: 10.1016/j.yrtph.2015.12.017
- McShane, L. M., Altman, D. G., Sauerbrei, W., Taube, S. E., Gion, M., Clark, G. M., et al. (2005). Reporting recommendations for tumour MARKER prognostic studies (REMARK). *Br. J. Cancer* 93, 387–391. doi: 10.1038/sj.bjc.6602678
- Moher, D. (1998). CONSORT: an evolving tool to help improve the quality of reports of randomized controlled trials. *JAMA* 279:1489. doi: 10.1001/jama.279.18.1489
- Moher, D., Liberati, A., Tetzlaff, J., and Altman, D. G. (2009). Preferred reporting items for systematic reviews and meta-analyses: the PRISMA statement. *PLoS Med.* 6:e1000097. doi: 10.1371/journal.pmed.1000097
- NC3Rs (2020). *The National Centre for the Replacement, Refinement and Reduction of Animals in Research (NC3Rs). The 3Rs*. Available online at: <https://www.nc3rs.org.uk/the-3rs> (accessed February 1, 2020).
- NIH (2017). *Principles and Guidelines for Reporting Preclinical Research. Rigor Reprod.* Available online at: <https://www.nih.gov/research-training/rigor-reproducibility/principles-guidelines-reporting-preclinical-research> (accessed February 1, 2020).
- NIH (2019). *Nih Guidelines For Research Involving Recombinant Or Synthetic Nucleic Acid Molecules*. Bethesda, MD: NIH.
- NIH-OER (2015). *Enhancing Reproducibility through Rigor and Transparency*. Available online at: <https://grants.nih.gov/grants/guide/notice-files/not-od-15-103.html> (accessed February 1, 2020).
- Nuffield Council on BioEthics (2005). *The Ethics of Research Involving Animals*. Available online at: <https://www.nuffieldbioethics.org/assets/pdfs/The-ethics-of-research-involving-animals-full-report.pdf> (accessed February 1, 2020).
- OECD (2004). *The Application of the Principles of GLP to *in vitro* studies (Advisory Document of the Working Group on Good Laboratory Practice)*. Paris: OECD.
- OECD (2005). *Guidance Document On The Validation And International Acceptance Of New Or Updated Test Methods For Hazard Assessment*. Paris: OECD.
- OECD (2018). *Guidance Document on Good In Vitro Method Practices*. Paris: OECD.
- Pamies, D., Bal-Price, A., Simeonov, A., Tagle, D., Allen, D., Gerhold, D., et al. (2017). Good cell culture practice for stem cells & stem-cell-derived models. *ALTEX* 34, 95–132. doi: 10.14573/altex.1607121
- QSR International (2018). *NVIVO*. Available online at: <https://www.qsrinternational.com/nvivo/home> (accessed February 1, 2020).

- Rooney, A. (2015). *Extending a Risk-of-Bias Approach to Address In Vitro Studies*. in *National Toxicology Program Office of Health Assessment and Translation (USA: Environmental Protection Agency (EPA))*. Available online at: https://ofmpub.epa.gov/eims/eimscomm.getfile?p_download_id=526750 (accessed February 1, 2020).
- Schmidt, B. Z., Lehmann, M., Gutbier, S., Nembo, E., Noel, S., Smirnova, L., et al. (2017). In vitro acute and developmental neurotoxicity screening: an overview of cellular platforms and high-throughput technical possibilities. *Arch. Toxicol.* 91, 1–33. doi: 10.1007/s00204-016-1805-9
- Schneider, K., Schwarz, M., Burkholder, I., Kopp-Schneider, A., Edler, L., Kinsner-Ovaskainen, A., et al. (2009). “ToxRTTool”, a new tool to assess the reliability of toxicological data. *Toxicol. Lett.* 189, 138–144. doi: 10.1016/j.toxlet.2009.05.013
- SNO (2017a). Abstracts from the 22nd annual scientific meeting and education day of the society for neuro-oncology. *Neuro-Oncology* 19(Suppl._6), vi1–vi314. doi: 10.1093/neuonc/nox168
- SNO (2017b). *Society for Neuro-oncology 22nd Annual Meeting and Education Day*. SNO. Available online at: https://www.soc-neuro-onc.org/UploadedFiles/2017_SNO_Program_final.pdf (accessed February 1, 2020).
- S-SANOC (2017). *Report of The First Sub-Saharan Africa Neuro-Oncology Collaborative (S-SANOC) Planning Meeting*. S-SANOC. Available online at: http://www.snossa.org/wp-content/uploads/2018/04/IBTA_SSANOC-Report_FINAL-20Mar2018.pdf (accessed February 1, 2020).
- Taylor, C. F., Field, D., Sansone, S. A., Aerts, J., Apweiler, R., Ashburner, M., et al. (2008). Promoting coherent minimum reporting guidelines for biological and biomedical investigations: the MIBBI project. *Nat. Biotechnol.* 26, 889–896. doi: 10.1038/nbt.1411
- UKCCCR (2000). UKCCCR guidelines for the use of cell lines in cancer research. *Br. J. Cancer* 82, 1495–1509. doi: 10.1054/bjoc.1999.1169
- WFNOS (2017a). *5th Quadrennial Meeting of the World Federation of Neuro-Oncology Societies*. Seoul: WFNOS.
- WFNOS (2017b). *World Federation of Neuro-oncology Societies (WFNOS) 2017 Meeting Final Programme*. Available online at: https://www.eano.eu/fileadmin/content/WFNOS_2017/2017_WFNOS_Final_Programme_for_print.pdf (accessed February 1, 2020).
- Xiao, Z., Li, C., Shan, J., Luo, L., Feng, L., Lu, J., et al. (2011). Mechanisms of renal cell apoptosis induced by cyclosporine a: a systematic review of in vitro studies. *Am. J. Nephrol.* 33, 558–566. doi: 10.1159/000328584

Conflict of Interest: The authors declare that the research was conducted in the absence of any commercial or financial relationships that could be construed as a potential conflict of interest.

Copyright © 2020 Bracher, Pilkington, Hanemann and Pilkington. This is an open-access article distributed under the terms of the Creative Commons Attribution License (CC BY). The use, distribution or reproduction in other forums is permitted, provided the original author(s) and the copyright owner(s) are credited and that the original publication in this journal is cited, in accordance with accepted academic practice. No use, distribution or reproduction is permitted which does not comply with these terms.



Advanced Microfluidic Models of Cancer and Immune Cell Extravasation: A Systematic Review of the Literature

Carlotta Mondadori^{1†}, Martina Crippa^{2,3†}, Matteo Moretti^{1,3}, Christian Candrian³, Silvia Lopa^{1*†} and Chiara Arrigoni^{3*†}

OPEN ACCESS

Edited by:

Davide Staedler,
University of Lausanne, Switzerland

Reviewed by:

Mara - Gilardi,
University of California, San Diego,
United States
Francis Lin,
University of Manitoba, Canada

*Correspondence:

Silvia Lopa
silvia.lopa@grupposandonato.it
Chiara Arrigoni
chiara.arrigoni@eoc.ch

[†]These authors have contributed
equally to this work

[‡]These authors have contributed
equally to this work and share
last authorship

Specialty section:

This article was submitted to
Nanobiotechnology,
a section of the journal
Frontiers in Bioengineering and
Biotechnology

Received: 18 May 2020

Accepted: 14 July 2020

Published: 26 August 2020

Citation:

Mondadori C, Crippa M, Moretti M,
Candrian C, Lopa S and Arrigoni C
(2020) Advanced Microfluidic Models
of Cancer and Immune Cell
Extravasation: A Systematic Review of
the Literature.
Front. Bioeng. Biotechnol. 8:907.
doi: 10.3389/fbioe.2020.00907

¹ IRCCS Istituto Ortopedico Galeazzi, Cell and Tissue Engineering Laboratory, Milan, Italy, ² Department of Chemistry, Materials, and Chemical Engineering "Giulio Natta", Politecnico di Milano, Milan, Italy, ³ Regenerative Medicine Technologies Laboratory, Ente Ospedaliero Cantonale (EOC), Lugano, Switzerland

Extravasation is a multi-step process implicated in many physiological and pathological events. This process is essential to get leukocytes to the site of injury or infection but is also one of the main steps in the metastatic cascade in which cancer cells leave the primary tumor and migrate to target sites through the vascular route. In this perspective, extravasation is a double-edged sword. This systematic review analyzes microfluidic 3D models that have been designed to investigate the extravasation of cancer and immune cells. The purpose of this systematic review is to provide an exhaustive summary of the advanced microfluidic 3D models that have been designed to study the extravasation of cancer and immune cells, offering a perspective on the current state-of-the-art. To this end, we set the literature search cross-examining PUBMED and EMBASE databases up to January 2020 and further included non-indexed references reported in relevant reviews. The inclusion criteria were defined in agreement between all the investigators, aimed at identifying studies which investigate the extravasation process of cancer cells and/or leukocytes in microfluidic platforms. Twenty seven studies among 174 examined each step of the extravasation process exploiting 3D microfluidic devices and hence were included in our review. The analysis of the results obtained with the use of microfluidic models allowed highlighting shared features and differences in the extravasation of immune and cancer cells, in view of the setup of a common framework, that could be beneficial for the development of therapeutic approaches fostering or hindering the extravasation process.

Keywords: extravasation, microfluidic, cancer cells, immune cells, *in vitro* models

INTRODUCTION

Extravasation is the process in which cells that are flowing into a vascular vessel interact with the endothelium lumen, adhere to it, and then cross the endothelial barrier to reach a target site, guided by various types of stimulation. This process represents a key step in several pathologic conditions, for this reason many researchers are focusing on trying to understand and control this phenomenon.

Leukocytes typically extravasate in inflammatory conditions and although the inflammatory response is fundamental to fight infection and in wound healing, the persistency of an active immune response is involved in several pathologies and chronic inflammatory disorders (Schnoor et al., 2015). Extravasation is also crucial during the metastatic cascade, whereby circulating cancer cells deriving from the primary tumor cross the endothelial barrier of specific organs to reach the targeted metastatic site (Reymond et al., 2013).

Extravasation consists in a series of sequential steps that are basically the same for each extravasating cell, and we refer the reader to specific reviews for the exhaustive description of activated pathways during leukocyte (Vestweber, 2015) and cancer cell (Reymond et al., 2013) extravasation. On a more general point of view, extravasation starts with the formation of adhesive interactions between circulating cells and endothelial cells which cover the lumen of the vessels. The process continues with tethering, rolling, and slow-rolling, followed by firm adhesion, crawling, and formation of the transmigratory cup on the endothelial surface. The next step consists in the transendothelial migration that can take place either in a paracellular (crossing the cell endothelial junctions) or in a transcellular (crossing endothelial cells) way. The paracellular way is largely studied due to the relation with the endothelial junction control that seems to be a promising therapeutic target. After passing the endothelial barrier, the extravasating cells must cross the pericyte layer and invade the basement membrane to reach the inflamed tissue or the target secondary organ. Even if the extravasation steps are essentially the same, according to the type of extravasating cells, there are differences in cell responsiveness to specific chemoattractants and diverse activation and/or expression of adhesion molecules mediating cell interactions with the endothelium (Schnoor et al., 2015).

Leukocyte extravasation is usually induced by tissue damage or by infection, which activate the defensive mechanisms of the body. The process starts with the release of proinflammatory cytokines in the damaged tissue, causing endothelial activation (Vestweber, 2012). This activation triggers a cascade of events that enables circulating leukocytes to recognize the vascular endothelium of the inflamed tissue and interact with the endothelial cells. Endothelial selectins (E-selectin, P-selectin) are expressed by the inflamed endothelium and capture leukocytes from the blood flow. Then, chemokines and other chemoattractants produced by endothelial cells and inflammatory cells increase the expression in leukocytes of integrins that bond specific endothelial adhesion molecules (e.g., intracellular adhesion molecule-1, ICAM-1, or vascular adhesion molecules 1, VCAM-1). This bond is essential and leads to leukocyte transendothelial migration (Vestweber, 2015).

Targeting leukocyte extravasation can be a promising approach either for the enhancement of immune defenses or for the suppression of inflammation-induced tissue destruction. For example, anti-adhesion therapies, contrasting self-destructive inflammation, are promising therapeutic options for multiple sclerosis (Vestweber, 2015). On the other hand, studies focusing on the extravasation of cancer cells are always aimed at contrasting this process. Indeed, extravasation is a crucial step

of metastasis formation, which leads to 90% of cancer related deaths (Reymond et al., 2013). Cancer cells that intravasate into the blood stream must survive to the aggression of immune cells and to the presence of elevated shear stress, only then they can eventually adhere to the blood vessel wall. Cancer cell extravasation preferentially takes place in small capillaries of the same diameter of the cells, suggesting that the process starts with a physical restriction where the formation of a stable adhesion occurs. The adhesion of cancer cells to the endothelium also requires the expression of ligands and related receptors on both cancer and endothelial cells, including integrins, selectins, cadherins, and immunoglobulin superfamily receptors. It is known that diverse tumors metastasize preferentially in specific tissues/organs, following metastatic patterns that can be related to the particular type of vasculature of the secondary site and to chemokine receptors and complementary chemokines expressed between target endothelium and cancer cells (Nguyen et al., 2009). There are specific chemokines frequently involved in cancer cells extravasation, such as CXC-chemokine ligand 12 (CXCL12), which are secreted by stromal cells placed in distant organs that stimulate cancer cells extravasation and migration to these secondary sites. The paracellular transendothelial migration of cancer cells is usually related to the disruption of endothelial junctions and it is the event that is principally observed *in vitro*. Although there is a small amount of evidence that the cancer transendothelial migration could also be transcellular, this behavior could be related to the characteristic of the vascular bed or the cancer type. This aspect has not yet been fully clarified (Reymond et al., 2013).

The extravasation process has been studied both in *in vivo* and *in vitro* models. Several types of animal models have been used, such as zebrafishes, rats, and mice and, less frequently, dogs for the study of cancer cell and leukocyte extravasation (Simmons et al., 2015; Brown et al., 2017; Gomez-Cuadrado et al., 2017; Marcovecchio et al., 2017). Among all these options, laboratory mice represent the most commonly used animal model, due to their superior physiological and genetic similarities with humans as compared to zebrafishes, but also by their ease of maintenance, breeding and short gestation time as compared to dogs. Moreover, the ability to genetically manipulate mice both by transgenic expression and knockout of specific genes makes mice more versatile for studying human cancer metastasis (Saxena and Christofori, 2013), but also for identifying the role of specific factors in leukocyte trafficking (Power, 2003). Cancer cell extravasation models can be based on the injection of human metastatic cancer cells into immune-compromised animals (xenograft) or on the creation of genetically engineered animals, reproducing the stages of tumor progression (Saxena and Christofori, 2013). In the first case, the use of immunocompromised mice, which is required for experiments using human cancer cells, hinders the possibility to study interactions between cancer and immune cells, that play a critical role in metastasis (Ma et al., 2018). On the other hand, the use of genetically modified mice allows the preservation of the immune system, although these models are not available for all tumor types (Kovar et al., 2016). In both cases, animal immune system, endothelium, and

specific tissue-secreted molecules are different from the human ones, possibly altering the observed mechanisms underlying cell behavior (Willyard, 2018). Furthermore, although *in vivo* models allow mimicking the complexity of cell extravasation in a physiological context, they do not permit to investigate how the different elements impact on the phenomenon.

Besides animal models, the study of cancer cell behavior has long been based on standard 2D and 3D *in vitro* cell culture models. The use of these models has allowed investigating many cancer-related events, although standard cell culture models present some critical issues. The principal limitation of 2D models is the lack of the 3D structure of human tissues, which can lead to an abnormal cell behavior. On the other hand, even if classical 3D *in vitro* models have succeeded in mimicking the cancer architecture, they are barely able to reproduce physiological features such as vascularization and blood flow, the presence of biochemical gradients, and the heterogeneity of cell populations that characterize cancer microenvironment (Sleeboom et al., 2018). More specifically, among *in vitro* systems, transwell inserts have been largely used to model the extravasation process. However, although these models allow studying cell adhesion to the endothelium and cell migration through it, they cannot reproduce the extravasation process in dynamic conditions and are not suitable to investigate tissue invasion. Furthermore, extravasation in transwell assays occurs through 2D circular pores measuring from 3 to 12 μm in diameter, which do not match the endothelial junction architecture, and the extravasation can be strongly influenced by gravity force (Kim et al., 2016). Toward a better modeling of the *in vivo* environment some hybrid models have been developed, such as transwell-microfluidic systems that allow including and controlling both luminal and transmural flow (Sleeboom et al., 2018).

Engineered microfluidic devices are promising *in vitro* tools that can overcome the above-mentioned limitations of *in vitro* models in the study of extravasation. The use of microfluidic devices spread out in the last decades thanks to the development of soft lithography. This technological advancement upgraded rapid prototyping allowing the researchers to increase the sophistication and complexity of microfluidic systems (Streets and Huang, 2013). The possibility to easily design and fabricate microfluidic devices also contributed to their versatility, enabling the addition of different features according to the specific microenvironment and phenomenon they are aimed to mimic. Microfluidic devices are all basically constituted by chambers and micro-scale fluidic circuits with a dimension around tens to hundreds of micrometers. The microscale dimension represents an important advantage in biological research, allowing more precise and quantitative measurements, dramatically reducing the number of cells and reagents needed, and hence decreasing also the cost of each experiment (Streets and Huang, 2013). These devices permit to include diverse cellular populations in a 3D microenvironment, allowing to mimic complex physiological microenvironments (Ma et al., 2018). It is also possible to precisely control biophysical and biochemical conditions, and directly visualize in real-time the investigated events. Another key aspect is the possibility to develop systems

entirely composed by human cells embedded in 3D extracellular matrices to recapitulate the *in vivo* behavior of cells (Coughlin and Kamm, 2020). In particular, microfluidic models allow including all the main elements involved in the process of extravasation (e.g., geometry of the blood vessel, presence of a 3D environment, etc.) within a cell culture device, thus reproducing the architecture of the *in vivo* milieu. These models can be further implemented to become even more sophisticated by incorporating non-cellular components of the tissue stroma or including multiple types of tissue-specific cells (Coughlin and Kamm, 2020).

Up to now, microfluidic models have been exploited to dissect specific effects of biophysical, biochemical and cellular elements on leukocyte or cancer cell extravasation. In the present systematic review, we will discuss the findings achieved through the use of microfluidic systems, highlighting specific model features which enabled to achieve the reported results.

METHODS

Search Strategy

The literature search was aimed to identify all the studies describing microfluidic models designed to investigate cancer cell and/or leukocyte extravasation. The literature search was carried out consulting PUBMED and EMBASE databases. We also checked the reference lists of relevant reviews to include other studies that had not been identified during the search process. The full search strategy is reported in **Appendix S1**.

Study Selection

Inclusion criteria were defined to select the studies. Specifically, we included studies describing the use of a microfluidic model and investigating the process of cancer cell and/or leukocyte extravasation. Two investigators (CM and MC) independently reviewed the literature and classified the references based on the title and abstract. The eligible articles were further screened through the available full-text, and the studies matching the inclusion criteria were selected. Upon full-text reading, some studies were excluded due to the reasons described in detail in section Study Selection and Features of the Study. Any disagreement on study eligibility was solved by discussion.

Data Extraction and Analysis

Data extraction was performed by three investigators (CM, MC, and SL). Any disagreement was solved by discussion. The following data were extracted: type of extravasating cells, type of endothelial setting (i.e., endothelial monolayer, endothelial channel, microvascular network), type of biophysical factor(s) applied in the system, type of biochemical factor(s) applied in the system, type of environmental factors present (i.e., presence of tissue-specific cells, features of the extracellular matrix), properties of extravasating cells (i.e., tissue of origin, metastatic potential, cell stiffness). We specifically focused on those factors that can be studied taking advantage of the features of microfluidic extravasation models, with the final aim to

illustrate their potential and provide examples of the scientific questions that can be addressed using this type of models.

Outcome(s)

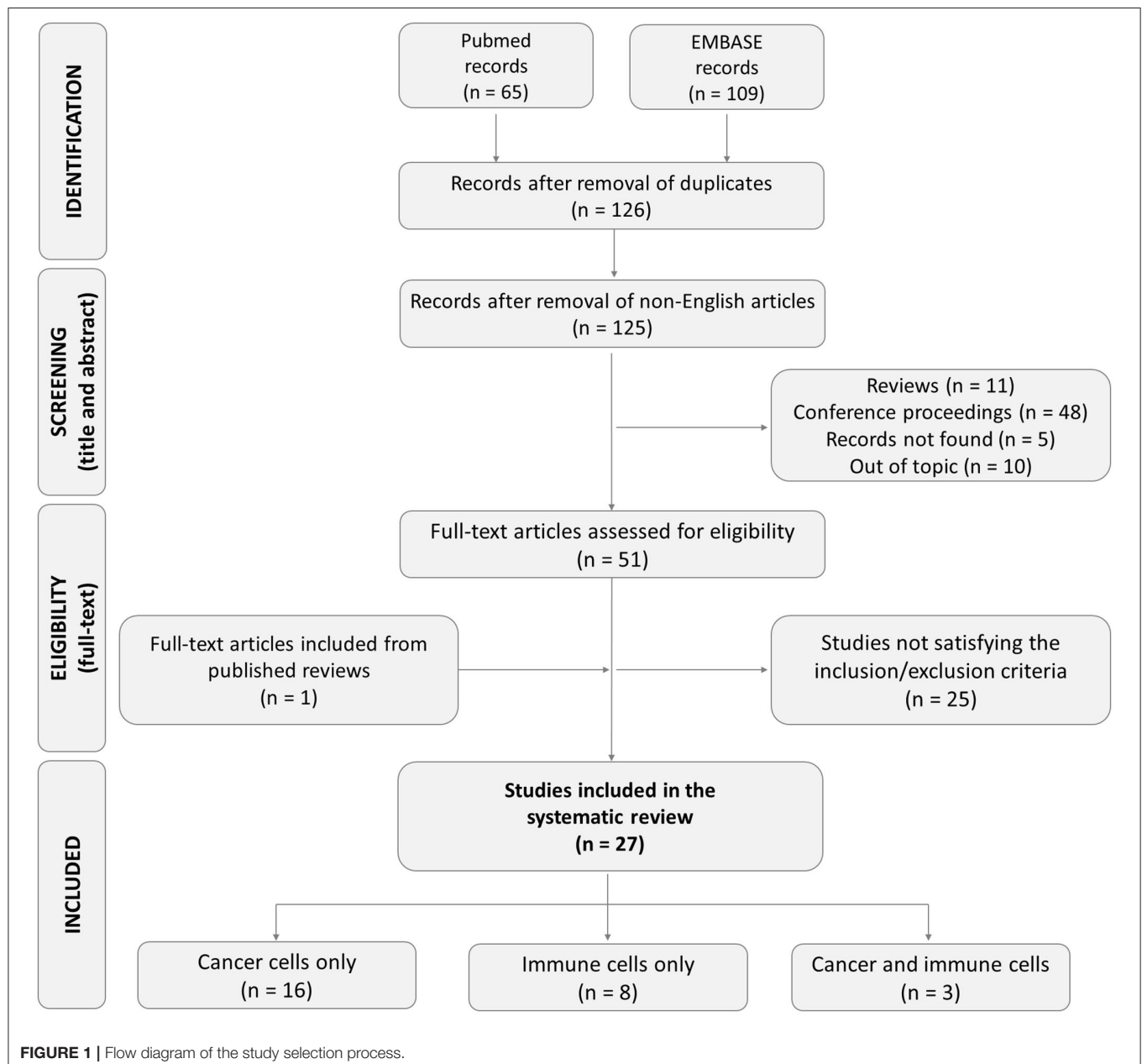
The primary outcome was the effect of any of the factors mentioned above (biochemical factors, biophysical factors, environmental factors, intrinsic cell properties) on the transendothelial migration of extravasating cells detected in the presence of any of these factors in comparison to a control condition.

The effect of the same factors on extravasation phases that precede or follow the transendothelial migration (i.e.,

rolling, adhesion, matrix invasion) were considered as secondary outcomes.

Quality and Risk of Bias Assessment

The methodological quality of the studies and the risk of bias were assessed adapting methodologies described in previous systematic reviews focusing on *in vitro* studies (AlShwaimi et al., 2016; Golbach et al., 2016). Two investigators (CM and SL) performed independently the quality assessment. The following biases were evaluated: (1) study design bias, (2) reporting bias, (3) detection bias. The scoring system included four possible answers to the questions reported in **Table 2**. If the paper satisfied totally or partially the request, the scores were respectively “Yes”



or “Partly.” If the paper did not satisfy the request, the score was “No.” “Unclear” was attributed when the paper lacked the necessary details to assess the risk and, hence, it was not possible to attribute any of the other three answers. The overall quality was then determined as follows: The articles that reported 1–3 “Yes” items were classified as high risk of bias, 4–6 as moderate risk of bias, and 6–9 as low risk of bias.

RESULTS

Study Selection and Features of the Study

Based on the literature search strategy, 174 studies were found (65 in PUBMED and 109 in EMBASE). Among them, 48 articles were excluded because they were doubly reported in the literature search. Of the remaining 126 records, one record was excluded because it was a non-English article. Other articles were excluded for different reasons: 5 records not found, 11 review articles, 48 conference proceedings, and 10 articles not satisfying the inclusion criteria. Of the remaining 51 articles, after reading the full-text, 25 were excluded for the following reasons: 3 studies describing non-microfluidic models, one study using animal cells, 5 methodological articles, 7 articles mentioning extravasation, but describing a model lacking endothelial cells, one study describing only the process of intravasation, 7 studies focusing only on the rolling and/or adhesion step and not analyzing the transendothelial migration phase, one study with unclear methodology. One additional eligible study was retrieved from the bibliography of a review and included. Overall, we finally included 27 studies meeting our eligibility criteria for the subsequent analysis (**Figure 1**). Among these, 16 studies investigated the extravasation of cancer cells only, 8 investigated the extravasation of immune cells only, and 3 studies investigated cancer and immune cell behavior in the same extravasation models. The studies included are reported and described in **Tables 1–3**.

Quality and Risk of Bias Assessment

The overall quality of the study was high (**Figure 2A**). For what concerns the study design, all the studies included control groups and in the vast majority of cases, the control groups were highly coherent with the scientific hypothesis. A higher heterogeneity was observed analyzing methodological reporting elements. About 25% of studies (7/27) did not provide a detailed and easily comprehensible description of the microfluidic model, which in some cases impeded the full comprehension of the results. All the studies clearly indicated the origin and type of cells, and the vast majority indicated the type of matrix included in the model. On the other hand, the detailed description of any biochemical and/or biophysical stimulation applied in the system was incomplete or missing in 25% of studies (7/27), leading to the impossibility to fully understand the experimental set-up. Almost all the studies (26/27) described the timing of the extravasation assay. Finally, regarding the detection phase, almost all the studies (26/27) applied a quantitative method to analyze cell extravasation, although 33% of studies (9/27) did not clearly indicate whether the data were obtained from independent experiments. Based on these elements, we classified

93% of studies (25/27) as affected by low risk of bias and 7% (2/27) by moderate risk of bias (**Figure 2B**).

Microfluidic Models Investigating Cancer and Immune Cells Extravasation

Cell extravasation is a multi-step process, subjected to influences deriving from biochemical and biochemical factors and from the microenvironment in which cells extravasate, but also from intrinsic cell properties and the interactions between cells. Different microfluidic models have been designed to consider the specific effects of those factors on the extravasation process and in the following sections we will describe the models applied and the results achieved for each category of factors (**Figures 3A,B**).

Effect of Biophysical Factors

The extravasation process takes place in an environment in which both extravasating cells and endothelial cells are exposed to the frictional force of the blood flow, called shear stress. Shear stress has a crucial role in regulating the interactions between leukocytes and endothelial cells during both physiological and pathological processes. In physiological conditions, leukocyte extravasation mostly occurs in post-capillary venules under shear stress conditions ranging from 1 to 5 dyn/cm² (Bianchi et al., 2013), whereas in some pathological conditions, such as atherosclerosis, leukocytes extravasate through the artery walls where the shear stress is much higher (Schimmel et al., 2017). Shear stress plays also a role in regulating tumor invasion and metastatic spreading. Cancer cells adhere to the endothelium and extravasate mainly within the range of 0.5–15 dyn/cm², shear stress conditions that are reached in capillaries, in veins, and in some arteries (Huang et al., 2018).

To study the effect of the shear stress on the extravasation process, advanced 3D microfluidic models have been proposed due to their compatibility with the application of a controlled shear stimulation, which can mimic the conditions experienced by cells *in vivo* (Zervantonakis et al., 2011). Moreover, microfluidic models can reproduce vessels with specific dimensions and geometrical features (e.g., bifurcations, curvatures, occlusions, etc.) that affect the fluid motion, thus giving the possibility to study the extravasation process in the most varied flow conditions, typical of healthy or pathological states (Wang et al., 2018).

Among the 27 studies included in this review, 13 included a fluid flow applied to the vascular compartment for different purposes: 3 studies used the fluid flow to pre-condition the endothelium before the extravasation assay, 8 to perfuse cells, 1 to induce cell deformation and one to remove non-adherent cells. Of those, only 5 studies analyzed the effect of the flow stimulation compared to a control group, all applied the fluid flow by means of a syringe pump.

To generate the vessels within microfluidic models, two different approaches are mainly used: in the first one, endothelial cells are introduced in a pre-formed microfluidic channel to generate an endothelialized channel, while in the other case endothelial cells embedded in a hydrogel form a 3D microvascular network by self-assembly. In both cases, a 3D endothelial structure with a lumen is obtained mimicking

TABLE 1 | Features of the studies focusing on cancer cell extravasation.

Extravasating cells	Endothelial setting	Biophysical factors	Biochemical factors	Environmental factors	Cell features	Primary outcome(s)	Secondary outcome(s)	First author Year
HepG2 (Hepatocellular carcinoma), HeLa (cervical cancer), MDA-MB-435S (breast cancer)	Endothelial monolayer Dermal HMECs	Flow shear stress (0.03 cm/s) to induce cancer cell deformation	-	Matrigel	Cell with different stiffness subjected to deformation	• Cell deformation = TEM	• Cell deformation = INV	Chaw et al., 2007
ACC-M cell aggregates (salivary gland adenoid cystic carcinoma)	Endothelial monolayer HUVECs	-	CXCL12 (200 ng/mL)	Basement membrane extract	-	• CXCL12 ↑ TEM	• CXCL12 ↑ INV	Zhang et al., 2012
HT-1080 (fibrosarcoma), MDA-MB-231 (breast cancer), MCF-10A (breast epithelial cells)	Self-assembled MVN HUVECs	Flow shear stress (range 0.012–0.48 Pa) to perfuse cancer cells	TNF- α (2, 5, 10 ng/mL)	Fibrin gel	Cells with higher or lower MP	• TNF- α ↑ TEM • ↑ MP ↑ TEM	-	Chen et al., 2013
MDA-MB-231 (breast cancer), MCF-10A (breast epithelial cells)	Endothelial channel HMECs	-	-	Collagen gel	-	-	-	Jeon et al., 2013
MDA-MB-231 (breast cancer)	Endothelialized channel HUVECs	-	CXCL5 (12 nM)	Collagen gel Osteo-cells in EVM	-	• Bone μ Env ↑ TEM • CXCL5 ↑ TEM	• Bone μ Env ↑ INV • CXCL5 ↑ INV	Bersini et al., 2014
PC3, BT-474 (prostate cancer)	Endothelial channel HUVECs	Flow shear stress (2.09 dyne/cm ²) to perfuse cancer cells	-	Collagen gel Pericytes and astrocytes in EVM	-	• ↑ MP ↑ TEM	-	Tourovskaia et al., 2014
BOKL clone MDA-MB-23 (breast cancer), MCF-10A (breast epithelial cells)	Self-assembled MVN HUVECs	Flow shear stress (0.25 dyn/cm ²) for endothelial cell pre-conditioning	-	Fibrin gel Osteo-cells in EVM or myoblasts in EVM	-	• Bone μ Env ↑ TEM • Muscle μ Env ↓ TEM • Shear stress ↓ TEM	• Bone μ Env = INV • Shear stress ↑ INV	Jeon et al., 2015
MDA-MB-231 (breast cancer), A-375 MA2 (melanoma)	Self-assembled MVN Endothelial monolayer HUVECs	Flow shear stress (5 dyne/cm ²) to remove non-adherent cancer cells	-	Fibrin/Collagen gel	-	-	-	Chen et al., 2016
MDA-MB-231 (breast cancer)	Endothelial channel HUVECs	-	CXCL12 (300 ng/mL)	Matrigel	-	• CXCL12 ↑ TEM	-	Roberts et al., 2016
MDA-MB-231 (breast cancer), T24 (bladder cancer), OVCAR-3 (ovarian cancer)	Endothelial channel HUVECs	-	-	Collagen gel Osteo-cells in EVM	Cancer cells with different MP	• Bone μ Env ↑ TEM • ↑ MP ↑ TEM	• Bone μ Env ↑ INV • ↑ MP ↑ INV	Bersini et al., 2018b
MDA-MB-231, LM2-4175 (breast cancer)	Endothelial channel HUVECs	Fluid flow (0.2 μ L/s) to perfuse cancer cells	-	Collagen gel	-	-	-	Bertulli et al., 2018
MDA-MB-231, HS578T, MCF7 (breast cancer)	Endothelial channel HUVECs	Flow shear stress (1–6 dyn/cm ²) to perfuse cancer cells	-	Collagen gel	Cancer cells with or without hyaluronic acid pericellular matrix	• Pericellular matrix ↑ TEM	• Pericellular matrix ↑ INV	Brett et al., 2018
MDA-MB-231, MCF7 (breast cancer), MCF-10A (breast epithelial cells)	Self-assembled MVN HUVECs	-	-	Fibrin gel	Hypoxic and normoxic cancer cells Cancer cells with different MP	• Hypoxic cancer cells ↑ TEM • ↑ MP ↑ TEM	-	Song et al., 2018

(Continued)

TABLE 1 | Continued

Extravasating cells	Endothelial setting	Biophysical factors	Biochemical factors	Environmental factors	Cell features	Primary outcome(s)	Secondary outcome(s)	First author Year
PC9, PC9-BrM3 (lung cancer)	Endothelial monolayer Brain HMECs	Fluid flow (0.1 $\mu\text{L}/\text{min}$) for endothelial cell pre-conditioning	-	Collagen and fibronectin Astrocytes	-	• \uparrow MP \uparrow TEM	-	Liu et al., 2019
MDA-MB-231 (breast cancer)	Endothelial channel HUVECs	Oscillatory flow (1 Pa, 1 Hz) to stimulate osteocytes in EVM	-	Collagen/Matrigel mix Osteocytes in EVM	Osteocytes stimulated or not by oscillatory fluid flow	• Mechanically-stimulated osteocytes \downarrow TEM	• Mechanically-stimulated osteocytes \downarrow INV	Mei et al., 2019
MDA-MB-231 (breast cancer)	Endothelial channel HUVECs	Flow shear rate* (10, 20 s^{-1}) to perfuse cells *Shear stress (0.08, 0.16 dyn/cm^2)	TNF- α (50 ng/mL)	Matrigel	-	-	• TNF- α \uparrow ADH \uparrow Flow \downarrow ADH	Mollica et al., 2019

When available, primary and secondary outcomes have been summarized. The symbol indicates if the analyzed factor increases (\uparrow) or decreases (\downarrow), or does not affect ($=$) any extravasation step (ADH, adhesion; TEM, transendothelial migration; INV, invasion). When a single symbol is present, the increase/decrease is defined respect to a control condition. In the case of factor intensity correlating with effect intensity, two symbols are present to indicate the direct or inverse correlation. When the shear rate was indicated in the paper, we calculated the corresponding shear stress value, considering a medium viscosity equal to $0.00082 \text{ Pa} \times \text{s}$ (Raimondi et al., 2002). (HMECs, human microvascular endothelial cells; HUVECs, human umbilical vein endothelial cells; MP, metastatic potential; EVM, extravascular matrix; μEnv , microenvironment).

the patency of native vessels. However, great differences exist between these two configurations. If the generation of endothelialized channels with well-defined geometry and dimensions allows controlling the shear stress imposed at the endothelium wall, the second strategy allows a better reproduction of the physiological geometrical structure of native vessels (Wang et al., 2018). To achieve a high control of the flow rate and, therefore, of the shear stress applied at the endothelium wall, the use of syringe pumps is recommended, even though it renders the experimental set-up more complex. A simpler, but less controllable, method exploits the difference in hydrostatic pressure between two reservoirs at the inlet and outlet of the channel, which generates a flow in the channel, defined as gravitational flow. Computational simulations can be carried out to precisely assess the shear stress within the microfluidic channels and correlate the values to the extravasation outcomes.

Shear stress has been shown to influence different steps of the extravasation process of both leukocytes and cancer cells as well as to modify the endothelium properties. Leukocyte extravasation was investigated in dynamic conditions within a synthetic microvascular network, composed by channels mimicking the dimension of post-capillary venules, the main focal sites of leukocyte-endothelium interactions. The microvascular network was obtained through soft-lithography techniques, starting from a digitalized image of the *in vivo* microvascular topology to reproduce a realistic geometry. In this model, computational fluid dynamic analysis allowed defining the shear stress values of specific regions to correlate the shear stress with either cell adhesion or transendothelial migration outcomes. In particular, the correlation between adherent and extravasated cells with shear stress values showed that neutrophil adhesion was reduced in regions where the shear rate was higher than 120 s^{-1} (corresponding to an estimated shear stress of 0.98

dyn/cm^2) and that transendothelial migration mainly occurred in regions characterized by a shear rate between 30 and 60 s^{-1} (corresponding to an estimated shear stress of $0.25\text{--}0.49 \text{ dyn}/\text{cm}^2$), as compared to regions with higher values. Rolling velocities measured from videos of neutrophils flowing in the microchannels, showed values closely mimicking the *in vivo* situation, corroborating the findings of this study (Lamberti et al., 2014). A shear stress lower than $0.1 \text{ dyn}/\text{cm}^2$ was also reported to enhance the positive effect of the Monocyte Chemoattractant Protein-1 (MCP-1) on monocyte transendothelial migration (Sharifi et al., 2019), suggesting that different types of leukocytes have a similar behavior in response to low shear stress conditions. Similar evidences emerged from a study in which a microfluidic model has been used to reproduce the stenotic occlusion typical of atherosclerosis and investigate the effect on neutrophil adhesion of flow and inflammation within the obstructed channel. Neutrophil adhesion along the channel was minimal at $1 \text{ dyn}/\text{cm}^2$ in healthy conditions, while it was enhanced when an inflammatory stimulus was present. On the other hand, neutrophil adhesion at higher shear stress values ($10 \text{ dyn}/\text{cm}^2$, value in the physiological shear stress range found in the arterioles, where atherosclerosis is favored), remained low along the channel even in the presence of an inflamed endothelium, indicating that the activation of the endothelium was not sufficient to counterbalance the effect of high shear stress. Differently, when neutrophils encountered obstacles in their trajectory, such as an obstruction in the microchannel mimicking the stenotic condition, they could adhere to the endothelium despite high shear stress levels (Menon et al., 2017).

Not surprisingly, shear stress has also a major role in cancer cell extravasation and consequently in the formation of tumor metastasis. Low shear stress ($0.25 \text{ dyn}/\text{cm}^2$) was shown to reduce breast cancer cell transendothelial migration compared to the

TABLE 2 | Features of the studies focusing on the extravasation of immune cells.

Extravasating Cells	Endothelial setting	Biophysical Factors	Biochemical factors	Environmental factors	Cell features	Primary outcome(s)	Secondary outcome(s)	References
Neutrophils	Endothelial channel Dermal HMECs	-	fMLP (10, 100, 1000 nM) IL8 (1, 10, 100 ng/mL)	Collagen gel with different stiffness	-	<ul style="list-style-type: none"> fMLP ↑ TEM IL8 ↑ TEM Effect on TEM : fMLP > IL8 ↑ EVM stiffness ↓ TEM 	<ul style="list-style-type: none"> fMLP ↑ INV IL8 = INV ↑ EVM stiffness ↓ INV 	Han et al., 2012
Neutrophils	Non-self-assembled MVN Porous membrane separating endothelial cells and EVM HUVECs	Shear rate* (<30, 30–60, 60–120, 120–280 s ⁻¹) to perfuse cells *Shear stress (<0.25, 0.25–0.49, 0.49–0.98, 0.98–1.48 dyn/cm ²)	TNF-α (10 U/mL) fMLP (1 μM)	n.d.	-	<ul style="list-style-type: none"> fMLP ↑ TEM Shear rate 30–60 s⁻¹ ↑ TEM 	<ul style="list-style-type: none"> Shear rate > 120 sec⁻¹ ↓ ADH 	Lamberti et al., 2014
Neutrophils	Endothelial monolayer Human endothelial cell line (hy926)	-	fMLP (10, 20, 50 ng/mL) IL-8 (10, 20, 50 ng/mL) LTB4 (10, 20, 50 ng/mL)	Collagen gel	-	<ul style="list-style-type: none"> fMLP ↑ TEM IL8 ↑ TEM LTB4 ↑ TEM Effect on TEM : fMLP = LTB4 > IL-8 	-	Wu et al., 2015
Neutrophils Neutrophils in whole blood	Endothelial channels HUVECs	Flow shear stress (1, 10 dyn/cm ²) to perfuse cells	TNF-α (10 ng/mL) fMLP (500 nM)	Collagen gel	-	<ul style="list-style-type: none"> fMLP ↑ TEM 	<ul style="list-style-type: none"> TNF-α ↑ ADH ↑ Shear stress ↓ ADH 	Menon et al., 2017
Neutrophils	Endothelial channel iPSC-ECs	-	<i>P aeruginosa</i> (bacterial strain)	Collagen gel	-	<ul style="list-style-type: none"> Presence of bacteria ↑ TEM 	<ul style="list-style-type: none"> Presence of bacteria ↑ INV 	Hind et al., 2018
Neutrophils Neutrophils in whole blood	Endothelial channel iPSC-ECs	-	fMLP (10 μM) IL8 (11 μM)	Collagen gel	-	<ul style="list-style-type: none"> Effect on TEM for purified neutrophils and whole blood : fMLP = IL-8 	<ul style="list-style-type: none"> Effect on INV for purified neutrophils : fMLP < IL8 Effect on INV for whole blood : fMLP > IL-8 	Ingram et al., 2018
Neutrophils	Endothelial Channel HUVECs	-	IL8 (n.d.)	Collagen gel	Migratory and non-migratory neutrophils	<ul style="list-style-type: none"> IL8 ↑ TEM of migratory neutrophils EVM continuity (no cells in gel) ↑ TEM 	-	McMinn et al., 2019
Monocytes	Endothelial monolayer Porous membrane separating endothelial cells and EVM HUVECs	Fluid flow (400 μL/min) for endothelial cell pre-conditioning	MCP-1 (50 ng/mL)	Titanium microbeads in the extravascular chamber	-	<ul style="list-style-type: none"> MCP-1 ↑ TEM Fluid flow ↑ TEM 	-	Sharifi et al., 2019

When available, primary and secondary outcomes have been summarized.

The symbols indicate if the analyzed factor increases (↑), decreases (↓), or does not affect (=) any extravasation step (ADH, adhesion; TEM, transendothelial migration; INV, invasion). When a single arrow is present, the increase/decrease is defined respect to a control condition. In the case of factor intensity correlating with effect intensity, two symbols are present to indicate the direct or inverse correlation. When the shear rate was indicated in the paper, we calculated the corresponding shear stress value, considering a medium viscosity equal to 0.0002 Pa × s (Raimondi et al., 2002). (MVN, microvascular network; HMECs, human microvascular endothelial cells; HUVECs, human umbilical vein endothelial cells; iPSC-ECs, induced pluripotent stem cell-derived endothelial cells; EVM, extravascular matrix).

static condition, whereas it increased the migration distance of cancer cells in the extracellular environment possibly due to the generation of an interstitial flow within the extravascular

environment (Jeon et al., 2015). Shear stress was also shown to negatively correlate with the adhesion of breast cancer cells to the endothelium, since a shear stress of 0.16 dyn/cm²

TABLE 3 | Features of the studies focusing on the interaction between cancer cell and immune cells in the process of extravasation.

Extravasating Cells	Endothelial setting	Biophysical Factors	Biochemical factors	Environmental factors	Cell features	Primary outcome(s)	Secondary outcome(s)	References
A375 and A375-MA2 (melanoma) and MDA-MB-231 (breast cancer)	Self-assembled MVN HUVECs	Flow shear stress (~1 Pa) to perfuse cancer cells	-	Fibrin gel	Unstimulated and LPS-stimulated neutrophils	• Neutrophils and LPS-stimulated neutrophils ↑ TEM of cancer cells	• LPS-stimulated neutrophils ↑ ADH of cancer cells	Chen et al., 2018
MDA-MB-231 (breast cancer) and MDA-MB-435 (melanoma) Monocytes	Self-assembled MVN HUVECs	-	-	Fibrin gel Lung fibroblasts in EVM	Inflammatory and patrolling monocytes	<ul style="list-style-type: none"> • Inflammatory monocytes ↑ TEM respect to patrolling monocytes • Intravascular monocytes ↓ TEM of cancer cells • Extravascular monocyte-derived • macrophages = TEM of cancer cells 	-	Boussommier-Calleja et al., 2019
MDA-MB-231 (breast cancer) Monocytes	Endothelial channel HMECs	-	-	Collagen gel	-	<ul style="list-style-type: none"> • Extravasating monocytes ↑ TEM of cancer cells • Extravascular monocyte-derived • macrophages ↑ TEM of cancer cells 	<ul style="list-style-type: none"> • Extravascular monocyte-derived macrophages ↑ INV of cancer cells 	Kim et al., 2019

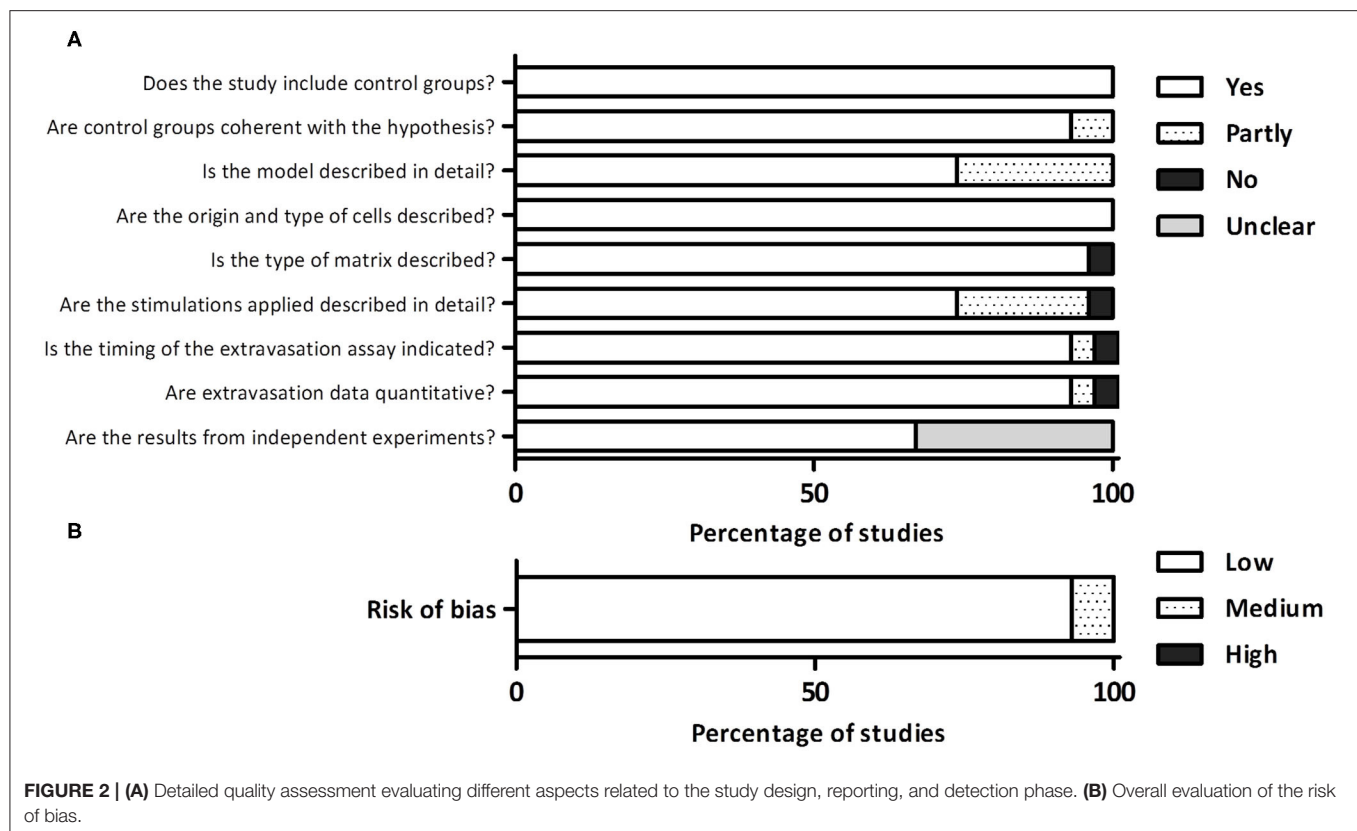
When available, primary and secondary outcomes have been summarized. The symbols indicate if the analyzed factor increases (↑), decreases (↓), or does not affect (≡) any extravasation step (ADH, adhesion; TEM, transendothelial migration; INV, invasion). When a single symbol is present, the increase/decrease is defined respect to a control condition. In the case of factor intensity correlating with effect intensity, two symbols are present to indicate the direct or inverse correlation (MVN, microvascular network; HMECs, human microvascular endothelial cells; HUVECs, human umbilical vein endothelial cells; EVM, extravascular matrix).

within an endothelialized channel reduced cancer cell adhesion compared to a half-shear stress value (0.08 dyn/cm²). This trend was present also when an inflammatory stimulus was added, once again showing the prevalent effect of shear stress over inflammation, although a higher number of cells adhered to the endothelium compared to a healthy condition (Mollica et al., 2019).

Besides the direct influence on the extravasating cells, shear stress can also have an indirect effect, through the modification of endothelial properties. A shear stress of 0.25 dyn/cm² applied in a microvascular network decreased the endothelial permeability compared to static conditions, possibly due to the tightening of endothelial cell junctions (Jeon et al., 2015). In line with this result, 10-fold lower shear stress values applied on an endothelial monolayer were sufficient to induce the expression of VE-cadherin and ZO-1, both involved in the formation of endothelial cell junctions (Liu et al., 2019). However, a minimal shear stress threshold to induce modifications in endothelial cell behavior seems to exist, since VE-cadherin and ICAM-1, an adhesion molecule involved in leukocyte-endothelial cells interactions, were not upregulated by a 100-fold lower value of shear stress (Sharifi et al., 2019). Altogether, these results suggest that shear

stress is important for the formation of an intact endothelial barrier mediating the first step of the extravasation process, even though the values of shear stress tested *in vitro* are far below the physiological values.

Although the shear stress stimulation is mostly used to mimic the flow conditions to which endothelial cells are exposed *in vivo*, it can also be used to mechanically stimulate the cells of the extracellular environment to investigate its effect on the process of cell extravasation. To this purpose, an oscillatory fluid flow (1 Pa, 1 Hz) was applied to stimulate osteocytes mimicking the interstitial shear stress experienced by bone cells *in vivo*. When bone cells were stimulated, the extravasation and migration distance of breast cancer cells decreased, highlighting how biophysical stimulation, modifying the behavior of the extravascular environment, can play a role in the extravasation of cancer cells (Mei et al., 2019). Beside shear stress, other biophysical stimuli can affect the extravascular environment and, subsequently, cell extravasation. For instance, microfluidic models applying mechanical stimuli, such as compression (Occhetta et al., 2019) or stretch/strain (Gaio et al., 2016), have been recently developed showing important effects on the stimulated tissues. Similar technological solutions could



be also implemented in models designed to investigate cell extravasation to correlate the behavior of extravasating cells with the reaction of the extravascular environment to biophysical stimuli. Furthermore, recent advances in microengineering have allowed the generation of more physiologically relevant microenvironments in which more than one type of biophysical stimuli can be applied (Kaarj and Yoon, 2019). However, despite these recent advances and the potential of microfluidic models to implement a variety of biophysical stimuli, among the 27 articles analyzed in this review, shear stress was the only biophysical stimulus that was investigated in relation to the cell extravasation process and, for this reason, the only one described here.

Summarizing, higher shear stress values decreased the extravasation of both immune and cancer cells, reducing their adhesion to the endothelium and increasing the tightness of the endothelial barrier. The ability of microfluidic systems to apply shear stress in vascularized channels allowed evaluating differences in endothelial permeability and in cell extravasation, which are hardly detectable with other models. Furthermore, the possibility to implement channels with a desired geometry highlighted that shear stress cannot be considered as a single element affecting the extravasation process, but it should be analyzed in combination with the geometrical features of the vascular environment because these two elements act together in determining cell trajectories and the probability of the circulating cells to adhere to the endothelium and, hence, transmigrate.

Effect of Biochemical Factors

Among different biochemical stimuli present in the microenvironment, those related to inflammation and chemotaxis play a key role in the extravasation of immune and cancer cells. Inflammation is a body response activated by toxic stimuli and pathological conditions, such as infections or tissue injuries (Medzhitov, 2008), but it is also a hallmark of cancer, involved in the development and progression of malignancies (Diakos et al., 2014). Inflammation influences cell extravasation mainly through a modulation of endothelial properties, decreasing the tightness of endothelial junction (Mollica et al., 2019) and leading to a higher permeability of the endothelial barrier (Chen et al., 2013; Menon et al., 2017; Mollica et al., 2019). Chemotaxis is fundamental for the homeostatic trafficking of immune cells and for the enrollment of leukocytes to infection and inflammation sites (Luster, 2001). Chemotaxis is also involved in each step of cancer spread, leading to metastasis formation (Roussos et al., 2011). Chemoattractants and their receptors act as mediators in the chemotaxis of cancer cells, stromal cells, and cancer-associated inflammatory cells. When the regulation of these mediators is unbalanced, spreading, and progression of cancer is favored, determining a dramatically more efficient cancer dissemination (Roussos et al., 2011).

Among the 27 selected articles, 13 studies investigated the effect of biochemical stimulations on the extravasation process. Among these, 4 studies applied an inflammatory stimulus and 10 tested the effect of chemoattractants.

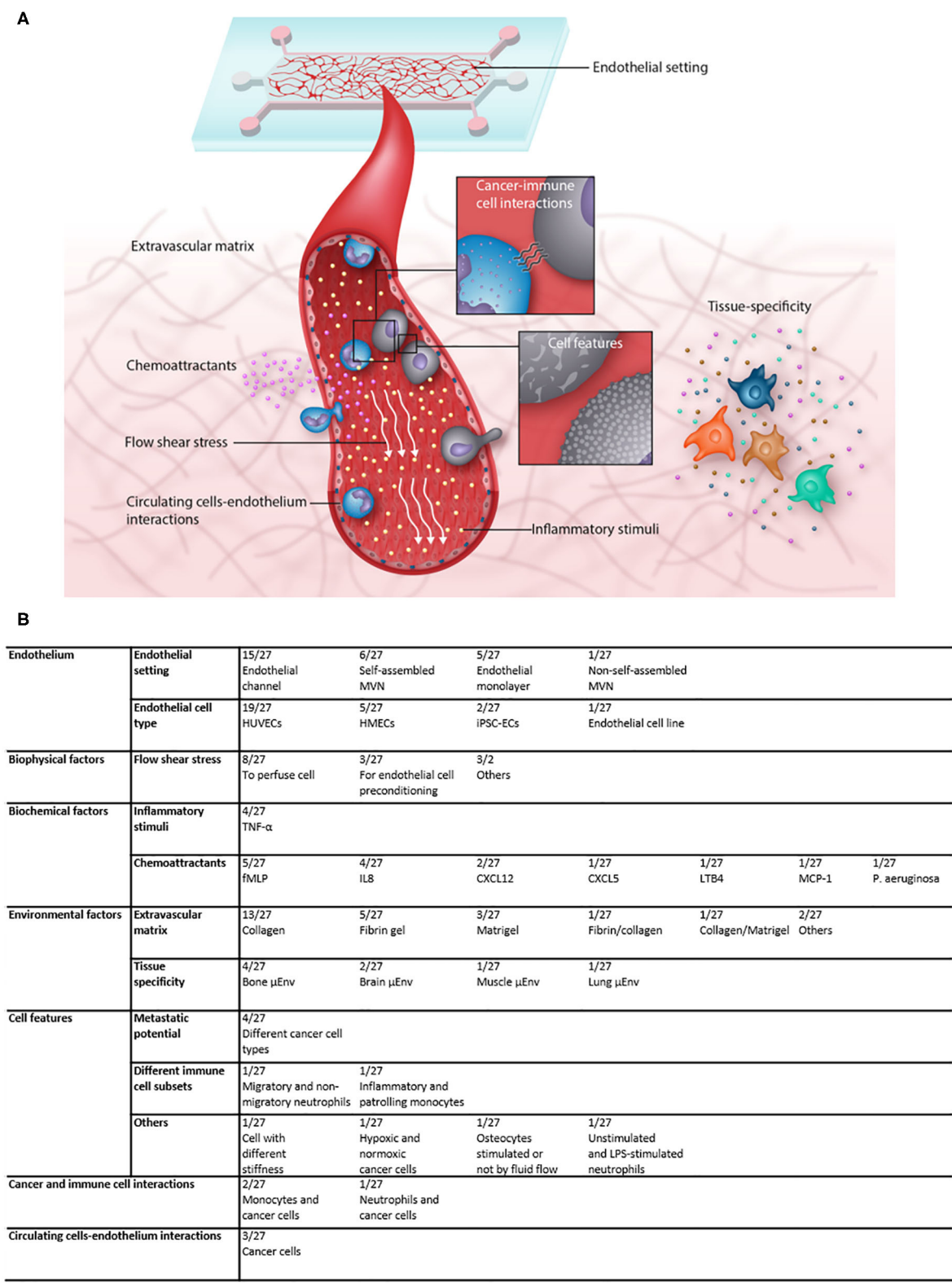


FIGURE 3 | (A) Illustration showing the multiple factors that contribute to the complexity of microfluidic extravasation models and the factors that can be investigated in such models. **(B)** Table recapitulating the features of the analyzed articles and the frequency with which each factor was applied and/or analyzed.

Microfluidic models are highly suitable for investigating the effects of biochemical stimuli on extravasation because they allow introducing external factors in the system to model specific *in vivo* conditions. This strategy consents to achieve the spatial and temporal control of biochemical gradients at relevant dimensions and time scales, which could not be obtained in traditional 2D cultures. The use of microfluidic models has allowed recapitulating gradients of hormones, growth factors, cytokines, and other biomolecules that play a fundamental role in processes such as angiogenesis, tumorigenesis, and cells migration, leading to an improvement in understanding of cells motility due to chemical gradients (Young and Beebe, 2010).

With regards to the investigation of the role of inflammation in extravasation, microfluidic models consent to generate gradients of inflammatory factors, usually TNF- α . These factors can be directly diluted into the culture medium (Chen et al., 2013; Menon et al., 2017) or incorporated into a gel (Mollica et al., 2019). The latter approach better mimics the physiological origin of the inflammatory stimuli, which usually takes place deep in the tissue, and eventually reaches the endothelial barrier. When supplemented directly in the medium, TNF- α is usually added in a concentration of 10 ng/mL, whilst its addition in the gel needs a higher concentration to reach a biological effect (Mollica et al., 2019). It is fundamental to apply the correct dose of inflammatory factors, considering that they can be cytotoxic when used at high concentrations, both on extravasating cells and on endothelial cells. As for the biological effect, also the cytotoxic effect depends on the mode of application and on the timing. A concentration of 10 ng/mL directly imposed on endothelial cells was reported to be toxic, leading to cell death and ruptures in a self-assembled microvasculature (Chen et al., 2013), while no toxic effect occurred at higher concentration of TNF- α (50 ng/mL) when the molecule was included in a gel (Mollica et al., 2019).

Exploiting microfluidic models, it has been demonstrated how TNF- α modulates endothelial intercellular adhesion and increases vascular permeability, allowing to better understand the influence of inflammatory stimuli on cell extravasation. These effects can be directly visualized by perfusing fluorescent dextran or μ m-sized fluorescent polystyrene beads into the endothelial channel (Chen et al., 2013; Menon et al., 2017; Mollica et al., 2019). The increase of the endothelial barrier permeability indicates a loosening of cell junctions and correlates with an increase in cancer cells transendothelial migration (Chen et al., 2013). Another effect of inflammation that has been observed in microfluidic models is the higher expression of specific molecules by endothelial cells, such as adhesion receptors and integrins, which promotes cancer-endothelial cell adhesion and contributes to increase the number of extravasated cancer cells (Mollica et al., 2019). Inflammatory stimuli have been also applied to promote the interaction between neutrophils and endothelium, which are essential to reproduce the pathological inflammatory state typical of cardiovascular diseases (Menon et al., 2017).

Beyond inflammatory factors, microfluidic models permit to create gradients of chemoattractants, by incorporating them

directly into the extravascular matrix (Han et al., 2012; Menon et al., 2017; Sharifi et al., 2019) or by diluting them into the medium placed in a separate compartment or channel of the microfluidic device (Lamberti et al., 2014; Wu et al., 2015; Roberts et al., 2016; Ingram et al., 2018). The profile and the stability of the chemical gradient can be simulated with a FEM (finite element method) software (Han et al., 2012; Wu et al., 2015), and the results can be easily compared with empirical tests conducted using a fluorescent tracer with a molecular weight comparable to that of the chemoattractant (Wu et al., 2015). As an alternative, chemoattractant factors imposed through the gel can be quantified in the medium collected over time to obtain a release profile (Sharifi et al., 2019).

Chemoattractants with a well-defined effect have been exploited in microfluidic models to validate their own ability to reproduce a specific pathologic microenvironment. In this scenario fMLP (formyl-methionyl-leucyl-phenylalanine) has been used to validate a new microfluidic system to study neutrophil motility and extravasation (Hind et al., 2018). MCP-1 (Monocyte Chemoattractant Protein-1) was used to validate a Foreign Body Response-on-a-Chip platform designed to study monocyte extravasation during implant-induced inflammation (Sharifi et al., 2019). Concerning cancer extravasation models, a gradient of SDF-1 α (Stromal Derived Factor-1 α) was applied to induce the extravasation of breast cancer cells and validate a platform for the study of single cell extravasation (Roberts et al., 2016).

Through the design of the microfluidic device, chemoattractant factors can also be studied in competition with each other to establish a chemoattractant hierarchy. The superior chemoattractant effect of fMLP as compared to IL8 (Interleukin-8) was proven analyzing neutrophils movement during the initial transendothelial migration phase and in the subsequent migration into the extravascular matrix (Han et al., 2012) in the presence of both molecules. Using another model, where neutrophils were simultaneously subjected to the stimuli of two diverse factors coming from two opposite ends of the migration channel, a similar chemoattractant hierarchy was proven. LTB4 and fMLP showed a similar ability in inducing neutrophil transendothelial migration, which was higher compared to that of IL8, in line with findings showing a prevalent effect for LTB4- and fMLP-activated signaling pathways (Wu et al., 2015).

Agents targeting chemotaxis have been tested in microfluidic models with the aim to develop new therapeutic strategies. Human monoclonal anti-FPR1 antibody and Wortmannin (a fungal metabolite), were shown to be effective in impeding neutrophil migration to fMLP (Han et al., 2012; Lamberti et al., 2014). A similar approach was applied to hinder the migration of cancer cells, using a CXCR4 (CXCL12 receptor) antagonist, which blocked the transendothelial migration of cancer aggregates (Zhang et al., 2012). Finally, cancer cell extravasation was blocked through the use of an antibody directed against a cancer cell surface receptor (CXCR2) specific for a chemokine, CXCL5, secreted by osteoblastic cells (Bersini et al., 2014).

To summarize, in the analyzed articles the effect of an induced inflammatory state was mainly studied in relation to its effect on endothelium activation and permeability, while the effect of chemoattractants was tested with different purposes depending on the scientific hypothesis of the study. In models investigating immune cells, chemoattractants were mainly applied to validate new microfluidic models or test different chemoattractant factors in competition. In cancer cell extravasation models, the studies were more focused in identifying strategies to block the effect of chemoattractants on cancer cells, with the final goal of finding a strategy to impede the metastatization process. The possibility to measure endothelial permeability in the context of a 3D microenvironment allowed correlating the modification of endothelial junctions induced by inflammatory factors with an increased cell extravasation. Furthermore, the possibility to generate controllable and measurable gradients of chemotactic factors empowered the identification of molecules and signaling pathways involved in the cell extravasation process, that can be pharmacologically inhibited or enhanced depending on the desired outcome. That leads to the exploitation of these models as platforms for the screening of new therapeutic agents.

Effect of Environmental Factors

The reproduction of some characteristics and properties of tissue-specific microenvironments in particular the 3D structure, in a microfluidic model is obtained through the use of hydrogels to form an extravascular matrix (EVM). *In vivo*, the EVM is a dynamic and intricate structure composed by hundreds of diverse proteins, including matrix proteins, growth factors, cytokines, and several bioactive products deriving from matrix degradation and impacting cellular differentiation, proliferation, and migration (Boyd and Thomas, 2017). In microfluidic models, the EVM is not so complex, but still provides cells with a 3D environment which facilitates the maintenance of cell function and is enriched over time by cell-produced molecules. The introduction of a 3D EVM in microfluidic devices for the study of extravasation represents a step forward compared to standard models, such as transwell models, due to a better reproduction of a functional endothelial barrier and the possibility to decouple the results from the gravitational effect. The EVM can also embed tissue-specific cells, allowing to reproduce even better a tissue-specific microenvironment in microfluidic models.

Among the 27 articles included in this review, 8 articles correlated the cellular extravasation process to the features of the extravascular matrix and 7 introduced tissue-specific cells to study the extravasation of cancer cells. Among these, 5 studies dissected the contribution of tissue-specific cells to the extravasation process compared to a control condition.

Collagen and fibrin gel, alone or in combination, are the hydrogels mainly used to reproduce the EVM. The use of collagen and fibrin allows modulating the mechanical features of EVM, since it is possible to vary collagen stiffness by adjusting the pH before the polymerization (Han et al., 2012), whilst fibrin stiffness can be easily tuned by modulating the concentrations of fibrinogen and thrombin as well as the polymerization conditions (Ingram et al., 2018). Alternatively, Matrigel, which is a widely used substrate for endothelial

cell culture and angiogenesis assays, has been also employed (Chaw et al., 2007; Roberts et al., 2016).

The choice of EVM is crucial, considering its role in the development of endothelial vessels. Vessels formed in fibrin gel show morphological elongation, characterized by tight cell junctions and vessel maturity, while vessels formed in collagen matrix lack morphological elongation, showing a leaky vessels phenotype and higher permeability, as demonstrated by FITC-dextran perfusion experiments (Ingram et al., 2018). These differences are particularly relevant considering the close correlation between the tightness of the endothelium and cell extravasation.

Beyond the effects on the endothelium, stiffness and porosity of the matrix can directly affect cancer and immune cell extravasation. Firstly, these matrix properties affect the passive diffusion of biochemical gradients imposed across the EVM. Additionally, EVM stiffness can directly influence cancer cell motility since cells tend to move toward more rigid ECM, with a process called durotaxis (Roberts et al., 2016). On the contrary, matrix stiffness can represent an obstacle for cell migration, as shown in the case of neutrophils whose migration was decreased in correspondence of higher stiffness of collagen matrix (Han et al., 2012).

The introduction of tissue-specific cells allows reproducing different tissue-specific microenvironments. Bone tissue represents one of the most investigated extravasation site, being acknowledged as a fertile metastatic target for various tumors, such as breast, prostate, thyroid, lung, bladder, renal carcinoma, and melanoma (Arrigoni et al., 2016, 2017; Macedo et al., 2017). The first reported approach aimed at reproducing bone tissue in microfluidic models was based on the inclusion of osteo-differentiated bone marrow-derived mesenchymal stem cells in a hydrogel matrix. Using this strategy, the extravasation and migration of breast cancer cells was shown to be higher in a bone microenvironment compared to empty EVM (i.e., without any cell), used as a control to prove that tissue specific cells do play a role in the process (Bersini et al., 2014). Additionally, bone- and muscle-mimicking microenvironments were compared, demonstrating the preferential extravasation of breast cancer cells toward the bone microenvironment (Jeon et al., 2015). These results are in accordance with the clinical data that indicate bone and muscle as a preferential and non-preferential metastatization site for breast cancer, respectively, proving that the model recapitulates the *in vivo* situation. The use of these muscle-specific models allowed also identifying the adenosine secreted by myoblasts as a protective agent against metastatization, leading to a better insight into the mutual interactions between microenvironment and extravasating cells (Jeon et al., 2015). The comparison between these two tissues also showed that the network developed into the muscle-mimicking microenvironment is characterized by higher permeability compared to the bone-like microenvironment, although the cancer extravasation rate was higher in the latter. This result decouples the direct correlation between the endothelial permeability and the extravasation rate, proving that this process is affected by multiple factors, among which the microenvironmental conditioning and the

presence of cell-secreted molecules play a critical role. *In vivo*, tissues are exposed also to specific mechanical stimuli, which are particularly important in the case of bone tissue. To study their influence on metastatic cell extravasation, bone cells cultured on a layer of collagen I in the EVM compartment were exposed to an oscillatory flow, to generate a mechanically-stimulated bone microenvironment that was compared to the unstimulated conditions. A decrease in the extravasation rate and migration distance of breast cancer cells was shown in the case of mechanical stimulation of bone cells, showing a protective effect of mechanical loading against the formation of bone metastasis (Mei et al., 2019).

The brain environment has been also object of study since brain metastases are among the most lethal events in cancer progression. In this context, to mimic *in vitro* the brain parenchyma toward which cancer cells extravasate, astrocytes were introduced in the EVM. The presence of brain specific cells combined with flow stimulation increased the tightness of brain-specific microvessels forming the blood-brain barrier by decreasing the endothelial permeability if compared to conditions without astrocytes and shear stimulus. These results indicate that astrocytes modify the endothelium properties and that this might change the cancer cell extravasation outcomes, approaching a condition more similar to the *in vivo* situation (Liu et al., 2019).

While tissue-specificity represents a key factor driving cancer cells extravasation, there is no evidence that it significantly influences the extravasation of leukocytes. Leukocyte extravasation has been generally considered as uniform between different tissues. However, in some organs the mechanisms guiding leukocyte extravasation can differ from the classical leukocyte adhesion cascade due to a peculiar structure of the endothelium, which can be fenestrated or discontinuous (e.g., in the bone marrow), and for the proteins involved in the different steps of leukocyte extravasation process (Maas et al., 2018). Among the analyzed studies, none investigated the influence of tissue-specific microenvironments on immune cell extravasation, probably due also to the difficulty in finely reproducing *in vitro* an endothelium with tissue-specific features in terms of endothelial cell organization and tightness.

In this context, beyond the presence of tissue-specific cells in the model, the presence of a tissue-specific endothelium would allow the study of cancer cell and leukocyte extravasation with a higher reliability, since the phenotypic traits of the endothelium strongly depends on its anatomical origin (Marcu et al., 2018). One of the studies analyzed in this review introduced a brain-specific endothelium mimicking the blood-brain barrier (Liu et al., 2019). However, the results on extravasation were not compared with those obtained with a non-specific endothelium, which did not allow a direct confirmation of the effects of a tissue-specific endothelium on extravasation. Among the 27 articles included in this review, 19 reproduced the endothelium by using HUVECs, regardless of the tissue under investigation. Indeed, HUVECs represent the most common source of primary endothelial cells used in *in vitro* models (Kocherova et al., 2019) due to the wide availability and easier culture protocols. On the contrary, tissue-specific endothelial cells are scarcely available

commercially and difficult to isolate from human tissues, which hampers their easy translation into *in vitro* settings. To overcome these major limitations, a possible alternative to the isolation of tissue-specific endothelial cells is the induction of a tissue-specific phenotype in HUVECs, by co-culturing them with tissue-specific cells, which has been shown to promote the acquisition of endothelial phenotypic tissue-specificity (Visone et al., 2016; Bersini et al., 2018a).

Summarizing, the presence of vascular channels or vascular networks associated to a tissue-specific environment in microfluidic models allowed evidencing the effect of EVM and tissue-specific cells on the properties of endothelium and on cell extravasation. The possibility to tailor the microenvironment (e.g., modifying matrix mechanical properties or including cells secreting tissue-specific molecules) allowed the study of the crosstalk between circulating and tissue-specific cells, thanks to the possibility of testing multiple combinations of cells in a standardized environment where circulating and tissue-specific cells are the only variables. Although this approach neglects some fundamental factors that play a role *in vivo*, such as the degree of vascularization, tissue-specific matrix composition and endothelium structure, it allows shading light on protective factors secreted by tissue-specific cells as well as on factors determining the pro-metastatic behavior of some tissues, which could find an application as preventive therapy against cancer metastatization.

Effect of Cell Features and Interactions Between Cancer and Immune Cells

The fate of a circulating cell from blood vessels to extravascular tissue-specific environments is not determined only by biochemical, biophysical, and environmental features, but also by own cell features that can determine its probability to extravasate. The intrinsic ability of a cancer cell to extravasate is related to its metastatic potential, defined as the ability to invade specific secondary organs. Similarly, leukocytes have different ability to extravasate during inflammation based on their phenotype and function. Among single cell features determining the ability to extravasate, cell deformability has been particularly studied, since it influences different steps of the metastatic cascade in which cells leave the primary site of tumor, circulate in the bloodstream, and extravasate (Swaminathan et al., 2011). Indeed, cancer cells deform to pass through endothelial cell junctions during both the intravasation and the extravasation processes and they need also to deform to avoid being stuck in small capillary vessels (Hu et al., 2018). Beside the properties of single circulating cells, the interplay between cancer cells and leukocytes is increasingly being investigated to determine its influence on cancer extravasation and metastasis formation. Leukocytes have been shown to be actively involved in tumor progression and metastasis formation with conflicting results. In some cases leukocytes have been shown to promote the extravasation of cancer cells (Liang et al., 2010), whilst in other cases they have been shown to hamper cancer dissemination by provoking tumor death, thus representing interesting candidates for the development of immunotherapies (Lanca and Silva-Santos, 2012).

Among the 27 studies included in this review, 4 studies investigated the effects of the cancer cell properties on extravasation, 2 papers studied the influence of leukocyte subpopulation (1 for monocytes and 1 for neutrophils), and 3 investigated the interactions between leukocytes and cancer cells.

To study the effect of circulating cells properties and of their interactions on the extravasation process, microfluidic models are key tools, since they permit to visualize cell deformation and interactions within an *in vivo*-like environment through high resolution imaging techniques. Furthermore, microfluidic models can well reproduce the organization of the intravascular and extravascular spaces if compared to standard 2D culture systems, allowing to monitor if leukocytes affect the metastasis formation when they are inside the vessels and/or when they are already infiltrated in the tissues. As mentioned before, the microfluidic models that can be used to investigate these processes can be classified in two different types, being either based on an endothelialized channel in which an endothelial monolayer divides the EVM from the intravascular space or through gel-embedded endothelial cells self-assembling in a 3D microvascular network surrounded by the EVM. This latter system, beyond providing a more physiological-like structure of the vessels, also allows a better real-time monitoring of cell interactions (e.g., clusters) within the vessel or with the endothelium.

To study the influence on extravasation of cell deformation in small vessels, microfluidic models including 10 μm microgaps mimicking blood capillaries were generated. Different types of cancer cells injected through these capillaries-like structures under flow showed a different mechanical deformation. Higher cell stiffness was correlated with higher cell viability after deformation, but it did not result in a different number of extravasated cells or migration distance (Chaw et al., 2007). The possibility to monitor in real-time cell transendothelial migration within a microvascular network allowed studying how cancer cells deform while crossing the endothelial barrier. Additionally, differences were observed in the extravasation of single circulating cells compared to cell clusters and of adherent cells compared to mechanically trapped cells (Chen et al., 2013).

Besides investigating the effects of cell deformation, microfluidic models were exploited to distinguish the extravasation ability of cancer cells with a different degree of malignancy (Chen et al., 2013) as well as of cancer cells originating from different primary tumors (Tourovskaya et al., 2014). For instance, the presence of hyaluronan in the pericellular matrix of breast cancer cells (Brett et al., 2018) or the expression of specific proteins implicated in brain cancer development (Liu et al., 2019) were studied in relation to the metastatic potential of cancer cells, demonstrating that microfluidic extravasation models are able to capture differences in cell malignancy and allow identifying some of the elements responsible of a high metastatic potential. Breast cancer cells with different metastatic potential were also pre-conditioned in hypoxic conditions before injection in a microfluidic device, demonstrating that hypoxic cells have a higher extravasation rate compared to normoxic cells (Song et al., 2018). The primary tumor from which metastatic cells originate can also heavily influence their extravasation

potential in relation to tissue-specific metastatization sites. Cells from breast, bladder and ovarian cancer in a microfluidic model displayed a different affinity toward a bone-mimicking microenvironment, with the bladder cancer cells showing the highest extravasation rate and migration distance and the ovarian cancer cells the lowest (Bersini et al., 2018b). These results are in line with clinical evidence demonstrating that different types of cancer preferentially invade different secondary organs.

Similar to cancer cells, leukocytes showed differences in the extravasation potential between different leukocyte subsets. Exploiting a microfluidic system allowing the physical separation of the extravascular and intravascular environment, a separate analysis of extravasated and non-extravasated neutrophils allowed studying the transcriptional profile of migratory and non-migratory neutrophil subsets (McMinn et al., 2019). Another model was applied to investigate the extravasation ability of different monocyte subsets, demonstrating that inflammatory monocytes have a superior TEM rate than patrolling monocytes (Boussommier-Calleja et al., 2019).

During extravasation, cancer cells interact with the endothelium and modify its microarchitecture. In this context, breast cancer cells characterized by invasive phenotype were shown to directly modify the function of the endothelium by increasing endothelial permeability compared to a non-tumorigenic cell line (Jeon et al., 2013). The negative influence of cancer cells in the maintenance of an intact endothelium was observed through fluorescence microscopy imaging. Immunofluorescence analysis allowed to obtain information about the endothelium integrity through the visualization of two tight junction proteins, ZO-1 and VE-cadherin, expressed by endothelial cells, both showing a decreased expression during cancer cell extravasation (Liu et al., 2019). The mechanisms that leads to endothelium disruption by cancer cells have not yet been clarified and can either depend on a local damage of the endothelium by cell contact or on the secretion of factors affecting the endothelial cell junctions. High resolution imaging showed the formation of gaps in the endothelial barrier during the physical passage of cancer cells, followed by intact endothelial cell-cell junctions immediately after the extravasation of cancer cells. This data reveals that the damage of the endothelial barrier is not irreversible, supporting the hypothesis that cancer cells might regulate the endothelial permeability through the secretion of biochemical factors (Chen et al., 2013).

Regarding the interactions between cancer cells and monocytes, both circulating monocytes and monocyte-derived macrophages resident in tissue EVM have been studied within microfluidic models. Circulating monocytes perfused together with breast cancer cells in a microvascular network were shown to decrease cancer cell extravasation rate. Since monocytes did not show prolonged contact with cancer cells in the microvessels, this effect probably depended on paracrine signaling rather than cell-cell contact. On the other hand, monocyte-derived macrophages present in the EVM did not affect cancer cell extravasation, suggesting a role of monocytes in cancer extravasation when they are inside the vessels but not when they are in the tissue (Boussommier-Calleja et al., 2019). Partially in contrast with this last result, human monocytes extravasated to

the EVM were shown to promote breast cancer cell extravasation as a result of MMP9 secretion, which caused the disruption of the endothelial barrier, and of the decreased expression of two tight junction proteins, ZO-1 and Occludin. The same study showed that monocyte-derived macrophages generated microtracks in the EVM, thus facilitating cancer cell migration and matrix invasion (Kim et al., 2019). The role of circulating leukocytes in cancer can be also influenced by the presence of inflammatory conditions. Indeed, inflamed neutrophils injected in a microvascular network model aggregated with circulating melanoma cells, facilitating the adhesion of cancer cells to endothelial cells. The confinement of these aggregates to the endothelium was favored by the secretion of IL8 from neutrophils and correlated with a higher extravasation of cancer cells (Chen et al., 2018).

Although the features of cancer and immune cells can be investigated also with standard *in vitro* and *in vivo* models, high-resolution real-time analyses that can be performed in microfluidic models allowed elucidating how certain cell features can impact on the ability of the cell to cross the endothelial barrier and evidencing the mechanisms which are activated during this process. Furthermore, microfluidic models allow studying how cancer and immune cells can interact with each other in the intravascular and extravascular environment, producing an effect on cancer cell extravasation, due to their ability to dissect the effects of cellular interactions during each specific extravasation step.

SUMMARY

Cell extravasation is a highly regulated process through which cells leave the bloodstream, cross the endothelium and finally migrate into the tissues. As evidenced from the literature, several studies investigated this process for immune or cancer cells exploiting microfluidic devices, which were analyzed and compared in this systematic review. As mentioned above, the overall quality of studies describing the application of microfluidic extravasation models is high. However, improvements could be pursued, mostly from a reporting aspect, in future studies. The understanding of microfluidic models design, as well as the localization of the different cell/matrix components in the systems is not always easy. The use of scientific illustrations, providing a graphical scheme of the model and highlighting how the different elements of the model mimic the *in vivo* situation, would significantly facilitate the comprehension of the studies. Additionally, we encourage authors applying biophysical and biochemical factors in their microfluidic models to describe in detail the methodology. For biochemical factors, it is essential to describe the concentration of the factor and the timing of application. Also, if a biochemical gradient is present, the way it is generated and maintained should be clearly indicated and the gradient should be characterized by computational modeling and/or experiments with fluorescent tracers over time. For what concerns biophysical factors, we found that flow shear stress is the factor most often applied. In this case, we encourage

authors to clearly state the purpose and the timing of flow shear stress application. It should be clearly indicated in the materials and methods whether the application of a fluid flow is used to pre-condition endothelial cells, to seed extravasating cells or for any other purpose. Most of the times, this information is present throughout the text, but not clearly reported in the methodological section. Additionally, when fluid flow is applied, it would be very useful to indicate the levels of flow shear stress (in dyn/cm² or Pa), to allow the comparison among different studies independently from the size of the vascular channel.

Overall, our analysis of the results obtained using advanced 3D models for studying immune and cancer cell extravasation, highlighted differences and similarities between the two processes. The use of microfluidic models allowed distinguishing between direct and endothelium-mediated effects on extravasation. As an example, it has been evidenced that shear stress application reduced endothelial permeability, leading to a decrease in extravasation, whilst inflammatory conditions increased permeability, eventually reflecting in an increased ability to extravasate of both immune and cancer cells. Concerning the direct effects of biophysical stimulation, both immune and cancer cells preferably adhered and transmigrated through the endothelium in lower shear conditions. Although shear stress values were not perfectly matched with the physiological ones, they still allowed evidencing a negative correlation between cell adhesion/TEM and shear stress, which is corroborated by *in vivo* data both on cancer (Follain et al., 2018) and immune cells (Yang et al., 2018). Similar to the correlation between extravasation and shear stress, also chemoattractants showed an analog effect on the extravasation of immune and cancer cells. In particular, leukocytes extravasated only in the presence of specific chemotactic stimuli, as reported *in vivo* (Mitroulis et al., 2015), and the presence of specific chemotactic factors facilitated cancer cell extravasation (Wendel et al., 2012; Borsig et al., 2014), although it was not strictly required to induce the phenomenon. In this context, microfluidic extravasation models were exploited to identify strategies to block the effect of chemoattractants on cancer cells, with the final goal of finding a strategy to stop the metastatization process. A factor differently affecting cancer and immune cell extravasation is represented by the presence of a specific extravascular tissue. Results from microfluidic devices incorporating tissue-like microenvironments showed that the presence of tissue-specific cells plays a relevant role in the metastasis formation, as already hypothesized in the past (Paget, 1989). On the other side, leukocyte extravasation follows a cascade common to most of the human tissues (Maas et al., 2018), even if differences in EVM mechanical properties and endothelium structure have been found to affect leukocyte migration in the tissue. Microfluidic devices proved particularly suitable also to investigate the effects of intrinsic cell properties and of their interactions. As an example, it was possible to visualize the mechanism through which cancer and immune cells cross the endothelial barrier, showing how cancer cells damage the endothelium integrity, and a similar but temporary modification of endothelial junctions was seen also in extravasating leukocytes (Strell and Entschladen, 2008; Sokeland and Schumacher, 2019). Taken together, all these

results highlight how cancer and immune cell extravasation shows a similar susceptibility toward factors including shear stress, presence of inflammation, or chemoattractants, whilst immune cell, as opposed to cancer cell, extravasation seems not to be so influenced by tissue-specific factors such as cells included in the 3D matrix.

As described, the majority of these models derives results and takes into account only the effects of single stimuli or specific combinations of few variables, despite the complexity of this physiologically dynamic scenario. Differences and commonalities in immune and cancer cell extravasation emerging from these first uses of microfluidic devices could help in elaborating a common model of the process. The construction of such a model requires the integration of further elements, bringing forward the reproduction of the *in vivo* environment, while maintaining the advantages of a controlled and easy-to-monitor *in vitro* system. The ideal model should hence be able to mimic in a single, detailed vascularized microenvironment all the different aspects of the extravasation process independently from the considered cells. Indeed, ideally only by changing the extravascular environment (tissue-specific cells and EVM) and the extravasating cells, the system would allow a multifaceted analysis of the extravasation process within several different human tissues. Increasing the level of detail and enriching the microfluidic models with more and more elements will lead to a better understanding of this complex process, in view of the development of therapeutic strategies counteracting or enhancing the extravasation of the desired cell type.

REFERENCES

- AlShwaimi, E., Bogari, D., Ajaj, R., Al-Shahrani, S., Almas, K., and Majeed, A. (2016). *In vitro* antimicrobial effectiveness of root canal sealers against *Enterococcus faecalis*: a systematic review. *J. Endod.* 42, 1588–1597. doi: 10.1016/j.joen.2016.08.001
- Arrigoni, C., Bersini, S., Gilardi, M., and Moretti, M. (2016). *In vitro* co-culture models of breast cancer metastatic progression towards bone. *Int. J. Mol. Sci.* 17:1405. doi: 10.3390/ijms17091405
- Arrigoni, C., Gilardi, M., Bersini, S., Candrian, C., and Moretti, M. (2017). Bioprinting and organ-on-chip applications towards personalized medicine for bone diseases. *Stem Cell Rev. Rep.* 13, 407–417. doi: 10.1007/s12015-017-9741-5
- Bersini, S., Gilardi, M., Ugolini, G. S., Sansoni, V., Talo, G., Perego, S., et al. (2018a). Engineering an environment for the study of fibrosis: a 3D human muscle model with endothelium specificity and endomysium. *Cell Rep.* 25, 3858–3868. doi: 10.1016/j.celrep.2018.11.092
- Bersini, S., Jeon, J. S., Dubini, G., Arrigoni, C., Chung, S., Charest, J. L., et al. (2014). A microfluidic 3D *in vitro* model for specificity of breast cancer metastasis to bone. *Biomaterials* 35, 2454–2461. doi: 10.1016/j.biomaterials.2013.11.050
- Bersini, S., Miermont, A., Pavesi, A., Kamm, R. D., Thiery, J. P., Moretti, M., et al. (2018b). A combined microfluidic-transcriptomic approach to characterize the extravasation potential of cancer cells. *Oncotarget* 9, 36110–36125. doi: 10.18632/oncotarget.26306
- Bertulli, C., Gerigk, M., Piano, N., Liu, Y., Zhang, D., Muller, T., et al. (2018). Image-assisted microvessel-on-a-chip platform for studying cancer cell transendothelial migration dynamics. *Sci. Rep.* 8:12480. doi: 10.1038/s41598-018-30776-0
- Bianchi, E., Molteni, R., Pardi, R., and Dubini, G. (2013). Microfluidics for *in vitro* biomimetic shear stress-dependent leukocyte adhesion assays. *J. Biomech.* 46, 276–283. doi: 10.1016/j.jbiomech.2012.10.024

DATA AVAILABILITY STATEMENT

The original contributions presented in the study are included in the article/**Supplementary Material**, further inquiries can be directed to the corresponding author/s.

AUTHOR CONTRIBUTIONS

CA, MM, and SL conceived and designed the study. CM and MC conducted the literature search and screened for eligibility the literature records. CM, MC, and SL conducted the data extraction. CM and SL performed the quality and risk of bias assessment. CM, MC, CA, and SL wrote the manuscript. MM revised the manuscript and supervised the discussion on result organization and presentation. All authors contributed to the article and approved the submitted version.

FUNDING

CA and MM are supported by the Swiss National Science Foundation (SNF 310030_179167). This study was partially funded by the Italian Ministry of Health (RicercaFinalizzata PE-2013-02356613).

SUPPLEMENTARY MATERIAL

The Supplementary Material for this article can be found online at: <https://www.frontiersin.org/articles/10.3389/fbioe.2020.00907/full#supplementary-material>

- Borsig, L., Wolf, M. J., Roblek, M., Lorentzen, A., and Heikenwalder, M. (2014). Inflammatory chemokines and metastasis—tracing the accessory. *Oncogene* 33, 3217–3224. doi: 10.1038/onc.2013.272
- Boussommier-Calleja, A., Atiyas, Y., Haase, K., Headley, M., Lewis, C., and Kamm, R. D. (2019). The effects of monocytes on tumor cell extravasation in a 3D vascularized microfluidic model. *Biomaterials* 198, 180–193. doi: 10.1016/j.biomaterials.2018.03.005
- Boyd, D. F., and Thomas, P. G. (2017). Towards integrating extracellular matrix and immunological pathways. *Cytokine* 98, 79–86. doi: 10.1016/j.cyt.2017.03.004
- Brett, M. E., Bomberger, H. E., Doak, G. R., Price, M. A., Mc carthy, J. B., and Wood, D. K. (2018). *In vitro* elucidation of the role of pericellular matrix in metastatic extravasation and invasion of breast carcinoma cells. *Integr. Biol.* 10, 242–252. doi: 10.1039/C7IB00173H
- Brown, H. K., Schiavone, K., Tazzyman, S., Heymann, D., and Chico, T. J. (2017). Zebrafish xenograft models of cancer and metastasis for drug discovery. *Expert Opin. Drug Discov.* 12, 379–389. doi: 10.1080/17460441.2017.1297416
- Chaw, K. C., Manimaran, M., Tay, E. H., and Swaminathan, S. (2007). Multi-step microfluidic device for studying cancer metastasis. *Lab Chip* 7, 1041–1047. doi: 10.1039/b707399m
- Chen, M. B., Lamar, J. M., Li, R., Hynes, R. O., and Kamm, R. D. (2016). Elucidation of the roles of tumor integrin beta1 in the extravasation stage of the metastasis cascade. *Cancer Res.* 76, 2513–2524. doi: 10.1158/0008-5472.CAN-15-1325
- Chen, M. B., Whisler, J. A., Jeon, J. S., and Kamm, R. D. (2013). Mechanisms of tumor cell extravasation in an *in vitro* microvascular network platform. *Integr. Biol.* 5, 1262–1271. doi: 10.1039/c3ib40149a
- Chen, Z., Tang, M., Huang, D., Jiang, W., Li, M., Ji, H., et al. (2018). Real-time observation of leukocyte-endothelium interactions in tissue-engineered blood vessel. *Lab Chip* 18, 2047–2054. doi: 10.1039/C8LC00202A

- Coughlin, M. F., and Kamm, R. D. (2020). The use of microfluidic platforms to probe the mechanism of cancer cell extravasation. *Adv. Healthc. Mater.* 9:e1901410. doi: 10.1002/adhm.201901410
- Diakos, C. I., Charles, K. A., Mcmillan, D. C., and Clarke, S. J. (2014). Cancer-related inflammation and treatment effectiveness. *Lancet Oncol.* 15, 493–503. doi: 10.1016/S1470-2045(14)70263-3
- Follain, G., Osmani, N., Azevedo, A. S., Allio, G., Mercier, L., Karreman, M. A., et al. (2018). Hemodynamic forces tune the arrest, adhesion, and extravasation of circulating tumor cells. *Dev. Cell* 45, 33–52. doi: 10.1016/j.devcel.2018.02.015
- Gaio, N., Van Meer, B., Quiros Solano, W., Bergers, L., Van De Stolpe, A., Mummery, C., et al. (2016). Cytostretch, an organ-on-chip platform. *Micromachines* 7:120. doi: 10.3390/mi7070120
- Golbach, L. A., Portelli, L. A., Savelkoul, H. F., Terwel, S. R., Kuster, N., De Vries, R. B., et al. (2016). Calcium homeostasis and low-frequency magnetic and electric field exposure: a systematic review and meta-analysis of *in vitro* studies. *Environ. Int.* 92–93, 695–706. doi: 10.1016/j.envint.2016.01.014
- Gomez-Cuadrado, L., Tracey, N., Ma, R., Qian, B., and Brunton, V. G. (2017). Mouse models of metastasis: progress and prospects. *Dis. Model. Mech.* 10, 1061–1074. doi: 10.1242/dmm.030403
- Han, S., Yan, J.-J., Shin, Y., Jeon, J. J., Won, J., Eun Jeong, H., et al. (2012). A versatile assay for monitoring *in vivo*-like transendothelial migration of neutrophils. *Lab Chip* 12, 3861–3865. doi: 10.1039/c2lc40445a
- Hind, L. E., Ingram, P. N., Beebe, D. J., and Huttenlocher, A. (2018). Interaction with an endothelial lumen increases neutrophil lifetime and motility in response to *P. aeruginosa*. *Blood* 132, 1818–1828. doi: 10.1182/blood-2018-05-848465
- Hu, S., Wang, R., Tsang, C. M., Tsao, S. W., Sun, D., and Lam, R. H. W. (2018). Revealing elasticity of largely deformed cells flowing along confining microchannels. *RSC Adv.* 8, 1030–1038. doi: 10.1039/C7RA10750A
- Huang, Q., Hu, X., He, W., Zhao, Y., Hao, S., Wu, Q., et al. (2018). Fluid shear stress and tumor metastasis. *Am. J. Cancer Res.* 8, 763–777.
- Ingram, P. N., Hind, L. E., Jimenez-Torres, J. A., Huttenlocher, A., and Beebe, D. J. (2018). An accessible organotypic microvessel model using iPSC-derived endothelium. *Adv. Healthc. Mater.* 7:1700497. doi: 10.1002/adhm.201700497
- Jeon, J. S., Bersini, S., Gilardi, M., Dubini, G., Charest, J. L., Moretti, M., et al. (2015). Human 3D vascularized organotypic microfluidic assays to study breast cancer cell extravasation. *Proc. Natl. Acad. Sci. U.S.A.* 112, 214–219. doi: 10.1073/pnas.1417115112
- Jeon, J. S., Zervantonakis, I. K., Chung, S., Kamm, R. D., and Charest, J. L. (2013). *In vitro* model of tumor cell extravasation. *PLoS ONE* 8:e56910. doi: 10.1371/journal.pone.0056910
- Kaarj, K., and Yoon, J. Y. (2019). Methods of delivering mechanical stimuli to organ-on-a-chip. *Micromachines* 10:700. doi: 10.3390/mi10100700
- Kim, H., Chung, H., Kim, J., Choi, D. H., Shin, Y., Kang, Y. G., et al. (2019). Macrophages-triggered sequential remodeling of endothelium-interstitial matrix to form pre-metastatic niche in microfluidic tumor microenvironment. *Adv. Sci.* 6:1900195. doi: 10.1002/adv.201900195
- Kim, Y., Williams, K. C., Gavin, C. T., Jardine, E., Chambers, A. F., and Leong, H. S. (2016). Quantification of cancer cell extravasation *in vivo*. *Nat. Protoc.* 11, 937–948. doi: 10.1038/nprot.2016.050
- Kocherova, I., Bryja, A., Mozdziak, P., Angelova Volponi, A., Dyszkiewicz-Konwinska, M., Piotrowska-Kempisty, H., et al. (2019). Human Umbilical Vein Endothelial Cells (HUVECs) co-culture with osteogenic cells: from molecular communication to engineering prevascularised bone grafts. *J. Clin. Med.* 8:1602. doi: 10.3390/jcm8101602
- Kovar, H., Amatruda, J., Brunet, E., Burdach, S., Cidre-Aranaz, F., De Alava, E., et al. (2016). The second European interdisciplinary Ewing sarcoma research summit—a joint effort to deconstructing the multiple layers of a complex disease. *Oncotarget* 7, 8613–8624. doi: 10.18632/oncotarget.6937
- Lamberti, G., Prabhakarandian, B., Garson, C., Smith, A., Pant, K., Wang, B., et al. (2014). Bioinspired microfluidic assay for *in vitro* modeling of leukocyte-endothelium interactions. *Anal. Chem.* 86, 8344–8351. doi: 10.1021/ac5018716
- Lanca, T., and Silva-Santos, B. (2012). The split nature of tumor-infiltrating leukocytes: implications for cancer surveillance and immunotherapy. *Oncoimmunology* 1, 717–725. doi: 10.4161/onci.20068
- Liang, S., Hoskins, M., and Dong, C. (2010). Tumor cell extravasation mediated by leukocyte adhesion is shear rate dependent on IL-8 signaling. *Mol. Cell. Biomech.* 7, 77–91.
- Liu, W., Song, J., Du, X., Zhou, Y., Li, Y., Li, R., et al. (2019). AKR1B10 (Aldo-keto reductase family 1 B10) promotes brain metastasis of lung cancer cells in a multi-organ microfluidic chip model. *Acta Biomater.* 91, 195–208. doi: 10.1016/j.actbio.2019.04.053
- Luster, A. (2001). Chemotaxis: role in immune response. *eLS.* doi: 10.1038/npg.els.0000507
- Ma, Y.-H. V., Middleton, K., You, L., and Sun, Y. (2018). A review of microfluidic approaches for investigating cancer extravasation during metastasis. *Microsyst. Nanoeng.* 4:17104. doi: 10.1038/micronano.2017.104
- Maas, S. L., Soehnlein, O., and Viola, J. R. (2018). Organ-specific mechanisms of transendothelial neutrophil migration in the lung, liver, kidney, and aorta. *Front. Immunol.* 9:2739. doi: 10.3389/fimmu.2018.02739
- Macedo, F., Ladeira, K., Pinho, F., Saraiva, N., Bonito, N., Pinto, L., et al. (2017). Bone metastases: an overview. *Oncol. Rev.* 11:321. doi: 10.4081/oncol.2017.321
- Marcovecchio, P. M., Thomas, G. D., Mikulski, Z., Ehinger, E., Mueller, K. A. L., Blatchley, A., et al. (2017). Scavenger receptor CD36 directs nonclassical monocyte patrolling along the endothelium during early atherogenesis. *Arterioscler. Thromb. Vasc. Biol.* 37, 2043–2052. doi: 10.1161/ATVBAHA.117.309123
- Marcu, R., Choi, Y. J., Xue, J., Fortin, C. L., Wang, Y., Nagao, R. J., et al. (2018). Human organ-specific endothelial cell heterogeneity. *iScience* 4, 20–35. doi: 10.1016/j.isci.2018.05.003
- McMinn, P. H., Hind, L. E., Huttenlocher, A., and Beebe, D. J. (2019). Neutrophil trafficking on-a-chip: an *in vitro*, organotypic model for investigating neutrophil priming, extravasation, and migration with spatiotemporal control. *Lab Chip* 19, 3697–3705. doi: 10.1039/C9LC00562E
- Medzhitov, R. (2008). Origin and physiological roles of inflammation. *Nature* 454, 428–435. doi: 10.1038/nature07201
- Mei, X., Middleton, K., Shim, D., Wan, Q., Xu, L., Ma, Y. V., et al. (2019). Microfluidic platform for studying osteocyte mechanoregulation of breast cancer bone metastasis. *Integr. Biol.* 11, 119–129. doi: 10.1093/intbio/zyz008
- Menon, N. V., Tay, H. M., Wee, S. N., Li, K. H. H., and Hou, H. W. (2017). Micro-engineered perfusable 3D vasculatures for cardiovascular diseases. *Lab Chip* 17, 2960–2968. doi: 10.1039/C7LC00607A
- Mitroulis, I., Alexaki, V. I., Kourtzelis, I., Ziogas, A., Hajishengallis, G., and Chavakis, T. (2015). Leukocyte integrins: role in leukocyte recruitment and as therapeutic targets in inflammatory disease. *Pharmacol. Ther.* 147, 123–135. doi: 10.1016/j.pharmthera.2014.11.008
- Mollica, H., Palomba, R., Primavera, R., and Decuzzi, P. (2019). Two-channel compartmentalized microfluidic chip for real-time monitoring of the metastatic cascade. *ACS Biomater. Sci. Eng.* 5, 4834–4843. doi: 10.1021/acsbiomaterials.9b00697
- Nguyen, D. X., Bos, P. D., and Massague, J. (2009). Metastasis: from dissemination to organ-specific colonization. *Nat. Rev. Cancer* 9, 274–284. doi: 10.1038/nrc2622
- Occhetta, P., Mainardi, A., Votta, E., Vallmajo-Martin, Q., Ehrbar, M., Martin, I., et al. (2019). Hyperphysiological compression of articular cartilage induces an osteoarthritic phenotype in a cartilage-on-a-chip model. *Nat. Biomed. Eng.* 3, 545–557. doi: 10.1038/s41551-019-0406-3
- Paget, S. (1989). The distribution of secondary growths in cancer of the breast. 1889. *Cancer Metastasis Rev.* 8, 98–101.
- Power, C. A. (2003). Knock out models to dissect chemokine receptor function *in vivo*. *J. Immunol. Methods* 273, 73–82. doi: 10.1016/S0022-1759(02)00419-2
- Raimondi, M. T., Boschetti, F., Falcone, L., Fiore, G. B., Remuzzi, A., Marinoni, E., et al. (2002). Mechanobiology of engineered cartilage cultured under a quantified fluid-dynamic environment. *Biomech. Model. Mechanobiol.* 1, 69–82. doi: 10.1007/s10237-002-0007-y
- Reymond, N., D'agui, B. B., and Ridley, A. J. (2013). Crossing the endothelial barrier during metastasis. *Nat. Rev. Cancer* 13, 858–870. doi: 10.1038/nrc3628
- Roberts, S. A., Waziri, A. E., and Agrawal, N. (2016). Development of a single-cell migration and extravasation platform through selective surface modification. *Anal. Chem.* 88, 2770–2776. doi: 10.1021/acs.analchem.5b04391
- Roussos, E. T., Condeelis, J. S., and Patsialou, A. (2011). Chemotaxis in cancer. *Nat. Rev. Cancer* 11, 573–587. doi: 10.1038/nrc3078
- Saxena, M., and Christofori, G. (2013). Rebuilding cancer metastasis in the mouse. *Mol. Oncol.* 7, 283–296. doi: 10.1016/j.molonc.2013.02.009

- Schimmel, L., Heemskerk, N., and Van Buul, J. D. (2017). Leukocyte transendothelial migration: a local affair. *Small GTPases* 8, 1–15. doi: 10.1080/21541248.2016.1197872
- Schnoor, M., Alcaide, P., Voisin, M. B., and Van Buul, J. D. (2015). Crossing the vascular wall: common and unique mechanisms exploited by different leukocyte subsets during extravasation. *Mediators Inflamm.* 2015:946509. doi: 10.1155/2015/946509
- Sharifi, F., Htwe, S. S., Righi, M., Liu, H., Pietralunga, A., Yesil-Celiktas, O., et al. (2019). A foreign body response-on-a-chip platform. *Adv. Healthc. Mater.* 8:e1801425. doi: 10.1002/adhm.201801425
- Simmons, J. K., Hildreth, B. E. III, Supsavhad, W., Elshafae, S. M., Hassan, B. B., Dirksen, W. P., Toribio, R. E., et al. (2015). Animal models of bone metastasis. *Vet. Pathol.* 52, 827–841. doi: 10.1177/0300985815586223
- Sleeboom, J. J. F., Eslami Amirabadi, H., Nair, P., Sahlgren, C. M., and Den Toonder, J. M. J. (2018). Metastasis in context: modeling the tumor microenvironment with cancer-on-a-chip approaches. *Dis. Model. Mech.* 11:dmm033100. doi: 10.1242/dmm.033100
- Sokeland, G., and Schumacher, U. (2019). The functional role of integrins during intra- and extravasation within the metastatic cascade. *Mol. Cancer* 18:12. doi: 10.1186/s12943-018-0937-3
- Song, J., Miermont, A., Lim, C. T., and Kamm, R. D. (2018). A 3D microvascular network model to study the impact of hypoxia on the extravasation potential of breast cell lines. *Sci. Rep.* 8:17949. doi: 10.1038/s41598-018-36381-5
- Streets, A. M., and Huang, Y. (2013). Chip in a lab: microfluidics for next generation life science research. *Biomicrofluidics* 7:11302. doi: 10.1063/1.4789751
- Strell, C., and Entschladen, F. (2008). Extravasation of leukocytes in comparison to tumor cells. *Cell Commun. Signal* 6:10. doi: 10.1186/1478-811X-6-10
- Swaminathan, V., Mythreye, K., O'Brien, E. T., Berchuck, A., Globe, G. C., and Superfine, R. (2011). Mechanical stiffness grades metastatic potential in patient tumor cells and in cancer cell lines. *Cancer Res.* 71, 5075–5080. doi: 10.1158/0008-5472.CAN-11-0247
- Tourovskaya, A., Fauver, M., Kramer, G., Simonson, S., and Neumann, T. (2014). Tissue-engineered microenvironment systems for modeling human vasculature. *Exp. Biol. Med.* 239, 1264–1271. doi: 10.1177/1535370214539228
- Vestweber, D. (2012). Novel insights into leukocyte extravasation. *Curr. Opin. Hematol.* 19, 212–217. doi: 10.1097/MOH.0b013e3283523e78
- Vestweber, D. (2015). How leukocytes cross the vascular endothelium. *Nat. Rev. Immunol.* 15, 692–704. doi: 10.1038/nri3908
- Visone, R., Gilardi, M., Marsano, A., Rasponi, M., Bersini, S., and Moretti, M. (2016). Cardiac meets skeletal: what's new in microfluidic models for muscle tissue engineering. *Molecules* 21:1128. doi: 10.3390/molecules21091128
- Wang, X., Sun, Q., and Pei, J. (2018). Microfluidic-based 3D engineered microvascular networks and their applications in vascularized microtumor models. *Micromachines* 9:493. doi: 10.3390/mi9100493
- Wendel, C., Hemping-Bovenkerk, A., Krasnyanska, J., Mees, S. T., Kochetkova, M., Stoeppeler, S., et al. (2012). CXCR4/CXCL12 participate in extravasation of metastasizing breast cancer cells within the liver in a rat model. *PLoS ONE* 7:e30046. doi: 10.1371/journal.pone.0030046
- Willyard, C. (2018). The mice with human tumours: growing pains for a popular cancer model. *Nature* 560, 156–157. doi: 10.1038/d41586-018-05890-8
- Wu, X., Newbold, M. A., and Haynes, C. L. (2015). Recapitulation of *in vivo*-like neutrophil transendothelial migration using a microfluidic platform. *Analyst* 140, 5055–5064. doi: 10.1039/C5AN00967G
- Yang, X. M., Chen, X. H., Lu, J. F., Zhou, C. M., Han, J. Y., and Chen, C. H. (2018). *In vivo* observation of cerebral microcirculation after experimental subarachnoid hemorrhage in mice. *Neural Regen. Res.* 13, 456–462. doi: 10.4103/1673-5374.228728
- Young, E. W., and Beebe, D. J. (2010). Fundamentals of microfluidic cell culture in controlled microenvironments. *Chem. Soc. Rev.* 39, 1036–1048. doi: 10.1039/b909900j
- Zervantonakis, I. K., Kothapalli, C. R., Chung, S., Sudo, R., and Kamm, R. D. (2011). Microfluidic devices for studying heterotypic cell-cell interactions and tissue specimen cultures under controlled microenvironments. *Biomicrofluidics* 5:13406. doi: 10.1063/1.3553237
- Zhang, Q., Liu, T., and Qin, J. (2012). A microfluidic-based device for study of transendothelial invasion of tumor aggregates in realtime. *Lab Chip* 12, 2837–2842. doi: 10.1039/c2lc00030j

Conflict of Interest: The authors declare that the research was conducted in the absence of any commercial or financial relationships that could be construed as a potential conflict of interest.

Copyright © 2020 Mondadori, Crippa, Moretti, Candrian, Lopa and Arrigoni. This is an open-access article distributed under the terms of the Creative Commons Attribution License (CC BY). The use, distribution or reproduction in other forums is permitted, provided the original author(s) and the copyright owner(s) are credited and that the original publication in this journal is cited, in accordance with accepted academic practice. No use, distribution or reproduction is permitted which does not comply with these terms.



Organoids to Study Intestinal Nutrient Transport, Drug Uptake and Metabolism – Update to the Human Model and Expansion of Applications

Tamara Zietek^{1*}, Pieter Giesbertz¹, Maren Ewers², Florian Reichart³, Michael Weinmüller³, Elisabeth Urbauer⁴, Dirk Haller^{4,5}, Ihsan Ekin Demir^{6,7,8,9}, Güralp O. Ceyhan^{6,7}, Horst Kessler³ and Eva Rath^{4*}

¹ Chair of Nutritional Physiology, Technische Universität München, Munich, Germany, ² Pediatric Nutritional Medicine, Klinikum Rechts der Isar, Else Kröner-Fresenius-Zentrum für Ernährungsmedizin, Technische Universität München, Munich, Germany, ³ Institute for Advanced Study, Department of Chemistry and Center for Integrated Protein Science (CIPSM), Technische Universität München, Garching, Germany, ⁴ Chair of Nutrition and Immunology, Technische Universität München, Munich, Germany, ⁵ ZIEL Institute for Food and Health, Technische Universität München, Munich, Germany, ⁶ Department of Surgery, Klinikum Rechts der Isar, Technische Universität München, Munich, Germany, ⁷ Department of General Surgery, HPB-Unit, School of Medicine, Acibadem Mehmet Ali Aydınlar University, Istanbul, Turkey, ⁸ German Cancer Consortium (DKTK), Munich, Germany, ⁹ CRC 1321 Modeling and Targeting Pancreatic Cancer, Klinikum rechts der Isar, School of Medicine, Technische Universität München, Munich, Germany

OPEN ACCESS

Edited by:

Davide Staedler,
University of Lausanne, Switzerland

Reviewed by:

Yongjun Hu,
Ann Arbor Pharmacometrics Group,
United States
Brahim Achour,
The University of Manchester,
United Kingdom

*Correspondence:

Tamara Zietek
zietek@tum.de
Eva Rath
eva.rath@tum.de

Specialty section:

This article was submitted to
Nanobiotechnology,
a section of the journal
Frontiers in Bioengineering and
Biotechnology

Received: 29 June 2020

Accepted: 19 August 2020

Published: 11 September 2020

Citation:

Zietek T, Giesbertz P, Ewers M, Reichart F, Weinmüller M, Urbauer E, Haller D, Demir IE, Ceyhan GO, Kessler H and Rath E (2020) Organoids to Study Intestinal Nutrient Transport, Drug Uptake and Metabolism – Update to the Human Model and Expansion of Applications. *Front. Bioeng. Biotechnol.* 8:577656. doi: 10.3389/fbioe.2020.577656

Intestinal transport and sensing processes and their interconnection to metabolism are relevant to pathologies such as malabsorption syndromes, inflammatory diseases, obesity and type 2 diabetes. Constituting a highly selective barrier, intestinal epithelial cells absorb, metabolize, and release nutrients into the circulation, hence serving as gatekeeper of nutrient availability and metabolic health for the whole organism. Next to nutrient transport and sensing functions, intestinal transporters including peptide transporter 1 (PEPT1) are involved in the absorption of drugs and prodrugs, including certain inhibitors of angiotensin-converting enzyme, protease inhibitors, antivirals, and peptidomimetics like β -lactam antibiotics. Here, we verify the applicability of 3D organoids for *in vitro* investigation of intestinal biochemical processes related to transport and metabolism of nutrients and drugs. Establishing a variety of methodologies including illustration of transporter-mediated nutrient and drug uptake and metabolomics approaches, we highlight intestinal organoids as robust and reliable tool in this field of research. Currently used *in vitro* models to study intestinal nutrient absorption, drug transport and enterocyte metabolism, such as Caco-2 cells or rodent explant models are of limited value due to their cancer and non-human origin, respectively. Particularly species differences result in poorly correlative data and findings obtained in these models cannot be extrapolated reliably to humans, as indicated by high failure rates in drug development pipelines. In contrast, human intestinal organoids represent a superior model of the intestinal epithelium and might help to implement the 3Rs (Reduction, Refinement and Replacement) principle in basic science as well as the preclinical and regulatory setup.

Keywords: peptidomimetics, acylcarnitine, glucose absorption, live cell imaging, fatty acid oxidation, PEPT1, competitive inhibition, 3R

INTRODUCTION

Since 2009, when Sato et al. (2009) reported the generation and long-term *in vitro* cultivation of intestinal organoids, this technology had a tremendous impact on research on stem cell biology, basic medical science, disease modeling and personalized medicine. Previously, we reported on murine intestinal organoids for assessing nutrient transport and sensing as well as incretin hormone secretion (Zietek et al., 2015). Intestinal nutrient transporters are not only involved in the absorption of nutrients from ingested food, they also serve as sensors e.g., for glucagon-like peptide 1 (GLP-1) secretion and are able to transport certain drugs (Wenzel et al., 2002; Zietek and Daniel, 2015). Hence, intestinal transport processes and their interconnection to intestinal epithelial cell (IEC) metabolism and whole body metabolic state are relevant to a variety of diseases and represent potential therapeutic targets. Among these pathologies are intestinal diseases such as malabsorption syndromes and intestinal inflammation, as well as metabolic disorders including obesity and type 2 diabetes, but also pathologies treated with drugs that are actively absorbed and/or metabolized by enterocytes. For example, peptidomimetics like β -lactam antibiotics are substrates of peptide transporters (Wenzel et al., 2002), and a broad range of drugs is metabolized by intestinal cytochrome P450 enzymes (Xie et al., 2016). Furthermore, IEC not only constitute a barrier separating the host from its microbiota, epithelial metabolism serves as a gatekeeper of nutrient availability for the whole organism, and IEC fatty acid oxidation has been implicated in the control of eating (Langhans et al., 2011; Ramachandran et al., 2018). Yet, many aspects of nutrient absorption, drug bioavailability and enterocyte metabolism remain elusive, e.g., underlying causes of fructose malabsorption are still unknown (Ebert and Witt, 2016) and a model to predict the impact of chemical modifications of a drug on its oral bioavailability is missing (Ovadia et al., 2011; Rader et al., 2018b). Consequently, there is growing interest in model systems allowing to study intestinal nutrient absorption, drug transport and enterocyte metabolism.

Here, we verify the transferability of our previous uptake studies in murine intestinal organoids (Zietek et al., 2015) to human organoids, improved experimental protocols and expanded readouts for visualization of transport processes and metabolic analyses. Previously existing *in vitro* models such as Caco-2 cells, Madin-Darby canine kidney cell culture (MDCK) or rodent explant models (Ussing chamber, everted gut sac models) suffer from severe limitations, as they do not reflect human physiology due to their cancer origin (Pinto et al., 1983; Hidalgo et al., 1989) or their non-human origin, respectively. In contrast, human organoids closely reflect epithelial physiology in a region-specific resolution, conserve the phenotype of the donor and concurrently offer advantages of easy handling, long-term culture and expansion, as well as cryo-conservation (Almeqdad et al., 2019). Since species-specific differences impede extrapolation of animal model-derived data to the human setup, focusing on human-based research models is essential for generating human-relevant data related to diseases and drug development. Currently, intestinal organoids are mostly discussed in the

context of personalized medicine, allowing for individualized drug screening and prediction of drug responses in cancer patients and patients with cystic fibrosis (Kondo and Inoue, 2019; Phan et al., 2019; Schutgens and Clevers, 2020). However, organoids as superior model of the intestinal epithelium may additionally be used for basic studies on bioavailability of drugs, drug development, and toxicology testing, complementing and partly replacing animal testing (Grabinger et al., 2014; Takahashi, 2019). Our data support that already simple organoid culture protocols hold great potential in improving the toolbox of metabolic research and facilitating animal-free approaches.

MATERIALS AND METHODS

All relevant methods and materials can be found in the **Supplementary Material**.

RESULTS

Culture Conditions Impact Organoid Cell Composition and Expression of Nutrient Transporters

Most nutrient and mineral uptake takes place in the small intestine, mediated by specific nutrient transporters located in the brush border membrane of enterocytes (Daniel and Zietek, 2015). A key property of intestinal organoids is that they are intrinsically programmed with their location-specific function and retain characteristics of their site of origin in culture (Middendorp et al., 2014). Consequently, differential expression of genes reported as site-specific (*GATA4*, *ABST*, *OSTB*) (Middendorp et al., 2014) as well as of *sodium-proton exchanger* (*NHE3*) and *epithelial sodium channel* (*ENaC*), involved in epithelial transport processes in the small and large intestine, respectively, could be detected in human organoids derived from different intestinal segments (**Figure 1A**). The ratio of *NHE3* and *ABST* mRNA expression in duodenal- versus ileal-derived organoids reflected the ratio seen in the primary tissues used for crypt isolation, underlining the physiological relevance (**Supplementary Figure 1A**). In line, mRNA expression of the enterocyte marker intestinal alkaline phosphatase (*ALPI*) as well as the main apical glucose transporter sodium-glucose co-transporter (*SGLT*) 1, glucose transporter (*GLUT*) 2 mediating glucose and fructose fluxes at the basolateral membrane via facilitated diffusion, the apical fructose transporter *GLUT5*, and peptide transporter 1 (*PEPT1*) were observed in human organoids derived from the different regions (duodenum, jejunum, ileum) of the small intestine (**Supplementary Figure 1B**). *SGLT1* and *PEPT1* expression could also be detected in human colonic organoids (**Supplementary Figure 1B**) and chromogranin A (*CHGA*), a marker for enterodendocrine cells (EEC), was expressed in all intestinal segments investigated (**Supplementary Figure 1B**). Mature, differentiated enterocytes are a prerequisite to study transport processes, downstream signaling and metabolic responses. However, intestinal organoid culture media, including commercial ready-to-use media optimized for permanent

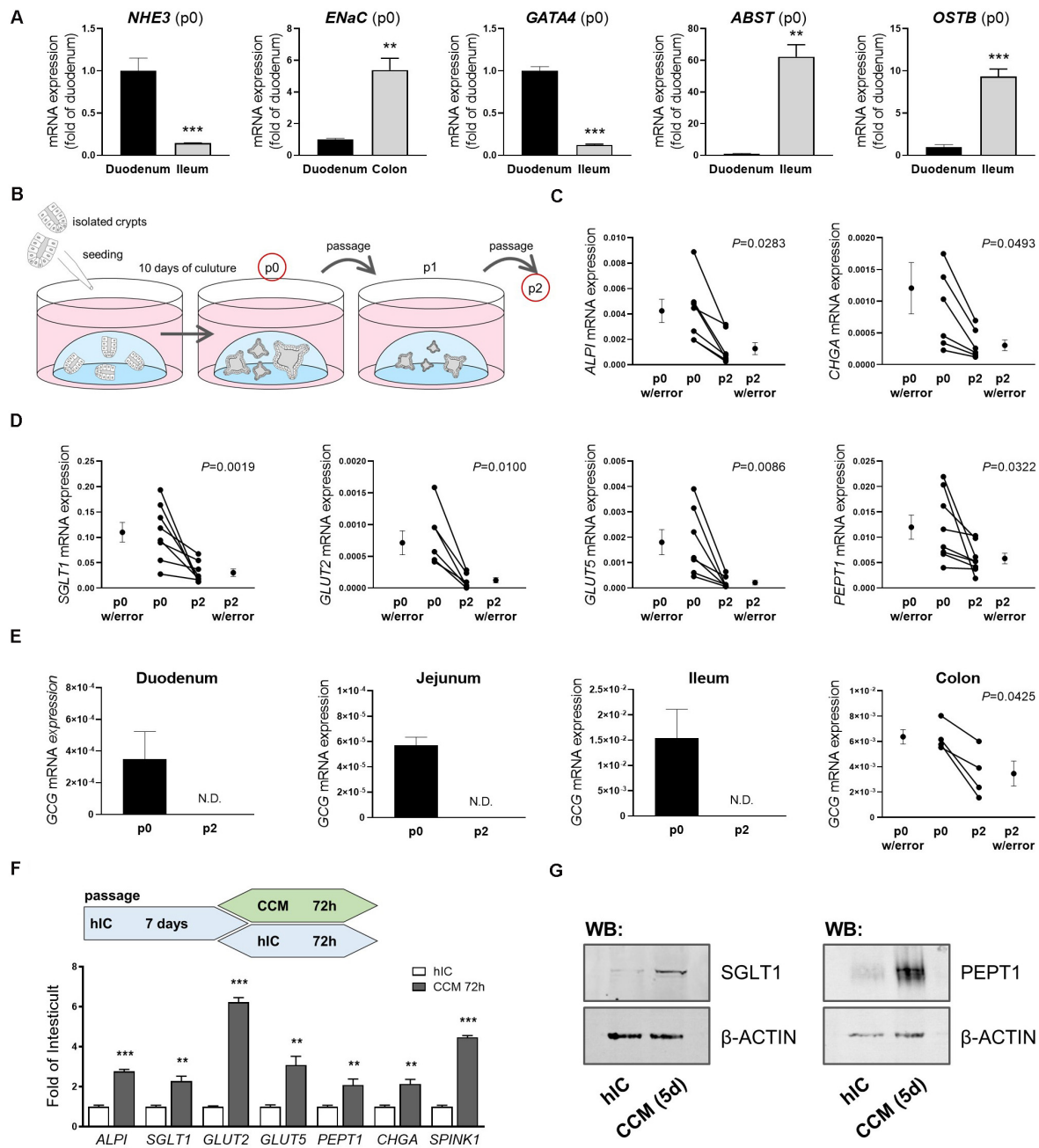


FIGURE 1 | Culture conditions impact intestinal organoid cell composition and expression of nutrient transporters. **(A)** mRNA expression analyses of human organoids derived from different intestinal segments; site-specific genes are depicted (passage p0) **(B)** Schematic representation of the organoid culture from which samples were derived for analyses. **(C,D)** mRNA expression analyses of duodenal human organoids from passages p0 and p2. **(E)** mRNA expression levels of GCG in human organoids derived from different intestinal segments from passages p0 and p2. **(C–E)** Target gene expression normalized to *HPRT*. **(F)** Upper panel: schematic representation of the experimental setup from which samples were derived for mRNA expression analysis; lower panel: relative gene expression of CCM-cultured human duodenal organoids as fold of organoids cultured in Wnt-containing hIC medium. *HPRT* was used as housekeeper. Bars represent mean + SEM. **(G)** Protein expression of SGLT1 and PEPT1 in human organoids cultured in hIC and CCM medium for 5 days, respectively. β-ACTIN serves as loading control. **(A,F)** unpaired t tests ($n = 5–6$). **(C–E)** paired t tests ($n = 5–6$). Asterisks indicate significant differences * $P < 0.05$, ** $P < 0.01$, *** $P < 0.001$; N.D. = Non-detectable; n.s. = non-significant; hIC = human IntestiCult medium, CCM = crypt culture medium.

propagation of human organoids contain Wnt factors and certain inhibitors that retain epithelial cells in an undifferentiated, stem cell-like state (Lindeboom et al., 2018). Accordingly, mRNA

levels of the investigated genes significantly dropped after the first passage of organoids (Figures 1B–D). During extended culture (passages 4 to 8), expression remained stable at low levels

(**Supplementary Figure 1C**). In particular, mRNA expression of *GCG*, encoding *i.a.* the incretin hormone glucagon-like peptide 1 (GLP-1) in EECs was rapidly lost. While completely undetectable in small intestinal organoids sampled after the second passage, expression levels were significantly diminished in colon-derived organoids (**Figure 1E**). Organoid differentiation can be steered into generation of distinct intestinal epithelial cell (IEC) subtypes like EECs (Petersen et al., 2015) or microfold (M) cells (de Lau et al., 2012) by addition of certain modulators like γ -secretase inhibitor or RANKL. *Vice versa*, withdrawal of compounds like Wnt3a or R-Spondin1 leads to general differentiation processes toward the enterocyte lineage (Foulke-Abel et al., 2016; Lindeboom et al., 2018). In line, changing the growth medium of organoids from a commercially available medium suitable for long-term culture of human organoids (human IC (hIC), that contains non-available concentrations of growth factors and inhibitors) to the standard medium used for murine small intestinal organoid culture (crypt culture medium, CCM) containing epidermal growth factor (EGF), Noggin1, and R-Spondin1 but no Wnt factors, induced expression levels of *ALPI*, *SGLT1*, *GLUT2*, *GLUT5*, *PEPT1*, *CHGA* and *SPINK1* (**Figure 1F**). *SPINK1* possesses structural similarities to EGF, and is associated with inflammatory states and various cancers, such as chronic pancreatitis (Hasan et al., 2018), inflammatory bowel disease and colon cancer (Ida et al., 2015). Western blot analysis of *SGLT1* and *PEPT1* protein expression confirmed the induction observed on mRNA levels (**Figure 1G**). A similar approach in murine small intestinal organoids, comparing CCM and murine IC (mIC) medium, yielded consistent results (**Supplementary Figure 1D**), highlighting the importance of appropriate culture conditions for functional readouts like transport assays or incretin hormone secretion in intestinal organoid cultures.

Nutrient and Drug Transport in Human Intestinal Organoids

Simple sugars can be taken up by enterocytes via passive or active transport – and exit the enterocyte likewise. The mechanism of intestinal sugar absorption is still not fully understood, given that a variety of transporters of the sodium glucose co-transporter (SGLT) family and the family of facilitative glucose transporters (GLUT) with partly unknown specificities is involved (Thorens and Mueckler, 2010). Genetic variants of transporters contributing to intestinal sugar transport are associated with human diseases, such as glucose-galactose malabsorption and Fanconi-Bickel syndrome caused by mutations in *SGLT1* (*SLC5A1*) and *GLUT2* (*SLC2A2*), respectively (Martin et al., 1996; Santer et al., 1997). Particularly, fructose uptake gained increasing attention, as fructose consumption is rising over the last decades and is associated with developing cardiovascular diseases and type 2 diabetes (Johnson et al., 2007). Furthermore, the molecular basis of fructose malabsorption still remains elusive, but defective absorption is most likely. Hence, intestinal organoids which can be directly derived from patients and allow to picture the complex interaction of transporters might considerably advance science in this field.

Previously, we established a straightforward approach to assess nutrient and drug transport in murine intestinal organoids (Zietek et al., 2015). By using fluorescently (FITC) labeled dextrans, we were able to show that molecules of a size of 4 kDa rapidly reach the luminal compartment of murine organoids. Hence, radiolabeled substrates were simply added to the culture plates, keeping the organoids in their 3-dimensional environment (a dome of laminin-rich gel) (Zietek et al., 2015). As species-specific differences might result in misleading outcomes (Youhanna and Lauschke, 2020), we validated experimental procedures for human intestinal organoids, allowing for tackling human-specific research questions. After confirming translocation of 4 kDa FITC-dextrans also into the lumen of human organoids (**Supplementary Figure 2A**), we applied the experimental procedures established in murine intestinal organoids (**Supplementary Figure 2B**) to human organoids. First investigating uptake of glucose and fructose, we used different inhibitors for functional characterization of monosaccharide transport, the SGLT1 inhibitor phloridzin, the GLUT inhibitor phloretin and rubusoside, inhibiting fructose transport by GLUT5 (**Figure 2A**).

Glucose is a substrate for both, apical and basolateral GLUT transporters, with the electrogenic solute carrier SGLT1 as the main apical glucose transporter in the small intestine. GLUT5 represents an exception, transporting exclusively fructose at the apical membrane. Opposing, the uniporter GLUT2 mediates glucose and fructose fluxes at the basolateral membrane via facilitated diffusion, providing import as well as export capacities (Thorens and Mueckler, 2010; Roder et al., 2014; **Figure 2A**). Due to the experimental setup, substrates first reach the outside, i.e., basolateral side of the organoids and only subsequently, after reaching the organoid lumen via the paracellular route or by simple diffusion, the apical side. Therefore, it is not possible to target apical or basolateral transporters separately, yet the use of inhibitors enables to illustrate contributions of certain transporters. Thus, using glucose as substrate in combination with either phloridzin or phloretin in human organoids derived from different regions of the small intestine, resulted in the expected pattern of blunted glucose uptake, which was more pronounced with the pan-GLUT inhibitor phloretin as compared to the SGLT1 inhibitor phloridzin (**Figure 2B**). In line, fructose transport could be diminished by phloretin, and to a lesser extent, by the GLUT5-inhibitor rubusoside (**Figure 2C**) as well as glucose (**Supplementary Figure 2C**) in human duodenal organoids.

Aiming at improving the experimental protocols, a second approach for investigating transport processes was established, using non-enzymatically dissociated (“broken up”) organoids instead of intact organoids (**Figure 2D**). In this case, human duodenal organoids were exposed to the radiolabeled dipeptide glycyl-sarcosine (Gly-Sar), a hydrolysis-resistant model substrate of the peptide transporter *PEPT1*. Peptide transport over the plasma membrane occurs in cotransport with protons and allows transport of di- and tripeptides against a substrate gradient [24]. Additionally, *PEPT1* also facilitates absorption of drugs and prodrugs, including certain inhibitors of angiotensin-converting enzyme (ACE), protease inhibitors, antivirals and peptidomimetics such as aminocephalosporins

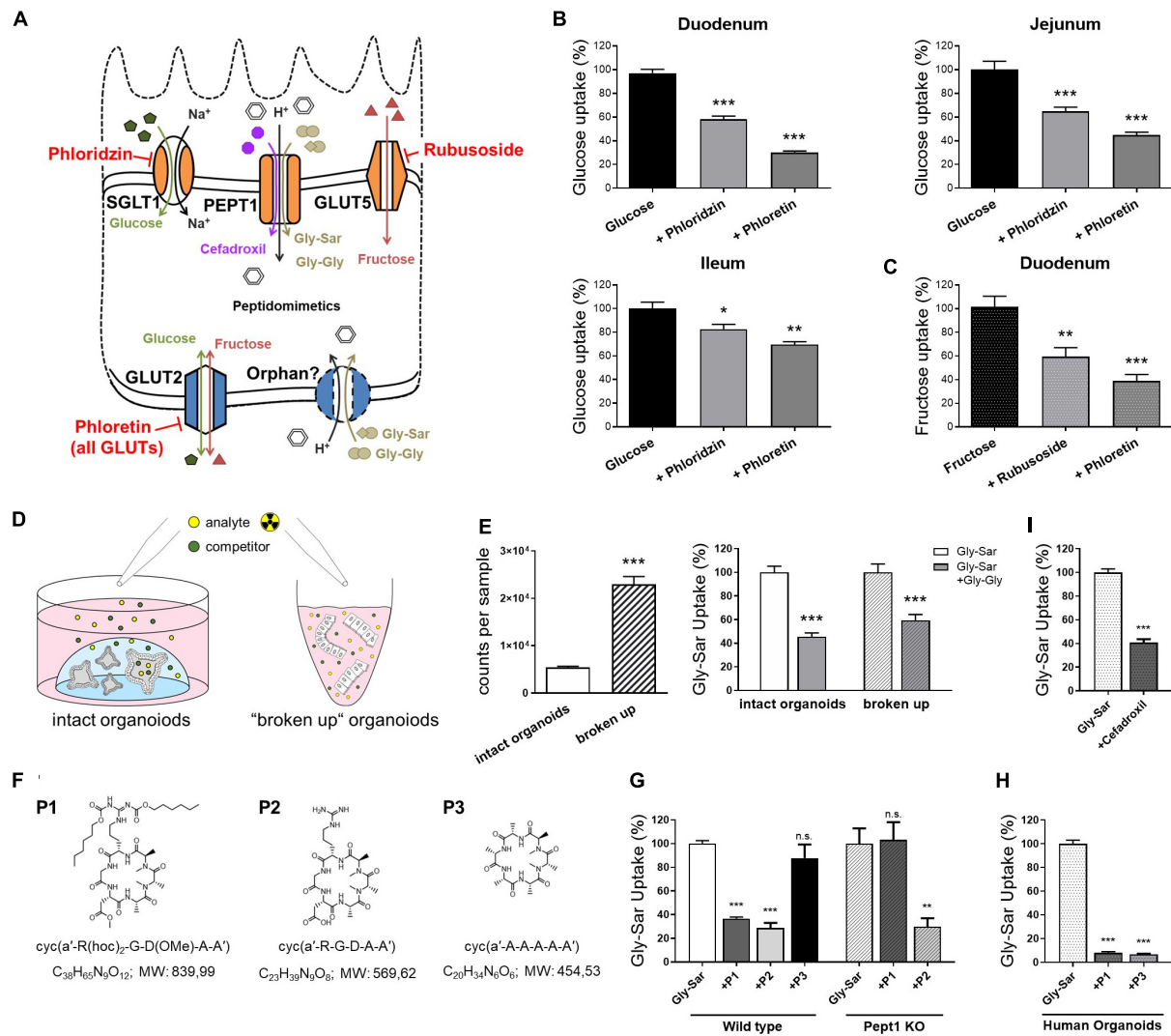


FIGURE 2 | Nutrient and drug transport in human intestinal organoids. **(A)** Schematic illustration of the transporters investigated and inhibitors used. **(B)** Uptake of radiolabeled glucose in human organoids derived from different small intestinal segments. **(C)** Uptake of radiolabeled fructose in human duodenal organoids. **(D)** Schematic representation of the intact organoids- and "broken up" organoids approach for measuring transport activities. **(E)** Left: comparison of detected counts per sample for both approaches using the same amount of radiolabeled substrates and right: reduction of radiolabeled Gly-Sar uptake by the competitive inhibitor Gly-Gly depicted for both approaches. Reduction of uptake was not significantly altered comparing both approaches; One-way analysis of variance (ANOVA) followed by Tukey's test. **(F)** Chemical structures and formulas of the peptidomimetics used. **(G)** Assessment of transport of peptidomimetics in a competition assay using radiolabeled Gly-Sar in murine small intestinal organoids derived from wild type and Pept1 knockout mice. **(H)** Similar approach to **(G)** using human duodenal organoids. **(I)** Reduction of radiolabeled Gly-Sar uptake using the antibiotic Cefadroxil as competitive inhibitor. **(B,C)** Unpaired t tests with Welch's correction. **(E,I)** Unpaired t tests. Bars represent mean + SEM. **(G,H)** One way ANOVA followed by Tukey's test. For all experiments $n = 5-6$. Asterisks indicate significant differences * $P < 0.05$, ** $P < 0.01$, *** $P < 0.001$.

(Ganapathy et al., 1995; Shu et al., 2001; Sugano et al., 2010; Kottra et al., 2013). Next to PEPT1-mediated substrate fluxes at the apical membrane, a not yet genetically identified system for basolateral peptide uptake with similar features to PEPT1 has been described (Berthelsen et al., 2013). Although radiolabeled transport assays are very sensitive, costs of labeled substrates are a major drawback. Hence, reducing the amount of substrates needed for experiments is desirable. Comparing intact organoids and "broken up" organoids exposed to the same concentrations of radiolabeled Gly-Sar, a 4-fold increase in signal intensity

was observed. Competitively inhibiting Gly-Sar uptake by the dipeptide glycyl-glycine (Gly-Gly) demonstrated a significant reduction of Gly-Sar uptake in both approaches, with the extent of reduction not being different between intact and "broken up" organoids (Figure 2E). Consequently, using "broken up" organoids instead of intact organoids represents a possibility not only to reduce costs but also to target basolateral and apical transporters at the same time.

As mentioned before, peptide transporters also play a role in drug uptake, including peptidomimetics. Peptidomimetics are

compounds mimicking a peptide or protein, which possess the ability to interact with a biological target to exert agonistic or antagonistic effects (Giannis and Kolter, 1993; Marshall and Ballante, 2017). Hence, they have a great potential in drug discovery, exerting drug-like properties (Rader et al., 2018a). For example, peptidomimetics have been designed for cancer therapy, e.g., to induce apoptosis (Walensky et al., 2004), sensitize cancer cells to chemotherapeutics (Greer et al., 2011), or specifically targeting integrins for interfering with angiogenesis and other aspects of tumor biology (Mas-Moruno et al., 2010; Nieberler et al., 2017). Primary goals in the development of orally available peptides are improving their intestinal transport and enhancing their stability to enzymatic degradation. Common strategies comprise the use of cyclic peptides, as well as D- instead of L-amino acids and N-methylation to increase metabolic stability (Rader et al., 2018a). For example, Cilengitide, a cyclic pentapeptide with one D-amino acid and one N-methylation is completely stable in humans and is excreted with a half-life of 4 h without any metabolism (Becker et al., 2015). Yet, intestinal permeation from the lumen into the bloodstream remains a major challenge. Structural changes affect intestinal and cellular permeability, and a change in one methyl position already can greatly impact permeability properties (Ovadia et al., 2011). Oral availability (crossing the gastrointestinal wall to reach the circulation) can be mediated via paracellular or transcellular mechanisms, including active transporters (Rader et al., 2018a). To date, it is not possible to predict the impact of certain chemical modifications on the transport/oral bioavailability of drug candidates (Rader et al., 2018b), therefore screening systems are required. Common tools to evaluate permeability properties of peptide drugs include Caco-2 monolayers and the side-by-side diffusion chamber (Ussing chamber), however, both systems are poorly correlative (Jezek et al., 1999; Bermejo et al., 2004; Ovadia et al., 2011) and face major disadvantages. Caco-2 cells, even though known to possess a rather small intestinal phenotype (Yee, 1997), were originally derived from a colon carcinoma, and phenotypic as well as functional characteristics highly differ from native human enterocytes (Harwood et al., 2016). For example, Caco-2 cells exhibit tighter junctions compared to the small intestine of human (Matsson et al., 2005) and were found not to be appropriate for evaluating active, carrier-mediated peptide drug absorption (Jezek et al., 1999). In contrast, Ussing chamber approaches, mainly using excised rat tissue better reflect physiology but suffer from potential species differences and large numbers of animals needed for screening. Hence, we tested the applicability of intestinal organoids as a new tool to evaluate the absorption properties of peptidomimetics. Three different cyclic hexapeptides (**P1**, **P2**, **P3**) (**Figure 2F**) were tested that were originally developed via a stepwise library approach: First a library of more than 55 different N-methylated alanine peptides of the general structure cyclo(D-Ala-L-Ala₅) were synthesized and investigated in a Caco-2 assay (Ovadia et al., 2011). Peptides identified as highly permeable (including **P3**) were subsequently functionalized by substitution of neutral Ala residues with the integrin-binding tripeptide sequence RGD. Among them, one compound (**P2**), has been identified with similar high activity and selectivity as Cilengitide (sub-nanomolar affinity for integrin

$\alpha\beta3$, high selectivity against other integrins) (Weinmuller et al., 2017). However, **P2** lacked permeability due to charges in the cyclic N-methylated alanine-peptides. To overcome this limitation, charged residues were protected with lipophilic protecting moieties (two hexyloxycarbonyl (Hoc) groups and conversion of the carboxylic side chain of Asp into a neutrally charged methyl ester). The resulting compound **P1** showed both, permeability in the Caco-2 assay and biological activity after oral administration in mice (Weinmuller et al., 2017). To test the involvement of active peptide transporter-mediated uptake in the permeability properties of **P1-P3**, we evaluated the ability of the three cyclic hexapeptides to competitively inhibit the uptake of radiolabeled Gly-Sar in murine small intestinal organoids derived from wild type and Pept1-deficient mice. In this assay, we identified **P1** as a potential substrate for active transport mediated by Pept1, **P2** to be actively transported independently of Pept1, and in contrast, **P3** showed no signs of peptide transporter-mediated uptake in murine organoids (**Figure 2G**). Subsequently testing **P1** and **P3** in human duodenal organoids, both peptides were able to significantly reduce radiolabeled Gly-Sar uptake, indicating **P1** and **P3** to be substrates for peptide transporter-mediated uptake in humans (**Figure 2H**). These data highlight the suitability of intestinal organoids to screen for transporter-mediated uptake of drug candidates, a process that might have been underappreciated in Caco-2 assays due to lack of physiological transporter expression, but contributes to oral availability. Additionally, efflux processes that limit drug absorption might be evaluated in detail in organoid systems (Schumacher-Klinger et al., 2018). Concomitantly, these data point toward potential species-specific transport phenotypes as already described for PEPT1 (Kottra et al., 2013). Accordingly, we could also confirm transport of the peptide-like β -lactam antibiotic cefadroxil, that has been previously described as PEPT1 substrate (Ganapathy et al., 1995; Zietek et al., 2015), in human duodenal organoids (**Figure 2I**).

In conclusion, these results underline the superior properties of human intestinal organoids for studying nutrient and drug uptake. Since organoids retain location-specific properties of their site of origin, absorption could even be determined at an intestinal region-specific resolution.

Visualization of Intestinal Peptide Transport Processes

It has been reported that fluorophore-conjugated dipeptides with a high-affinity for PEPT1 were able to block transport of Gly-Sar, however, they failed to be transported (Abe et al., 1999; Kottra et al., 2013). To exclude similar effects, either specific inhibitors can be applied (for example Lys-z-NO₂-Val, a specific PEPT1-inhibitor) or downstream effects of transport processes can be investigated. Thus, we extended our previously established protocol for visualization of intracellular signaling by life-cell imaging of murine intestinal organoids (Zietek et al., 2015), to human organoids and drug transport-induced signaling events. As mentioned before, peptide transport over the plasma membrane occurs in cotransport with protons, leading to cytosolic acidification of enterocytes (Chen et al., 2010). Hence,

intracellular changes immediately reflect transport activities and provide direct evidence for substrate fluxes. A drop in pH can be visualized by live-cell imaging using fluorescent probes (Chen et al., 2010; Zietek et al., 2015). Employing the pH-indicator BCECF-AM, intracellular acidification was

demonstrated in human duodenal organoids upon exposure to Gly-Sar, Gly-Gly as well as cefadroxil and the carbonyl cyanide m-chlorophenyl hydrazine (CCCP, an ionophore used as a positive control) (Figures 3A–D). Stimulating organoids with CCCP subsequent to administration of Gly-Sar, Gly-Gly,

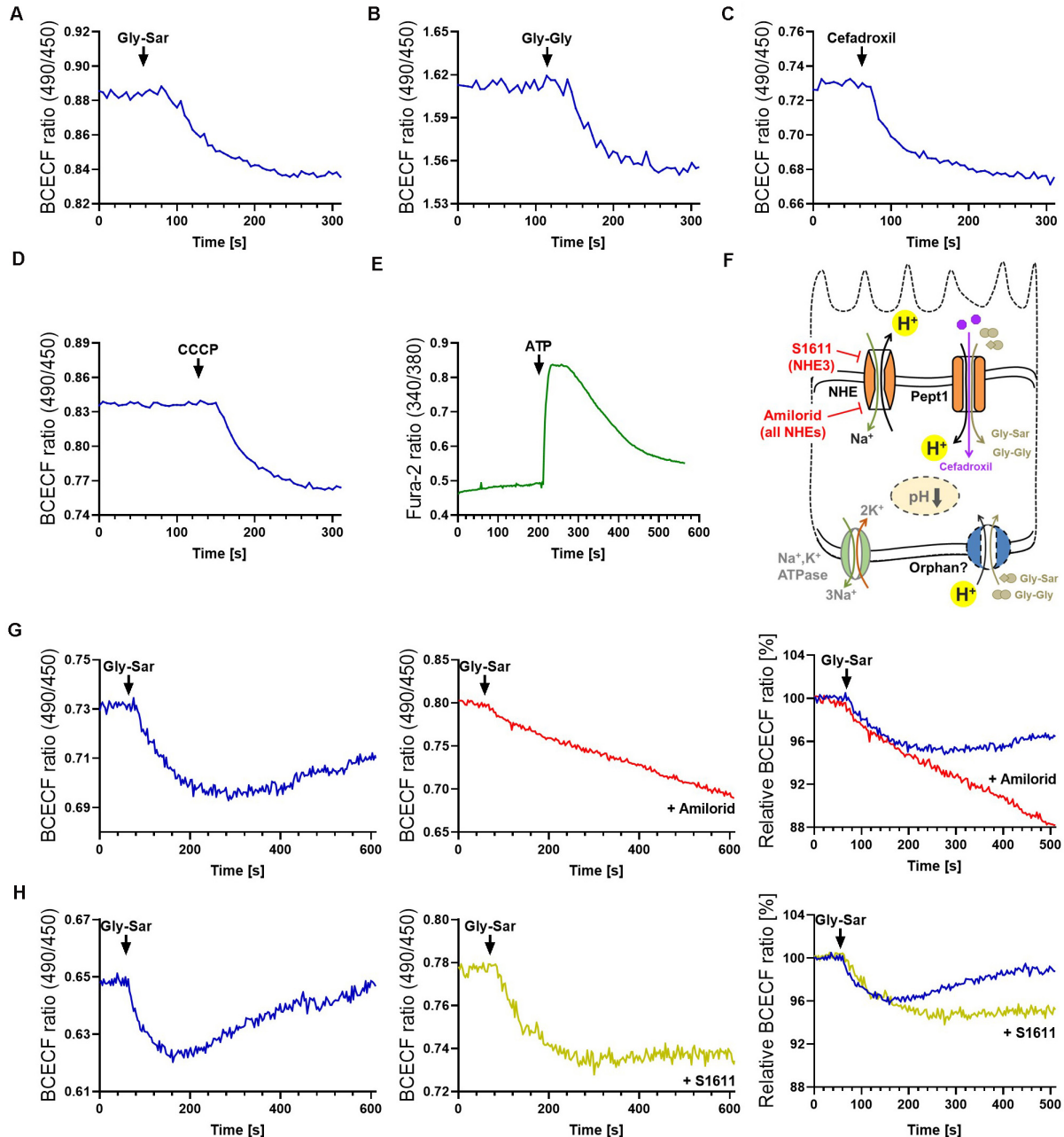


FIGURE 3 | Visualization of intestinal peptide transport processes. Intracellular acidification visualized by BCECF-AM induced by transport of peptide-transporter substrates (A) Gly-Sar and (B) Gly-Gly, (C) by the antibiotic Cefadroxil and (D) the protonophore CCCP. (E) Calcium responses to ATP stimulation visualized by Fura-2. Intracellular acidification induced by the antibiotic Cefadroxil. (F) Schematic illustration of the transporters investigated and inhibitors used. (G) Course of intracellular acidification induced by Gly-Sar exposure for an extended time frame (left) with and (middle) without the NHE-inhibitor Amilorid; right: overlay of both curves giving relative BCECF ratios. (H) Similar approach to (G) using the NHE3-inhibitor S1611. (A–E) human duodenal organoids, (G,H) murine small intestinal organoids. For data analysis, whole organoids were selected and no background correction was applied. Analyses were performed on several organoids derived from independent cultures and representative measurements are shown.

and cefadroxil caused an additional decline in intracellular pH, indicating the physiological range of observed responses (**Supplementary Figure 3A**). As expected, neither glucose nor fructose (used as negative controls) led to an intracellular acidification of enterocytes (**Supplementary Figure 3B**). Since live-cell imaging of calcium fluxes is routinely applied in pharmacological screenings to detect activation of receptors by a putative ligand/drug, and many transporter activities (e.g., PEPT1) (Wenzel et al., 2002) and intracellular translocation events (e.g., GLUT2) (Kellett et al., 2008) are regulated via intracellular calcium, we confirmed the applicability of the calcium-indicator Fura-2-AM in human organoids. In accordance to literature, robust signals were obtained upon ATP-mediated increases in intracellular calcium (**Figure 3E**). For both dyes, BCECF-AM and Fura-2-AM, excellent dye-loading efficiency was observed (**Supplementary Figure 3C**).

For continuous peptide uptake, IECs need to maintain the transmembrane ionic gradients and furthermore, augmented or prolonged acidification of the cell by proton symport of peptide transporters has to be avoided. Hence, protons are exported in exchange with Na^+ by sodium–proton exchangers (NHEs) (**Figure 3F**, **Supplementary Figure 1A**). In enterocytes, several types of NHEs are expressed, and NHE3 specifically has been shown to be required for proper PEPT1-mediated transport (Chen et al., 2010). Importantly, NHE-function is targeted by both, clinically relevant drugs as well as bacterial toxins. The distinct role of NHE3 in Na^+ absorption during normal digestion and in acute and chronic diarrheal diseases has been explored in human enteroids by Foulke-Abel et al. (2016), underlining the possibility to identify drug targets in this system. To illustrate the function of NHEs in general and NHE3 in particular in the context of active peptide transport in organoids, we used two different inhibitors: Amiloride, an FDA-approved inhibitor of NHEs, and S1611, which predominantly acts on NHE3 (Wiemann et al., 1999). As expected, both inhibitors prevented the recovery of intracellular pH to basal levels as observed in non-treated murine organoids following exposure to Gly-Sar (**Figures 3G,H** left). In accordance to their specific inhibitory spectrum, amiloride led to a continuous influx of protons in the observed time span (**Figure 3G**), while S1611 treatment resulted in a stable intracellular pH level below base line (**Figure 3H**). To decipher biology and functional characteristics of intestinal transporters it is very important not only to quantify transport of substrates, but also to take intracellular downstream effects and signaling into account, as presented above. These data highlight the high-resolution measurements possible in intestinal organoids.

Metabolite Analysis in Intestinal Organoids

Metabolism in IECs has gained increasing attention, not only due to the expression of key drug metabolizing enzymes, including cytochrome P450 3A4 (CYP3A4), in small intestinal epithelial cells, that are prone to diet-drug interactions (Lown et al., 1997). IEC and whole body metabolism are tightly interrelated via production of incretine hormones (Zietek and Rath, 2016)

and factors like Fgf15 (Kliwer and Mangelsdorf, 2015) by enteroendocrine cells and enterocytes, respectively, and vice versa, IECs are targets of remote-tissue metabolic signals such as insulin and leptin signaling (Yilmaz et al., 2012; Le Drian and Segain, 2014). In the gastrointestinal tract, carbohydrates, peptides and lipids are broken down and absorbed by enterocytes. Subsequently, they serve as substrates for cellular energy generation or for interconversions and distribution to the whole organism via transfer into the circulation. Hence, IEC metabolism also profoundly impacts availability and quality of nutrients, constituting an initial check point between diet and host. In this context, the intestinal microbiota plays an additional key role, as a source of bacterial metabolites such as short chain fatty acids (SCFAs) including butyrate. IEC metabolism and exposure to certain nutrients furthermore relates to diseases, for example high-fat diets were shown to enhance tumorigenicity of intestinal progenitors (Beyaz et al., 2016) and SCFAs and lactate promote intestinal healing processes (Lee et al., 2018; Parada Venegas et al., 2019). Despite the fact that general metabolic functions of enterocytes are understood, many open questions remain, including whether the small intestine can act as a site for gluconeogenesis, which seems to be species-dependent (Sinha et al., 2017; Potts et al., 2018; Varga et al., 2019) or how carbohydrate and lipid absorption and metabolism interact. Metabolomic approaches are key technologies allowing to tackle such questions by enabling analysis of metabolic events in a large scale and high throughput manner.

To test the feasibility of metabolic measurements in intestinal organoids, we applied different experimental schemes to replicate/validate effects described in literature. First, we determined the effect of insulin on amino acid (AA) and acylcarnitine levels in small intestinal organoids. Murine intestinal organoids were deprived of insulin-containing N2 medium supplement (yet, the B27 supplement contains residual insulin in a n/a concentration) over night, stimulated with 1 μM insulin and AAs and acylcarnitines were measured after 0, 30, 60, and 120 min (**Figure 4A**). All proteinogenic amino acids could be detected in small intestinal organoids at concentration ranges given in **Figure 4B**. Insulin is known to promote anabolism, affecting both, processes of protein synthesis and proteolysis. Enterocytes respond to insulin signals and develop insulin resistance under conditions of obesity-related inflammation (Monteiro-Sepulveda et al., 2015), and in particular, it was demonstrated that insulin deprivation reduces small intestinal protein biosynthesis, an effect that could be rescued by insulin treatment (Charlton et al., 2000). In line, concentrations of valine and alanine responded fast to insulin stimulation showing maximal reduction 30 min after addition of insulin (**Figure 4C**), consistently with most other AAs (data not shown), indicating a shift in protein turnover toward an enhanced net incorporation of AAs in proteins. In parallel, tau-methylhistidine, a marker compound for proteolysis and propionylcarnitine (C3), a typical intermediate in the breakdown of valine, isoleucine, methionine and threonine were diminished with lowest levels observed 60 min after insulin stimulation (**Figure 4D**), confirming also the inhibitory effect of insulin on proteolysis in intestinal organoids.

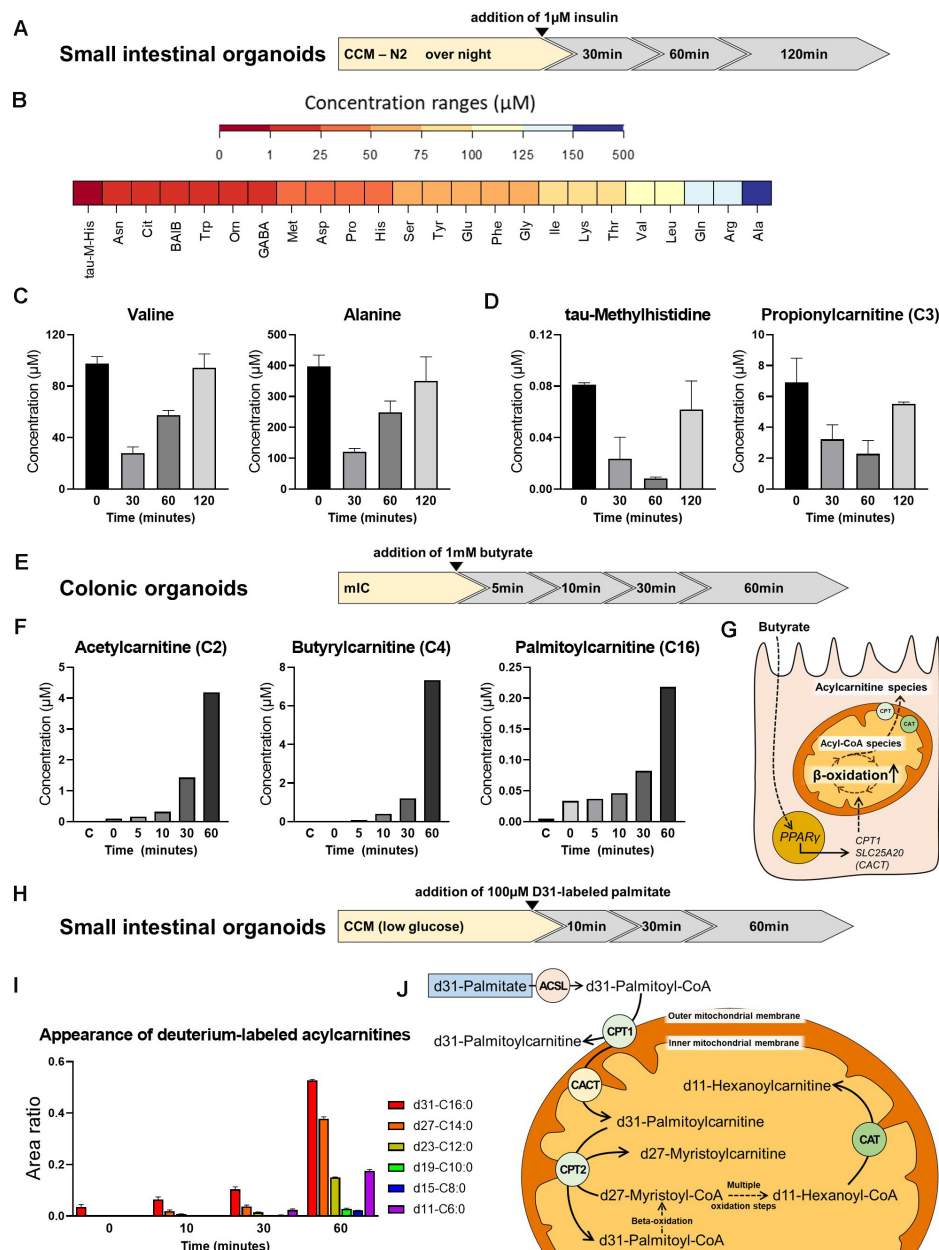


FIGURE 4 | Metabolite analysis in intestinal organoids. **(A)** Schematic representation of the experimental setup from which samples were derived for analyses shown in panel **(B,C)**. **(B)** Range of amino acid (AA) concentrations detected in organoids. **(C)** Concentration of valine and alanine at different time points after insulin stimulation. **(D)** Concentration of tau-methylhistidine, a marker compound for proteolysis, and propionylcarnitine (C3), a typical intermediate in the breakdown of valine, at different time points after insulin stimulation. **(E)** Schematic representation of the experimental setup from which samples were derived for analyses shown in panel **(F)**. **(F)** Concentration of the acylcarnitine species Acetylcarnitine (C2), Butyrylcarnitine (C4), and Palmitoylcarnitine (C16) at different time points after addition of butyrate. **(G)** Proposed mode of action for the effect of butyrate on beta-oxidation. **(H)** Schematic representation of the experimental setup from which samples were derived for analyses shown in panel **(I)**. **(I)** Appearance of deuterium-labeled acylcarnitines at different time points after addition of deuterium-labeled d31-palmitate. **(J)** Schematic illustration of carnitine acyltransferases involved in the generation of the acylcarnitine species detected. **(B,C,F,I)** Representative results from three independent organoid cultures. ASCL, long-chain acyl-CoA synthetase; CPT, carnitine palmitoyltransferase; CAT, carnitine acetyltransferase; CACT, carnitine-acylcarnitine translocase.

Next, we depict the effect of butyrate on acylcarnitine profiles in murine large intestinal organoids. In this approach, 1mM butyrate was added and shifts in acylcarnitines were measured 0, 5, 10, 30, and 60 min afterward (**Figure 4E**). Butyrate has

been shown to broadly affect colonocyte metabolism, including glucose utilization (Donohoe et al., 2012) and fat oxidation (den Besten et al., 2015), in turn regulating cell cycle progression and proliferation (Donohoe et al., 2012). In accordance to literature,

a clear effect of butyrate on saturated acylcarnitines, comprising short-, medium- and long-chain acylcarnitines was observed, with acetylcarnitine, butyrylcarnitine and palmitoylcarnitine increasing to maximal concentrations 60 min after butyrate addition (**Figure 4F**). A proposed mechanism explaining the effect of butyrate involves the butyrate transporter SLC5A8 and the butyrate receptor GPR109A expressed by colonocytes (Cresci et al., 2010), mediating activation of PPAR γ signaling, in turn increasing expression of carnitine palmitoyl-CoA transferase (CPT1) and carnitine-acylcarnitine translocase (SLC25A20/CACT) to enhance mitochondrial beta-oxidation (Vanhoutvin et al., 2009; den Besten et al., 2015; **Figure 4G**).

Last but not least, we followed the breakdown of d31-labeled palmitic acid, in which all 31 hydrogen atoms are replaced by deuterium atoms, in small intestinal organoids. Stable isotope labeling enables following the fate of the labeled fatty acid within the enterocyte, being either subjected to chain-shortening during beta-oxidation and conversion to the respective acylcarnitine species for energy generation, or being reesterified, and incorporated into chylomicrons for systemic supply. Importantly, sensing dietary fat via fatty acid oxidation in enterocytes has been implicated in the control of eating (Langhans et al., 2011), and modulation of enterocyte metabolism might affect whole body glucose homeostasis and the development of diet-induced obesity (Schober et al., 2013; Ramachandran et al., 2018). Prior to addition of d31-labeled palmitic acid, murine small intestinal organoids were incubated with CCM prepared with low-glucose DMEM/F12 for 24 h. Low-glucose DMEM/F12 contains 1g/L glucose, corresponding to 5.5 mM glucose, which is within the physiological range. Appearance of deuterium-labeled acylcarnitines were determined 0, 10, 30, and 60 min after addition of d31-palmitic acid (**Figure 4H**). Indicating beta-oxidation, we could detect chain-shortened, deuterium-labeled acylcarnitine species (**Figure 4I**). The conversion of the long-chain fatty acids to their acylcarnitine species is known to be mediated by carnitine palmitoyltransferase 1 and 2 (CPT1 and CPT2), while short-chain acylcarnitine species are formed by carnitine acetyltransferase (CAT) (**Figure 4J**). Carnitine octanoyltransferase (COT) located in peroxisomes is responsible for the conversion of medium-chain fatty acids (Violante et al., 2013). Contrarily, CPT1 is located in the outer mitochondrial membrane and thus may convert the added d31-palmitic acid directly to d31-palmitoylcarnitine (Bonfont et al., 2004). In line, immediately after addition of d31-palmitic acid ($t = 0$), a peak of d31-palmitoylcarnitine (d31-C16:0) was detected, that increased in subsequent time points (**Figure 4I**). Shorter fatty acid intermediates are formed within the mitochondria and their respective acylcarnitine species are generated by CPT2 and CAT, located in the inner mitochondrial membrane. Consistent with the sequential removal of 2-carbon units during beta-oxidation, d27-myristoylcarnitine (d27-C14:0) and to a lesser extent d23-dodecanoylcarnitine (d23-C12:0) could already be seen after 10 min of incubation, whereas d19-decanoyl-, d15-octanoyl- and d11-hexanoylcarnitine appeared 30 min after addition of d31-palmitic acid. All of these

intermediates showed increasing peaks for $t = 60$ (**Figure 4I**). Of note, the larger peaks of d11-C6, as compared to d19-C10 and d15-C8 after 30 and 60 min might be explained by a higher preference of CAT for short-chain fatty acid substrates (C2 to C6).

In summary, intestinal organoids are an excellent model system close to physiology to explore cellular metabolism and the applied metabolic readouts could be adapted easily to the 3D culture. Human organoids, constituting the most relevant model, are superior to animal (rodent)-derived organoids and (cancer) cell lines, especially in the context of metabolism and diseases, since metabolic properties differ between species and alterations in the cellular metabolism are part of many pathologies. Thus, human organoids hold great potential to answer remaining questions on intestinal metabolism and to identify drug targets to improve overall metabolic health.

CONCLUSION

Taken together, our results demonstrate that intestinal organoids cultured in 3D, embedded in a laminin-rich gel dome, the most basic and probably least cost and labor extensive culture protocol, is suitable for a broad range of measurements in the field of intestinal transport and metabolic studies. Beyond these applications, many other readouts are possible in this setup, for example assessment of proteasome activity (**Supplementary Figure 2D**), which is of interest in the context of proteasome inhibitors, an important class of drugs in the treatment of different types of cancer (Fricker, 2020).

Simple improvements and “tricks” like changing the medium composition to promote differentiation or to “break up” organoids prior to uptake studies help further enhancing results and reducing costs. Implementing other culture protocols like organoids with reversed polarity (in which the apical side faces outward) (Co et al., 2019) or organoids seeded in a 2D layer in transwell plates (VanDussen et al., 2015; Wang et al., 2019) are additional roads to go. Paracellular transport of fluorescein, transcellular transport of propranolol, and basolateral efflux of rhodamin123, a substrate of p-glycoprotein (MDR1) have been measured in a model in which human organoid-derived cells are seeded as a 2D monolayer on a porcine small intestinal scaffold (Schweinlin et al., 2016), complementing our animal-free approach focusing on active, transporter-mediated substrate uptake.

The field of applications for organoids is still rapidly growing, and there is a trend toward more complex and sophisticated organoid-based model systems. For example, co-cultures with bacterial and viral pathogens and immune cells (Yin et al., 2015; Dutta and Clevers, 2017), as well as approaches to reproduce the complex tissue environment comprising continuously flowing fluid systems, or to reflect multi-organ interactions (organoids on a chip), have been developed (Almeqdadi et al., 2019). These systems provide a microenvironment to study the impact of oxygenation, mechanical stress, and tissue communication via soluble factors and will further advance intestinal research.

Yet, to date they remain very expensive tools in highly specialized laboratories not suitable for broad applications (Almeqdadi et al., 2019). In contrast, the intestinal organoid culture protocols and methods presented here represent *in vitro* models that already now allow for partly replacement and reduction of animal numbers needed for research and testing.

Although the methodologies that we have established are applicable to mouse and human organoids, the human organoid technology should be focused when targeting human-related issues. Drug development success rates are particularly low in widespread diseases such as diabetes (Ali et al., 2018) or cancer (Mak et al., 2014). Only 5 to 10 percent of drugs proven as safe and effective in preclinical animal studies make it to the market (Arrowsmith, 2012; Thomas et al., 2016). Species-specific differences and hence poor transferability from animal models to humans is the main reason for this high failure rate (Arrowsmith and Miller, 2013; Cook et al., 2014; Mullard, 2016).

In light of this, we provide innovative approaches for physiologically relevant *in vitro* testing in the field of intestinal research and metabolomics. In particular, the use of human organoids in this context is a highly valuable tool for drug discovery and testing as well as for human-relevant disease modeling.

DATA AVAILABILITY STATEMENT

All datasets presented in this study are included in the article/**Supplementary Material**.

ETHICS STATEMENT

The studies involving human participants were reviewed and approved by the Ethics Committee of the Medical Faculty of TUM. The patients/participants provided their written informed consent to participate in this study. The animal study was reviewed and approved by the Committee on Animal Health and Care of the local government body of the state of Upper Bavaria (Regierung von Oberbayern).

REFERENCES

- Abe, H., Satoh, M., Miyauchi, S., Shuto, S., Matsuda, A., and Kamo, N. (1999). Conjugation of dipeptide to fluorescent dyes enhances its affinity for a dipeptide transporter (PEPT1) in human intestinal Caco-2 cells. *Bioconjug. Chem.* 10, 24–31. doi: 10.1021/bc980049i
- Ali, Z., Chandrasekera, P. C., and Pippin, J. J. (2018). Animal research for type 2 diabetes mellitus, its limited translation for clinical benefit, and the way forward. *Altern. Lab. Anim.* 46, 13–22. doi: 10.1177/026119291804600101
- Almeqdadi, M., Mana, M. D., Roper, J., and Yilmaz, O. H. (2019). Gut organoids: mini-tissues in culture to study intestinal physiology and disease. *Am. J. Physiol. Cell. Physiol.* 317, C405–C419.
- Arrowsmith, J. (2012). A decade of change. *Nat. Rev. Drug Discov.* 11, 17–18.
- Arrowsmith, J., and Miller, P. (2013). Trial watch: phase II and phase III attrition rates 2011–2012. *Nat. Rev. Drug Discov.* 12:569. doi: 10.1038/nrd4090

AUTHOR CONTRIBUTIONS

TZ contributed to study conception and design, human organoid culture, data acquisition, analysis and interpretation, and drafting and revising the article. PG contributed to data acquisition, analysis and interpretation, and drafting and revising the article. ME contributed to data acquisition, organoid culture, and analysis and interpretation. FR and MW contributed to synthesis of peptidomimetics. EU contributed to organoid culture and analysis of protein expression. DH contributed to critically revising the article. ID and GC provided material for organoid preparation. HK contributed to study conception and critically revising the article. ER contributed to study conception and design, murine and human organoid culture, data acquisition, analysis and interpretation, and drafting and revising the article. All authors contributed to the article and approved the submitted version.

FUNDING

This work was supported by the Reinhart Koselleck Grant of the Deutsche Forschungsgemeinschaft (DFG KE 147/42-1) to HK and the Center of Integrated Protein Science Munich. ID and GC were funded by the Deutsche Forschungsgemeinschaft (DFG, German Research Foundation) – Project number 329628492 – SFB 1321.

ACKNOWLEDGMENTS

The authors gratefully acknowledge the Bavarian NMR Center (BNMRZ) for covering publication costs. We thank Beate Rauscher for excellent technical support.

SUPPLEMENTARY MATERIAL

The Supplementary Material for this article can be found online at: <https://www.frontiersin.org/articles/10.3389/fbioe.2020.577656/full#supplementary-material>

- Becker, A., Von Richter, O., Kovar, A., Scheible, H., Van Lier, J. J., and John, A. (2015). Metabolism and disposition of the α -v-integrin ss3/ss5 receptor antagonist cilengitide, a cyclic polypeptide, in humans. *J. Clin. Pharmacol.* 55, 815–824. doi: 10.1002/jcph.482
- Bermejo, M., Avdeef, A., Ruiz, A., Nalda, R., Ruell, J. A., Tsinman, O., et al. (2004). PAMPA—a drug absorption in vitro model 7. Comparing rat in situ, Caco-2, and PAMPA permeability of fluoroquinolones. *Eur. J. Pharm. Sci.* 21, 429–441.
- Berthelsen, R., Nielsen, C. U., and Brodin, B. (2013). Basolateral glycylsarcosine (Gly-Sar) transport in Caco-2 cell monolayers is pH dependent. *J. Pharm. Pharmacol.* 65, 970–979. doi: 10.1111/jphp.12061
- Beyaz, S., Mana, M. D., Roper, J., Kedrin, D., Saadatpour, A., Hong, S. J., et al. (2016). High-fat diet enhances stemness and tumorigenicity of intestinal progenitors. *Nature* 531, 53–58. doi: 10.1038/nature17173
- Bonnefont, J. P., Djouadi, F., Prip-Buus, C., Gobin, S., Munnich, A., and Bastin, J. (2004). Carnitine palmitoyltransferases 1 and 2: biochemical, molecular and medical aspects. *Mol. Aspects Med.* 25, 495–520. doi: 10.1016/j.mam.2004.06.004

- Charlton, M., Ahlman, B., and Nair, K. S. (2000). The effect of insulin on human small intestinal mucosal protein synthesis. *Gastroenterology* 118, 299–306. doi: 10.1016/S0016-5085(00)70212-5
- Chen, M., Singh, A., Xiao, F., Dringenberg, U., Wang, J., Engelhardt, R., et al. (2010). Gene ablation for PEPT1 in mice abolishes the effects of dipeptides on small intestinal fluid absorption, short-circuit current, and intracellular pH. *Am. J. Physiol. Gastrointest Liver Physiol.* 299, G265–G274.
- Co, J. Y., Margalef-Catala, M., Li, X., Mah, A. T., Kuo, C. J., Monack, D. M., et al. (2019). Controlling epithelial polarity: a human enteroid model for host-pathogen interactions. *Cell Rep.* 26:e2504.
- Cook, D., Brown, D., Alexander, R., March, R., Morgan, P., Satterthwaite, G., et al. (2014). Lessons learned from the fate of AstraZeneca's drug pipeline: a five-dimensional framework. *Nat. Rev. Drug Discov.* 13, 419–431. doi: 10.1038/nrd4309
- Cresci, G. A., Thangaraju, M., Mellinger, J. D., Liu, K., and Ganapathy, V. (2010). Colonic gene expression in conventional and germ-free mice with a focus on the butyrate receptor GPR109A and the butyrate transporter SLC5A8. *J. Gastrointest Surg.* 14, 449–461. doi: 10.1007/s11605-009-1045-x
- Daniel, H., and Zietek, T. (2015). Taste and move: glucose and peptide transporters in the gastrointestinal tract. *Exp. Physiol.* 100, 1441–1450. doi: 10.1113/ep085029
- de Lau, W., Kujala, P., Schneeberger, K., Middendorp, S., Li, V. S., Barker, N., et al. (2012). Peyer's patch M cells derived from Lgr5(+) stem cells require SpiB and are induced by RankL in cultured "miniguts". *Mol. Cell Biol.* 32, 3639–3647. doi: 10.1128/mcb.00434-12
- den Besten, G., Bleeker, A., Gerding, A., Van Eunen, K., Havinga, R., Van Dijk, T. H., et al. (2015). Short-chain fatty acids protect against High-fat diet-induced obesity via a PPARgamma-dependent switch from Lipogenesis to fat oxidation. *Diabetes* 64, 2398–2408. doi: 10.2337/db14-1213
- Donohoe, D. R., Wali, A., Brylawski, B. P., and Bultman, S. J. (2012). Microbial regulation of glucose metabolism and cell-cycle progression in mammalian colonocytes. *PLoS One* 7:e46589. doi: 10.1371/journal.pone.0046589
- Dutta, D., and Clevers, H. (2017). Organoid culture systems to study host-pathogen interactions. *Curr. Opin. Immunol.* 48, 15–22. doi: 10.1016/j.coi.2017.07.012
- Ebert, K., and Witt, H. (2016). Fructose malabsorption. *Mol. Cell. Pediatr.* 3, 10.
- Foulke-Abel, J., In, J., Yin, J., Zachos, N. C., Kovbasnjuk, O., Estes, M. K., et al. (2016). Human enteroids as a model of upper small intestinal ion transport physiology and pathophysiology. *Gastroenterology* 150: e638.
- Fricker, L. D. (2020). Proteasome inhibitor drugs. *Annu. Rev. Pharmacol. Toxicol.* 60, 457–476. doi: 10.1146/annurev-pharmtox-010919-023603
- Ganapathy, M. E., Brandsch, M., Prasad, P. D., Ganapathy, V., and Leibach, F. H. (1995). Differential recognition of beta-lactam antibiotics by intestinal and renal peptide transporters, PEPT 1 and PEPT 2. *J. Biol. Chem.* 270, 25672–25677. doi: 10.1074/jbc.270.43.25672
- Giannis, A., and Kolter, T. (1993). Peptidomimetics for receptor ligands-discovery, development, and medical perspectives. *Angew. Chem. Int. Ed.* 32, 1244–1267. doi: 10.1002/anie.199312441
- Grabinger, T., Luks, L., Kostadinova, F., Zimmerlin, C., Medema, J. P., Leist, M., et al. (2014). Ex vivo culture of intestinal crypt organoids as a model system for assessing cell death induction in intestinal epithelial cells and enteropathy. *Cell Death Dis.* 5:e1228. doi: 10.1038/cddis.2014.183
- Greer, R. M., Peyton, M., Larsen, J. E., Girard, L., Xie, Y., Gazdar, A. F., et al. (2011). SMAC mimetic (JP1201) sensitizes non-small cell lung cancers to multiple chemotherapy agents in an IAP-dependent but TNF-alpha-independent manner. *Cancer Res.* 71, 7640–7648. doi: 10.1158/0008-5472.can-10-3947
- Harwood, M. D., Achour, B., Neuheoff, S., Russell, M. R., Carlson, G., Warhurst, G., et al. (2016). In vitro-In vivo extrapolation scaling factors for intestinal P-Glycoprotein and breast cancer resistance protein: part I: a cross-laboratory comparison of transporter-protein abundances and relative expression factors in human intestine and Caco-2 Cells. *Drug Metab. Dispos.* 44, 297–307. doi: 10.1124/dmd.115.067371
- Hasan, A., Moscoso, D. I., and Kastrinos, F. (2018). The role of genetics in pancreatitis. *Gastrointest Endosc. Clin. N. Am.* 28, 587–603.
- Hidalgo, I. J., Raub, T. J., and Borchardt, R. T. (1989). Characterization of the human colon carcinoma cell line (Caco-2) as a model system for intestinal epithelial permeability. *Gastroenterology* 96, 736–749. doi: 10.1016/0016-5085(89)90897-4
- Ida, S., Ozaki, N., Araki, K., Hirashima, K., Zaitu, Y., Taki, K., et al. (2015). SPINK1 status in colorectal cancer, impact on proliferation, and role in colitis-associated cancer. *Mol. Cancer Res.* 13, 1130–1138. doi: 10.1158/1541-7786.mcr-14-0581
- Jezyk, N., Li, C., Stewart, B. H., Wu, X., Bockbrader, H. N., and Fleisher, D. (1999). Transport of pregabalin in rat intestine and Caco-2 monolayers. *Pharm. Res.* 16, 519–526.
- Johnson, R. J., Segal, M. S., Sautin, Y., Nakagawa, T., Feig, D. I., Kang, D. H., et al. (2007). Potential role of sugar (fructose) in the epidemic of hypertension, obesity and the metabolic syndrome, diabetes, kidney disease, and cardiovascular disease. *Am. J. Clin. Nutr.* 86, 899–906.
- Kellett, G. L., Brot-Laroche, E., Mace, O. J., and Leturque, A. (2008). Sugar absorption in the intestine: the role of GLUT2. *Annu. Rev. Nutr.* 28, 35–54. doi: 10.1146/annurev.nutr.28.061807.155518
- Kliwer, S. A., and Mangelsdorf, D. J. (2015). Bile acids as hormones: the FXR-FGF15/19 pathway. *Dig. Dis.* 33, 327–331. doi: 10.1159/000371670
- Kondo, J., and Inoue, M. (2019). Application of cancer organoid model for drug screening and personalized therapy. *Cells* 8:470. doi: 10.3390/cells8050470
- Kottra, G., Spanier, B., Verri, T., and Daniel, H. (2013). Peptide transporter isoforms are discriminated by the fluorophore-conjugated dipeptides beta-Ala- and d-Ala-Lys-N-7-amino-4-methylcoumarin-3-acetic acid. *Physiol. Rep.* 1:e00165. doi: 10.1002/phy2.165
- Langhans, W., Leitner, C., and Arnold, M. (2011). Dietary fat sensing via fatty acid oxidation in enterocytes: possible role in the control of eating. *Am. J. Physiol. Regul. Integr. Comp. Physiol.* 300, R554–R565.
- Le Drian, G., and Segain, J. P. (2014). Connecting metabolism to intestinal barrier function: the role of leptin. *Tissue Barriers* 2:e970940. doi: 10.4161/21688362.2014.970940
- Lee, Y. S., Kim, T. Y., Kim, Y., Lee, S. H., Kim, S., Kang, S. W., et al. (2018). Microbiota-derived acetate accelerates intestinal stem-cell-mediated epithelial development. *Cell Host Microbe* 24:e836.
- Lindeboom, R. G., Van Voorthuisen, L., Oost, K. C., Rodriguez-Colman, M. J., Luna-Velez, M. V., Furlan, C., et al. (2018). Integrative multi-omics analysis of intestinal organoid differentiation. *Mol. Syst. Biol.* 14: e8227.
- Lown, K. S., Bailey, D. G., Fontana, R. J., Janardan, S. K., Adair, C. H., Fortlage, L. A., et al. (1997). Grapefruit juice increases felodipine oral availability in humans by decreasing intestinal CYP3A protein expression. *J. Clin. Invest.* 99, 2545–2553. doi: 10.1172/jci119439
- Mak, I. W., Evaniew, N., and Ghert, M. (2014). Lost in translation: animal models and clinical trials in cancer treatment. *Am. J. Transl. Res.* 6, 114–118.
- Marshall, G. R., and Ballante, F. (2017). Limiting assumptions in the design of peptidomimetics. *Drug Dev. Res.* 78, 245–267. doi: 10.1002/ddr.21406
- Martin, M. G., Turk, E., Lostao, M. P., Kerner, C., and Wright, E. M. (1996). Defects in Na⁺/glucose cotransporter (SGLT1) trafficking and function cause glucose-galactose malabsorption. *Nat. Genet.* 12, 216–220. doi: 10.1038/ng0296-216
- Mas-Moruno, C., Rechenmacher, F., and Kessler, H. (2010). Cilengitide: the first anti-angiogenic small molecule drug candidate design, synthesis and clinical evaluation. *Anticancer Agents Med. Chem.* 10, 753–768.
- Matsson, P., Bergstrom, C. A., Nagahara, N., Tavelin, S., Norinder, U., and Artursson, P. (2005). Exploring the role of different drug transport routes in permeability screening. *J. Med. Chem.* 48, 604–613. doi: 10.1021/jm049711o
- Middendorp, S., Schneeberger, K., Wiegerinck, C. L., Mokry, M., Akkerman, R. D., Van Wijngaarden, S., et al. (2014). Adult stem cells in the small intestine are intrinsically programmed with their location-specific function. *Stem Cells* 32, 1083–1091. doi: 10.1002/stem.1655
- Monteiro-Sepulveda, M., Touch, S., Mendes-Sa, C., Andre, S., Poitou, C., Allatif, O., et al. (2015). Jejunal T cell inflammation in human obesity correlates with

- decreased enterocyte insulin signaling. *Cell Metab* 22, 113–124. doi: 10.1016/j.cmet.2015.05.020
- Mullard, A. (2016). Parsing clinical success rates. *Nat. Rev. Drug Discov.* 15:447. doi: 10.1038/nrd.2016.136
- Niebler, M., Reuning, U., Reichart, F., Notni, J., Wester, H. J., Schwaiger, M., et al. (2017). Exploring the role of RGD-recognizing integrins in cancer. *Cancers* 9:116. doi: 10.3390/cancers9090116
- Ovadia, O., Greenberg, S., Chatterjee, J., Laufer, B., Opperer, F., Kessler, H., et al. (2011). The effect of multiple N-methylation on intestinal permeability of cyclic hexapeptides. *Mol. Pharm.* 8, 479–487. doi: 10.1021/mp1003306
- Parada Venegas, D., De La Fuente, M. K., Landskron, G., Gonzalez, M. J., Quera, R., Dijkstra, G., et al. (2019). Corrigendum: short chain fatty acids (SCFAs)-mediated gut epithelial and immune regulation and its relevance for inflammatory bowel diseases. *Front. Immunol.* 10:1486. doi: 10.3389/fimmu.2019.01486
- Petersen, N., Reimann, F., Van Es, J. H., Van Den Berg, B. M., Kroone, C., Pais, R., et al. (2015). Targeting development of incretin-producing cells increases insulin secretion. *J. Clin. Invest.* 125, 379–385. doi: 10.1172/jci75838
- Phan, N., Hong, J. J., Tofig, B., Mapua, M., Elashoff, D., Moatamed, N. A., et al. (2019). A simple high-throughput approach identifies actionable drug sensitivities in patient-derived tumor organoids. *Commun. Biol.* 2:78.
- Pinto, M., Robineleon, S., Appay, M. D., Kedinger, M., Triadou, N., Dussaulx, E., et al. (1983). Enterocyte-like differentiation and polarization of the human colon carcinoma cell-line Caco-2 in culture. *Biol. Cell* 47, 323–330.
- Potts, A., Uchida, A., Deja, S., Berglund, E. D., Kucejova, B., Duarte, J. A., et al. (2018). Cytosolic phosphoenolpyruvate carboxykinase as a cataplerotic pathway in the small intestine. *Am. J. Physiol. Gastrointest Liver Physiol.* 315, G249–G258.
- Rader, A. F. B., Reichart, F., Weinmuller, M., and Kessler, H. (2018a). Improving oral bioavailability of cyclic peptides by N-methylation. *Bioorg. Med. Chem.* 26, 2766–2773. doi: 10.1016/j.bmc.2017.08.031
- Rader, A. F. B., Weinmuller, M., Reichart, F., Schumacher-Klinger, A., Merzbach, S., Gilon, C., et al. (2018b). Orally active peptides: is there a magic bullet? *Angew. Chem. Int. Ed. Engl.* 57, 14414–14438. doi: 10.1002/anie.201807298
- Ramachandran, D., Clara, R., Fedele, S., Michel, L., Burkard, J., Kaufman, S., et al. (2018). Enhancing enterocyte fatty acid oxidation in mice affects glycemic control depending on dietary fat. *Sci. Rep.* 8:10818.
- Roder, P. V., Geillinger, K. E., Zietek, T. S., Thorens, B., Koepsell, H., and Daniel, H. (2014). The role of SGLT1 and GLUT2 in intestinal glucose transport and sensing. *PLoS One* 9:e89977. doi: 10.1371/journal.pone.0089977
- Santer, R., Schneppenheim, R., Dombrowski, A., Gotze, H., Steinmann, B., and Schaub, J. (1997). Mutations in GLUT2, the gene for the liver-type glucose transporter, in patients with Fanconi-Bickel syndrome. *Nat. Genet.* 17, 324–326. doi: 10.1038/ng1197-324
- Sato, T., Vries, R. G., Snippert, H. J., Van De Wetering, M., Barker, N., Stange, D. E., et al. (2009). Single Lgr5 stem cells build crypt-villus structures in vitro without a mesenchymal niche. *Nature* 459, 262–265. doi: 10.1038/nature07935
- Schober, G., Arnold, M., Birtles, S., Buckett, L. K., Pacheco-Lopez, G., Turnbull, A. V., et al. (2013). Diacylglycerol acyltransferase-1 inhibition enhances intestinal fatty acid oxidation and reduces energy intake in rats. *J. Lipid Res.* 54, 1369–1384. doi: 10.1194/jlr.m035154
- Schumacher-Klinger, A., Fanous, J., Merzbach, S., Weinmuller, M., Reichart, F., Rader, A. F. B., et al. (2018). Enhancing oral bioavailability of cyclic RGD hexa-peptides by the lipophilic prodrug charge masking approach: redirection of peptide intestinal permeability from a paracellular to transcellular pathway. *Mol. Pharm.* 15, 3468–3477. doi: 10.1021/acs.molpharmaceut.8b00466
- Schutgens, F., and Clevers, H. (2020). Human organoids: tools for understanding biology and treating diseases. *Annu. Rev. Pathol.* 15, 211–234. doi: 10.1146/annurev-pathmechdis-012419-032611
- Schweinlin, M., Wilhelm, S., Schwedhelm, I., Hansmann, J., Rietscher, R., Jurowich, C., et al. (2016). Development of an advanced primary human in vitro model of the small intestine. *Tissue Eng. Part C Methods* 22, 873–883. doi: 10.1089/ten.tec.2016.0101
- Shu, C., Shen, H., Hopfer, U., and Smith, D. E. (2001). Mechanism of intestinal absorption and renal reabsorption of an orally active ace inhibitor: uptake and transport of fosinopril in cell cultures. *Drug Metab. Dispos.* 29, 1307–1315.
- Sinha, N., Suarez-Diez, M., Van Schothorst, E. M., Keijer, J., Martins Dos Santos, V. A. P., and Hooiveld, G. (2017). Predicting the murine enterocyte metabolic response to diets that differ in lipid and carbohydrate composition. *Sci. Rep.* 7:8784.
- Sugano, K., Kansy, M., Artursson, P., Avdeef, A., Bendels, S., Di, L., et al. (2010). Coexistence of passive and carrier-mediated processes in drug transport. *Nat. Rev. Drug Discov.* 9, 597–614. doi: 10.1038/nrd3187
- Takahashi, T. (2019). Organoids for drug discovery and personalized medicine. *Annu. Rev. Pharmacol. Toxicol.* 59, 447–462. doi: 10.1146/annurev-pharmtox-010818-021108
- Thomas, D., Burns, J., Audette, J., Carroll, A., Dow-Hygelund, C., and Hay, M. (2016). “Clinical development success rates 2006–2015,” in *BIO Industry Analysis, Amplion, Inc., Biomedtracker, Biotechnology Innovation Organization (BIO)*, 1–16.
- Thorens, B., and Mueckler, M. (2010). Glucose transporters in the 21st Century. *Am. J. Physiol. Endocrinol. Metab.* 298, E141–E145.
- VanDussen, K. L., Marinsaw, J. M., Shaikh, N., Miyoshi, H., Moon, C., Tarr, P. I., et al. (2015). Development of an enhanced human gastrointestinal epithelial culture system to facilitate patient-based assays. *Gut* 64, 911–920. doi: 10.1136/gutjnl-2013-306651
- Vanhoutvin, S. A., Troost, F. J., Hamer, H. M., Lindsey, P. J., Koek, G. H., Jonkers, D. M., et al. (2009). Butyrate-induced transcriptional changes in human colonic mucosa. *PLoS One* 4:e6759. doi: 10.1371/journal.pone.0006759
- Varga, V., Muranyi, Z., Kurucz, A., Marcolongo, P., Benedetti, A., Banhegyi, G., et al. (2019). Species-specific glucose-6-phosphatase activity in the small intestine-studies in three different Mammalian models. *Int. J. Mol. Sci.* 20:5039. doi: 10.3390/ijms20205039
- Violante, S., Ijst, L., Te Brinke, H., Koster, J., Tavares De Almeida, I., Wanders, R. J., et al. (2013). Peroxisomes contribute to the acylcarnitine production when the carnitine shuttle is deficient. *Biochim. Biophys. Acta* 1831, 1467–1474. doi: 10.1016/j.bbalip.2013.06.007
- Walensky, L. D., Kung, A. L., Escher, I., Malia, T. J., Barbuto, S., Wright, R. D., et al. (2004). Activation of apoptosis in vivo by a hydrocarbon-stapled BH3 helix. *Science* 305, 1466–1470. doi: 10.1126/science.1099191
- Wang, Y., Chiang, I. L., Ohara, T. E., Fujii, S., Cheng, J., Muegge, B. D., et al. (2019). Long-term culture captures injury-repair cycles of colonic stem cells. *Cell* 179, 1144.e15–1159.e15.
- Weinmuller, M., Rechenmacher, F., Kiran Marelli, U., Reichart, F., Kapp, T. G., Rader, A. F. B., et al. (2017). Overcoming the lack of oral availability of cyclic Hexapeptides: design of a selective and orally available ligand for the integrin alphavbeta3. *Angew. Chem. Int. Ed. Engl.* 56, 16405–16409.
- Wenzel, U., Kuntz, S., Diestel, S., and Daniel, H. (2002). PEPT1-mediated cefixime uptake into human intestinal epithelial cells is increased by Ca²⁺ channel blockers. *Antimicrob. Agents Chemother.* 46, 1375–1380. doi: 10.1128/aac.46.5.1375-1380.2002
- Wiemann, M., Schwark, J. R., Bonnet, U., Jansen, H. W., Grinstein, S., Baker, R. E., et al. (1999). Selective inhibition of the Na⁺/H⁺ exchanger type 3 activates CO₂/H⁺-sensitive medullary neurones. *Pflugers Arch.* 438, 255–262. doi: 10.1007/s004240050907
- Xie, F., Ding, X., and Zhang, Q. Y. (2016). An update on the role of intestinal cytochrome P450 enzymes in drug disposition. *Acta Pharm. Sin. B* 6, 374–383. doi: 10.1016/j.apsb.2016.07.012
- Yee, S. (1997). In vitro permeability across Caco-2 cells (colonic) can predict in vivo (small intestinal) absorption in man—fact or myth. *Pharm. Res.* 14, 763–766.
- Yilmaz, O. H., Katajisto, P., Lamming, D. W., Gultekin, Y., Bauer-Rowe, K. E., Sengupta, S., et al. (2012). mTORC1 in the Paneth cell niche couples intestinal stem-cell function to calorie intake. *Nature* 486, 490–495. doi: 10.1038/nature11163
- Yin, Y., Bijvelds, M., Dang, W., Xu, L., Van Der Eijk, A. A., Knipping, K., et al. (2015). Modeling rotavirus infection and antiviral therapy using primary intestinal organoids. *Antiviral Res.* 123, 120–131. doi: 10.1016/j.antiviral.2015.09.010

- Youhanna, S., and Lauschke, V. M. (2020). The past, present and future of intestinal in vitro cell systems for drug absorption studies. *J. Pharm. Sci.* doi: 10.1016/j.xphs.2020.07.001 [Epub ahead of print].
- Zietek, T., and Daniel, H. (2015). Intestinal nutrient sensing and blood glucose control. *Curr. Opin. Clin. Nutr. Metab. Care* 18, 381–388. doi: 10.1097/mco.000000000000187
- Zietek, T., and Rath, E. (2016). Inflammation meets metabolic disease: gut feeling mediated by GLP-1. *Front. Immunol.* 7:154. doi: 10.3389/fimmu.2016.00154
- Zietek, T., Rath, E., Haller, D., and Daniel, H. (2015). Intestinal organoids for assessing nutrient transport, sensing and incretin secretion. *Sci. Rep.* 5:16831.

Conflict of Interest: The authors declare that the research was conducted in the absence of any commercial or financial relationships that could be construed as a potential conflict of interest.

Copyright © 2020 Zietek, Giesbertz, Ewers, Reichart, Weinmüller, Urbauer, Haller, Demir, Ceyhan, Kessler and Rath. This is an open-access article distributed under the terms of the Creative Commons Attribution License (CC BY). The use, distribution or reproduction in other forums is permitted, provided the original author(s) and the copyright owner(s) are credited and that the original publication in this journal is cited, in accordance with accepted academic practice. No use, distribution or reproduction is permitted which does not comply with these terms.



Ex vivo Live Cell Imaging of Nanoparticle-Cell Interactions in the Mouse Lung

Fernanda Ramos-Gomes¹, Nathalia Ferreira¹, Alexander Kraupner², Frauke Alves^{1,3} and M. Andrea Markus^{1*}

¹ Translational Molecular Imaging, Max-Planck-Institute for Experimental Medicine, Göttingen, Germany, ² nanoPET Pharma GmbH, Berlin, Germany, ³ Clinic of Hematology and Medical Oncology/Institute of Diagnostic and Interventional Radiology, University Medical Center Göttingen, Göttingen, Germany

OPEN ACCESS

Edited by:

Adrielle Prina-Mello,
Trinity College Dublin, Ireland

Reviewed by:

Harini Kantamneni,
Rutgers, The State University of New
Jersey, United States

Jyothi U. Menon,
University of Rhode Island,
United States

*Correspondence:

M. Andrea Markus
markus@em.mpg.de

Specialty section:

This article was submitted to
Nanobiotechnology,
a section of the journal
Frontiers in Bioengineering and
Biotechnology

Received: 29 July 2020

Accepted: 21 September 2020

Published: 30 October 2020

Citation:

Ramos-Gomes F, Ferreira N,
Kraupner A, Alves F and Markus MA
(2020) Ex vivo Live Cell Imaging of
Nanoparticle-Cell Interactions in the
Mouse Lung.
Front. Bioeng. Biotechnol. 8:588922.
doi: 10.3389/fbioe.2020.588922

A successful clinical translation of novel nanoparticle-based cancer therapeutics requires a thorough preclinical investigation of their interaction with immune, tumor and endothelial cells as well as components of the tumor-microenvironment. Although high-resolution microscopy images of fixed tumor tissue specimens can provide valuable information in this regard, they are only static snapshots of a momentary event. Here we describe a superior alternative fluorescence microscopy approach to assess the feasibility of investigating nanoparticle-cell interactions in the mouse lung live and over time at nanometer resolution. We applied fluorescent lung tumor cells and Barium-based fluorescently labeled nanoparticles to nude mice or to CD68-EGFP transgenic mice for visualization of the monocyte-macrophage lineage. Shortly before imaging, fluorescently labeled lectin was intravenously injected for staining of the blood vessels. The lung was filled *ex vivo* with 1% agarose and individual lung lobes were imaged over time using a confocal microscope with Airyscan technology. Time series demonstrate that live cell imaging of lung lobes can be performed for at least 4 h post mortem. Time-lapse movies illustrate the dynamics of the nanoparticles within the pulmonary circulation and their uptake by immune cells. Moreover, the exchange of nanoparticle material between cancer cells was observed over time. Fluorescent monocytes in lungs of CD68-EGFP transgenic mice could be visualized within blood vessels in the process of interaction with tumor cells and nanoparticles. This high resolution *ex vivo* live cell imaging approach provides an excellent 4D tool to obtain valuable information on the behavior of tumor and immune cells at first encounter with nanoparticles and may contribute to the understanding of how nanoparticles interact with cells supporting the development of therapeutic strategies based on nanoparticulate drug delivery systems.

Keywords: nanoparticles, live cell imaging, fluorescence microscopy, cancer, experimental lung metastasis, phagocytosis, extracellular vesicles, cell dynamics

INTRODUCTION

Routinely used chemotherapy has a number of weaknesses, including poor pharmacokinetics, low specificity and off target effects, leading to substantial side-effects. Nanoparticle (NP)-based cancer therapeutics have therefore been increasingly explored, because NPs have a number of advantages compared to “naked” therapies: (i) improved drug solubility and stability, (ii) prolonged drug half-life in plasma, (iii) minimized off-target effects, (iv) improved accumulation of drugs at a target site due to the possibility of functionalization and (v) better controlled concentration of drugs by packaging in NPs. Furthermore, recent efforts allowed the incorporation of therapeutic agents into biocompatible NPs, therefore, reducing undesirable local or systemic effects (Li et al., 2012). Combining all these characteristics, some NPs have been successfully approved by the FDA or are currently being tested in clinical trials (Ventola, 2017). However, most NP-based cancer drugs have either not made it into the clinic or have failed to significantly improve patient outcome. This is most likely due to the inter- and intra-individual heterogeneity of tumors and to the complexity of tumor and immune response that has been underestimated. For instance, the Enhanced Permeability and Retention (EPR) effect, was widely believed to be a general and homogenous feature of most tumors, a phenomenon caused by leaky vessels by which nanodrugs would predominantly accumulate in the tumor. It has now been recognized that the EPR effect is greatly influenced by a number of parameters, including the tumor microenvironment, vessel density and permeability and stroma composition (Dasgupta et al., 2020).

A further deciding factor for the success of nanotherapies, in particular nanoparticulate immunotherapies, is the specific immune response induced by these (Khalil et al., 2016). As Blank et al. recently summarized, modulation of immune response progresses in different steps of the immune cell-antigen interaction, comprising antigen uptake, trafficking, processing and presentation to T cells. These steps require thorough analysis, also as part of pharmacologic and biocompatibility testing in the development process of novel NP-based cancer therapeutic strategies. The safe design of nanotherapies should therefore include the careful characterization of the interaction of NPs with immune cells, tumor cells, the microenvironment and endothelial cells (blood vessels) (Blank et al., 2017). Moreover, a thorough assessment of the targeted accumulation of nanoparticulate drugs at the desired site is crucial, as the EPR effect is not a reliable feature of all tumors.

To avoid side effects upon systemic delivery of therapies, local applications of nanoparticulate therapies have been already tested, for instance by intratumoral injection (Marabelle et al., 2014) or in the case of lung cancer by inhalation (Liu et al., 2019). A rapid uptake of NPs by pulmonary antigen-presenting cells (APCs) has been repeatedly demonstrated and the targeted delivery of immunostimulants to intratumoral APCs in the lung has recently been shown (Liu et al., 2019). Studies *in vitro* and *in vivo* further suggested both dendritic cells (DCs) and T cells as promising targets for pulmonary NP therapies (Nembrini et al., 2011; Blank et al., 2017; Jia et al., 2018). The lung thus

seems to be an ideal organ for specific delivery of nanoparticulate drugs as the relevant immune cells can be directly targeted by inhalation and intravenous application also results in deposition in the lung. A particular close look should be taken at the interaction of NPs with the monocyte/macrophage lineage, which plays a key role in both innate adaptive immune response and is involved in all common pulmonary diseases, including allergic asthma, chronic obstructive pulmonary dysplasia (COPD) and lung cancer (Arora et al., 2017). Tumor associated macrophages (TAMs) not only play a key role in tumor therapy response (Cassetta and Kitamura, 2018; Rodell et al., 2018), but have also been successfully used as theranostic targets for the combined treatment and imaging of lung tumors (Markus et al., 2015; Cuccarese et al., 2017; Napp et al., 2018).

Imaging of the numerous processes and interactions of NPs with lung immune cells, microenvironment and/or tumor cells and the elimination of NPs from the lung has traditionally been done by histology and immunohistochemistry. While these microscopic methods provide cellular nanoscale resolution, they are only static snapshots of momentary events and cannot provide the same information as live cell imaging. Other live cell or *in vivo* technologies, such as near infrared fluorescence optical imaging, computed tomography (CT), magnetic resonance imaging (MRI), and positron emission tomography (PET) or ultrasound do not provide the resolution to image at the cellular or nanomaterial resolution.

Here we demonstrate an alternative technique for monitoring the live interaction of monocytes/macrophages and tumor cells with NPs in the lung. We show that *ex vivo* live cell confocal microscopy of entire mouse lung lobes provides an excellent 4D tool for imaging of several dynamic processes in tumor tissue, such as the traffic of cells, shedding of extracellular vesicles (EVs) and the accumulation of NPs in tumor tissue.

METHODS AND MATERIALS

Materials

Barium sulfate (BaSO₄)-based nanoparticles (Ba-NPs) were produced by chemical precipitation at ambient conditions. After a purification step the particles were sterically stabilized using a biocompatible polymer. The so obtained highly stable colloidal suspension was sterilized and formulated for *in vitro/in vivo* use. The hydrodynamic diameter of the particles was around 120 nm. Fluorescent labeling of Ba-NPs was performed via EDC/NHS coupling chemistry of amino-functionalized Atto488 (Atto-Tec GmbH, Siegen) or Cy3 fluorescent dyes to COOH groups of the stabilizing polymer. Subsequently, the labeled particles were dialyzed against water in order to remove non-bound dye. The Ba-NPs were tested *in vitro* and were found to be non-toxic and had no effect on the vitality of mammalian cells.

Lectin-Alexa647 (Alexa647 labeled Isolectin B4 from Bandeiraea simplicifolia) was a kind gift from Roche Pharma, Penzberg.

Cell Culture

A cell proliferation assay (MTT-assay) was performed using the MCF-7 in order to assess the cytotoxicity of the Ba-NPs. The

experiments ($n = 5$ per test series) were conducted at 4 h and 24 h incubation time and with a final Ba-NP concentration of 15–45 mg/ml. The results were compared against a positive (100% death cells) and negative control (100% vital cells). The same experiments were performed with A549 cells with a Ba-NPs concentration of 30 mg/mL and 24 h incubation time.

Human A549-mCherry lung tumor cells (a kind gift from Dr. Winkler, German Primate Centre, Germany) and murine LL/2-red fluorescence protein (RFP) (Lewis Lung) cancer cells (a kind gift from Prof. Augustin, Deutsches Krebsforschungszentrum, Heidelberg) were kept at 37°C and 5% CO₂ atmosphere. A549-mCherry cells were grown in DMEM high glucose (Gibco) supplemented with 10% fetal calf serum (FCS) (Gibco). LL/2-RFP cells were grown in DMEM high glucose supplemented with 1% penicillin/streptomycin, 1% non-essential amino acids (Gibco) and 10% FCS. When indicated, 1×10^6 A549-mCherry cells were incubated with 13 mg/ml Ba-Atto488 NPs overnight, washed of excess NPs the next morning and run over a 40 µm cell strainer (Corning) before application to the mice.

Animal Experiments

All animal *in-vivo* procedures were performed in compliance with the guidelines of the European Directive (2010/63/EU) and the German ethical laws and were approved by the administration of Lower Saxony, Germany.

Pathogen-free male NMRI-Fox1nu/nu mice, 6–8 weeks of age were purchased from Charles River Laboratories Inc. C57BL/6-Tg(CD68-EGFP)1Drg/J were originally purchased from The Jackson Laboratory and then bred in house. All animals were housed in a controlled environment with a regular 12 h dark:light cycle, at 22°C and were fed laboratory chow and tap water *ad libitum*.

Healthy mice were injected intravenously (i.v.) either with 1×10^6 LL/2-RFP cells or 1×10^6 Ba-Atto488-NP-loaded A549-mCherry cells or with 6 mg Ba-Cy3 NPs, 5 min before sacrifice.

Experimental lung metastases were obtained by i.v. injection of 1×10^6 A549-mCherry cells into male NMRI-Fox1^{nu/nu} mice. The development of lung metastasis was assessed by microCT (Quantum FX, Perkin Elmer) every other week. Once lung metastasis were visible (about 8 weeks after induction), 6 mg Ba-Atto488 NPs were injected i.v. 5 min before sacrifice.

All mice were i.v. injected with 100 µg Lectin-Alexa647 shortly before sacrifice.

Preparation of Lungs for Live Cell Imaging

The lungs were prepared as described previously with some modifications (van den Bijgaart et al., 2016). Briefly, mice were sacrificed by isoflurane overdose and cervical dislocation and the trachea exposed. Following a small incision at the top of the trachea, a blunt cannula (20G, the tips cut-off) was inserted max. 1 cm into the trachea and fixed with common cotton thread. The lungs were immediately filled with 600 µl of 37°C warm 1% agarose (BioFroxx) in DMEM w/o phenol red (Gibco 31053-028). The agarose filled lungs were tied with a cotton thread at the trachea underneath the inserted cannula to prevent leaking of the agarose before setting and were then dissected from the mouse. Individual lung lobes were then placed on uncoated ibidi

35 mm cell culture dishes (ibidi GmbH) with the flat side down, covered entirely with warm 1% agarose-DMEM and imaged by confocal microscopy as soon as the agarose was set.

Confocal Microscopy

A Zeiss LSM880 confocal laser scanning microscope (CLSM, Carl Zeiss Microscopy GmbH) was used, equipped with an Airyscan detection unit and GaAsP-PMT/Spectral detectors, a 20 × air objective lens (Plan-APOCHROMAT, NA: 0.45, air, DIC), a motorized stage, incubator for live cell conditions and a tuneable laser (470–670 nm). mCherry and Red Fluorescence Protein (RFP) were excited at 561 nm, Ba-Atto488 NPs and CD68-EGFP were excited at 488 nm and Lectin-Alexa647 was excited at 633 nm. The experiments were performed under live cell environmental conditions (37°C/5% CO₂) and the whole equipment was turned on the evening before imaging to minimize tissue movement due to temperature changes.

Light Sheet Microscopy

Following confocal microscopy the same lung lobes were fixed in 4% paraformaldehyde (PFA) overnight and then cleared using the ethyl-3-phenylprop-2-enoate (ethyl cinnamate, ECi) protocol described before (Klingberg et al., 2017). Images were acquired with an UltraMicroscope II (LaVision BioTec) with an Olympus MVX10 Zoom Microscope Body (Olympus), a white light laser module, an Andor Neo sCMOS camera, and detection optics with an optical magnification range from 1.26× to 12.6× and an NA of 0.6 were used. The following filter settings were used for excitation/emission of: EGFP 520 ± 40/585 ± 40 nm; mCherry 560 ± 40/620 ± 60 nm and LectinA647 630 ± 30/680 ± 30 nm. Z-step size was set to 20 µm and a 2× optical zoom factor was used. Stitched 3D mosaics were composed of 8 tiles of 215 Z-stacks in a total range of 4,280 µm.

Histology

Following light sheet microscopy the same lung lobe was paraffin embedded and 2 µm sections were cut using a Leica EG 1150C Microtome. Deparaffinized sections were stained with Haematoxylin and Eosin (H&E) and imaged using an Axiovert 200 M inverted microscope (Carl Zeiss Microscopy GmbH).

Image Analysis

All images, including volumetric 3D images of microscopy z-stacks, were processed and analyzed with the software Imaris 9.1.2 (Bitplane), Imaris Stitcher, FIJI (an image-processing package based on ImageJ) and Graph Pad Prism 7.05 (Graph Pad Software, Inc.). Maximum 3D projections of z-stacks are presented. Videos were produced from time series using Imaris 9.1.2.

RESULTS AND DISCUSSION

Set-Up of ex vivo Live Cell Imaging of the Mouse Lung

To demonstrate the feasibility of *ex vivo* live cell imaging we chose three biological scenarios in the mouse lung:

(i) To evaluate the immediate interaction of NPs and tumor cells with the immune cells and the surrounding lung tissue we either i.v. injected LL/2-RFP cells (Bertram and Janik, 1980) or fluorescently labeled Ba-NPs (Ba-Atto488 or Ba-Cy3) in CD68-EGFP or Nu/Nu mice.

(ii) To evaluate the inter-cellular behavior of tumor cells, we incubated A549-mCherry cells with Ba-Atto488 NPs overnight and injected them i.v. into Nu/Nu mice.

(iii) To visualize the tumor cell dynamics in the tumor mass and the interactions of NPs with tumor tissue we used the model of experimental lung metastasis.

The use of the fluorescent protein-expressing-cancer cells (A549-mCherry and LL/2-RFP), transgenic fluorescent protein expressing animals (CD68-EGFP), and fluorescent tags (Lectin-A647 and Ba-NPs) enabled the easy discrimination of tumor cells, tumor masses, blood vessels and NPs and their specific interactions (Hoffman, 2009). The human tumor cell line A549 is commonly used for experimental metastasis and produced solid nodules in the lungs of Nu/Nu mice after i.v. application, as previously described (Liu et al., 2012).

As an illustrative example for NPs we chose Ba-based NPs of about 120 nm in size that are non-toxic. Cell proliferation tests (MTT assay) at 4 h incubation showed no cytotoxic effects over the tested concentration range while incubation at 24 h time showed a concentration dependent trend, but still no relevant cytotoxic effects (cell vitality > 80 %) (**Supplementary Figure 1**). MTT assay with A549 cells at 24 h incubation time showed identical results (data not shown). Ba-NPs were either labeled with Atto488 or Cy3 fluorescent dyes that resulted in a detectable resolution range due to their formation of small agglomerates. Furthermore, they were efficiently taken up by macrophage/monocytes and tumor cells *in vitro* (data not shown).

Blood vessels were stained *in vivo* with the widely used protein Lectin, which is known to bind to glycoproteins located in the glycocalyx and in the basal membrane of endothelial cells. The visualization of the blood vessels provided a good “counterstain” of the lung tissue structure and excellent means to monitor the stability of the tissue over the time measurements.

We chose to sacrifice the animals shortly after injection of NPs because we were interested in visualizing the immediate reaction of tumor and immune cells to NPs in the lung. The filling of the lungs with agarose following the sacrifice of the mice prevented the collapse of the lungs and maintained the structural integrity of the lung. Environmental control settings during the image acquisition process provided physiological conditions to maximize the length of cell viability within the explanted lung. The total process from i.v. injection of NPs or tumor cells to acquisition of the first image took on average 40–60 min.

Combined, this *ex vivo* imaging approach allowed us to assess several live cell processes in the lung tissue at cellular resolution and up to a time period of at least 4 h. These findings are in accordance with results previously described by van den Bijgaart et al. (2016). While they showed the suitability of the technique to monitor the activity of metastatic and immune cells over a similar time period, we were able to additionally demonstrate the interaction with NPs and shedding of extracellular vesicles

(EVs) at a substantially improved resolution. Most importantly, we were able to demonstrate cell dynamics and motility at quantifiable numbers by assuring minimal tissue movement during acquisition.

Live cell imaging of the mouse lung has been attempted before by intravital lung imaging using intercostal windows, however this is a very complicated technique and stressful for the animal (Headley et al., 2016). Other imaging approaches such as endoscopy or fluorescence reflectance imaging provide significantly lower resolution. The *ex vivo* live cell imaging method presented here also requires no *ex vivo* staining procedures if fluorescently labeled nanoparticles and fluorescently tagged cell lines are used for the induction of tumors. The approach described here thus provides a powerful 4D tool for monitoring nanoparticle-cell and cell-cell interactions.

In the following we present several scenarios where this technique has proven to be useful for *ex vivo* live cell imaging of the lung.

Reaction of Macrophages and Monocytes Toward Tumor Cells

The i.v. injection of tumor cells is a common method to mimic circulating tumor cells (CTCs) which can be generated by primary tumors and can lead to metastasis. From the circulation, the cells reach the lung within minutes. We therefore i.v. injected LL/2-RFP cells into CD68-EGFP transgenic mice to examine the behavior of tumor cells at the immediate contact with immune cells.

In the first hour of acquisition we could observe the recruitment of macrophages/monocytes to the tumor cell-rich regions and their surveillance (**Figure 1**). **Supplementary Movie 1A**, which includes the Lectin-A647 stained blood vessel imaging, shows minimal movement of the lung tissue and high focus stability over a period of 3 h 20 min. Moreover, **Supplementary Movie 1B** shows that the interaction of monocytes and macrophages with the tumor cells is a very immediate process, where within 5 min frame intervals we observed immune cells which directly contacted the tumor cells and appeared and disappeared from the video frame. Furthermore, **Supplementary Movie 1B** illustrates that tumor cells produce extensive extracellular vesicles (EVs), which are partly captured by CD68-positive cells (white arrow). Blebbing of cells was also observed at about 2 h of acquisition, suggesting apoptotic processes of tumor cells around 3 h after their arrival in the lung tissue. Moreover, the phagocytosis of tumor cells by macrophages/monocytes is seen in **Supplementary Movie 1B** (yellow arrow).

The dynamic movement of monocytes/macrophages and tumor cells were tracked over time in lungs of CD68-EGFP mice which received an i.v. injection of LL/2-RFP tumor cells as shown in **Figure 2A** and **Supplementary Movie 2**. The displacement dynamics of both cell types were recorded over 87 min (**Figure 2B**) and were quantified in **Figure 2C**.

No other cell is more appropriate than the macrophage to show the need that cells have to be examined in their natural

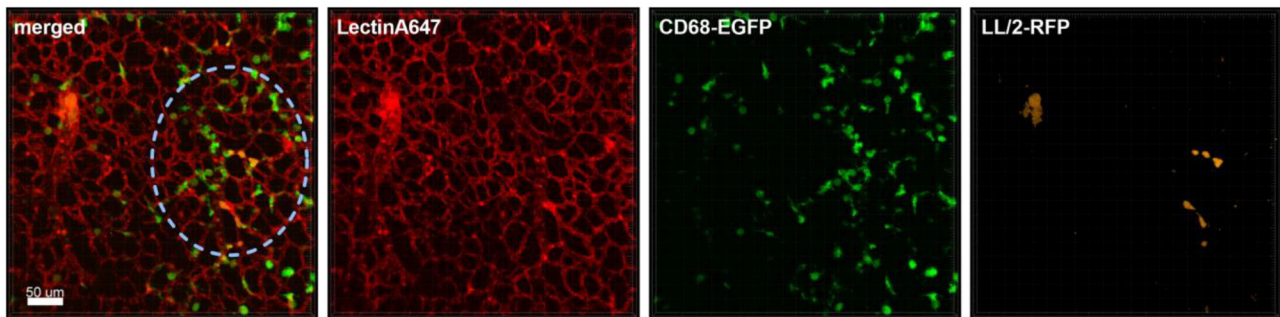
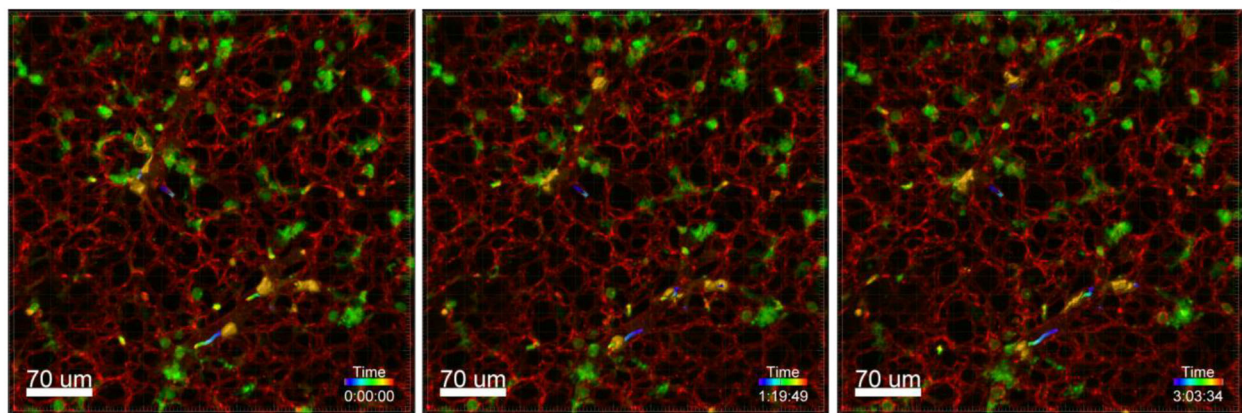
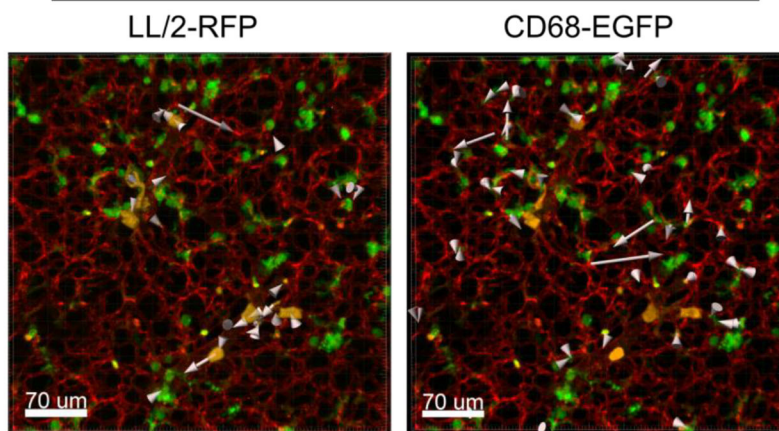


FIGURE 1 | Monocyte recruitment and surveillance of tumor cells within the lung. Representative confocal images of a lung lobe from a CD68-EGFP mouse (macrophages and monocytes green), showing the macrophages/monocytes distribution in the lung parenchyma/vessels visualized by staining of blood vessels with Lectin-A647 (red) in close proximity to LL/2-RFP tumor cells (yellow). Tumor cells and Lectin-A647 were applied shortly before sacrifice. Images show the overlay (merged) of Lectin-A647 (red), CD68-EGFP cells (green), and LL/2-RFP cells (yellow). Scale bar represents 50 μm .

A Time Series



B dynamics over time



C displacement dynamics

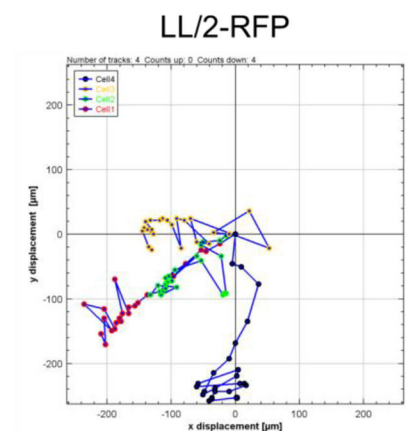


FIGURE 2 | Tracking of cell dynamics. Confocal images of a lung lobe from a CD68-EGFP mouse (macrophages and monocytes green), injected with Lectin-A647 (red), and LL/2-RFP cells (yellow) i.v. 5 min before sacrifice. **(A)** Representative frames of a time series over 3 h at an interval of 300 s showing the trajectories of LL/2-RFP cells within blood vessels. **(B)** Two representative examples of how individual cells can be tracked over time. Arrow length represents the distance of displacement of individual cells over time. **(C)** Exemplary measurement of the 2D displacement dynamic of 4 LL/2-RFP cells. Scale bars represent 70 μm .

setting. Only recently, Hussell and Bell stressed in a review that alveolar macrophages exist in a unique microenvironment of the airway lumen which can have a considerable influence on many aspects of their phenotype, function and turnover (Hussell and Bell, 2014). There is for instance little understanding of the extent to which alveolar macrophages interact with the epithelium, blood vessels or with one another in their response to pathogens, allergens, or environmental challenges. Additionally, different macrophage lineages, for example tissue-resident and monocyte-derived macrophages, may respond differently to cytokines and other signals received from tumor cells (Ham et al., 2020).

However, our knowledge on TAMs, monocytes and the interaction of these with tumor cells, microenvironment mainly comes from *in vitro* and histological examinations, leaving a large information gap on how these cell lineages behave *in vivo*. Recently, Headley et al. used intravital microscopy using an intercostal window to describe the reaction of macrophages to freshly arrived CTCs in the lung tissue (Headley et al., 2016). Their results show the dynamic generation of tumor microparticles by the CTCs in capillaries and the loading of such material onto cells of the myeloid lineage. Our *ex vivo* live cell imaging approach confirms such findings using a much simpler technique and demonstrates the feasibility to shed some light on some of the processes involving the monocyte/macrophage lineage and the behavior of CTCs.

Reaction of Macrophages and Monocytes Toward Nanoparticles

TAMs and monocytes are also important for the specific accumulation of NPs, which are increasingly explored for therapeutic drug delivery in oncology (Cuccarese et al., 2017). Nanomedicines can also be engineered to inhibit the recruitment, kill or re-educate TAMs, and imaging TAMs with NPs can support diagnosis and prognosis of cancer (Andón et al., 2017).

Different to the behavior of immune cells toward tumor cells described above, the i.v. injection of NPs into healthy CD68-EGFP mice did not produce the same recruitment effect of blood monocytes and alveolar macrophages, since the NPs have a more homogenous dispersion throughout the lung tissue. **Figure 3** and **Supplementary Movie 3** are produced from lung lobes of CD68-EGFP mice that received an i.v. injection of Ba-Cy3 NPs. The images show that CD68 positive blood monocytes (green) which appear smaller than the also CD68-positive alveolar macrophages, are excellent phagocytes, internalizing the Ba-Cy3 NPs and possibly processing them (**Figure 3B**). **Figure 3A** and **Supplementary Movie 3** also show how active the Ba-Cy3-NP-loaded monocytes move up and down the blood vessels, which can be tracked over time.

A limitation of the technique is the necessity to use agarose to fill the lung in order to prevent collapsing of the lung. This evidently implies a somewhat unphysiological environment in the bronchial and alveolar spaces and most certainly represents a barrier for alveolar macrophages and their mobility. Processes that occur in these spaces can therefore only be observed in limits. Especially the phagocytosis of NPs and tumor cells by alveolar macrophages are likely to be hampered. We have

attempted to image *ex vivo* lungs which we filled with air via the trachea and immediately enclosed in 1% agarose on a microscopy chamber to mimic the outside pressure of the pleural space and rib cage and thus prevent loss of air. Visualization of live cells, including alveolar macrophages is still possible up to 1 h post preparation, but the instability of the lung then causes movement and consequently imaging artifacts (data not shown). The described technique using agarose to fill the lung is thus mostly suited for visualization of processes that occur within the blood and lymphatic vessels and interaction of NPs with blood residing immune cells as well as endothelial cells. However, some aspects such as the induction of cell apoptosis by drugs or the internalization of NPs by alveolar macrophages may well be studied by including the drugs or NPs in the agarose. We included Ba-Cy3 NPs in the agarose and could indeed detect the phagocytosis of NPs by macrophages (data not shown).

Another interesting finding was that Ba-based NPs injected i.v. into Nu/Nu mice were mostly detected in blood vessels, but some were also found moving in lectin-unstained vessels, suggestive of lymphatic channel drainage (**Figure 4**). For the use of NPs as drug delivery systems, the understanding of their clearance is very important. NPs can be transported to the lymph nodes through the lymphatic vessels where they could accumulate or also be transported back to the blood stream and end up in the liver or kidneys for elimination, depending on their size. NPs can also be designed to be favorably delivered to immune-rich organs such as lymph nodes or spleens (Reddy et al., 2007). In future, *ex vivo* live cell imaging may thus be used to test whether nanovaccines can be efficiently drained into the lymphatic system, enabling accumulation in lymph nodes which contain a high number of immune cells and which coordinate diverse immunomodulation events. This method may be also used to test the size dependency of NPs for lymphatic drainage of NPs. Reddy et al. reported for instance that after intradermal injection, interstitial flow transported 25 nm small nanoparticles highly efficiently into lymphatic capillaries and their draining lymph nodes, targeting half of the lymph node-residing dendritic cells, whereas 100 nm NPs were only 10% as efficient (Reddy et al., 2007).

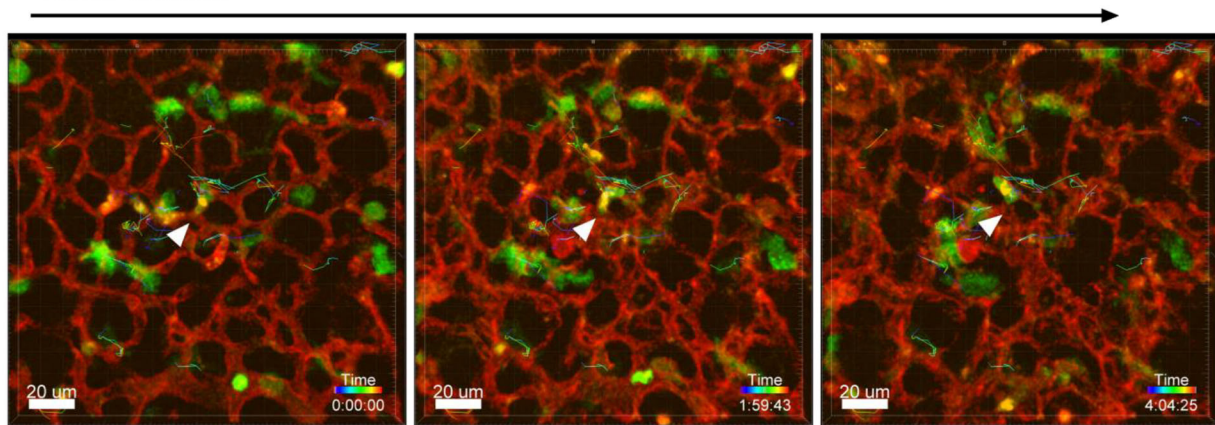
Delivery of Nanoparticles to the Tumor

Targeting NP-based therapies to the tumor site is obviously crucial for specific and effective treatment. It is therefore important to assess the capability of nanoparticulate drugs to reach the tumor, as we show in the following examples.

Experimental lung metastasis was obtained by i.v. injection of A549-mCherry cells in NMRI-Fox1nu/nu mice that led to the formation of tumor nodules in the lung that were easily detectable by their fluorescence (**Figure 5**). Blood vessel staining of the nodules revealed that they are poorly perfused and possess a strong connective tissue capsule (**Figure 5**).

Although NPs have progressively been used as drug delivery systems their successful transport to the tumor lesion or TAMs is not always a given. We tested the feasibility of *ex vivo* lung live cell imaging for assessing the penetration and accumulation of Ba-NPs at the tumor site. **Figure 5** shows a lung lobe of a mouse with an A549-mCherry positive lung metastasis which

A Time Series



B

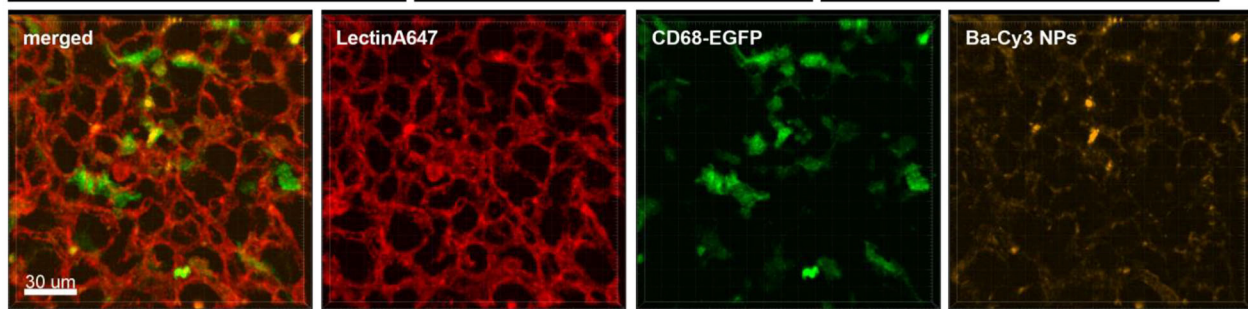


FIGURE 3 | Uptake of NPs by monocytes and their tracking. Representative confocal images of a lung lobe from a CD68-EGFP mouse (macrophages and monocytes green). Lectin-A647 for visualization of blood vessels (red) and Ba-Cy3 NPs (yellow) were injected i.v. 5 min before sacrifice. **(A)** Representative frames of a time series over 4 h at an interval of 300 s showing the trajectory of individual monocytes. Scale bar represents 20 μm . **(B)** shows the co-localization of the Ba-Cy3 NPs with the CD68-EGFP positive monocytes within blood vessels. Images show the overlay (merged) of Lectin-A647 (red), CD68-EGFP cells (green), and Ba-Cy3 NPs (yellow). Scale bar represents 30 μm .

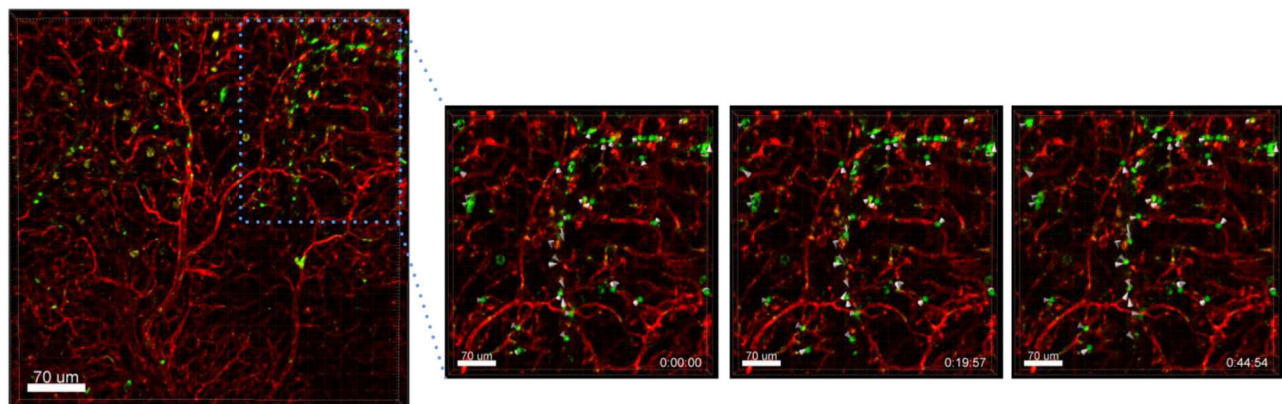


FIGURE 4 | Drainage of Ba-488 NPs by lymphatic vessels. Confocal microscopy images of lung lobes which received i.v. injected Ba-Atto488 NPs (green) and Lectin-A647 (red) 30 min before sacrifice of the mouse. Left: overview image. Right: representative higher magnification images of a time series over 45 min of a selected area tracking NPs in a non-lectin-stained vessel. Scale bars represent 70 μm .

received an i.v. injection of Ba-Atto488 NPs. It is clearly visible that the type and size of NPs used here strike a barrier around the tumor mass that they cannot penetrate and only a very

small proportion of NPs reach the core of the tumor, due to the limited vascularization of the nodule, as illustrated by the lack of lectin staining.

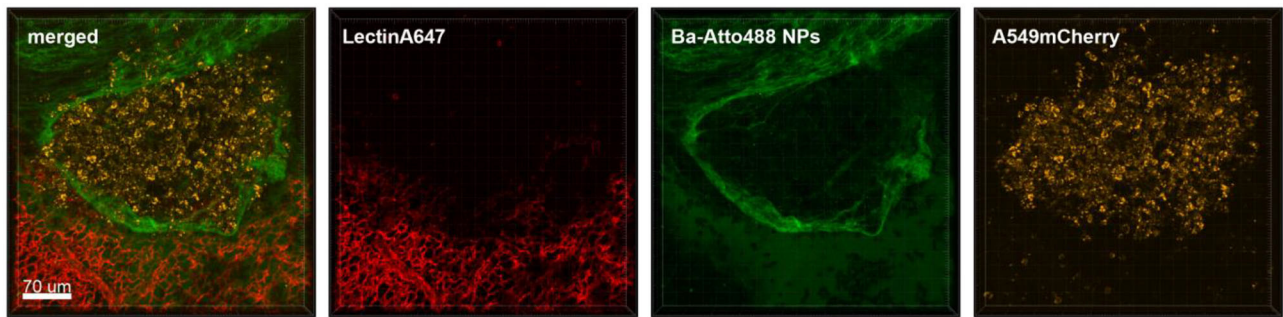


FIGURE 5 | Ba-NPs barely penetrate the tumor capsule due to poor tumor vascularization. Confocal images of a lung lobe from a mouse with A549-mCherry induced lung tumor nodules that received Ba-Atto488 NPs i.v. shortly before sacrifice. Images show the overlay (merged) of Lectin-A647 for blood vessel staining (red), Ba-Atto488 NPs (green), and A549-mCherry positive nodules (yellow). Scale bar represents 70 μm .

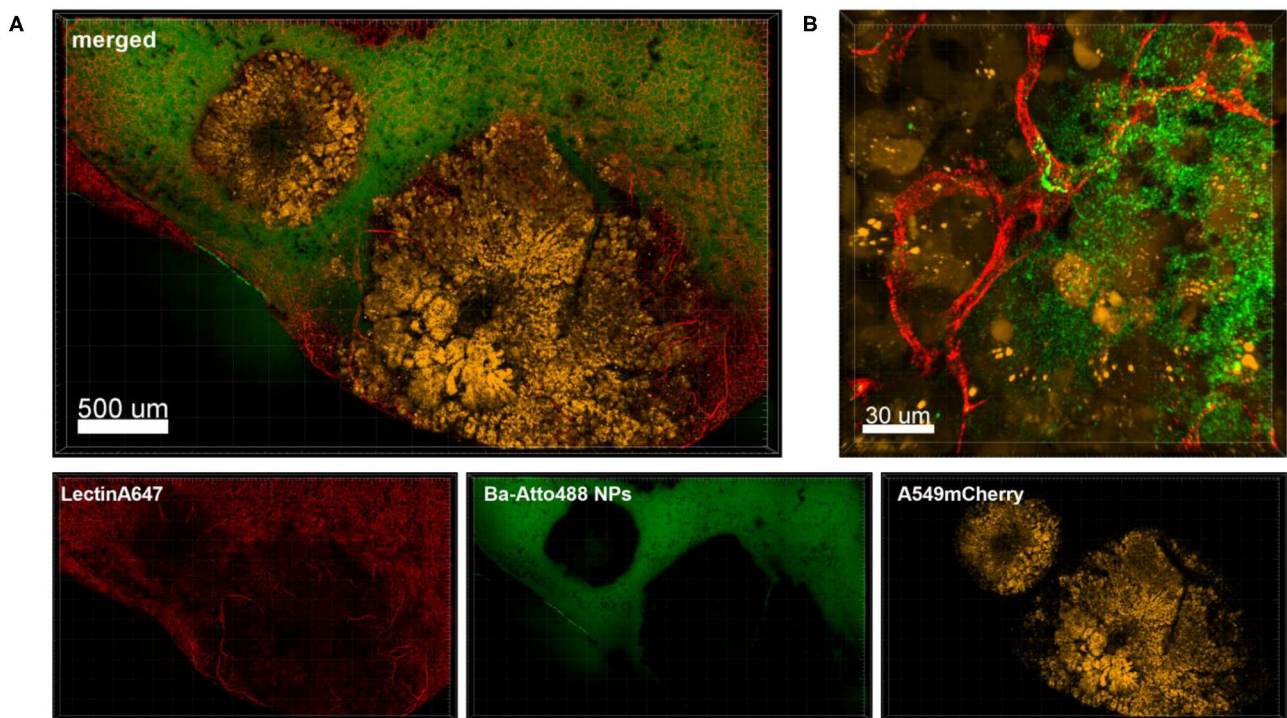
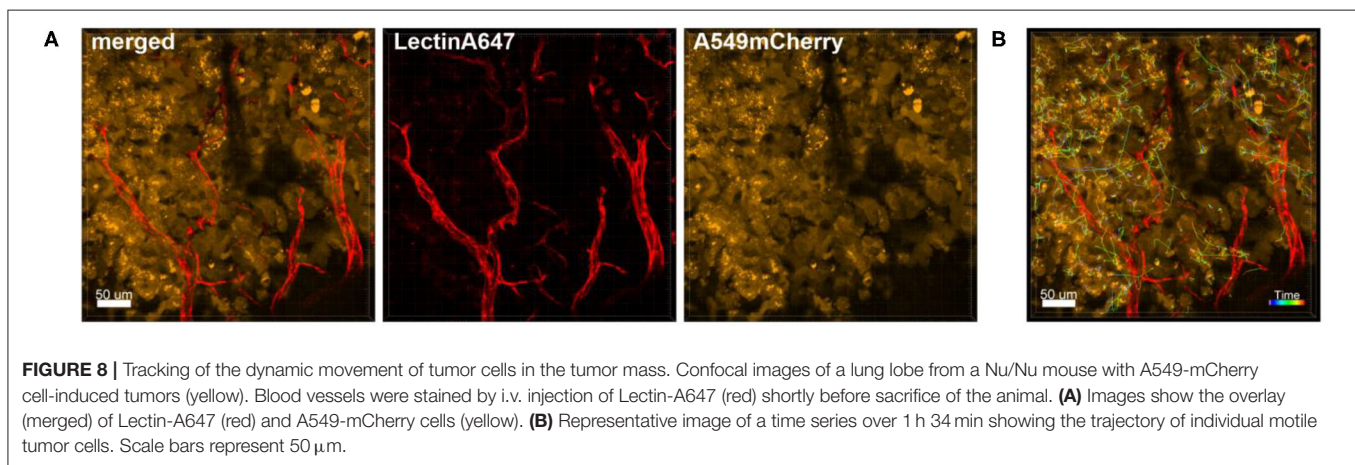
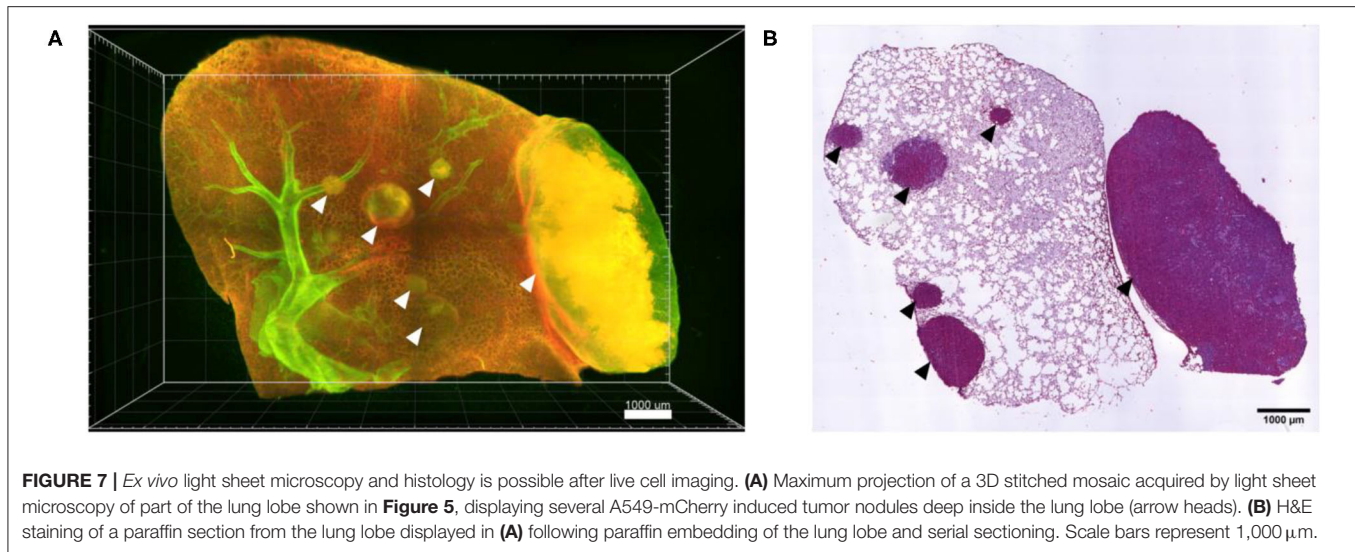


FIGURE 6 | Penetration of Ba-Atto488-NPs into the tumor tissue. Representative confocal images of a lung lobe from a Nu/Nu mouse with A549-mCherry (yellow) lung tumor nodules. Lectin-A647 (red) for blood vessel staining and Ba-Atto488 NPs (green) were injected i.v. shortly before sacrifice. **(A)** Overview of two tumor nodules in the lung with central necrotic areas and poor vascularization. Images show the overlay (merged) of Lectin-A647 (red), Ba-Atto488 NPs (green), and A549-mCherry cells (yellow). Scale bar represents 500 μm . **(B)** shows a magnified region at the border of the tumor represented in **(A)**, with a leaky vessel within one of the nodules and Ba-Atto488-NPs that entered the surrounding tumor tissue in close proximity to the vessel. Ba-Atto488 NPs were detected with Airyscan technology. Scale bar represents 30 μm .

Figure 6 shows an overview of part of a lung lobe with several A549-mCherry induced tumor nodules and Ba-Atto488 NPs as well as Lectin-A647 injected shortly before sacrifice. The tumor nodules displayed a mixed intensity of mCherry fluorescent protein, which may be either due to different levels of mCherry expression or heterogeneous development of the tumor cells (**Figure 6A**, yellow signals). Furthermore, dark areas were visible

in the center of the nodules, suggestive of necrosis (**Figure 6A**). The nodules are generally poorly vascularized as seen by a lack of bound Lectin-A647 (**Figure 6A**, red signals). This led to a very limited distribution of Ba-Atto488 NPs in the tumor nodules when compared to the healthy lung tissue, where the NPs were generally well-dispersed throughout. Some lectin-stained vessels are present at the border of the tumor and these are partly

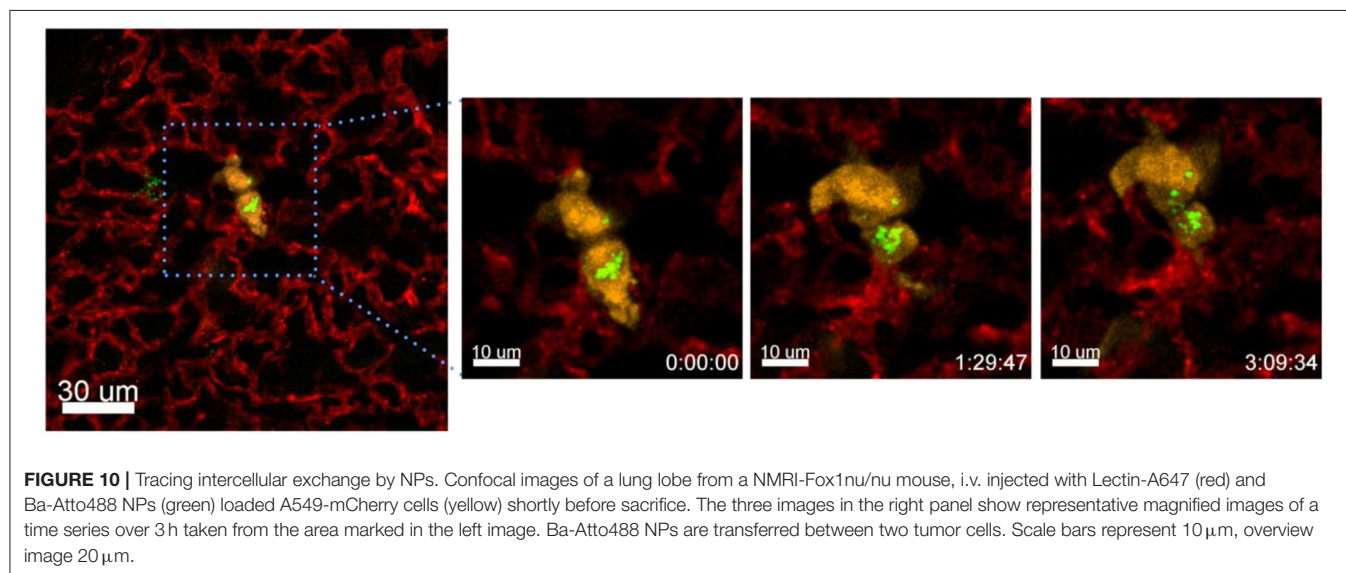
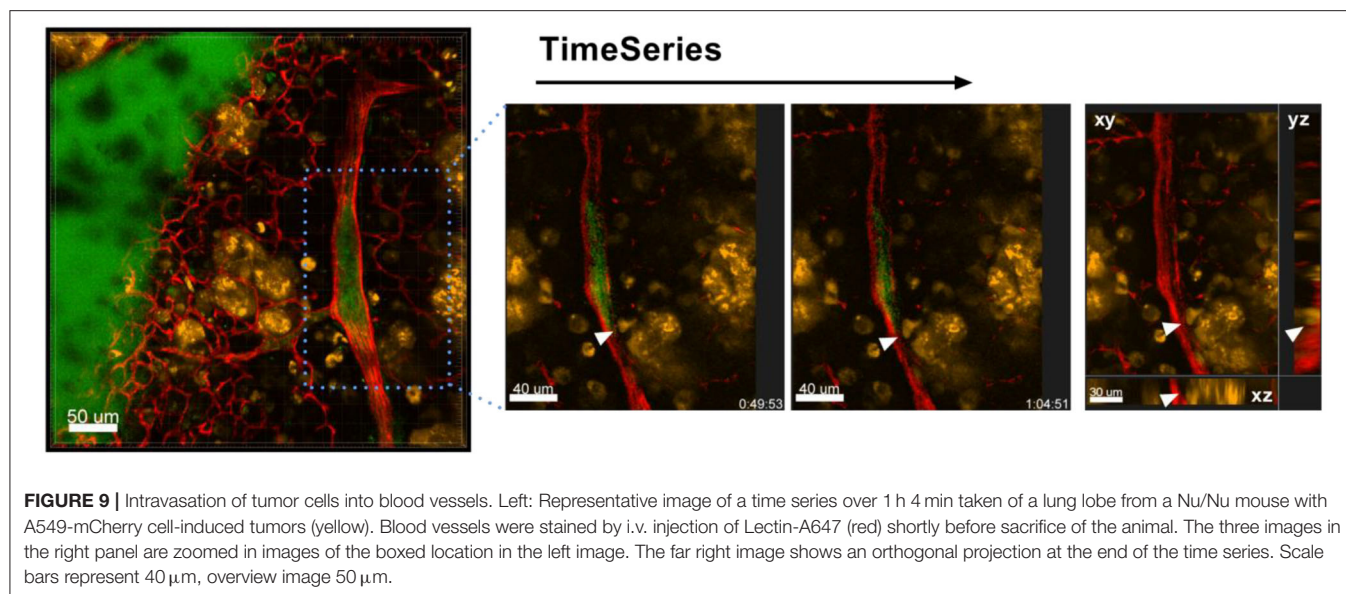


leaky, which is demonstrated by an accumulation of NPs in the surrounding tumor tissue (**Figure 6B**).

These results confirm earlier problems with the specific delivery of nanoparticulate drugs to tumor sites. Despite the fact that nanoencapsulated drugs have been shown preclinically to accumulate in tumors via the enhanced permeability and retention effect (EPR) (Sanna and Sechi, 2020) as well as attempts to actively target the tumors by functionalization of nanotherapies with specific antibodies, most efforts showed a very large intra- and inter-individual heterogeneity, explaining the mixed response of patients to the therapies (Dasgupta et al., 2020). It appears that tumors show vast differences in EPR-contributing parameters, such as vessel density, perfusion and permeability, tumor stroma composition and lymphatic vessel functionality (Dasgupta et al., 2020) and these differences largely contribute to the heterogenic response of tumors to nanotherapies. Our approach vividly depicts this problem by showing that the limited accumulation of NPs at the tumor site can be related to both a lack in vascularization as well as a dense stroma capsule around the tumor, offering an exemplary

explanation for the frequently poor efficacy found when such strategies are implemented. Moreover, the delivery of NPs to the tumor and lymph nodes, the elimination pathway as well as their intracellular processing is dependent on the size and shape of NPs (Stylianopoulos, 2013). A fine balance has to be found between NP sizes that are large enough to avoid a rapid renal clearance, but small enough to penetrate the leaky tumor vessel pores. The *ex vivo* live cell imaging method may therefore be a useful tool for the evaluation of differently sized and composed NPs and the effect these parameters have on EPR, lymphatic drainage and modification of the extracellular matrix (Fernandes et al., 2018; Wang et al., 2019).

Following confocal live cell visualization, the tissues can be prepared for all other common *ex vivo* visualization procedures, including light sheet microscopy and histology, as shown in **Figure 7**. Light sheet microscopy, which uses cleared fixed tissue revealed additional tumor nodules deep within the same lung lobe, which were not identified by confocal microscopy due to limited optical penetration. H&E staining of a 2D paraffin section from the same lung tissue confirmed several locations of tumor



lesions. Combined, *ex vivo* live cell confocal imaging of entire lung lobes is thus a good preclinical method of pre-assessing the accumulation of NP-based drugs at the desired site of action, in particular in the case of tumor masses.

Tumor Cell Dynamics

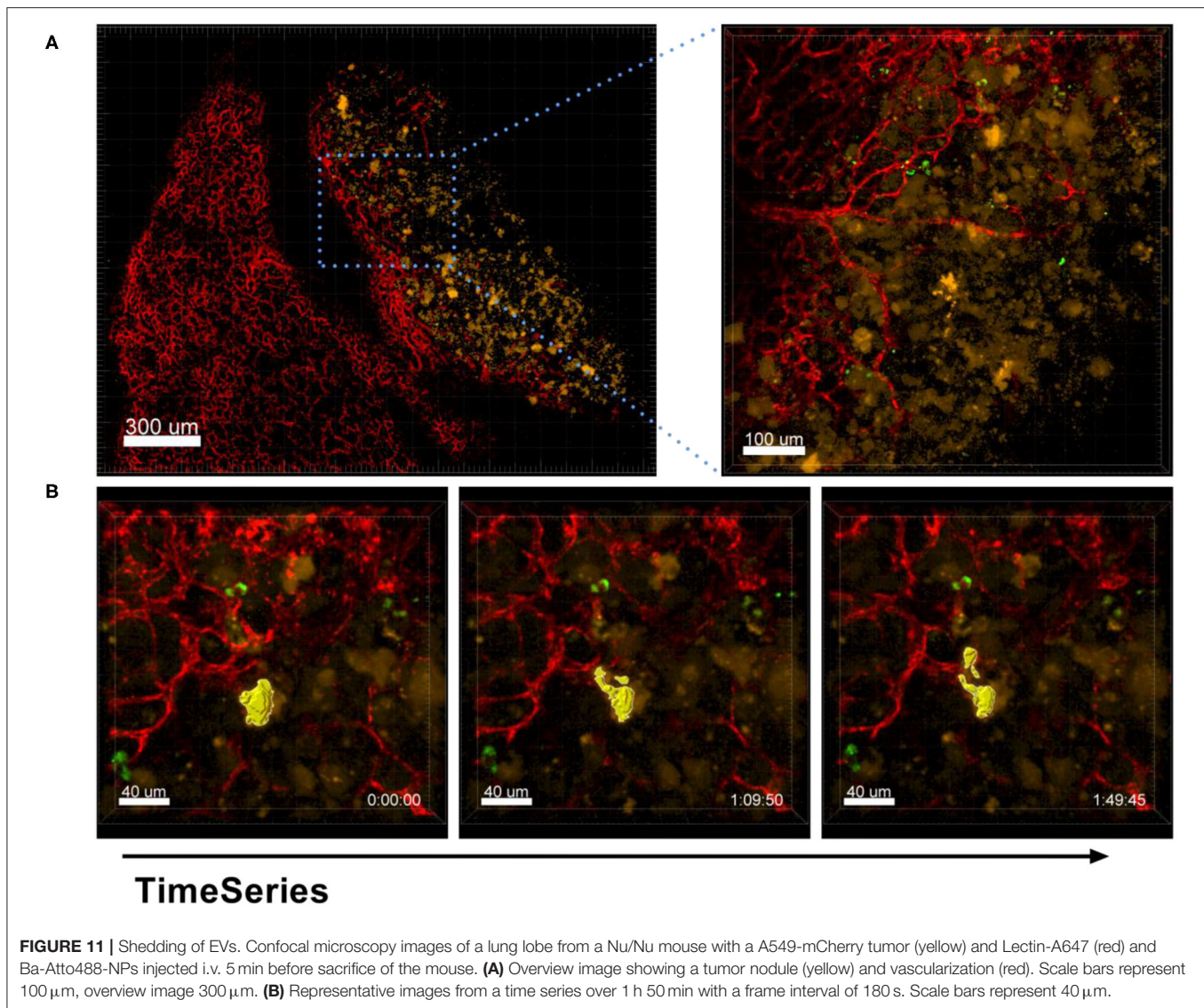
Also the behavior of individual or clusters of cells within a tumor mass can be studied. We have for instance observed astonishingly strong movement of tumor cells in already established tumor masses that were induced several weeks before imaging (**Figure 8** and **Supplementary Movie 4**). This suggests that tumors are extremely active structures with dynamic cell displacement.

The process of extra- and intravasation of tumor cells into and from blood vessels are also processes that could be studied in detail by *ex vivo* lung live cell imaging, an example of which can

be seen in **Figure 9**. Imaging of the direct crossing of the tumor vascular barrier through intercellular gaps may be achieved by Airyscan technology.

Exchange of Nanomaterial Between Tumor Cells

Another process that we observed with the presented technique is the exchange of material between different cells. In the following example we have incubated A549-mCherry cells with Ba-Atto488 overnight and then injected them i.v. in a NMRI-Fox1nu/nu mouse. **Figure 10** and **Supplementary Movie 5** clearly show the exchange of Ba-NPs between two tumor cells active in the lung. The exchange of nanomaterial took place over 3 h. As we have labeled the A549-mCherry cells with Ba-Atto488-NPs before injecting them i.v., it is most likely that



the NPs are already located in late endosomes/lysosomes, which can be then transferred by extracellular shedding. Fluorescent NPs are of advantage here for the visualization of this process.

Intercellular organelle and EV exchange has been described many times, but most have only been shown in cell culture (Rogers and Bhattacharya, 2013). Moreover, the transfer of exosomes from one cell to another is a common feature especially in immune cells. EVs are vehicles for bidirectional communication between cells and carry bioactive molecular cargoes, including proteins, lipids and nucleic acids that can affect the functions and phenotypes of recipient cells by altering gene expression or by activating various signaling pathways (Maacha et al., 2019). EVs can carry their cargo from the parent cell and can be captured by neighboring or distant recipient cells through the interaction of vesicular ligands with cellular receptors, but the precise mechanisms of interaction remain poorly characterized.

Tumor-derived EVs may contain tumor-specific antigens on their surface or miRNAs and brings an advantage to cells that can share this material with other cells. Studies suggest that vesicles can be internalized and could fuse with the recipient cell either at the plasma membrane or after internalization (Théry et al., 2009). While we cannot directly show that the transfer of NPs happened through EVs, we speculate that this is the most likely process. Importantly, to our knowledge this is the first description of material exchange between tumor cells in live lung tissue imaging.

Shedding of Membrane Vesicles

The process of EV production by tumor cells was also captured by our *ex vivo* live cell microscopy approach. As shown in **Figure 11** and **Supplementary Movie 6A**, A549-mCherry tumor cells from an established tumor nodule were observed in the process of

producing vesicles of about 10 μm in size and releasing them in a blebbing manner.

A second example of EVs shedding of similar size can be seen in **Supplementary Movie 6B**, which was produced shortly after i.v. injection of A549-mCherry cells. This movie also shows that ex-vivo live cell imaging visualized the active movement of tumor cells within a blood vessel over about 3 h 19 min hours. Furthermore, several tumor cells were observed that undergo apoptosis, or others seem to be more resistant and release EVs and rapidly explore the surrounding tissue. The lung is the organ with the highest vascular density in humans and thus substantially contributes to the circulation of EVs, lipid bilayer-delimited particles that contribute to the development of metastasis. Exosomes, microvesicles and oncosomes secreted by tumors have been shown to inhibit immune responses, but in conjunction with adjuvants they can also induce potent antitumor responses (Théry et al., 2009). Moreover, all these EVs have been shown to be key players in signaling of tumor cells over long distances, contributing to the promotion of a pre-metastatic niche and reprogramming of the stroma (Minciocchi et al., 2017; Wortzel et al., 2019). While exosomes may be too small (up to 150 nm) to visualize by our described approach, microvesicles (100–1,000 nm) and oncosomes (1–10 μm) are in the range of good visibility by confocal microscopy. It is therefore probable that the EVs we detected by *ex vivo* live cell imaging are oncosomes. Thus, this method may support the better understanding of EVs and their distinctive roles and may also contribute to the clarification of the controversy that exists to date on the nomenclature of EVs (Meehan et al., 2016; Witwer and Théry, 2019). This method is thus a valuable tool to identify the continuous formation of EVs by the tumor cells, which most of the time cannot be detected by slice imaging methodologies once that the EVs lose the expression of key cancer biomarkers used to identify the tumor cells.

CONCLUSION AND POTENTIAL

Ex vivo live cell confocal microscopy provides a new way of studying the interactions of nanoparticles with immune and tumor cells and the vessel endothelium. As we show by several examples in the mouse lung, the method presents a notable alternative to more demanding techniques such as intravital lung microscopy using windows and to *in vivo* optical imaging that provide substantially lower resolution. It is mostly suitable for the visualization of processes that occur within the vessel/tumor interfaces, such as delivery of NPs to the tumor, interaction of NPs with blood monocytes, intra- and extravasation. Thus, the method may support the characterization of nanoparticulate therapies, studying the dependence of NP uptake on the heterogeneity and microenvironmental features of tumors as well as the optimization of NPs size and functionalization for specific targeting. By engineering specific NP surfaces it should in theory be possible to modulate and control host responses. Such processes may also be studied by this technique. While we are using fluorescently tagged cell lines and transgenic

mice to visualize specific cells, an alternative or additional approach could be the injection of fluorescent antibodies before sacrifice and imaging of the lung. Moreover, the approach is able to supply new information on cell processes that are not directly and instantaneously affected by a loss of air flow or breathing mechanics, such as the behavior of tumor masses in the lung, including the production of extracellular vesicles and their fate, intercellular exchange of material/organelles and the processing of tumor material by immune cells. While we focus on interactions with nanoparticles, this method may provide novel information on a number of other cellular events, such as the phagocytosis of tumor cells by macrophages and other cells; the immediate cellular effects of treatments such as chemotherapies, including the live visualization of apoptotic events; the immediate reaction of immune cells at encounter of allergens and real-time detection of intracellular and metabolic processes in live cells.

DATA AVAILABILITY STATEMENT

All datasets generated for this study are included in the article/**Supplementary Material**.

ETHICS STATEMENT

The animal study was reviewed and approved by Nds. Landesamt für Verbraucherschutz und Lebensmittelsicherheit.

AUTHOR CONTRIBUTIONS

FR-G conceived and designed the experiments, acquired and analyzed the data, and wrote the paper. NF acquired and analyzed the light sheet microscopy data. AK designed and prepared the nanoparticles. FA conceived the experiments and contributed to writing the paper. MM conceived, designed, prepared the experiments, and wrote the paper. All authors contributed to the article and approved the submitted version.

FUNDING

This project has received funding from the European Union's Horizon 2020 research and innovation program under the Marie Skłodowska-Curie grant agreement No. 861190 (PAVE) and from the BMBF (VDI) funded projects THERAKON (No. 13GW0218A) and ELICIT (No. 13N14346).

ACKNOWLEDGMENTS

We thank Bärbel Heidrich and Regine Kruse for excellent technical assistance. We further acknowledge the Microscopy Facility of the Max-Planck-Institute of Experimental Medicine. A549-mCherry lung tumor cells were a kind gift from Dr. Michael Winkler, Deutsches Primatenzentrum Göttingen and LL/2-RFP (Lewis Lung) cancer cells were a kind gift from Prof. Hellmut Augustin, Deutsches

Krebsforschungszentrum, Heidelberg. Lectin-Alexa647 was a kind gift from Jörg Peter Müller und Dr. Thomas Pöschinger, Preclinical Imaging Laboratory, Discovery Oncology Pharmacology, Roche Innovation Center Munich, Roche Diagnostics GmbH.

REFERENCES

- Andón, F. T., Digifico, E., Maeda, A., Erreni, M., Mantovani, A., Alonso, M. J., et al. (2017). Targeting tumor associated macrophages: the new challenge for nanomedicine. *Semin. Immunol.* 34, 103–113. doi: 10.1016/j.smim.2017.09.004
- Arora, S., Dev, K., Agarwal, B., Das, P., and Syed, M. A. (2017). Macrophages: their role, activation and polarization in pulmonary diseases. *Immunobiology* 223, 383–396. doi: 10.1016/j.imbio.2017.11.001
- Bertram, J. S., and Janik, P. (1980). Establishment of a cloned line of lewis lung carcinoma cells adapted to cell culture. *Cancer Lett.* 11, 63–73. doi: 10.1016/0304-3835(80)90130-5
- Blank, F., Fytianos, K., Seydoux, E., Rodriguez-Lorenzo, L., Petri-Fink, A., von Garnier, C., et al. (2017). Interaction of biomedical nanoparticles with the pulmonary immune system. *J. Nanobiotechnol.* 15:6. doi: 10.1186/s12951-016-0242-5
- Cassetta, L., and Kitamura, T. (2018). Macrophage targeting: opening new possibilities for cancer immunotherapy. *Immunology* 155, 285–293. doi: 10.1111/imm.12976
- Cuccarese, M. F., Dubach, J. M., Pfirschke, C., Engblom, C., Garriss, C., Miller, M. A., et al. (2017). Heterogeneity of macrophage infiltration and therapeutic response in lung carcinoma revealed by 3D organ imaging. *Nat. Commun.* 8:14293. doi: 10.1038/ncomms14293
- Dasgupta, A., Biancacci, I., Kiessling, F., and Lammers, T. (2020). Imaging-assisted anticancer nanotherapy. *Theranostics* 10, 956–967. doi: 10.7150/thno.38288
- Fernandes, C., Soares, D., and Yergeri, M. C. (2018). Tumor microenvironment targeted nanotherapy. *Front. Pharmacol.* 9:1230. doi: 10.3389/fphar.2018.01230
- Ham, S., Lima, L. G., Lek, E., and Möller, A. (2020). The impact of the cancer microenvironment on macrophage phenotypes. *Front. Immunol.* 11:1308. doi: 10.3389/fimmu.2020.01308
- Headley, M. B., Bins, A., Nip, A., Roberts, E. W., Looney, M. R., Gerard, A., et al. (2016). Visualization of immediate immune responses to pioneer metastatic cells in the lung. *Nature* 531, 513–517. doi: 10.1038/nature16985
- Hoffman, R. M. (2009). Imaging cancer dynamics *in vivo* at the tumor and cellular level with fluorescent proteins. *Clin. Exp. Metastasis* 26, 345–355. doi: 10.1007/s10585-008-9205-z
- Hussell, T., and Bell, T. J. (2014). Alveolar macrophages: plasticity in a tissue-specific context. *Nat. Rev. Immunol.* 14, 1–93. doi: 10.1038/nri3600
- Jia, J., Zhang, Y., Xin, Y., Jiang, C., Yan, B., and Zhai, S. (2018). Interactions between nanoparticles and dendritic cells: from the perspective of cancer immunotherapy. *Front. Oncol.* 8:404. doi: 10.3389/fonc.2018.0404
- Khalil, D. N., Smith, E. L., Brentjens, R. J., and Wolchok, J. D. (2016). The future of cancer treatment: immunomodulation, CARs and combination immunotherapy. *Nat. Rev. Clin. Oncol.* 13, 273–90. doi: 10.1038/nrclinonc.2016.65
- Klingberg, A., Hasenberg, A., Ludwig-Portugall, I., Medyukhina, A., Männ, L., Brenzel, A., et al. (2017). Fully automated evaluation of total glomerular number and capillary tuft size in nephritic kidneys using lightsheet microscopy. *JASN* 28, 452–459. doi: 10.1681/ASN.201602.0232
- Li, X., Lee, S. C., Zhang, S., and Akasaka, T. (2012). Biocompatibility and toxicity of nanobiomaterials. *J. Nanomater.* 2012:e591278. doi: 10.1155/2012/591278
- Liu, X., Liu, J., Guan, Y., Li, H., Huang, L., Tang, H., et al. (2012). Establishment of an orthotopic lung cancer model in nude mice and its evaluation by spiral CT. *J. Thorac. Dis.* 4, 141–145. doi: 10.3978/j.issn.2072-1439.2012.03.04
- Liu, Y., Crowe, W. N., Wang, L., Lu, Y., Petty, W. J., Habib, A. A., et al. (2019). An inhalable nanoparticulate STING agonist synergizes with radiotherapy to confer long-term control of lung metastases. *Nat. Commun.* 10:5108. doi: 10.1038/s41467-019-13094-5
- Maacha, S., Bhat, A. A., Jimenez, L., Raza, A., Haris, M., Uddin, S., et al. (2019). Extracellular vesicles-mediated intercellular communication: roles in the tumor microenvironment and anti-cancer drug resistance. *Mol. Cancer* 18:55. doi: 10.1186/s12943-019-0965-7
- Marabelle, A., Kohrt, H., Caux, C., and Levy, R. (2014). Intratumoral immunization: a new paradigm for cancer therapy. *Clin. Cancer Res.* 20, 1747–1756. doi: 10.1158/1078-0432.CCR-13-2116
- Markus, M. A., Napp, J., Behnke, T., Mitkovski, M., Monecke, S., Dullin, C., et al. (2015). Tracking of inhaled near-infrared fluorescent nanoparticles in lungs of SKH-1 mice with allergic airway inflammation. *ACS Nano* 9, 11642–11657. doi: 10.1021/acsnano.5b04026
- Meehan, B., Rak, J., and Di Vizio, D. (2016). Oncosomes – large and small: what are they, where they came from? *J. Extracell. Vesicles* 5:10.3402/jev.v5.33109. doi: 10.3402/jev.v5.33109
- Minciacchi, V. R., Spinelli, C., Reis-Sobreiro, M., Cavallini, L., You, S., Zandian, M., et al. (2017). MYC mediates large oncosome-induced fibroblast reprogramming in prostate cancer. *Cancer Res.* 77, 2306–2317. doi: 10.1158/0008-5472.CAN-16-2942
- Napp, J., Markus, M. A., Heck, J. G., Dullin, C., Möbius, W., Gorpas, D., et al. (2018). Therapeutic fluorescent hybrid nanoparticles for traceable delivery of glucocorticoids to inflammatory sites. *Theranostics* 8, 6367–6383. doi: 10.7150/thno.28324
- Nembrini, C., Stano, A., Dane, K. Y., Ballester, M., van der Vlies, A. J., Marsland, B. J., et al. (2011). Nanoparticle conjugation of antigen enhances cytotoxic T-cell responses in pulmonary vaccination. *Proc. Natl. Acad. Sci. U.S.A.* 108, E989–E997. doi: 10.1073/pnas.1104264108
- Reddy, S. T., Vlies, A. J., van der, Simeoni, E., Angeli, V., Randolph, G. J., O'Neil, C. P., et al. (2007). Exploiting lymphatic transport and complement activation in nanoparticle vaccines. *Nat. Biotechnol.* 25, 1159–1164. doi: 10.1038/nbt1332
- Rodell, C. B., Arlauckas, S. P., Cuccarese, M. F., Garriss, C. S., Li, R., Ahmed, M. S., et al. (2018). TLR7/8-agonist-loaded nanoparticles promote the polarization of tumour-associated macrophages to enhance cancer immunotherapy. *Nat. Biomed. Eng.* 2, 578–588. doi: 10.1038/s41551-018-0236-8
- Rogers, R. S., and Bhattacharya, J. (2013). When cells become organelle donors. *Physiology* 28, 414–422. doi: 10.1152/physiol.00032.2013
- Sanna, V., and Sechi, M. (2020). Therapeutic potential of targeted nanoparticles and perspective on nanotherapies. *ACS Med. Chem. Lett.* 11, 1069–1073. doi: 10.1021/acsmchemlett.0c00075
- Stylianopoulos, T. (2013). EPR-effect: utilizing size-dependent nanoparticle delivery to solid tumors. *Ther. Deliv.* 4, 421–423. doi: 10.4155/tde.13.8
- Théry, C., Ostrowski, M., and Segura, E. (2009). Membrane vesicles as conveyors of immune responses. *Nat. Rev. Immunol.* 9, 581–593. doi: 10.1038/nri2567
- van den Bijgaart, R. J. E., Kong, N., Maynard, C., and Plaks, V. (2016). *Ex vivo* live imaging of lung metastasis and their microenvironment. *J. Vis. Exp.* 3:e53741. doi: 10.3791/53741

SUPPLEMENTARY MATERIAL

The Supplementary Material for this article can be found online at: <https://www.frontiersin.org/articles/10.3389/fbioe.2020.588922/full#supplementary-material>

- Ventola, C. L. (2017). Progress in nanomedicine: approved and investigational nanodrugs. *P T* 42, 742–755.
- Wang, L., Subasic, C., Minchin, R. F., and Kaminskas, L. M. (2019). Drug formulation and nanomedicine approaches to targeting lymphatic cancer metastases. *Nanomedicine* 14, 1605–1621. doi: 10.2217/nnm-2018-0478
- Witwer, K. W., and Théry, C. (2019). Extracellular vesicles or exosomes? On primacy, precision, and popularity influencing a choice of nomenclature. *J. Extracell. Vesicles* 8:1648167. doi: 10.1080/20013078.2019.1648167
- Wortzel, I., Dror, S., Kenific, C. M., and Lyden, D. (2019). Exosome-mediated metastasis: communication from a distance. *Dev. Cell* 49, 347–360. doi: 10.1016/j.devcel.2019.04.011

Conflict of Interest: AK was employed by nanoPET Pharma GmbH.

The remaining authors declare that the research was conducted in the absence of any commercial or financial relationships that could be construed as a potential conflict of interest.

Copyright © 2020 Ramos-Gomes, Ferreira, Kraupner, Alves and Markus. This is an open-access article distributed under the terms of the Creative Commons Attribution License (CC BY). The use, distribution or reproduction in other forums is permitted, provided the original author(s) and the copyright owner(s) are credited and that the original publication in this journal is cited, in accordance with accepted academic practice. No use, distribution or reproduction is permitted which does not comply with these terms.



Mechanical Stimulation: A Crucial Element of Organ-on-Chip Models

Clare L. Thompson¹, Su Fu¹, Hannah K. Heywood¹, Martin M. Knight¹ and Stephen D. Thorpe^{2*}

¹ Centre for Predictive *in vitro* Models, School of Engineering and Materials Science, Queen Mary University of London, London, United Kingdom, ² UCD School of Medicine, UCD Conway Institute of Biomolecular and Biomedical Research, University College Dublin, Dublin, Ireland

OPEN ACCESS

Edited by:

Adriele Prina-Mello,
Trinity College Dublin, Ireland

Reviewed by:

Ravi Sinha,
Maastricht University, Netherlands
Virginia Pensabene,
University of Leeds, United Kingdom

*Correspondence:

Stephen D. Thorpe
stephen.thorpe@ucd.ie

Specialty section:

This article was submitted to
Nanobiotechnology,
a section of the journal
Frontiers in Bioengineering and
Biotechnology

Received: 03 September 2020

Accepted: 20 November 2020

Published: 10 December 2020

Citation:

Thompson CL, Fu S,
Heywood HK, Knight MM and
Thorpe SD (2020) Mechanical
Stimulation: A Crucial Element
of Organ-on-Chip Models.
Front. Bioeng. Biotechnol. 8:602646.
doi: 10.3389/fbioe.2020.602646

Organ-on-chip (OOC) systems recapitulate key biological processes and responses *in vitro* exhibited by cells, tissues, and organs *in vivo*. Accordingly, these models of both health and disease hold great promise for improving fundamental research, drug development, personalized medicine, and testing of pharmaceuticals, food substances, pollutants etc. Cells within the body are exposed to biomechanical stimuli, the nature of which is tissue specific and may change with disease or injury. These biomechanical stimuli regulate cell behavior and can amplify, annul, or even reverse the response to a given biochemical cue or drug candidate. As such, the application of an appropriate physiological or pathological biomechanical environment is essential for the successful recapitulation of *in vivo* behavior in OOC models. Here we review the current range of commercially available OOC platforms which incorporate active biomechanical stimulation. We highlight recent findings demonstrating the importance of including mechanical stimuli in models used for drug development and outline emerging factors which regulate the cellular response to the biomechanical environment. We explore the incorporation of mechanical stimuli in different organ models and identify areas where further research and development is required. Challenges associated with the integration of mechanics alongside other OOC requirements including scaling to increase throughput and diagnostic imaging are discussed. In summary, compelling evidence demonstrates that the incorporation of biomechanical stimuli in these OOC or microphysiological systems is key to fully replicating *in vivo* physiology in health and disease.

Keywords: microphysiological systems, organ-on-chip, mechanobiology, biomechanics, biomechanical stimulation, pre-clinical model, tensile strain, fluid shear

INTRODUCTION

Pre-clinical drug development requires physiologically relevant *in vitro* models which successfully recapitulate the human tissue or organ scenario *in vivo*. These predictive models are also extremely valuable for fundamental research into health and disease and for testing the response to manufactured products, food substances, toxins, pollutants, etc., providing potential as platforms

for personalized medicine. Organ-on-chip (OOC) technology holds great promise in this regard as it facilitates the design of biomimetic microfluidic models incorporating multiple cell types and extracellular matrix (ECM) cues within a 2- or 3-dimensional (3D) environment, thereby replicating functional units of human tissues and organs *in vitro* (Huh et al., 2013; Caplin et al., 2015; Skardal et al., 2016; Caballero et al., 2017). These OOCs, also known as microphysiological systems, are increasingly being used to model both healthy and diseased organs and as drug screening platforms (Esch et al., 2015). This positions OOC technology as a potential route toward delivering safer and more effective treatments and unblocking the drug development pipeline which currently suffers substantial and costly attrition. As a result, there is significant interest and investment in this area from the biotech and pharmaceutical industries. Indeed, it is estimated that OOC technology could reduce pharmaceutical research and development costs by 10–26% (Franzen et al., 2019).

Organ-on-chip systems facilitate the application of multiple biochemical and biomechanical cues which direct cell behavior and ultimately replicate key aspects of tissue and organ function (Bhatia and Ingber, 2014). Biomechanical cues influence the growth and form of practically all tissues in the human body and are well established as modulators of cell signaling in health and disease (Jalalouk and Lammerding, 2009). While biomechanical stimuli can alter mass transport within tissues to modulate biochemical signaling gradients, cells can also sense these signals through mechanotransduction. Mechanobiology is the study of the cellular interpretation of biomechanical stimuli which, over the past 25 years, has become a burgeoning field of interdisciplinary research. The fundamental role of mechanobiology in many physiological processes, including the response to pharmaceuticals and other stimuli, necessitates the incorporation of biomechanical cues into OOC systems. For example, the incorporation of cyclic tensile strain mimicking lung epithelial stretch while breathing into an OOC lung-on-a-chip device is crucial to obtaining a physiological inflammatory response (Huh et al., 2010). The use of microfluidic platforms such as OOC systems for the study of mechanobiology is well established (Polacheck et al., 2013), while the innovative OOC field is producing novel approaches toward incorporating biomechanical cues into chip design as recently reviewed by Kaarj and Yoon (2019). However, to satisfy regulators and ensure reliability, OOC models with application in pre-clinical research or personalized medicine require standardized systems with validated biological models. In this review we highlight some instances where mechanical stimuli can drastically alter a given biochemical response with relevance to pre-clinical models. We summarize commercially available OOC model systems incorporating biomechanical stimuli, and review efforts to utilize these systems across different anatomical systems. The versatility of many of these OOC systems facilitates their application toward multiple organ models in addition to those validated to date, and we discuss future perspectives for this technology. As the field looks to build biological complexity in these OOC systems, it remains to be seen whether it is necessary to precisely mimic the diverse biomechanical stimuli found *in vivo*, or whether an approximation of *in vivo* biomechanics is sufficient.

MECHANOBIOLOGY AND THE IMPORTANCE OF BIOMECHANICAL STIMULI IN OOC

The Nature of Biomechanical Stimuli

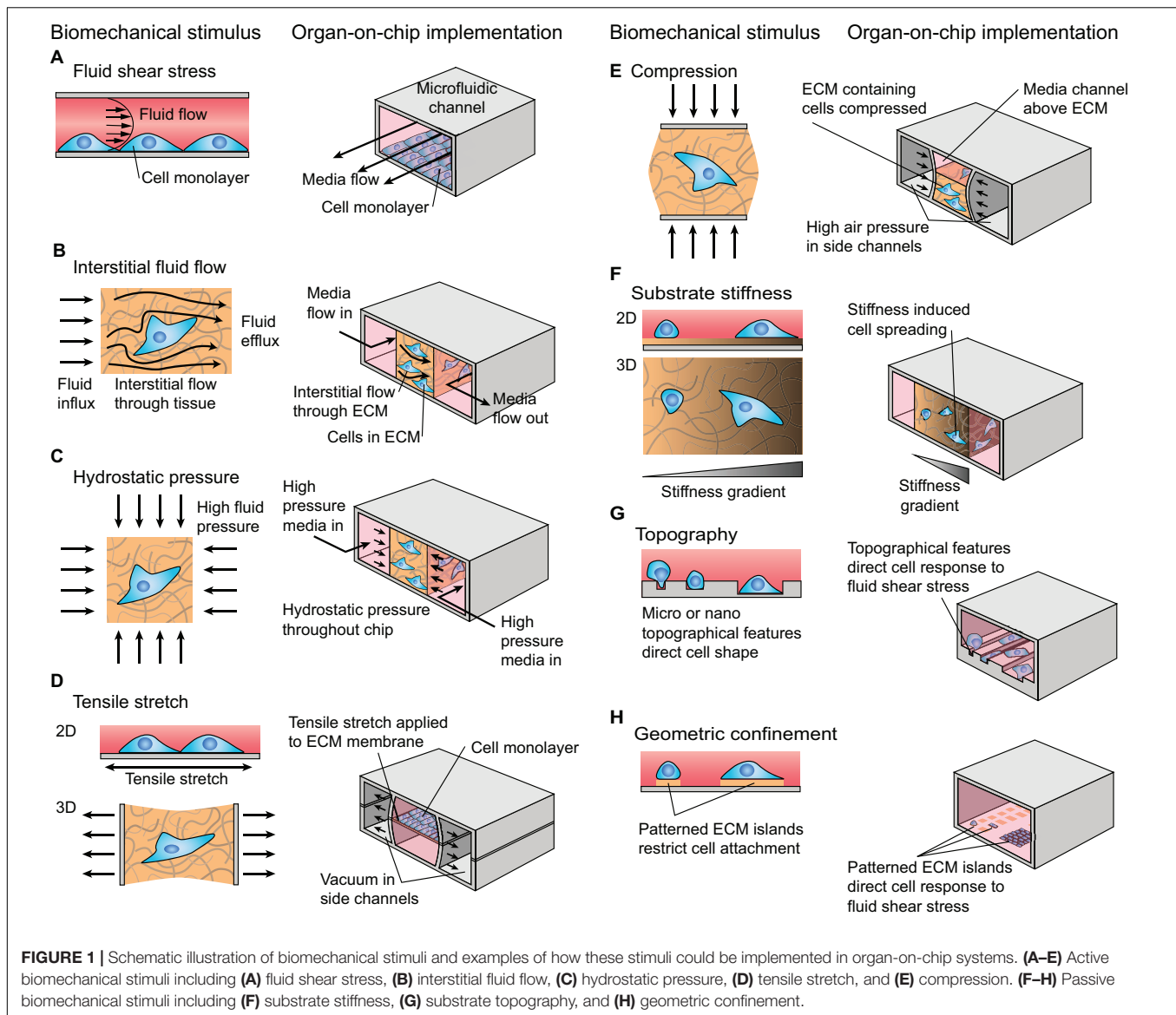
In vivo, cells are subjected to combinations of biomechanical and biochemical stimuli, which can interact to modulate the cellular response. Biomechanical cues are often extrinsic to the cell and can take passive or active forms. Passive biomechanical stimuli include substrate stiffness, geometric confinement, or topographic cues. Active stimuli include connective tissue tensile stretch and compression, fluid shear stress, interstitial fluid flow, and hydrostatic pressure (Figure 1).

While the nature of the biomechanical signal is important, the cellular response is also heavily dependent on the duration, magnitude, and frequency of the active biomechanical cue. Efforts to engineer connective tissues have used biomechanical signals as drivers of anabolic tissue formation and stem cell differentiation (Potier et al., 2010; Delaine-Smith and Reilly, 2012). Dynamic compression has long been applied to chondrocytes (Kim et al., 1994), with physiological loading duration, magnitude and frequency capable of eliciting anabolic responses (Anderson and Johnstone, 2017), while supraphysiological strain rates via high magnitude or frequency can drive a catabolic response (Leong et al., 2011). Experiments in fracture healing have demonstrated that mesenchymal stem cell (MSC) lineage specification can be driven *in vivo* by both magnitude and type of biomechanical signal, e.g., interstitial fluid flow or hydrostatic pressure (McMahon et al., 2008; Lee et al., 2011). These active stimuli can be further tuned to modulate stem cell differentiation through their interactions with passive stimuli such as substrate stiffness (Engler et al., 2006) and cellular confinement (McBeath et al., 2004; Gao et al., 2010).

An instance where strain magnitude and frequency can have physiological consequences is in mechanical lung ventilation, commonly used in very prematurely born infants. Children who received high frequency oscillatory ventilation as neonates had superior lung function at 11–14 years than those receiving conventional mechanical ventilation (Zivanovic et al., 2014). When the associated strain magnitudes were investigated *in vitro* using A549 alveolar analog cells, lower strain amplitudes associated with high frequency oscillatory ventilation resulted in a reduced inflammatory response which may provide an explanation for superior lung function years later (Harris et al., 2019). A great deal of literature has focused on identifying appropriate and pathological biomechanical parameters for specific cell types and tissues, and such studies involving microphysiological systems relevant to OOC models have been reviewed by Polacheck et al. (2013) and Kaarj and Yoon (2019).

Mechanobiology Regulates Cell Behavior and Response to Pharmaceuticals

Biomechanical signals can direct cell behavior in numerous contexts. Interactions between biomechanical signals can have unexpected effects, with dynamic compression overriding the influence of hydrogel substrate to divert MSC differentiation

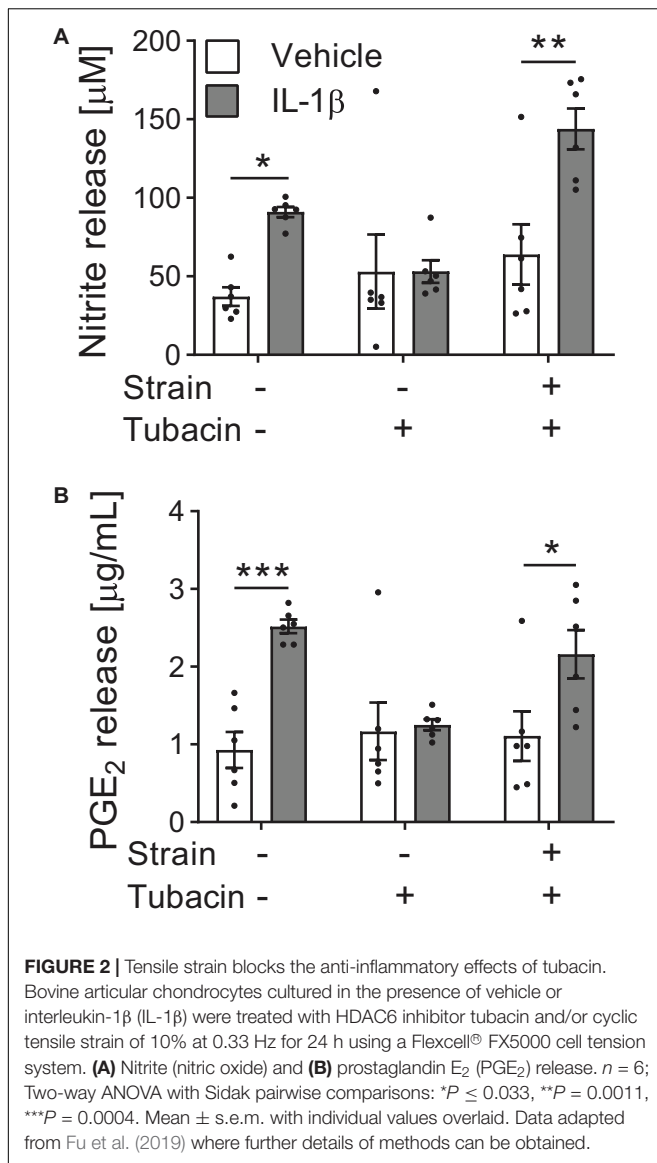


from myogenic to chondrogenic (Thorpe et al., 2012). Biomechanical signals can also modulate the cellular response to biochemical signals including pharmaceuticals. For example, matrix rigidity can switch the functional response to the cytokine transforming growth factor- β 1 (TGF- β 1) in epithelial cells, with TGF- β 1 inducing apoptosis in cells on soft substrates in contrast to epithelial-mesenchymal transition (EMT) in cells on rigid substrates (Leight et al., 2012). This demonstrates how changes in tissue mechanics, as often occur in disease, could confound the cellular response to a given pharmaceutical.

Active biomechanical cues can also switch the cellular response to pharmaceuticals. We have shown that dynamic tensile strain applied to cultured cells in 2D using the Flexcell® system can regulate chondrocyte response to histone deacetylase 6 (HDAC6) inhibition (Fu et al., 2019). The inflammatory cytokine interleukin-1 β (IL-1 β) triggers nitric oxide and prostaglandin E₂ (PGE₂) release from articular chondrocytes,

ultimately leading to the destruction of articular cartilage in disease. Tubacin, a specific inhibitor of the cytoplasmic tubulin deacetylase HDAC6, is anti-inflammatory and inhibits nitric oxide and PGE₂ release in the absence of tensile strain (Figure 2). However, the application of biomechanical strain nullifies the anti-inflammatory effects of tubacin leading to elevated nitric oxide and PGE₂ release (Figure 2). This compound's efficacy as an anti-inflammatory agent is dependent on the biomechanical environment and highlights the need to include mechanical stimuli in pre-clinical testing.

The importance of biomechanical stimuli in models of the respiratory system is highlighted by studies demonstrating the ability of these stimuli to both modify disease behavior and drug responsiveness. The addition of biomechanical stimuli to an orthotopic model of human non-small cell lung carcinoma (NSCLC) decreased the sensitivity of tumor cells to tyrosine kinase therapy (Hassell et al., 2017). While this study



found application of breathing motions reduced NSCLC cell proliferation and cluster formation within an Alveolus-Chip, it also resulted in the downregulation of epidermal growth factor receptor (EGFR) expression and signaling which ultimately led to the accumulation of tumor cells resistant to tyrosine kinase inhibitor mediated growth inhibition (Hassell et al., 2017). This may explain the high therapeutic resistance observed in regions of the lung which remain functionally aerated, and further demonstrates the importance of considering biomechanical stimuli in pre-clinical models.

Intrinsic Drivers of Biomechanical Response in OOC

Mechanobiological responses are cell type dependent, and this is evident as stem cells change their mechanosensitivity with differentiation (Thorpe et al., 2010). Indeed, cellular sensitivity to mechanics may fluctuate in response to various intrinsic

factors which act on timescales ranging from seconds for biomechanical memory (Heo et al., 2015), to years in the case of aging (Boers et al., 2018). Biomechanical stimuli provide integral cues to direct cell behavior, however there are several emerging intrinsic factors which influence the cellular response on the timescale of a typical study and should be considered in OOC strategies.

Biomechanical Memory

The response to a given biomechanical stimulus often results in changes in the cells and ECM that make up the cellular microenvironment. This in turn alters the biomechanical stimuli to which cells are exposed. The resulting mechano-reciprocal relationship between cell and biomechanical microenvironment is fundamental to tissue development and remodeling (van Helvert et al., 2018).

In addition, prior exposure to biomechanical stimuli leads to epigenetic changes determining the transcriptional response to subsequent stimuli (Downing et al., 2013; Heo et al., 2015; Li et al., 2017). Thus, the encoding of the history of biomechanical stimuli as epigenetic marks can lead to a faster more robust response upon subsequent stimulation or may temporally silence a genomic reaction to provide a refractory period of biomechanical unresponsiveness. Furthermore, different cell lineages have well documented changes in epigenetic state (Atlasi and Stunnenberg, 2017), which may impact cell behavior in response to strain.

Due to both tissue remodeling and epigenetic factors, previous exposure to biomechanical stimuli influences the response to repeat stimulation. Hence OOC systems may need to use pre-stimulated cells or precondition the model with biomechanical stimuli prior to testing the biological response to an intervention.

Inflammation

Chronic inflammation is associated with the deregulation of matrix signaling, tissue fibrosis and stiffening. It is well established that such changes will alter the biomechanical response of the cell and can influence a cell's inherent biomechanical memory (Heo et al., 2015; Nowell et al., 2016). However, the direct effect of inflammatory signaling upon cellular mechanosensitivity itself is unclear. Cytokines can influence actin, focal adhesions, mechanoreceptor expression and primary cilia (Wann and Knight, 2012; Wang et al., 2018). Indeed, preconditioning of synoviocytes with inflammatory cytokines enhances mechanosensitivity (Estell et al., 2017). Therefore, it may be important to build OOC models that incorporate this interaction between inflammation and biomechanical stimuli to accurately predict *in vivo* behavior.

Time of Day

Cells possess an internal timing system, or circadian rhythm, allowing synchronization to predictable environmental fluctuations of the 24 h day/night cycle. This biological clock enables the temporal compartmentalization of key cell processes according to the time of day. The recent findings on Clock regulation of expression of mechanoreceptors Piezo1 and TRPV4 in bladder cells (Ihara et al., 2017), the body temperature sensitivity of TRPV4 activation (Gao et al., 2003), and diurnal

actin dynamics (Hoyle et al., 2017), supports the concept of circadian fluctuations in mechanosensitivity. In addition, biomechanical stimulation, particularly in musculoskeletal tissues, may be important in regulating the clock, such that alterations in patterns of loading may disrupt clock function altering cellular behavior. Consequently, there is increasing suggestion that protocols for applying biomechanical stimuli via OOC systems should be coordinated around a physiological diurnal cycle.

Metabolism

Glycolysis and oxidative phosphorylation are the two major energy producing pathways in the cell. The shift between these two processes is a driving force in lineage commitment and environmental adaptation (Folmes and Terzic, 2016). Cytoskeletal remodeling and cell traction are energetically dependent upon glycolytic flux (Shiraishi et al., 2015; Hu et al., 2016), and it has recently been shown that increasing substrate stiffness leads to the downregulation of glycolysis (Park et al., 2020). Furthermore, the mechanosensor polycystin-1 has a dual function as an essential mitochondrial protein (Lin et al., 2018), together demonstrating direct connectivity of cell metabolism and mechanosensitivity. The metabolic status of cells within an OOC system will therefore influence the effect of biomechanical stimuli on regulating cell function and drug response.

COMMERCIAL ORGAN-ON-CHIP PLATFORMS INCORPORATING BIOMECHANICAL STIMULI

Organ-on-chip platforms vary greatly in their design (Figure 3), however the majority of commercial systems incorporate microfluidics to supply cells with nutrients and remove waste materials, thus also providing biomechanical stimuli in the form of fluid shear and interstitial flow. A small number of systems can also stimulate cells with mechanical strain to mimic biological processes such as breathing, peristalsis or the pumping of blood through the vasculature. Other systems that apply electrical stimuli have also been developed (Feric et al., 2019). In this section we summarize several well established, commercially available OOC model systems that incorporate biomechanical stimuli (Table 1). In the subsequent section, we review efforts to validate these systems across different anatomical systems. We have focused on nine of the leading manufacturers of OOC technology who not only supply hardware but focus on the biological development of these systems.

AlveoliX

The ^{AX}Lung-on-Chip System is a medium throughput system which mimics the biomechanical microenvironment of the air-blood barrier of the human lung (Figure 3A). It has the footprint of a standard culture plate (127 mm × 85 mm) and comprises two chips per plate which each have six “alveolar wells.” These wells are comprised of an ultrathin (3.5 μm), porous (3 μm diameter pores) alveolar membrane. Lung cells can be

cultured under air-liquid interface (ALI) on the apical side of the membrane, and endothelial cells cultured on the basal side. The membrane is cyclically deflected in three dimensions using a “micro-diaphragm” beneath the membrane which is deflected by applying negative and positive pressures through an electro-pneumatic setup. Consequently, this strain (8%, 0.25 Hz) is transferred to the alveolar membrane in a manner comparable to that observed in the human lung.

BI/OND

The inCHIPitTM offers a medium throughput organ chip with up to six cultures running in parallel. Each chip is comprised of two compartments which can be subjected to flow (1–300 μL/min) and are connected by a porous membrane. The top channel (fluid shear: 1.58×10^{-6} – 2.10×10^{-4} Pa) is open for added flexibility while the bottom functions as a microfluidic channel (fluid shear: 0.011–9.722 Pa) and can be subjected to cyclic strain (2.5–10%, 1 Hz). It is suitable for the cultivation of complex 3D tissues (organoids, *ex vivo* tissue, spheroids, micro tissues) as well as tissue-tissue interface models.

CNBio

The PhysioMimixTM OOC system uses open-well plates (standard footprint: 127 mm × 85 mm) which are compatible with commercial inserts, tissue-specific scaffolds and scaffold-free cultures for easy scaling and on-boarding of validated or bespoke model systems. Up to six plates can be used simultaneously to run multiple independent experiments. This system allows real-time sampling and supports long-term, automated culture, refreshing culture media at a rate of 50–5,000 μL/min with limited user input and are suitable for single-organ, two-organ, or multi-organ experiments.

Emulate

The “Human Emulation System” platform comprises Organ-Chips, instrumentation, software, and applications to create a micro engineered system that replicates human *in vivo*-relevant physiology (Figure 3B). The Chip-S1 is composed of an elastomeric polymer, PDMS, with an upper channel (1 mm high × 1 mm wide) separated from a parallel lower channel (0.2 mm high × 1 mm wide) by a thin, flexible, porous (pore size 7 μm) membrane coated with ECM and lined with human cells. Multiple cell sources can be used including primary cells or organoids and the chips support a 3D microenvironment. The Zoë Cell Culture Module supports the culture of the chips, application of pressure-driven flow (0–1,000 μL/h, fluid shear: top channel; 0–0.009 Pa, bottom channel; 0–0.03 Pa) and stretch (0–12%, 0.01–0.4 Hz). The application of biomechanical forces (shear stress and tensile strain) and the ECM environment can be optimized for different organs or tissues to recreate a more physiological microenvironment.

Kirkstall

The Quasi Vivo[®] system is an advanced interconnected cell culture flow system. It is engineered to provide *in vivo* like conditions for cell growth. Available in three configurations

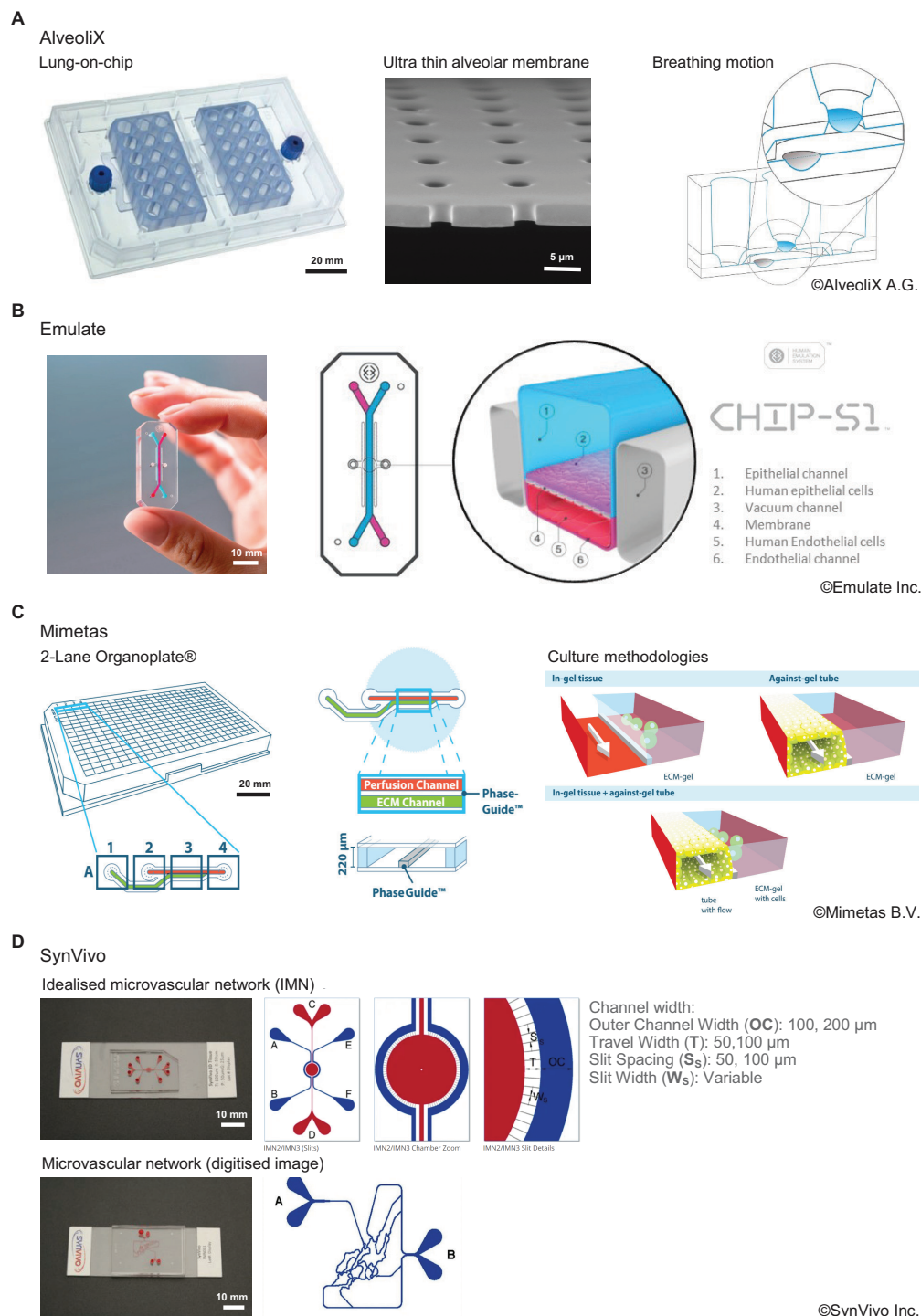


FIGURE 3 | Comparison of commercially available organ-on-chip platforms incorporating a form of active biophysical stimulus. **(A)** AX12 lung chip based on a 96-well plate format, consisting of two chips supported by a plate, each of which comprise six independent units. The ultrathin membrane (blue) is deflected by negative pressure inside the basal chip chamber through an integrated micro-diaphragm (gray). Images® Alveolix A.G. **(B)** The Human Emulation system from Emulate Inc. comprising organ chips which fit into the Pod™ carrier. The Zoë™ culture module controls the rate of flow and stretch for up to 12 chips. The Orb™ provides the precise mixture of gas, power, and vacuum stretch required by the Zoë™ culture module. Images® Emulate Inc. **(C)** The 2-lane Organoplate™ from Mimetas. Based on a 384-well plate format, it can support 96-individual models. Cells are cultured in/on ECM alongside a perfusion channel created using unique phase guide technology. Images® Mimetas B.V. **(D)** SynVivo's microfluidic chips create an idealized microvascular network to mimic the formation of, and transport across, tight and gap junctions. Networks can also be created from digitised images to replicate *in vivo* physiology more accurately. Natural tissue regions can also be incorporated within the network topology. Images® SynVivo Inc.

TABLE 1 | Commercially available organ on chip systems with integrated mechanical stimulation.

Company	Mechanical stimulation	Validated models
AlveoliX http://www.alveolix.com/	Strain: 10%, 0.16 Hz Fluid flow: passive	Alveolus: Inflammation, toxicology, fibrosis (Stucki et al., 2015, 2018; Artzy-Schnirman et al., 2019; Krempaska et al., 2020; Wang et al., 2020)
BI/OND https://www.gobiond.com/	Strain: 2.5–10%, 0–1 Hz Fluid flow: 1–300 $\mu\text{L}/\text{min}$ Fluid shear: upper channel: 1.58×10^{-6} – 2.10×10^{-4} Pa lower channel: 0.011–9.722 Pa	Heart, midbrain organoid, cancer
CNBio https://cn-bio.com/	Fluid flow: 50–5,000 $\mu\text{L}/\text{min}$ Fluid shear: dependent on model	Liver (Domansky et al., 2010; Vinci et al., 2011; Wheeler et al., 2014; Long et al., 2016; Kostrzewski et al., 2017, 2020; Sarkar et al., 2017; Rowe et al., 2018; Ortega-Prieto et al., 2019; Vacca et al., 2020). Liver/Intestine (Chen et al., 2017), Brain, Heart, Kidney, Lung, Pancreas, Skin.
Emulate, Inc. https://www.emulatebio.com/	Strain: 0–12%, 0.01–0.4 Hz Fluid Flow: 0–1,000 $\mu\text{L}/\text{min}$ Fluid shear: upper channel: 0–0.009 Pa lower channel: 0–0.03 Pa	Blood-brain barrier (Sances et al., 2018; Park et al., 2019; Vatine et al., 2019) Blood vessel: Micro vessel (Jain et al., 2016) Bone marrow (Torisawa et al., 2014, 2016) Bone: Osteogenic differentiation (Sheyn et al., 2019) Lung: Small airway (Huh et al., 2010, 2013; Benam et al., 2016a,b; Jain et al., 2016; Henry et al., 2017; Si et al., 2020) Lung: Alveolus (Huh et al., 2012; Jain et al., 2018) Intestine (Kim et al., 2012; Henry et al., 2017; Villenave et al., 2017; Jallil-Firoozinezhad et al., 2018; Kasendra et al., 2018, 2020; Workman et al., 2018; Grassart et al., 2019) Kidney: Glomerulus (Musah et al., 2018) Kidney: Proximal Tubule (Jang et al., 2013; Vriend et al., 2020; Xu et al., 2020) Liver (Foster et al., 2019; Jang K. J. et al., 2019; Peel et al., 2019) Neuronal development (Sances et al., 2018)
Kirkstall https://www.kirkstall.com/	Fluid flow: 75–250 $\mu\text{L}/\text{min}$ Fluid shear: dependent on model	Blood-brain barrier (Miranda-Azpiazu et al., 2018; Elbakary and Badhan, 2020) Brain: Mid brain organoids (Berger et al., 2018) Heart: cardiac tissue (Pagliari et al., 2014) Intestine (Giusti et al., 2014) Liver (Ramachandran et al., 2015; Pedersen et al., 2016; Rashidi et al., 2016; Shannahan et al., 2016) Lung (Chandorkar et al., 2017) Pancreas/Liver (Faure et al., 2016) Kidney
Micronit https://www.micronit.com/microfluidics/smart-organ-on-a-chip-platform.html	Fluid shear: 0.01–5 dyne/cm ²	Intestine (Kulthong et al., 2020) Liver (Li et al., 2018) Pancreas (Navarro-Tableros et al., 2019; Gomez et al., 2020) Skin, Lung, Bone marrow, Neural or cardiovascular network
Mimetas https://mimetas.com/	Fluid flow: Gravity driven leveling Fluid shear: 0–0.3 Pa	Blood-brain barrier (Wilmer et al., 2016; Koo et al., 2018) Blood vessel (van Duinen et al., 2017; Beekers et al., 2018; Poussin et al., 2020) Blood vessel: Angiogenesis (van Duinen et al., 2019) Breast cancer (Lanz et al., 2017) Liver (Jang et al., 2015, 2018; Jang M. et al., 2019) Neural: CNS toxicity (Moreno et al., 2015; Wevers et al., 2018; Bolognin et al., 2019; Kane et al., 2019) Intestine (Trietsch et al., 2017; Beaurivage et al., 2019) Kidney: glomerulus (Petrosyan et al., 2019) Kidney: proximal tubule (Wilmer et al., 2016; Vormann et al., 2018; Vriend et al., 2018, 2020; Schutgens et al., 2019) Pancreas (Kramer et al., 2019) Brain: Glioma,
SynVivo https://www.synvivobio.com/	Fluid Flow: 10 nL/min–10 $\mu\text{L}/\text{min}$ Fluid shear: 0.001–2 Pa	Blood-brain barrier (Prabhakarpandian et al., 2013; Deosarkar et al., 2015; Tang et al., 2018; Brown et al., 2019; Da Silva-Candal et al., 2019) Blood vessel (Silvani et al., 2019) Blood vessel: Microvascular network (Rosano et al., 2009; Prabhakarpandian et al., 2011; Lamberti et al., 2013) Cancer models (Tang et al., 2017; Terrell-Hall et al., 2017; Vu et al., 2019) Lung (Kolhar et al., 2013; Liu et al., 2019; Soroush et al., 2020)
TissUse https://www.tissuse.com/en/	Fluid shear: 0.02–2 Pa	Multi-tissue models: Intestine-Liver-Brain-Kidney (Ramme et al., 2019) Intestine-Liver-Skin-Kidney (Maschmeyer et al., 2015b) Liver-Brain (Materne et al., 2015) Liver-Intestine (Maschmeyer et al., 2015a) Liver-Kidney (Lin et al., 2020) Liver-Lung (Schimek et al., 2020) Liver-Pancreatic islets (Bauer et al., 2017)

(Continued)

TABLE 1 | Continued

Company	Mechanical stimulation	Validated models
		Liver-Skin (Wagner et al., 2013) Liver-Skin-Vasculature (Maschmeyer et al., 2015a) Liver-Testis (Baert et al., 2020) Skin-Lung cancer (Hubner et al., 2018) Single tissue models: Blood vessels (Schimek et al., 2013; Maschmeyer et al., 2015b) Blood vessels: Micro capillaries (Hasenberg et al., 2015) Bone marrow (Sieber et al., 2018) Brain (Materne et al., 2015) Hair follicle biopsies (Atac et al., 2013) Intestine (Maschmeyer et al., 2015a) Kidney (Ramme et al., 2019) Liver (Maschmeyer et al., 2015a; Materne et al., 2015; Bauer et al., 2017) Lung (Schimek et al., 2020) Pancreas: Pancreatic islets (Bauer et al., 2017) Skin (Atac et al., 2013; Maschmeyer et al., 2015a; Schimek et al., 2018) Testis (Baert et al., 2020)

(QV500, QV600, and QV900) this system is compatible with coverslips, membranes, barrier models, ALI culture and a range of 3D scaffolds. The Quasi Vivo® system uses a peristaltic pump to create flow (75–250 $\mu\text{L}/\text{min}$).

Micronit

Provide a range of OOC products in a variety of formats. Their core device is open and re-sealable consisting of a top and bottom layer completed by a central membrane layer. These are secured by dedicated and customizable clamps to create a cell culture platform with separately controllable fluid-flows above and below (fluid shear: 0.001–0.5 Pa). Microplate formats with active flow control systems are also offered based on fully integrated membrane valves and external actuation. Such solutions are developed and produced in a business-to-business fashion according to customer specific requirements. The open formats support sensory integration with focus applied to the optical sensing of oxygen.

Mimetas

The OrganoPlate® is a high throughput, microfluidic 3D cell culture plate capable of supporting up to 96 individual models concurrently with the footprint of a single 384-well plate (127 mm \times 85 mm) and is available in 2-lane and 3-lane configurations (Figure 3C). For the 2-lane configuration, each individual model consists of two channels, a perfusion channel, and a gel channel, which are uniquely separated using phase guides rather than a physical membrane barrier. Tissues can be grown embedded in an ECM gel (lane width 375 μm) or as a perfused tubule (lane width 325 μm) against the ECM gel (surface area 1 mm^2). Continuous gravity driven pump-free perfusion is provided using a rocker system to generate bi-directional flow (fluid shear: 0–0.3 Pa). This technology supports 3D cell culture, up to 3-layer co-culture, barrier integrity and transport, angiogenesis, and gradient formation.

SynVivo

Microfluidic chips are functionalized to recreate complex *in vivo* like microenvironments including scale, morphology and hemodynamics along with endothelial barrier function. They can support a microvascular network that simulates the circulation inside any tissue with respect to flow, shear and pressure conditions. These microfluidic chips are available in several configurations based on the desired geometry and tissue conditions and include linear channels, bifurcating channels (comprising *in vivo* geometries), micro vascular networks (obtained from *in vivo* imaging), and idealized network designs (Figure 3D). Within the idealized network, a central chamber, flanked by vascularized micro channels, allows creation of 3D tissue OOC models for real-time studies of cellular interactions, extravasation, and drug delivery. The devices include customized micro fabricated pores to allow communication between the tissue and vascular cells while maintaining tight and gap junctions between cells. The side-by-side architecture of the chips allows for development of complex cellular morphology while maintaining real time visualization and quantitation of cell-cell and cell-drug interactions. These models are also customizable with multiple options for channel size, tissue chamber size, number of chambers, scaffolding, and barrier design. Various tissue/OOC models have been validated against *in vivo* measurements in oncology, neuroscience, and inflammation studies. A syringe pump or peristaltic pump provides continuous flow in this system (1 nL/min –100 $\mu\text{L}/\text{min}$, fluid shear: 0.001–2 Pa).

TissUse

The HUMIMIC™ platform is a miniaturized construct that closely simulates the activity of multiple human organs. The platform is available in multiple configurations and can support up to four different organ models simultaneously on a chip the size of a standard microscope slide. The organ models are supplied with media and connected by microfluidic channels (fluid shear: 0.02–2 Pa) supported by an on-chip pump. Cells and

tissues can be used to emulate biological barriers as well as to grow spheroidal and matrix-supported cultures.

INCORPORATION OF BIOMECHANICAL CUES IN OOC MODELS FOR DIFFERENT ORGAN SYSTEMS

In the following section we outline some of the major biological systems where mechanical stimulation is well established to influence tissue function. We outline how different commercial OOC systems have been used to generate some of the most developed models of the cardiovascular, intestine, kidney and respiratory systems, and discuss how the development of the biology within these are influenced by the mechanical environment. However, the importance of mechanical stimuli to tissue development and function goes beyond these anatomical systems and will be an important component for the development of many if not all models, for example muscle, skin or fetal membrane and would similarly be expected to influence functionality and drug responses.

Cardiovascular Models

The cardiovascular system is subject to various types and levels of biomechanical stimuli. Within the heart, highly coordinated contractions of cardiac muscle pump blood into the vessels of the circulatory system. In the vasculature, endothelial cells lining the inner surface of the blood vessels are exposed to shear stress, tensile strain, and changes in hydrostatic pressure as the result of pulsatile blood flow. These stimuli influence cell morphology, proliferation and the permeability of the vessel. Shear stress is the most significant and prominent of these forces and disruption as a result of altered flow conditions is associated with disease such as atherosclerosis, thrombosis, and aneurysm (Chiu and Chien, 2011). In straight regions of arterial trees, the vascular endothelium experiences laminar blood flow that provides high and constant pressure (>1.5 Pa). Whereas regions that branch and curve experience non-uniform, irregular, and disturbed blood flow and as such shear stress is lower (<0.4 Pa) (Gomel et al., 2018).

Key features of the cardiovascular system have been replicated using OOC technology from blood vessel-on-chip models used to study single vessels or microvasculature, to heart-on-chip models (Table 1). Drug-induced cardiotoxicity is a critical issue in drug development. However, the complex environment of mechanical and electrical stimulation means that while several heart-on-chip devices have been published, validated models using commercial systems are limited. Perhaps the most advanced of these is the Biowire IITM platform from Tara Biosystems, which uses biomimetic electrical stimulation to examine the functionality of engineered cardiac tissue (Nunes et al., 2013). This heart-on-a-chip device gauges contractile activity generated by the engineered tissue as a measure of tissue function. As this review focuses on systems which directly apply mechanical stimulation, this system is not discussed here. For further review of recent developments in heart-on-a-chip models please see (Beverung et al., 2020).

Vascular components are a common feature of barrier models such as blood-brain barrier, liver, kidney, and intestine models. Disruption of the vascular barrier plays a key role in the onset and progression of several diseases, thus preventing disruption or restoring function are attractive targets for drug discovery. In the Chip-S1 from Emulate Inc., organ-specific epithelial cells are cultured within the larger upper channel, while endothelial cells are cultured in the bottom channel. These endothelial cells proliferate until a continuous channel lining is formed creating a micro-vessel that represents the supporting microvasculature of the tissue. This micro-vessel has been used to study neutrophil adhesion, rolling and intravasation in lung-chip models of asthma and chronic obstructive pulmonary disease (COPD) (Benam et al., 2016a,b). At 0.3 Pa, maximum shear stress in these systems is significantly lower than observed *in vivo*. More recently, a developmental aorta-on-chip was constructed on this platform. The shear stress values were increased to 0.5 Pa using a generic multichannel peristaltic pump, and together with cyclic membrane stretching (10%, 2 Hz) to replicate the heart rate at this stage of development (~ 120 beats per minute), promoted hematopoietic stem cell formation in response to blood flow (Lundin et al., 2020).

The SynRAMTM 3D inflammation model from SynVivo uses this barrier concept in a more complex chip design to study real-time rolling, adhesion, and migration processes within a microvasculature network. While simplified idealized networks can be used to reproduce constant shear and flow conditions from 0.05 to 0.4 Pa (Lamberti et al., 2013), a unique feature of this chip is that network design can also be derived from complex *in vivo* microvascular networks obtained from digitized images (Figure 3D). This produces a vascular morphology with converging and diverging bifurcations which result in varying shear and flow conditions permitting the study of inflammation and particle adhesion in a realistic and dynamic environment (Rosano et al., 2009; Prabhakarapandian et al., 2011; Lamberti et al., 2013). Indeed, the disruption to flow patterns and morphology generated near to bifurcations within the chip replicates increased adhesion of cells (platelets, leukocytes, etc.) and particles observed at these sites *in vivo* under pathological conditions (Prabhakarapandian et al., 2011).

Using OrganoPlate[®] technology, Mimetis have created the first high throughput blood vessel-on-chip system. Human coronary artery endothelial cells seeded in the perfusion channel proliferate to cover the surface forming a micro vessel with a perfusable lumen (van Duinen et al., 2019). Fluid shear (0.16 Pa) is applied to this system in a gravity-driven manner to generate a bidirectional, oscillating flow rather than the unidirectional linear flow observed *in vivo*. Crucially, the tubular shape of this vessel only develops within the chip when adherent endothelial cells are exposed to flow thus highlighting the importance of biomechanical stimuli. This system has been used to investigate drug delivery (Beekers et al., 2018), angiogenesis (van Duinen et al., 2019) and to explore the effects of inflammation on monocyte-to-endothelium adhesion under flow (Poussin et al., 2020). In the latter, adhesion of monocytic cells to endothelial microvessels is observed in response to aerosols (Poussin et al., 2020) similar to

what is observed in chip systems utilizing unidirectional flow (Benam et al., 2016b).

Respiratory Models

Current models of the respiratory system typically focus on the alveolus or airway epithelium. As the alveolus expands and contracts during normal breathing the alveolar epithelium is exposed to cyclic tensile strain while also receiving a low level of shear stress due to air flow. Healthy epithelium typically experiences up to 12% strain, however these levels can become much higher in scarred areas which are less elastic (Waters et al., 2012). The mechanical environment of the airway itself is complex, while the contribution of strain is less, low level circumferential and longitudinal expansion and contraction will accompany normal breathing. This environment will be greatly affected under diseased conditions such as asthma where bronchoconstriction results in compressive loading of the epithelium as the result of smooth muscle activation (Tschumperlin and Drazen, 2001).

Few commercially available systems combine the ALI culture required for these models with cellular stretching to incorporate the tensile strain. The ^{AX}Lung-on-a-chip, from AlveoliX is one such system (Figure 3A), it replicates the alveolar barrier whereby alveolar epithelial cells and endothelial cells are cultured in tight monolayers upon either side of a thin, porous membrane (Stucki et al., 2015, 2018). The inclusion of cyclic strain in this model (10% strain, 0.2 Hz) influences the metabolic activity of primary human pulmonary alveolar epithelial cells and increases the permeability of the epithelial barrier with no effect on cell layer integrity. Cytokine secretion by the epithelial cells is altered by the inclusion of mechanics such that interleukin-8 release is greater after 24–48 h of stretching relative to static conditions (Stucki et al., 2015).

In the Alveolus chip from Emulate Inc., human or mouse alveolar epithelial cells and endothelial cells are cultured within the Chip-S1 on opposite sides of the PDMS membrane described above (Figure 3B). The membrane is subjected to cyclic stretch to represent physiological breathing (10% strain, 0.2 Hz). This biomechanical input is essential for the replication of lung function and results in a 10-fold enhancement of the uptake of nano particulates into the alveolar epithelium over static conditions dramatically increasing reactive oxygen species production and promoting neutrophil capture and transmigration (Huh et al., 2010). Pulmonary surfactant production is enhanced within the chip further promoting epithelium integrity and barrier function while functioning as an important defense mechanism against bacterial infection (Thacker et al., 2020). Several commercial systems have been used to generate lung-on-a-chip models that mimic the complex solid and fluid microenvironment of the airway epithelium such as SynVivo's SynALI lung model which comprises an apical channel functionalized with lung epithelial cells and surrounded by "vasculature" comprised of endothelial cells separated by a porous scaffold (Kolhar et al., 2013; Liu et al., 2019; Soroush et al., 2020). This structure allows the formation of airway tubules through ALI culture within the apical channel that transport mucus and are maintained by the

surrounding endothelium (Kolhar et al., 2013; Liu et al., 2019; Soroush et al., 2020).

In the Airway-chip from Emulate Inc. primary human lung airway basal stem cells are cultured under ALI on one side of the membrane, while primary human lung endothelium is cultured on the parallel vascular channel and exposed to continuous fluid flow with a volumetric flow rate of 60 μ L/h resulting in wall shear stress of 0.0017 Pa (Huh et al., 2012; Jain et al., 2018). The basal stem cells differentiate into a functional mucociliary pseudostratified epithelium containing ciliated cells, mucus-producing goblet cells, club cells, and basal cells in relevant *in vivo* proportions. The underlying human pulmonary microvascular endothelium forms a continuous cell monolayer linked by VE-cadherin containing adherens junctions. This chip accurately replicates viral infection by SARS-CoV-2 and influenza virus and can be used to study the recruitment of circulating immune cells, such as neutrophils, under dynamic flow to the site of infection. In a recent study, this chip model successfully recapitulated the effects of clinically used viral therapeutics for influenza (Si et al., 2020).

Other systems combine ALI culture with flow to generate lung models from tissue culture inserts such as CNBio's PhysioMimixTM and Kirkstall's Quasi Vivo system (Table 1). Mazzei et al. (2010) have used the Quasi Vivo system to generate co-culture models of lung epithelium and immune cells [dendritic cells (DCs), macrophages]. In the QV600 system, lung epithelium cultured on transwell inserts is subjected to ALI culture, which coupled with perfusion accelerates development of the lung epithelium with higher ciliogenesis, cilia movement, mucus-production and improved barrier function relative to static conditions (Chandorkar et al., 2017). In SynVivo's SynALI model, epithelial and endothelial co-cultures are grown in a tubular structure to generate a central *in vitro* 3D hollow airway lumen with continuous airflow which is flanked by two *in vitro* 3D microvascular structures. The central lumen communicates via pores to these vascular channels which are cultured with living endothelium around a central lumen filled with fluid, mimicking blood flow (Liu et al., 2019).

In recent work, Si et al. (2020) demonstrated that in the Airway-chip from Emulate, only two of seven compounds identified by drug repurposing screens in 2D culture systems were effective at inhibiting viral entry of a pseudotyped SARS-CoV-2 virus. These findings in the chip have been corroborated by *in vivo* studies that similarly found one of these compounds, amodiaquine and its active metabolite (desethylamodiaquine) significantly reduced viral load in hamsters in both direct infection and animal-to-animal transmission models of native SARS-CoV-2 infection (Si et al., 2020). Thus, this study highlights the enormous potential of OOC technology to screen drug candidates more stringently prior to their use in animal studies and thus accelerate both the development and rapid repurposing of drugs.

Intestine Models

As part of normal gut function, the intestinal epithelium is subjected to complex biomechanics. During peristalsis, waves of highly synchronized contraction move digested food through

the intestinal tract deforming the intestinal mucosal layer and generating irregular compressive and tensile strains, and fluid shear stress, which vary along the length of the digestive tract as the viscosity of the digesta is altered (Brandstaeter et al., 2019). The digestive system has been another key area of focus for OOC technology as intestinal models are crucial for drug research and development, providing platforms for drug adsorption, efficacy and toxicity testing in addition to providing a range of disease models for conditions including inflammatory bowel disease and colitis.

The replication of peristaltic motions within the intestinal microenvironment is key to generation of 3D tissue architecture within organ-chips. The application of flow at 30 $\mu\text{L/h}$ (0.0346 mPa) and cyclic stretch (10%, 0.15 Hz) to the human intestinal colorectal adenocarcinoma cell line (Caco-2) cultured in Emulate's Chip-S1 (**Figure 3B**) promotes formation of a columnar epithelium which spontaneously grows into folds recapitulating the structure of intestinal villi (Kim et al., 2012; Grassart et al., 2019). This platform can support the co-culture of intestinal microbes for extended periods without compromising epithelial viability (Kim et al., 2012). Moreover, it is compatible with human organoid culture such that organ chips representing small intestine (Kasendra et al., 2018), adult duodenum (Kasendra et al., 2020) and colon (Sontheimer-Phelps et al., 2020) have been successfully generated in combination with co-cultures of intestine-specific endothelium. For the colon chip in particular, the use of this technology to generate a continuously perfused culture at 60 $\mu\text{L/h}$ (~ 0.0692 mPa) supports accumulation of a mucus bilayer with impenetrable and penetrable layers, and a thickness similar to that observed in the human colon which can be analyzed non-invasively in real time (Sontheimer-Phelps et al., 2020).

In Micronit's gut-on-chip model, Caco-2 cells are subjected to flow at 100 $\mu\text{L/h}$ producing a shear stress of ~ 0.02 – 0.17 mPa at the cell surface (Kulthong et al., 2020). Following culture in this manner for 21 days, caco-2 cells form a continuous epithelium with greater height than equivalent transwell cultures that have an enhanced barrier function. Caco-2 cell differentiation was comparable with static cultures in this model (Kulthong et al., 2020).

In Mimetas' 3-lane Organoplate®, perfused intestinal tubules can be cultured in a high throughput manner as a mono-culture or co-culture with immune cells or blood vessels and stromal tissue to generate a model of the intestinal epithelium (Trietsch et al., 2017). The inclusion of stromal tissue interactions is an important factor for replicating physiological cellular interactions. In this system, Trietsch et al. (2017) cultured Caco-2 cells against an ECM gel, which proliferate upon application of bi-directional flow to form a confluent tube. Perfusion is critical for tubule formation. Beaurivage et al. (2019) have recently used this model to mimic the effects of *Escherichia coli*-activated DCs on the intestinal epithelium. Through the addition of a cytokine cocktail of IL-1 β , tumor necrosis factor α (TNF- α) and interferon- γ (IFN- γ), they were able to replicate the loss of barrier function observed in irritable bowel disease (Beaurivage et al., 2019). Similar results were achieved using iPSCs which can be induced to undergo differentiation within the Organoplate® to express mature intestinal markers, including

markers for Paneth cells, enterocytes and neuroendocrine cells (Naumovska et al., 2020).

In addition to drug efficacy, biomechanics can also mediate pathogen infectivity. In the small intestine, the incorporation of both fluid flow (30 $\mu\text{L/h}$, fluid shear: 0.346 mPa) and tensile strain (10%, 0.15 Hz) mimicking peristalsis promotes formation of a more physiologically relevant 3D architecture. Grassart et al. (2019) observed that these mechanically active intestine chip cultures better replicate bacterial infection uncovering a mechanism whereby *Shigella flexneri* exploits the epithelial crypt microarchitecture and active biomechanics to efficiently invade the intestine. In the region of 70% of all drugs are administered orally (Brandstaeter et al., 2019). Their processing and effectiveness depend crucially on gastric mechanics thus the incorporation of active biomechanical stimuli into OOC gut models is essential to the successful use of this technology.

Kidney Models

Several OOC models have focused on the kidney proximal tubule as the site at which active clearance, reabsorption, intracellular concentration, and local interstitial accumulation of drugs primarily occurs. The epithelium in this region is continually exposed to shear stress in the region of 0.02 Pa as the result of constant flow of the glomerular filtrate which influences cell morphology causing alignment and elongation of kidney epithelial cells in the direction of flow (Vriend et al., 2020), and modulates expression of apical and basolateral transporters and sodium transport (Duan et al., 2010).

Nephrotoxicity is a major cause of drug attrition during pre-clinical pharmaceutical development and is responsible for almost 20% of failures during Phase 3 clinical trials underlying the limitation of current methodologies (i.e., 2D cell culture and animal models) to predict the human response. The inclusion of biomechanical stimuli in kidney models examining drug toxicity is essential as exemplified by the use of both the OrganoPlate® (Mimetas) and Chip-S1 (Emulate) systems which show that both albumin uptake and drug efflux are enhanced in response to fluid shear stress despite the differential use of uni-directional and bi-directional flow in these models (Jang et al., 2013; Vriend et al., 2020). Jang et al. (2013) report that cisplatin toxicity more closely replicates the *in vivo* response observed than traditional culture techniques. Thus, the use of these models which incorporate biomechanics to screen for kidney injury early in the drug discovery process will provide greater capacity to predict responses in humans.

Musculoskeletal Models

The nature and magnitude of biomechanical stimuli experienced by the musculoskeletal system are highly varied both between connective tissue types and within them due to the extreme forces that must be endured during physical activity. These mechanical stimuli are essential to the health and maintenance of the tissue; regulating cell morphology, proliferation matrix production and catabolism. Articular cartilage is routinely exposed to diverse mechanical stimuli consisting of compressive, shear and tensile strains as well as associated alterations in fluid shear and osmolality as a result of normal physical activity (Knecht et al., 2006). Energy-storing tendons like the Achilles are designed

to stretch and recoil to increase efficiency during locomotion and are thus subjected to high magnitude stresses and strains during exercise. In the bone, oscillatory fluid flow generated by compressive loading generates shear stress in the lacunar-canalicular network which influences both the maintenance and healing of bone tissue and is essential for bone health. Inappropriate cellular responses to these stimuli result in the disruption of tissue homeostasis and can lead to conditions such as tendinopathy and osteoarthritis (Felson, 2013; Dean et al., 2017). Thus, the incorporation of biomechanical stimuli into OOC models of the musculoskeletal system is essential. However, few commercial systems have been used to develop models in this field to date.

Existing models from Emulate, Micronit and TissUse have focused on bone or bone marrow while models for muscle, cartilage or tendon are overlooked. This is likely due to the difficulty in replicating the complex architecture of these tissues and the more dynamic biomechanical environment the cells experience. A bone-on-a-chip generated using Emulate's Chip-S1 (**Figure 3B**) utilizes an inducible, MSC-bone morphogenic protein-2 (BMP-2) overexpression system cultured on one side of the membrane to examine osteogenic differentiation under flow (Sheyn et al., 2019). In this system, cells grown on Bone-chips under flow (30 $\mu\text{L/h}$, shear stress: 0.346 mPa) showed enhanced survival and proliferation relative to cells grown under static conditions. MSCs cultured in this manner exhibited greater expression of the osteogenic markers osteopontin, bone sialoprotein, and collagen type I, despite the use of constant flow in this system (Sheyn et al., 2019).

Hydroxyapatite coated zirconium oxide scaffolds incorporated within the multiorgan chip (MOC) from TissUse combine tissue engineering techniques with OOC technology and have been used to generate bone-marrow-on-chip (Sieber et al., 2018). In this model, a cell seeded scaffold of MSC and multipotent haematopoietic stem and progenitor cells (HSPC) is cultured within the MOC which comprises two separate independent channel circuits, each hosting a single culture compartment interconnected by the channel system. One of these compartments is used for the cell scaffold, while the other functions as a medium reservoir. The flow rate (5 $\mu\text{L/min}$) is controlled by an on-chip peristaltic micro pump (frequency of 2 Hz for continuous dynamic operation) integrated into each circuit (Sieber et al., 2018). Long term culture of HSPCs is maintained in the MOC for a period of 28 days. The cells form a microenvironment reminiscent of the *in vivo* bone marrow niche within the scaffold, and remain in their primitive, undifferentiated state (Sieber et al., 2018).

PERSPECTIVES

Challenges Associated With Incorporating Biomechanical Stimuli in OOC Models

Incorporating appropriate physiologically representative biomechanical stimuli into OOC models is challenging. A major

confounding factor in the replication of *in vivo* biology is tissue structure. Cells within their native environment can withstand significantly higher levels of mechanical stimulation due to the structural organization of the tissue. For example, joint loading during physical activity subjects articular cartilage to forces several times greater than body weight. However the unique anisotropic structure of this tissue (depth dependent variation in collagen fibril alignment and confinement of hydrated proteoglycan) allows these forces to be dissipated such that the cellular strains experienced by chondrocytes are actually much lower (Bergmann et al., 1993). Thus, further integration of OOC technology with tissue engineering techniques such as 3D bioprinting to achieve structurally aligned matrices or generate 3D scaffolds within chips, has the potential to create better representations of the mechanical environment within organ models. This could unlock new application areas for OOC, such as modeling fibrosis and tumor stroma.

The successful recapitulation of the *in vivo* biomechanical environment will also be dependent upon the ability of organ chips to incorporate multiple forms of mechanical stimuli within a single device. Thus far commercial systems have achieved the integration of stretch and flow (Emulate Inc., BI/OND; **Figures 1A,B,D**). However, to date no commercial systems are available which apply compression in organ chips. The incorporation of compressive strain into OOC systems will be essential to the development of multiple models particularly those mimicking the musculoskeletal system. Topography and geometric confinement (**Figures 1G,H**) provide two biomechanical cues which while not yet incorporated into the above reviewed commercial systems, could be easily integrated into future iterations of these to build biomechanical complexity. Moreover, integrating these stimuli into a single model presents significant technical challenges both in terms of the interactive effects these stimuli will exert upon each other (e.g., flow rate changes as the result of stretch induced changes in channel volume and shape) and the increased complexity of the biological outcome. To replicate the body's fluid shear conditions more accurately, organ chips should feature greater ranges of fluid shear levels and more variable types of flow such as oscillatory or pulsatile flow. Once again, the successful integration of these stimuli will enhance the accuracy of organ models and thus better replicate tissue function in health and disease.

A caveat to increasing the biological complexity of these models is the conflict this represents with analytical requirements such as real-time imaging, sampling, and scaling to increase throughput. Moreover, more complex models will likely produce more complex outputs due to additional cellular and matrix interactions which could be difficult to interpret.

One of the many advantages of OOC systems are that they have the potential to be accessible in ways that cannot easily be achieved *in vivo*. Thus, the ability to culture cells for extended periods with regular sampling of culture media and cellular by-products are a necessary feature. Mechanical stimuli within OOC systems could also be used more generally to improve mechanobiological studies. Therefore, researchers must be able to monitor both the cells and their responses in real-time in a non-destructive manner using existing research methodologies

for this technology to be adopted more readily. At the same time, for these systems to be successful within the pharmaceutical industry, they need to be high throughput and have the potential for significant automation of downstream analyses. This undoubtedly presents significant technical challenges relating to the development of robust standardized equipment supporting these organ chips for the application of multiple types of stimuli at consistent, and tightly controlled levels.

The use of OOC technology for diagnostic approaches or to deliver personalized medicine is highly attractive. The incorporation of this technology into clinical practice to determine drug responsiveness of patient samples and inform clinical decisions means that these models must be established in a highly standardized manner and subjected to well-defined mechanical input to deliver clear outcomes.

How Much Mechanobiology Do We Need?

Organ-on-chip models incorporating active mechanical stimuli have arrived at similar findings demonstrating the crucial role of biomechanics in replicating *in vivo* behavior and dictating drug response. In this review, we identify several studies demonstrating that incorporation these stimuli into OOC models has the potential to create more sophisticated organ models that better represent the *in vivo* scenario. In vascular models, appropriate modulation of inflammatory responses is observed at shear stress levels far below those found *in vivo* (Benam et al., 2016a,b; Poussin et al., 2020). In the airway, stretch influences viral entry and drug efficacy (Si et al., 2020). In the kidney, the application of apical shear stress modulates drug uptake and nephrotoxicity (Duan et al., 2010; Vriend et al., 2020). While in the intestine, the inclusion of peristalsis-like stretch creates a more accurate representation of bacterial infection (Grassart et al., 2019).

These examples from different organ systems provide strong evidence to support the consideration of mechanobiology when designing *in vitro* OOC model systems to obtain a more accurate, reliable prediction of the human response prior to clinical trials. Ultimately, this will accelerate the drug development process by both identifying potential drug candidates earlier in the pipeline and by ruling out many of those that will fail in subsequent clinical trials. However, none of these models precisely mimic the entire *in vivo* biomechanical environment, rather focusing

on a key stimulus delivered at approximately physiological intensities. These systems also do not account for pathological patient-specific biomechanics which typically deviate from what is considered physiologically normal and may be important in the use of OOC for personalized medicine. This begs the question, how accurately do biomechanical stimuli need to be replicated? Several commercial systems already incorporate a sufficient level of biomechanical stimulation to modulate drug efficacy in multiple organ models and are beginning to be adopted by the pharmaceutical industry in their current forms. The requirement for standardized systems suggests future research should focus on developing the biology within these existing systems. Validation of these OOC systems in a clinical context requires the replication of *in vivo* human biology, which must provide the benchmark when considering the extent to which mechanical stimuli should be incorporated. A greater understanding of how individual forms of biomechanical stimuli influence cell behavior in both health and disease is therefore required to develop these models and enhance their ability to predict drug performance in humans.

AUTHOR CONTRIBUTIONS

CT, HH, and ST reviewed and evaluated the literature and drafted the manuscript. MK was involved in the conception of the review and critically revised the manuscript. SF provided pre-clinical data. All authors contributed to manuscript revision and approved the submitted version.

FUNDING

Experimental data included in this review was generated with the support of funding from the Medical Research Council (MRC grant no. MR/L002876/1) and Ph.D. studentship funding from the China Scholarship Council.

ACKNOWLEDGMENTS

We are grateful for the input from the various manufactures indicated in the text who provided technical information about their commercially available organ-on-chip systems.

REFERENCES

- Anderson, D. E., and Johnstone, B. (2017). Dynamic mechanical compression of chondrocytes for tissue engineering: a critical review. *Front. Bioeng. Biotechnol.* 5:76. doi: 10.3389/fbioe.2017.00076
- Artzy-Schnirman, A., Hobi, N., Schneider-Daum, N., Guenat, O. T., Lehr, C. M., and Sznitman, J. (2019). Advanced in vitro lung-on-chip platforms for inhalation assays: from prospect to pipeline. *Eur. J. Pharm. Biopharm.* 144, 11–17. doi: 10.1016/j.ejpb.2019.09.006
- Atac, B., Wagner, I., Horland, R., Lauster, R., Marx, U., Tonevitsky, A. G., et al. (2013). Skin and hair on-a-chip: in vitro skin models versus ex vivo tissue maintenance with dynamic perfusion. *Lab. Chip* 13, 3555–3561. doi: 10.1039/c3lc50227a
- Atasi, Y., and Stunnenberg, H. G. (2017). The interplay of epigenetic marks during stem cell differentiation and development. *Nat. Rev. Genet.* 18, 643–658. doi: 10.1038/nrg.2017.57
- Baert, Y., Ruetschle, I., Cools, W., Oehme, A., Lorenz, A., Marx, U., et al. (2020). A multi-organ-chip co-culture of liver and testis equivalents: a first step toward a systemic male reprotoxicity model. *Hum. Reprod.* 35, 1029–1044. doi: 10.1093/humrep/deaa057
- Bauer, S., Wennberg Hultdt, C., Kanebratt, K. P., Durieux, I., Gunne, D., Andersson, S., et al. (2017). Functional coupling of human pancreatic islets and liver spheroids on-a-chip: towards a novel human ex vivo type 2 diabetes model. *Sci. Rep.* 7:14620. doi: 10.1038/s41598-017-14815-w
- Beaurivage, C., Naumovska, E., Chang, Y. X., Elstak, E. D., Nicolas, A., Wouters, H., et al. (2019). Development of a gut-on-a-chip model for high throughput

- disease modeling and drug discovery. *Int. J. Mol. Sci.* 2:5661. doi: 10.3390/ijms20225661
- Beekers, I., van Rooij, T., Verweij, M. D., Versluis, M., de Jong, N., Trietsch, S. J., et al. (2018). Acoustic characterization of a vessel-on-a-chip microfluidic system for ultrasound-mediated drug delivery. *IEEE Trans. Ultrason. Ferroelectr. Freq. Control* 65, 570–581. doi: 10.1109/TUFFC.2018.2803137
- Benam, K. H., Novak, R., Nawroth, J., Hirano-Kobayashi, M., Ferrante, T. C., Choe, Y., et al. (2016a). Matched-comparative modeling of normal and diseased human airway responses using a microengineered breathing lung chip. *Cell Syst.* 3, 456–466e454. doi: 10.1016/j.cels.2016.10.003
- Benam, K. H., Villenave, R., Lucchesi, C., Varone, A., Hubeau, C., Lee, H. H., et al. (2016b). Small airway-on-a-chip enables analysis of human lung inflammation and drug responses in vitro. *Nat. Methods* 13, 151–157. doi: 10.1038/nmeth.3697
- Berger, E., Magliaro, C., Paczia, N., Monzel, A. S., Antony, P., Linster, C. L., et al. (2018). Millifluidic culture improves human midbrain organoid vitality and differentiation. *Lab. Chip* 18, 3172–3183. doi: 10.1039/c8lc00206a
- Bergmann, G., Graichen, F., and Rohlmann, A. (1993). Hip joint loading during walking and running, measured in two patients. *J. Biomech.* 26, 969–990. doi: 10.1016/0021-9290(93)90058-m
- Beverung, S., Wu, J., and Steward, R. Jr. (2020). Lab-on-a-chip for cardiovascular physiology and pathology. *Micromachines (Basel)* 11:898. doi: 10.3390/mi1100898
- Bhatia, S. N., and Ingber, D. E. (2014). Microfluidic organs-on-chips. *Nat. Biotechnol.* 32, 760–772. doi: 10.1038/nbt.2989
- Boers, H. E., Haroon, M., Le Grand, F., Bakker, A. D., Klein-Nulend, J., and Jaspers, R. T. (2018). Mechanosensitivity of aged muscle stem cells. *J. Orthop. Res.* 36, 632–641. doi: 10.1002/jor.23797
- Bolognin, S., Fossepre, M., Qing, X., Jarazo, J., Scancar, J., Moreno, E. L., et al. (2019). 3D cultures of Parkinson's disease-specific dopaminergic neurons for high content phenotyping and drug testing. *Adv. Sci. (Weinh)* 6:1800927. doi: 10.1002/advs.201800927
- Brandstaeter, S., Fuchs, S. L., Aydin, R. C., and Cyron, C. J. (2019). Mechanics of the stomach: a review of an emerging field of biomechanics. *GAMMMitteilungen* 42:e201900001. doi: 10.1002/gamm.201900001
- Brown, T. D., Nowak, M., Bayles, A. V., Prabhakarapandian, B., Karande, P., Lahann, J., et al. (2019). A microfluidic model of human brain (muHuB) for assessment of blood brain barrier. *Bioeng. Transl. Med.* 4:e10126. doi: 10.1002/btm2.10126
- Caballero, D., Kaushik, S., Corrello, V. M., Oliveira, J. M., Reis, R. L., and Kundu, S. C. (2017). Organ-on-chip models of cancer metastasis for future personalized medicine: from chip to the patient. *Biomaterials* 149, 98–115. doi: 10.1016/j.biomaterials.2017.10.005
- Caplin, J. D., Granados, N. G., James, M. R., Montazami, R., and Hashemi, N. (2015). Microfluidic organ-on-a-chip technology for advancement of drug development and toxicology. *Adv. Health. Mater.* 4, 1426–1450. doi: 10.1002/adhm.201500040
- Chandorkar, P., Posch, W., Zaderer, V., Blatzer, M., Steger, M., Ammann, C. G., et al. (2017). Fast-track development of an in vitro 3D lung/immune cell model to study *Aspergillus* infections. *Sci. Rep.* 7:11644. doi: 10.1038/s41598-017-11271-4
- Chen, W. L. K., Edington, C., Suter, E., Yu, J., Velazquez, J. J., Velazquez, J. G., et al. (2017). Integrated gut/liver microphysiological systems elucidates inflammatory inter-tissue crosstalk. *Biotechnol. Bioeng.* 114, 2648–2659. doi: 10.1002/bit.26370
- Chiu, J. J., and Chien, S. (2011). Effects of disturbed flow on vascular endothelium: pathophysiological basis and clinical perspectives. *Physiol. Rev.* 91, 327–387. doi: 10.1152/physrev.00047.2009
- Da Silva-Candal, A., Brown, T., Krishnan, V., Lopez-Loureiro, I., Avila-Gomez, P., Pusuluri, A., et al. (2019). Shape effect in active targeting of nanoparticles to inflamed cerebral endothelium under static and flow conditions. *J. Control Release* 309, 94–105. doi: 10.1016/j.jconrel.2019.07.026
- Dean, B. J. F., Dakin, S. G., Millar, N. L., and Carr, A. J. (2017). Review: emerging concepts in the pathogenesis of tendinopathy. *Surgeon* 15, 349–354. doi: 10.1016/j.surge.2017.05.005
- Delaine-Smith, R. M., and Reilly, G. C. (2012). Mesenchymal stem cell responses to mechanical stimuli. *Muscles Ligaments Tendons J.* 2, 169–180.
- Deosarkar, S. P., Prabhakarapandian, B., Wang, B., Sheffield, J. B., Krynska, B., and Kiani, M. F. (2015). A novel dynamic neonatal blood-brain barrier on a chip. *PLoS One* 10:e0142725. doi: 10.1371/journal.pone.0142725
- Domansky, K., Inman, W., Serdy, J., Dash, A., Lim, M. H., and Griffith, L. G. (2010). Perfused multiwell plate for 3D liver tissue engineering. *Lab. Chip* 10, 51–58. doi: 10.1039/b913221j
- Downing, T. L., Soto, J., Morez, C., Houssin, T., Fritz, A., Yuan, F., et al. (2013). Biophysical regulation of epigenetic state and cell reprogramming. *Nat. Mater.* 12, 1154–1162. doi: 10.1038/nmat3777
- Duan, Y., Weinstein, A. M., Weinbaum, S., and Wang, T. (2010). Shear stress-induced changes of membrane transporter localization and expression in mouse proximal tubule cells. *Proc. Natl. Acad. Sci. U.S.A.* 107, 21860–21865. doi: 10.1073/pnas.1015751107
- Elbakary, B., and Badhan, R. K. S. (2020). A dynamic perfusion based blood-brain barrier model for cytotoxicity testing and drug permeation. *Sci. Rep.* 10:3788. doi: 10.1038/s41598-020-60689-w
- Engler, A. J., Sen, S., Sweeney, H. L., and Discher, D. E. (2006). Matrix elasticity directs stem cell lineage specification. *Cell* 126, 677–689. doi: 10.1016/j.cell.2006.06.044
- Esch, E. W., Bahinski, A., and Huh, D. (2015). Organs-on-chips at the frontiers of drug discovery. *Nat. Rev. Drug Discov.* 14, 248–260. doi: 10.1038/nrd4539
- Estell, E. G., Murphy, L. A., Silverstein, A. M., Tan, A. R., Shah, R. P., Ateshian, G. A., et al. (2017). Fibroblast-like synovocyte mechanosensitivity to fluid shear is modulated by interleukin-1 α . *J. Biomech.* 60, 91–99. doi: 10.1016/j.jbiomech.2017.06.011
- Faure, M., Guibert, E., Alves, S., Pain, B., Rame, C., Dupont, J., et al. (2016). The insulin sensitiser metformin regulates chicken Sertoli and germ cell populations. *Reproduction* 151, 527–538. doi: 10.1530/REP-15-0565
- Felson, D. T. (2013). Osteoarthritis as a disease of mechanics. *Osteoarthritis Cartilage* 21, 10–15. doi: 10.1016/j.joca.2012.09.012
- Feric, N. T., Pallotta, I., Singh, R., Bogdanowicz, D. R., Gustilo, M., Chaudhary, K., et al. (2019). Engineered cardiac tissues generated in the Biowire II: a platform for human-based drug discovery. *Toxicol. Sci.* 172, 89–97. doi: 10.1093/toxsci/kfz168
- Folmes, C. D., and Terzic, A. (2016). Energy metabolism in the acquisition and maintenance of stemness. *Semin. Cell Dev. Biol.* 52, 68–75. doi: 10.1016/j.semcdb.2016.02.010
- Foster, A. J., Chouhan, B., Regan, S. L., Rollison, H., Amberntsson, S., Andersson, L. C., et al. (2019). Integrated in vitro models for hepatic safety and metabolism: evaluation of a human Liver-Chip and liver spheroid. *Arch. Toxicol.* 93, 1021–1037. doi: 10.1007/s00204-019-02427-4
- Franzen, N., van Harten, W. H., Retel, V. P., Loskill, P., van den Eijnden-van Raaij, J., and IJzerman, M. (2019). Impact of organ-on-a-chip technology on pharmaceutical R&D costs. *Drug Discov. Today* 24, 1720–1724. doi: 10.1016/j.drudis.2019.06.003
- Fu, S., Thompson, C. L., Ali, A., Wang, W., Chapple, J. P., Mitchison, H. M., et al. (2019). Mechanical loading inhibits cartilage inflammatory signalling via an HDAC6 and IFT-dependent mechanism regulating primary cilia elongation. *Osteoarthritis Cartilage* 27, 1064–1074. doi: 10.1016/j.joca.2019.03.003
- Gao, L., McBeath, R., and Chen, C. S. (2010). Stem cell shape regulates a chondrogenic versus myogenic fate through Rac1 and N-cadherin. *Stem Cells* 28, 564–572. doi: 10.1002/stem.308
- Gao, X., Wu, L., and O'Neil, R. G. (2003). Temperature-modulated diversity of TRPV4 channel gating: activation by physical stresses and phorbol ester derivatives through protein kinase C-dependent and -independent pathways. *J. Biol. Chem.* 278, 27129–27137. doi: 10.1074/jbc.M302517200
- Giusti, S., Sbrana, T., La Marca, M., Di Patria, V., Martinucci, V., Tirella, A., et al. (2014). A novel dual-flow bioreactor simulates increased fluorescein permeability in epithelial tissue barriers. *Biotechnol. J.* 9, 1175–1184. doi: 10.1002/biot.201400004
- Gomel, M. A., Lee, R., and Grande-Allen, K. J. (2018). Comparing the role of mechanical forces in vascular and valvular calcification progression. *Front. Cardiovasc. Med.* 5:197. doi: 10.3389/fcvm.2018.00197
- Gomez, Y., Navarro-Tableros, V., Tetta, C., Camussi, G., and Brizzi, M. F. (2020). A Versatile model of microfluidic perfusion system for the evaluation of c-peptide secretion profiles: comparison between human pancreatic islets and HLSC-derived Islet-like structures. *Biomedicines* 8:26. doi: 10.3390/biomedicines8020026

- Grassart, A., Malarde, V., Gobaa, S., Sartori-Rupp, A., Kerns, J., Karalis, K., et al. (2019). Bioengineered human organ-on-chip reveals intestinal microenvironment and mechanical forces impacting *Shigella* infection. *Cell Host Microbe* 26, 435–444.e434. doi: 10.1016/j.chom.2019.08.007
- Harris, C., Thorpe, S. D., Rushwan, S., Wang, W., Thompson, C. L., Peacock, J. L., et al. (2019). An in vitro investigation of the inflammatory response to the strain amplitudes which occur during high frequency oscillation ventilation and conventional mechanical ventilation. *J. Biomech.* 88, 186–189. doi: 10.1016/j.jbiomech.2019.03.024
- Hasenberg, T., Muhleder, S., Dotzler, A., Bauer, S., Labuda, K., Holnthoner, W., et al. (2015). Emulating human microcapillaries in a multi-organ-chip platform. *J. Biotechnol.* 216, 1–10. doi: 10.1016/j.jbiotec.2015.09.038
- Hassell, B. A., Goyal, G., Lee, E., Sontheimer-Phelps, A., Levy, O., Chen, C. S., et al. (2017). Human organ chip models recapitulate orthotopic lung cancer growth, therapeutic responses, and tumor dormancy in vitro. *Cell Rep.* 21, 508–516. doi: 10.1016/j.celrep.2017.09.043
- Henry, O. Y. F., Villenave, R., Crouce, M. J., Leineweber, W. D., Benz, M. A., and Ingber, D. E. (2017). Organs-on-chips with integrated electrodes for trans-epithelial electrical resistance (TEER) measurements of human epithelial barrier function. *Lab. Chip* 17, 2264–2271. doi: 10.1039/c7lc00155j
- Heo, S. J., Thorpe, S. D., Driscoll, T. P., Duncan, R. L., Lee, D. A., and Mauck, R. L. (2015). Biophysical regulation of chromatin architecture instills a mechanical memory in mesenchymal stem cells. *Sci. Rep.* 5:16895. doi: 10.1038/srep16895
- Hoyle, N. P., Seinkmane, E., Putker, M., Feeney, K. A., Krogager, T. P., Chesham, J. E., et al. (2017). Circadian actin dynamics drive rhythmic fibroblast mobilization during wound healing. *Sci. Transl. Med.* 9:eal2774. doi: 10.1126/scitranslmed.aal2774
- Hu, H., Juvekar, A., Lyssiotis, C. A., Lien, E. C., Albeck, J. G., Oh, D., et al. (2016). Phosphoinositide 3-kinase regulates glycolysis through mobilization of aldolase from the actin cytoskeleton. *Cell* 164, 433–446. doi: 10.1016/j.cell.2015.12.042
- Hubner, J., Raschke, M., Rutschle, I., Grassle, S., Hasenberg, T., Schirrmann, K., et al. (2018). Simultaneous evaluation of anti-EGFR-induced tumour and adverse skin effects in a microfluidic human 3D co-culture model. *Sci. Rep.* 8:15010. doi: 10.1038/s41598-018-33462-3
- Huh, D., Kim, H. J., Fraser, J. P., Shea, D. E., Khan, M., Bahinski, A., et al. (2013). Microfabrication of human organs-on-chips. *Nat. Protoc.* 8, 2135–2157. doi: 10.1038/nprot.2013.137
- Huh, D., Leslie, D. C., Matthews, B. D., Fraser, J. P., Jurek, S., Hamilton, G. A., et al. (2012). A human disease model of drug toxicity-induced pulmonary edema in a lung-on-a-chip microdevice. *Sci. Transl. Med.* 4:159ra147. doi: 10.1126/scitranslmed.3004249
- Huh, D., Matthews, B. D., Mammoto, A., Montoya-Zavala, M., Hsin, H. Y., and Ingber, D. E. (2010). Reconstituting organ-level lung functions on a chip. *Science* 328, 1662–1668. doi: 10.1126/science.1188302
- Ihara, T., Mitsui, T., Nakamura, Y., Kira, S., Nakagomi, H., Sawada, N., et al. (2017). Clock genes regulate the circadian expression of Piezo1, TRPV4, Connexin26, and VNUT in an ex vivo mouse bladder mucosa. *PLoS One* 12:e0168234. doi: 10.1371/journal.pone.0168234
- Jaalouk, D. E., and Lammerding, J. (2009). Mechanotransduction gone awry. *Nat. Rev. Mol. Cell Biol.* 10, 63–73. doi: 10.1038/nrm2597
- Jain, A., Barrile, R., van der Meer, A. D., Mammoto, A., Mammoto, T., De Ceunynck, K., et al. (2018). Primary human lung alveolus-on-a-chip model of intravascular thrombosis for assessment of therapeutics. *Clin. Pharmacol. Ther.* 103, 332–340. doi: 10.1002/cpt.742
- Jain, A., van der Meer, A. D., Papa, A. L., Barrile, R., Lai, A., Schlechter, B. L., et al. (2016). Assessment of whole blood thrombosis in a microfluidic device lined by fixed human endothelium. *Biomed. Microdevices* 18:73. doi: 10.1007/s10544-016-0095-6
- Jalili-Firoozinezhad, S., Prantil-Baun, R., Jiang, A., Potla, R., Mammoto, T., Weaver, J. C., et al. (2018). Modeling radiation injury-induced cell death and countermeasure drug responses in a human Gut-on-a-Chip. *Cell Death Dis.* 9:223. doi: 10.1038/s41419-018-0304-8
- Jang, K. J., Mehr, A. P., Hamilton, G. A., McPartlin, L. A., Chung, S., Suh, K. Y., et al. (2013). Human kidney proximal tubule-on-a-chip for drug transport and nephrotoxicity assessment. *Integr. Biol. (Camb)* 5, 1119–1129. doi: 10.1039/c3ib40049b
- Jang, K. J., Otieno, M. A., Ronxhi, J., Lim, H. K., Ewart, L., Kodella, K. R., et al. (2019). Reproducing human and cross-species drug toxicities using a Liver-Chip. *Sci. Transl. Med.* 11:eaax5516. doi: 10.1126/scitranslmed.aax5516
- Jang, M., Kleber, A., Ruckelshausen, T., Betzholz, R., and Manz, A. (2019). Differentiation of the human liver progenitor cell line (HepaRG) on a microfluidic-based biochip. *J. Tissue Eng. Regen. Med.* 13, 482–494. doi: 10.1002/term.2802
- Jang, M., Manz, A., Volk, T., and Kleber, A. (2018). Study of melatonin-mediated effects on various hepatic inflammatory responses stimulated by IL-6 in a new HepG2-on-a-chip platform. *Biomed. Microdevices* 20:54. doi: 10.1007/s10544-018-0300-x
- Jang, M., Neuzil, P., Volk, T., Manz, A., and Kleber, A. (2015). On-chip three-dimensional cell culture in phaseguides improves hepatocyte functions in vitro. *Biomicrofluidics* 9:034113. doi: 10.1063/1.4922863
- Kaarj, K., and Yoon, J. Y. (2019). Methods of delivering mechanical stimuli to organ-on-a-chip. *Micromachines (Basel)* 10:700. doi: 10.3390/mi10100700
- Kane, K. I. W., Moreno, E. L., Hachi, S., Walter, M., Jarazo, J., Oliveira, M. A. P., et al. (2019). Automated microfluidic cell culture of stem cell derived dopaminergic neurons. *Sci. Rep.* 9:1796. doi: 10.1038/s41598-018-34828-3
- Kasendra, M., Luc, R., Yin, J., Manatakis, D. V., Kulkarni, G., Lucchesi, C., et al. (2020). Duodenum intestine-chip for preclinical drug assessment in a human relevant model. *eLife* 9:e50135. doi: 10.7554/eLife.50135
- Kasendra, M., Tovaglieri, A., Sontheimer-Phelps, A., Jalili-Firoozinezhad, S., Bein, A., Chalkiadaki, A., et al. (2018). Development of a primary human Small Intestine-on-a-Chip using biopsy-derived organoids. *Sci. Rep.* 8:2871. doi: 10.1038/s41598-018-21201-7
- Kim, H. J., Huh, D., Hamilton, G., and Ingber, D. E. (2012). Human gut-on-a-chip inhabited by microbial flora that experiences intestinal peristalsis-like motions and flow. *Lab. Chip* 12, 2165–2174. doi: 10.1039/c2lc40074j
- Kim, Y. J., Sah, R. L., Grodzinsky, A. J., Plaas, A. H., and Sandy, J. D. (1994). Mechanical regulation of cartilage biosynthetic behavior: physical stimuli. *Arch. Biochem. Biophys.* 311, 1–12. doi: 10.1006/abbi.1994.1201
- Knecht, S., Vanwanseele, B., and Stüssi, E. (2006). A review on the mechanical quality of articular cartilage—implications for the diagnosis of osteoarthritis. *Clin. Biomech.* 21, 999–1012.
- Kolhar, P., Anselmo, A. C., Gupta, V., Pant, K., Prabhakarapandian, B., Ruoslahti, E., et al. (2013). Using shape effects to target antibody-coated nanoparticles to lung and brain endothelium. *Proc. Natl. Acad. Sci. U.S.A.* 110, 10753–10758. doi: 10.1073/pnas.1308345110
- Koo, Y., Hawkins, B. T., and Yun, Y. (2018). Three-dimensional (3D) tetra-culture brain on chip platform for organophosphate toxicity screening. *Sci. Rep.* 8:2841. doi: 10.1038/s41598-018-20876-2
- Kostrzewski, T., Cornforth, T., Snow, S. A., Ouro-Gnao, L., Rowe, C., Large, E. M., et al. (2017). Three-dimensional perfused human in vitro model of non-alcoholic fatty liver disease. *World J. Gastroenterol.* 23, 204–215. doi: 10.3748/wjg.v23.i2.204
- Kostrzewski, T., Maraver, P., Ouro-Gnao, L., Levi, A., Snow, S., Miedzick, A., et al. (2020). A Microphysiological system for studying nonalcoholic steatohepatitis. *Hepatology* 71, 77–91. doi: 10.1002/hep4.1450
- Kramer, B., Haan, L., Vermeer, M., Olivier, T., Hankemeier, T., Vulto, P., et al. (2019). Interstitial flow recapitulates gemcitabine chemoresistance in a 3D microfluidic pancreatic ductal adenocarcinoma model by induction of multidrug resistance proteins. *Int. J. Mol. Sci.* 20:4647. doi: 10.3390/ijms20184647
- Krempaska, K., Barnowski, S., Gavini, J., Hobi, N., Ebener, S., Simillion, C., et al. (2020). Azithromycin has enhanced effects on lung fibroblasts from idiopathic pulmonary fibrosis (IPF) patients compared to controls. *Respir. Res.* 21:25. doi: 10.1186/s12931-020-1275-8
- Kulthong, K., Duivenvoorde, L., Sun, H., Confederat, S., Wu, J., Spenkelink, B., et al. (2020). Microfluidic chip for culturing intestinal epithelial cell layers: characterization and comparison of drug transport between dynamic and static models. *Toxicol. In Vitro* 65:104815. doi: 10.1016/j.tiv.2020.104815
- Lamberti, G., Tang, Y., Prabhakarapandian, B., Wang, Y., Pant, K., Kiani, M. F., et al. (2013). Adhesive interaction of functionalized particles and endothelium in idealized microvascular networks. *Microvasc. Res.* 89, 107–114. doi: 10.1016/j.mvr.2013.03.007
- Lanz, H. L., Saleh, A., Kramer, B., Cairns, J., Ng, C. P., Yu, J., et al. (2017). Therapy response testing of breast cancer in a 3D high-throughput perfused microfluidic platform. *BMC Cancer* 17:709. doi: 10.1186/s12885-017-3709-3
- Lee, D. A., Knight, M. M., Campbell, J. J., and Bader, D. L. (2011). Stem cell mechanobiology. *J. Cell Biochem.* 112, 1–9. doi: 10.1002/jcb.22758

- Leight, J. L., Wozniak, M. A., Chen, S., Lynch, M. L., and Chen, C. S. (2012). Matrix rigidity regulates a switch between TGF- β 1-induced apoptosis and epithelial-mesenchymal transition. *Mol. Biol. Cell* 23, 781–791. doi: 10.1091/mbc.E11-06-0537
- Leong, D. J., Li, Y. H., Gu, X. I., Sun, L., Zhou, Z., Nasser, P., et al. (2011). Physiological loading of joints prevents cartilage degradation through CITED2. *FASEB J.* 25, 182–191. doi: 10.1096/fj.10-164277
- Li, C. X., Talele, N. P., Boo, S., Koehler, A., Knee-Walden, E., Balestrini, J. L., et al. (2017). MicroRNA-21 preserves the fibrotic mechanical memory of mesenchymal stem cells. *Nat. Mater.* 16, 379–389. doi: 10.1038/nmat4780
- Li, X., George, S. M., Vernetti, L., Gough, A. H., and Taylor, D. L. (2018). A glass-based, continuously zonated and vascularized human liver acinus microphysiological system (vLAMPS) designed for experimental modeling of diseases and ADME/TOX. *Lab. Chip* 18, 2614–2631. doi: 10.1039/c8lc00418h
- Lin, C. C., Kurashige, M., Liu, Y., Terabayashi, T., Ishimoto, Y., Wang, T., et al. (2018). A cleavage product of Polycystin-1 is a mitochondrial matrix protein that affects mitochondria morphology and function when heterologously expressed. *Sci. Rep.* 8:2743. doi: 10.1038/s41598-018-20856-6
- Lin, N., Zhou, X., Geng, X., Drewell, C., Hubner, J., Li, Z., et al. (2020). Repeated dose multi-drug testing using a microfluidic chip-based coculture of human liver and kidney proximal tubules equivalents. *Sci. Rep.* 10:8879. doi: 10.1038/s41598-020-65817-0
- Liu, Z., Mackay, S., Gordon, D. M., Anderson, J. D., Haithcock, D. W., Garson, C. J., et al. (2019). Co-cultured microfluidic model of the airway optimized for microscopy and micro-optical coherence tomography imaging. *Biomed. Opt. Express* 10, 5414–5430. doi: 10.1364/BOE.10.005414
- Long, T. J., Cosgrove, P. A., Dunn, R. T., Stolz, D. B., Hamadeh, H., Afshari, C., et al. (2016). Modeling therapeutic antibody-small molecule drug-drug interactions using a three-dimensional perfusable human liver coculture platform. *Drug Metab. Dispos.* 44, 1940–1948. doi: 10.1124/dmd.116.071456
- Lundin, V., Sugden, W. W., Theodore, L. N., Sousa, P. M., Han, A., Chou, S., et al. (2020). YAP regulates hematopoietic stem cell formation in response to the biomechanical forces of blood flow. *Dev. Cell* 52, 446–460. doi: 10.1016/j.devcel.2020.01.006
- Maschmeyer, I., Hasenberg, T., Jaenicke, A., Lindner, M., Lorenz, A. K., Zech, J., et al. (2015a). Chip-based human liver-intestine and liver-skin co-cultures – a first step toward systemic repeated dose substance testing in vitro. *Eur. J. Pharm. Biopharm.* 95(Pt A), 77–87. doi: 10.1016/j.ejpb.2015.03.002
- Maschmeyer, I., Lorenz, A. K., Schimek, K., Hasenberg, T., Ramme, A. P., Hubner, J., et al. (2015b). A four-organ-chip for interconnected long-term co-culture of human intestine, liver, skin and kidney equivalents. *Lab. Chip* 15, 2688–2699. doi: 10.1039/c5lc00392j
- Materne, E. M., Ramme, A. P., Terrasso, A. P., Serra, M., Alves, P. M., Brito, C., et al. (2015). A multi-organ chip co-culture of neurospheres and liver equivalents for long-term substance testing. *J. Biotechnol.* 205, 36–46. doi: 10.1016/j.jbiotec.2015.02.002
- Mazzei, D., Guzzardi, M. A., Giusti, S., and Ahluwalia, A. (2010). A low shear stress modular bioreactor for connected cell culture under high flow rates. *Biotechnol. Bioeng.* 106, 127–137. doi: 10.1002/bit.22671
- McBeath, R., Pirone, D. M., Nelson, C. M., Bhadriraju, K., and Chen, C. S. (2004). Cell shape, cytoskeletal tension, and RhoA regulate stem cell lineage commitment. *Dev. Cell* 6, 483–495. doi: 10.1016/s1534-5807(04)00075-9
- McMahon, L. A., O'Brien, F. J., and Prendergast, P. J. (2008). Biomechanics and mechanobiology in osteochondral tissues. *Regen. Med.* 3, 743–759. doi: 10.2217/17460751.3.5.743
- Miranda-Azpiroz, P., Panagiotou, S., Jose, G., and Saha, S. (2018). A novel dynamic multicellular co-culture system for studying individual blood-brain barrier cell types in brain diseases and cytotoxicity testing. *Sci. Rep.* 8:8784. doi: 10.1038/s41598-018-26480-8
- Moreno, E. L., Hachi, S., Hemmer, K., Trietsch, S. J., Baumratov, A. S., Hankemeier, T., et al. (2015). Differentiation of neuroepithelial stem cells into functional dopaminergic neurons in 3D microfluidic cell culture. *Lab. Chip* 15, 2419–2428. doi: 10.1039/c5lc00180c
- Musah, S., Dimitrakakis, N., Camacho, D. M., Church, G. M., and Ingber, D. E. (2018). Directed differentiation of human induced pluripotent stem cells into mature kidney podocytes and establishment of a Glomerulus Chip. *Nat. Protoc.* 13, 1662–1685. doi: 10.1038/s41596-018-0007-8
- Naumovska, E., Aalderink, G., Wong Valencia, C., Kosim, K., Nicolas, A., Brown, S., et al. (2020). Direct on-chip differentiation of intestinal tubules from induced pluripotent stem cells. *Int. J. Mol. Sci.* 21:4964. doi: 10.3390/ijms21144964
- Navarro-Tableros, V., Gai, C., Gomez, Y., Giunti, S., Pasquino, C., Derigibus, M. C., et al. (2019). Islet-like structures generated in vitro from adult human liver stem cells revert hyperglycemia in diabetic SCID mice. *Stem Cell Rev. Rep.* 15, 93–111. doi: 10.1007/s12015-018-9845-6
- Nowell, C. S., Odermatt, P. D., Azzolin, L., Hohnel, S., Wagner, E. F., Fantner, G. E., et al. (2016). Chronic inflammation imposes aberrant cell fate in regenerating epithelia through mechanotransduction. *Nat. Cell Biol.* 18, 168–180. doi: 10.1038/ncb3290
- Nunes, S. S., Miklas, J. W., Liu, J., Aschar-Sobbi, R., Xiao, Y., Zhang, B., et al. (2013). Biowire: a platform for maturation of human pluripotent stem cell-derived cardiomyocytes. *Nat. Methods* 10, 781–787. doi: 10.1038/nmeth.2524
- Ortega-Prieto, A. M., Skelton, J. K., Cherry, C., Briones-Orta, M. A., Hateley, C. A., and Dörner, M. (2019). “Liver-on-a-chip” cultures of primary hepatocytes and kupffer cells for Hepatitis B virus infection. *J. Vis. Exp.* 144:e58333. doi: 10.3791/58333
- Pagliari, S., Tirella, A., Ahluwalia, A., Duim, S., Goumans, M. J., Aoyagi, T., et al. (2014). A multistep procedure to prepare pre-vascularized cardiac tissue constructs using adult stem cells, dynamic cell cultures, and porous scaffolds. *Front. Physiol.* 5:210. doi: 10.3389/fphys.2014.00210
- Park, J. S., Burckhardt, C. J., Lazzano, R., Solis, L. M., Isogai, T., Li, L., et al. (2020). Mechanical regulation of glycolysis via cytoskeleton architecture. *Nature* 578, 621–626. doi: 10.1038/s41586-020-1998-1
- Park, T. E., Mustafaoğlu, N., Herland, A., Hasselkus, R., Mannix, R., FitzGerald, E. A., et al. (2019). Hypoxia-enhanced Blood-Brain Barrier Chip recapitulates human barrier function and shuttling of drugs and antibodies. *Nat. Commun.* 10:2621. doi: 10.1038/s41467-019-10588-0
- Pedersen, J. M., Shim, Y. S., Hans, V., Phillips, M. B., Macdonald, J. M., Walker, G., et al. (2016). Fluid dynamic modeling to support the development of flow-based hepatocyte culture systems for metabolism studies. *Front. Bioeng. Biotechnol.* 4:72. doi: 10.3389/fbioe.2016.00072
- Peel, S., Corrigan, A. M., Ehrhardt, B., Jang, K. J., Caetano-Pinto, P., Boeckeler, M., et al. (2019). Introducing an automated high content confocal imaging approach for Organs-on-Chips. *Lab. Chip* 19, 410–421. doi: 10.1039/c8lc00829a
- Petrosyan, A., Cravedi, P., Villani, V., Angeletti, A., Manrique, J., Renieri, A., et al. (2019). A glomerulus-on-a-chip to recapitulate the human glomerular filtration barrier. *Nat. Commun.* 10:3656. doi: 10.1038/s41467-019-11577-z
- Polachek, W. J., Li, R., Uzel, S. G., and Kamm, R. D. (2013). Microfluidic platforms for mechanobiology. *Lab. Chip* 13, 2252–2267. doi: 10.1039/c3lc41393d
- Potier, E., Noailly, J., and Ito, K. (2010). Directing bone marrow-derived stromal cell function with mechanics. *J. Biomech.* 43, 807–817. doi: 10.1016/j.jbiomech.2009.11.019
- Poussin, C., Kramer, B., Lanz, H. L., Van den Heuvel, A., Laurent, A., Olivier, T., et al. (2020). 3D human microvessel-on-a-chip model for studying monocyte-to-endothelium adhesion under flow - application in systems toxicology. *ALTEX* 37, 47–63. doi: 10.14573/altex.1811301
- Prabhakarandian, B., Shen, M. C., Nichols, J. B., Mills, I. R., Sidoryk-Wegrzynowicz, M., Aschner, M., et al. (2013). SyM-BBB: a microfluidic Blood Brain Barrier model. *Lab. Chip* 13, 1093–1101. doi: 10.1039/c2lc41208j
- Prabhakarandian, B., Wang, Y., Rea-Ramsey, A., Sundaram, S., Kiani, M. F., and Pant, K. (2011). Bifurcations: focal points of particle adhesion in microvascular networks. *Microcirculation* 18, 380–389. doi: 10.1111/j.1549-8719.2011.00099.x
- Ramachandran, S. D., Schirmer, K., Munst, B., Heinz, S., Ghafoory, S., Wolff, S., et al. (2015). In vitro generation of functional liver organoid-like structures using adult human cells. *PLoS One* 10:e0139345. doi: 10.1371/journal.pone.0139345
- Ramme, A. P., Koenig, L., Hasenberg, T., Schwenk, C., Magauer, C., Faust, D., et al. (2019). Autologous induced pluripotent stem cell-derived four-organ-chip. *Future Sci. OA* 5:FSO413. doi: 10.2144/foa-2019-0065
- Rashidi, H., Alhaque, S., Szkolnicka, D., Flint, O., and Hay, D. C. (2016). Fluid shear stress modulation of hepatocyte-like cell function. *Arch. Toxicol.* 90, 1757–1761. doi: 10.1007/s00204-016-1689-8
- Rosano, J. M., Tousi, N., Scott, R. C., Krynska, B., Rizzo, V., Prabhakarandian, B., et al. (2009). A physiologically realistic in vitro model of microvascular

- networks. *Biomed. Microdevices* 11, 1051–1057. doi: 10.1007/s10544-009-9322-8
- Rowe, C., Shaeri, M., Large, E., Cornforth, T., Robinson, A., Kostrzewski, T., et al. (2018). Perfused human hepatocyte microtissues identify reactive metabolite-forming and mitochondria-perturbing hepatotoxins. *Toxicol. In Vitro* 46, 29–38. doi: 10.1016/j.tiv.2017.09.012
- Sances, S., Ho, R., Vatine, G., West, D., Laperle, A., Meyer, A., et al. (2018). Human iPSC-derived endothelial cells and microengineered organ-chip enhance neuronal development. *Stem Cell Reports* 10, 1222–1236. doi: 10.1016/j.stemcr.2018.02.012
- Sarkar, U., Ravindra, K. C., Large, E., Young, C. L., Rivera-Burgos, D., Yu, J., et al. (2017). Integrated assessment of diclofenac biotransformation, pharmacokinetics, and omics-based toxicity in a three-dimensional human liver-immunocompetent coculture system. *Drug Metab. Dispos.* 45, 855–866. doi: 10.1124/dmd.116.074005
- Schimek, K., Busek, M., Brincker, S., Groth, B., Hoffmann, S., Lauster, R., et al. (2013). Integrating biological vasculature into a multi-organ-chip microsystem. *Lab. Chip* 13, 3588–3598. doi: 10.1039/c3lc50217a
- Schimek, K., Frenzel, S., Luetlich, K., Bovard, D., Rutschle, I., Boden, L., et al. (2020). Human multi-organ chip co-culture of bronchial lung culture and liver spheroids for substance exposure studies. *Sci. Rep.* 10:7865. doi: 10.1038/s41598-020-64219-6
- Schimek, K., Hsu, H. H., Boehme, M., Kornet, J. J., Marx, U., Lauster, R., et al. (2018). Bioengineering of a full-thickness skin equivalent in a 96-well insert format for substance permeation studies and organ-on-a-chip applications. *Bioengineering (Basel)* 5:43. doi: 10.3390/bioengineering5020043
- Schutgens, F., Rookmaaker, M. B., Margaritis, T., Rios, A., Ammerlaan, C., Jansen, J., et al. (2019). Tubuloids derived from human adult kidney and urine for personalized disease modeling. *Nat. Biotechnol.* 37, 303–313. doi: 10.1038/s41587-019-0048-8
- Shannahan, J. H., Fritz, K. S., Raghavendra, A. J., Podila, R., Persaud, I., and Brown, J. M. (2016). From the cover: disease-induced disparities in formation of the nanoparticle-biocrona and the toxicological consequences. *Toxicol. Sci.* 152, 406–416. doi: 10.1093/toxsci/kfw097
- Sheyn, D., Cohn-Yakubovich, D., Ben-David, S., De Mel, S., Chan, V., Hinojosa, C., et al. (2019). Bone-chip system to monitor osteogenic differentiation using optical imaging. *Microfluid. Nanofluidics* 23:99. doi: 10.1007/s10404-019-2261-7
- Shiraishi, T., Verdone, J. E., Huang, J., Kahlert, U. D., Hernandez, J. R., Torga, G., et al. (2015). Glycolysis is the primary bioenergetic pathway for cell motility and cytoskeletal remodeling in human prostate and breast cancer cells. *Oncotarget* 6, 130–143. doi: 10.18632/oncotarget.2766
- Si, L., Bai, H., Rodas, M., Cao, W., Oh, C. Y., Jiang, A., et al. (2020). Human organ chip-enabled pipeline to rapidly repurpose therapeutics during viral pandemics. *bioRxiv* [Preprint]. doi: 10.1101/2020.04.13.039917
- Sieber, S., Wirth, L., Cavak, N., Koenigsmark, M., Marx, U., Lauster, R., et al. (2018). Bone marrow-on-a-chip: long-term culture of human haematopoietic stem cells in a three-dimensional microfluidic environment. *J. Tissue Eng. Regen. Med.* 12, 479–489. doi: 10.1002/term.2507
- Silvani, G., Scognamiglio, C., Caprini, D., Marino, L., Chinappi, M., Sinibaldi, G., et al. (2019). Reversible cavitation-induced junctional opening in an artificial endothelial layer. *Small* 15:e1905375. doi: 10.1002/sml.201905375
- Skardal, A., Devarasetty, M., Forsythe, S., Atala, A., and Soker, S. (2016). A reductionist metastasis-on-a-chip platform for in vitro tumor progression modeling and drug screening. *Biotechnol. Bioeng.* 113, 2020–2032. doi: 10.1002/bit.25950
- Sontheimer-Phelps, A., Chou, D. B., Tovaglieri, A., Ferrante, T. C., Duckworth, T., Fadel, C., et al. (2020). Human colon-on-a-chip enables continuous in vitro analysis of colon mucus layer accumulation and physiology. *Cell Mol. Gastroenterol. Hepatol.* 9, 507–526. doi: 10.1016/j.jcmgh.2019.11.008
- Soroush, F., Tang, Y., Mustafa, O., Sun, S., Yang, Q., Kilpatrick, L. E., et al. (2020). Neutrophil-endothelial interactions of murine cells is not a good predictor of their interactions in human cells. *FASEB J.* 34, 2691–2702. doi: 10.1096/fj.201900048R
- Stucki, A. O., Stucki, J. D., Hall, S. R., Felder, M., Mermoud, Y., Schmid, R. A., et al. (2015). A lung-on-a-chip array with an integrated bio-inspired respiration mechanism. *Lab. Chip* 15, 1302–1310. doi: 10.1039/c4lc01252f
- Stucki, J. D., Hobi, N., Galimov, A., Stucki, A. O., Schneider-Daum, N., Lehr, C. M., et al. (2018). Medium throughput breathing human primary cell alveolus-on-chip model. *Sci. Rep.* 8:14359. doi: 10.1038/s41598-018-32523-x
- Tang, Y., Soroush, F., Sheffield, J. B., Wang, B., Prabhakarapandian, B., and Kiani, M. F. (2017). A biomimetic microfluidic tumor microenvironment platform mimicking the EPR effect for rapid screening of drug delivery systems. *Sci. Rep.* 7:9359. doi: 10.1038/s41598-017-09815-9
- Tang, Y., Soroush, F., Sun, S., Liverani, E., Langston, J. C., Yang, Q., et al. (2018). Protein kinase C-delta inhibition protects blood-brain barrier from sepsis-induced vascular damage. *J. Neuroinflammation* 15:309. doi: 10.1186/s12974-018-1342-y
- Terrell-Hall, T. B., Nounou, M. I., El-Amrawy, F., Griffith, J. I. G., and Lockman, P. R. (2017). Trastuzumab distribution in an in-vivo and in-vitro model of brain metastases of breast cancer. *Oncotarget* 8, 83734–83744. doi: 10.18632/oncotarget.19634
- Thacker, V. V., Dhar, N., Sharma, K., Barrile, R., Karalis, K., and McKinney, J. D. (2020). A lung-on-chip model reveals an essential role for alveolar epithelial cells in controlling bacterial growth during early tuberculosis. *bioRxiv* [Preprint]. doi: 10.1101/2020.02.03.931170
- Thorpe, S. D., Buckley, C. T., Steward, A. J., and Kelly, D. J. (2012). European Society of Biomechanics S.M. Perren Award 2012: the external mechanical environment can override the influence of local substrate in determining stem cell fate. *J. Biomech.* 45, 2483–2492. doi: 10.1016/j.jbiomech.2012.07.024
- Thorpe, S. D., Buckley, C. T., Vinardell, T., O'Brien, F. J., Campbell, V. A., and Kelly, D. J. (2010). The response of bone marrow-derived mesenchymal stem cells to dynamic compression following TGF-beta3 induced chondrogenic differentiation. *Ann. Biomed. Eng.* 38, 2896–2909. doi: 10.1007/s10439-010-0059-6
- Torisawa, Y. S., Mammoto, T., Jiang, E., Jiang, A., Mammoto, A., Watters, A. L., et al. (2016). Modeling hematopoiesis and responses to radiation countermeasures in a bone marrow-on-a-chip. *Tissue Eng. Part C Methods* 22, 509–515. doi: 10.1089/ten.TEC.2015.0507
- Torisawa, Y. S., Spina, C. S., Mammoto, T., Mammoto, A., Weaver, J. C., Tat, T., et al. (2014). Bone marrow-on-a-chip replicates hematopoietic niche physiology in vitro. *Nat. Methods* 11, 663–669. doi: 10.1038/nmeth.2938
- Trietsch, S. J., Naumovska, E., Kurek, D., Setyawati, M. C., Vormann, M. K., Wilschut, K. J., et al. (2017). Membrane-free culture and real-time barrier integrity assessment of perfused intestinal epithelium tubes. *Nat. Commun.* 8:262. doi: 10.1038/s41467-017-00259-3
- Tschumperlin, D. J., and Drazen, J. M. (2001). Mechanical stimuli to airway remodeling. *Am. J. Respir. Crit. Care Med.* 164(10 Pt 2), S90–S94. doi: 10.1164/ajrccm.164.supplement_2.2106060
- Vacca, M., Leslie, J., Virtue, S., Lam, B. Y. H., Govaere, O., Tiniakos, D., et al. (2020). Bone morphogenetic protein 8B promotes the progression of non-alcoholic steatohepatitis. *Nat. Metab.* 2, 514–531. doi: 10.1038/s42255-020-0214-9
- van Duinen, V., van den Heuvel, A., Trietsch, S. J., Lanz, H. L., van Gils, J. M., van Zonneveld, A. J., et al. (2017). 96 perfusable blood vessels to study vascular permeability in vitro. *Sci. Rep.* 7:18071. doi: 10.1038/s41598-017-14716-y
- van Duinen, V., Zhu, D., Ramakers, C., van Zonneveld, A. J., Vulto, P., and Hankemeier, T. (2019). Perfused 3D angiogenic sprouting in a high-throughput in vitro platform. *Angiogenesis* 22, 157–165. doi: 10.1007/s10456-018-9647-0
- van Helvert, S., Storm, C., and Friedl, P. (2018). Mechanoreciprocity in cell migration. *Nat. Cell Biol.* 20, 8–20. doi: 10.1038/s41556-017-0012-0
- Vatine, G. D., Barrile, R., Workman, M. J., Sances, S., Barriga, B. K., Rahnama, M., et al. (2019). Human iPSC-derived blood-brain barrier chips enable disease modeling and personalized medicine applications. *Cell Stem Cell* 24, 995–1005.e1006. doi: 10.1016/j.stem.2019.05.011
- Villanave, R., Wales, S. Q., Hamkins-Indik, T., Papafragkou, E., Weaver, J. C., Ferrante, T. C., et al. (2017). Human gut-on-A-Chip supports polarized infection of coxsackie B1 virus in vitro. *PLoS One* 12:e0169412. doi: 10.1371/journal.pone.0169412
- Vinci, B., Duret, C., Klieber, S., Gerbal-Chaloin, S., Sa-Cunha, A., Laporte, S., et al. (2011). Modular bioreactor for primary human hepatocyte culture: medium flow stimulates expression and activity of detoxification genes. *Biotechnol. J.* 6, 554–564. doi: 10.1002/biot.201000326

- Vormann, M. K., Gijzen, L., Hutter, S., Boot, L., Nicolas, A., van den Heuvel, A., et al. (2018). Nephrotoxicity and kidney transport assessment on 3D perfused proximal tubules. *AAPS J.* 20:90. doi: 10.1208/s12248-018-0248-z
- Vriend, J., Nieskens, T. T. G., Vormann, M. K., van den Berge, B. T., van den Heuvel, A., Russel, F. G. M., et al. (2018). Screening of drug-transporter interactions in a 3D microfluidic renal proximal tubule on a chip. *AAPS J.* 20:87. doi: 10.1208/s12248-018-0247-0
- Vriend, J., Peters, J. G. P., Nieskens, T. T. G., Skovronova, R., Blaimschein, N., Schmidts, M., et al. (2020). Flow stimulates drug transport in a human kidney proximal tubule-on-a-chip independent of primary cilia. *Biochim. Biophys. Acta Gen. Subj.* 1864:129433. doi: 10.1016/j.bbagen.2019.12.9433
- Vu, M. N., Rajasekhar, P., Poole, D. P., Khor, S. Y., Truong, N. P., Nowell, C. J., et al. (2019). Rapid assessment of nanoparticle extravasation in a microfluidic tumor model. *ACS Appl. Nano Mater.* 2, 1844–1856. doi: 10.1021/acsanm.8b02056
- Wagner, I., Materne, E. M., Brincker, S., Sussbier, U., Fradrich, C., Busek, M., et al. (2013). A dynamic multi-organ-chip for long-term cultivation and substance testing proven by 3D human liver and skin tissue co-culture. *Lab. Chip* 13, 3538–3547. doi: 10.1039/c3lc50234a
- Wang, L., Dorn, P., Zeinali, S., Froment, L., Berezowska, S., Kocher, G. J., et al. (2020). CD90(+)CD146(+) identifies a pulmonary mesenchymal cell subtype with both immune modulatory and perivascular-like function in postnatal human lung. *Am. J. Physiol. Lung Cell Mol. Physiol.* 318, L813–L830. doi: 10.1152/ajplung.00146.2019
- Wang, Q., Delcorde, J., Tang, T., Downey, G. P., and McCulloch, C. A. (2018). Regulation of IL-1 signaling through control of focal adhesion assembly. *FASEB J.* 32, 3119–3132. doi: 10.1096/fj.201700966R
- Wann, A. K., and Knight, M. M. (2012). Primary cilia elongation in response to interleukin-1 mediates the inflammatory response. *Cell. Mol. Life Sci.* 69, 2967–2977. doi: 10.1007/s00018-012-0980-y
- Waters, C. M., Roan, E., and Navajas, D. (2012). Mechanobiology in lung epithelial cells: measurements, perturbations, and responses. *Compr. Physiol.* 2, 1–29. doi: 10.1002/cphy.c100090
- Wevers, N. R., Kasi, D. G., Gray, T., Wilschut, K. J., Smith, B., van Vught, R., et al. (2018). A perfused human blood-brain barrier on-a-chip for high-throughput assessment of barrier function and antibody transport. *Fluids Barriers CNS* 15:23. doi: 10.1186/s12987-018-0108-3
- Wheeler, S. E., Clark, A. M., Taylor, D. P., Young, C. L., Pillai, V. C., Stolz, D. B., et al. (2014). Spontaneous dormancy of metastatic breast cancer cells in an all human liver microphysiologic system. *Br. J. Cancer* 111, 2342–2350. doi: 10.1038/bjc.2014.533
- Wilmer, M. J., Ng, C. P., Lanz, H. L., Vulto, P., Suter-Dick, L., and Masereeuw, R. (2016). Kidney-on-a-chip technology for drug-induced nephrotoxicity screening. *Trends Biotechnol.* 34, 156–170. doi: 10.1016/j.tibtech.2015.11.001
- Workman, M. J., Gleeson, J. P., Troisi, E. J., Estrada, H. Q., Kerns, S. J., Hinojosa, C. D., et al. (2018). Enhanced utilization of induced pluripotent stem cell-derived human intestinal organoids using microengineered chips. *Cell. Mol. Gastroenterol. Hepatol.* 5, 669–677.e662. doi: 10.1016/j.jcmgh.2017.12.008
- Xu, Y., Qin, S., Niu, Y., Gong, T., Zhang, Z., and Fu, Y. (2020). Effect of fluid shear stress on the internalization of kidney-targeted delivery systems in renal tubular epithelial cells. *Acta Pharm. Sin. B* 10, 680–692. doi: 10.1016/j.apsb.2019.11.012
- Zivanovic, S., Peacock, J., Alcazar-Paris, M., Lo, J. W., Lunt, A., Marlow, N., et al. (2014). Late outcomes of a randomized trial of high-frequency oscillation in neonates. *N. Engl. J. Med.* 370, 1121–1130. doi: 10.1056/NEJMoa1309220

Conflict of Interest: MK is Director of the Queen Mary + Emulate Organs-on-Chips Centre and CT is the centre scientist of the Queen Mary + Emulate Organs-on-Chips Centre which is part funded by Emulate Inc. Emulate Inc. were not involved in the preparation of this review other than the provision of data on device specifications as provided by all featured manufacturers.

The remaining authors declare that the research was conducted in the absence of any commercial or financial relationships that could be construed as a potential conflict of interest.

Copyright © 2020 Thompson, Fu, Heywood, Knight and Thorpe. This is an open-access article distributed under the terms of the Creative Commons Attribution License (CC BY). The use, distribution or reproduction in other forums is permitted, provided the original author(s) and the copyright owner(s) are credited and that the original publication in this journal is cited, in accordance with accepted academic practice. No use, distribution or reproduction is permitted which does not comply with these terms.



Building Scaffolds for Tubular Tissue Engineering

Alexander J. Boys, Sarah L. Barron, Damyan Tilev and Roisin M. Owens*

Department of Chemical Engineering and Biotechnology, University of Cambridge, Cambridge, United Kingdom

OPEN ACCESS

Edited by:

Dania Movia,
Trinity College Dublin, Ireland

Reviewed by:

Francesca Taraballi,
Center for Musculoskeletal
Regeneration, Houston Methodist
Research Institute, United States
Silvia Baiguera,
University of Rome Tor Vergata, Italy

*Correspondence:

Roisin M. Owens
rmo37@cam.ac.uk

Specialty section:

This article was submitted to
Nanobiotechnology,
a section of the journal
Frontiers in Bioengineering and
Biotechnology

Received: 31 July 2020

Accepted: 04 November 2020

Published: 10 December 2020

Citation:

Boys AJ, Barron SL, Tilev D and
Owens RM (2020) Building Scaffolds
for Tubular Tissue Engineering.
Front. Bioeng. Biotechnol. 8:589960.
doi: 10.3389/fbioe.2020.589960

Hollow organs and tissue systems drive various functions in the body. Many of these hollow or tubular systems, such as vasculature, the intestines, and the trachea, are common targets for tissue engineering, given their relevance to numerous diseases and body functions. As the field of tissue engineering has developed, numerous benchtop models have been produced as platforms for basic science and drug testing. Production of tubular scaffolds for different tissue engineering applications possesses many commonalities, such as the necessity for producing an intact tubular opening and for formation of semi-permeable epithelia or endothelia. As such, the field has converged on a series of manufacturing techniques for producing these structures. In this review, we discuss some of the most common tissue engineered applications within the context of tubular tissues and the methods by which these structures can be produced. We provide an overview of the general structure and anatomy for these tissue systems along with a series of general design criteria for tubular tissue engineering. We categorize methods for manufacturing tubular scaffolds as follows: casting, electrospinning, rolling, 3D printing, and decellularization. We discuss state-of-the-art models within the context of vascular, intestinal, and tracheal tissue engineering. Finally, we conclude with a discussion of the future for these fields.

Keywords: biomaterials, 3D printing, electrospinning, decellularization, lumen, vascular, intestine, trachea

INTRODUCTION

Function of the human body is dependent on tubular tissues and tissue structures. These tissues, including vasculature, the intestines, the trachea, and many others, serve various roles in the body, ranging from absorption of nutrients to transport of oxygen. As may be expected given the broad assortment of functions associated with tubular tissues, these structures are susceptible to a variety of diseases and traumas. As such, significant focus has been placed on the generation of models of tubular systems for studies in disease, basic science, and drug discovery/efficacy. Many of these models utilize tissue engineering principles to recreate the function of these systems on the benchtop without requiring use of animal models (Bitar and Raghavan, 2012; Seifu et al., 2013; Law et al., 2016). The methods used to manufacture these tissue engineered systems play a major role in their resultant function. Here, we review the construction of tissue engineered systems for generating tubular models.

Tubular tissues have many unifying structural characteristics despite their various functions. Generally, these tissues are constructed in a lamellar manner, with sequential layers of tissue surrounding an internal opening. This opening, called the lumen, is where transport and containment of the specific medium for a particular tubular tissue occurs. This lumen is lined with

a set of barrier-forming cells, called an epithelium (or endothelium in the case of vasculature). This structure functions to separate the internal contents of the lumen from the surrounding tissues and organs, while allowing selective permeation and transport across the epithelium. The epithelium is situated on a bed of extracellular matrix (ECM), which provides structural support for the lumen and the epithelium (Hendow et al., 2016). This ECM layer can be present in various forms, but it generally consists of cells embedded in connective tissue, including various proteins like collagen, elastin, etc. Depending on the function of the particular tissue, other tissue layers may also be present. For example, given the role of vasculature in moving blood throughout the body, blood vessels often contain a layer of smooth muscle, which assists in the vasodilation and constriction in the vascular system. Regardless of the particular function for a tubular tissue, the main purpose of these structures involves the separation of one media from another, guiding and transporting various fluids, gases, and solids.

Tissue engineering is the combination of cells and a template to generate a structure that recapitulates the native function of a specific tissue or tissue system. Often the template is a scaffold or hydrogel on which the cells can proliferate and produce ECM. Here, we discuss scaffolds and hydrogels nearly synonymously, as the manufacturing methods for producing a tubular scaffold versus a tubular hydrogel do not necessarily differ. However, these structures possess different fundamental properties, and each should be considered independently for a given application. An understanding of the native function and physiology of a tissue is often sufficient to inform the choice of cells and scaffold materials for a tissue engineered application. However, scaffold design is challenging, given the need to create a supportive structure for cells to grow and create the desired tissue, without impinging on the overall function of the resultant structure. These challenges are especially prominent in the design of tubular systems, given the need to create an intact lumen that can support the formation of an epithelium and other components. Various manufacturing approaches have been utilized for production of scaffolds, including casting, electrospinning, rolling, three-dimensional (3D) printing, and decellularization.

Determination of the resultant properties in tubular systems can be difficult, particularly due to geometry. Besides the manufacture of a tubular scaffold, characterization of the interaction between cellular and scaffold components, as well as their combined structural integrity, is fundamental. For example, the formation and continued integrity of the epithelial or endothelial barrier ensures the selective permeability of essential nutrients and metabolic by-products, while preventing the entrance of noxious or pathogenic compounds. Thus, without successful barrier formation, and characterization of such, the functionality and even survival of these models would be limited. Equally, any drug transport studies would be rendered invalid if barrier formation was insufficient. Intercellular junctions, provide this barrier function and consist of various proteins, such as cadherins, zonulin-1 (ZO-1), etc. Generally, membranes like the intestinal epithelium possess tight junctions, which highly regulate ionic/molecular passage across the epithelium, whereas the vascular endothelium, for example, is more permeable.

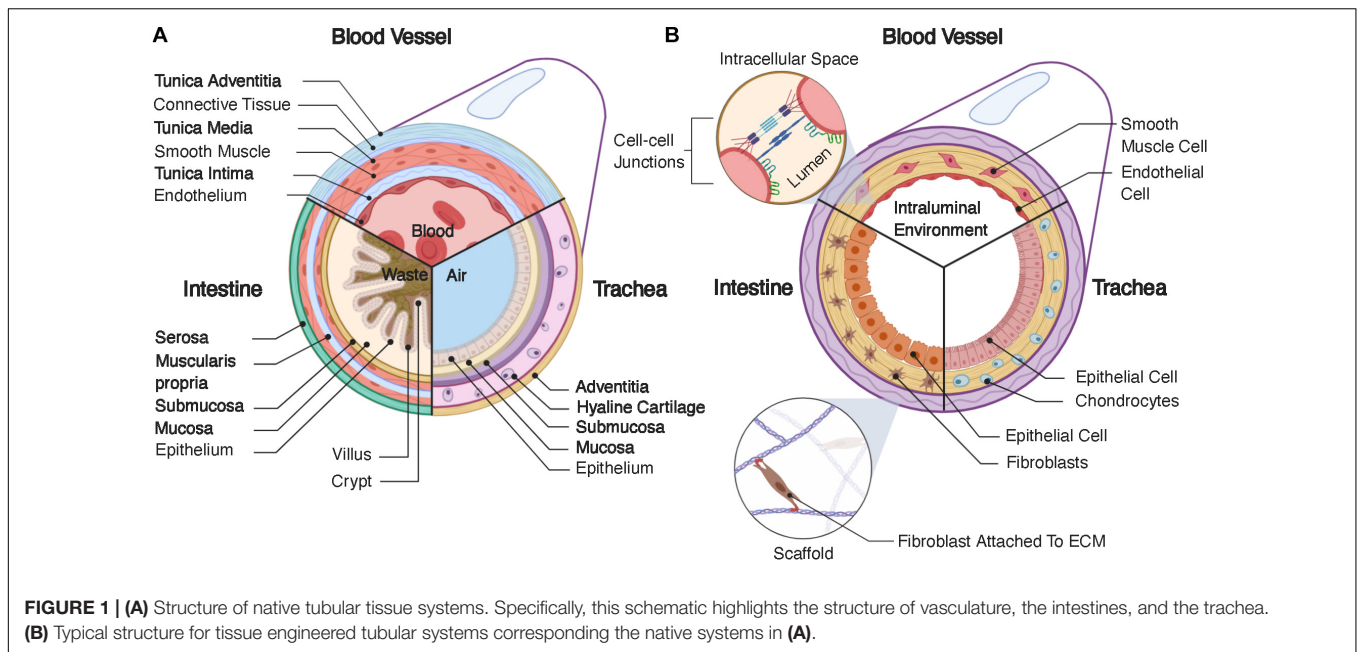
In this review, we discuss techniques commonly used to generate tissue engineered scaffolds for tubular systems. Our aim is to provide a categorization of the available methodologies for scaffold production to assist tissue engineers in navigating this extensive field. As such, we have chosen to focus on three specific tissue systems that represent various design challenges in the field: vasculature, the intestine, and the trachea for recapitulating the functions of many tubular tissue systems present in the body. Initially, we discuss the anatomy of these systems and some of the general criteria for tubular scaffold design. Then, we categorize the available scaffold manufacturing techniques. We proceed to examine some the applications of these techniques for our chosen tissue systems. Finally, we conclude with a discussion of the future for tissue engineered scaffold design for tubular tissue systems.

Structure of Native Tubular Tissues

Various tubular tissues are present in the body, including the vascular system, digestive system, respiratory system, lymphatic system, reproductive system, and many others. As discussed above, we have chosen to highlight vasculature, intestines, and the trachea, as these applications are some of the most widely researched in terms of generation of tubular tissue engineered models (Bitar and Raghavan, 2012; Seifu et al., 2013; Hendow et al., 2016; Law et al., 2016). Additionally, these systems possess various functions that differentiate them from one another with respect to design. Below, we discuss the specifics of the structure and physiology for each of these systems.

Vascular Structure

The primary role of the vascular system is the transport of blood throughout the body at relatively high velocities (Riva et al., 1985; Klarhöfer et al., 2001), generating significant fluid shear stress on the walls of a blood vessel (Akintewe et al., 2017). Additionally, the vascular endothelium is relatively permeable, allowing transport of biochemical factors through the vascular wall and even cells during some disease states (Park-Windhol and D'Amore, 2016). Blood vessels range in size from capillaries and microvasculature, which are only microns in diameter (Sieminski and Gooch, 2000), to larger veins and arteries, which can be ~30mm in diameter in the case of the pulmonary artery (Kuriyama et al., 1984). Small capillaries, such as those that make up the blood brain barrier, can consist of only one cell, wrapped onto itself to create the interior lumen (Abbott et al., 2006). However, we will focus on larger blood vessels that have a lamellar structure divided into three layers (**Figure 1A**): the tunica intima, tunica media, and tunica adventitia. Generally, the intima contains the endothelium, the media is composed of a layer of smooth muscle, and the adventitia consists of a layer of connective tissue (James and Allen, 2018). The endothelial layer of cells makes up the vascular wall. These cells form a semi-permeable membrane that allows transport of nutrients, oxygenation, and waste removal from surrounding tissues (Park-Windhol and D'Amore, 2016). The layer of smooth muscle in the tunica media aids in control of vasodilation, which can regulate local blood flow. Lastly, the tunica adventitia provides support for the internal layers in addition to housing a variety of



nerves, immune cells, and other support systems for vasculature (James and Allen, 2018). The heart pumps blood through the luminal compartment of these vessels. This pumping creates relatively high rates of fluid flow, ~ 30 mL/min (Klarhöfer et al., 2001), thereby generating significant fluid shear on the walls of vasculature, which is an additional necessary consideration in any tissue engineered model.

Intestinal Structure

The intestines are a portion of the gastrointestinal tract, which extends from the mouth, through the esophagus, the stomach, the small intestines, the large intestines, and finally to the rectum and anus. The main function of the intestine is to absorb nutrients from food and liquids we ingest and expel the remaining waste out of the body, with each portion of the gastrointestinal tract consisting of four layers. Starting from the interior lining of the lumen, these layers are the mucosa, submucosa, muscularis propria, and serosa (Figure 1A). In this review, we focus on the intestines and describe the layers in the context of these organs, versus other portions of the gastrointestinal tract. The mucosa contains the intestinal epithelium and has absorptive, secretory, and protective functions. The intestinal epithelium is a tight barrier system, robustly separating the interior contents of the lumen from the surrounding tissue (Suzuki, 2013). Intestinal epithelial tissue has a complex 3D structure, consistent of luminal projections, called villi, with intermediate invaginations, called crypts (Santos et al., 2018). This 3D architecture maximizes interior surface area, aiding in nutrient adsorption (Rao and Wang, 2010). The intestinal epithelium consists of numerous cell types with various functions, which have a semi-regimented distribution along this 3D structure. Generally, these cells and their respective functions are as follows: enterocytes – absorption of nutrients and formation of intestinal barrier; goblet cells – secretion of mucin; enteroendocrine cells – sensing of nutrients

and microbes and communication with the enteric nervous system; transit amplifying cells – differentiation toward secretory or absorptive lineages; as well as tuft cells, Paneth cells, intestinal stem cells, and others (Santos et al., 2018). These epithelial cells are adhered to the lamina propria, a layer of connective tissue, which is surrounded by a sheet of smooth muscle cells. The next layer is the submucosa, which contains a series of immune cells, nerves, and lymphatic cells. This layer is surrounded by the muscularis propria, which provides peristaltic pumping through muscle cells, performing the critical function of gut motility. Finally, the outermost layer is the serosa, or in some cases the adventitia depending on the present populations of cells, which forms a barrier around the gastrointestinal tract (Rao and Wang, 2010). The gut also possesses a complex series of nerves called the enteric nervous system, which consist of two parallel nerve plexi, the submucosal plexus and myenteric plexus, which run along the length of the gastrointestinal tract (Furness, 2012). Lastly, the interior of the gut contains a large cohort of bacteria, called the gut microbiome, which can influence various other organs throughout the body (Cryan et al., 2019), in addition to further complicating tissue engineered design.

Tracheal Structure

The trachea is fundamental in swallowing, speech and respiratory processes. It resides below the upper airways (nasal cavity, larynx, pharynx) and forms part of the lower airways (trachea, bronchi, bronchioles, alveoli), with its main function to conduct and warm air (Brand-Saberi and Schäfer, 2014). The trachea is comprised of four main layers (Figure 1A): mucosa, submucosa, hyaline cartilage, and adventitia. The mucosa contains a pseudostratified epithelium, which lines the lumen and contains many cell types including secretory club cells, ciliated cells, mucus producing goblet cells, basal stem cells, and pulmonary neuroendocrine cells. Ciliated, mucus-producing, and secretory cells act in

coordination to aid mucociliary clearance and protection against infection, while basal cells aid in regenerative processes (Brand-Saberi and Schäfer, 2014). The submucosa is a connective tissue layer containing submucosal glands, which contribute to mucus secretion. The cartilage layer consists of horseshoe-like rings of hyaline cartilage joined by fibroelastic tissue, which, is closed posteriorly by a membranous structure consisting of longitudinally oriented smooth muscle. Lastly, the adventitia consists of connective tissue. Both the cartilage and adventitial layers are fundamental in producing the unique structural and mechanical properties of the trachea. For example, the specific flexibility which permits the rotation and flexion of the neck while also maintaining sufficient structural strength to withstand compression and pressure alterations during respiratory processes. In order to reflect and integrate with the *in vivo* environment, tracheal tissue engineered models must adhere to these mechanical requirements (Boazak and Auguste, 2018). The adventitia also houses numerous other cell types, such as fibroblasts, adipocytes, nerves, and connections to vasculature, which is essential in meeting blood, nutrient, and metabolic demands. The respiratory system requires an air-liquid interface between the interior of the lumen and the surrounding epithelium (Pezzulo et al., 2011; de Souza Carvalho et al., 2014), creating a different environment from the fluidic environments of the vascular and intestinal systems, which can be difficult to produce in tissue engineered models. Unlike the *in vitro* models discussed for vasculature and the intestine, the outlook for tracheal tissue engineering so far largely concerns implantable scaffolds for tracheal replacement (Bogan et al., 2016; Law et al., 2016; Etienne et al., 2018). Indeed, the trachea is subject to a range of airway disorders which may result from infection, stenosis, collapse, or cancer (Etienne et al., 2018). The rise of biomedical engineering approaches, which recapitulate tracheal tissue, have been largely motivated by these applications. Here, we will discuss some of these studies, which focus on implant generation, and how they can be further developed for use as benchtop disease models.

Design Criteria for Tissue Engineering Tubular Systems

The physiology of tubular tissues is often complex, requiring various factors to produce an approximate model of the desired tissue. Generally, tissue engineered systems utilize a cell type (or types) in combination with a scaffold to recreate the primary function (or functions) of the tissue. However, choosing

appropriate cell types and scaffold architectures can be difficult. Here, we have highlighted some of the necessary design criteria to consider for manufacturing a scaffold for tubular tissue engineering (Table 1).

Scaffold design for tubular systems presents a variety of challenges. First, one must consider the source and types of cells, with any tubular system requiring a source of epithelial cells. However, the exact behavior of these cells will vary depending on the tissue in question. Epithelial cells are often co-cultured with ECM-producing cells like fibroblasts or smooth muscle cells (Boland et al., 2004; Yoshikawa et al., 2011; Chen et al., 2015), but even the type of matrix-producing cell can vary depending on application. For example, the trachea requires production of cartilaginous ECM using chondrocytes (Lin et al., 2009) or mesenchymal stem cells differentiated along chondrogenic pathways (Asnaghi et al., 2009; Haykal et al., 2014). Different tissues will also require different supporting cells. For example, native intestinal epithelium contains goblet cells for producing mucus (Dosh et al., 2019). Both native vasculature and intestine possess a layer of musculature (Boland et al., 2004), necessitating sourcing of appropriate muscle cells. We have summarized some common cell lines or primary cells used to reconstitute native function in tissue engineered models (Table 2).

A major requirement for every tubular scaffold is the formation of a contiguous epithelial or endothelial lining (Figure 1B). Cells are most effectively seeded homogeneously on two-dimensional (2D), non-porous surfaces, such as cell culture flasks, or in injectable media, such as hydrogels. However, tubular scaffolds are not flat and, generally, are porous. Therefore, the necessity for homogenous seeding on a 3D surface, requires alternative methodologies. For example, researchers have seeded cells onto flat membranes and then rolled these membranes into tubes (Yuan et al., 2012; Cheng et al., 2017; Zhao et al., 2018). Other studies have used dynamic methods, relying on the cells to adhere homogeneously to the surrounding walls through rotational or pressurized actuation (Niklason and Langer, 1997; Godbey et al., 2004; Nieponice et al., 2008). Porous scaffolds are beneficial in that they provide greater access to media by cells, but these pores also make the formation of a contiguous epithelium difficult. Some studies have back-filled pores with ECM-producing cells or depositing cells in a layered approach to assist in the formation of an epithelium (Liu et al., 2015; Chen et al., 2015). Many implant-driven studies also rely on cell infiltration *in vivo*. All of these methods have limitations, but continuous iteration has improved the feasibility of accomplishing this particular task for tubular tissue engineering.

TABLE 1 | Design criteria for tubular tissue engineered scaffold development as a function of tissue type.

Tissue System	Cellular				Mechanical			Other	
	Contiguous Epithelium/Endothelium	Smooth Muscle Layer	Supporting Connective Tissue Layer	Mucous Layer	Fluid Shear	Pressurization	Mechanical Stimulation (Peristalsis)	Separation of Luminal Chamber	Air-liquid Interface
Vasculature	X	X	X		X	X			
Intestine	X	X	X	X	X	X	X	X	
Trachea	X		X	X		X		X	X

TABLE 2 | Commonly used cells for tissue engineered models of vasculature, the intestine, and the trachea.

Tissue System	Native Tissue Layer	Cell Model	Cell Function	References
Blood Vessel	Tunica Intima	Human Umbilical Vein Endothelial Cell (HUVEC)	Endothelial Cell	Boland et al., 2004; Lovett et al., 2007; Du et al., 2012; Wang et al., 2014; Cui et al., 2019
		Endothelial Progenitor Cell (EPC)	Endothelial Cell	Neff et al., 2011; Ju et al., 2017; Atchison et al., 2017
		Primary Endothelial Cell	Endothelial Cell	Matsuda, 2004, 200; Opitz et al., 2004; Zang et al., 2013
	Tunica Media	Primary Smooth Muscle Cells	Smooth Muscle Cell	Seliktar et al., 2003; Opitz et al., 2004; Swartz et al., 2005; Lee et al., 2007; Zhang et al., 2013; Fu et al., 2014; Cui et al., 2019
	Tunica Adventitia	Dermal Fibroblasts	Fibroblast	Seliktar et al., 2003; Boland et al., 2004
Intestine	Mucosa	Caco-2 Cells	Enterocyte	Costello et al., 2014; Chen et al., 2015; Ladd et al., 2018
		HT-29-MTX Cells	Goblet Cell	Chen et al., 2015
	Submucosa	Primary Intestinal Myofibroblast	Myofibroblast	Chen et al., 2015
	Muscularis Propria	Smooth Muscle Cell	Smooth Muscle Cell	Zakhem et al., 2012; Knight et al., 2013
	Serosa			
Trachea	Mucosa	Primary Respiratory Epithelial Cell	Epithelial Cell	Butler et al., 2017; Kreimendahl et al., 2019; Park et al., 2019
		Turbinate Mesenchymal Stromal Cell	Epithelial Cell	Park et al., 2018; Ahn et al., 2019
	Submucosa			
	Hyaline Cartilage	Mesenchymal Stem Cell	Chondrocyte	Wang et al., 2020
		Adipose-derived Stem Cell	Chondrocyte	Giraldo-Gomez et al., 2019
		Auricular Chondrocyte	Chondrocyte	Park et al., 2019
	Adventitia	Nasal Fibroblast	Fibroblast	Kreimendahl et al., 2019

Another necessary design consideration is provision of nutrients to all cells in the system. Tubular systems will inherently contain epithelial cells, but they may also contain supporting cells, present underneath the epithelium (**Figure 1B**). In the case of vascular systems, these underlying cells can theoretically receive nutrients through the endothelial wall, as the vascular endothelium is inherently permeable for this purpose. However, intestinal and respiratory tissue engineering presents a particular challenge, as the lumen should not be used to provide nutrients to any of the cells in the system, given the function of these tissues (Bitar and Raghavan, 2012). In the body, nutrients are provided to the tissues underlying the epithelium by surrounding vasculature. To mimic native tissues, tissue engineered models rely on perfusion of the scaffold with media to simulate nutrient transport. However, separation of the luminal compartment from the surrounding scaffold is difficult. Custom bioreactors can accomplish this task (Haykal et al., 2014; Zhou et al., 2018), but bioreactor design and setup also complicate culture for the system.

Secondary design criteria relate to the specific function of the tubular system. For example, vascular systems often induce fluid movement to mimic blood flow. As such, vascular systems utilize external pumps, typically with pulsatile pumping patterns (Niklason and Langer, 1997; Niklason et al., 1999; Opitz et al., 2004), which also necessitates the ability of the scaffold to withstand mechanical forces that result from pumping, i.e. pressurization and fluid shear (**Figure 2**). Fluid shear is also

known to drive vascular endothelial phenotype and morphology (Wang et al., 2013; Wang et al., 2016a; Polacheck et al., 2017) and regulates angiogenesis *in vitro* (Song and Munn, 2011; Galie et al., 2014), which can be beneficial in different tissue engineering models. An accurate intestinal model requires peristaltic pumping to mimic gut motility. Peristalsis has been achieved using external bioreactors (Zhou et al., 2018), but

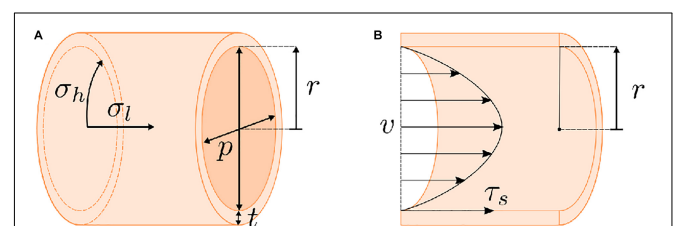


FIGURE 2 | Stresses present for dynamic flow of a fluid through a tube. **(A)** Pumping a liquid or gaseous medium through a tube will generate a pressure on the tube walls. The highest stress resultant from this pressurization is the hoop stress (σ_h). Any scaffold must possess sufficient strength to compensate for this hoop stress. **(B)** Fluid movement will also result in a shear stress (τ_s) on the walls of the tube. Generally, these factors (σ_h and τ_s) can be calculated based on the geometry of the tube, i.e., wall thickness (t) and inner radius (r), the pressure (p) on the tube walls, the flow rate of the fluid (v), and the viscosity of the fluid. However, these calculations are complicated by scaffold porosity and the potential for effects of cell growth on the scaffold over the course of an experiment.

bioreactors are often custom-made, requiring further design and optimization. Secondly, native intestinal environments contain a bacterial cohort. Inputting of bacteria into a tissue engineered lumen is feasible (Costello et al., 2014) but also further complicates culture conditions. Other systems, like the trachea, require the presence of air in the lumen, which can make culture condition more complex. Many studies have utilized bioreactors that rotate the tubular tracheal scaffold along its axis with half of the scaffold submerged in media and the other half in air to create an air-liquid interface (Lin et al., 2009). However, this approach is not ideal for biomimetic studies assessing drug delivery, given its dissimilarities to the native tracheal environment.

METHODS FOR FABRICATING TUBULAR SCAFFOLDS

Various methodologies can be used to produce tubular scaffolds for tissue engineering. We have divided these techniques into five categories (Table 3) to assist in experimental design and planning. Below, we have discussed the general methodologies for each technique, while also addressing their benefits and limitations. Other reviews have also examined general strategies for tissue engineering tubular systems (Bitar and Raghavan, 2012; Seifu et al., 2013; Hendow et al., 2016; Law et al., 2016; Song et al., 2018).

Casting

Casting is one of the most commonly used manufacturing techniques across the entirety of the tissue engineering field. The basis for this methodology is the pouring or injection of a liquid into a mold, at which point the liquid is induced to form a solid structure. The liquid can be derived from a variety of means, including the melting and solidification of a material (Im et al., 2019), the solubilization of a material in a solvent and subsequent evaporation of the solvent (Mooney et al., 1995; Opitz et al., 2004; Nieponice et al., 2008; Ma et al., 2010; Zakhem et al., 2012), or the cross-linking (Matsuda, 2004; Guo et al., 2017) or gelation of a material into a solid or semi-solid structure, such as a hydrogel (Wang et al., 2014; Strobel et al., 2018b). Casting is also applicable within the context of more complex molding techniques, such as vacuum-assisted tube formation (Singh et al., 2017), and for the formation of more complex structures (Ladd et al., 2018). As may be expected, the chosen material will dictate the mechanism. In the case of some hydrogels, particularly biomolecular gels, e.g., collagen, fibrin, etc., cells can be cast with the gel (Seliktar et al., 2003; Swartz et al., 2005; Liu et al., 2007; Naito et al., 2011; Atchison et al., 2017, 2020). This method is convenient and widely applicable, as it can be used to produce a variety of geometries and shapes with homogenous cell populations and is compatible with other manufacturing methods (Atchison et al., 2017; Iannucci et al., 2019). However, a secondary seeding step is often still necessary to create the stratified cellular structure of native tubular tissues, even when using homogeneously seeded hydrogels.

In tissue engineering cases, the inclusion of pores in the final structure is often necessary to provide nutrient access for seeded cells. Pores can be created in variety of manners but are often


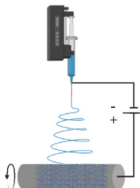
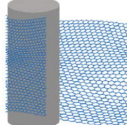

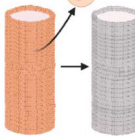
produced using a secondary material or porogen that can be removed through post-processing, leaving a pore in its place. Various porous scaffolds have been produced using ice templating (Boccaccini et al., 2005; Shin'oka et al., 2005; Nieponice et al., 2008; Ma et al., 2010; Zakhem et al., 2012; Chen et al., 2015; Roh et al., 2019). This process involves freezing a solution or mixture of water and the scaffold material, followed by sublimation of the ice, also called lyophilization, leaving pores in the resultant solid structure. Alternatively, pores can be produced by including orthogonally soluble solids in the casting solution. For example, salt can be included in solvent-cast polymeric solutions and then washed out with water after solvent evaporation (Mooney et al., 1995; Sin et al., 2010; Costello et al., 2014). This technique is only feasible for highly porous materials, because lower porosities will prevent access for porogen removal.

Casting is simple, convenient, and compatible with a wide range of materials, with examples showing the application of casting techniques for the production of complex models with stratified layers of cells (Figure 3). However, various factors can complicate the casting process, including the construction of larger objects, objects with inconsistent cross-sections, or objects with internal cavities. In these cases, mold design is particularly important. Inclusion of vents can ensure filling of the entire mold. However, releasing the resultant material from a mold can also be difficult, depending on the material. Regardless, complex shapes can be cast to generate useful, tissue-like structures (Wang et al., 2014). Another negative factor affecting casts, particularly solvent cast polymers and some porogen forming techniques, is the presence of remnant solvent or toxic porogens that can negatively affect cell growth. These issues can be avoided with proper handling and preparation of the cast. Seeding cells into cast tubes can also be difficult, as discussed above. Many studies seed cells into the lumen through pipetting. However, the scaffolds often need to be rotated (Opitz et al., 2004; Atchison et al., 2017, 2020) or subjected to another form of dynamic seeding (Godbey et al., 2004; Nieponice et al., 2008) to reach homogeneous seeding on the interior lining of the scaffold. Nevertheless, casting remains a commonly used mechanism for tubular scaffold production given its customizability and wide range of accessible materials. Further, the resultant tubular scaffolds are repeatably manufacturable, requiring no further steps for assembly after the initial cast. These factors make this technique widely applicable in the field of tubular tissue engineering and beyond.

Electrospinning

Electrospinning techniques involve the solubilization of a polymeric or biomolecular material, which is ejected from a syringe. During the electrospinning processes, the fluid is charged through an applied voltage and directed toward a neutral or oppositely charged mandrel. The solvent evaporates as the material travels toward the mandrel, creating nanofibers. For the formation of tubular scaffolds, the mandrel is typically rotated during the extrusion process. The resultant mesh of nanofibers can be removed from the mandrel, producing a mesh-tube (Rocco et al., 2014), with examples producing contiguous tubular structures that are compatible with cell-seeding (Figure 4). In many cases these meshes are combined with secondary electrospinning, deposition, or casting techniques to change

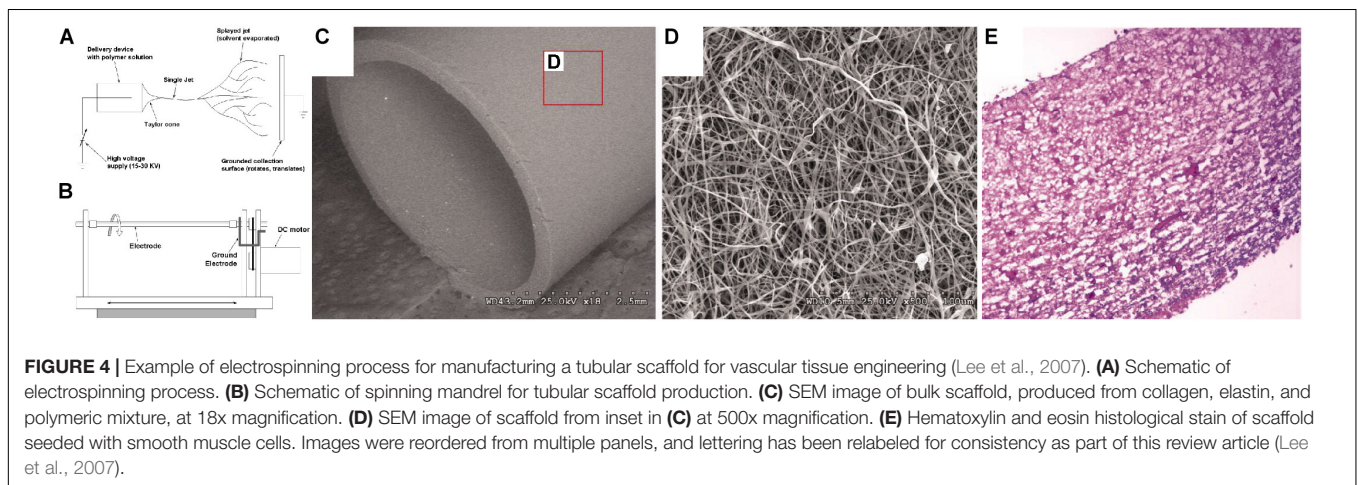
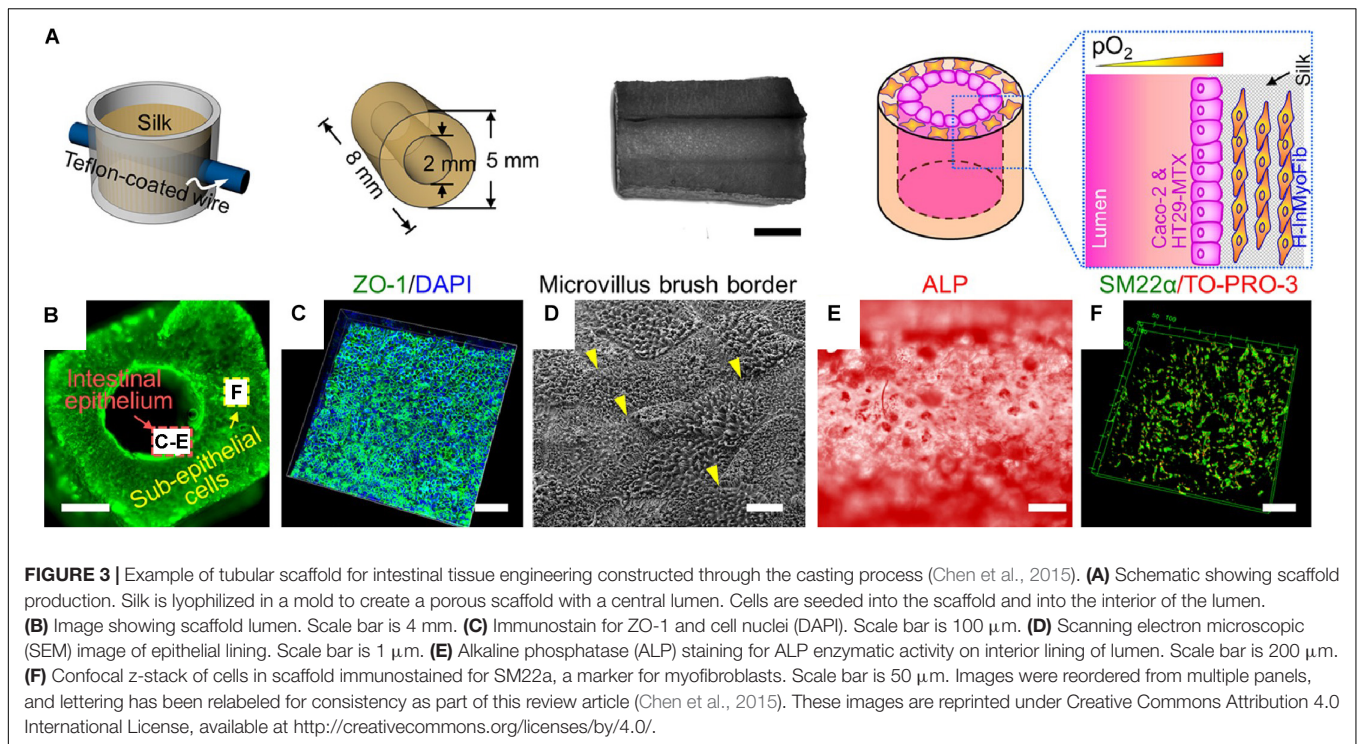
TABLE 3 | Categorization of techniques for manufacturing tubular scaffolds for tissue engineering.

Fabrication method	Advantages	Disadvantages	References
Casting 	<ul style="list-style-type: none"> Compatible with most material types Simple and easy to implement Applicable with cell-seeded materials 	<ul style="list-style-type: none"> Difficult to produce complex shapes Processing can result in toxic byproducts Secondary cell seeding method required 	Vasculature Seliktar et al., 2003; Matsuda, 2004; Opitz et al., 2004; Swartz et al., 2005; Liu et al., 2007; Nieponice et al., 2008; Ma et al., 2010; Wang et al., 2014; Guo et al., 2017; Atchison et al., 2017; Strobel et al., 2018b; Im et al., 2019 Intestine Yu et al., 2012; Zakhem et al., 2012; Chen et al., 2015; Zhou et al., 2018; Ladd et al., 2018, 2019; Roh et al., 2019 Trachea Naito et al., 2011 Vascular Boland et al., 2004; Lee et al., 2007; Smith et al., 2008; Wang et al., 2009; Han et al., 2011; Du et al., 2012; Zhang et al., 2013; Fu et al., 2014; Zhou et al., 2016; Ju et al., 2017; Strobel et al., 2018a; Rodriguez et al., 2019 Intestine Yoon and Kim, 2010; Knight et al., 2013 Trachea Hinderer et al., 2012; Mahoney et al., 2016; Wu et al., 2017; Best et al., 2018; Kang et al., 2019; O'Leary et al., 2020 Vascular Niklason et al., 2001; Shen et al., 2003; L'Heureux et al., 2006; Pricci et al., 2009; Konig et al., 2009; Gauvin et al., 2010; Rayatpisheh et al., 2014; Jung et al., 2015; Gui et al., 2016; Zhao et al., 2018; Wang et al., 2018 Intestine Grikscheit et al., 2002, 2004
Electrospinning 	<ul style="list-style-type: none"> High degree of control over scaffold properties (porosity, mechanics, etc.) Easily applied for tube formation Directly compatible with proteins 	<ul style="list-style-type: none"> Processing can result in toxic byproducts Secondary cell seeding method required Optimization necessary for experimental setup 	Vascular Boland et al., 2004; Lee et al., 2007; Smith et al., 2008; Wang et al., 2009; Han et al., 2011; Du et al., 2012; Zhang et al., 2013; Fu et al., 2014; Zhou et al., 2016; Ju et al., 2017; Strobel et al., 2018a; Rodriguez et al., 2019 Intestine Yoon and Kim, 2010; Knight et al., 2013 Trachea Hinderer et al., 2012; Mahoney et al., 2016; Wu et al., 2017; Best et al., 2018; Kang et al., 2019; O'Leary et al., 2020 Vascular Niklason et al., 2001; Shen et al., 2003; L'Heureux et al., 2006; Pricci et al., 2009; Konig et al., 2009; Gauvin et al., 2010; Rayatpisheh et al., 2014; Jung et al., 2015; Gui et al., 2016; Zhao et al., 2018; Wang et al., 2018 Intestine Grikscheit et al., 2002, 2004
Rolling 	<ul style="list-style-type: none"> Cells can be seeded in 2D and rolled into 3D tube Simple and easy to implement 	<ul style="list-style-type: none"> Production may require handling of cell-seeded scaffold Sealing of tube can be difficult 	Vascular Niklason et al., 2001; Shen et al., 2003; L'Heureux et al., 2006; Pricci et al., 2009; Konig et al., 2009; Gauvin et al., 2010; Rayatpisheh et al., 2014; Jung et al., 2015; Gui et al., 2016; Zhao et al., 2018; Wang et al., 2018 Intestine Grikscheit et al., 2002, 2004
3D Printing 	<ul style="list-style-type: none"> High degree of customization and control over scaffold production Compatible with most material types Applicable with cell-seeded materials 	<ul style="list-style-type: none"> Expensive equipment requires for production of scaffolds Optimization necessary for experimental setup Some printing techniques do not currently possess high resolution 	Vascular Melchiorri et al., 2016; Rabionet et al., 2018; Cui et al., 2019 Trachea Johnson et al., 2016; Gao et al., 2017; Taniguchi et al., 2018; Hsieh et al., 2018; Park et al., 2018; Park et al., 2019; Machino et al., 2019; Xia et al., 2019; Kang et al., 2019; Ahn et al., 2019; Gao et al., 2019
Decellularization 	<ul style="list-style-type: none"> Scaffold material is highly biocompatible Intrinsic biochemical factors can benefit production of tissue engineered model 	<ul style="list-style-type: none"> Secondary cell seeding method required Decellularized scaffold can contain biochemical factors that negatively affect production of tissue engineered model Extensive characterization and quality control are necessary 	Vascular McFetridge et al., 2007; Xi-Xun et al., 2008; Yang et al., 2009; Neff et al., 2011; Lee et al., 2012 Intestine Totonelli et al., 2012 Trachea Johnson et al., 2016; Butler et al., 2017; Ghorbani et al., 2017; Zhong et al., 2019; Batioglu-Karaaltin et al., 2019; Giraldo-Gomez et al., 2019; Wang et al., 2020

the properties and/or structure of the scaffold. The process of electrospinning, particularly for scaffold production, has been covered extensively in previous reviews (Pham et al., 2006; Rocco et al., 2014).

Electrospinning provides a high degree of control over the resultant “pore” size of the mesh and the mechanical properties of the fibers. This process is also compatible with numerous materials that are suitable for scaffold production (Figure 4). Most electrospun scaffolds have been produced using polymers,

or polymers mixed with ECM proteins (Vaz et al., 2005; Buttafoco et al., 2006; Lee et al., 2007; Smith et al., 2008; Wang et al., 2009; Yoon and Kim, 2010, 2011; Han et al., 2011; Du et al., 2012; Hinderer et al., 2012; Zhang et al., 2013; Knight et al., 2013; Fu et al., 2014; Ott et al., 2016; Mahoney et al., 2016; Zhou et al., 2016; Wu et al., 2017; Ju et al., 2017; Best et al., 2018; Strobel et al., 2018a; O'Leary et al., 2020). However, some scaffolds have purely utilized proteins (Boland et al., 2004). Electrospun scaffolds suffer from the same disadvantages as

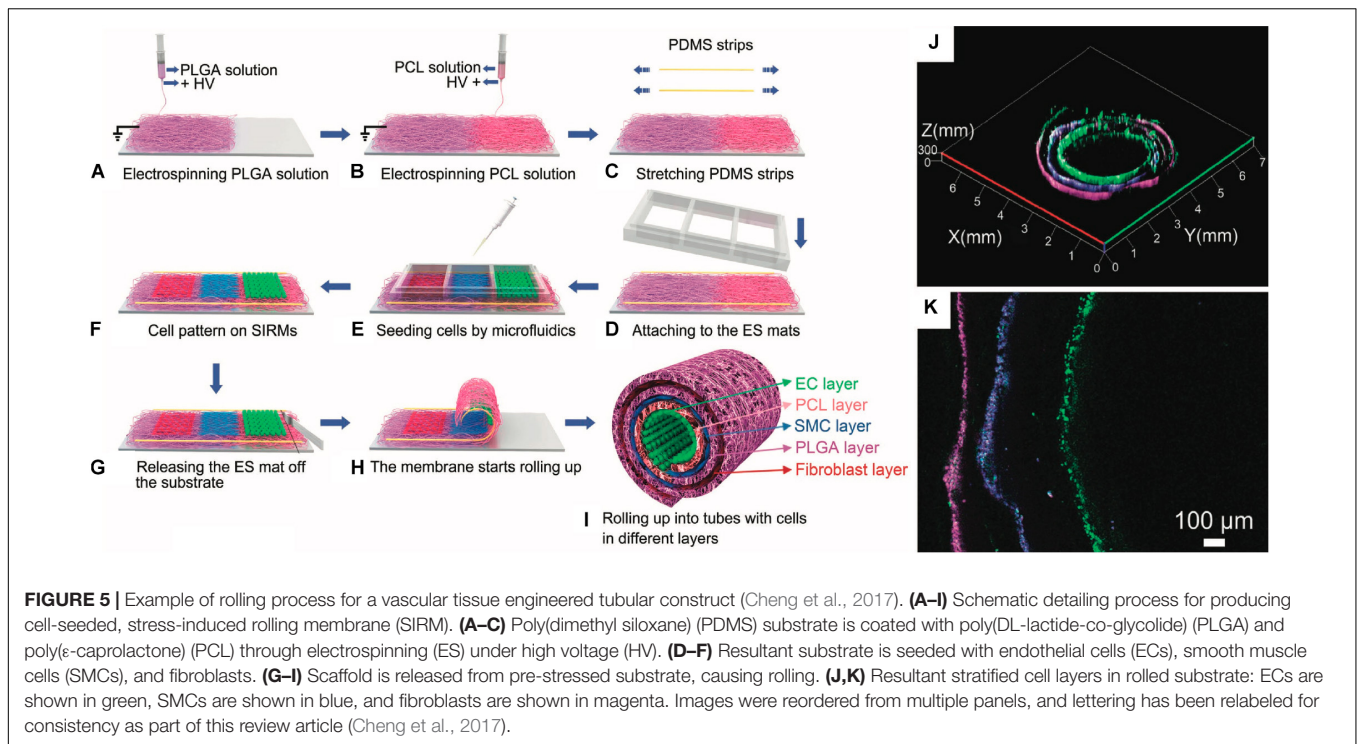


the cast scaffolds above, namely toxicity from remnant solvent and potential difficulties in homogeneous cell seeding. However, both of these criteria have been examined extensively. A similar technique to electrospinning, called gel spinning, has also been used for tubular scaffold production, where high viscosity gels are extruded onto a spinning mandrel (Lovett et al., 2008; Rodriguez et al., 2019). Generally, electrospinning and other similar techniques have been widely and successfully applied for the production of tubular scaffolds.

Rolling

Rolling mechanisms involve the rolling of a flat substrate into a tube. Rolling is usually accomplished using a mandrel to manually roll the substrate. However, some studies have

generated tubes with stratified cell layers using a self-assembly mechanism based on properties of the underlying substrate (**Figure 5**). Some of the earlier studies to produce tubular scaffolds for tissue engineering used rolling methodologies. Generally, these studies would produce a polymeric sheet and stitch the sheet into a tube (Niklason and Langer, 1997; Niklason et al., 1999; Niklason et al., 2001; Gui et al., 2011; 2016). Other studies developed the use of cell-derived ECM sheets that were rolled into tubes using a mandrel (L'Heureux et al., 1998, 2006; Pricci et al., 2009; König et al., 2009; Gauvin et al., 2010; Jung et al., 2015). This approach was particularly interesting in its use of only biological materials. In these studies, ECM-producing cells were grown to confluence. The resulting ECM sheet was then detached and rolled into a tube, where further



cells could be seeded. One study used an electrospun scaffold to assist in rolling a cell sheet into a tubular construct (Rayatpisheh et al., 2014). Other studies also focused on rolling polymeric sheets around a mandrel (Shen et al., 2003; Wang et al., 2016b, 2018). More recently, groups have developed self-assembling tubes. Self-assembly mechanisms or other rolling strategies that can be performed sterily have the major benefit of allowing for cell seeding prior to rolling. Rolling is initiated in these studies using either mechanically tensioned sheets bound (Cheng et al., 2017) or shape-memory polymers (Zhao et al., 2018). In either of these scenarios, cells can be homogeneously seeded and cultured in 2D and then rolled into a 3D tube (Figure 5). This strategy allows for the effective production of a confluent monolayer of epithelial cells on a structure easily compatible with typical cell culture techniques, while still ultimately producing a tubular tissue engineered structure. However, once the structure has been rolled, the sealing of the tube from the free edges of the rolled substrate needs to be addressed. Many strategies simply use multi-layered tubes, but this approach can potentially limit media access to the basal side of the seeded cells. Alternatively, tubes can be closed with stitching, as described above, or through use of a sealant to seal the free edges of the tube (Grikscheit et al., 2002, 2004). Rolling is perhaps the only manufacturing method that most specifically applies to tubular scaffold production, and, as such, has had significant impact on this field.

3D Printing

3D printing, also known as additive manufacturing or bioprinting in some tissue engineering cases, is the process of forming a 3D structure in a layer-by-layer manner. Printing processes typically involve extrusion of a material from a nozzle or

photo-crosslinking of an object from a liquid precursor. In extrusion-based 3D printing, a liquid material, similar to those used for casting approaches, is extruded from a nozzle onto a platform. The nozzle follows a fabrication path across the platform, generating a single layer of the ultimate desired shape. Once this layer has set, the nozzle ejects a second layer of material on top of the initial layer, thereby constructing a 3D object (Zhu et al., 2016). This type of 3D printing is compatible with most material types, including hydrogels and hydrogels containing live cellular populations. One study used polymeric scaffolds and cell-seeded hydrogels to produce layered structures containing multiple cell populations for construction of a tissue engineered trachea (Figure 6). For bioprinting applications, cell-seeded hydrogels or other cell-compatible, printable materials are often called bioinks. However, specialized printers can be required depending on the material. Another format of 3D printing involves the photo-crosslinking of a polymer precursor from a liquid bath. In these printers, the precursor is cross-linked and fused to a baseplate, which is moved in 3D as subsequent layers are crosslinked onto the initial layer, generating 3D structures in this manner. This type of printing is typically performed using a photo-initiated cross-linker, meaning that material choices are limited to those which can be constructed as such. Inkjet printing is also frequently used in biological applications, but this type of printing is not typically compatible with the creation of large, 3D scaffolds like those used for tissue engineering and, as such, will not be discussed here. Other novel types of printing are also being developed, which will undoubtedly apply to the production of tubular scaffolds. Various reviews have specifically focused on 3D printing for tissue engineering and the available methods (Wang et al., 2015; Zhu et al., 2016; Galliger et al., 2019).

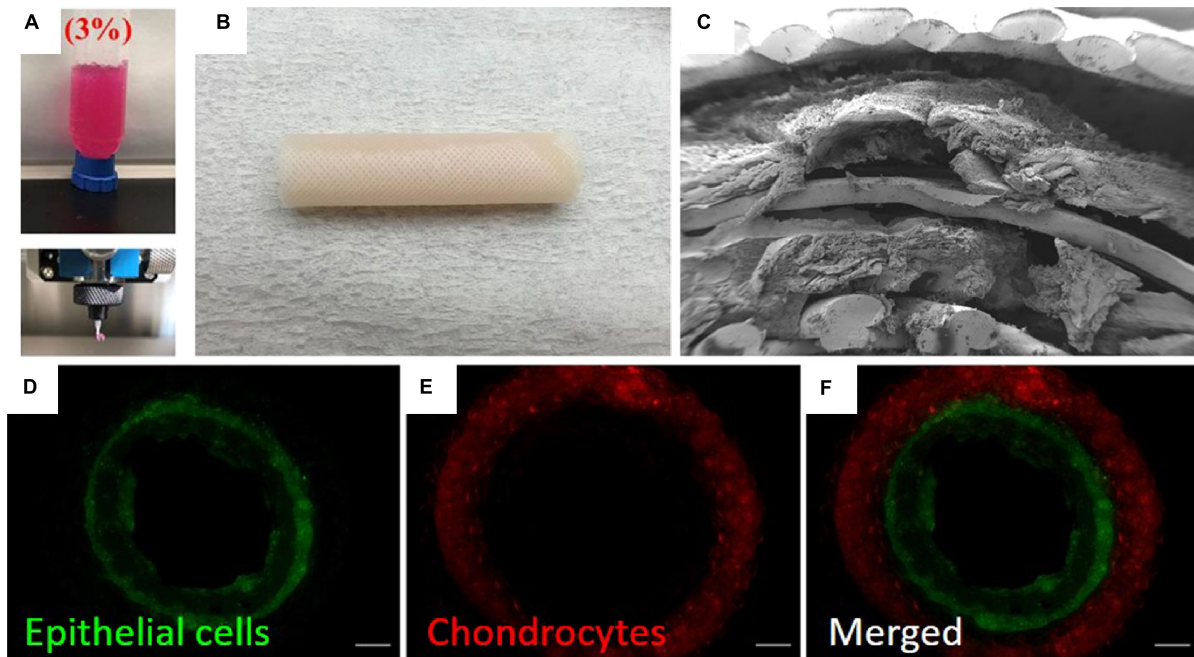


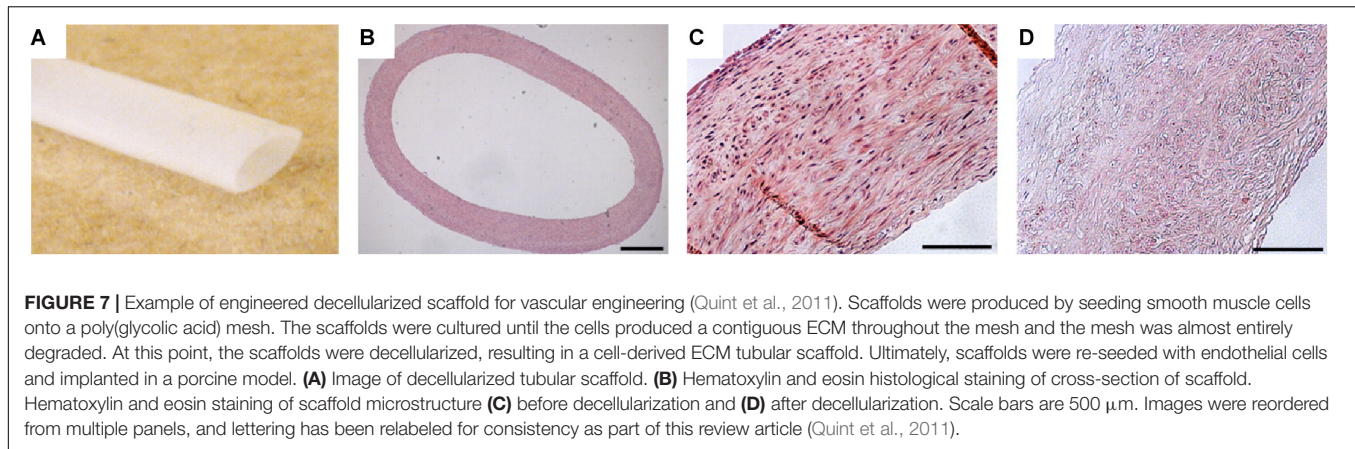
FIGURE 6 | Example of 3D printing process for construction of tissue engineered trachea (Park et al., 2019). **(A)** Image showing 3D printing of alginate into a cell-compatible hydrogel. **(B)** Image of 3D printed trachea. Scaffold consisted of 5 layers (innermost to outermost): gridded pattern of poly(caprolactone), alginate hydrogel containing primary nasal epithelial cells, cylindrical pattern of poly(caprolactone), alginate hydrogel containing primary auricular chondrocytes, gridded pattern of poly(caprolactone). **(C)** SEM image showing lamellar structure of scaffold. **(D–F)** Fluorescence microscopy images showing stratified cell layers in scaffold cross-section. Epithelial cells are shown in green, and chondrocytes are shown in red. Images were reordered from multiple panels, and lettering has been relabeled for consistency as part of this review article (Park et al., 2019). These images are reprinted under Creative Commons Attribution 4.0 International License, available at <http://creativecommons.org/licenses/by/4.0/>.

A major advantage to the 3D printing process is the potential for easily customizable scaffolds and, when using compatible printers, the potential print materials containing live cells (Park et al., 2019; Cui et al., 2019). Unlike casting, this type of bioprinting is more easily compatible with the generation of stratified layers of cells. However, the resolution of bioprinters is often limited due to the viscous properties of biomolecular pre-gel solutions. Studies have directly examined the optimization of these properties to enhance bioprinting efforts (Diamantides et al., 2019). Excluding bioprinting, other 3D printed scaffolds suffer from the same drawbacks in cell seeding as cast or electrospun scaffolds but can still produce functional tubular scaffolds (Melchiorri et al., 2016; Gao et al., 2017; Rabionet et al., 2018; Hsieh et al., 2018; Park et al., 2018; Xia et al., 2019). 3D printing methodologies are also compatible with other techniques discussed in this review. For example, one study focused on the construction of a 3D printed scaffold, which was then molded with a cell-laden hydrogel through casting (Gao et al., 2019). Another study used a combination of 3D printing and electrospinning techniques (Ahn et al., 2019). Studies are now increasingly focusing on the use of 3D printing to create vascular structures (Abaci et al., 2016; Lei et al., 2019), which could potentially be used to provide nutrients to larger structures, such as intestinal models. Recently, some studies have printed a trachea directly using spheroid cell cultures (Taniguchi et al., 2018; Machino et al., 2019). These studies and others demonstrate

the wide applicability and relevance of 3D printing in various areas of these fields.

Decellularization

Decellularization involves the production of a scaffold from native tissue. This field encompasses a wide variety of applications, from whole organ decellularization (Gilbert et al., 2006; Crapo et al., 2011) to decellularization of specific tissues and engineering of these structures for other uses (Lee et al., 2012; Boys et al., 2019). Generally, decellularization proceeds through the explanation of a native tissue and then treatment for the complete removal of cells from the tissue. For cell removal, the tissue is typically subjected to a series of washes with enzymes or detergents to lyse and remove the native population of cells. After removal, the resultant tissues are washed further or lyophilized to prepare the structure as a scaffold for tissue engineering (Gilbert et al., 2006). In tissue engineering applications, decellularized scaffolds may be used for allograft transplantation or implantation. However, the scaffold must also be re-seeded with an appropriate cellular population to recapitulate the desired tissue system *in vitro* (McPetridge et al., 2007; Xi-Xun et al., 2008; Yang et al., 2009; Neff et al., 2011; Zang et al., 2013; Bertanha et al., 2014). Recellularization is often accomplished through perfusion of the scaffold with a new cellular population. Decellularization methods are not reserved exclusively for mammalian tissues. Some studies have shown



viable cell attachment and growth on cellulose scaffolds derived from apples (Modulevsky et al., 2014).

Decellularization has multiple advantages. First, the scaffold will inherently consist of a highly biocompatible material, which can assist in tissue production and maturation of the scaffold, with studies showing that similar cellular populations can be effectively re-seeded onto decellularized scaffolds. Typically, these scaffolds are also of sufficient mechanical strength for the specified application, given their origin. The scaffolds will also likely contain matrix-bound growth factors and other biochemical cues that can influence cell behavior upon re-seeding (Zhou et al., 2020). Some studies have also tissue engineered cell sheets, decellularized these sheets, and then used them for re-seeding with a new cellular population (L'Heureux et al., 1998; Quint et al., 2011). This approach can produce entirely biologically derived scaffolds (Figure 7), with the particular advantage of potential usage of only autologous cells and components. Decellularization has been used jointly with many other methods for tubular scaffold production. One study wrapped a cell-seeded, electrospun scaffold around decellularized aorta fitted with a cast polymeric stent as mechanical support for tracheal tissue engineering application (Ghorbani et al., 2017).

Decellularized tissue will also usually maintain its native structure to some extent (Totonelli et al., 2012), which can be useful. However, the resultant properties of the decellularized tissue will likely be altered during the decellularization process (Partington et al., 2013). Decellularized tissues need to undergo significant characterization to ensure that the resulting scaffold can still be used in the desired application. Many studies have utilized decellularized tissues originating in regions differing from the ultimate region of application, i.e., use of decellularized amniotic membrane as a vascular scaffold (Lee et al., 2012). While this strategy may be very effective, the presence of matrix-bound growth factors that are not associated with the desired tissue can affect the behavior of the newly seeded cells. A major disadvantage to the use of decellularized scaffolds is sourcing the tissue for decellularization. Typically, researchers use xenografts, which can potentially initiate negative responses depending on the origin of the scaffold and re-seeded cells. Secondly, the use of tissue derived from organisms can induce high variability

between scaffolds. However, with proper quality control and analysis, decellularized scaffolds are a powerful tool in the tissue engineering of tubular systems.

Other Methods

Various other methods exist for modeling tubular systems. Most notable among these is the use of microfluidic systems. Microfluidic systems typically utilize 2D cell culture, which is compatible with epithelial cultures. As such, various advancements in our understanding of cellular mechanisms have been developed through microfluidics. These structures are generally not tubular or 3D, and we, therefore, have not included them in our review of available manufacturing mechanisms for tissue engineered scaffolds. However, microfluidic technologies for epithelial engineering have been extensively reviewed elsewhere (Wong et al., 2012; Ahadian et al., 2018).

STATE-OF-THE-ART FOR TUBULAR TISSUE ENGINEERING

Here, we discuss specific applications for the manufacturing techniques discussed above. As mentioned in the introduction, we will focus on tissue engineered vasculature, intestine, and trachea, particularly considering systems that have applications in drug testing and discovery.

Vascular Systems

Vasculature is one of the most commonly tissue engineered structures in the body. Various reviews have been specifically written about tissue engineering vasculature (Nerem and Seliktar, 2001; Stegemann et al., 2007; Song et al., 2018), with reviews even written specifically about using electrospinning for vascular tissue engineering (Rocco et al., 2014). Here, we seek to highlight some of the innovations in vascular tissue engineering from a tubular scaffold manufacturing standpoint in addition to discussing recent approaches.

Many tissue engineered vascular models rely on a population of smooth muscle cells to produce the relevant ECM on the scaffold support (Seliktar et al., 2003; McFetridge et al., 2007;

Lee et al., 2007; Nieponice et al., 2008; Zhang et al., 2013; Strobel et al., 2018a). However, some systems have also used fibroblasts, mesenchymal stem cells, or other stem-like progenitors for this purpose (Shin'oka et al., 2005; Vaz et al., 2005; Wang et al., 2009; Rayatpisheh et al., 2014; Bertanha et al., 2014; Jung et al., 2015; Gui et al., 2016; Rabionet et al., 2018; Strobel et al., 2018b). Much of the literature regarding vascular design is targeted at the ultimate use of the structure as an implant or vascular graft. This objective allows for the endothelialization of the structure *in vivo*. However, for benchtop models, endothelial cells must also be included. Some models have utilized only endothelial cells (Matsuda, 2004; Lovett et al., 2007; Xi-Xun et al., 2008; Zhang et al., 2013; Wang et al., 2014; Zhou et al., 2016; Zhao et al., 2018), but many of the more complex models involve a co-culture of endothelial cells with an ECM-depositing cell type (Niklason and Langer, 1997; L'Heureux et al., 1998; Niklason et al., 1999; Boland et al., 2004; Opitz et al., 2004; Swartz et al., 2005; L'Heureux et al., 2006; Lovett et al., 2008; Yang et al., 2009; Neff et al., 2011; Han et al., 2011; Cheng et al., 2017; Ju et al., 2017; Atchison et al., 2017; Cui et al., 2019; Atchison et al., 2020).

Given the layered structure of native blood vessels (Figure 1A), many models utilize an approach where the ECM-forming cell type is first seeded, followed by a secondary seeding step of endothelial cells. This seeding method is compatible with virtually any tubular scaffold construction. An earlier model for tissue engineered vasculature used a series of three layers to mimic native vascular structure. The basis for the scaffold was formed through a fibroblast-derived cell sheet that was rolled into a multi-layered tube. The layers fused together in culture before subsequent dehydration, resulting in decellularization, for further seeding. This support tubing was wrapped with a second, living sheet of fibroblasts followed by injection of endothelial cells into the lumen, at which point the vessel was subjected to fluid shear (L'Heureux et al., 2006). This model was not used as a benchtop system but was ultimately implanted into humans (L'Heureux et al., 2007), significantly driving the field of vascular tissue engineering forward. However, this technique, while generally successful, took an extended period of culture (~28 weeks) to produce the finalized vessel.

Various early studies solidified the usage of stratified cell layers in vascular tissue engineering, particularly with regard to different tubular scaffold construction methodologies. Some studies focused on the initial seeding of the scaffold with smooth muscle cells or fibroblasts (Boland et al., 2004; Yang et al., 2009; Neff et al., 2011). Other studies used cell-compatible injection molding techniques to create a tissue-like structure as the scaffold (Swartz et al., 2005; Liu et al., 2007). Some of these studies were able to demonstrate response of smooth muscle cells to vasoactive reagents, indicating the potential of these constructs for drug testing (Swartz et al., 2005; Liu et al., 2007). However, these particular studies produced structures that lacked an endothelium for these tests (Swartz et al., 2005; Liu et al., 2007), limiting similarity to native tissue. A more recent study used a rolling technique to produce the medial/adventitial regions of the blood vessel (Jung et al., 2015). Mesenchymal

stem cells were used to produce cell sheets, which were rolled into a tube with four concentric layers. These sheets fused together during culture in a bioreactor. The lumen was then seeded with a population of endothelial progenitor cells and cultured under flow conditions. Exposure of the vessels to a vasoconstrictor, phenylephrine, elicited a constrictive response by the cells. The vessels also dilated under increased flow. The study also examined the adhesion of monocyte-like cells under exposure of the vessel to TNF- α , an inflammatory cytokine. TNF- α can upregulate production of adhesion molecules on vascular walls to aid in leukocyte binding. Increased binding was observed for this system with exposure to TNF- α . However, the researchers did not analyze their structures for the formation of endothelial junctions (Jung et al., 2015).

Another study focused on the development of a bioink and a co-axial extrusion printer system to enable the direct printing of tubular structures containing cells (Cui et al., 2019). In this setup, the walls of the resultant vessel were constructed of crosslinked gelatin methacrylate, containing smooth muscle cells. The lumen was formed by extruding Pluronic F127, a bioinert polymer surfactant hydrogel which can be dissolved under certain conditions, containing endothelial cells. The structure was allowed to set before the Pluronic F127 layer was removed from the lumen. During the removal process, some of the endothelial cells adhered to the interior walls of the lumen, resulting in a gelatin methacrylate layer containing smooth muscle cells with an interior lining of endothelial cells, remnant after the lumen clearance. Vascular permeability was assessed on similar structures possessing a non-tubular geometry, finding that the endothelial layer showed decreased permeability. The structures were also subjected to a vasodilator, acetylcholine, and showed dilation upon exposure (Cui et al., 2019). A major benefit to structures produced in this manner, or similar manners, is the vast array of feasible shapes and channels that can be produced through 3D printing. Studies are increasingly focusing on the development of microvasculature (Wang et al., 2014; Abaci et al., 2016; Lei et al., 2019), which can provide more realistic environments in other models, such as the intestine.

Various models have also been produced to mimic and study specific disease states. Tissue engineered vasculature was developed to model Hutchinson-Gilford Progeria Syndrome (HGPS), which is associated with increased prevalence of cardiovascular disease and is associated with dysfunctional smooth muscle cells in vasculature (Atchison et al., 2017, 2020). This model was developed using induced pluripotent stem cells (iPSCs) and endothelial progenitor cells. The iPSCs were derived from healthy fibroblasts or fibroblasts an HGPS mutation, then differentiated toward smooth muscle cells. Tissue engineered vasculature was constructed by injecting collagen, containing smooth muscle cells, into a mold, following by gelation of the cell-seeded collagen. Endothelial progenitors were then perfused into the lumen for seeding (Atchison et al., 2017, 2020). The authors were able to observe differences in vasoactivity between healthy and diseased cells, as monitored by examining vasodilation and vasoconstriction using acetylcholine and phenylephrine, respectively (Atchison et al., 2020). This

study and others highlight the major potential for use of tissue engineered vasculature as a model for drug testing/discovery.

Intestinal Systems

Intestinal tissue engineering represents a particularly challenging field in the difficulty of producing a functional intestinal epithelium, given the numerous types of epithelial cells present in the native intestine. Further, the intestine has a complex 3D cross-section of villi and crypts, which also relates to the cellular distribution in the intestine (Santos et al., 2018). To reconstitute these structures, numerous studies have developed intestinal models using microfluidics or 2D cell culture substrates. However, these models do not fully mimic the complex native environment of the intestine (Bein et al., 2018). As such, 3D tissue engineered models have also been developed, which allow for the recapitulation of some of the aspects of the native intestine.

Some of the earlier tissue engineered models of the intestine were developed by rolling polymeric tubes and seeding these scaffolds with organoids derived from native murine colons. These structures were successfully transplanted into rats (Grikscheit et al., 2002). These structures were also used to treat induced short bowel syndrome in rats. The tissue engineered structures were beneficial for survival and gut function versus sham controls (Grikscheit et al., 2004). These studies indicated the possibility for the development of further tissue engineered benchtop models.

One model developed non-tubular 3D villus and crypt geometries using casting techniques (Yu et al., 2012). Scaffold construction was performed by casting collagen onto a negative of the villus-crypt structure. These structures were seeded with an enterocyte-like cell line (Caco-2 cells) and analyzed versus a flat system, i.e., without villi. The permeability of the cellularized structures was gauged using electrical measurements and permeation by two drugs, finding higher permeability coefficients in the 3D structures (Yu et al., 2012). This experimental design has since been used with various other materials, mainly porous polymeric structures, to monitor the effects of bacterial culture with enterocytes (Costello et al., 2014; Ladd et al., 2019) and has recently been formed into tubular structures for implantation (Ladd et al., 2018).

Perhaps one of the most complete tissue engineered tubular models was developed for the intestine, using a cellularized, stratified silk scaffold (Chen et al., 2015) with a bioreactor, designed to simulate gut motility (Zhou et al., 2018). A casting approach was used to generate tubular silk scaffolds (Figure 3). Primary intestinal myofibroblasts were seeded within collagen into the silk scaffold and the interior lumen was subsequently lined with a co-culture of an enterocyte-like cell line (Caco-2) and goblet-like cell line (HT29-MTX) by luminal injection. The resultant cultures showed mucus production and tight junctional formation throughout the epithelial cell layer. Further, an intraluminal oxygen gradient was detected (Chen et al., 2015). Iterations on this model have also included colonoid-derived epithelium (Chen et al., 2017) with monocyte cultures and examination for macrophage infiltration through the epithelium (Roh et al., 2019). A bioreactor was also developed and applied

to this system to provide pulsatile, peristaltic-like stimulation to these constructs (Zhou et al., 2018).

Many other non-tubular systems have also successfully modeled various aspects of the gastrointestinal tract. For example, an extensive bioreactor system was developed to simulate the microbial populations of the intestine (Van den Abbeele et al., 2012). A recently developed microfluidic model was also able to recapitulate the intestinal epithelium and associated microbial population with an adjacent vascular structure (Jalili-Firoozinezhad et al., 2019). This design resulted in the formation of a villus-crypt structure with polarized epithelial cells. This device also included sensors for monitoring oxygen content non-invasively, allowing for monitoring of oxygen gradients between the intestinal lumen and adjacent vascular lumen chambers (Jalili-Firoozinezhad et al., 2019). These types of devices are particularly useful as basic science platforms and can help inform the design of larger tubular systems. Currently, many of the tissue engineered intestinal models are focusing on the examination of the gut microbiome or immune components. As these models are developed further and our understanding of some of these aspects of intestinal biology improves, focus will likely shift to the testing of drugs in these tissue engineered systems.

Tracheal Systems

Unlike the *in vitro* models discussed for vasculature and the intestine, the outlook for tracheal tissue engineering to date largely concerns implantable scaffolds for tracheal replacement. In recent years, research has been targeted toward improving *in vitro* preparation methods such as optimizing decellularization through enzymatic, detergent (Zhong et al., 2019), vacuum-assisted (Butler et al., 2017), and chemical-based techniques (Batioglu-Karaaltin et al., 2019). For example, enhanced enzymatic approaches have drastically reduced tracheal decellularization time (Giraldo-Gomez et al., 2019; Wang et al., 2020). Importantly, the reduced preparation time had no adverse effects on tracheal ECM structure or biomechanical properties and evaded immunogenic or inflammatory responses when implanted *in vivo*. This result highlights the promise of advanced decellularization methods for production of tracheal implants. Despite success in these areas, decellularization methods require availability of human tracheal donors, and decellularized scaffolds can possess altered mechanical properties compared to native (Partington et al., 2013).

A major requirement for tracheal tissue engineering is sufficient mechanical support to resist pressurization. As such, many tissue engineered tracheal models have been created through combination of different manufacturing methods, incorporating a mechanical support structure with a cell-seedable scaffold. Tissue engineered trachea have been produced using a combination of 3D printing and decellularization methodologies (Johnson et al., 2016). This approach offers many advantages, including improved structural and mechanical support versus decellularized tissue alone, while maintaining biocompatibility and a native-like ECM. These hybrid 3D printed-decellularized scaffolds showed comparable resistance

to compression versus native tissue and higher resistance to compression versus a decellularized scaffold alone (Johnson et al., 2016). Scaffolds produced through combination of 3D printing and electrospinning also possessed sufficient mechanics (rotation angle, elastic modulus, elongation ratio, and tensile strength) for recapitulation of the trachea, while still demonstrating a high degree of cellular attachment (Ahn et al., 2019). Other studies have mimicked native tracheal structure by incorporating C-shaped rings onto 3D printed tubular designs, thusly producing similar mechanical profiles to *in vivo* (Ott et al., 2016; Best et al., 2018).

Other studies have looked to characterize biocompatibility and regenerative capabilities of tracheal grafts via transplantation into rabbit models. For example, 3D solvent-based casting techniques have been utilized to fabricate tubular scaffolds, which demonstrate vascularization and differentiation of ciliated, mucus producing tracheal epithelium 4 weeks post-implantation (Park et al., 2015). Similarly, 3D bioprinting of a tubular tracheal tissue, containing layers of PCL and autologous epithelial cells and chondrocytes (Figure 6), demonstrated complete regeneration of respiratory epithelium and long-term stability of tracheal function (Park et al., 2019). However, further studies are needed to assess possibility of adverse immune or inflammatory processes and to promote chondrocyte regeneration of cartilage for mechanical support. Additionally, sufficient luminal airflow and gas tightness is necessary (Hsieh et al., 2018) and fundamental to the success of tracheal implants when positioned at the native air-liquid interface.

In summary, many studies have shown the successful fabrication of layered, flexible and structurally supportive tubular tracheal models, with characterization and comparisons made *in vitro* using techniques such as high-resolution microscopy, immunofluorescence, histological staining, and mechanical testing. Although some studies have looked to address microbial properties and response to pathogen invasion (Kang et al., 2019), to date, most tissue engineered tracheal model systems focus on developing implantable scaffolds. The limited examples of models which address toxicology or drug testing may be associated with the difficulty of established a 3D air-liquid interface *in vitro*. Further, the use of high throughput microfluidic and 2D systems for drug stimulation and discovery is well-established in this field (Ahadian et al., 2018).

FUTURE PERSPECTIVES

The field of tissue engineering for tubular systems has undergone various innovative steps over the course of its history. However, tissue engineered models still do not fully resemble native tissue. This lack of resemblance is partially due to the numerous cell types that require representation. For example, few systems include neural and immune components, which are increasingly connected to tissue function and homeostasis (Veiga-Fernandes and Artis, 2018). Further, in intestinal tissue engineering, numerous cell types are necessary for making only the epithelium, which can drastically complicate culture setup. Further innovations in scaffold manufacturing have the potential

to solve these issues. Bioprinting can potentially place various cell types in a stratified manner, increasing the feasibility of producing cellularly complex systems. However, the cost of producing or purchasing a bioprinter capable of constructing such stratified structures is currently too high to be widely available. As such, innovations in the surrounding technologies, i.e., multi-nozzle systems, integrated culture capabilities, etc., can significantly increase feasibility. Other techniques involving tubular self-assembly can accomplish some of these tasks at lower cost. Researchers should also consider the production of modular systems for improving model complexity. Designing scaffolds that can be placed into a co-culture upon reaching maturity allows for a wider range of culture conditions and experiments without necessarily requiring expensive fabrication equipment.

Other factors complicating current efforts in tubular tissue engineering involve the application of native-like conditions to the resultant scaffolds. For example, while some studies have developed native-like culture conditions using bioreactors (Zhou et al., 2018), most studies rely on media conditions to produce tissue models. Many of the cells present in these systems are mechanoresponsive, as evidenced by the dynamic physiological conditions *in vivo*, indicating that further stimuli must be applied to reach native-like conditions *in vitro*. For this particular limitation, study designs must consider compatibility of the scaffold with a subsequent bioreactor system. Scaffolds can potentially be fabricated inside a bioreactor using many of the techniques above, such casting and printing. Alternatively scaffolds can be produced with dynamic material components, like piezoelectric materials, that can potentially provide mechanical stimuli to a scaffold using an inherent material property.

A final piece to consider for improving tubular scaffold efficacy is engineering of scaffold walls to generate multiple cellular microenvironments within a singular scaffold. For example, scaffolds can be produced to support formation of microvasculature (Chang and Niklason, 2017). Use of such a scaffold in an intestinal tissue engineering application can provide cells with nutrients through microvasculature channels, which can theoretically simplify bulk fluidic bioreactor designs. Similar concepts can be applied to tracheal tissue engineering, in designing scaffolds that can support cartilage formation, while simultaneously providing a face for epithelial formation. Many of the scaffold manufacturing techniques presented in this review have the potential for microstructural engineering within the scaffold bulk, and consideration of desired microenvironments when designing a fabrication process can have considerable benefits in the final results.

As tissue engineered tubular systems progress toward functional tissues, these systems can be used for drug testing and discovery. Many systems have already begun to show active responses to different drugs (Jung et al., 2015; Atchison et al., 2017, 2020). However, a major factor that is still lacking is the ability to monitor these systems in real-time. Most tissue engineered systems, particularly those with 3D structural features, require endpoint analysis. Studies typically use analytical techniques like immunostaining or blotting to determine the cellular response and activity in the tissue engineered system.

While these techniques are very useful and informative, they can also result in a lengthened study period, in that they will often require titration or larger sample numbers to reach sufficient statistical power for analysis.

Some studies have begun to integrate non-invasive techniques, like electrical measurements, that can be performed during culture. These techniques provide real-time data on the tissue engineered system that can be compared to typical endpoint analyses. For example, a common method for assessing epithelial barrier formation, with reference to drug or toxicology studies, is transepithelial electrical resistance (TEER) (Benson et al., 2013; Srinivasan et al., 2015). However, TEER apparatus are somewhat limited due to the rigid structure of electrode probes, which fails to conform to the complex architecture of advanced tissue engineered models. Other common means for monitoring tissue engineered tubular models include various material analyses, such as mechanical analysis, or biological analytical methods, such as histology and immunostaining. However, these methods are also more difficult to apply in tubular scaffolds due to their geometry, further complicating assessment in these tissue engineered systems. In answer to these limitations, some innovative solutions have been demonstrated including the use of an electroactive polymer scaffold, which can monitor real-time cell adhesion, growth, and migration during culture (Pitsalidis et al., 2018), with potential for a tubular setup for tissue engineering. Additionally, electrodes have been fabricated in organ-on-chip devices (Henry et al., 2017), microfluidics (Curto et al., 2017), and flexible polymer substrates (Ferro et al., 2019; Kalmykov et al., 2019) to monitor barrier integrity in complex cell cultures. These examples highlight the potential of flexible and microelectronic fabrication methods in monitoring complete barrier formation in future 3D tissue-engineered models. However, while measurements like TEER, are very common in 2D systems, these measurements have not yet been widely adapted to larger-scale 3D systems.

REFERENCES

- Abaci, H. E., Guo, Z., Coffman, A., Gillette, B., Lee, W., Sia, S. K., et al. (2016). Human skin constructs with spatially controlled vasculature using primary and iPSC-Derived endothelial cells. *Adv. Healthcare Mater.* 5, 1800–1807. doi: 10.1002/adhm.201500936
- Abbott, N. J., Rönnebeck, L., and Hansson, E. (2006). Astrocyte-Endothelial interactions at the blood-brain barrier. *Nat. Rev. Neurosci.* 7, 41–53. doi: 10.1038/nrn1824
- Ahadian, S., Civitarese, R., Bannerman, D., Mohammadi, M. H., Lu, R., Wang, E., et al. (2018). Organ-On-A-Chip platforms: a convergence of advanced materials, cells, and microscale technologies. *Adv. Healthcare Mater.* 7:1700506. doi: 10.1002/adhm.201700506
- Ahn, C. B., Son, K. H., Yu, Y. S., Kim, T. H., Lee, J. I., and Lee, J. W. (2019). Development of a flexible 3D printed scaffold with a cell-adhesive surface for artificial trachea. *Biomed. Mater.* 14:055001. doi: 10.1088/1748-605X/ab2a6c
- Akintewe, O. O., Roberts, E. G., Rim, N., Ferguson, M. A. H., and Wong, J. Y. (2017). Design approaches to myocardial and vascular tissue engineering. *Ann. Rev. Biomed. Eng.* 19, 389–414. doi: 10.1146/annurev-bioeng-071516-44641
- Asnaghi, M. A., Jungebluth, P., Raimondi, M. T., Dickinson, S. C., Rees, L. E. N., Go, T., et al. (2009). A double-chamber rotating bioreactor for the development of tissue-engineered hollow organs: from concept to clinical trial. *Biomaterials* 30, 5260–5269. doi: 10.1016/j.biomaterials.2009.07.018
- Atchison, L., Abutaleb, N. O., Snyder-Mounts, E., Gete, Y., Ladha, A., Ribar, T., et al. (2020). iPSC-Derived endothelial cells affect vascular function in a tissue-engineered blood vessel model of hutchinson-gilford progeria syndrome. *Stem Cell Rep.* 14, 325–337. doi: 10.1016/j.stemcr.2020.01.005
- Atchison, L., Zhang, H., Cao, K., and Truskey, G. A. (2017). A tissue engineered blood vessel model of hutchinson-gilford progeria syndrome using human iPSC-Derived smooth muscle cells. *Sci. Rep.* 7:8168. doi: 10.1038/s41598-017-08632-8634
- Batioglu-Karaaltin, A., Ovali, E., Karaaltin, M. V., Yener, M., Yilmaz, M., Eyüpoğlu, F., et al. (2019). Decellularization of trachea with combined techniques for tissue-engineered trachea transplantation. *Clin. Exp. Otorhinolaryngol.* 12, 86–94. doi: 10.21053/ceo.2018.00486
- Bein, A., Shin, W., Jalili-Firoozinezhad, S., Park, M. H., Sontheimer-Phelps, A., Tovaglieri, A., et al. (2018). Microfluidic organ-on-a-chip models of human intestine. *Cell. Mol. Gastroenterol. Hepatol.* 5, 659–668. doi: 10.1016/j.jcmgh.2017.12.010
- Benson, K., Cramer, S., and Galla, H. (2013). Impedance-Based cell monitoring: barrier properties and beyond. *Fluids Barr. CNS* 10:5. doi: 10.1186/2045-8118-10-15
- Bertanha, M., Moroz, A., Almeida, R., Alves, F. C., Valério, M. J. A., Moura, R., et al. (2014). Tissue-Engineered blood vessel substitute by reconstruction of endothelium using mesenchymal stem cells induced by platelet growth factors. *J. Vascular Surg.* 59, 1677–1685. doi: 10.1016/j.jvs.2013.05.032

Overall, we have discussed the various mechanisms by which tubular scaffolds can be constructed for tissue engineering. We divided the available manufacturing methodologies into five major categories: casting, electrospinning, rolling, 3D printing, and decellularization. Innovations for every one of these methodologies are still being generated today, with continuous new advancements in fabrication of scaffolds and tissue engineered systems. Methods like 3D printing and self-assembled rolling scaffolds allow for simultaneous advancements in ease of manufacturing and system complexity, driving toward tissue engineered systems that truly mimic native tissues. As these systems are developed, we will soon see their viable use in testing drug safety and efficacy in future biomedical studies.

AUTHOR CONTRIBUTIONS

AB, DT, and RO were responsible for design of the contents of the article, including the subject and general outline. AB and SB were responsible for the majority of the writing of the article. DT assisted in writing initial drafts of the article. SB and DT designed and produced the custom figures for the article. RO provided feedback and guidance for construction of the article. All authors have read the article, provided feedback, and given approval.

FUNDING

The authors wish to acknowledge funding from the European Research Council (ERC) under the European Union's Horizon 2020 Research and Innovation Program (Grant Agreement No. 723951) (AB and RO). The authors also wish to acknowledge funding by the Engineering and Physical Sciences Research Council Centre for Doctoral Training in Sensor Technologies and Applications (EP/L015889/1) (SB).

- Best, C. A., Pepper, V. K., Ohst, D., Bodnyk, K., Heuer, E., Onwuka, E. A., et al. (2018). Designing a tissue-engineered tracheal scaffold for preclinical evaluation. *Int. J. Pediatric Otorhinolaryngol.* 104, 155–160. doi: 10.1016/j.ijporl.2017.10.036
- Bitar, K. N., and Raghavan, S. (2012). Intestinal tissue engineering: current concepts and future vision of regenerative medicine in the gut. *Neurogastroenterol. Motil.* 24, 7–19. doi: 10.1111/j.1365-2982.2011.01843.x
- Boazak, E. M., and Auguste, D. T. (2018). Trachea mechanics for tissue engineering design. *ACS Biomater. Sci. Eng.* 4, 1272–1284. doi: 10.1021/acsbomaterials.7b00738
- Boccaccini, A. R., Blaker, J. J., Maquet, V., Day, R. M., and Jérôme, R. (2005). Preparation and characterisation of Poly(Lactide-Co-Glycolide) (PLGA) and PLGA/Bioglass® composite tubular foam scaffolds for tissue engineering applications. *Mater. Sci. Eng.: C* 25, 23–31. doi: 10.1016/j.msec.2004.03.002
- Bogan, S. L., Teoh, G. Z., and Birchall, M. A. (2016). Tissue engineered airways: a prospects article. *J. Cell. Biochem.* 117, 1497–1505. doi: 10.1002/jcb.25512
- Boland, E. D., Matthews, J. A., Pawlowski, K. J., Simpson, D. G., Wnek, G. E., and Bowlin, G. L. (2004). Electrospinning collagen and elastin: preliminary vascular tissue engineering. *Front. Biosci.* 9:1422–1432. doi: 10.2741/1313
- Boys, A. J., Zhou, H., Harrod, J. B., McCorry, M. C., Estroff, L. A., and Bonassar, L. J. (2019). Top-Down fabrication of spatially controlled mineral-gradient scaffolds for interfacial tissue engineering. *ACS Biomater. Sci. Eng.* 5, 2988–2997. doi: 10.1021/acsbomaterials.9b00176
- Brand-Saberi, B. E. M., and Schäfer, T. (2014). Trachea: anatomy and physiology. *Thorac. Surg. Clin.* 24, 1–5. doi: 10.1016/j.thorsurg.2013.09.004
- Butler, C. R., Hynds, R. E., Crowley, C., Gowers, K. H. C., Partington, L., Hamilton, N. J., et al. (2017). Vacuum-Assisted decellularization: an accelerated protocol to generate tissue-engineered human tracheal scaffolds. *Biomaterials* 124, 95–105. doi: 10.1016/j.biomaterials.2017.02.001
- Buttafoco, L., Kolkman, N. G., Engbers-Buijtenhuijs, P., Poot, A. A., Dijkstra, P. J., Vermes, I., et al. (2006). Electrospinning of collagen and elastin for tissue engineering applications. *Biomaterials* 27, 724–734. doi: 10.1016/j.biomaterials.2005.06.024
- Chang, W. G., and Niklason, L. E. (2017). A short discourse on vascular tissue engineering. *NPJ Regen. Med.* 2:7. doi: 10.1038/s41536-017-0011-16
- Chen, Y., Lin, Y., Davis, K. M., Wang, Q., Rnjak-Kovacina, J., Li, C., et al. (2015). Robust bioengineered 3D functional human intestinal epithelium. *Sci. Rep.* 5:13708. doi: 10.1038/srep13708
- Chen, Y., Zhou, W., Roh, T., Estes, M. K., and Kaplan, D. L. (2017). In vitro enteroid-derived three-dimensional tissue model of human small intestinal epithelium with innate immune responses. edited by shree ram singh. *PLoS One* 12:e0187880. doi: 10.1371/journal.pone.0187880
- Cheng, S., Jin, Y., Wang, N., Cao, F., Zhang, W., Bai, W., et al. (2017). Self-Adjusting, polymeric multilayered roll that can keep the shapes of the blood vessel scaffolds during biodegradation. *Adv. Mater.* 29:1700171. doi: 10.1002/adma.201700171
- Costello, C. M., Sorna, R. M., Goh, Y., Cengic, I., Jain, N. K., and March, J. C. (2014). 3-D intestinal scaffolds for evaluating the therapeutic potential of probiotics. *Mol. Pharmaceut.* 11, 2030–2039. doi: 10.1021/mp5001422
- Crapo, P. M., Gilbert, T. W., and Badylak, S. F. (2011). An overview of tissue and whole organ decellularization processes. *Biomaterials* 32, 3233–3243. doi: 10.1016/j.biomaterials.2011.01.057
- Cryan, J. F., O'Riordan, K. J., Cowan, C. S. M., Sandhu, K. V., Bastiaanssen, T. F. S., Boehme, M., et al. (2019). The microbiota-gut-brain axis. *Physiol. Rev.* 99, 1877–2013. doi: 10.1152/physrev.00018.2018
- Cui, H., Zhu, W., Huang, Y., Yu, Z., Nowicki, M., et al. (2019). In vitro and in vivo evaluation of 3d bioprinted small-diameter vasculature with smooth muscle and endothelium. *Biofabrication* 12:015004. doi: 10.1088/1758-5090/ab402c
- Curto, V. F., Marchiori, B., Hama, A., Pappa, A. M., Ferro, M. P., Braendlein, M., et al. (2017). Organic transistor platform with integrated microfluidics for in-line multi-parametric in vitro cell monitoring. *Microsystems Nanoeng.* 3:17028. doi: 10.1038/micronano.2017.28
- de Souza Carvalho, C., Daum, N., and Lehr, C. (2014). Carrier interactions with the biological barriers of the lung: advanced in vitro models and challenges for pulmonary drug delivery. *Adv. Drug Delivery Rev.* 75, 129–140. doi: 10.1016/j.addr.2014.05.014
- Diamantides, N., Dugopolski, C., Blahut, E., Kennedy, S., and Bonassar, L. J. (2019). High density cell seeding affects the rheology and printability of collagen bioinks. *Biofabrication* 11:045016. doi: 10.1088/1758-5090/ab3524
- Dosh, R. H., Jordan-Mahy, N., Sammon, C., and Le Maitre, C. L. (2019). Long-Term in vitro 3d hydrogel co-culture model of inflammatory bowel disease. *Sci. Rep.* 9:1812. doi: 10.1038/s41598-019-38524-38528
- Du, F., Wang, H., Zhao, W., Li, D., Kong, D., Yang, J., et al. (2012). Gradient nanofibrous chitosan/poly ϵ -Caprolactone scaffolds as extracellular microenvironments for vascular tissue engineering. *Biomaterials* 33, 762–770. doi: 10.1016/j.biomaterials.2011.10.037
- Etienne, H., Fabre, D., Caro, A. G., Kolb, F., Mussot, S., Mercier, O., et al. (2018). Tracheal replacement. *Eur. Respiratory J.* 51:1702211. doi: 10.1183/13993003.02211-2017
- Ferro, M. P., Leclerc, L., Sleiman, M., Marchiori, B., Pourchez, J., Owens, R. M., et al. (2019). Effect of E cigarette emissions on tracheal cells monitored at the air-liquid interface using an organic electrochemical transistor. *Adv. Biosystems* 3:1800249. doi: 10.1002/adb.201800249
- Fu, W., Liu, Z., Feng, B., Hu, R., He, X., Wang, H., et al. (2014). Electrospun Gelatin/PCL and Collagen/PLCL scaffolds for vascular tissue engineering. *Int. J. Nanomed.* 9, 2335–2344. doi: 10.2147/IJN.S61375
- Furness, J. B. (2012). The enteric nervous system and neurogastroenterology. *Nat. Rev. Gastroenterol. Hepatol.* 9, 286–294. doi: 10.1038/nrgastro.2012.32
- Galie, P. A., Nguyen, D.-H. T., Choi, C. K., Cohen, D. M., Janmey, P. A., and Chen, C. S. (2014). Fluid shear stress threshold regulates angiogenic sprouting. *Proc. Natl. Acad. Sci. U S A* 111, 7968–7973. doi: 10.1073/pnas.1310842111
- Galliger, Z., Vogt, C. D., and Panoskaltis-Mortary, A. (2019). 3D Bioprinting for lungs and hollow organs. *Transl. Res.* 211, 19–34. doi: 10.1016/j.trsl.2019.05.001
- Gao, B., Jing, H., Gao, M., Wang, S., Fu, W., Zhang, X., et al. (2019). Long-Segmental tracheal reconstruction in rabbits with pedicled tissue-engineered trachea based on a 3d-printed scaffold. *Acta Biomater.* 97, 177–186. doi: 10.1016/j.actbio.2019.07.043
- Gao, M., Zhang, H., Dong, W., Bai, J., Gao, B., Xia, D., et al. (2017). Tissue-Engineered trachea from a 3D-Printed scaffold enhances whole-segment tracheal repair. *Sci. Rep.* 7:5246. doi: 10.1038/s41598-017-05518-5513
- Gauvin, R., Ahsan, T., Larouche, D., Lévesque, P., Dubé, J., Auger, F. A., et al. (2010). A novel single-step self-assembly approach for the fabrication of tissue-engineered vascular constructs. *Tissue Eng. Part A* 16, 1737–1747. doi: 10.1089/ten.tea.2009.0313
- Ghorbani, F., Moradi, L., Shadmehr, M. B., Bonakdar, S., Droodinia, A., and Safshekan, F. (2017). In-Vivo characterization of a 3D hybrid scaffold based on pcl/decellularized aorta for tracheal tissue engineering. *Mater. Sci. Eng. C* 81, 74–83. doi: 10.1016/j.msec.2017.04.150
- Gilbert, T. W., Sellaro, T. L., and Badylak, S. F. (2006). Decellularization of Tissues and organs. *Biomaterials* 27, 3675–3683. doi: 10.1016/j.biomaterials.2006.02.014
- Giraldo-Gomez, D. M., García-López, S. J., Tamay-de-Dios, L., Sánchez-Sánchez, R., Villalba-Caloca, J., Sotres-Vega, A., et al. (2019). Fast cyclical-decellularized trachea as a natural 3d scaffold for organ engineering. *Mater. Sci. Eng. C* 105:110142. doi: 10.1016/j.msec.2019.110142
- Godbey, W. T., Hindy, B. S. S., Sherman, M. E., and Atala, A. (2004). A novel use of centrifugal force for cell seeding into porous scaffolds. *Biomaterials* 25, 2799–2805. doi: 10.1016/j.biomaterials.2003.09.056
- Grikscheit, T. C., Ogilvie, J. B., Ochoa, E. R., Alsberg, E., Mooney, D., and Vacanti, J. P. (2002). Tissue-Engineered colon exhibits function in vivo. *Surgery* 132, 200–204. doi: 10.1067/msy.2002.125310
- Grikscheit, T. C., Siddique, A., Ochoa, E. R., Srinivasan, A., Alsberg, E., Hodin, R. A., et al. (2004). Tissue-Engineered small intestine improves recovery after massive small bowel resection. *Ann. Surg.* 240:748–754. doi: 10.1097/01.sla.0000143246.07277.73
- Gui, L., Dash, B. C., Luo, J., Qin, L., Zhao, L., Yamamoto, K., et al. (2016). Implantable tissue-engineered blood vessels from human induced pluripotent stem cells. *Biomaterials* 102, 120–129. doi: 10.1016/j.biomaterials.2016.06.010
- Gui, L., Zhao, L., Spencer, R. W., Burghouwt, A., Taylor, M. S., Shalaby, S. W., et al. (2011). Development of novel biodegradable polymer scaffolds for vascular tissue engineering. *Tissue Eng. Part A* 17, 1191–1200. doi: 10.1089/ten.tea.2010.0508
- Guo, Z., Grijpma, D. W., and Poot, A. A. (2017). Preparation and characterization of flexible and elastic porous tubular PTMC scaffolds for vascular tissue

- engineering: porous tubular PTMC scaffolds for vascular tissue engineering. *Pol. Adv. Technol.* 28, 1239–1244. doi: 10.1002/pat.3954
- Han, J., Lazarovici, P., Pomerantz, C., Chen, X., Wei, Y., and Lelkes, P. I. (2011). Co-Electrospun blends of PLGA, gelatin, and elastin as potential nonthrombogenic scaffolds for vascular tissue engineering. *Biomacromolecules* 12, 399–408. doi: 10.1021/bm101149r
- Haykal, S., Salna, M., Zhou, Y., Marcus, P., Fatehi, M., Frost, G., et al. (2014). Double-Chamber rotating bioreactor for dynamic perfusion cell seeding of large-segment tracheal allografts: comparison to conventional static methods. *Tissue Eng. Part C: Methods* 20, 681–692. doi: 10.1089/ten.tec.2013.0627
- Hendow, E. K., Guhmann, P., Wright, B., Sofokleous, P., Parmar, N., and Day, R. M. (2016). Biomaterials for hollow organ tissue engineering. *Fibrogenesis Tissue Repair* 9:3. doi: 10.1186/s13069-016-0040-46
- Henry, O. Y. F., Villenave, R., Cronic, M. J., Leineweber, W. D., Benz, M. A., and Ingber, D. J. (2017). Organs-on-Chips with Integrated Electrodes for Trans-Epithelial Electrical Resistance (TEER) measurements of human epithelial barrier function. *Lab Chip* 17, 2264–2271. doi: 10.1039/C7LC00155J
- Hinderer, S., Schesny, M., Bayrak, A., Ibold, B., Hampel, M., Walles, T., et al. (2012). Engineering of fibrillar decorin matrices for a tissue-engineered trachea. *Biomaterials* 33, 5259–5266. doi: 10.1016/j.biomaterials.2012.03.075
- Hsieh, C., Liao, C., Dai, N., Tseng, C., Yen, B. L., and Hsu, S. (2018). 3D printing of tubular scaffolds with elasticity and complex structure from multiple waterborne polyurethanes for tracheal tissue engineering. *Appl. Mater. Today* 12, 330–341. doi: 10.1016/j.apmt.2018.06.004
- Iannucci, L. E., Boys, A. J., McCorry, M. C., Estroff, L. A., and Bonassar, L. J. (2019). Cellular and chemical gradients to engineer the meniscus-to-bone insertion. *Adv. Healthcare Mater.* 8:1800806. doi: 10.1002/adhm.201800806
- Im, S. H., Park, S. J., Chung, J. J., Jung, Y., and Kim, S. H. (2019). Creation of poly(lactide) vascular scaffolds with high compressive strength using a novel melt-tube drawing method. *Polymer* 166, 130–137. doi: 10.1016/j.polymer.2019.01.067
- Jalili-Firoozinezhad, S., Gazzaniga, F. S., Calamari, E. L., Camacho, D. M., Fadel, C. W., Bein, A., et al. (2019). A complex human gut microbiome cultured in an anaerobic intestine-on-a-chip. *Nat. Biomed. Eng.* 3, 520–531. doi: 10.1038/s41551-019-0397-390
- James, B. D., and Allen, J. B. (2018). Vascular endothelial cell behavior in complex mechanical microenvironments. *ACS Biomater. Sci. Eng.* 4, 3818–3842. doi: 10.1021/acsbomaterials.8b00628
- Johnson, C., Sheshadri, P., Ketchum, J. M., Narayanan, L. K., Weinberger, P. M., and Shirwaiker, R. A. (2016). In vitro characterization of design and compressive properties of 3d-biofabricated/decellularized hybrid grafts for tracheal tissue engineering. *J. Mech. Behav. Biomed. Mater.* 59, 572–585. doi: 10.1016/j.jmbm.2016.03.024
- Ju, Y. M., Ahn, H., Arenas-Herrera, J., Kim, C., Abolbashari, M., Atala, A., et al. (2017). Electrospun vascular scaffold for cellularized small diameter blood vessels: a preclinical large animal study. *Acta Biomater.* 59, 58–67. doi: 10.1016/j.actbio.2017.06.027
- Jung, Y., Ji, H., Chen, Z., Chan, H. F., Atchison, L., Klitzman, B., et al. (2015). Scaffold-Free, human mesenchymal stem cell-based tissue engineered blood vessels. *Sci. Rep.* 5:15116. doi: 10.1038/srep15116
- Kalmykov, A., Huang, C., Bliley, J., Shiwerski, D., Tashman, J., Abdullah, A., et al. (2019). Organ-on-e-Chip: three-dimensional self-rolled biosensor array for electrical interrogations of human electrogenic spheroids. *Sci. Adv.* 5:eaax0729. doi: 10.1126/sciadv.aax0729
- Kang, Y., Wang, C., Qiao, Y., Gu, J., Zhang, H., Peijs, T., et al. (2019). Tissue-Engineered trachea consisting of electrospun patterned Sc-PLA/GO- g -IL fibrous membranes with antibacterial property and 3d-printed skeletons with elasticity. *Biomacromolecules* 20, 1765–1776. doi: 10.1021/acs.biomac.9b00160
- Klarhöfer, M., Csapo, B., Balassy, C., Szeles, J. C., and Moser, E. (2001). High-Resolution blood flow velocity measurements in the human finger: blood flow velocities in the human finger. *Magnet. Resonance Med.* 45, 716–719. doi: 10.1002/mrm.1096
- Knight, T., Basu, J., Rivera, E. A., Spencer, T., Jain, D., and Payne, R. (2013). Fabrication of a multi-layer three-dimensional scaffold with controlled porous micro-architecture for application in small intestine tissue engineering. *Cell Adhesion Migrat.* 7, 267–274. doi: 10.4161/cam.24351
- König, G., McAllister, T. N., Dusserre, N., Garrido, S. A., Iyican, C., Marini, A., et al. (2009). Mechanical properties of completely autologous human tissue engineered blood vessels compared to human saphenous vein and mammary artery. *Biomaterials* 30, 1542–1550. doi: 10.1016/j.biomaterials.2008.11.011
- Kreimendahl, F., Ossenbrink, S., Köpf, M., Westhofen, M., Schmitz-Rode, T., Fischer, H., et al. (2019). Combination of vascularization and cilia formation for three-dimensional airway tissue engineering. *J. Biomed. Mater. Res. Part A* 107, 2053–2062. doi: 10.1002/jbm.a.36718
- Kuriyama, K., Gamsu, G., Stern, R. G., Cann, C. E., Herfkens, R. J., and Brundage, B. H. (1984). CT-Determined pulmonary artery diameters in predicting pulmonary hypertension. *Invest. Radiol.* 19, 16–22.
- Ladd, M. R., Costello, C. M., Gosztyla, C., Werts, A. D., Johnson, B., Fulton, W. B., et al. (2019). Development of intestinal scaffolds that mimic native mammalian intestinal tissue. *Tissue Eng. Part A* 25, 1225–1241. doi: 10.1089/ten.tea.2018.0239
- Ladd, M. R., Martin, L. Y., Werts, A., Costello, C., Sodhi, C. P., Fulton, W. B., et al. (2018). The development of newborn porcine models for evaluation of tissue-engineered small intestine. *Tissue Eng. Part C: Methods* 24, 331–345. doi: 10.1089/ten.tec.2018.0040
- Law, J. X., Liao, L. L., Aminuddin, B. S., and Ruszymah, B. H. I. (2016). Tissue-Engineered trachea: a review. *Int. J. Pediatric Otorhinolaryngol.* 91, 55–63. doi: 10.1016/j.ijporl.2016.10.012
- Lee, P., Tsai, S., Kuo, L., Hwang, C., Kuo, C., Yang, V. C., et al. (2012). A prototype tissue engineered blood vessel using amniotic membrane as scaffold. *Acta Biomater.* 8, 3342–3348. doi: 10.1016/j.actbio.2012.05.012
- Lee, S. J., Yoo, J. J., Lim, G. J., Atala, A., and Stitzel, J. (2007). In vitro evaluation of electrospun nanofiber scaffolds for vascular graft application. *J. Biomed. Mater. Res. Part A* 83A, 999–1008. doi: 10.1002/jbm.a.31287
- Lei, D., Yang, Y., Liu, Z., Yang, B., Gong, W., Chen, S., et al. (2019). 3D printing of biomimetic vasculature for tissue regeneration. *Mater. Horizons* 6, 1197–1206. doi: 10.1039/C9MH00174C
- L'Heureux, N., Dusserre, N., König, G., Victor, B., Keire, P., Wight, T. N., et al. (2006). Human tissue-engineered blood vessels for adult arterial revascularization. *Nat. Med.* 12, 361–365. doi: 10.1038/nm1364
- L'Heureux, N., McAllister, T. N., and de la Fuente, L. M. (2007). Tissue-Engineered blood vessel for adult arterial revascularization. *N. E. J. Med.* 357, 1451–1453. doi: 10.1056/NEJMc071536
- L'Heureux, N., Pâquet, S., Labbé, R., Germain, L., and Auger, F. A. (1998). A completely biological tissue-engineered human blood vessel. *FASEB J.* 12, 47–56. doi: 10.1096/psb2fasebj.12.1.47
- Lin, C., Hsu, S., Huang, C., Cheng, W., et al. (2009). A scaffold-bioreactor system for a tissue-engineered trachea. *Biomaterials* 30, 4117–4126. doi: 10.1016/j.biomaterials.2009.04.028
- Liu, J., Swartz, D., Peng, H., Gugino, S., Russell, J., and Andreadis, S. (2007). Functional tissue-engineered blood vessels from bone marrow progenitor cells. *Cardiovascular Res.* 75, 618–628. doi: 10.1016/j.cardiores.2007.04.018
- Liu, Y., Lu, J., Li, H., Wei, J., and Li, X. (2015). Engineering blood vessels through micropatterned co-culture of vascular endothelial and smooth muscle cells on bilayered electrospun fibrous mats with PDNA inoculation. *Acta Biomater.* 11, 114–125. doi: 10.1016/j.actbio.2014.10.004
- Lovett, M., Cannizzaro, C., Daheron, L., Messmer, B., Vunjak-Novakovic, G., and Kaplan, D. L. (2007). Silk fibroin microtubes for blood vessel engineering. *Biomaterials* 28, 5271–5279. doi: 10.1016/j.biomaterials.2007.08.008
- Lovett, M. L., Cannizzaro, C. M., Vunjak-Novakovic, G., and Kaplan, D. L. (2008). Gel spinning of silk tubes for tissue engineering. *Biomaterials* 29, 4650–4657. doi: 10.1016/j.biomaterials.2008.08.025
- Ma, H., Hu, J., and Ma, P. X. (2010). Polymer scaffolds for small-diameter vascular tissue engineering. *Adv. Functional Mater.* 20, 2833–2841. doi: 10.1002/adfm.201000922
- Machino, R., Matsumoto, K., Taniguchi, D., Tsuchiya, T., Takeoka, Y., Taura, Y., et al. (2019). Replacement of rat tracheas by layered, trachea-like, scaffold-free structures of human cells using a bio-3d printing system. *Adv. Healthcare Mater.* 8:1800983. doi: 10.1002/adhm.201800983
- Mahoney, C., Conklin, D., Waterman, J., Sankar, J., and Bhattarai, N. (2016). Electrospun nanofibers of Poly(ϵ -Caprolactone)/Depolymerized chitosan for respiratory tissue engineering applications. *J. Biomater. Sci. Pol. Edit.* 27, 611–625. doi: 10.1080/09205063.2016.1144454
- Matsuda, T. (2004). Poly(N-Isopropylacrylamide)-Grafted gelatin as a thermoresponsive cell-adhesive, mold-releasable material for shape-engineered tissues. *J. Biomater. Sci. Pol. Edit.* 15, 947–955. doi: 10.1163/1568562041271101

- McPetridge, P. S., Abe, K., Horrocks, M., and Chaudhuri, J. B. (2007). Vascular tissue engineering: bioreactor design considerations for extended culture of primary human vascular smooth muscle cells. *ASAIO J.* 53, 623–630. doi: 10.1097/MAT.0b013e31812f3b7e
- Melchiorri, A. J., Hibino, N., Best, C. A., Yi, T., Lee, Y. U., Kraynak, C. A., et al. (2016). 3D-Printed biodegradable polymeric vascular grafts. *Adv. Healthcare Mater.* 5, 319–325. doi: 10.1002/adhm.201500725
- Modulevsky, D. J., Lefebvre, C., Haase, K., Al-Rekabi, Z., and Pelling, A. E. (2014). Apple derived cellulose scaffolds for 3d mammalian cell culture. Edited by Irina Kerkis. *PLoS One* 9, e97835. doi: 10.1371/journal.pone.0097835
- Mooney, D. J., Breuer, C., McNamara, K., Vacanti, J. P., and Langer, R. (1995). Fabricating tubular devices from polymers of lactic and glycolic acid for tissue engineering. *Tissue Eng.* 1, 107–118. doi: 10.1089/ten.1995.1.107
- Naito, H., Tojo, T., Kimura, M., Dohi, Y., Zimmermann, W., Eschenhagen, T., et al. (2011). Engineering bioartificial tracheal tissue using hybrid fibroblast-mesenchymal stem cell cultures in collagen hydrogels. *Int. CardioVascular Thoracic Surg.* 12, 156–161. doi: 10.1510/icvts.2010.253559
- Neff, L. P., Tillman, B. W., Yazdani, S. K., Machingal, M. A., Yoo, J. J., Soker, S., et al. (2011). Vascular smooth muscle enhances functionality of tissue-engineered blood vessels in vivo. *J. Vascular Surg.* 53, 426–434. doi: 10.1016/j.jvs.2010.07.054
- Nerem, R. M., and Seliktar, D. (2001). Vascular tissue engineering. *Annu. Rev. Biomed. Eng.* 3, 225–243.
- Nieponce, A., Soletti, L., Guan, J., Deasy, B., Huard, J., Wagner, W., et al. (2008). Development of a tissue-engineered vascular graft combining a biodegradable scaffold, muscle-derived stem cells and a rotational vacuum seeding technique. *Biomaterials* 29, 825–833. doi: 10.1016/j.biomaterials.2007.10.044
- Niklason, L., and Langer, R. (1997). Advances in tissue engineering of blood vessels and other tissues. *Transplant Immunol.* 5, 303–306. doi: 10.1016/S0966-3274(97)80013-80015
- Niklason, L. E., Abbott, W., Gao, J., Klagges, B., Hirschi, K. K., Ulubayram, K., et al. (2001). Morphologic and mechanical characteristics of engineered bovine arteries. *J. Vascular Surg.* 33, 628–638. doi: 10.1067/mva.2001.111747
- Niklason, L. E., Gao, J., Abbott, W. M., Hirschi, K. K., Houser, S., Marini, R., et al. (1999). Functional arteries grown in vitro. *Science* 284, 489–493. doi: 10.1126/science.284.5413.489
- O'Leary, C., Soriano, L., Fagan-Murphy, A., Ivankovic, I., Cavanagh, B., O'Brien, F. J., et al. (2020). The fabrication and in vitro evaluation of retinoic acid-loaded electrospun composite biomaterials for tracheal tissue regeneration. *Front. Bioeng. Biotechnol.* 8:190. doi: 10.3389/fbioe.2020.00190
- Opitz, F., Schenke-Layland, K., Richter, W., Martin, D. P., Degenkolbe, I., Wahlers, T., et al. (2004). Tissue engineering of ovine aortic blood vessel substitutes using applied shear stress and enzymatically derived vascular smooth muscle cells. *Ann. Biomed. Eng.* 32, 212–222. doi: 10.1023/B:ABME.0000012741.85600.f1
- Ott, L. M., Zabel, T. A., Walker, N. K., Farris, A. L., Chakroff, J. T., Ohst, D. G., et al. (2016). Mechanical evaluation of gradient electrospun scaffolds with 3d printed ring reinforcements for tracheal defect repair. *Biomed. Mater.* 11:025020. doi: 10.1088/1748-6041/11/2/025020
- Park, J., Yoon, J., Lee, J. B., Shin, Y. M., Lee, K., Bae, S. et al. (2019). Experimental tracheal replacement using 3-dimensional bioprinted artificial trachea with autologous epithelial cells and chondrocytes. *Sci. Rep.* 9:2103. doi: 10.1038/s41598-019-38565-z
- Park, J. H., Park, J. Y., Nam, I., Ahn, M., Lee, J. Y., Choi, S. H., et al. (2018). A rational tissue engineering strategy based on three-dimensional (3d) printing for extensive circumferential tracheal reconstruction. *Biomaterials* 185, 276–283. doi: 10.1016/j.biomaterials.2018.09.031
- Park, J. H., Park, J. Y., Nam, I., Hwang, S., Kim, C., Jung, J. W., et al. (2015). Human turbinate mesenchymal stromal cell sheets with bellows graft for rapid tracheal epithelial regeneration. *Acta Biomater.* 25, 56–64. doi: 10.1016/j.actbio.2015.07.014
- Park-Windhol, C., and D'Amore, P. A. (2016). Disorders of vascular permeability. *Ann. Rev. Pathol. Mechan. Dis.* 11, 251–281. doi: 10.1146/annurev-pathol-012615-044506
- Partington, L., Mordan, N. J., Mason, C., Knowles, J. C., Kim, H., Lowdell, M. W., et al. (2013). Biochemical changes caused by decellularization may compromise mechanical integrity of tracheal scaffolds. *Acta Biomater.* 9, 5251–5261. doi: 10.1016/j.actbio.2012.10.004
- Pezzulo, A. A., Starner, T. D., Scheetz, T. E., Traver, G. L., Tilley, A. E., Harvey, B., et al. (2011). The air-liquid interface and use of primary cell cultures are important to recapitulate the transcriptional profile of in vivo airway epithelia. *Am. J. Physiology-Lung Cell. Mol. Physiol.* 300, L25–L31. doi: 10.1152/ajplung.00256.2010
- Pham, Q. P., Sharma, U., and Mikos, A. G. (2006). Electrospinning of polymeric nanofibers for tissue engineering applications: a review. *Tissue Eng.* 12, 1197–1211. doi: 10.1089/ten.2006.12.1197
- Pitsalidis, C., Ferro, M. P., Iandolo, D., Tzounis, L., Inal, S., and Owens, R. M. (2018). Transistor in a tube: a route to three-dimensional bioelectronics. *Sci. Adv.* 4:eat4253. doi: 10.1126/sciadv.aat4253
- Polacheck, W. J., Kutys, M. L., Yang, J., Eyckmans, J., Wu, Y., Vasavada, H., et al. (2017). A non-canonical notch complex regulates adherens junctions and vascular barrier function. *Nature* 552, 258–262. doi: 10.1038/nature24998
- Pricci, M., Bourget, J., Robitaille, H., Porro, C., Soletti, R., Mostefai, H. A., et al. (2009). Applications of human tissue-engineered blood vessel models to study the effects of shed membrane microparticles from T-Lymphocytes on vascular function. *Tissue Eng. Part A* 15, 137–145. doi: 10.1089/ten.tea.2007.0360
- Quint, C., Kondo, Y., Manson, R. J., Lawson, J. H., Dardik, A., and Niklason, L. E. (2011). Decellularized tissue-engineered blood vessel as an arterial conduit. *Proc. Natl. Acad. Sci.* 108, 9214–9219. doi: 10.1073/pnas.1019506108
- Rabionet, M., Guerra, A. J., Puig, T., and Ciurana, J. (2018). 3D-Printed tubular scaffolds for vascular tissue engineering. *Procedia CIRP* 68, 352–357. doi: 10.1016/j.procir.2017.12.094
- Rao, J. N., and Wang, J. Y. (2010). *Intestinal Architecture and Development. In Regulation of Gastrointestinal Mucosal Growth.* San Rafael, CA: Morgan & Claypool Life Sciences.
- Rayatpisheh, S., Heath, D. E., Shakouri, A., Rujitanaroj, P., Chew, S. Y., and Chan-Park, M. B. (2014). Combining cell sheet technology and electrospun scaffolding for engineered tubular, aligned, and contractile blood vessels. *Biomaterials* 35, 2713–2719. doi: 10.1016/j.biomaterials.2013.12.035
- Riva, C. E., Grunwald, J. E., Sinclair, S. H., and Petrig, B. L. (1985). Blood velocity and volumetric flow rate in human retinal vessels. *Invest. Ophthalmol. Visual Sci.* 26, 1124–1132.
- Rocco, K. A., Maxfield, M. W., Best, C. A., Dean, E. W., and Breuer, C. K. (2014). In vivo applications of electrospun tissue-engineered vascular grafts: a review. *Tissue Eng. Part B: Rev.* 20, 628–640. doi: 10.1089/ten.teb.2014.0123
- Rodriguez, M., Kluge, J. A., Smoot, D., Kluge, M. A., Schmidt, D. F., Paetsch, C. R., et al. (2019). Fabricating mechanically improved silk-based vascular grafts by solution control of the gel-spinning process. *Biomaterials* 230:119567. doi: 10.1016/j.biomaterials.2019.119567
- Roh, T. T., Chen, Y., Paul, H. T., Guo, C., and Kaplan, D. L. (2019). 3D bioengineered tissue model of the large intestine to study inflammatory bowel disease. *Biomaterials* 225:119517. doi: 10.1016/j.biomaterials.2019.119517
- Santos, A. J. M., Lo, Y., Mah, A. T., and Kuo, C. J. (2018). The intestinal stem cell niche: homeostasis and adaptations. *Trends Cell Biol.* 28, 1062–1078. doi: 10.1016/j.tcb.2018.08.001
- Seifu, D. G., Purnama, A., Mequanint, K., and Mantovani, D. (2013). Small-Diameter vascular tissue engineering. *Nat. Rev. Cardiol.* 10, 410–421. doi: 10.1038/nrcardio.2013.77
- Seliktar, D., Nerem, R. M., and Galis, Z. S. (2003). Mechanical strain-stimulated remodeling of tissue-engineered blood vessel constructs. *Tissue Eng.* 9, 657–666. doi: 10.1089/107632703768247359
- Shen, G., Tsung, H. C., Wu, C. F., Liu, X. Y., Wang, X., Liu, W., et al. (2003). Tissue engineering of blood vessels with endothelial cells differentiated from mouse embryonic stem cells. *Cell Res.* 13, 335–341. doi: 10.1038/sj.cr.7290178
- Shin'oka, T., Matsumura, G., Hibino, N., Naito, Y., Watanabe, M., Konuma, T., et al. (2005). Midterm clinical result of tissue-engineered vascular autografts seeded with autologous bone marrow cells. *J. Thoracic Cardiovascular Surg.* 129, 1330–1338. doi: 10.1016/j.jtcvs.2004.12.047
- Sieminski, A. L., and Gooch, K. J. (2000). Biomaterial–Microvasculature interactions. *Biomaterials* 21, 2233–2241. doi: 10.1016/S0142-9612(00)00149-146
- Sin, D., Miao, X., Liu, G., Wei, F., Chadwick, G., Yan, C., et al. (2010). Polyurethane (PU) scaffolds prepared by solvent casting/particulate leaching (scpl) combined with centrifugation. *Mater. Sci. Eng. C* 30, 78–85. doi: 10.1016/j.msec.2009.09.002

- Singh, A., Lee, D., Sopko, N., Matsui, H., Sabnekar, P., Liu, X. J., et al. (2017). Biomanufacturing seamless tubular and hollow collagen scaffolds with unique design features and biomechanical properties. *Adv. Healthcare Mater.* 6:1601136. doi: 10.1002/adhm.201601136
- Smith, M. J., McClure, M. J., Sell, S. A., Barnes, C. P., Walpoth, B. H., Simpson, D. G., et al. (2008). Suture-Reinforced electrospun polydioxanone-elastin small-diameter tubes for use in vascular tissue engineering: a feasibility study. *Acta Biomater.* 4, 58–66. doi: 10.1016/j.actbio.2007.08.001
- Song, H.-H. G., Rumma, R. T., Ozaki, C. K., Edelman, E. R., and Chen, C. S. (2018). Vascular tissue engineering: progress, challenges, and clinical promise. *Cell Stem Cell* 22, 340–354. doi: 10.1016/j.stem.2018.02.009
- Song, J. W., and Munn, L. L. (2011). Fluid forces control endothelial sprouting. *Proc. Natl. Acad. Sci.* 108, 15342–15347. doi: 10.1073/pnas.1105316108
- Srinivasan, B., Kolli, A. R., Esch, M. B., Abaci, H. E., Shuler, M. L., and Hickman, J. J. (2015). TEER measurement techniques for in vitro barrier model systems. *J. Lab. Automat.* 20, 107–126. doi: 10.1177/2211068214561025
- Stegemann, J. P., Kaszuba, S. N., and Rowe, S. L. (2007). Review: advances in vascular tissue engineering using protein-based biomaterials. *Tissue Eng.* 13, 2601–2613. doi: 10.1089/ten.2007.0196
- Strobel, H. A., Calamari, E. L., Beliveau, A., Jain, A., and Rolle, M. W. (2018a). Fabrication and characterization of electrospun polycaprolactone and gelatin composite cuffs for tissue engineered blood vessels. *J. Biomed. Mater. Res. Part B: Appl. Biomater.* 106, 817–826. doi: 10.1002/jbm.b.33871
- Strobel, H. A., Hookway, T. A., Piola, M., Fiore, G. B., Soncini, M., Alsberg, E., et al. (2018b). Assembly of tissue-engineered blood vessels with spatially controlled heterogeneities. *Tissue Eng. Part A* 24, 1492–1503. doi: 10.1089/ten.tea.2017.0492
- Suzuki, T. (2013). Regulation of intestinal epithelial permeability by tight junctions. *Cell. Mol. Life Sci.* 70, 631–659. doi: 10.1007/s00018-012-1070-x
- Swartz, D. D., Russell, J. A., and Andreadis, S. T. (2005). Engineering of fibrin-based functional and implantable small-diameter blood vessels. *Am. J. Physiol.-Heart Circulat. Physiol.* 288, H1451–H1460. doi: 10.1152/ajpheart.00479.2004
- Taniguchi, D., Matsumoto, K., Tsuchiya, T., Machino, R., Takeoka, Y., Elgalad, A., et al. (2018). Scaffold-Free trachea regeneration by tissue engineering with bio-3d printing. *Int. Cardiovascular Thoracic Surg.* 26, 745–752. doi: 10.1093/icvts/ivx444
- Totonelli, G., Maghsoudlou, P., Garriboli, M., Riegler, J., Orlando, G., Burns, A. J., et al. (2012). A rat decellularized small bowel scaffold that preserves villus-crypt architecture for intestinal regeneration. *Biomaterials* 33, 3401–3410. doi: 10.1016/j.biomaterials.2012.01.012
- Van den Abbeele, P., Roos, S., Eeckhaut, V., MacKenzie, D. A., Derde, M., Verstraete, W., et al. (2012). Incorporating a mucosal environment in a dynamic gut model results in a more representative colonization by lactobacilli: incorporating a mucosal environment in a gut model. *Microbial Biotechnol.* 5, 106–115. doi: 10.1111/j.1751-7915.2011.00308.x
- Vaz, C. M., van Tuijl, S., Bouten, C. V. C., and Baaijens, F. P. T. (2005). Design of scaffolds for blood vessel tissue engineering using a multi-layering electrospinning technique. *Acta Biomater.* 1, 575–582. doi: 10.1016/j.actbio.2005.06.006
- Veiga-Fernandes, H., and Artis, D. (2018). Neuronal-immune system cross-talk in homeostasis. *Science* 359, 1465–1466. doi: 10.1126/science.aap9598
- Wang, C., Baker, B. M., Chen, C. S., and Schwartz, M. A. (2013). Endothelial cell sensing of flow direction. *Art. Thrombosis Vascular Biol.* 33, 2130–2136. doi: 10.1161/ATVBAHA.113.301826
- Wang, K., Yeh, Y., Nguyen, P., Limquenco, E., Lopez, J., Thorossian, S., et al. (2016a). Flow-Dependent YAP/TAZ activities regulate endothelial phenotypes and atherosclerosis. *Proc. Natl. Acad. Sci. U S A* 113, 11525–11530. doi: 10.1073/pnas.1613121113
- Wang, N., Tang, L., Zheng, W., Peng, Y., Cheng, S., Lei, Y., et al. (2016b). A strategy for rapid and facile fabrication of controlled, layered blood vessel-like structures. *RSC Adv.* 6, 55054–55063. doi: 10.1039/C6RA12768A
- Wang, M. O., Vorwald, C. E., Dreher, M. L., Mott, E. J., Cheng, M., Cinar, A., et al. (2015). Evaluating 3D-Printed biomaterials as scaffolds for vascularized bone tissue engineering. *Adv. Mater.* 27, 138–144. doi: 10.1002/adma.201403943
- Wang, N., Peng, Y., Zheng, W., Tang, L., Cheng, S., Yang, J., et al. (2018). A strategy for rapid construction of blood vessel-like structures with complex cell alignments. *Macromol. Biosci.* 18:1700408. doi: 10.1002/mabi.20170408
- Wang, S., Zhang, Y., Yin, G., Wang, H., and Dong, Z. (2009). Electrospun polylactide/silk fibroin-gelatin composite tubular scaffolds for small-diameter tissue engineering blood vessels. *J. Appl. Pol. Sci.* 113, 2675–2682. doi: 10.1002/app.30346
- Wang, X., Jin, Z., Gan, B., Lv, S., Xie, M., and Huang, W. (2014). Engineering interconnected 3D vascular networks in hydrogels using molded sodium alginate lattice as the sacrificial template. *Lab Chip* 14, 2709–2716. doi: 10.1039/C4LC00069B
- Wang, Z., Sun, F., Lu, Y., Pan, S., Yang, W., Zhang, G., et al. (2020). Rapid preparation of decellularized trachea as a 3D scaffold for organ engineering. *Int. J. Art. Organs* doi: 10.1177/0391398820924041 Online ahead of print.
- Wong, K. H. K., Chan, J. M., Kamm, R. D., and Tien, J. (2012). Microfluidic models of vascular functions. *Ann. Rev. Biomed. Eng.* 14, 205–230. doi: 10.1146/annurev-bioeng-071811-150052
- Wu, T., Zheng, H., Chen, J., Wang, Y., Sun, B., Morsi, Y., et al. (2017). Application of a bilayer tubular scaffold based on electrospun Poly(l-Lactide-Co-Caprolactone)/Collagen fibers and yarns for tracheal tissue engineering. *J. Mater. Chem. B* 5, 139–150. doi: 10.1039/C6TB02484J
- Xia, D., Jin, D., Wang, Q., Gao, M., Zhang, J., Zhang, H., et al. (2019). Tissue-engineered trachea from a 3d-printed scaffold enhances whole-segment tracheal repair in a goat model. *J. Tissue Eng. Regenerat. Med.* 13, 694–703. doi: 10.1002/term.2828
- Xi-Xun, Y., Chang-xiu, W., and Huai-qing, C. (2008). Preparation and endothelialization of decellularised vascular scaffold for tissue-engineered blood vessel. *J. Mater. Sci. Mater. Med.* 19, 319–326. doi: 10.1007/s10856-007-3157-3158
- Yang, D., Guo, T., Nie, C., and Morris, S. F. (2009). Tissue-Engineered blood vessel graft produced by self-derived cells and allogenic acellular matrix: a functional performance and histologic study. *Ann. Plastic Surg.* 62, 297–303. doi: 10.1097/SAP.0b013e318197eb19
- Yoon, H., and Kim, G. (2010). Micro/Nanofibrous scaffolds electrospun from pcl and small intestinal submucosa. *J. Biomater. Sci. Pol. Edit.* 21, 553–562. doi: 10.1163/156856209X429166
- Yoshikawa, T., Hamada, S., Otsuji, E., Tsujimoto, H., and Hagiwara, A. (2011). Endocrine differentiation of rat enterocytes in long-term three-dimensional co-culture with intestinal myofibroblasts. *Vitro Cell. Dev. Biol. Animal* 47, 707–715. doi: 10.1007/s11626-011-9458-8
- Yu, J., Peng, S., Luo, D., and March, J. C. (2012). In vitro 3d human small intestinal villous model for drug permeability determination. *Biotechnol. Bioeng.* 109, 2173–2178. doi: 10.1002/bit.24518
- Yuan, B., Jin, Y., Sun, Y., Wang, D., Sun, J., Wang, Z., et al. (2012). A strategy for depositing different types of cells in three dimensions to mimic tubular structures in tissues. *Adv. Mater.* 24, 890–896. doi: 10.1002/adma.201104589
- Zakhem, E., Raghavan, S., Gilmont, R. R., and Bitar, K. N. (2012). Chitosan-Based scaffolds for the support of smooth muscle constructs in intestinal tissue engineering. *Biomaterials* 33, 4810–4817. doi: 10.1016/j.biomaterials.2012.03.051
- Zang, M., Zhang, Q., Chang, E. I., Mathur, A. B., and Yu, P. (2013). Decellularized tracheal matrix scaffold for tracheal tissue engineering: in vivo host response. *Plastic Reconstruct. Surg.* 132, 549e–559e. doi: 10.1097/PRS.0b013e3182a013fc
- Zhang, H., Jia, X., Han, F., Zhao, J., Zhao, Y., Fan, Y., et al. (2013). Dual-Delivery of VEGF and PDGF by double-layered electrospun membranes for blood vessel regeneration. *Biomaterials* 34, 2202–2212. doi: 10.1016/j.biomaterials.2012.12.005
- Zhao, Q., Wang, J., Cui, H., Chen, H., Wang, Y., and Du, X. (2018). Programmed shape-morphing scaffolds enabling facile 3d endothelialization. *Adv. Funct. Mater.* 28:1801027. doi: 10.1002/adfm.201801027
- Zhong, Y., Jiang, A., Sun, F., Xiao, Y., Gu, Y., Wu, L., et al. (2019). A comparative study of the effects of different decellularization methods and genipin-cross-linking on the properties of tracheal matrices. *Tissue Eng. Regenerat. Med.* 16, 39–50. doi: 10.1007/s13770-018-0170-176
- Zhou, F., Jia, X., Yang, Y., Yang, Q., Gao, C., Hu, S., et al. (2016). Nanofiber-Mediated MicroRNA-126 delivery to vascular endothelial cells for blood vessel regeneration. *Acta Biomater.* 43, 303–313. doi: 10.1016/j.actbio.2016.07.048

- Zhou, H., Boys, A. J., Harrod, J. B., Bonassar, L. J., and Estroff, L. A. (2020). Mineral distribution spatially patterns bone marrow stromal cell behavior on monolithic bone scaffolds. *Acta Biomater.* 112, 274–285. doi: 10.1016/j.actbio.2020.05.032
- Zhou, W., Chen, Y., Roh, T., Lin, Y., Ling, S., Zhao, S., et al. (2018). Multifunctional bioreactor system for human intestine tissues. *ACS Biomater. Sci. Eng.* 4, 231–239. doi: 10.1021/acsbiomaterials.7b00794
- Zhu, W., Ma, X., Gou, M., Mei, D., Zhang, K., and Chen, S. (2016). 3D Printing of functional biomaterials for tissue engineering. *Curr. Opin. Biotechnol.* 40, 103–112. doi: 10.1016/j.copbio.2016.03.014

Conflict of Interest: The authors declare that the research was conducted in the absence of any commercial or financial relationships that could be construed as a potential conflict of interest.

Copyright © 2020 Boys, Barron, Tilev and Owens. This is an open-access article distributed under the terms of the Creative Commons Attribution License (CC BY). The use, distribution or reproduction in other forums is permitted, provided the original author(s) and the copyright owner(s) are credited and that the original publication in this journal is cited, in accordance with accepted academic practice. No use, distribution or reproduction is permitted which does not comply with these terms.



Mass Generation, Neuron Labeling, and 3D Imaging of Minibrains

Subashika Govindan^{1,2}, Laura Batti³, Samira F. Osterop^{3†}, Luc Stoppini^{1,4} and Adrien Roux^{1,4*}

¹ Tissue Engineering Laboratory, Haute école du paysage, d'ingénierie et d'architecture de Genève, Haute école spécialisée de Suisse occidentale (HEPIA HES-SO), University of Applied Sciences and Arts Western Switzerland, Geneva, Switzerland,

² ARIMA Lifesciences PVT Ltd., Chennai, India, ³ Wyss Center for Bio and Neuroengineering, Geneva, Switzerland, ⁴ Swiss Center for Applied Human Toxicology (SCAHT), Bern, Switzerland

OPEN ACCESS

Edited by:

Dania Movia,
Trinity College Dublin, Ireland

Reviewed by:

Lisa Maria Smits,
University of Luxembourg,
Luxembourg
Davide Staedler,
University of Lausanne, Switzerland

*Correspondence:

Adrien Roux
adrien.roux@hesge.ch

†ORCID:

Samira F. Osterop
orcid.org/0000-0002-8233-2660

Specialty section:

This article was submitted to
Nanobiotechnology,
a section of the journal
Frontiers in Bioengineering and
Biotechnology

Received: 13 July 2020

Accepted: 23 November 2020

Published: 07 January 2021

Citation:

Govindan S, Batti L, Osterop SF,
Stoppini L and Roux A (2021) Mass
Generation, Neuron Labeling, and 3D
Imaging of Minibrains.
Front. Bioeng. Biotechnol. 8:582650.
doi: 10.3389/fbioe.2020.582650

Minibrain is a 3D brain *in vitro* spheroid model, composed of a mixed population of neurons and glial cells, generated from human iPSC derived neural stem cells. Despite the advances in human 3D *in vitro* models such as aggregates, spheroids and organoids, there is a lack of labeling and imaging methodologies to characterize these models. In this study, we present a step-by-step methodology to generate human minibrain nurseries and novel strategies to subsequently label projection neurons, perform immunohistochemistry and 3D imaging of the minibrains at large multiplexable scales. To visualize projection neurons, we adapt viral transduction and to visualize the organization of cell types we implement immunohistochemistry. To facilitate 3D imaging of minibrains, we present here pipelines and accessories for one step mounting and clearing suitable for confocal microscopy. The pipelines are specifically designed in such a way that the assays can be multiplexed with ease for large-scale screenings using minibrains and other organoid models. Using the pipeline, we present (i) dendrite morphometric properties obtained from 3D neuron morphology reconstructions, (ii) diversity in neuron morphology, and (iii) quantified distribution of progenitors and POU3F2 positive neurons in human minibrains.

Keywords: 3D cell culture, 3D imaging, tissue clearing, neuron labeling, human iPSC derived models, brain spheroids, tissue engineering

INTRODUCTION

In vitro culture models have been integral in studying aspects of brain development and function in real time. The advent of human induced pluripotent stem cells (iPSCs) has accelerated the development of miniature *in vitro* 3D human brain models for the purpose of disease modeling, drug testing and molecular screening. 2D *in vitro* modeling of the human brain involves either (i) derivation of neural progenitor cells from primary human sources at gestational ages, (ii) differentiation of embryonic stem cells or iPSCs to neural progenitors or (iii) forced expression of neuronal transcription factor to transdifferentiate iPSCs to neurons (Pang et al., 2011; Zhang et al., 2013). These differentiated neurons or neural progenitor cells can then be used to generate 3D brain *in vitro* models (containing different types of CNS neurons and glial cells) by (i) culturing on low adhesion cell culture surfaces under agitation, (ii) hanging drop techniques, and (iii) seeding cells at high compaction ratio which are variably termed as neurospheres, brain spheroids, brain micro physiological systems and brain aggregates models (Hogberg et al., 2013; Smirnova et al., 2016; Krencik et al., 2017; Pamies et al., 2017). Alternatively, embryoid bodies, i.e., spherical ensemble

of human iPSCs or embryonic stem cells (ESCs) can be directed into neuronal differentiation that leads to formation of 3D cultures with the cytoarchitecture of the cerebral cortex (Pasca et al., 2015; Otani et al., 2016) which are termed either as spheroids or brain microphysiological system. The more advanced and complex 3D brain *in vitro* models are brain organoids that have been recently been developed by Kadoshima et al. (2013) and Lancaster et al. (2017) which recapitulated the self-organizing principle of forebrain structures while differentiating iPSC to the neuronal lineage using non-guided differentiation protocol.

Despite the advances in the field of 3D brain *in vitro* models, the smaller size of these models presents some challenges in performing classical histological and imaging techniques. On the other hand, some 3D *in vitro* brain models such as the cortical organoids are rather bigger in size but offer challenges for multiplexing for large scale screening studies and necrose relatively rapidly over a few months (Wang, 2018). Here, we present a protocol optimized for generating a brain spheroid model termed as minibrains, where the size of the spheroids and subsequent imaging techniques are optimized for large-scale screening studies at affordable cost, time and labor efficiency.

Minibrains: Miniature 3D Brain Spheroids Generated From Neural Stem Cells Derived From Human iPSCs

In this study, we present minibrains, a brain spheroid model generated by non-directed differentiation of neural stem cells derived from human iPSCs (NSC^{hiPS}) (Figures 1, 2) (protocol was modified and adapted from Sandström et al., 2017). By 8 weeks minibrains display synchronized neural networks (Figure 3; Sandström et al., 2017). Genes characteristic to neurons, oligodendrocytes and astrocytes were expressed in the minibrain. Transcriptomic analysis of minibrain vs NSC^{hiPS} revealed activation of biological process such as synaptic signaling, neuron morphology projection, neuron differentiation and neurotransmitter release. Minibrain expressed genes that is typically enriched in cortical regions such as striatum, sub pallium, layer 6 of motor cortex, piriform, anterior cingulate and occipital cortex (Figure 4).

The size, simplicity and cost efficiency of generating minibrains make them an ideal choice for mass production for the purpose of large-scale screening and modeling studies (Figure 2 and Supplementary Table 1). The average size of minibrains is around 550.64 (\pm) 75.19 μ m and around 50–100 minibrains can be generated and maintained in one well of a 6-well plate (Figure 5 and Table 1). The cost of generating approximately 100 minibrains is 33.50 CHF, the cost of generating and maintaining a “nursery” of approximately 6,000 minibrains for about 1-year costs about 3740 CHF. The smaller size of minibrains, allows efficient diffusion of nutrients to cells until the center of the minibrains, reducing the occurrence of necrosis and maintaining minibrain for up to 15 months and above. Minibrains can subsequently be maintained on an air-liquid interface (ALI) to facilitate brain on chip methodologies for

neuronal network activity measurement using micro-electrode-array integrated biochip (Figure 3).

Labeling neurons and subsequent morphological reconstruction of the neurons provides information about the dendrite morphometric and axonal properties that are crucial for network establishment. These properties can give valuable insight in large scale disease modeling and drug testing screens (DePoy et al., 2014; Miguéns et al., 2015; Cheng et al., 2017; Martínez-Cerdeño, 2017; Patnaik et al., 2020). Much is yet to be understood as to how human neuron morphology is driven in 3D brain *in vitro* models where all connectivity pathways are miniaturized. Labeling of live neuron morphology involves artificial gene transfer techniques that enable expression of fluorescent reporters under the regulation of selective promoters. In previous studies, neurons were labeled in live brain organoids either through electroporation or viral infection of organoid slices, which are laborious processes (Lancaster et al., 2017; Giandomenico et al., 2019). In our pipeline, we implement a novel strategy to label projection neurons with tdTomato fluorescence reporter in the minibrains using retrograde adeno associated viral particles (AAVrg) (Figures 7A–C). Sparse neuronal labeling, together with a high signal to noise ratio of the labeled neurons, enabled 3D reconstructions of distinct neurons within the minibrain (Figures 7B,C). For the first time, we show reconstruction of single neuron morphologies from an 3D *in vitro* brain model, which would allow us in the future to understand neuron differentiation, diversity and connectivity in 3D brain *in vitro* models (Figures 7C–F and Supplementary Figure 3).

3D imaging techniques are critical for reconstructing whole neuron morphology, assessing anatomical distribution of cell types and their interaction across 3D brain *in vitro* models. Here we present a novel 3D imaging pipeline that allows imaging of whole 3D brain *in vitro* models. 2D imaging methodologies require slicing of 3D brain *in vitro* models which can be laborious, time consuming and leads to loss of tissue given the smaller sample size. In contrast, our 3D imaging pipeline relies on easily multiplexable one step non-invasive tissue clarification technique on whole minibrains. We tested multiple tissue clarification protocols on our minibrains. While active CLARITY techniques are too harsh on the minibrains, passive CLARITY technique required embedding the minibrains in agarose gel, a cumbersome process when processing multiple minibrains. Tissue clarification method using fructose-glycerol solution lead to distortion of the minibrain morphology (Figure 5C). On the other hand, RapiClearTM, a commercial tissue clearing agent, allowed direct mounting of minibrains without loss of morphology and best signal preservation for viral labeling, immunohistochemistry and Golgi-Cox staining (Figures 6–8 and Supplementary Videos 1–4). We achieved efficient clarification by permeabilizing fixed minibrains using Triton X-100 before clearing with RapiClearTM (Figures 6A,B). RapiClearTM allows preservation of mounted minibrains at 4°C and –20°C for long term storage. The cleared minibrains were compatible for both confocal and light sheet microscopy (Supplementary Videos 1–4 and Figure 6). For high resolution imaging using upright microscopy, we have used an upright confocal imaging and designed sample holders and microscopy support to facilitate whole mount minibrain

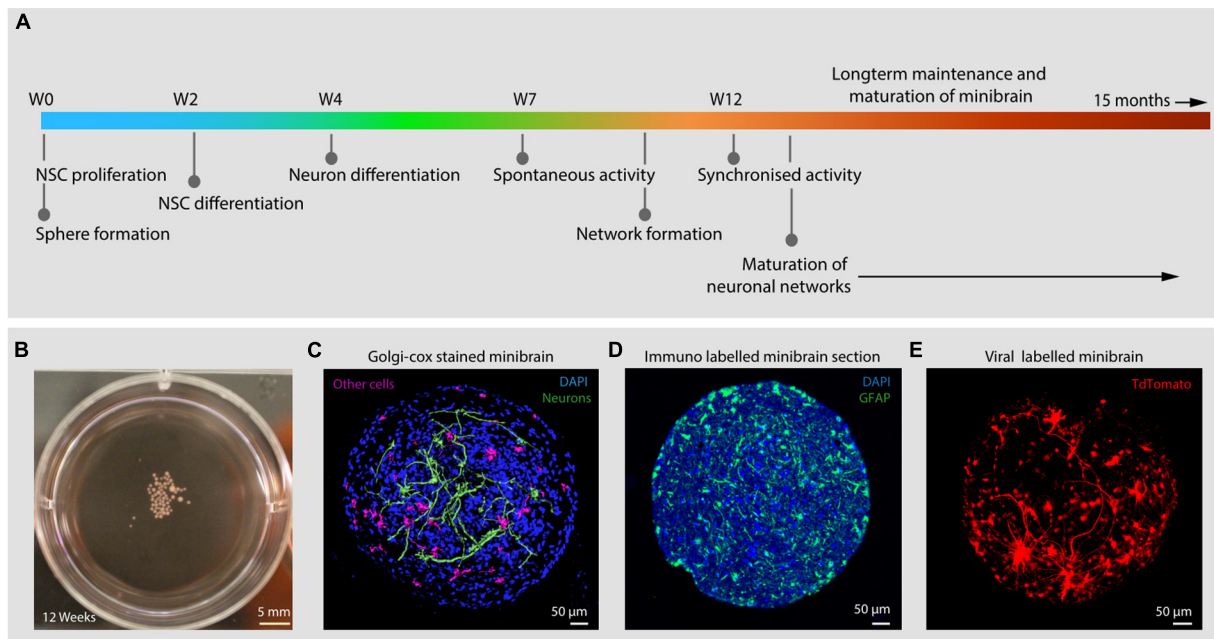


FIGURE 1 | Introduction to minibrains. **(A)** Schematics show the timeline of processes involved in minibrain development. **(B)** Shows 12-week-old minibrains in a 6-well plate. **(C)** Volume rendered image of Golgi-Cox and DAPI stained (a nuclear stain) 12-week-old whole minibrain showing neurons with elaborate projections (color coded in green) and cells with short protrusions (color coded in pink) (see **Supplementary Video 1**). **(D)** Shows microtome cut 12-week-old minibrain section stained with GFAP, a marker of glial cells and DAPI. **(E)** Shows volume rendered image of viral labeled 12-week-old whole minibrain showing tdTomato (a fluorescent protein) labeled projection neurons. W, Week of minibrain generation.

imaging in high refractive index (RI) solution, while multiplexing up to 9 samples (**Supplementary Figure 2**). The long travel distance of the immersion objectives (5.6 mm) allowed us to scan through the whole thickness of the cleared samples (**Figure 6** and **Supplementary Videos 1, 3**). The minibrains can be imaged until a depth of 150–250 µm using inverted microscopy allowing multiplexing up to 96 or 384 samples by using multi-well imaging plates (**Supplementary Video 5**).

We present here a step-by-step methodology for generation and maintenance of minibrain nurseries, ALI maintenance of minibrain, projection neuron labeling, optimized whole minibrain immunohistochemistry, one step mounting clarification, 3D imaging and design of imaging accessories that facilitate 3D imaging using confocal microscopy on cleared minibrains. We present dendrite morphometric properties, diverse reconstructed neuron morphologies, distribution of progenitors and POU3F2⁺ neurons in our minibrain (**Figures 7, 8**). Our novel pipeline is designed to facilitate the usage of minibrains as an *in vitro* 3D human neuronal model for large scale modeling and mass screening studies.

MATERIALS

Reagents

GelTrexTM (ThermoFisher, #A1413301)
StemproTM NSC SFM kit (ThermoFisher, #A1050901) containing

KnockOutTM DMEM/F-12 medium
StemProTM Neural Supplement
FGF-basic (AA 10–155) Recombinant Human Protein
EGF Recombinant Human Protein
GlutaMAXTM Supplement (ThermoFisher, #35050038)
B27TM Plus Neuronal Culture System (ThermoFisher, #A3653401) containing
NeurobasalTM Plus
B-27 Plus Supplement (50X)
Accutase (ThermoFisher, #00-4555-56)
StemProTM hESC SFM (ThermoFisher, #A1000701) containing
DMEM/F12 + GlutaMAXTM
Bovine serum albumin (BSA) 25%
Stempro[®] hESC Supplement
Brain-Derived Neurotrophic Factor (BDNF) Recombinant Human Protein (ThermoFisher, #PHC7074)
Glial-Derived Neurotrophic Factor (GDNF) Recombinant Human Protein (ThermoFisher, #PHC7044)
Dibutyl cyclic AMP (AMPC) (Merck Sigma, #D0627)
2-phospho-Ascorbic Acid (Merck Sigma, #49752)
RapiClearTM 1.47 (SUNJin Lab, #RC147001)
DAPI (4',6-Diamidino-2-Phenylindole, Dihydrochloride) (Invitrogen, #D1306)
Triton X-100 (Merck Sigma Aldrich, #T8787-50ML)
Tween 20 (Merck Sigma Aldrich, #P9416-50ML)
1X Dulbecco's PBS (DPBS) (ThermoFisher, #14040133)
PierceTM 16% Formaldehyde (w/v), Methanol-free (ThermoFisher, #28906)

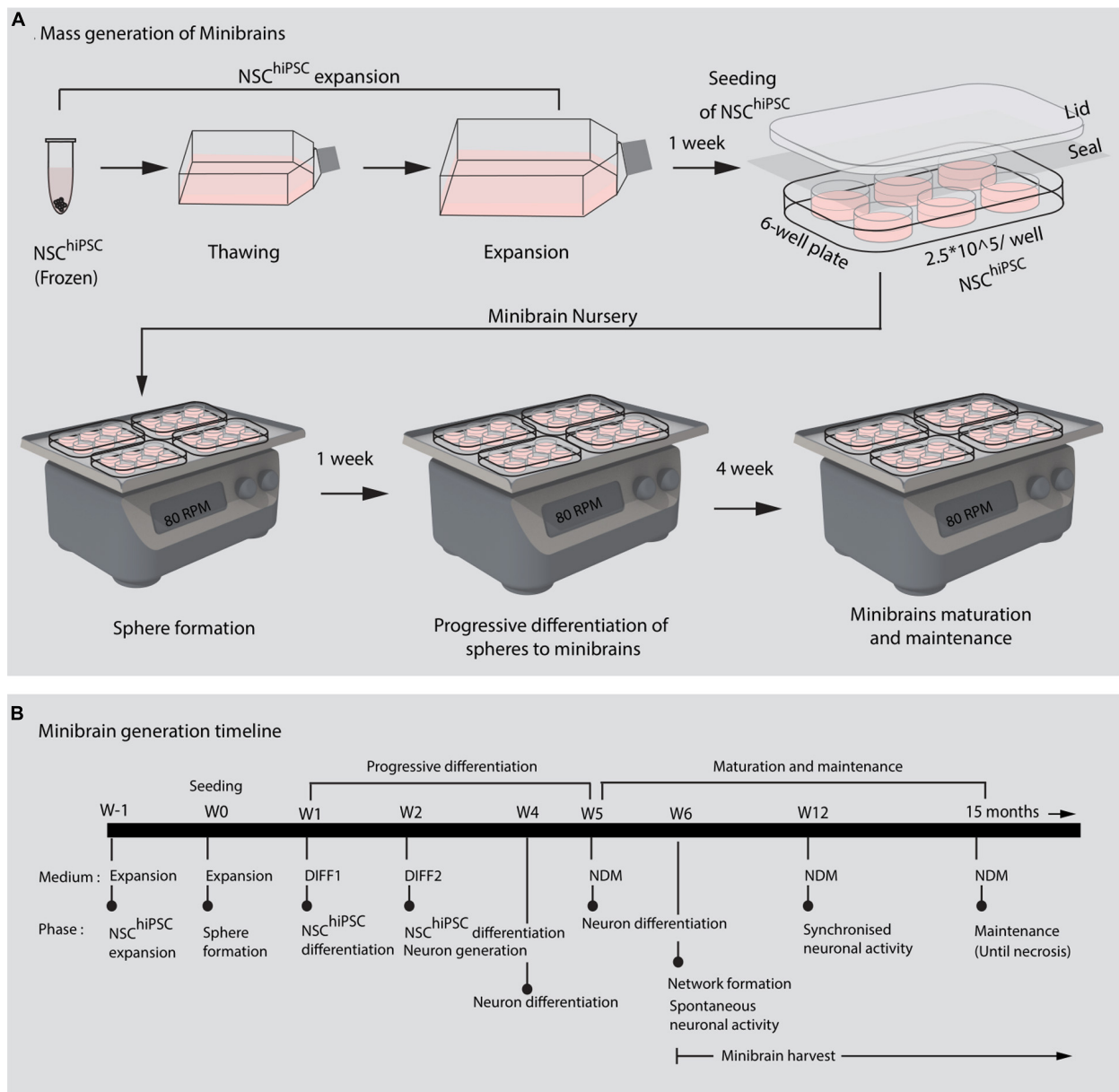


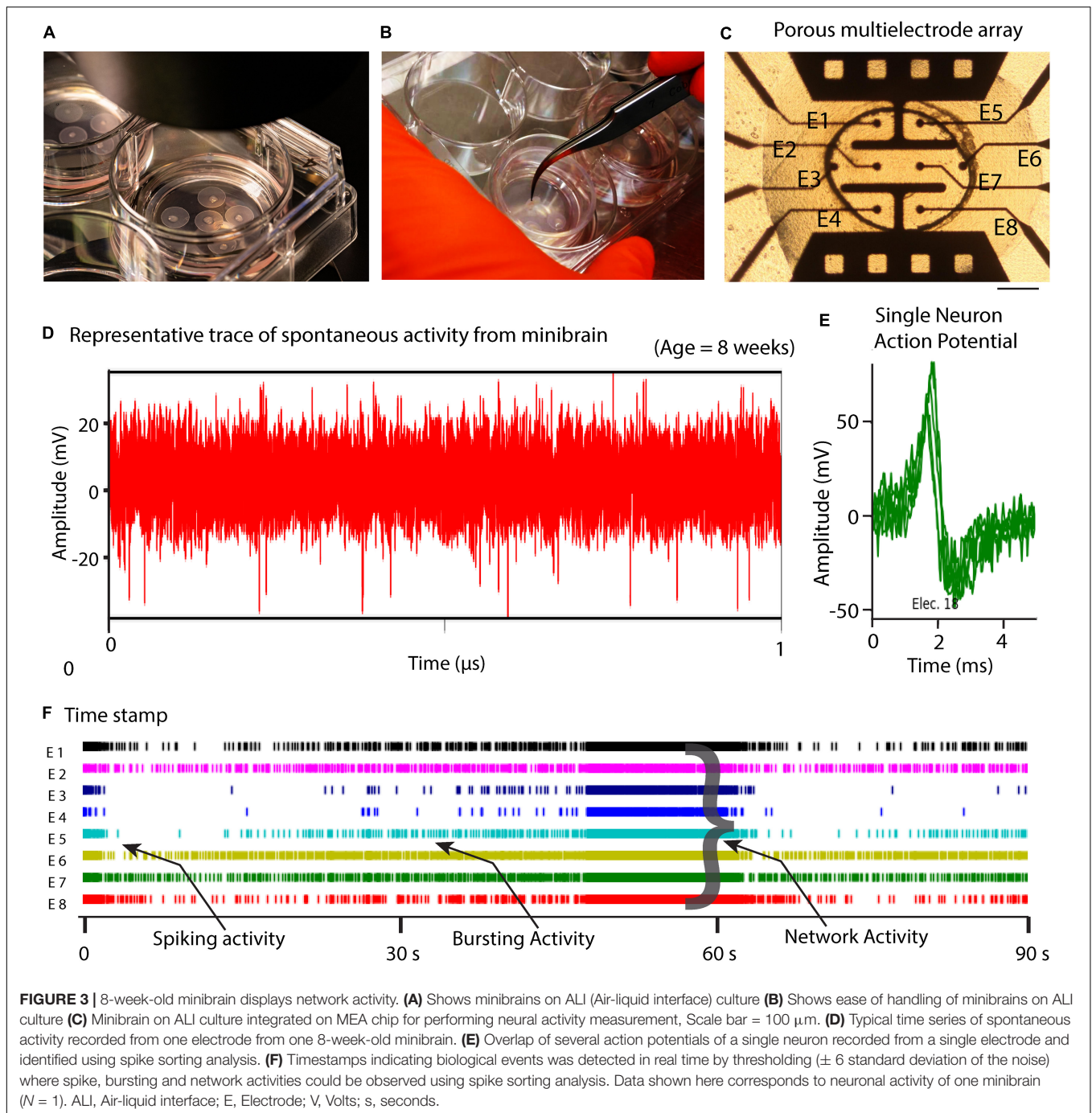
FIGURE 2 | Mass generation of minibrains. **(A,B)** Shows the processes and timeline of establishing and maintaining minibrain “nursery” NSC^{hiPSC}, Neural stem cells derived from human induced pluripotent stem cells; W, Week of minibrain generation; DIFF1, Differentiation 1 medium; DIFF2, Differentiation 2 medium; NDM, Neuron differentiation medium.

Trypan Blue Stain (0.4%) (ThermoFisher, #15250-061).
 Purified Mouse Anti-Human Ki67 antibody (BD Bioscience, #556003)
 Mouse Anti-Human POU3F2 antibody (DSHB, #PCR-POU3F2-1A3-s)
 HistodenzTM (Sigma, #D2158)
 Goat anti-mouse TRITC (Abcam, #ab6786).

Plastics and Tools

6-well culture plate (Greiner Bio-One, #657 160)
 96-well culture plate for imaging (Greiner bio-one, #655090)

384 well culture plate for imaging (Greiner bio-one, #781091)
 24 well culture plate non-treated (Nunc, #144530)
 Breathable plate sealer (Greiner Bio-One, #676051)
 25 cm² cell culture flask (T25) (Corning Falcon, #353109)
 75 cm² cell culture flask (T75) Flask (Corning Falcon, #353136)
 175 cm² cell culture flask (T175) Flask (Corning Falcon, #353112)
 Sterile Hydrophilic PTFE membrane for tissue cultures, 2 mm diameter (named as « confetti ») (PTFE-005, HEPIA Biosciences)
 Cell culture inserts for 6-well plate (Merck Millipore, #044003)
 0.2 ml PCR tube (Thermoscientific, #AB-0784)
 1.5 ml microfuge tubes (Eppendorf, #0030125150)



15 ml tube with conical bottom (Corning Falcon, #352096)
 50 ml tube with conical bottom (Corning Falcon, #352070)
 Pointe 10–20 μ l cleanpack clearline sterile (Milan, #010320)
 Pointe 20 μ l cleanpack clearline sterile (Milan, #713178)
 Pointe 200 μ l cleanpack clearline sterile (Milan, #713179)
 Pointe 1,000 μ l cleanpack clearline sterile (Milan, #713180)
 10 μ l pipette (Rainin, #17014388)
 20 μ l pipette (Rainin, #17014392)
 200 μ l pipette (Rainin, #17014391)
 1,000 μ l pipette (Rainin, #17014382)

2 ml sterile aspirating pipets (Corning Falcon, #357558)
 12 mm glass coverslips (SPL Life Sciences, #20012)
 Luna Cell Counting Slides (Logos biosystems, #L12001)
 Sample holder (HEPIA, **Supplementary Figure 2**).

Cells

NSC^{hiPS} (Human Neural Stem Cells derived from the human induced pluripotent stem (iPS) cell line) (ThermoFisher, #A3890101).

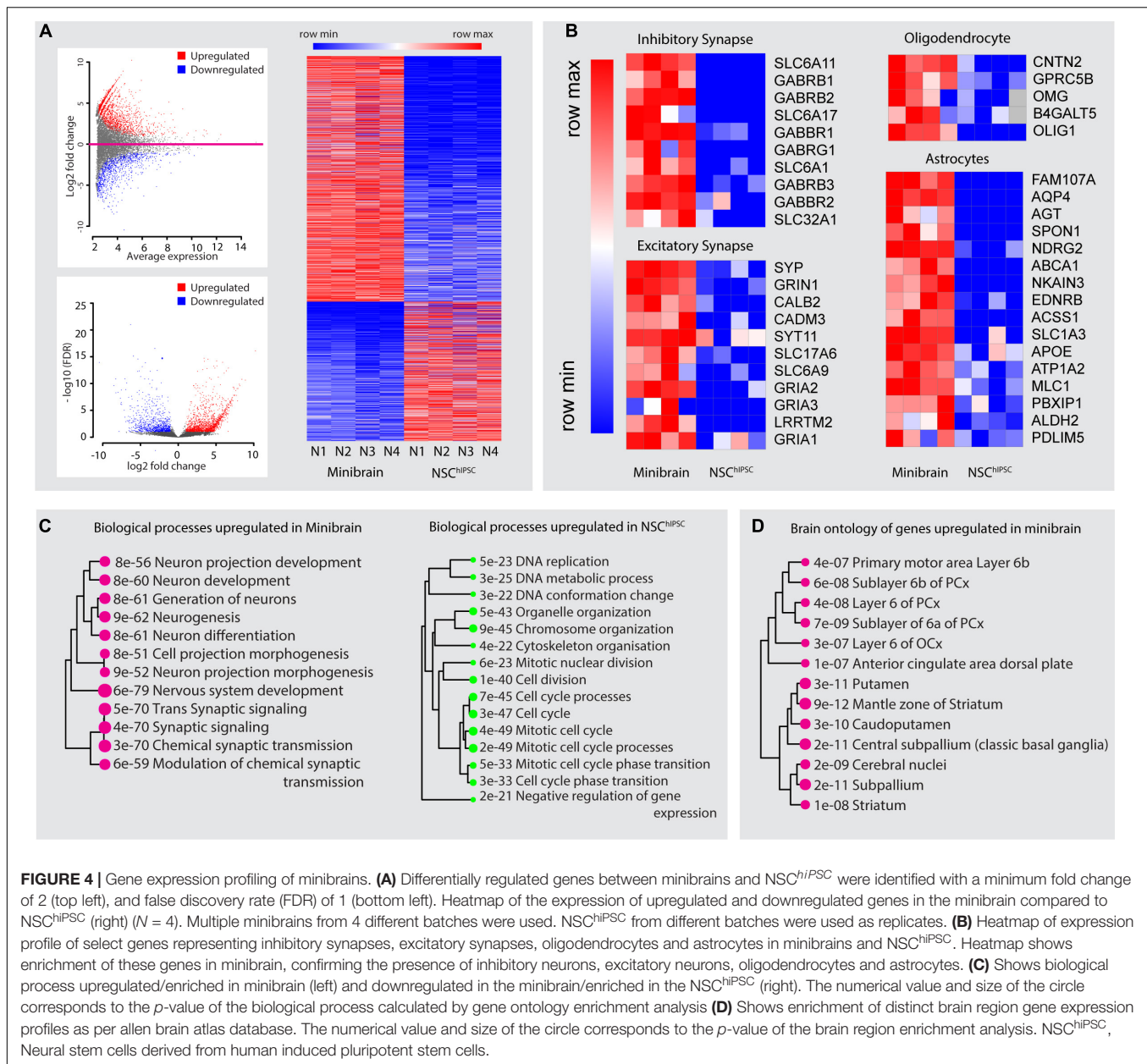


FIGURE 4 | Gene expression profiling of minibrains. **(A)** Differentially regulated genes between minibrains and NSC^{hiPSC} were identified with a minimum fold change of 2 (top left), and false discovery rate (FDR) of 1 (bottom left). Heatmap of the expression of upregulated and downregulated genes in the minibrain compared to NSC^{hiPSC} (right) ($N = 4$). Multiple minibrains from 4 different batches were used. NSC^{hiPSC} from different batches were used as replicates. **(B)** Heatmap of expression profile of select genes representing inhibitory synapses, excitatory synapses, oligodendrocytes and astrocytes in minibrains and NSC^{hiPSC}. Heatmap shows enrichment of these genes in minibrain, confirming the presence of inhibitory neurons, excitatory neurons, oligodendrocytes and astrocytes. **(C)** Shows biological process upregulated/enriched in minibrain (left) and downregulated in the minibrain/enriched in the NSC^{hiPSC} (right). The numerical value and size of the circle corresponds to the p -value of the biological process calculated by gene ontology enrichment analysis. **(D)** Shows enrichment of distinct brain region gene expression profiles as per allen brain atlas database. The numerical value and size of the circle corresponds to the p -value of the brain region enrichment analysis. NSC^{hiPSC}, Neural stem cells derived from human induced pluripotent stem cells.

Virus

AAVrg-CAG-tdTomato (codon diversified), titer value $\geq 7 \times 10^{12}$ vg/ml (Addgene, #59462-AAVrg).

Important: Virus must be handled in biosafety level 2 (BSL2) facility

Note: Upon receipt of the virus, prepare 5 μ l aliquots on ice and store at -80°C .

Equipment

CO₂ resistant orbital Shakers (ThermoFisher, #88881102)

CO₂ incubator (ThermoFisher, #371)

Confocal microscope (Zeiss, LSM880)

20X/1.0 water immersion objective, with adjustable RI correction collar (RI 1.42–1.48) (Zeiss, #421459-9972-000)

Confocal Microscope (Leica, TCS SPE-II) HC PL APO 10.0 \times 0.30NA objective (Leica, #507902)

HXC PL FLUOTAR L 20X/0.40NA objective (Leica, #506242)

Specimen holder for cleared tissue imaging (HEPIA, **Supplementary Figure 2**)

Laminar hood (SKAN AG, #MSF120)

Centrifuge (Eppendorf, #5804 R)

Media Warmer (Lab ArmorTM Beads, #M706)

Elliptical shaker 3D Polymax 1040 complete (Heidolph Instruments, #543-42210-00)

Thermal cycler (MJ Research, #PTC-200)

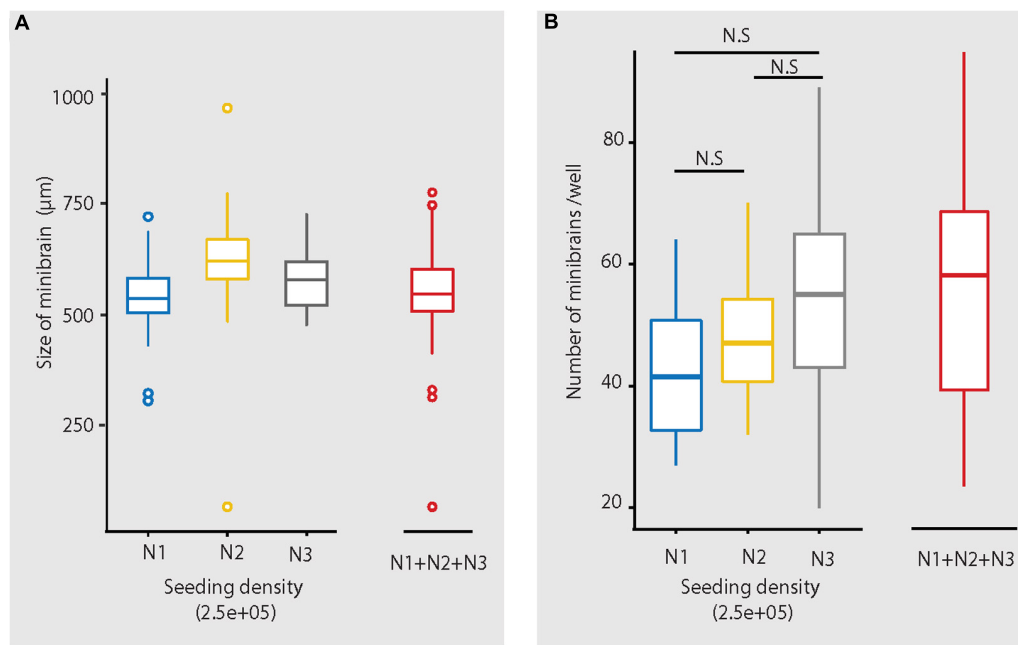


FIGURE 5 | Size and number of minibrains generated using the protocol. **(A)** Shows the distribution of size of minibrains older than 8 weeks across three different batches (N1, N2, and N3) (with seeding density of 2.5×10^5 cells per well) as a whisker plot. Mean \pm Standard deviation (SD) of N1, N2, and N3 are 546.80 ± 62.40 , 623.61 ± 68.52 and 584.73 ± 79.02 , respectively. Collective mean \pm SD of all the three batches is 550.64 ± 75.19 . N1 = 199 minibrains, N2 = 304 minibrains, N3 = 93 minibrains. **(B)** Shows the number of minibrains (more than 8 weeks old) generated per well in a 6-well plate across three different batches (N1, N2 and N3 with seeding density of 2.5×10^5 cells per well) as a whisker plot. The number of minibrains generated across three batches are not significantly different ($p = 0.028$) as per Kruskal Wallis statistical test. Mean \pm SD of N1, N2, and N3 are 42.93 ± 12.00 , 47.75 ± 8.37 , 52.47 ± 16.38 , respectively. Collective mean \pm SD all the three batches is 48.97 ± 12.68 . N1 = 15 wells, N2 = 45 wells and N3 = 60 wells.

Luna Automated Cell Counter (Logos biosystems, #L10001)
 Inverted microscope (Zeiss, #Axiovert 25)
 Laboratory vacuum pump (Milian, #886083)
 Regine Horlogery watchmaker tweezers, type 7 (Beco Technic, #220337)
 Mr. Frosty™ Freezing Container (ThermoFisher, #5100-0001).

REAGENT SETUP

GelTrex (1:200)

Thaw 1 ml vial of GelTrex at 4°C overnight, without agitation (!!! Attention: Agitation will cause clumping). Aseptically add 1 ml of GelTrex to 199 ml of cold KnockOut™ D-MEM/F12 medium. Can be stored at 4°C for up to 1 month.

Stock Solutions of Supplements

Prepare stock solution for EGF, FGF, BDNF (20 ng/ml), GDNF (20 ng/ml), and 2phospho-Ascorbic Acid (20 mM) by resuspending the powder in DPBS, 0.1% BSA, prepare 20 μl or 100 μl aliquots, and freeze at -20°C . Aliquots can be kept for 2 years.

Prepare stock solution for Dibutyl cAMP (100 mM) by resuspending the powder in sterile water, prepare 20 μl or 100 μl aliquots and freeze at -20°C . Aliquots can be kept for 2 years.

Expansion Medium

Prepare expansion medium by aseptically mixing components of Stempro™ NSC SFM kit:

- 500 ml, KnockOut™ D-MEM/F12
- 5 ml, GlutaMAX™ Supplement
- 10 ml, StemPro™ Neural supplement

This medium can be stored at 4°C for up to 3 months.

Before use, aseptically add 100 μl of EGF stock and 100 μl of FGF stock to 50 ml of the above media mix. This solution can be stored at 4°C for up to 1 week.

Differentiation 1 Medium (DIFF1)

For 50 ml of medium aseptically mix

- 44.45 ml, D-MEM/F12 + GlutaMAX
- 3.6 ml, 25% BSA

TABLE 1 | Plating guideline for Minibrain formation.

	No. of cells	Medium volume	Average number of spheres	Required volume of cell suspension
6-well	1×10^6	3 ml	95 ± 34 ($N = 12$ wells)	$2 \times 10^6/X$
6-well	2.5×10^5	3 ml	49 ± 13 ($N = 129$ wells)	$5 \times 10^5/X$
24 well	2×10^4	500 μl	1 or 2	$4 \times 10^5/X$

X, number of living cells/ml in cell suspension.

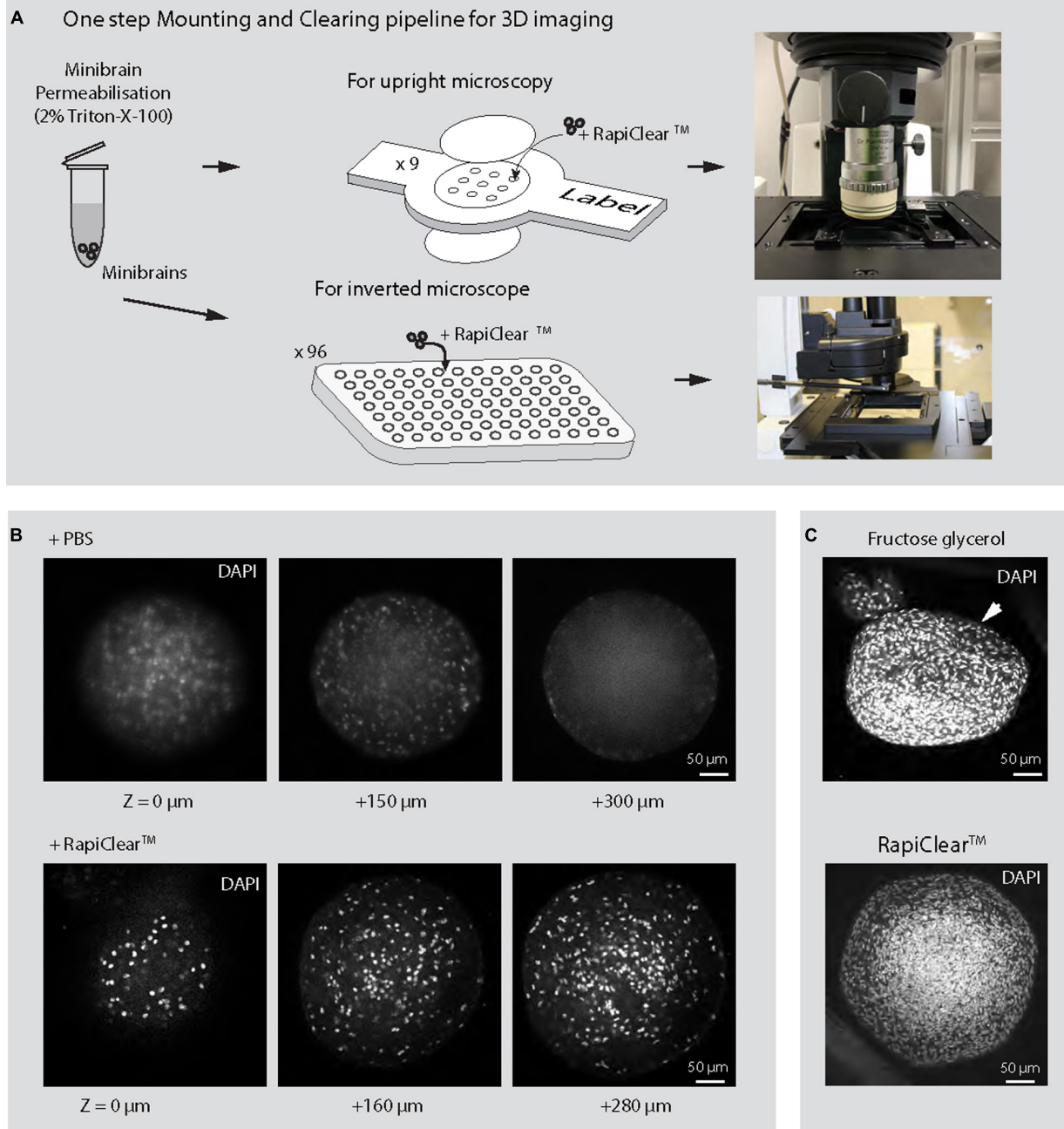


FIGURE 6 | 3D imaging of minibrains. (A) Shows the pipeline for imaging minibrains using upright and inverted confocal microscopes. **(B)** Shows the representative 2D optical sections of 10-week-old minibrains stained with DAPI (a nuclear stain) ($N = 3$ minibrains) without clearing (top) and upon clearing with RapiClear™ at different Z imaging depth. **(C)** Shows morphological changes in 10-week-old minibrains upon clearing with fructose glycerol (top) and intact morphology while using RapiClear™ (bottom). The images are representative maximum intensity projection of approximately 600 μm confocal Z-stack of the minibrain ($N = 5$ minibrains).

1 ml, Stempro hESC Supplement
 100 μl, BDNF stock solution
 100 μl, GDNF stock solution
 250 μl, Dibutyl cyclic AMP stock solution
 500 μl, 2phospho-Ascorbic Acid stock solution
 Note: Do not overheat this medium (for a long time) because several factors (BDNF-GDNF) are sensitive to heat!

This medium can be stored at 4°C for 1 week, but it is best to prepare it fresh before use.

Neuron Differentiation/Maintenance Medium (NDM)

Aseptically mix:

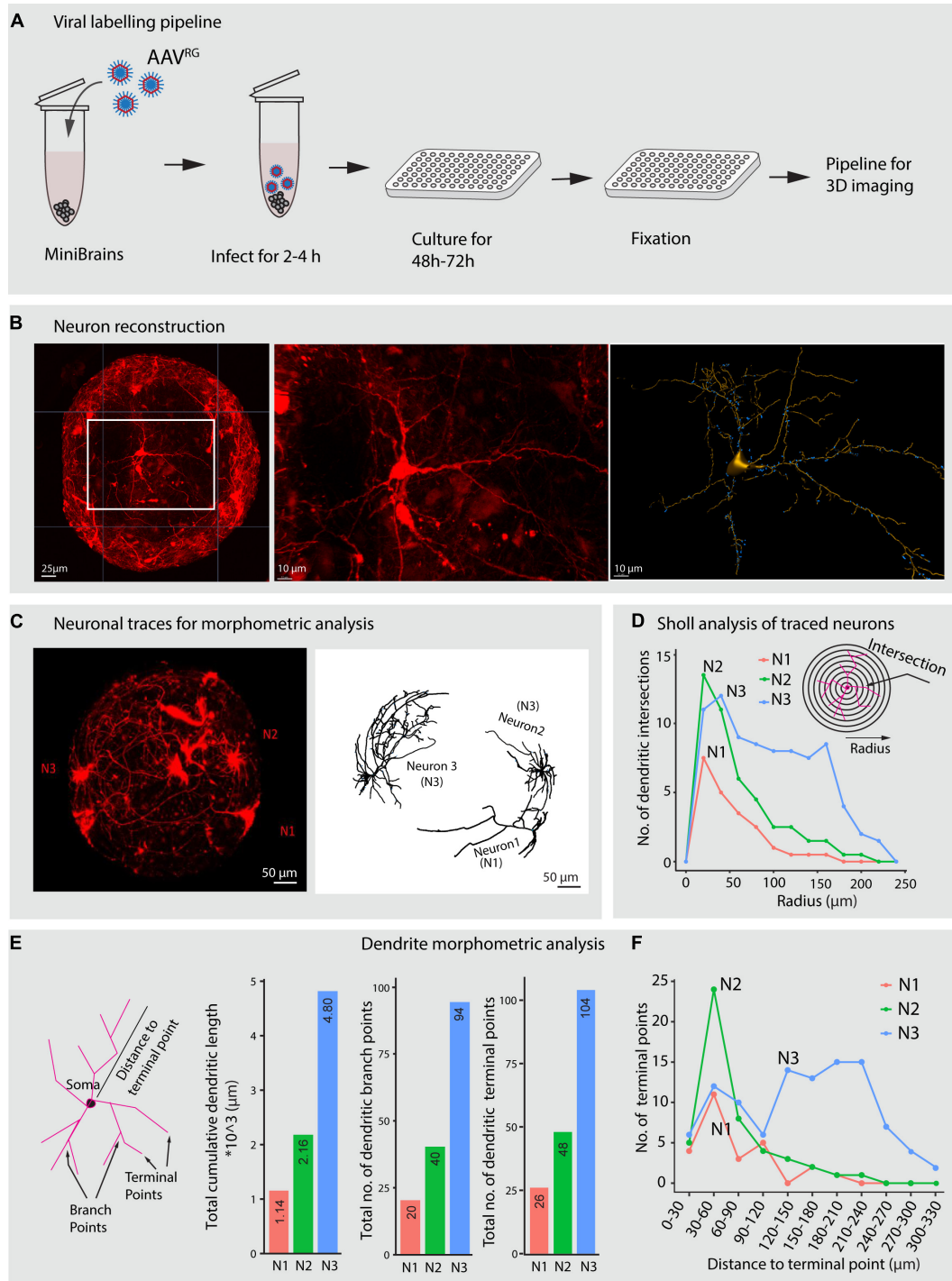


FIGURE 7 | Viral labeling and neuron morphology reconstruction in minibrains. **(A)** Shows a multiplexable viral infection pipeline to label and 3D reconstruct projection neurons in minibrains. **(B)** Shows representative maximum intensity projection of approximately 300 μm confocal Z-stack of minibrain labeled with tdTomato by AAV^{RG} infection (left), an inset zoom on one neuron (center) and the 3D segmentation of the neuron using filament pipeline in Imaris (right) (Age of minibrain = 7 months, $N = 20$ minibrains). **(C)** Shows a representative maximum intensity projection of approximately 600 μm confocal Z-stack of a whole minibrains with tdTomato labeled neurons (Age of minibrain = 3 months) (left), neuron morphology traces of 3 selected neurons (N1, N2, and N3) from the same minibrain segmented by Imaris software (right). **(D)** Sholl analysis of dendrites of the three selected neurons N1, N2, and N3 within the one minibrain in **(C)**. **(E)** Shows dendrite morphometric features (left) and quantification of three properties across three neurons. The bar graphs from left to right show cumulative summation of all dendritic branch length, dendritic branch points and dendritic terminal in three traced neurons shown in **(C)**. **(F)** Shows distribution of the number of the dendritic terminal points at different distances from the soma across the 3 neurons N1, N2, and N3 traced in **(C)**. AAV^{RG}, Adeno associated virus retrograde serotype; h, hours post infection. Neuron morphological analysis performed from three more minibrains are presented in **Supplementary Figure 3**.

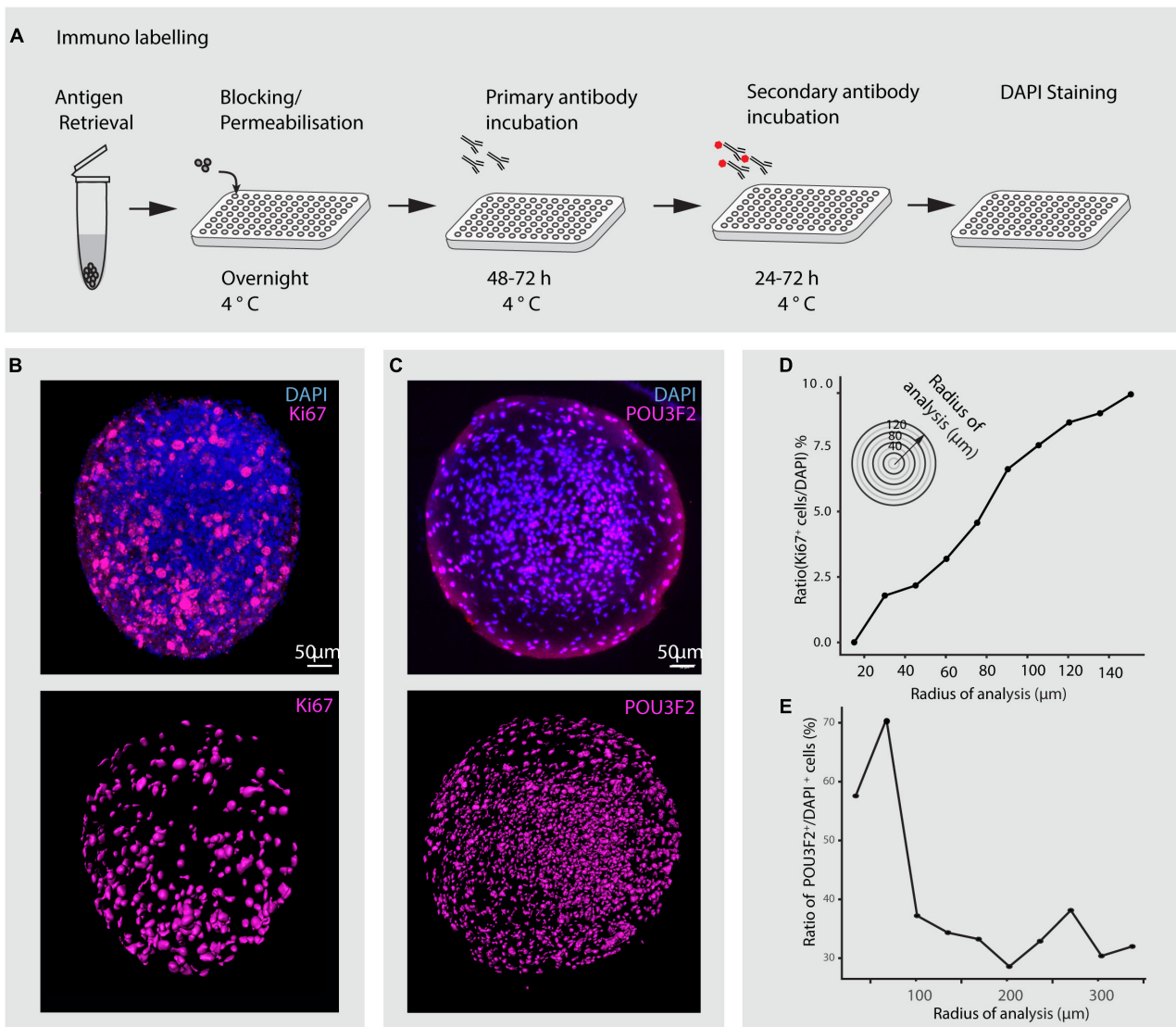


FIGURE 8 | Immunohistochemical analysis of minibrains. **(A)** Shows a multiplexable immunohistochemistry pipeline for minibrains. **(B)** Shows a representative rendered maximum intensity projection of 3D whole minibrain image stained for Ki67 (progenitor marker) and DAPI (top), subsequent segmentation of Ki67 cells (bottom) by Imaris pipeline. Age = 1 week, $N = 9$ minibrains. **(C)** Shows a representative maximum intensity projection (15 μm) of whole minibrain image (age of minibrain = 16 weeks) stained for POU3F2 (excitatory neuronal marker) and DAPI (top), subsequent segmentation of POU3F2+ neurons cells (bottom) by Imaris pipeline. The images are representative of multiple tests $N = 9$ minibrains. Age = 12 weeks. **(D)** Graph shows the distribution of the ratio of Ki67 expressing progenitors to DAPI stained nuclei across minibrain ($N = 1$ minibrain), illustrating the increase in progenitor density toward the periphery in the minibrain in **(B)**. **(E)** Graph shows the distribution of the ratio of POU3F2+ expressing neurons to DAPI stained nuclei across one minibrain, illustrating neurons enriched in the center of the minibrain in **(C)** ($N = 1$ minibrain). Analysis in **(D,E)** was performed only in one minibrain to illustrate an example of cell distribution analysis using 3D imaging. h, hours post staining.

500 ml, NeurobasalTM Plus 1 \times 10 ml, 50x B27 Plus Supplement
1.25 ml, GlutaMAXTM Supplement
This medium can be stored at 4°C for up to 3 months.

Differentiation 2 Medium (DIFF 2)

Aseptically mix DIFF1 medium and NDM medium at 1:1 ratio.

Note: Do not overheat this medium (for a long time) because several factors (BDNF-GDNF) are sensitive to heat!

This medium can be stored at 4°C for 1 week, the best is to prepare it fresh before use.

4% PFA

Aseptically dilute 0.5 ml of 16% PFA to 1.5 ml of 1X DPBS. Store at 4°C for up to 1 month.

Post-fixation Rinse Buffer: DPBS-Tween

Dissolve 1 ml of Tween-20 in 1000 ml of 1X DPBS.

Store at 4°C for up to 6 months.

Antigen Retrieval Buffer

Dissolve 1.5 g of sodium citrate (10 mM) in 450 ml water, adjust pH to 6 with 1 N HCl. Make up the final volume to 500 ml and add 450 µl of Tween 20.

Store at 4°C for up to 6 months.

Blocking Buffer

Dissolve 1 g of BSA and 2 ml of Triton X-100 in 100 ml of 1X DPBS.

Store at 4°C for up to 6 months.

Wash Buffer

Dissolve 2 ml of Triton X-100 in 100 ml of 1X DPBS.

Store at 4°C for up to 6 months.

Primary Antibody Dilution

Dilute primary antibody in blocking buffer as per antibody manufacturer's instructions. Always prepare the dilution freshly before use.

Dilute Ki67 antibody (BD Bioscience, #556003) at 1:25 dilution in blocking buffer.

Dilute POU3F2 antibody (DSHB, #PCRP-POU3F2-1A3-s) at 1:5 dilution in blocking buffer.

Secondary Antibody Dilution

Dilute anti-mouse TRITC secondary antibody (Abcam, #ab6786) at 1:500 dilution in blocking buffer.

DAPI Stock Solution

Make a 5 mg/ml DAPI stock solution by dissolving 10 mg in 2 ml deionized water.

Make sure to dissolve the powder completely by vortexing the tube.

Prepare aliquots and freeze at −20°C for long term storage. Once an aliquot is open, it can be kept at 4°C for 6 months.

METHODS AND PROTOCOLS

Generation of Minibrains

Thawing Frozen Aliquots of NSC^{hiPS}

Before starting the experiment

1. Coat a T25 flask by adding 3 ml of GelTrex stock. Make sure it covers the entire surface area and incubate for 37°C for 1 h.
Note: optionally the coated flasks can be stored at 4°C for 1 month and pre warmed to room temperature before use.
2. Warm 9 ml expansion medium in a 50 ml conical tube to room temperature and 5 ml expansion medium in a 15 ml conical tubes to 37°C.
3. Warm water bath to 37°C.
4. Thaw a vial containing 1 ml of NSC^{hiPS} quickly in a 37°C water bath for not more than 30 s.

5. Transfer 1 ml of the thawed NSC^{hiPS} to a 50 ml tube under the hood using a 1 ml micropipette.
6. Rinse the vial with 1 ml prewarmed expansion medium (at room temperature) and add the contents using a 1 ml micropipette to the cells in the 50 ml tube.
7. Slowly add 8 ml of prewarmed expansion medium (at room temperature) to the thawed cells in the 50 ml tube while mixing gently.
8. Centrifuge the thawed cells at $250 \times g$ for 5 min at room temperature. A cell pellet will be visible after centrifugation.
9. Aspirate medium without disturbing the pellet using an 1 ml micropipette and resuspend the cell pellet in 5 ml expansion medium in the 15 ml conical tube at 37°C using an aspirating pipette.
10. Add 5 ml of the resuspended cells to a GelTrex coated T25 flask and spread evenly.
11. Every second day change the expansion medium.
12. When the cells reach 80% confluency (typically in 2–3 days), passage with Accutase as described in step 13.

Passaging and Expansion of NSC^{hiPS}

Before starting the experiment: warm Accutase and expansion medium (aliquots or the whole bottle) at 37°C. Coat flasks with GelTrex as described in step 1.

13. Aspirate all medium from the flask and add 2 ml of Accutase. Incubate at room temperature for 1–2 min.
Tip: Swirl the plate gently to better visualize the detachment of the cells.
14. To collect the cells, add 2 ml of expansion medium to the detached cells and collect in a 15 ml tube using an aspirating pipette.
15. Rinse the remaining cells with an additional 2 ml of expansion medium and collect in the same tube.
16. Centrifuge cells at $250 \times g$ for 5 min at room temperature.
17. Aspirate medium and resuspend pellet in 2–5 ml of expansion medium (depending on the size of the pellet) using an aspiration pipette.
18. Count live cells per ml on cell counter
 - a. Mix 10 µl of Trypan Blue and 10 µl cell suspension in an 0.5 ml microcentrifuge tube.
 - b. Transfer 10 µl of the mix on a counting slide
 - c. Insert the counting slide in the Luna Automated Cell Counter, adjust the focus and press “count.”
 - d. $\text{Number of live cells/ml} = \text{Number of counted cells} \times 2$
19. Calculate the volume of cell suspension needed for each T75 flask using the formula below.

$$\text{Number of cells required} = 25 \times 10^3 \text{ cells/cm}^2$$

$$\text{Surface area of T75 flask} = 75 \text{ cm}^2$$

$$\text{Number of live cells/ml} = X$$

$$\text{Volume of cell suspension required} = \text{Number of cells required} \times \text{surface area of culture plate}/(X)$$
20. Add the calculated volume of cell suspension using aspiration pipette and 10 ml of prewarmed expansion medium to a new GelTrex coated T75 flask.

21. Culture the cells in an incubator at 37°C and 5% CO₂ until they reach 80% confluency, typically in 2–3 days.

Week 0: Formation of Spheres (3D)

22. Prepare NSC^{hiPS} cell suspension and calculate the number of live cells per ml (X) as described in Step 13–18.
23. Calculate volume of cell suspension to be added based on the guidelines in **Table 1** and as described in step 19.
24. Add calculated volume of cell suspension and required volume of medium using an aspiration pipette required based on the guidelines in **Table 1**.
25. Seal the plate with breathable adhesive paper by detaching the plastic layer protecting the paper and carefully covering the plate using the adhesive side. Make sure all wells are covered by the paper. Close the lid of the plate (**Supplementary Figure 1A**).
26. To form spheres, place the cells on an orbital shaker at 80 rpm and culture for 7 days at 37°C and 5% CO₂.
Note: Spherical nascent minibrains are apparent after 24 h and increase in size is visible after 7 days due to proliferation.
Important!!! From this point on, the culture plates should always be sealed with adhesive paper while culturing minibrains in suspension.

Week 1: Differentiation Phase I

27. Position the plates at a slanted angle allowing minibrains to settle down, aspirate the medium gently from the top without losing any minibrains.
28. Add 2.5 ml of DIFF1 medium per well (for a 6-well plate). Culture the minibrains for 7 days at 80 rpm at 37°C and 5% CO₂.

Weeks 2–4: Differentiation Phase II

29. Aspirate medium as described in step 27, add 2.5 ml of DIFF2 medium (for a 6-well plate). Culture the minibrains for 3 weeks at 80 rpm in the cell culture incubator at 37°C and 5% CO₂. Change DIFF2 medium twice per week.

Week 5 Until 1 Year and Above: Shifting to Maintenance Phase of the Minibrains

30. Aspirate medium as described in step 27. Add 2.5 ml of NDM medium (for a 6-well plate). Change the NDM once per week and check the luminosity of the minibrain.

Troubleshooting: Minibrains can go through fusion upon shifting to maintenance medium (**Supplementary Figure 1B**). Shift one well of minibrains to the maintenance medium, check for fusion of minibrains after 24–48 h. If minibrains have fused in the test well, prolong differentiation phase II until the next medium change (1 week), repeat testing for fusion until minibrains stop to fuse before shifting to maintenance medium.

Troubleshooting: Health of the minibrains can be monitored by screening of necrosis in the minibrains (**Supplementary Figure 1C**). If a minibrain displays complete necrosis, discard the entire well of minibrains.

Note: Minibrains can survive for 15 months and more, with neuronal activity (data not included). The minibrains are termed as early minibrains starting from the 6th week, as that is when they display synchronized neuronal network activity. Mature activity is observed at 8 weeks.

ALI Culture of Minibrain on Confetti

1. Add 1 ml of NDM medium to a 6-well plate.
2. Place cell culture insert on the 6-well plate and place the confetti on the insert, enabling absorption of medium.
3. Warm the medium in the plate in the cell culture incubator for 30 min.
4. Set a 1 ml pipette at 20 µl and transfer one sphere onto the center of a confetti (check the sphere for luminosity before transfer).
5. Add 5 ml of water in the spaces between the well, to ensure humidity as the plates will not be sealed with breathable adhesive paper.
6. Change the medium twice per week by removing the maximum by aspiration and add 1 ml of NDM medium.

Note: Monitor necrosis under a light microscope to monitor health of minibrains.

Viral Labeling of Projection Neurons in Live Minibrains

Viral labeling must be done in biosafety level 2 equipped facility under a hood.

Before starting the experiment:

1. Prepare an ice box and place the viral aliquots in the ice to thaw.
2. Set the centrifuge temperature to 4°C.
3. Warm 5 ml of media in a 15 ml conical tube in the cell culture incubator.
4. Centrifuge the virus at 100 × g for 10 minutes at 4°C, to avoid loss of virus and any spill.
5. Cut a 200 µl tip and transfer 3–4 minibrains to a 1.5 ml microcentrifuge tube.
6. Remove the excess media.
7. Add exactly 30 µl of media in each tube, let the minibrains settle to the bottom.
8. Add 0.5 µl of virus (3.5×10^9 particles) in each tube.
Note: The pipette tip must contact the minibrain while adding the virus. Do not mix the tube after the addition of the virus.
Using higher concentration of virus leads to more neurons labeled making it difficult to reconstruct single neuron morphologies.
9. Incubate the minibrains with virus in the cell culture incubator at 37°C and 5% CO₂ for 2–4 h.
10. In the meantime, add 200 µl NDM medium to a 96-well plate and incubate at 37°C and 5% CO₂.
11. Cut the tip of a 200 µl pipette tip and transfer 1 minibrain per well in the prepared 96-well plate and culture the minibrains for a minimum of 48 h.

Immuno-Histochemical Staining of Minibrains

Minibrain Fixation

1. Remove media from the wells and add 100 μ l of 4% PFA for a 96-well plate, 1 ml of PFA for a 24-well plate and 3 ml of PFA for a 6-well plate and incubate for 45 min at room temperature.
2. Wash the minibrains at room temperature by rinsing with DPBS-Tween for 10 min at 60 rpm on the elliptical shaker. Repeat two more times.

Antigen Retrieval

3. Transfer minibrains to a PCR tube using a cut 200 μ l tip. Remove excess DPBS-Tween, add 100 μ l of antigen retrieval buffer and incubate at 95°C for 1 h in a PCR cyclor.
4. Wash the minibrains at room temperature by rinsing with wash buffer for 5 min at 60 rpm on the elliptical shaker. Repeat one more time.

Permeabilization and Blocking

5. Using a cut 200 μ l tip transfer minibrains to a 96-well plate and remove excess buffer.
6. Resuspend the minibrains in 70 μ l of blocking buffer and incubate for minimum 4 h at room temperature or overnight at 4°C on a rocker at 80 rpm.

Primary and Secondary Antibody Labeling

7. Remove the blocking buffer and add 70 μ l of primary antibody dilution. Incubate at 4°C on a rocker at 80 rpm for 48–72 h.
8. Remove the primary antibody, add 70 μ l of wash buffer, incubate for 30 min on a rocker at 80 rpm. Repeat two more times.
9. Remove the wash buffer and add 70 μ l of secondary antibody dilution. Incubate at 4°C on a rocker at 80 rpm for 24–48 h, protected from light.
Note: From this point on, protect the samples from light to avoid bleaching of the fluorescence.
10. Remove the secondary antibody and add 70 μ l of wash buffer and place in a rocker at 80 rpm for 10 min.

Nuclei Staining With DAPI

11. Dilute DAPI stock solution 1:1,000 in wash buffer and incubate the minibrains for a minimum of 1 h.
12. Remove the DAPI solution, add 70 μ l of wash buffer and place on a rocker at 80 rpm for 30 min. Repeat 2 more times.

Minibrain Preparation for Microscopy

Permeabilization of Minibrain for Tissue Clearing

1. If the minibrains are fixed but were not processed further for immunohistochemistry, incubate minibrains with wash buffer for 2 h.

Mounting and Clearing Minibrains for 3D Confocal Imaging Using Upright Confocal Microscopy

2. In the meantime, prepare the inserts for confocal imaging as shown in **Figure 6** and **Supplementary Figure 2**. Peel the adhesive protector from the middle on one side of the imaging insert and seal the open well holes on one side using an 18 mm glass cover slip.
3. Cut the tip of a 200 μ l pipette tip, transfer minibrains in the wells of the imaging insert, remove excess buffer. One well can hold as much as 4–5 minibrains.
4. Add 20–30 μ l of RapiClear™ to the well as shown in **Supplementary Figure 2**. Make sure wells are completely filled.
5. Remove excess RapiClear™ outside the wells using a 20 μ l pipette.
6. Peel the adhesive tape in the middle and seal the wells of the imaging insert using another 18 mm coverslips.
7. Incubate the minibrains mounted with RapiClear™ for 24 h at room temperature, protected from light.
Note: Optionally lift the minibrains using a pipette tip before sealing the top of the imaging insert. This allows easier location of the minibrains during confocal imaging.

Minibrain Preparation for 3D Imaging Using Inverted Fluorescence Microscopy

8. Transfer permeabilized minibrains to an imaging grade 96 or 384-well plate.
9. Remove any remaining buffer completely and add 80 μ l of RapiClear™ per well for a 96-well plate and 50 μ l of RapiClear™ per well for 384-well plate. Incubate in RapiClear™ for 18–24 h and proceed for imaging.

Imaging Minibrains

Imaging Using Upright Confocal Microscopy

1. Mount the 20X/1 water immersion objective, with adjustable RI correction collar (RI 1.42–1.48) onto the LSM-880 confocal microscope (Zeiss).
2. Prepare the mounting insert by cleaning it. Place the imaging insert as in **Supplementary Figure 2** and secure the insert tightly using the screws on the image insert holder.
3. Fill the mounting insert with Histodenz solution (RI = 1.46).
Note: if the imaging insert is not secured using the brace, the insert will start lifting up while imaging.
4. Perform multi-tile and Z-stack imaging, using confocal or Airy scan module, with step-size of 3 μ m for neuron reconstructions, and 10 μ m for profiling the minibrain for signal.

Note: Alternatively, lightsheet microscopy technique can be used to image cluster of minibrains all at once, by using a lightsheet microscope optimized for large cleared samples (Clarity Optimized Light-sheet Microscope – COLM) (**Supplementary Video 2**).

Note: To perform image analysis and 3D rendering on the z-stack use FIJI or Imaris software (filament tracer and surface modules). Confocal images were denoised with despeckle filter and a background correction was applied by using FIJI software. The Imaris filament tracer pipeline can be applied upon background subtraction to reconstruct neuron morphology by using Imaris Bitplane software.

Imaging Using Inverted Microscopy Multiplexed at 96 or 384 Samples

5. Choose a lens with large working distances and adjustable RI. Match the RI of the lens to match RapiClear™.
6. To ensure the minibrains are close to the imaging surface, remove 30 µl of RapiClear™ from each well for a 96-well plate and 30 µl of RapiClear™ from each well for a 384 well plate.
7. Proceed for imaging using required Z step size, 3 µm for volume rendering, and 10 µm for profiling the minibrain for signal.

Troubleshooting: If the imaging is blurry, choose appropriate RapiClear™ or change the objective with the correct RI to match the refractive indices of both.

TIMING

Generation of Minibrains

- I. Thawing frozen aliquots of NSC^{hiPS}
Step 1–10: 1 h and 30 min
- II. Passaging and expansion of NSC^{hiPS}
Step 13–20: 1 h and 30 min
- III. Week 0: Formation of spheres (3D)
Step 22–26: 1 h
- IV. Week 1: Differentiation phase I
Step 27–28: 30 min
- V. Week 2–4: Differentiation phase II
Step 29: 15 min for one plate
- VI. Week 3–5: Shifting to maintenance phase of the minibrains
Step 30: 15 min for one plate.

ALI Culture of Minibrain on Confetti

Step 1–5: 30–45 min for one plate.

Viral Labeling of Projection Neurons in Live Minibrains

Step 1–8: 30 min
Step 9–10: 2 h and 15 min
Step 11: 48 h.

Immuno-Histochemical Staining of Minibrains

- I. Minibrain fixation
Step 1–2: 1 h 30 min
- II. Antigen retrieval
Step 3–4: 1 h 15 min

- III. Permeabilization and blocking of the minibrain
Step 5–6: 5–18 h
- IV. Primary and secondary antibody labeling
Step 7–10: 3 days
- V. Nuclei staining with DAPI.
Step 11–12: 4 h

Minibrain Preparation for Microscopy

- I. Permeabilization of minibrain for tissue clearing
Step 1: 1 h 30 min
- II. Mounting and clearing minibrains for 3D confocal imaging for upright confocal microscopy
Step 2–6: 20 min to mount 3 minibrains per well onto 9 wells of the sample holder.
Step 7: 24 h
- III. Minibrain preparation for 3D imaging using inverted fluorescence microscopy
Step 8–9: 3 min for one well.

Imaging Minibrains

- I. Imaging in upright confocal microscopy
Step 1–3: 20 min for mounting 3 minibrains per well in 9 wells of the sample holder.
Step 4: 30 min to 2 h for one minibrain
- II. Imaging in inverted microscopy multiplexed at 96 or 384 samples
Step 6: 1 min for 1 well
Step 7: 10–30 min per minibrain (250 µm of imaging).

ANTICIPATED RESULTS

Minibrain is a brain spheroid model, a complex ensemble of various types of excitatory neurons, inhibitory neurons and glial cells (**Figure 4**). The protocol allows generation of minibrains in large numbers and longitudinal maintenance of minibrain for long periods of time. The protocol generates minibrains ranging approximately between 500 and 600 µm, allowing viability of the minibrain for over 15 months. The viral labeling protocol is easy and quick, allowing visualization of neurons as early as 24 h after infection. Projection neurons with different morphologies are labeled through the protocol (**Figure 7** and **Supplementary Figure 3**). Immunohistochemistry protocol is optimized to enable complete penetration of antibodies across the minibrain (**Figure 8**). The clearing of minibrains is suitable for lightsheet, upright and inverted microscopy allowing imaging of minibrains in 3D (**Figures 6–8** and **Supplementary Videos 1–5**). The protocol allows complete imaging of the minibrain from which whole neuron morphology can be reconstructed (**Figure 7** and **Supplementary Figure 3**). Using Imaris, neuron morphology properties can be extracted and analyzed (**Figure 7**). The protocol allows 3D rendering of minibrain immunohistochemistry allowing assessment of anatomical distribution of markers across the minibrain (**Figure 8**).

LIMITATIONS

The viral labeling protocol we developed is currently limited to strong ubiquitous CAG promoters. Further testing is required to check efficiency of weak promoters that would allow labeling of specific cell types. The time required for imaging the minibrains in their whole thickness using a laser scanning technique can take up to 1–2 h when using a step size of 3 μm . This limitation can be circumvented by the use of lightsheet technology. We show that by using a clarity optimized lightsheet system (COLM), aggregates of minibrains can be quickly imaged all at once (**Supplementary Video 2**). Localizing single minibrains and vertically mounting minibrains is complicated and not convenient, hence it is difficult to multiplex imaging using this kind of light sheet microscopy set up. Further protocol establishment is required for light sheet imaging of minibrains. Dispensing minibrains to 96-well and 384 well plates for assays is time consuming and careful attention is required to avoid mix-up of the samples. This limitation can be partly overcome by using multi-channel pipettes and using printed sample/reagent layouts while dispensing minibrains and performing any further assays. For large screening studies, we show that clarified minibrains can be imaged using 384 well imaging culture plates (**Supplementary Video 5**) but images can be clearly obtained only until partial depth due to the quality of the lens used that is not optimized for tissue clarified samples.

DISCUSSION

Minibrains are an excellent choice of *in vitro* models to study early human neuronal development, aspects of gliogenesis, neurogenesis and neuronal connectivity. The iPSCs technology allows us to generate patient-specific minibrain models for various neurological disorders (Costamagna et al., 2019). Minibrains are cost-efficient, reliable and reproducible for testing drug therapeutic options, screening for toxicological effects and assaying for biocompatibility of human neural tissue (Sandström et al., 2017). The ability to maintain the minibrains for over a year allows the researcher to monitor and follow neuronal differentiation and network maturity longitudinally over time.

In this study, we present methodology for mass generation and maintenance of minibrains for large scale studies. In our methodology we adopt generation of minibrains from NSC^{hiPSC} instead of directly from iPSCs to circumvent multiple stem cell differentiation steps. We follow a slow progressive differentiation protocol that was modified from Sandström et al. (2017) published from our lab which allows us to generate relatively smaller brain spheroids in comparison to the brain organoid protocols (Paşca, 2016; Bagley et al., 2017; Lancaster et al., 2017; Xiang et al., 2017; Karzbrun and Reiner, 2019). The use of breathable, adhesive seals in our protocol reduces the frequency of medium changes and increased humidity maintenance, assuring

better health of minibrains and longitudinal maintenance for over 15 months and above. ALI maintenance of minibrain allows integration of minibrains on micro-electrode array biochips and test biocompatibility of neural tissue on neuroprosthetic devices.

In this study, we present novel methodologies to study minibrains using neuronal labeling, immunohistochemistry, clearing and 3D imaging at multiplexed scales. The development of a custom multi-sample holder for the clarity confocal modules enables to image up to 9 wells, and at least 5 minibrains per well. Using immunohistochemistry and 3D imaging, we show that unlike cerebral organoids, in minibrains the progenitors (expressing Ki67) are not distributed to a central core but spread throughout the minibrains (**Figure 8**). Using our pipeline, we were able to confirm the presence of POU3F2 positive neurons and its distribution across minibrains in 3D (**Supplementary Figure 4** and **Figure 8**). With our imaging pipeline, 2D imaging or partial 3D imaging of 3D brain models can be multiplexed for up to 96 or 384 samples using inverted microscopy, investing in long distance lenses, could possibly allow whole mount imaging using inverted microscopy (**Supplementary Video 5**).

It is not yet well understood how neurons shape their morphology in 3D *in vitro* brain models where spontaneous neuronal activity-based networks are the main source of input and where anatomical distribution of molecules like in human developing brains is absent. Thus, studying neuron morphology in 3D brain *in vitro* models, will allow us to study intrinsic self-organizing mechanisms that guide neuron morphology across distinct neuronal subtypes. By combining viral labeling, tissue clearing and confocal imaging, we were able to produce high resolution imaging dataset from whole minibrains revealing diverse neuron morphology reconstructions. By using Imaris Filament tracer we were able to segment 3D labeled cells and model neuronal dendrites allowing us to map various dendrite morphometric properties of neurons. We were able to confirm both long and short projecting neurons in minibrains using our pipeline. Combining neuronal markers with our protocol will allow users to reconstruct neuron morphology specific to distinct subtypes of neurons in minibrains.

More light sheet microscopes and 3D imaging systems have been recently developed for the purpose of imaging small biological samples at multiplexed scales (Alladin et al., 2019; Rakotoson et al., 2019). Our pipeline can easily be adapted for light sheet microscopy systems that have been designed for imaging small-sized biological samples and organoids, which will allow easy multiplexing and shorter time scales for imaging. We show by light sheet imaging of aggregates of minibrains that our pipeline can also be extended to larger brain organoids (**Supplementary Video 2**). In prevue of the fact that most researchers do not have access to light sheet microscopes, and the prevalence of the confocal microscopes our protocol will allow many researchers to image 3D *brain in vitro* models.

In summary, the novel methodologies presented here will serve as a blueprint in using minibrains for large scale screening and modeling studies for the purpose of studying neuronal disorders, drug testing and chemical screening.

DATA AVAILABILITY STATEMENT

The original contributions presented in the study are included in the article/**Supplementary Material**, further inquiries can be directed to the corresponding author/s.

AUTHOR CONTRIBUTIONS

SG and AR designed, conceived the project, and developed the protocols and pipelines. SG, LS, and SO performed the experiments. SG, SO, and LB performed the imaging. SG and LB performed the image processing and analysis. SG wrote the manuscript. LS and AR supervised the project and provided critical inputs. All authors assisted in the preparation of the manuscript.

REFERENCES

- Alladin, A., Chaible, L., Reither, S., Löscher, M., Wachsmuth, M., Hériché, J. K., et al. (2019). Tracking the cells of tumor origin in breast organoids by light sheet microscopy. *bioRxiv* [Preprint]. doi: 10.1101/617837
- Bagley, J. A., Reumann, D., Bian, S., Lévi-Strauss, J., and Knoblich, J. A. (2017). Fused cerebral organoids model interactions between brain regions. *Nat. Methods* 14, 743–751. doi: 10.1038/nmeth.4304
- Cheng, N., Alshammari, F., Hughes, E., Khanbabaei, M., and Rho, J. M. (2017). Dendritic overgrowth and elevated ERK signaling during neonatal development in a mouse model of autism. *PLoS One* 12:e0179409. doi: 10.1371/journal.pone.0179409
- Costamagna, G., Andreoli, L., Corti, S., and Faravelli, I. (2019). iPSCs-Based Neural 3D systems: a multidimensional approach for disease modeling and drug discovery. *Cells* 8:1438. doi: 10.3390/cells8111438
- DePoy, L. M., Perszyk, R. E., Zimmermann, K. S., Koleske, A. J., and Gourley, S. L. (2014). Adolescent cocaine exposure simplifies orbitofrontal cortical dendritic arbors. *Front. Pharmacol.* 5:228. doi: 10.3389/fphar.2014.00228
- Giandomenico, S. L., Mierau, S. B., Gibbons, G. M., Wenger, L. M. D., Masullo, L., Sit, T., et al. (2019). Cerebral organoids at the air–liquid interface generate diverse nerve tracts with functional output. *Nat. Neurosci.* 22, 669–679. doi: 10.1038/s41593-019-0350-2
- Hogberg, H. T., Bressler, J., Christian, K. M., Harris, G., Makri, G., O'Driscoll, C., et al. (2013). Toward a 3D model of human brain development for studying gene/environment interactions. *Stem Cell Res. Ther.* 4(Suppl. 1):S4. doi: 10.1186/scrt365
- Kadoshima, T., Sakaguchi, H., Nakano, T., Soen, M., Ando, S., Eiraku, M., et al. (2013). Self-organization of axial polarity, inside-out layer pattern, and species-specific progenitor dynamics in human ES cell-derived neocortex. *Proc. Natl. Acad. Sci. U.S.A.* 110, 20284–20289. doi: 10.1073/pnas.1315710110
- Karzbrun, E., and Reiner, O. (2019). Brain Organoids—a bottom-up approach for studying human neurodevelopment. *Bioengineering* 6:9. doi: 10.3390/bioengineering6010009
- Krencik, R., Seo, K., van Asperen, J. V., Basu, N., Cvetkovic, C., Barlas, S., et al. (2017). Systematic three-dimensional coculture rapidly recapitulates interactions between human neurons and astrocytes. *Stem Cell Rep.* 9, 1745–1753. doi: 10.1016/j.stemcr.2017.10.026

FUNDING

BNF, HEPIA HES-SO, SCAHT, Wyss Center for Bio and Neuroengineering provided financial support for this project.

ACKNOWLEDGMENTS

Laetitia Nikles and Enes Karavdic for technical support. Audrey Tissot for light sheet microscopy imaging. Loris Gomez Baisac, Jeremy Laedermann and Fabien Moreillon for engineering. Drs. Stéphane Pagès and Corinne Brana for critical input. Daniel Alpern for his help with establishing BRB-seq, Marc Heuschkel and Flavio F. Mor for the design of the MEA and the design of the MEA analysis software respectively.

SUPPLEMENTARY MATERIAL

The Supplementary Material for this article can be found online at: <https://www.frontiersin.org/articles/10.3389/fbioe.2020.582650/full#supplementary-material>

- Lancaster, M. A., Corsini, N. S., Wolfinger, S., Gustafson, E. H., Phillips, A., Burkard, T. R., et al. (2017). Guided self-organization and cortical plate formation in human brain organoids. *Nat. Biotechnol.* 35, 659–666. doi: 10.1038/nbt.3906
- Martínez-Cerdeño, V. (2017). Dendrite and spine modifications in autism and related neurodevelopmental disorders in patients and animal models. *Dev. Neurobiol.* 77, 393–404. doi: 10.1002/dneu.22417
- Miguéns, M., Kastanauskaite, A., Coria, S. M., Selvas, A., Ballesteros-Yañez, I., DeFelipe, J., et al. (2015). The effects of cocaine self-administration on dendritic spine density in the rat hippocampus are dependent on genetic background. *Cereb. Cortex* 25, 56–65. doi: 10.1093/cercor/bht200
- Otani, T., Marchetto, M. C., Gage, F. H., Simons, B. D., and Livesey, F. J. (2016). 2D and 3D stem cell models of primate cortical development identify species-specific differences in progenitor behavior contributing to brain size. *Cell Stem Cell* 18, 467–480. doi: 10.1016/j.stem.2016.03.003
- Pamies, D., Barrera, P., Block, K., Makri, G., Kumar, A., Wiersma, D., et al. (2017). A human brain microphysiological system derived from induced pluripotent stem cells to study neurological diseases and toxicity. *ALTEX* 34, 362–376. doi: 10.14573/altex.1609122
- Pang, Z. P., Yang, N., Vierbuchen, T., Ostermeier, A., Fuentes, D. R., Yang, T. Q., et al. (2011). Induction of human neuronal cells by defined transcription factors. *Nature* 476, 220–223. doi: 10.1038/nature10202
- Pasca, A. M., Sloan, S. A., Clarke, L. E., Tian, Y., Makinson, C. D., Huber, N., et al. (2015). Functional cortical neurons and astrocytes from human pluripotent stem cells in 3D culture. *Nat. Methods* 12, 671–678. doi: 10.1038/nmeth.3415
- Paşca, S. P. (2016). Personalized human cortical spheroids. *Am. J. Psychiatry* 173, 332–333. doi: 10.1176/appi.ajp.2016.16020133
- Patnaik, A., Spiombi, E., Frasca, A., Landsberger, N., Zagrebelsky, M., and Korte, M. (2020). Fingolimod modulates dendritic architecture in a BDNF-dependent manner. *Int. J. Mol. Sci.* 21:3079. doi: 10.3390/ijms21093079
- Rakotoson, I., Delhomme, B., Djian, P., Deeg, A., Brunstein, M., Seebacher, C., et al. (2019). Fast 3-D imaging of brain organoids with a new single-objective planar-illumination two-photon microscope. *Front. Neuroanat.* 13:77. doi: 10.3389/fnana.2019.00077
- Sandström, J., Eggermann, E., Charvet, I., Roux, A., Toni, N., Greggio, C., et al. (2017). Development and characterization of a human embryonic stem

- cell-derived 3D neural tissue model for neurotoxicity testing. *Toxicol. In Vitro* 38, 124–135. doi: 10.1016/j.tiv.2016.10.001
- Smirnova, L., Harris, G., Delp, J., Valadares, M., Pamies, D., Hogberg, H. T., et al. (2016). A LUHMES 3D dopaminergic neuronal model for neurotoxicity testing allowing long-term exposure and cellular resilience analysis. *Arch. Toxicol.* 90, 2725–2743. doi: 10.1007/s00204-015-1637-z
- Wang, H. (2018). Modeling neurological diseases with human brain organoids. *Front. Synaptic Neurosci.* 10:15. doi: 10.3389/fnsyn.2018.00015
- Xiang, Y., Tanaka, Y., Patterson, B., Kang, Y.-J., Govindaiah, G., Roselaar, N., et al. (2017). Fusion of regionally specified hPSC-derived organoids models human brain development and interneuron migration. *Cell Stem Cell* 21:383. doi: 10.1016/j.stem.2017.07.007
- Zhang, Y., Pak, C. H., Han, Y., Ahlenius, H., Zhang, Z., Chanda, S., et al. (2013). Rapid single-step induction of functional neurons from human pluripotent stem cells. *Neuron* 78, 785–798. doi: 10.1016/j.neuron.2013.05.029

Conflict of Interest: SG was employed by HEPIA and is currently employed by company ARMIA Lifesciences PVT Ltd.

The remaining authors declare that the research was conducted in the absence of any commercial or financial relationships that could be construed as a potential conflict of interest.

Copyright © 2021 Govindan, Batti, Osterop, Stoppini and Roux. This is an open-access article distributed under the terms of the Creative Commons Attribution License (CC BY). The use, distribution or reproduction in other forums is permitted, provided the original author(s) and the copyright owner(s) are credited and that the original publication in this journal is cited, in accordance with accepted academic practice. No use, distribution or reproduction is permitted which does not comply with these terms.

Advantages of publishing in Frontiers



OPEN ACCESS

Articles are free to read
for greatest visibility
and readership



FAST PUBLICATION

Around 90 days
from submission
to decision



HIGH QUALITY PEER-REVIEW

Rigorous, collaborative,
and constructive
peer-review



TRANSPARENT PEER-REVIEW

Editors and reviewers
acknowledged by name
on published articles

Frontiers

Avenue du Tribunal-Fédéral 34
1005 Lausanne | Switzerland

Visit us: www.frontiersin.org

Contact us: frontiersin.org/about/contact



REPRODUCIBILITY OF RESEARCH

Support open data
and methods to enhance
research reproducibility



DIGITAL PUBLISHING

Articles designed
for optimal readership
across devices



FOLLOW US

@frontiersin



IMPACT METRICS

Advanced article metrics
track visibility across
digital media



EXTENSIVE PROMOTION

Marketing
and promotion
of impactful research



LOOP RESEARCH NETWORK

Our network
increases your
article's readership